LECTURES ON LIGHT

NONLINEAR AND QUANTUM OPTICS

USING THE DENSITY MATRIX

STEPHEN C. RAND

Lectures on Light

This page intentionally left blank

Lectures on Light

Nonlinear and Quantum Optics using the Density Matrix

Stephen C. Rand
University of Michigan

OXFORD
UNIVERSITY PRESS

This book owes its existence to the abiding support of my wife Paula, the soaring spirit of my mother Margaret, and the wisdom of my father Charles Gordon Rand.

This page intentionally left blank

Contents

This page intentionally left blank

Preface

This book, and the course from which it sprang, attempts to bridge the enormous gap between introductory quantum mechanics and the research front of modern optics and other fields that make use of light. This would be an impossibly daunting task, were it not for the fact that most of us love to hear things again and again that we already know. Taking that into account, this book uses a single approach repeatedly to tackle progressively more exciting topics in the science of light, moving systematically and swiftly from very basic concepts to sophisticated topics.

The reader should be aware from the outset that the approach taken here is unconventional. It is highly selective instead of encyclopedic, and it teaches the reader only how to use the density matrix on new problems. Nowadays, scientific answers are being sought to an ever-expanding array of problems across numerous disciplines. The trend in textbooks on quantum optics is understandably to cover an increasing number of topics comprehensively, and to familiarize students with an ever-widening array of analytic tools, exhaustively. There are many fine texts that fulfill this function, but this book is not one of them. Instead, important topics and alternative methods of analysis have been omitted here to keep it as brief as possible, with a single-minded pedagogical purpose in mind. The main objective of the book is to provide students and researchers with one reliable tool, and the confidence that comes from practice, to analyze new optical phenomena in their chosen field successfully and rigorously.

Thus, the one and only analytic tool developed here for attacking research-level problems in optical science is the density matrix. A systematic procedure is applied to representative problems of "critical subjects" – usually only one example each – to show how virtually any problem can be analyzed with the density matrix. Each successive example adds one system property at a time, with the result that one qualitatively new feature appears in the dynamics each time. By using a systematic "building-up" principle to approach complicated interactions, students begin to recognize what terms in the analysis are associated with particular changes in the dynamics. Following two slow-paced introductory chapters on review material, the text shifts focus to the development of insights as to when atomic motion, or multilevel structure, or coherence effects dominate the behavior of complicated systems. It ends with fast-paced coverage of selected topics and applications.

The organization of the book follows the original sequence of lectures on light prepared for applied physics graduates with typical undergraduate physics, chemistry, and engineering preparation, expected to handle interdisciplinary research topics during their careers. Present-day graduate students who use light often face important problems that no longer fall into the neat categories of unique models from the early days of quantum mechanics, and require broad perspective and reliable mathematical tools to handle new cross-disciplinary topics quickly. This course therefore embraces not only students from traditional subject areas that make use of light (physics, chemistry,

electrical engineering, and materials science), but also the biophysicist who needs laser tweezers, the photochemist who wants coherent control, the biomedical engineer who needs to image through scattering media, the mechanical engineer interested in molecular design of new materials, and others. The greatest theoretical challenge faced by most students is to make appropriate connections between standard models and the bewildering landscape of new research questions on intersecting boundaries of hyphenated subjects like bio-physics, bio-medicine, photo-chemistry, etc. For them, the systematic progression of *Lectures on Light* offers an approach to quantum optical analysis that should help bridge the gaps.

Why choose the density matrix? After all, there are many mathematical tools available to treat nonlinear and quantum optics. The answer is that the density matrix has features that make it a natural choice. For example, it permits one to ignore parts of a problem that appear to be irrelevant and to focus mathematically on the dynamics of interest to the researcher. Also, if desired, it can be reduced to a rate equation treatment – a familiar approach to analysis that all students of science encounter. In addition, it is particularly well suited for dealing with coherence in isolated or interactive systems. This makes it an excellent point of departure for anyone who wishes to use light either to probe or control systems about which little is known. By focusing on this adaptable tool, readers can cover a lot of intellectual ground with the minimum investment in mathematical complexity. What emerges is a reliable analytic framework for use in any research where light probes or controls or alters a system, regardless of whether the problems are classical or quantum.

Another hurdle that is addressed explicitly in this book, and that is very important, is the persistent issue of whether simplified models provide reliable representations of complicated systems. That is why the last part of Chapter 3 examines in detail the question of whether sodium atoms can ever legitimately be viewed as two-level systems given the complexity of their energy level structure. It turns out that the experimentalist is much more in control of the effective number of levels than one might guess. By the end of this course, graduate students in interdisciplinary science are able to exercise considerable judgment in the creation of useful models for their own frontier research problems and analyze them by drawing on solid examples and the explicit methodology of the text.

Some familiarity with introductory quantum mechanics is assumed. However, advanced preparation in optics is not essential to learn and use this material. Over the years, students from disciplines as diverse as the ones mentioned above – mechanical engineering, materials science, electrical and biomedical engineering together with physics, applied physics, and chemistry – have found it to provide the essential insights and analysis they need for immediate application in their research. Some material that is ordinarily omitted from advanced quantum mechanics texts is included to set the stage for the broadest possible applicability. An example of this is third-order perturbation theory. This topic provides an important bridge to understanding nonlinear behavior of even the simplest quantum mechanical systems. Since self-saturation effects, cross-saturation, four-wave mixing processes, and other third-order phenomena are encountered much more commonly in pump-probe experiments than one might expect, it is important that readers become familiar with third-order

effects early in the course of their research. Another unusual feature of this book is that a few procedural errors are presented early on to illustrate what can go wrong when quantum mechanical calculations are formulated inconsistently. These humbling examples remind us all that in research, and most especially in cross-disciplinary work, there is no substitute for the use of common sense and no shortcut to pioneering science.

This book progresses as rapidly as possible from a simple and easy review to challenging modern applications. One layer of conceptual or computational complexity is added in each new section. The technical material begins with some uncommon examples of introductory quantum mechanics that force students from the start to revisit the basic physical principles of optics and quantum mechanics studied as undergraduates. Potential pitfalls are also pointed out that arise from the inclusion of relaxation processes in system dynamics. Once the density matrix approach to dynamics is motivated, formulated, and understood, the course progresses at an accelerated rate through important applications. Hence, the material is best studied in sequence.

This lecture material will be most useful to students interested in acquiring rigorous, broadly applicable analysis quickly. However, the systematic application of one mathematical tool to many forefront topics in nonlinear and quantum optics will be of interest to seasoned researchers as well. The heavy reliance in late chapters on the insights and dynamic effects described in earlier chapters helps to keep the treatment short. Much of the course relies on the semiclassical description in which only the atoms are quantized – the light field is not. This is intended to encourage intuitive thinking to as late a stage as possible. However, in Chapters 6 and 7 several topics are covered where both the atoms and the light field are quantized and intuitive notions are sometimes poor guides. Finally, the selected research topics of Chapter 7 not only illustrate the power of systematic density matrix analysis but give students confidence that, as they approach the exciting frontiers of their own research, the combination of density matrix analysis and common sense perspectives developed throughout this course will facilitate success.

I would like to acknowledge all the help I have received during various stages of preparation of this monograph. First and foremost, I am grateful for the comments and questions of students who took this course over a period of two decades. Along with my own graduate students, they helped to make the presentation compact by forcing me to provide concise answers about confusing notions. I am indebted to Philbrick Bridgess of Roxbury Latin School for imparting to me his respect for analytic geometry, which ultimately led to the discovery of transverse optical magnetism, covered in Sec. 7.4 of this book. On a few topics I have drawn liberally from existing texts, but most especially from "Elements of Quantum Optics" by Meystre and Sargent, "Quantum Electronics" by Yariv, "Quantum Optics" by Zhubary and Scully, "Laser Physics" by Sargent, Scully, and Lamb, "Optical Resonance and Two-level Atoms" by Allen and Eberley, and "Foundations of Laser Spectroscopy" by Stenholm. I am thankful for their fine examples of concise pedagogy. Also I thank my colleagues at the University of Michigan for creating the intellectual environment that made this book possible.

List of Abbreviations

EIT	electromagnetically induced transparency
FID	free induction decay
FWHM	full width at half maximum
QED	quantum electrodynamics
MODFET	modulation-doped field-effect transistor
NDFWM	nearly degenerate four-wave mixing
rms	root-mean-square
RWA	rotating wave approximation
SHO	simple harmonic oscillator
SVEA	slowly varying envelope approximation
VSCPT	velocity-selective coherent population trapping
2DEG	two-dimensional electron gas

This page intentionally left blank

1
Basic Classical Concepts

1.1 Introduction

In classical physics, light interacts with matter as described by a compact set of equations formulated by James Clerk Maxwell in 1885, namely Maxwell's equations. Solutions for the propagation of electromagnetic fields in arbitrary media can generally be built up from solutions to these equations for individual frequency components, and are particularly easy to find if the fields have slowly varying electric and magnetic field magnitudes. The medium through which light passes must also be uniform, and the timescale of interest must greatly exceed the optical period. Fortunately, these conditions are not terribly restrictive. They encompass most (though not all) distinctive phenomena in classical as well as quantum optics. Perhaps more importantly, they form a useful framework for lectures on light without unnecessarily limiting our horizons.

Nowadays, the optical characteristics of media can often be engineered to enhance specific interactions deliberately. For example, quasi-phase-matching crystals can be prepared with periodically inverted domain structure to allow the buildup of new frequency components in the optical field. Similarly, in so-called metamaterials, deliberate variation in microstructure from point to point within a medium is intended to permit light fields to evolve in complicated but controllable ways. It has been shown in recent years that metamaterials can be designed to distort the way electromagnetic waves move through an occupied region of space, in such a way as to render objects located there effectively invisible. Yet even the passage of light through these nonuniform media is again entirely predictable using Maxwell's equations and modern computational tools. The relative maturity of the subject of electromagnetism and the power of modern computers have put us in a position to predict in great detail how light moves, and how it is attenuated, emitted, amplified, or scattered as it progresses through practically any kind of matter. So why is it that light is still such a vital topic today, and when do we have to treat problems quantum mechanically? How can it be that so many new marvels have emerged from the study of electromagnetism and optical science in the last decade or two? The pace of major discoveries continues unabated. How can light tantalize and surprise experts in the twenty-first century with an ever-expanding landscape of discovery and applications at a time when Maxwell's equations are 150 years old?

In addition to being a manual for applications of the density matrix, this book seeks to answer this question. One of its goals is to teach students how to explore and analyze the unknown without already knowing everything. For this journey, the density

matrix is a perfect companion, since one finds that with it the wavefunction of complex systems is no longer needed to calculate most things of interest in optical interactions. The content of this course has been presented now for two decades as an advanced lecture course on light for graduate students at the University of Michigan – primarily those with backgrounds in physics, chemistry, and engineering. It seeks to give students familiarity with a single analytic tool, the density matrix, by applying it systematically to a great many forefront problems in modern optics. It presents a concise, broad (though admittedly incomplete) picture of active research fronts in optical science that students can absorb in a single semester. It does not pretend to be a comprehensive reference for research in any specialty area from which one or more examples may have been drawn. Instead, it shows students how to get started on virtually any research problem using a standard toolbox, and gives them the requisite perspective on what is physically possible and essential in the analysis. Students acquire a sense for when classical, semiclassical, or quantum optical approaches need to be applied, when coherence plays an important role and when it does not, when an exact solution is required and when it is not, through an approach that adds one concept at a time systematically with a single mathematical tool.

Among the more advanced topics that are included in this course are free induction decay, photon echoes, nutation, spectral and spatial hole-burning, light shifts, two- and three-level coherence, Zeeman coherence, coherent population transfer, electro-magnetically induced transparency (EIT), slow light, high-order perturbation theory, laser cooling, optical magnetism, squeezed light, dressed atoms, and cavity quantum electrodynamics. Although some of these subjects are typically omitted from standard textbooks on light, experience has shown that they can be handled by intermediate or beginning graduate students when the progression through these topics is presented in sufficiently small steps. Moreover, this process succeeds in providing a framework for understanding optical phenomena in a way that is quite different from that of books that emphasize a sequence of different mathematical techniques to handle quantum mechanics. For this reason, most of the book utilizes a "semiclassical" approach that treats the system under study as a quantum system but avoids the introduction of operators to describe the electromagnetic field itself. This has the merit of postponing operator mathematics required for the quantization of the electromagnetic field until the final chapters when they are really needed.

Analysis of many forefront topics in optics with a single approach gives readers confidence that they can proceed into virtually any developing field where light is used to probe or control dynamics, and confidently formulate an initial attack on *their* research problem. Naturally it also has the disadvantage of being just one approach. Many of us are familiar with the mathematical handicap that can result from a bad choice of coordinate system, or an ill-suited choice of variables. However, the density matrix is a remarkably complete and forgiving tool that accomplishes the essential things. First, it incorporates the all-important phases of fields and polarizations responsible for some of the surprising phenomena encountered in optical science. It can describe dephasing, coherent control, and relaxation processes in a manner consistent with the occupation of various states of the system. Second, it eliminates the need for detailed wavefunctions in the prediction of most of the important dynamics in new systems. In beginning courses in quantum mechanics we are taught that the

wavefunction contains all the details of the quantum system and is essential for understanding or predicting its behavior. Unfortunately, solutions are available for wavefunctions of only the simplest systems like atomic hydrogen. Consequently, it is fortunate, to say the least, that the density matrix provides a method for computing all the "interesting" dynamics of new systems given only limited information on energy levels and symmetries. One can even ignore parts of multicomponent systems through the use of the reduced density matrix. In this way, it becomes possible to analyze complicated systems like macromolecules, for which analytic wavefunctions are not likely to be available at any time in the foreseeable future.

1.2 Electric and magnetic interactions

1.2.1 Classical electromagnetism

The interaction of electromagnetic waves with matter is more complex at optical frequencies than at radio or microwave frequencies. There are innumerable possibilities for resonance in the optical range which do not exist at frequencies below 10 GHz, for example. Such resonances result in large changes to absorption, dispersion, and scattering when only small changes in frequency are made. In addition, relatively large variations of constitutive parameters, namely permittivity ε and permeability μ, over the frequency ranges between resonances can be exploited to cause energy exchange between waves of different frequencies. This emphasizes the importance of finding a general approach to optical analysis that incorporates resonant, dispersive, and quantum mechanical character of atomic and molecular interactions with light. So we shall develop a formalism that combines Maxwell's equations and quantum properties of matter from the outset, and seek perspective by applying it systematically to a variety of problems.

1.2.2 Maxwell's equations

The fundamental equations relating time-varying electric and magnetic fields are

$$\bar{\nabla} \times \bar{H} = \bar{J} + \frac{\partial \bar{D}}{\partial t}, \tag{1.2.1}$$

$$\bar{\nabla} \times \bar{E} = -\frac{\partial \bar{B}}{\partial t}, \tag{1.2.2}$$

$$\bar{\nabla} \cdot \bar{D} = \rho_v, \tag{1.2.3}$$

$$\bar{\nabla} \cdot \bar{B} = 0. \tag{1.2.4}$$

Constitutive relations describe the response of charges to applied electric or magnetic fields in real materials. The displacement field $\bar{D}$ in Maxwell's equations is

$$\bar{D} = \varepsilon \bar{E} = \varepsilon_0 \bar{E} + \bar{P}, \tag{1.2.5}$$

and the magnetic flux density in Maxwell's equations is

$$\bar{B} = \mu \bar{H} = \mu_0 \left(\bar{H} + \bar{M} \right). \tag{1.2.6}$$

At optical frequencies or in nonmagnetic systems, we typically assume $\bar{M} = 0$, because magnetic Lorentz forces are small compared to electric forces at high frequencies. In media with linear response, the polarization is $\bar{P} = \varepsilon_0 \chi_e^{(1)} \bar{E}$, $\chi_e^{(1)}$ being the linear electric susceptibility. Thus, the displacement field is

$$\bar{D} = \varepsilon_0 \big(1 + \chi_e^{(1)}\big) \bar{E}, \tag{1.2.7}$$

and the relative, linear dielectric constant $\varepsilon_r = \varepsilon/\varepsilon_0$ is given by $\varepsilon_r = 1 + \chi_e^{(1)}$.

In nonlinear or strongly excited media, there are higher-order terms ($P = P^{(1)} + P^{(2)} + \ldots = \varepsilon_0(\chi_e^{(1)} E + \chi_e^{(2)} E^2 + \ldots)$) that introduce field-induced effects. We deal with nonlinear response when multiphoton transitions of isolated atoms are considered in later chapters. Nonlinear response can also arise from the finite response time of bound electrons or charge motion in the case of free carriers. Either mechanism can produce a "nonlocal" relationship between the polarization and the field ($P(\bar{r}, t) \sim \varepsilon_0 \chi_e(t - t', \bar{r} - \bar{r}') E(\bar{r}', t)$). If we are interested only in slow dynamics in dielectrics we can often ignore such effects. However, finite response times cannot be ignored on ultrafast timescales in semiconductors, plasmas, or organic electronic materials. They also cannot be ignored in photorefractive media, where charges diffuse slowly from place to place, or in multilevel media, where long-lived states lead to time-delayed response.

1.2.3 The wave equation

The key equation describing propagation of classical light is the wave equation, obtained by applying the curl operator to combine Eqs. (1.2.1) and (1.2.2).

$$\bar{\nabla} \times \bar{\nabla} \times \bar{E} = -\bar{\nabla} \times \frac{\partial \bar{B}}{\partial t} = -\frac{\partial}{\partial t} \left[\mu \left(\bar{J} + \frac{\partial \bar{D}}{\partial t} \right) + \mu \left(\bar{\nabla} \times \bar{M} \right) \right]$$

$$= -\mu \frac{\partial \bar{J}}{\partial t} - \mu\varepsilon \frac{\partial^2 E}{\partial t^2} - \mu \frac{\partial^2 \bar{P}}{\partial t^2} - \mu\bar{\nabla} \times \frac{\partial \bar{M}}{\partial t}. \tag{1.2.8}$$

If we restrict ourselves to nonmagnetic, insulating materials ($\bar{M} = 0$; $\bar{J} = 0$), then we can use a vector identity in Eq. (1.2.8) to find

$$\bar{\nabla} \times \bar{\nabla} \times \bar{E} = -\nabla^2 \bar{E} + \bar{\nabla} \left(\bar{\nabla} \cdot \bar{E} \right) = -\nabla^2 E + \frac{\bar{\nabla}}{\varepsilon} \left[\bar{\nabla} \cdot \bar{D} - \bar{\nabla} \cdot \bar{P} \right]. \tag{1.2.9}$$

Provided that the local free charge density ρ_v is zero and there are no spatial variations of polarization due to charge migration or field gradients, we find $\bar{\nabla} \cdot \bar{D} = \bar{\nabla} \cdot \bar{P} = 0$ and in non-magnetic insulators ($M = J = 0$) the wave equation becomes

$$\nabla^2 \bar{E} - \frac{1}{c^2} \frac{\partial^2 \bar{E}}{\partial t^2} = \mu_0 \frac{\partial^2 \bar{P}}{\partial t^2}, \tag{1.2.10}$$

where $c \equiv (\mu_0 \varepsilon_0)^{-1/2}$ is the speed of light in vacuum.

1.2.4 Absorption and dispersion

Solutions of Eq. (1.2.10) are useful in describing many important classical phenomena in linear dielectrics $(P = P^{(1)})$, such as absorption and dispersion. As an example of such a solution, consider a linearly polarized plane wave $E(z, t)$ propagating along $\hat{z}$. If the wave is polarized along $\hat{x}$, meaning that it points along the direction x, this wave can be written in the form

$$\bar{E}(z, t) = \frac{1}{2} E_{0x}(z) \, \hat{x} \exp[i(kz - \omega t)] + c.c., \tag{1.2.11}$$

where c.c. stands for complex conjugate. Other possible polarization states are considered in the next section. Here, however, we show, by substituting Eq. (1.2.11) into Eq. (1.2.10), that the wave equation can often be written in a scalar form that ignores the vector character of light. After substitution, the orientation of the field emerges as a common factor, which may therefore simply be dropped from the equation. In this way, we find

$$\frac{\partial^2 E_{0x}(z)}{\partial z^2} + 2ik\frac{\partial E_{0x}(z)}{\partial z} - k^2 E_{0x}(z) + \frac{\omega^2}{c^2} E_{0x}(z) = -\frac{\omega^2}{c^2}\chi^{(e)} E_{0x}(z). \tag{1.2.12}$$

An important mathematical simplification can be introduced at this point, called the slowly varying envelope approximation (SVEA), by assuming that the amplitude $E_{0x}(z)$ varies slowly over distance scales comparable to the wavelength. This permits neglect of small terms like $\partial^2 E_0(z)/\partial z^2$ in Eq. (1.2.12), whereupon the wave equation reduces to

$$2ik\frac{\partial E_{0x}(z)}{\partial z} - \left(k^2 - \frac{\omega^2}{c^2}\right) E_{0x}(z) = -\frac{\omega^2}{c^2}\chi^{(e)} E_{0x}(z). \tag{1.2.13}$$

Recognizing that the electric susceptibility $\chi^{(e)}$ can be complex $\left(\chi^{(e)} = \chi' + i\chi''\right)$, we can equate the real parts of Eq. (1.2.13) to find

$$k^2 = \frac{\omega^2}{c^2}\left(1 + \chi'\right). \tag{1.2.14}$$

This relationship between frequency ω and wavenumber k is known as the linear dispersion relation. It is a defining relationship for light, usually written as

$$\omega = c_n k, \tag{1.2.15}$$

where

$c_n(\omega) = c/n(\omega)$ is the phase velocity of the wave,
c is the speed of light in vacuum, and
n is the refractive index given by $n^2 = 1 + \chi'$.

Equating the imaginary parts of Eq. (1.2.13), one finds

$$-2k\frac{\partial E_{0x}(z)}{\partial z} = \frac{\omega^2}{c^2}\chi'' E_{0x}(z). \tag{1.2.16}$$

Multiplication of both sides of Eq. (1.2.16) by the conjugate field amplitude $E_{0x}^*(z)$ yields

$$\frac{\partial |E_0|^2}{\partial z} = -\frac{\omega^2}{c^2}\frac{\chi''}{k}|E_0|^2, \tag{1.2.17}$$

and thus

$$\frac{\partial I}{\partial z} = -\alpha I, \tag{1.2.18}$$

where I is the optical intensity. By defining the absorption coefficient

$$\alpha \equiv \frac{\omega^2}{c^2}\frac{\chi''}{k}, \tag{1.2.19}$$

we find that the solution of Eq. (1.2.18) can be written as

$$I(z) = I_0 \exp[-\alpha z], \tag{1.2.20}$$

which is Beer's Law. When $\alpha > 0$ the electromagnetic wave undergoes exponential absorption (loss). When $\alpha < 0$, there is exponential amplification (gain). Beer's Law applies to optical propagation in many systems. Exceptions include systems where radiation trapping, saturation, and multiple scattering take place.

1.2.5   Resonant response

So far, we have characterized the electric response by introducing a polarization P that depends on the incident field. The proportionality constant is the classical macroscopic susceptibility χ, and we find that we can describe some well-known propagation effects such as the dependence of the phase velocity c_n on refractive index and the exponential nature of absorption or gain in simple materials. However, to this point we have no model or fundamental theory for the electric susceptibility χ itself.

For this purpose, we turn to a classical harmonic oscillator model based on linear response (and Hooke's Law). The electron and proton comprising a fictitious atom are joined by a mechanical spring with a restoring force constant k_0. It is assumed that the proton does not move significantly in response to the applied field (Born approximation), whereas the displacement $x(t)$ about equilibrium of the bound electron depends on the applied field according to $\bar{F} = -e\bar{E} = -k_0\bar{x}$. If $\bar{E}$ is harmonic in time, solutions will have the form $x(t) = x_0 \exp(-i\omega t)$. Upon substitution into Newton's second law

$$m_e \frac{\partial^2 x(t)}{\partial t^2} - m_e \gamma \frac{\partial x(t)}{\partial t} + k_0 x(t) = -eE_{0x}\exp(-i\omega t), \tag{1.2.21}$$

one can solve for the amplitude $x(t)$ of driven charge motion, which is given by

$$x_0 = \frac{eE_{0x}/m_e}{\omega^2 - i\omega\gamma - \omega_0^2}, \tag{1.2.22}$$
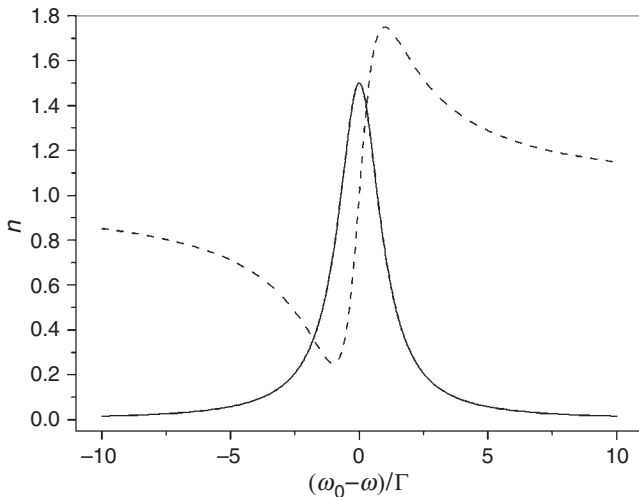
Figure 1.1 *Frequency dependence of absorption (solid curve) and dispersion (refractive index – dashed curve) near a resonance at frequency ω_0 in the classical model.*

where $\omega_0 \equiv \sqrt{k_0/m_{\rm e}}$ is the resonant frequency of the oscillator and γ is an empirical damping constant. The total polarization is

$$P(t) = -\sum_{1}^{N} ex(t) = -Nex(t), \qquad (1.2.23)$$

for N identically prepared atoms. A comparison with our former expression $P = \varepsilon_0 \chi E$ determines the frequency-dependent susceptibility components, and through them the absorption and dispersion curves shown in Fig. 1.1.

Although this Lorentz model is strictly empirical, it provides a qualitatively useful picture of the frequency dependence of system response near electronic resonances. Regrettably, it does not provide a way to derive the spring and damping constants from first principles or to explain the stability of atoms. We turn to quantum mechanics to remedy such deficiencies.

1.2.6   The vectorial character of light

The wave equation (Eq.1.2.10) is a vector relation. Often, as shown in Section 1.2.4, it can be reduced to a scalar relation because the vector character of light plays no role in the particular atom–field interaction of interest. However, this is certainly not always true, and it is helpful to identify what circumstances require full vector analysis. In later chapters, a few topics such as Zeeman coherence and transverse optical magnetism are covered that are strongly governed by vectorial aspects of light. In anticipation of these subjects, we close this introductory chapter by describing the basic polarization states of light that are possible and the angular momentum carried by them.

In Section 1.2.4, the polarization of light was introduced as a property of light specifying the direction in which the optical electric field is oriented. Since the field orientation may vary in time, this definition still admits three fundamentally different states of polarization which are called linear, right circular, and left circular. Linear polarization describes light waves in which the electric field points in a fixed direction. For example, x-polarized light propagating along $\hat{z}$ has an E field oriented along the unit vector $\hat{x}$. Hence it may be written in the form $\bar{E}(z,t) = E_x(z,t)\hat{x}$ or $\bar{E}(z,t) = E(z,t)\hat{e}$, if we let $\hat{e}$ represent a more general polarization unit vector. Circular polarization describes light with an electric field vector that executes a circle around the propagation axis. The electric field rotates once per cycle, either clockwise or counterclockwise, as the wave propagates forward. The circular basis vectors for these polarizations are

$$\hat{\varepsilon}_\pm = -(1/\sqrt{2})(\hat{x} \mp i\hat{y}). \qquad (1.2.24)$$

In the case of circular polarization, the vector $\hat{e} = \hat{\varepsilon}_\pm$ is an axial rather than a polar vector. The 90° difference in phase of oscillations along $\hat{x}$ and $\hat{y}$ in Eq. (1.2.24) results in fields of the form $\bar{E}(z,t) = E_x(z,t)\hat{\varepsilon}_\pm$ that do not point in a fixed direction. Instead, they rotate as the wave propagates. Circular and linear states of polarization are illustrated in Fig. 1.2.

Circular polarizations carry spin angular momentum of $\pm\hbar$ as indicated in the figure. The field direction and the energy density associated with the field twists as it moves,
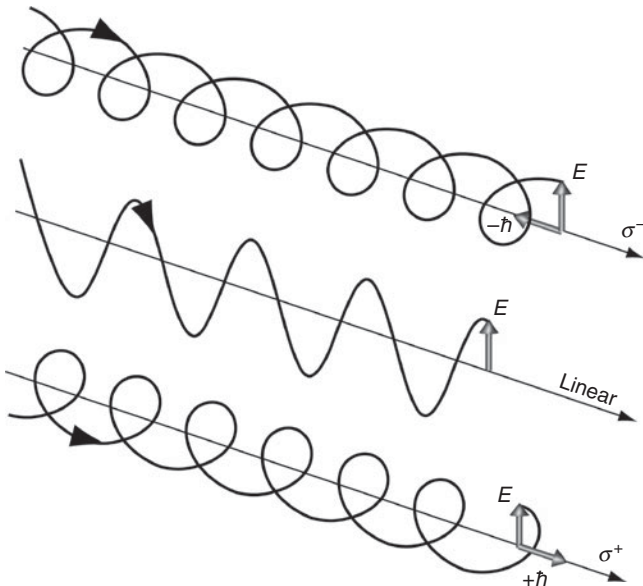
Figure 1.2 *Fundamental polarizations of light, illustrating light fields that carry spin angular momenta of $-\hbar$, 0, $+\hbar$ (top to bottom respectively). Angular momentum carried by a light wave affects the way it interacts with matter.*

undergoing a helical rotation with respect to $\hat{z}$. Linear polarization carries no angular momentum, since the electric field vector does not rotate about $\hat{z}$ at all. This latter state of polarization is a special combination or superposition state, consisting of the sum of two equal-amplitude, circularly polarized fields of opposite helicity.

Exercise: (*a*) Show that light which is linearly polarized along $\hat{x}$ can be written as the sum of two opposite circularly polarized fields. That is, show from Eq. (1.2.24) that x-polarized light is a phased, superposition state of two equal amplitude right and left circularly polarized components:

$$\hat{x} = -(1/\sqrt{2})(\hat{\varepsilon}_+ + \hat{\varepsilon}_-). \tag{1.2.25}$$

(*b*) Conversely, show that circular polarization can be expressed as a superposition of two orthogonal, linearly polarized waves of equal amplitude.

Since momentum must be conserved in optical interactions, just as energy must be conserved, we can anticipate that any angular momentum carried by light may affect the way it interacts with materials. This point is addressed in later chapters.

Supplementary reading

G.R. Fowles, *Introduction to Modern Optics*, Dover, New York, 1987.

W.K.H. Panofsky and M. Phillips, *Classical Electricity and Magnetism*, Second edition, Addison-Wesley Publishing Co., London, 1962.

2
Basic Quantum Mechanics

2.1 Particles and waves

Quantum mechanics postulates a concept known as wave–particle duality in the description of dynamical systems by associating a de Broglie wavelength λ_B with each particle. This wavelength depends on the linear momentum p of the particle, and is given by

$$\lambda_B = h/p, \qquad (2.1.1)$$

where h is Planck's constant. The de Broglie wave causes particles to exhibit wave interference effects whenever the wavelength becomes comparable to, or larger than, the space occupied by the wave. In fact de Broglie derived the Bohr-Sommerfeld quantization rules from (2.1.1). Remarkably, this is the only essentially new idea of "wave" mechanics that is missing in "classical mechanics", and curiously, although matter can exhibit particle or wavelike properties, its particle and wave characteristics are never observed together.

It follows specifically from Eq. (2.1.1) that electron waves can form self-consistent standing wave patterns ("stationary" states, "orbitals," or "eigenstates") that have constant angular momentum and energy. Charge distributions can be simultaneously localized and stable. The forces from Coulomb attraction between an electron and a nucleus, together with nuclear repulsion must balance within atoms at equilibrium. This balance, and the requirement that the standing wave be self-consistent, uniquely determine the ground state of atoms. Excited states must similarly satisfy the boundary conditions imposed by the de Broglie wavelength, but tend to be short-lived because the forces on the electron are no longer balanced. Consequently, excitation of such a state is quickly followed by a transition to the ground state, accompanied by emission of the energy difference between the ground and excited state as electromagnetic energy.

Conversely, light of frequency ν_0 has particle-like properties and may cause resonant transitions of atoms between well-defined initial and final states of an atom with energies E_i and E_f. To effect a transition between two specific states, light must supply the energy difference, according to the formula

$$h\nu_0 = E_f - E_i. \qquad (2.1.2)$$

ν_0 is called the transition frequency. Individual transitions are rarely observable because even small particles of bulk matter contain a great many atoms, and light

of even modest intensity $I \propto |E|^2$ consists of a high density $(N/V = I/ch\nu)$ of energy-bearing particles (photons) which cause transitions at random times. Therefore, individual interactions generally go unnoticed. Particle-like interactions of light waves are rarely observed unless intensities are extremely low. If a light field is pictured as a collection of quantum particles of energy $h\nu_0$, then at low intensity the particles must be widely separated in time, presuming they are all the same. We then require a description of light in terms of mathematical operators that produce discrete changes of the field when they interact. The particle nature of light is therefore an important factor determining the noise and statistical correlation properties of weak fields. However, a great many important aspects of light–matter interactions can be described adequately by treating only the atomic variables quantum mechanically as operators and the light field classically, with an amplitude and phase that are continuous scalar functions. This approach, called the semiclassical approach, is the one adopted throughout the first few chapters of this book. Aspects of light–matter interactions that depend explicitly on the discrete character of the field are reserved for the final chapters.

Charge motion caused by light is typically a dipolar response such as that determined in our classical model (Eq. (1.2.21)). However, in systems of bound charges excited near internal resonant frequencies, the dipole polarization that develops must clearly depend on the stationary quantum states and the corresponding resonant frequencies. Hence, under these conditions, polarization of the medium becomes a quantum mechanical observable determined to first order by nonzero values of the first moment of the microscopic polarization operator $\hat{p}$. Hence we shall need a procedure for determining the expected values of the dipole moment and other operators weighted by available states of the atomic system (specified by the probability amplitude ψ of finding the system in a given state at a given time and location) to predict the outcome of experimental measurements. This predictor of repeated measurements is called the expectation value, and it resembles an average weighted by the probability amplitude of the state of the system. The most important physical observable considered throughout this book is the electric dipole $\hat{p} = -e\bar{r}$, which has an expectation value given by

$$\langle \hat{p} \rangle = - \langle \psi | e\bar{r} | \psi \rangle \equiv -e \int \psi^* \bar{r} \psi \, dV. \tag{2.1.3}$$

Here, the wavefunction $\psi(r, t)$ accounts for the proportion of eigenstates contributing to the actual state of the system. (See Section. 2.2 and Appendix A for a more complete discussion of the definition of expectation value.) The bra–ket symbols used in Eq. (2.1.3) were introduced by Dirac to represent not only the conjugate state functions $\psi \leftrightarrow |\psi\rangle$ and $\psi^* \leftrightarrow \langle\psi|$, respectively but also to simplify spatial integrals where $|\psi\rangle$ and $\langle\psi|$ appear in combination, as in the dipole moment $\langle\psi| e\bar{r} |\psi\rangle$ of Eq. (2.1.3). This notation provides a convenient shorthand and will be used to shorten calculations throughout the book.

The total polarization for N identical atomic dipoles in the quantum mechanical limit is obtained by summing individual contributions with an expression similar to Eq. (2.1.3). However, the notation now implicitly includes functions (wavefunctions)

on which the operator of interest must operate for the expression to have meaning:

$$\langle \bar{P} \rangle = - \left\langle \sum_{i=1}^{N} e\bar{r}_i \right\rangle. \tag{2.1.4}$$

Dipoles may be static or time-varying. When $\langle \bar{P} \rangle$ is time-varying, it may have observable effects even if its time average is zero, because the charge distribution oscillates and may cause a change of state of the atom or lead to radiation. Indeed, the magnitude of the dipole operator $e\bar{r}$ evaluated between *different* states of a single atom, molecule, or optical center will be shown to be the dominant factor determining the rate of optically induced transitions between quantum states. For a collection of atoms however, we shall find that the relative phase variation of $e\bar{r}_i$ from one atom to the next also plays an important role in determining the magnitude and temporal development of the ensemble-averaged or *macroscopic* polarization $\langle \bar{P} \rangle$ in Eq. (2.1.4). The behavior of $\langle \bar{P} \rangle$ due to initial phasing, dephasing, and even rephasing is important in coherent optical processes, and the density matrix is especially well suited to keep track of important phase information.

2.2   Quantum observables

2.2.1   Calculation of quantum observables

Operators generate eigenvalues corresponding to specific energy states by their action on components of a wavefunction ψ. However, all systems, particularly systems undergoing transition, contain components with a spread in energy and momentum. So for a system described by a wavefunction $\psi(\bar{r}, t)$ that is in general not an eigenstate, measurement of an observable O yields a simple average or first moment of O. This moment is weighted by the states the system is in or passing through. The only quantum mechanical aspect of this calculation is that O must be replaced by the corresponding operator $\hat{O}$:

$$\left\langle \hat{O} \right\rangle = \langle \psi | \hat{O} | \psi \rangle = \int d^3 r \psi^* \hat{O} \psi. \tag{2.2.1}$$

This expression will then incorporate commutation properties, as discussed in Appendix A.

Because quantum theory deals with wavelike properties of matter, its predictions reflect the delocalization of waves and include a certain amount of "inexactitude." This is not a defect of the theory, but merely reflects the difficulty inherent in answering the question "Where is a wave?" Once a wave-based, probabilistic description of matter is introduced, there is a minimum uncertainty associated with measurements. To be more precise, conjugate variables cannot be determined simultaneously with infinite precision. For example, linear momentum p_x and position x are conjugate variables that have uncertainties Δp_x and Δx that are mutually related.

$$\Delta p_x \Delta x \geq \hbar/2. \tag{2.2.2}$$
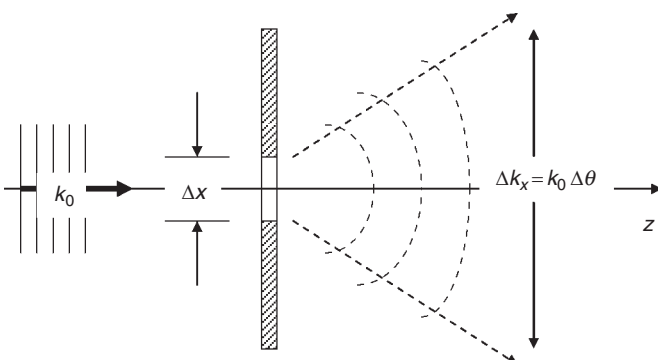
Figure 2.1 *Illustration of a typical uncertainty relationship between spatial resolution Δx and the corresponding angular spread that accompanies optical diffraction at an aperture according to the relation $\Delta p_x \Delta x = \hbar k_0 \Delta\theta \Delta x \geq \hbar/2$.*

The exact form of this Heisenburg uncertainty relation is justified and generalized in Appendix B for all pairs of conjugate variables. A simple example of the reciprocal relationship between spatial and angular resolution governed by Eq. (2.2.2) is illustrated by diffraction from an aperture (Fig. 2.1), when a plane wave develops a spread of propagation directions as it passes through a small aperture.

Measurements acquire minimum uncertainty when the product in Eq. (2.2.2) takes on its minimum value. For the variables above, the minimum product is $\Delta p_x \Delta x = \hbar/2$. When systems are prepared in minimum uncertainty or coherent states, they obey this equality, as discussed in Chapter 6. However, it will be shown that despite the inescapable uncertainty associated with wave mechanics, the Heisenberg limit expressed by Eq. (2.2.2) can be partly circumvented by preparing systems in special states called coherent states.

2.2.2 Time development

The wavefunction $\psi(\bar{r}, t)$ that we use to describe a material system gives the probability amplitude for finding the particle at $(\bar{r}, t)$, and its square modulus $|\psi(\bar{r}, t)|^2$ yields the probability density. Typically, experiments measure $|\psi(\bar{r}, t)|^2$, but we note in passing that it is possible to measure the eigenstates forming the basis of $\psi(\bar{r}, t)$ directly [2.1]. We expect to find the particle (with unit probability) if we search through all space. Hence the wavefunction is assumed to be normalized according to

$$\int \psi^*(\bar{r}, t)\psi(\bar{r}, t)\, d^3r = 1. \tag{2.2.3}$$

Evolution of the wavefunction in time is described by Schrödinger's wave equation

$$i\hbar \frac{\partial \psi}{\partial t} = H\psi. \tag{2.2.4}$$

In classical mechanics, the Hamiltonian H describing system energy is expressible in terms of canonically conjugate variables q_i and p_i of the motion. The operator form of

the Hamiltonian, designated by $\hat{H}$, is obtained by replacing the Poisson bracket $\{q_i, p_j\}$ in Hamilton's classical equations of motion by a similar bracket that keeps track of operator commutation properties, namely the commutator $[\hat{q}_i, \hat{p}_j] \equiv \hat{q}_i \hat{p}_j - \hat{p}_j \hat{q}_i = i\hbar \delta_{ij}$. An analogous procedure is used in a later chapter to quantize the electromagnetic field, and the essential role played by commutation in optical interactions will be discussed there further.

Solutions to the Schrödinger equation can be constructed from the spatial energy eigenfunctions U_n of the Hamiltonian, together with harmonic functions of time. For example,

$$\psi_n(r, t) = U_n(r) \exp(-i\omega_n t) \tag{2.2.5}$$

is a particular solution which satisfies Schrödinger's equation when the system energy is constant (i.e. $\hat{H}\psi_n = i\hbar \frac{\partial}{\partial t}\psi_n = \hbar\omega_n\psi_n$ and $\hbar\omega_n$ must be the energy eigenvalue E of the spatial eigenstate).

$$\hat{H}U_n = \hbar\omega_n U_n.$$

The energy of real, non-decaying systems is constant and observable, so the eigenvalues of such systems are real. It is the adjoint nature of $\hat{H}$ that assures us mathematically that the eigenvalues are real, that the corresponding eigenfunctions U_n can be ortho-normalized, and that they collectively furnish a complete description of the system. That is,

$$\int U_n^* U_m d^3 r = \delta_{nm}, \tag{2.2.6}$$

$$U_n^*(\bar{r}) U_n(\bar{r}') = \delta(\bar{r} - \bar{r}'). \tag{2.2.7}$$

Formally, the U_n form a complete basis set that can represent an arbitrary state of the system. The most general solution for the wavefunction is formed from linear combinations of solutions like Eq. (2.3.3), such as

$$\psi(\bar{r}, t) = \sum_n C_n U_n(\bar{r}) e^{-i\omega_n t}. \tag{2.2.8}$$

If the total probability $|\psi|^2$ for the system to occupy the space defined by the basis functions U_n is to be normalized to unity, one can easily show from Eq. (2.2.8) that the constant coefficients must satisfy

$$\sum_n |C_n|^2 = 1. \tag{2.2.9}$$

In Eq. (2.2.9), $|C_n|^2$ gives the occupation probability associated with a particular eigenstate n. This closure relation is exploited in Section 2.4 as the main tool for changing between alternative descriptions of a system, expressed in terms of various basis sets.

2.2.3   Symmetry

When researchers are confronted by a new problem, the greatest simplifications arise from considering system symmetries. Symmetry can be exploited to reduce complex
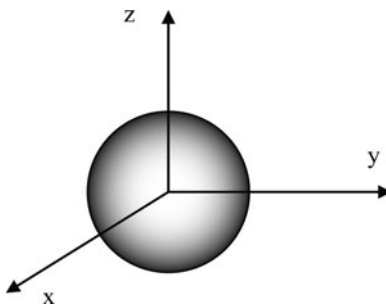
Figure 2.2 *Example of a three-dimensional object with inversion symmetry. A featureless sphere looks the same if the coordinates are all reversed.*

problems to simpler ones and to derive general rules for atom–field interactions. The optimal approach to using symmetry in this way is the domain of group theory, which is too extensive a topic to be included here. However, we review one important symmetry here, inversion symmetry, because it has important implications for many problems in optical science. It affects both linear and nonlinear interactions of light with matter. In a later chapter we encounter the Wigner–Eckart theorem (see also Appendix H), which can be used to implement other symmetry considerations, without group theory. For a broader discussion of symmetry see Ref. 2.2.

When a system has inversion symmetry, it is energetically indistinguishable in inverted and non-inverted states (see Fig. 2.2). Then, one can conclude from symmetry alone that (*a*) the wavefunctions for different stationary states may be classified into odd or even "parity," (*b*) the system cannot sustain a permanent dipole moment, and (*c*) "parity" must change when an electromagnetic transition occurs. Hence, the presence or absence of this symmetry often determines whether electromagnetic transitions are allowed or not. To confirm these results, we introduce parity operator $\hat{I}$, defined by its inverting action on all three spatial coordinates, and allow it to operate on the energy eigenvalue equation:

$$\hat{I}\left(\hat{H}(\bar{r})\psi(\bar{r})\right) = \hat{I}E\psi(\bar{r}) = E\psi(-\bar{r}) \tag{2.2.10}$$

The left side can be rewritten as

$$\hat{I}\left(\hat{H}(\bar{r})\psi(\bar{r})\right) = \hat{H}(-\bar{r})\psi(-\bar{r}) = \hat{H}(\bar{r})\hat{I}\psi(\bar{r}), \tag{2.2.11}$$

since $\hat{H}(\bar{r}) = \hat{H}(-\bar{r})$. This last point is the result of the system being physically indistinguishable in inverted or non-inverted states. Equation (2.2.11) shows that the commutator $[\hat{H}, \hat{I}] = 0$. Since $\hat{I}$ commutes with $\hat{H}$, the energy eigenfunctions of $\hat{H}$ are also eigenfunctions of $\hat{I}$. The eigenvalues I of the parity operator are easily found by applying inversion twice to return the original wavefunction. Thus

$$\hat{I}^2\psi = I^2\psi = \psi, \tag{2.2.12}$$

and wavefunctions of the system separate into two groups distinguished by $I = \pm 1$.

In the presence of inversion symmetry we reach three conclusions:

1. Energy eigenfunctions in systems with inversion symmetry have a definite parity. That is, with respect to inversion of the coordinates they are either even (e) or odd (o).

$$\psi^{(e)} = \psi(r) + \psi(-r) \text{ for } I = +1, \tag{2.2.13}$$

$$\psi^{(o)} = \psi(r) - \psi(-r) \text{ for } I = -1. \tag{2.2.14}$$

2. The system has no permanent dipole moment.

$$\langle \psi(r) \,|er|\, \psi(r)\rangle = \hat{I} \,\langle \psi(r) \,|er|\, \psi(r)\rangle = \langle \pm\psi \,|-er|\pm \psi\rangle = - \,\langle \psi(r) \,|er|\, \psi(r)\rangle.$$

Since the dipole moment must equal its negative, the only solution is

$$\langle \psi \,|er|\, \psi\rangle = 0, \tag{2.2.15}$$

regardless of the state ψ of the system.

3. Transition dipole moments (where the initial and final states are different) only exist between states of opposite parity.

$$\left\langle \psi^{(o)}(r)\big|er\big|\psi^{(e)}(r)\right\rangle = \hat{I} \left\langle \psi^{(o)}(r)\big|er\big|\psi^{(e)}(r)\right\rangle = \left\langle -\psi^{(o)}(r)\big|-er\big|\psi^{(e)}(r)\right\rangle$$

$$= \left\langle \psi^{(o)}(r)\big|er\big|\psi^{(e)}(r)\right\rangle \neq 0 \tag{2.2.16}$$

$$\left\langle \psi_1^{(o)}\big|er\big|\psi_2^{(o)}\right\rangle = \hat{I} \left\langle \psi_1^{(o)}\big|er\big|\psi_2^{(o)}\right\rangle = \left\langle -\psi_1^{(o)}\big|-er\big|-\psi_2^{(o)}\right\rangle$$

$$= - \left\langle \psi_1^{(o)}\big|er\big|\psi_2^{(o)}\right\rangle = 0, \tag{2.2.17}$$

$$\left\langle \psi_1^{(e)}\big|er\big|\psi_2^{(e)}\right\rangle = \hat{I} \left\langle \psi_1^{(e)}\big|er\big|\psi_2^{(e)}\right\rangle = \left\langle \psi_1^{(e)}\big|-er\big|\psi_2^{(e)}\right\rangle$$

$$= - \left\langle \psi_1^{(e)}\big|er\big|\psi_2^{(e)}\right\rangle = 0. \tag{2.2.18}$$

These selection rules based on inversion symmetry play an important role in some of the simple examples of quantum systems that follow.

2.2.4   Examples of simple quantum systems

2.2.4.1   Simple harmonic oscillator

One of the simplest dynamical systems with inversion symmetry consists of a simple harmonic oscillator, exemplified by a spring that obeys Hooke's law of motion on an immovable support attached to a mass m. Its allowed energy levels are depicted in Fig. 2.3.

In such a system, the restoring force of the spring is linear in the displacement x from equilibrium in accord with $\bar{F} = -k\bar{x}$ (where $k = m\omega_0^2$) and the system energy consists of potential and kinetic energy terms that appear explicitly in the Hamiltonian

$$\hat{H} = \hat{p}^2/2m + m\omega_0^2\hat{x}^2/2. \tag{2.2.19}$$
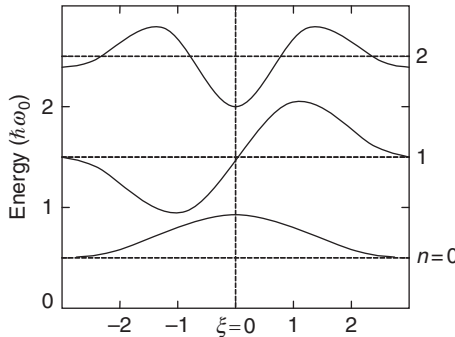
Figure 2.3 *The lowest three eigenfunctions of the simple harmonic oscillator.*

By solving Schrodinger's equation one finds

$$U_n = \left(\frac{m\omega_0}{\hbar\sqrt{\pi}2^n n!} \right)^{1/2} H_n\left(\xi\right)\exp(-\xi^2/2), \tag{2.2.20}$$

where $\xi \equiv \sqrt{m\omega_0/\hbar}\,x$ and $H_n(\xi)$ is a Hermite polynomial. The eigenvalues are

$$\hbar\omega_n = \left(n + \frac{1}{2} \right)\hbar\omega_0, \quad n = 0, 1, 2, \ldots. \tag{2.2.21}$$

Note that the eigenfunctions separate into even and odd sets, reflecting the inversion symmetry of the motion about the origin.

2.2.4.2   Particle in a one-dimensional (symmetric) potential well
The situation of a particle in an infinitely deep potential is illustrated in Fig. 2.4.

$$\hat{H} = \frac{\hat{p}^2}{2m} + \hat{V}, \quad \hat{V} = \begin{cases} 0, & 0 \leq z \leq L \\ \infty, & z < 0, z > L \end{cases}. \tag{2.2.22}$$

The momentum operator is $\hat{p} = -i\hbar\partial/\partial z$. Energy eigenfunctions are therefore

$$U_n\left(z\right) = \begin{cases} \sqrt{2/L}\sin k_n z, & 0 \leq z \leq L \\ 0, & z < 0, z > L \end{cases}, \tag{2.2.23}$$

where $k_n = n\pi/L$ and $n = 1, 2, 3, \ldots$.
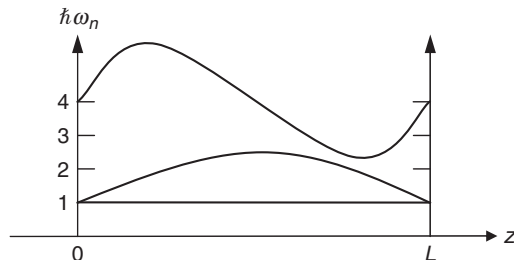
Figure 2.4 *The two lowest eigenfunctions of a one-dimensional infinite square well.*

The energy eigenvalues are

$$\hbar\omega_n = \frac{1}{2}\frac{\hbar^2 k_n^2}{m},$$

(2.2.24)

and a general wavefunction for this problem is

$$\psi = \left(\frac{2}{L}\right)^{1/2} \sum_n C_n \sin\left(k_n z\right) e^{-i\omega_n t}.$$

(2.2.25)

Note that the solutions in Eq. (2.2.25) again separate into contributions with n even or odd, reflecting the inversion symmetry of the potential, as in Section 2.2.3.

2.2.4.3   *Particle in a one-dimensional (asymmetric) potential well*

In modulation-doped field-effect transistor (MODFET) structures, energy bands near interfaces bend in such a way that carriers can be trapped in shallow potential wells that lack inversion symmetry, forming a two-dimensional electron gas, as illustrated in Fig. 2.5.
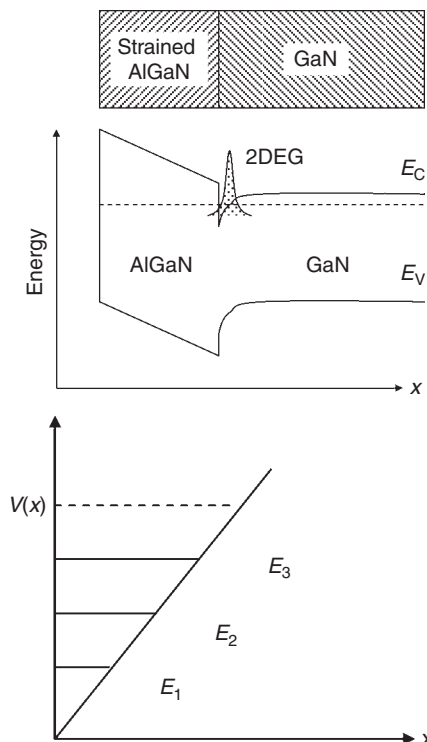
Figure 2.5 *(Top) Schematic cross section of a ternary nitride semiconductor structure giving rise to a two-dimensional electron gas (2DEG) at the AlGaN/GaN interface (in the middle). (Bottom) The linear potential well and quantized energy levels at the 2DEG interface.*

The potential $V(x)$ is approximately proportional to the distance x from the interface.

$$V(x) = V_0 x. \tag{2.2.26}$$

Hence the time-independent Schrödinger equation is

$$\left[\frac{-\hbar^2}{2m_e}\frac{d^2}{dx^2} + (V_0 x - E)\right] U(x) = 0. \tag{2.2.27}$$

By introducing the dimensionless variable

$$\xi_n \equiv \left(x - \frac{E_n}{V_0}\right)\left(\frac{2m_e V_0}{\hbar^2}\right)^{1/3}, \tag{2.2.28}$$

where $n = 1, 2, 3, \ldots$ is an integer index for the various solutions, this equation simplifies to

$$\left[\frac{d^2}{d\xi_n{}^2} - \xi_n\right] U_n(\xi_n) = 0. \tag{2.2.29}$$

The solution of this equation is an Airy function, related to Bessel functions of fractional order. A suitable integral form of this function can be written as

$$\Phi_n(\xi_n) = \frac{1}{\pi}\int\limits_0^\infty \cos(\frac{1}{3}u^3 + u\xi_n)\,du, \tag{2.2.30}$$

with the explicit eigenfunctions being

$$U_n(\xi_n) = A_n\Phi_n(-\xi_n), \tag{2.2.31}$$

where A_n is a constant amplitude for the nth solution. To find energy eigenvalues, it is necessary to apply boundary conditions. For this we can approximate the well height at the origin as infinite, so that $U(\xi) = 0$ at $x = 0$. That is,

$$U_n\left(-\frac{E_n}{V_0}\left[\frac{2m_e V_0}{\hbar^2}\right]^{1/3}\right) = U_n\left(-R_n\right) = 0. \tag{2.2.32}$$

This shows that the eigenvalues are proportional to roots (R_n) of the Airy function. The first few roots are $R_1 = 2.34$, $R_2 = 4.09$, $R_3 = 5.52$, and $R_4 = 6.78$. Hence the eigenvalues, obtained from the expression above, are

$$E_n = \left(\frac{V_0^2\hbar^2}{2m_e}\right)^{1/3} R_n. \tag{2.2.33}$$

The wavefunctions must be normalized to unity. This requires that

$$\int\limits_{-R_n}^\infty U_n^*(\xi)U_n(\xi)d\xi = |A_n|^2, \tag{2.2.34}$$

showing that the undetermined coefficients are given by

$$
A_n = \left(\int\limits_{-R_n}^{\infty} |U_n(\xi_n)|^2 \, d\xi_n \right)^{-1/2}. \tag{2.2.35}
$$

In this example, no reduction of the wavefunction into sets of even and odd energy levels takes place. Because of the lack of inversion symmetry, the wavefunctions do not separate into different parity classes. (See *Handbook of Math. Functions*, NBS, 1964, p.446–7, Eqs. 10.4.1 and 10.4.32, and Ref. [2.3].)

2.2.4.4   Particle in an adjustable three-dimensional box

F-centers in alkali halides are excellent examples of real particles in real cubic boxes of adjustable size. These color centers consist of an electron in an anion vacancy of an ionic crystal (a defect of the crystal structure), and give rise to dramatic coloration of otherwise transparent crystals [2.3]. One does not need to know much in the way of specifics about them to make quite detailed, verifiable predictions about them. We picture an electron in a cubic space left by a missing anion, a space somewhat larger than a hydrogen atom (Fig. 2.6), with a positive charge and an infinitely high potential at the walls. Because it is caged in by the otherwise perfect crystal, the wavefunction must vanish at the "walls" comprised of neighboring cations. Hence, borrowing from the one-dimensional symmetric case above, we would guess that possible wavefunctions have the form

$$
\psi(x, y, z) = \sin(k_x x) \sin(k_y y) \sin(k_z z), \tag{2.2.36}
$$

where

$$
k_x = \frac{\pi}{a} n_x, \; k_y = \frac{\pi}{a} n_y, \; \text{and} \; k_z = \frac{\pi}{a} n_z.
$$

The energy eigenvalues are

$$
E(n_x, n_y, n_z) = \frac{\hbar^2 k^2}{2m} = \frac{\hbar^2 \left(k_x^2 + k_y^2 + k_z^2 \right)}{2m} = \frac{\hbar^2 \pi^2}{2ma^2} \left(n_x^2 + n_y^2 + n_z^2 \right). \tag{2.2.37}
$$

The ground state energy is

$$
E_0 = \frac{3h^2}{8ma^2}, \tag{2.2.38}
$$

since $n_x = n_y = n_z = 1$. The energy of the first excited state is

$$
E_1 = \frac{6h^2}{8ma^2}, \tag{2.2.39}
$$

since $n_x = 2$ and $n_y = n_z = 1$. The transition frequency of the first resonance of the F-center is therefore given by

$$
h\nu = E_1 - E_0 = \frac{3n^2}{8ma^2}, \tag{2.2.40}
$$

(a)

(b)
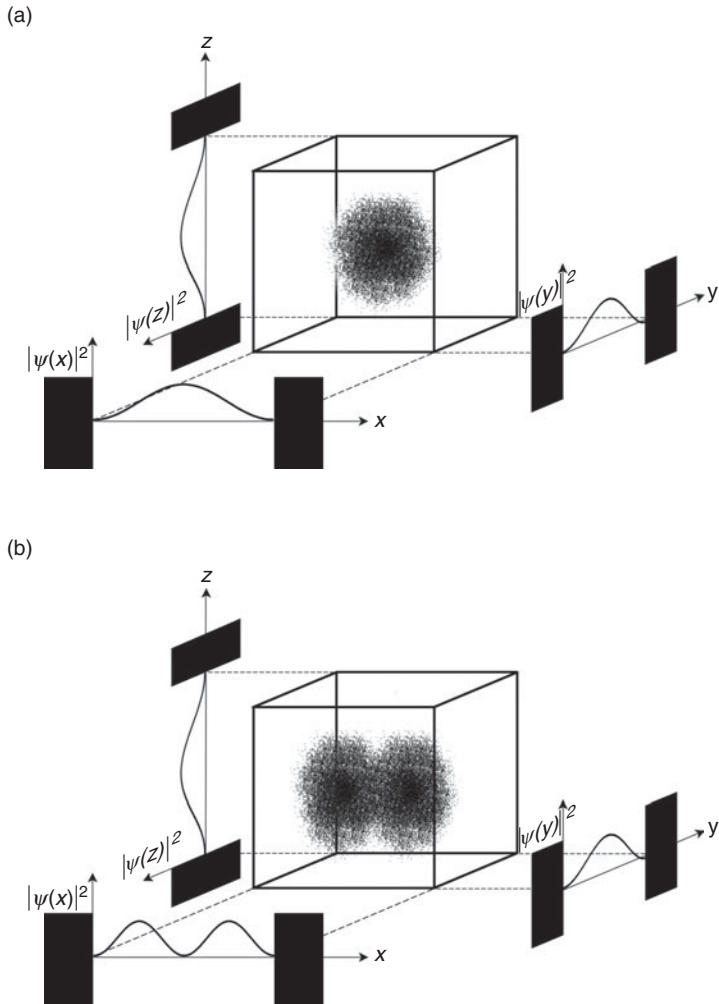
Figure 2.6 *Pictorial representation of the wavefunctions and charge distributions of an F-center in the (a) ground state and (b) the first excited state. (After Ref. [2.4]).*

from which one obtains directly the Mollwo-Ivey relation [2.4] for the relationship between the edge length of the crystal unit cell and the frequency of resonant absorption:

$$\ln(a) = \frac{1}{2}\ln(\nu) + c. \qquad (2.2.41)$$

As shown in Fig. 2.7, this relation has been confirmed by measurements on various alkali halide crystals.

Multi-electron color centers are not only good examples of particle-in-a-box analysis, but have been widely used in high gain tunable laser technology [2.5]. Another
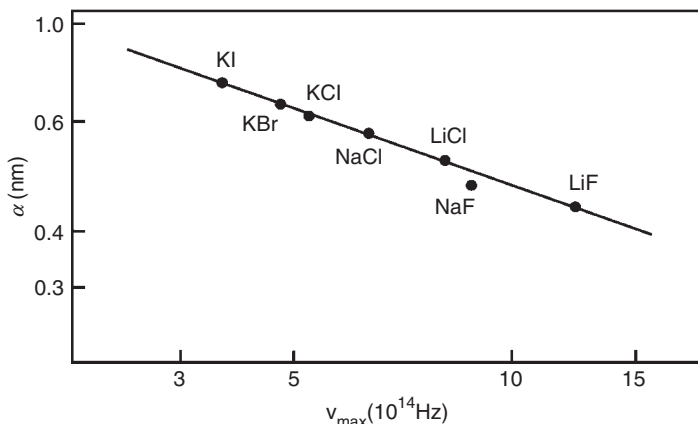
Figure 2.7 *Plot of experimental measurements of the first absorption resonance of F-centers in several alkali halides, compared with the prediction of the Mollwo-Ivey relation (solid curve). (After Ref. [2.4]).*

important application relies on their mobility under applied fields. Oxygen vacancies in semiconducting rutile (TiO_2) are thermally more stable than the alkali F-centers and can be made to migrate by the application of voltage across the crystal, causing a change in resistance of the medium proportional to the integral of voltage over time. This understanding led to the first realization of a fundamental circuit element called the memristor [2.6].

2.3 Dynamics in two-level systems

Knowledge of system symmetries and eigenenergies is often enough to predict dynamics in systems where the wavefunction and Hamiltonian H_0 are unknown. This is fortunate, because systems encountered in research often have unknown properties and structure that is complicated enough to prevent determination of the wavefunction. The limited number of models available for which ψ can be found analytically might even suggest that these case studies are irrelevant to new problems in which ψ is essentially unknowable. However, there are at least three reasons why this is not so. The first is that many aspects of dynamics are dominated by the interaction of light with only the upper and lower levels coupled by the light. Other levels in the system are often not strongly coupled by the electromagnetic field and play a secondary role. So, two-level models capture dominant aspects of the dynamics in complex systems. The second reason is that even complicated systems can sometimes be converted into truly two-level systems by a judicious choice of experimental conditions. Thirdly, as illustrated below, the development that a system undergoes as time progresses depends on its resonant frequencies and state symmetries, not on any particular mathematical representation of H_0 or ψ.

Consider a solid known to have two levels separated by an energy in the range of an available light source. When light propagates along the z-axis of the crystal, the structure absorbs strongly regardless of polarization. What, if anything, can be said about such a system, its dynamics, and transitions? Presuming that the absorption process involves a single electron as in the vast majority of cases, and recalling that the classical energy of an electric dipole formed by the electron in a field $\bar{E}$ is given by the projection of the moment on the external field, the interaction energy should be

$$\hat{H}_I = -\bar{\mu} \cdot \bar{E}\,(z,t)\,. \tag{2.3.1}$$

Since the light field is under the experimentalist's control, assume it is a plane wave traveling along z with no variation of its amplitude in x or y. The dipole moment could be oriented in an arbitrary, fixed direction described by

$$\bar{\mu} = \mu_x \hat{x} + \mu_y \hat{y} + \mu_z \hat{z}. \tag{2.3.2}$$

Perpendicular to z, only the x and y components of the moment are relevant for interaction with the wave. In free space, the orientation of $\bar{E}$ is perpendicular to the direction of propagation, so $\mu_z \hat{z} \cdot \bar{E}(z,t) = 0$. Since we are told the absorption is isotropic, we may also assume $\mu_x = \mu_y = \mu_0$, and without loss of generality reduce Eq. (2.3.1) to

$$\hat{H}_{\text{int}} = -\mu_0 E_0, \tag{2.3.3}$$

where E_0 is the amplitude of the electromagnetic wave. The charge oscillations excited by the field are restricted to the x–y plane. So the interaction spans a two-dimensional Hilbert space. Equation (2.3.3) therefore describes a two-dimensional interaction operator, and can be represented using 2×2 matrices – the Pauli spin matrices that (together with the unit matrix σ_I) form a complete basis set.

$$\hat{\sigma}_x = \begin{bmatrix} 0 & 1 \\ 1 & 0 \end{bmatrix}, \quad \hat{\sigma}_y = \begin{bmatrix} 0 & -i \\ i & 0 \end{bmatrix}, \quad \text{and } \hat{\sigma}_z = \begin{bmatrix} 1 & 0 \\ 0 & -1 \end{bmatrix}. \tag{2.3.4}$$

This set of matrices is called complete because any complex two-component vector can be written as a linear combination of σ_x, σ_y, σ_z, and the unit matrix σ_I with appropriate coefficients. Also the product of any two Pauli matrices is a Pauli matrix, showing that they form a complete group. Since light can at most transform the state of the atom among its available states in Hilbert space, the interaction Hamiltonian $\hat{H}_I$ must be an operator that can convert a two-vector into another two-vector in the same Hilbert space. Therefore, its matrix representation must also be 2×2 and we choose the Pauli matrices as basis operators. The operator representation of Eq. (2.3.3) must change state $\begin{bmatrix} 0 \\ 1 \end{bmatrix}$ into $\begin{bmatrix} 1 \\ 0 \end{bmatrix}$ and vice versa. Hence it is given by

$$\hat{H}_{\text{int}} = -\mu_0 E_0 \hat{\sigma}_x. \tag{2.3.5}$$

Exercise: Confirm that the form of $\hat{H}_I$ in Eq. (2.3.5) is correct by applying it to either eigenstate of the two-level atom and showing that it causes a transition to the other.

Now, $\hat{\sigma}_x$ can be written in terms of raising and lowering operators for atomic states to simplify interpretation of dynamics. Consider the following two matrices:

$$\hat{\sigma}^+ \equiv \frac{1}{2}\left(\hat{\sigma}_x + i\hat{\sigma}_y\right) = \begin{bmatrix} 0 & 1 \\ 0 & 0 \end{bmatrix} \rightarrow \hat{\sigma}^+ \begin{bmatrix} 0 \\ 1 \end{bmatrix} = \begin{bmatrix} 1 \\ 0 \end{bmatrix} \tag{2.3.6}$$

$$\hat{\sigma}^- \equiv \frac{1}{2}\left(\hat{\sigma}_x - i\hat{\sigma}_y\right) = \begin{bmatrix} 0 & 0 \\ 1 & 0 \end{bmatrix} \rightarrow \hat{\sigma}^- \begin{bmatrix} 1 \\ 0 \end{bmatrix} = \begin{bmatrix} 0 \\ 1 \end{bmatrix}. \tag{2.3.7}$$

Writing the interaction Hamiltonian in terms of these operators, which raise or lower the state of the atom, Eq. (2.3.5) becomes

$$\hat{H}_{\text{int}} = -\mu_0 E_0 \begin{bmatrix} 0 & 1 \\ 1 & 0 \end{bmatrix} = -\mu_0 E_0 \left(\hat{\sigma}^+ + \hat{\sigma}^-\right). \tag{2.3.8}$$

It may now be deduced that a continuous field–atom interaction causes the atom to make periodic transitions up and down between states 1 and 2 by stimulated absorption and emission, respectively, at a frequency related to the absorption coefficient (since it depends on the transition moment μ_0).

As shown by the exercise above, discrete applications of the interaction Hamiltonian show the individual transitions caused by optical irradiation:

$$\hat{H}_{\text{int}} \begin{bmatrix} 0 \\ 1 \end{bmatrix} = -\mu_0 E_0 \begin{bmatrix} 1 \\ 0 \end{bmatrix}, \tag{2.3.9}$$

and

$$\hat{H}_{\text{int}} \begin{bmatrix} 1 \\ 0 \end{bmatrix} = -\mu_0 E_0 \begin{bmatrix} 0 \\ 1 \end{bmatrix}. \tag{2.3.10}$$

A more detailed picture of system dynamics can only emerge by solving explicitly for temporal evolution of the state of the system. In the present problem, there is no information on the stationary states of the system. So we do not know the wavefunction itself, but we do know there are at least two states in the system. There is a ground state that might be represented as ψ^- and an excited state ψ^+. The challenge of predicting what the system will do in response to irradiation requires the determination of the most general wavefunction we can write based on this information. This is $\psi(t) = c^+\psi^+ + c^-\psi^-$, where c^+ and c^- are time-dependent coefficients. So the time-dependent Schrödinger equation yields

$$\frac{d}{dt}\left(c^+(t)\psi^+ + c^-(t)\psi^-\right) = i\Omega\left(\hat{\sigma}^+ + \hat{\sigma}^-\right)\left(c^+(t)\psi^+ + c^-(t)\psi^-\right)$$
$$= i\Omega\left(c^+(t)\psi^- + c^-(t)\psi^+\right), \tag{2.3.11}$$

where $\Omega \equiv \mu_0 E_0/\hbar$. Hence

$$\left[\frac{\partial c^+(t)}{\partial t}\psi^+ + \frac{\partial c^-(t)}{\partial t}\psi^-\right] = i\Omega\left[c^+(t)\psi^- + c^-(t)\psi^+\right], \tag{2.3.12}$$

and because ψ^+ and ψ^- are independent vector states, Eq. (2.3.12) may be decomposed into the following two equations:

$$\frac{\partial c^+}{\partial t} = i\Omega c^-, \tag{2.3.13}$$

$$\frac{\partial c^-}{\partial t} = i\Omega c^+. \tag{2.3.14}$$

These two coupled equations are readily solved by differentiation and cross substitution.

$$\frac{\partial^2 c^\pm}{\partial t^2} = -\Omega^2 c^\pm \tag{2.3.15}$$

By taking into account the normalization condition $|c^+|^2 + |c^-|^2 = 1$ and initial condition $c^-(0) = 1$, the overall wavefunction can therefore be written as

$$\psi(t) = c^+\psi^+ + c^-\psi^- = \psi^+ \sin\Omega t + \psi^- \cos\Omega t. \tag{2.3.12}$$

The system oscillates between the ground state ψ^- and the excited state ψ^+ at a frequency Ω called the resonant Rabi frequency. This oscillatory behavior is called Rabi flopping. What is interesting here is that we have predicted some system dynamics – an oscillation at a very specific rate in a poorly characterized system – without knowing the functional form of the wavefunction ψ or even the unperturbed system Hamiltonian H_0. It was sufficient to know a little about system symmetry, the energy eigenvalues, and to assume the optical interaction was dominated by the electric dipole Hamiltonian. It is particularly important to realize that one can calculate optical properties and dynamic response to light without knowing the wavefunction, since the wavefunction itself is rarely known in systems of interest.

2.4   Representations

2.4.1   Representations of vector states and operators

The Hamiltonian describing the interaction of matter with a perturbing influence is often written as the sum of a static portion $\hat{H}_0$ and an interaction term $\hat{V}$. (The electric dipole interaction between light and matter is considered in detail in Appendix C.)

$$\hat{H} = \hat{H}_0 + \hat{V}. \tag{2.4.1}$$

The Schrödinger equation then becomes

$$\frac{d}{dt}\left|\psi(t)\right\rangle = -\frac{i}{\hbar}(\hat{H}_0 + \hat{V})\left|\psi(t)\right\rangle. \tag{2.4.2}$$

If the entire Hamiltonian $\hat{H}$ itself is time-independent, direct integration of Eq. (2.4.2) yields

$$\left|\psi(t)\right\rangle = \exp\left(-\frac{i}{\hbar}\hat{H}t\right)\left|\psi(0)\right\rangle, \tag{2.4.3}$$

showing that the system wavefunction can still evolve by changing the admixture of its eigenstates. Hence an observable O acquires a time dependence which, if not too rapid, is reflected in the measured matrix element

$$\langle \hat{O}(t) \rangle = \langle \psi | \hat{O} | \psi \rangle. \tag{2.4.4}$$

There are three common ways to partition the time dependence in Eq. (2.4.4) between the state vector $|\psi\rangle$ and the operator $\hat{O}$. The most common divisions are the following.

Schrödinger picture:

$$\langle \hat{O} \rangle = \langle \psi^{\mathrm{S}}(t) | \hat{O}^{\mathrm{S}}(0) | \psi^{\mathrm{S}}(t) \rangle, \tag{2.4.5}$$

where $|\psi^{\mathrm{S}}(t)\rangle \equiv \exp(-i\hat{H}t/\hbar)|\psi^{\mathrm{S}}(0)\rangle$.

Interaction picture:

$$\langle \hat{O} \rangle = \langle \psi^{\mathrm{I}}(t) | \hat{O}^{\mathrm{I}}(t) | \psi^{\mathrm{I}}(t) \rangle, \tag{2.4.6}$$

where $|\psi^{\mathrm{I}}(t)\rangle \equiv \exp(i\hat{H}_0 t/\hbar)|\psi^{\mathrm{S}}(t)\rangle$,
   and $\hat{O}^{\mathrm{I}}(t) \equiv \exp(i\hat{H}_0 t/\hbar)\hat{O}^{\mathrm{S}}(0) \exp(-i\hat{H}_0 t/\hbar)$.

Heisenberg picture:

$$\langle \hat{O} \rangle = \langle \psi^{\mathrm{H}} | \hat{O}^{\mathrm{H}}(t) | \psi^{\mathrm{H}} \rangle, \tag{2.4.7}$$

where $\hat{O}^{\mathrm{H}}(t) \equiv \exp(i\hat{H}t/\hbar)\hat{O}^{\mathrm{S}}(0) \exp(-i\hat{H}t/\hbar)$,
   and $|\psi^{\mathrm{H}}\rangle \equiv |\psi^{\mathrm{S}}(0)\rangle$.

These options for representing problems are explored further in Section 2.4.2. One of the three pictures is generally preferable to another for a given problem. The choice of representation is determined by what aspect of system dynamics is to be emphasized in calculations.

2.4.2   Equations of motion in different representations

The basic equation of motion is Schrödinger's equation, given by Eq. (2.4.2). However, it is a matter of convenience as to whether one views the physical effects of system dynamics as being associated primarily with the atomic wavefunction, or the perturbing field operator, or as being divided between the two. For easy analysis, the choice of representation should reflect whether it is the state of the atom, the state of the field, or the interaction between them (i.e., coherent atom–field coupling) that is of most interest, respectively. Why is this a concern? This matters because we generally have in mind experiments of a specific type with which we plan to probe a system. It may be just the atomic state that we wish to monitor. Or, alterations in the spectrum and intensity of the perturbing field itself may be the chief interest. Or, the chief concern might be measurement of the amplitude of a transient coherent polarization that simultaneously reflects the harmonic oscillation of a superposition state of the atom and its phase-dependent coupling with the applied field. For ease of interpretation, our calculations should reflect the way we choose to view the problem.

A. Time-independent $\hat{H}$

Direct integration of the Schrödinger Equation when $\hat{H}$ is time-independent gives

$$\left|\psi\left(t\right)\right\rangle = \exp(-i\hat{H}t/\hbar)\left|\psi\left(0\right)\right\rangle, \tag{2.4.8}$$

$$\text{where} \quad \exp\left(-i\hat{H}t/\hbar\right) \equiv 1 - i(\hat{H}t/\hbar) - \frac{1}{2}(\hat{H}t/\hbar)^2 + \dots. \tag{2.4.9}$$

This result can then be used to develop slightly different equations of motion for the various pictures of system dynamics.

(i) *Schrödinger picture:*

$$i\hbar\frac{d}{dt}\left|\psi^{\mathrm{S}}\left(t\right)\right\rangle = \hat{H}\left|\psi^{\mathrm{S}}\left(t\right)\right\rangle, \tag{2.4.10}$$

$$\left\langle\hat{O}(t)\right\rangle = \left\langle\psi^{\mathrm{S}}\left(t\right)\right|\hat{O}(0)\left|\psi^{\mathrm{S}}\left(t\right)\right\rangle, \tag{2.4.11}$$

where

$$\left|\psi^{\mathrm{S}}\left(t\right)\right\rangle = \exp(-i\hat{H}t/\hbar)\left|\psi\left(0\right)\right\rangle. \tag{2.4.12}$$

In Eq. (2.4.11) the expectation value of the operator has been written in terms of its initial value $\hat{O}(0)$ to emphasize that it does not change with time. All time dependence is associated with the wavefunctions in the Schrödinger picture.

(ii) *Interaction picture:*

To extract the purely sinusoidal dynamics associated with the static Hamiltonian H_0 in our description of the time development of the state vector, the contribution of H_0 can be removed with the transformation

$$\left|\psi^{\mathrm{S}}\left(t\right)\right\rangle = \exp\left(-i\hat{H}_0t/\hbar\right)\left|\psi^{\mathrm{I}}\left(t\right)\right\rangle. \tag{2.4.13}$$

Then

$$i\hbar\frac{d}{dt}\exp\left(-i\hat{H}_0t/\hbar\right)\left|\psi^{\mathrm{I}}\left(t\right)\right\rangle = \left(\hat{H}_0^{\mathrm{S}} + \hat{V}^{\mathrm{S}}\right)\exp\left(-i\hat{H}_0t/\hbar\right)\left|\psi^{\mathrm{I}}\left(t\right)\right\rangle,$$

$$i\hbar\frac{d}{dt}\left|\psi^{\mathrm{I}}\left(t\right)\right\rangle = \exp\left(i\hat{H}_0t/\hbar\right)\hat{V}^{\mathrm{S}}\exp\left(-i\hat{H}_0t/\hbar\right)\left|\psi^{\mathrm{I}}\left(t\right)\right\rangle.$$

This result may be rewritten in the form

$$i\hbar\frac{d}{dt}\left|\psi^{\mathrm{I}}\left(t\right)\right\rangle = \hat{V}^{\mathrm{I}}\left(t\right)\left|\psi^{\mathrm{I}}\left(t\right)\right\rangle, \tag{2.4.14}$$

where

$$\hat{V}^{\mathrm{I}}\left(t\right) \equiv \exp(i\hat{H}_0t/\hbar)\hat{V}^{\mathrm{S}}\exp(-i\hat{H}_0t/\hbar) \tag{2.4.15}$$

is an effective Hamiltonian for the transformed state vector $|\psi^{\mathrm{I}}(t)\rangle$. This representation is called the interaction picture, because according to Eq. (2.4.14) the development of $|\psi^{\mathrm{I}}(t)\rangle$ is determined by the interaction $\hat{V}^{\mathrm{I}}(t)$ rather than $\hat{H}_0$ or $\hat{H}$.

On the other hand, the time development of *operators* in this picture is determined by $\hat{H}_0$. To make a comparison with the Schrödinger picture, we note from Eq. (2.4.15) that an arbitrary operator in the interaction picture relates to one in the Schrödinger picture according to

$$\hat{O}^{\mathrm{I}} = \exp(i\hat{H}_0 t/\hbar)\hat{O}^{\mathrm{S}}(0)\exp(-i\hat{H}_0 t/\hbar). \tag{2.4.16}$$

Consequently, its expectation value may be evaluated by making use of Eq. (2.4.13).

$$\begin{aligned}
\langle \hat{O}^I(t)\rangle &= \langle \psi^{\mathrm{I}}(t)| \exp(i\hat{H}_0 t/\hbar)\hat{O}^{\mathrm{S}}(0)\exp(-i\hat{H}_0 t/\hbar) |\psi^{\mathrm{I}}(t)\rangle \\
&= \langle \psi^{\mathrm{S}}(t)\exp(-i\hat{H}_0 t/\hbar)| \exp(i\hat{H}_0 t/\hbar)\hat{O}^{\mathrm{S}}(0)\exp(-i\hat{H}_0 t/\hbar)|\exp(i\hat{H}_0 t/\hbar)\psi^{\mathrm{S}}(t)\rangle \\
&= \langle \hat{O}^{\mathrm{S}}(t)\rangle. \tag{2.4.17}
\end{aligned}$$

This shows that expectation values of operators are *independent of representation*. However, in the interaction picture operators are assigned part of the overall time dependence, unlike the Schrödinger picture. Hence we shall need an equation of motion for the operator $\hat{O}^{\mathrm{I}}(t)$. Direct differentiation of Eq. (2.4.16) yields

$$\frac{d}{dt}\hat{O}^{\mathrm{I}}(t) = \frac{i}{\hbar}\left[\hat{H}_0, \hat{O}^{\mathrm{I}}\right]. \tag{2.4.18}$$

Note that the expansion coefficients in the Schrödinger and interaction pictures are different. The complete time dependence is described by Schrödinger coefficients $c_n(t)$ in the expansion $|\psi\rangle = \sum_n c_n(t)|n\rangle$, whereas the time dependence due only to the interaction is described by interaction picture coefficients $C_n(t)$ in the $|\psi\rangle = \sum_n C_n(t)\exp(-i\omega_n t)|n\rangle$. For each eigenfrequency ω_n, the coefficients are therefore related by

$$c_n(t) = C_n(t)\exp(-i\omega_n t). \tag{2.4.19}$$

(iii) *Heisenberg picture:*

$$\begin{aligned}
\langle \hat{O}(t)\rangle &= \langle \psi^{\mathrm{S}}(0)| \exp(i\hat{H}t/\hbar)\hat{O}\exp(-i\hat{H}t/\hbar) |\psi^{\mathrm{S}}(0)\rangle \\
&= \langle \psi^{\mathrm{H}}| \hat{O}^{\mathrm{H}}(t) |\psi^{\mathrm{H}}\rangle, \tag{2.4.20}
\end{aligned}$$

where

$$\hat{O}^{\mathrm{H}}(t) \equiv \exp\left(i\hat{H}t/\hbar\right)\hat{O}\exp\left(-i\hat{H}t/\hbar\right), \tag{2.4.21}$$

and

$$|\psi^{\mathrm{H}}\rangle = |\psi^{\mathrm{S}}(0)\rangle. \tag{2.4.22}$$

By direct differentiation of Eq. (2.4.21), we obtain

$$\frac{d}{dt}\psi^{\mathrm{H}} = \frac{d}{dt}\psi(0) = 0, \tag{2.4.23}$$

$$\frac{d}{dt}\hat{O}^H = \frac{i}{\hbar}\left[\hat{H}^H, \hat{O}^H\right]. \tag{2.4.24}$$

Great care must be exercised when manipulating functions of operators for the simple reason that operators do not generally commute with one another. Some decompositions of the time dependence that might suggest themselves intuitively are invalid.

For example,

$$|\psi(t)\rangle = \exp(-i\hat{H}t/\hbar)|\psi(0)\rangle = \exp(-i\hat{H}_0 t/\hbar)\exp(-i\hat{V}t/\hbar)|\psi(0)\rangle \qquad (2.4.25)$$

is incorrect unless $[\hat{H}_0, \hat{V}] = 0$, because factorization of exponential functions of operators is prohibited when the operators in the argument do not commute. The Weyl formula (see Problem 6.1) prescribes $\exp[\hat{A} + \hat{B}] = \exp[\hat{A}]\exp[\hat{B}]\exp(-[\hat{A}, \hat{B}]/2)]$. While the physical meaning of commutation in quantum mechanics is not obvious or intuitive at first, it may be physically understood by simply considering the different effects that reversed sequences of interactions have on optical systems. In the next section, we discuss a sequence of light pulses as an example of complex time-varying interactions where commutation keeps track of the order of events.

As a final note on representations, although different choices of representation are available, the Schrödinger representation will be used for most of the analysis presented in this book. This choice helps maintain consistency from one topic to another to the maximum extent possible. Also, for Chapters 3–5, the optical interactions do not change the energy level structure of the atom itself, so occupation of the various levels and transition rates between them are the main concern. For this purpose, calculations of the probability amplitudes in the Schrödinger picture are generally adequate. An exception is the analysis of photon echoes covered in Chapter 4, where a combination of Schrödinger and interaction pictures makes the analysis tractable. Other exceptions appear in Chapters 6 and 7, where the state of the field rather than the state of the atom is of primary interest. Such cases are best treated in the Heisenberg picture which assigns the time development to the field operator as we have seen above.

B. Time-dependent $\hat{H}$

A useful approach when the Hamiltonian is time-dependent is to introduce an evolution operator $U_R(t)$. This operator is defined by

$$|\psi(t)\rangle = U_R(t)|\psi(0)\rangle. \qquad (2.4.26)$$

Hence the equation of motion may be obtained directly as

$$\frac{d}{dt}|\psi(t)\rangle = \frac{d}{dt}U_R(t)|\psi(0)\rangle. \qquad (2.4.27)$$

But the Schrödinger equation yields

$$\frac{d}{dt}|\psi(t)\rangle = -\frac{i}{\hbar}\hat{H}(t)|\psi(t)\rangle = -\frac{i}{\hbar}\hat{H}(t)U_R(t)|\psi(0)\rangle \qquad (2.4.28)$$

$$\frac{d}{dt}U_R(t) = -\frac{i}{\hbar}\hat{H}(t)U_R(t). \qquad (2.4.29)$$

Solutions to Eq. (2.4.29) can be obtained by an iterative approach over small time intervals, and should reduce to $U_R(t, t_0) = \exp(-i\hat{H}(t - t_0)/\hbar)$ in the limit that $\hat{H}$ is time-independent. For the time interval t_0 to t, formal integration yields

$$\int_{t_0}^{t} dU_R(t', t_0)dt' = -\frac{i}{\hbar} \int_{t_0}^{t} \hat{H}(t')U_R(t', t_0)dt'. \tag{2.4.30}$$

This result permits the first iterative contribution to the evolution operator to be identified as

$$U_R(t, t_0) = 1 - \frac{i}{\hbar} \int_{t_0}^{t} \hat{H}(t') U_R(t', t_0) dt', \tag{2.4.31}$$

since the 0th order term is $U_R(t_0, t_0) = 1$. By successive substitutions for $U_R(t', t_0)$ into Eq. (2.4.31), a series expansion may be found for $U(t_1, t_0)$.

$$U(t, t_0) = 1 - \frac{i}{\hbar} \int_{t_0}^{t} \hat{H}(t_1)dt_1 + \left(\frac{-i}{\hbar}\right)^2 \int_{t_0}^{t} \int_{t_0}^{t} dt_1 dt_2 \hat{H}(t_1)\hat{H}(t_2) \dots . \tag{2.4.32}$$

Standard perturbative approaches to static and dynamic interactions are considered further in the review section of Appendix D. Note that Eq. (2.4.32) is a *time-ordered* expression, because the operators $\hat{H}(t_1)$, $\hat{H}(t_2)$, etc. do not commute in general.

What is the meaning of the restriction on the time order of operators? Among other things, it reflects the difference in dynamics caused by different sequences of interactions. If three pulses are incident on a system at separate times t_1, t_2, and t_3, it may easily be anticipated that the outcome depends on which pulse arrives first and whether its frequency is close to resonance. This situation is depicted in Fig. 2.8, where three different sequences are compared. In the 123 sequence on the left, the ground state absorption transition is driven first, so the upper state can be reached if pulses 2 and 3 arrive before the atom decays back to ground. In the 321 sequence in the middle of the figure, however, the pulse connecting excited state 3 to the intended final state 4 is applied first. Since state 3 is presumably unoccupied prior to the arrival of the pulses, there is no population in this state to absorb the first arriving pulse and nothing happens – no atoms reach state 4 in this case. This illustrates the fact that permutation of the time of arrival is important in pulsed optical interactions. The third sequence in Fig. 2.8 illustrates that the permutation of frequencies leads to still other excitation channels. Different time-domain and frequency-domain sequences of pulses lead to physically distinct processes and outcomes, and commutation algebra automatically accounts for this.

2.4.3   Matrix representations of operators

To this point, we have described how one can divide the overall time dependence of changes effected by operators, but we have not discussed the notation with
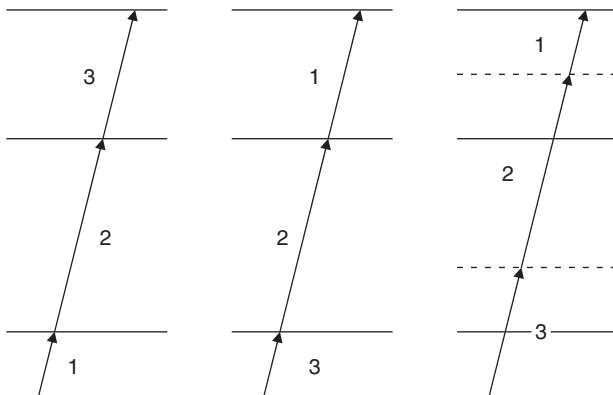
Figure 2.8 *Schematic diagram showing three different sequences of pulses with a fixed set of frequencies applied to excite the upper state of a four-level system. The sequence on the left begins from a populated state. All transitions are resonant. Because the transitions progress sequentially toward the upper level, this sequence is the most effective. The one in the middle illustrates a time-reversed sequence initiated from an excited state. It is ineffective if the excited states are unpopulated, but constitutes an independent excitation channel otherwise. The final sequence on the right permutes the frequencies of the first, by imagining them to excite unintended transitions in an off-resonant fashion. This illustrates a third independent excitation channel that could be effective, if the detunings are not too large. What should be concluded from the figure is that the result of each sequence is different.*

which we plan to represent the operators themselves. There are several options, if we wish to avoid approaches that presume we know the wavefunction itself. For example, in a system with a finite number of energy levels, we know in advance that there is a finite number of expectation values and matrix elements between the available states. For the operator $\hat{O}$ in a two-level system, these quantities are $\langle 1|\hat{O}|1\rangle$, $\langle 1|\hat{O}|2\rangle$, $\langle 2|\hat{O}|1\rangle$, and $\langle 2|\hat{O}|2\rangle$. These four quantities represent all the reproducible, measurable properties of the system. In this respect, these eigenvalues provide a complete description of the role of the operator $\hat{O}$ on the system. Thus, a complete representation of the operator can be written as a collection of matrix entries as

$$\begin{bmatrix} \langle 2|\,\hat{O}\,|2\rangle & \langle 2|\,\hat{O}\,|1\rangle \\ \langle 1|\,\hat{O}\,|2\rangle & \langle 1|\,\hat{O}\,|1\rangle \end{bmatrix} = \begin{bmatrix} O_{22} & O_{21} \\ O_{12} & O_{11} \end{bmatrix}.$$

Alternatively, in Dirac notation, the representation of $\hat{O}$ can be written as $\hat{O} = O_{11}|1\rangle\langle 1| + O_{12}|1\rangle\langle 2| + O_{21}|2\rangle\langle 1| + O_{22}|2\rangle\langle 2|$. Any matrix element O_{ij} in the basis of states $|1\rangle$ and $|2\rangle$ can be retrieved by calculating $\langle i|\hat{O}|j\rangle = \langle i|\{O_{11}|1\rangle\langle 1| + O_{12}|1\rangle\langle 2| + O_{21}|2\rangle\langle 1| + O_{22}|2\rangle\langle 2|\}|j\rangle$ with $i,j = 1, 2$. For example, one finds $\langle 1|\hat{O}|2\rangle = \langle 1|\{O_{11}|1\rangle\langle 1| + O_{12}|1\rangle\langle 2| + O_{21}|2\rangle\langle 1| + O_{22}|2\rangle\langle 2|\}|2\rangle = O_{12}$.

In a system with an arbitrary number of states, use can therefore be made of the expansion

$$\hat{O} = \sum_{m',n'} O_{m',n'} \,|n'\rangle\,\langle m'|\,, \tag{2.4.33}$$

which represents the operator as a matrix of its coefficients between various states, as in the example. It may readily be checked whether Eq. (2.4.33) yields the appropriate matrix element in the basis $|n\rangle$ when evaluated between states n and m. The n, m entry in the matrix should be given by

$$\langle n|\,\hat{O}\,|m\rangle = \langle n|\sum_{n'm'} O_{m'n'}\,|n'\rangle\,\langle m'\,|\,m\rangle\,. \tag{2.4.34}$$

Since the $O_{m'n'}$ on the right of Eq. (2.4.34) are merely scalar coefficients and the sum is over primed variables only, this can be reordered as follows:

$$\langle n|\,\hat{O}\,|m\rangle = \sum_{n'm'} O_{m'n'}\,\langle n\,|\,n'\rangle\,\langle m'\,|\,m\rangle = \sum_{n'm'} O_{m'n'}\delta_{nn'}\delta_{mm'} = O_{mn}. \tag{2.4.35}$$

In obtaining Eq. (2.4.35), use has been made of the Kronecker delta δ_{ij} which is equal to 1 or 0, depending on whether the indices i, j are the same or different. The point is that the representation given by Eq. (2.4.33) reproduces all possible matrix elements for an operator in the space spanned by $|n\rangle$.

Matrix representations are very useful for calculations in systems with only a few levels. For example, the Hamiltonian of a two-level system is

$$\hat{H} = \sum_{n_1 m}^{2} H_{mn}\,|n\rangle\,\langle m| = H_{11}\,|1\rangle\,\langle 1| + H_{21}\,|1\rangle\,\langle 2| + H_{12}\,|2\rangle\,\langle 1| + H_{22}\,|2\rangle\,\langle 2|$$

$$= \begin{pmatrix} H_{11} & H_{12} \\ H_{21} & H_{22} \end{pmatrix}. \tag{2.4.36}$$

Using this kind of representation of an operator in terms of its matrix elements instead of its explicit mathematical form makes it easy to write a full equation of motion for a system based on minimal information about it. For example, in the presence of an electric dipole perturbation $\hat{V}$, the equation of motion (Schrödinger's equation) can be written

$$i\hbar \frac{d}{dt}\begin{pmatrix} C_1 \exp(-i\omega_1 t) \\ C_2 \exp(-i\omega_2 t) \end{pmatrix} = \begin{pmatrix} \hbar\omega_1 & V_{12} \\ V_{21} & \hbar\omega_2 \end{pmatrix}\begin{pmatrix} C_1 \exp(-i\omega_1 t) \\ C_2 \exp(-i\omega_2 t) \end{pmatrix}. \tag{2.4.37}$$

2.4.4   Changing representations

Any continuous regular function ψ can be expanded in terms of a complete set of discrete basis functions U_n. Provided the functions U_n are mutually orthogonal and normalized, the expansion has the form

$$\psi = \sum_n C_n U_n, \tag{2.4.38}$$

where each expansion coefficient C_n gives the relative contribution of a single basis function. If we consider the functions U_n to constitute a set of basis vectors $|n\rangle$ which span the space, then ψ becomes a state vector, denoted in the Dirac notation introduced earlier by

$$|\psi\rangle = \sum_n C_n |n\rangle, \tag{2.4.39}$$

and the coefficient C_i is the result of vectorial projection of $|\psi\rangle$ on the basis vector $|i\rangle$. The projection procedure thus projects out of the full state $|\psi\rangle$ the probability amplitude of finding it in a particular eigenstate $|i\rangle$ in the basis of states $|n\rangle$.

$$\langle i \mid \psi \rangle = \langle i| \sum_n C_n |n\rangle = \sum_n C_n \langle i \mid n \rangle = \sum_n C_n \delta_{in} = C_i. \tag{2.4.40}$$

The set of all coefficients C_i constitutes a representation of ψ in the basis n.

It often happens that initial information about a system is available in a representation that is inconvenient for solving dynamics. Also sometimes solutions are needed in the laboratory reference frame, whereas the basis states that make a problem mathematically tractable (perhaps by better reflecting the symmetry of the problem) are in a different frame. This situation can be rectified by changing representations. Provided the basis states form complete sets, the procedure for transforming between two arbitrary basis sets $|\xi\rangle$ and $|n\rangle$ is straightforward, as described below.

If we think of the set of coefficients C as the representation itself, then the problem of changing representations becomes one of relating an initial set of expansion coefficients C_n from a description like Eq. (2.4.39) to another set C_ξ in the desired expansion

$$|\psi\rangle = \sum_\xi C_\xi |\xi\rangle. \tag{2.4.41}$$

The tool for finding the relationship between C_n and C_ξ is obtained by multiplying Eq. (2.4.41) from the left by ψ^* and integrating over all space. Since $\langle \psi | \psi \rangle = 1$, the result equals unity.

$$\langle \psi| \sum_n C_n |n\rangle = \sum_{m,n} \langle m| C_m^* C_n |n\rangle = 1. \tag{2.4.42}$$

With the help of Eq. (2.4.40), one can substitute for the coefficients in Eq. (2.4.42) to obtain

$$1 = \sum_{m,n} \langle m|\langle \psi|m\rangle \langle n|\psi\rangle |n\rangle, \tag{2.4.43}$$

and then rearrangement of the right side yields

$$1 = \sum_{m,n} \langle m|n\rangle \langle \psi|m\rangle \langle n|\psi\rangle$$

$$= \sum_{m,n} \delta_{mn} \langle \psi|m\rangle \langle n|\psi\rangle. \tag{2.4.44}$$

Since ψ does not depend on m, n, it can be removed from the summation. Hence

$$1 = \langle \psi | \left\{ \sum_n |n\rangle \langle n| \right\} |\psi\rangle . \tag{2.4.45}$$

For this equation to be valid the sum in parentheses must equal 1. Hence this furnishes a representation of the identity operator $\hat{I}$ namely

$$\hat{I} = \sum_n |n\rangle \langle n| . \tag{2.4.46}$$

Equation (2.4.46) is the most convenient mathematical tool for changing representations. With it, one can change from the $|n\rangle$ basis to the $|\xi\rangle$ basis or from (x,y,z) configuration space coordinates to (r, θ, ϕ) coordinates by simply inserting the identity operator for the desired basis into the original expansion of the wavefunction. That is,

$$|\psi\rangle = \sum_n C_n |n\rangle = \sum_{\xi,n} |\xi\rangle \langle \xi | C_n |n\rangle$$

$$= \sum_{\xi,n} \left[C_n \langle \xi \mid n \rangle \right] |\xi\rangle. \tag{2.4.47}$$

The square bracket in Eq. (2.4.47) encloses all but the desired basis vectors $|\xi\rangle$. Hence Eq. (2.4.47) is a representation of $|\psi\rangle$ in terms of basis vectors $|\xi\rangle$ with new coefficients $C_\xi \equiv \sum_n C_n \langle \xi | n \rangle$. Since the new basis was chosen for convenience, it is helpful to know that the states $|\xi\rangle$ need not be orthogonal to $|n\rangle$ for this procedure to work. The new basis needs only to be complete.

One final point about representations bears mentioning. Throughout this book, wavefunctions for collections of particles are written without imposing additional restrictions due to the Pauli Principle. Although atoms are typically bosons, actually assuming them to be bosons represents a significant assumption. Stable atoms consist of protons, neutrons, and electrons all of which are fermions. But they contain an even total number of such particles and are found to obey Bose statistics. Consequently, we usually assume any number of them may occupy the same state. Nevertheless in semiconductors, as one counterexample, the occupation of valence and conduction band spin states is governed by the Pauli Exclusion Principle, so spin statistics must be reflected in wavefunctions for the energy bands. As another example, bosonic atoms can sometimes be converted into fermions near Feshbach resonances [2.6], so in principle the occupation of spin states should reflect the Pauli Principle in dense phases of such matter. Because the wavefunctions of fermionic systems must be written differently from Eq. (2.4.47) to account for spin exclusion, Appendix F provides an elementary introduction to the anti-commutation properties of spin systems for the sake of completeness.

Problems

2.1. The initial state of an "entangled" pair of identical two-level atoms A and B located at the origin is $\psi = \frac{|1\rangle|0\rangle+|0\rangle|1\rangle}{\sqrt{2}}$, where the ket products denote the products of the wavefunctions for atoms A and B in the order $|A\rangle|B\rangle$. A and B may be 0 or 1. This state is the result of excitation by a single photon capable of providing enough energy to excite atom A or atom B of the pair but not both.

   (*a*) Show that ensemble average measurements of the probability for finding the atoms in particular combination states, as given by the pair density matrix elements $\langle\psi|\rho_{AB}|\psi\rangle$ where $\rho_{AB} = |A\rangle|B\rangle\langle B|\langle A|$, confirm that half the time one finds atom A excited and half the time one finds B excited. (Find ρ_{01} and ρ_{10}.)

   (*b*) Next, consider separating the two atoms *of a single pair* by a distance on the order of 100 km, without causing any phase or state change and making a sequential determination of the states of each separate atom. Because the pair is initially in a superposition state (and given the fundamental postulate of quantum mechanics) the state of atom A is unknowable until a measurement is made. Similarly the state of atom B is indeterminate until measured. Find the probability amplitude for ψ to yield each possible product state of A and B by projecting ψ directly onto each of the four possible eigenstate products in turn.

   (*c*) In part (*b*), compare the probabilities of finding B in state 0 or 1 after A is found in 0. Suggest a resolution of the surprising fact that B seems to "know" the measured state of atom A and always conserves energy even though it has an overall 50% probability of being found in either state and is measured at a different location.

2.2. A particle in a one-dimensional well has the Hamiltonian

$$H = \begin{cases} \dfrac{p^2}{2m} = -\dfrac{\hbar^2}{2m}\dfrac{d^2}{dz^2}, & 0 \le z \le L \\ \infty, & z < 0, z > L \end{cases}$$

and is in a superposition state described by

$$\Psi = \left(\frac{2}{L}\right)^{1/2} \sum_n C_n \sin(k_n z)e^{-i\omega_n t}$$

   (*a*) What is the expectation value of its energy?

   (*b*) Under what condition might we expect the expectation value of energy to equal the energy of an individual state, for example the mth state?

   (*c*) Taking into account restrictions on the allowed values of k_n, what is the average result of repeated measurements of the momentum of particles in state Ψ?

2.3. A two-level atom has a Hamiltonian $H = \begin{pmatrix} H_{11} & H_{12} \\ H_{21} & H_{22} \end{pmatrix}$. Find the appropriate expansion coefficients to write this completely in terms of the three Pauli spin matrices plus the unit matrix.

2.4. An electron with spin angular momentum $S = \frac{\hbar}{2}\sigma$, where σ is a Pauli spin matrix experiences a static magnetic field $\bar{B}$ oriented along the z-axis. Assume that the spin is initially oriented perpendicular to the field, in state

$$\Psi(0) = \frac{1}{\sqrt{2}} \begin{pmatrix} 1 \\ 1 \end{pmatrix}.$$

Find $\Psi(t)$ and show that the expectation value of the spin in the x-direction precesses according to

$$\langle S_x \rangle = \frac{\hbar}{2} \cos \omega t.$$

(The magnetic moment of the spin is related to the spin angular momentum by $\mu_s = g\mu_B S/\hbar$, where g is the spin g factor, and the Hamiltonian is $H = -\bar{\mu}_s \cdot \bar{B}$).

2.5. Show that the Pauli spin matrices have the properties
   (a) $\sigma_i \sigma_j = i\sigma_k$ for cyclic (and $\sigma_i \sigma_j = -i\sigma_k$ for anti-cyclic) permutations, and
   (b) $[\sigma_i, \sigma_j] = 2i\sigma_k$ for cyclic (and $[\sigma_i, \sigma_j] = -2i\sigma_k$ for anti-cyclic) permutations of the indices $i, j, k = x, y, z$.

2.6. Pauli spin matrices, and transition operators $\sigma^{\pm}$ based on them, are commonly encountered in calculations of photon echoes and resonance fluorescence. Products of these matrices must be simplified on the basis of their commutation relations. Show that
   (a) $[\sigma^{\pm}, \sigma_z] = \mp 2\sigma^{\pm}$,
   (b) $[\sigma^+, \sigma^-] = \sigma_z$,
   where $\sigma^{\pm} \equiv \frac{1}{2}(\sigma_x \pm i\sigma_y)$.

2.7. Pauli matrices anticommute.
   (a) Show that $[\sigma_i, \sigma_j]_+ \equiv \sigma_i \sigma_j + \sigma_j \sigma_i = 2\delta_{ij}$, where δ_{ij} is a Kronecker delta whose value is 0 unless the subscripts are equal.
   (b) Use an inductive argument and part (a) to show that $\sigma_i(\sigma_j)^k = (-\sigma_j)^k \sigma_i$, when $i \neq j$ and k is an arbitrary positive integer.
   (c) Prove that $\exp[-i\theta_3\sigma_3]\exp[-i\theta_i\sigma_i] = \exp[i\theta_i\sigma_i]\exp[-i\theta_3\sigma_3]$, when $i = 1, 2$.

2.8. The Pauli spin matrices are useful because as representations of angular momentum operators, they are generators of important unitary transformations. For example, an exponential function of the three Pauli spin 1/2 operators generates rotations about the $x-$, $y-$, and z-axes of a two-level atom as verified below. Since the static and interaction Hamiltonians, and the transformation of arbitrary superposition states into other states of the atom, can all be represented by these matrices, the Pauli matrices can provide a complete representation of static and dynamic aspects of atoms in their "spin" space.

(a) Let ξ be a real number and suppose $\hat{A}$ is a matrix operator that satisfies $\hat{A}\hat{A} = 1$. Show that $\exp(i\xi\hat{A}) = \hat{I}\cos(\xi) + i\hat{A}\sin(\xi)$, where $\hat{I}$ is the unit operator.

(b) Show that if $\hat{A} = \hat{\sigma}_y$, the exponential operator in part (a) produces a rotation through an angle ξ about the $\hat{y}$ axis, by showing that it reduces to the usual 2×2 rotation matrix for transforming the two (x and z) components of a state vector projected onto the plane perpendicular to the rotation axis.

(c) Finally, if $\hat{n} = n_x\hat{x} + n_y\hat{y} + n_z\hat{z}$ is an arbitrary real unit vector in three dimensions, prove that $(\hat{n} \cdot \vec{\sigma})^2 = \hat{I}$ and use part (a) to find the explicit 2×2 matrix form of the operator $R_{\hat{n}}(\theta) \equiv \exp(-i\theta\hat{n} \cdot \vec{\sigma}/2)$ that produces a rotation by θ about the axis $\hat{n}$. The symbol $\vec{\sigma}$ in these expressions denotes the three-component vector $(\sigma_x, \sigma_y, \sigma_z)$ of Pauli spin matrices. (Note: The factor of 2 difference between the angular arguments of R and the exponential operator merely accounts for the rotational degeneracy of real space with respect to rotations in spin space.)

(d) Write the interaction Hamiltonian for electric dipole response in a two-level atom in terms of Pauli spin matrices – both (i) as a single Hermitian matrix, and (ii) as a sum of two non-Hermitian matrices (that are raising and lowering operators).

2.9. Use a symmetry argument to find the expectation value of the electric dipole moment $< e\bar{r} >$ of an atom in an eigenstate.

2.10. Show that the expectation value of the magnetic dipole moment $\bar{\mu}^{(m)} = e(\bar{r} \times \bar{p})/2m$ of a system with inversion symmetry is not necessarily 0 in an eigenstate.

2.11. (a) Calculate the expectation value of the dipole moment $< e\bar{r} >$ of an atom with the specific wavefunction

$$\psi(\bar{r}, t) = C_{210}u_{210}(\bar{r})\exp(-i\omega_{210}t) + C_{100}u_{100}(\bar{r})\exp(-i\omega_{100}t),$$

where

$$u_{100}(r, \theta, \varphi) = \left(\pi a_0^3\right)^{-1/2}\exp(-r/a_0),$$

$$u_{210}(r, \theta, \varphi) = \left(32\pi a_0^3\right)^{-1/2}(r/a_0)\cos\theta\exp(-r/2a_0),$$

and a_0 is a constant (the Bohr radius). Use spherical coordinates and write the position vector as $\bar{r} = \frac{1}{2}r\sin\theta[(\hat{x} - i\hat{y})\exp(i\varphi) + (\hat{x} + i\hat{y})\exp(-i\varphi)] + \hat{z}r\cos\theta$.

(b) Give a physical reason why the result of part (a) is not zero.

2.12. A system is placed in a linear superposition state with the (unnormalized) wavefunction

$$\psi_1(t) = \exp(-i\pi t)\cos x + \exp(-i5\pi t)\cos 5x + \exp(-i11\pi t)\cos 11x.$$

(a) Plot the probability $|\psi_1(x,t)|^2$ of finding the system at $x = \pi/60$ as a function of time for $0 < t < 40$.

(b) Recalculate and plot the squared probability amplitude for finding the system at $x = \pi/60$ for $0 < t < 40$ when relaxation of the excited states is introduced by modifying the wavefunction to

$$\psi_2(t) = e^{-i\pi t}\cos x + e^{-t/10}(e^{-i5\pi t}\cos 5x + e^{-i11\pi t}\cos 11x).$$

(c) On the basis of your plots, interpret the large amplitude features in the temporal evolution of the system with and without dissipation. Identify two fundamental differences in the basic dynamics of non-dissipative and dissipative systems.

2.13. A beam of light propagating in the z-direction is in a state of polarization that is expressed in terms of linearly polarized basis states $|x\rangle = \begin{pmatrix} 1 \\ 0 \end{pmatrix}$ and $|y\rangle = \begin{pmatrix} 0 \\ 1 \end{pmatrix}$ according to $|\psi\rangle = \psi_x |x\rangle + \psi_y |y\rangle$.

(a) Find the expansion coefficients ψ_x and ψ_y of the wavefunction in Dirac notation.

(b) Change representations by inserting the identity operator to show that a completely equivalent description of $|\psi\rangle$ exists that is based on left and right circularly polarized states $|L\rangle = \frac{1}{\sqrt{2}} \begin{pmatrix} 1 \\ -i \end{pmatrix}$ and $|R\rangle = \frac{1}{\sqrt{2}} \begin{pmatrix} 1 \\ i \end{pmatrix}$. Find the coefficients c_1 and c_2 in the new representation $|\psi\rangle = c_1 |R\rangle + c_2 |L\rangle$.

(c) Configuration space representations can be given in terms of *rotated* basis vector states. This is done by noting that

$$|x\rangle = \cos\varphi |x'\rangle - \sin\varphi |y'\rangle,$$

and

$$|y\rangle = \sin\varphi |x'\rangle + \cos\varphi |y'\rangle.$$

Hence $\langle x' \mid x \rangle = \cos\phi$ and $\langle y' \mid y \rangle = \sin\phi$, where ϕ is the angle by which x' is rotated with respect to x about z. Show that a state vector in the transformed (primed) basis becomes

$$|\psi'\rangle = \begin{pmatrix} \psi_{x'} \\ \psi_{y'} \end{pmatrix} = \begin{pmatrix} \langle x' \mid \psi \rangle \\ \langle y' \mid \psi \rangle \end{pmatrix} = \begin{pmatrix} \cos\varphi & \sin\varphi \\ -\sin\varphi & \cos\varphi \end{pmatrix} \begin{pmatrix} \langle x \mid \psi \rangle \\ \langle y \mid \psi \rangle \end{pmatrix} = R(\varphi) |\psi\rangle,$$

where $R(\phi)$ is the rotation operator.

(d) Circularly polarized representations can be expressed in terms of rotated bases too. Separate the rotation operator into two parts: a diagonal matrix and the Pauli matrix σ_y, each with an appropriate coefficient. Then find the eigenvalues and eigenvectors of the Pauli matrix (the part of R which is traceless). Interpret the meaning of the eigenvalues in the context of photon polarization.

(e) Operate with $R(\phi)$, *after reduction into symmetric and antisymmetric parts* as in part (d), on the basis states $|L\rangle$ and $|R\rangle$ directly to show that a rotation

multiplies each of them by a complex phase factor. (Note that the phase factor differs in sign in $|L'\rangle$ and $|R'\rangle$.) Is this consistent with part (d)?

(*f*) Show that an arbitrary linear superposition of rotated basis states is not an eigenvector of the rotation operator. (Hint: Apply the reduced operator to a superposition state like $|\psi\rangle = |R\rangle\langle R \mid \psi\rangle + |L\rangle\langle L \mid \psi\rangle$.) What does this mean in general with regard to the angular momentum of linear superposition states of right and left circularly polarized light?

References

2.1. J. Itatani, J. Levesque, D. Zeidler, H. Niikura, H. Pepin, J.C. Kieffer, P.B. Corkum and D.M. Villeneuve, *Nature* **432**, 867(2004).

2.2. M. Tinkham, *Group Theory and Quantum Mechanics*, Courier Dover Publications, New York, 2003.

2.3. P.W. Langhoff, *Am. J. Phys.* **39**, 954(1971).

2.4. W. Kuhn, *Eur. J. Phys.* **1**, 65 (1980); see also W.B. Fowler, *The Physics of Color Centers*, Academic Press, New York, 1968.

2.5. T.T. Basiev, S.B. Mirov, and V.V. Osiko, *IEEE J.Q.E.* **24**, 1052(1988).

2.6. D.B. Strukov, G.S. Snider, D.R. Stewart, and R.S. Williams, *Nature* **453**, 80–3(2008).

2.7. C.A. Regal, M. Greiner, and D.S. Jin, *Phys. Rev. Lett.* **92**, 040403(2004).

3

Atom–Field Interactions

3.1 The interaction Hamiltonian

In the description of atoms interacting with light, the system Hamiltonian H accounts in principle for everything – for the energetics of each atom, the energy density of the light field itself, and the modification of system energy due to the coupling of atoms to the field. Our ability to understand and predict behavior relies on an accurate determination of H and subsequent solution of Schrödinger's equation for the wavefunction, which is usually deemed essential. However, in the century or so that has passed since the discovery of quantum mechanics, analytic solutions for the wavefunctions of only a handful of simple, isolated atoms like hydrogen and helium have emerged. It is therefore hard to imagine applying this approach successfully to modern research on new materials. However, its limitations can be overcome by realizing that the vast majority of optical problems involve the same interaction Hamiltonian, do not require knowledge of the wavefunction itself, and can be enormously simplified by experimental as well as theoretical procedures. Moreover, with the so-called reduced density matrix, mathematically rigorous ways can be found to ignore parts of complicated systems while focusing on specific portions of interest. In this chapter we prepare for this by identifying the one interaction Hamiltonian to be used in all subsequent chapters, by introducing the density matrix to replace the wavefunction, and discussing experimental tricks that can be used to convert multilevel systems into simple two-level systems.

When it is chiefly the *dynamics* of an atom or some other system that are of interest, it is natural to separate the total Hamiltonian into a part H_0 that describes the isolated (static) system and an electromagnetic interaction Hamiltonian $V(t)$ which initiates dynamics:

$$H = H_0 + V(t). \tag{3.1.1}$$

H_0 determines the allowed energies and wavefunction of the unperturbed system, but knowledge of the exact wavefunction is fortunately not necessary to predict the effects of $V(t)$. For this, knowledge of the placement of energy levels and system symmetries is adequate, and these properties of the system can be determined experimentally without ever knowing H_0 or the wavefunction. $V(t)$ can be derived (see Appendix C) in a general multipole form that is not only the same for all problems considered in this book, but can be readily quantized and that displays dependences on (*a*) the electric and magnetic fields of light and (*b*) the main charge motions induced by its

passage. The largest induced moments are the electric dipole moment $\bar{\mu}^{(e)} = e\bar{r}$ and the magnetic dipole moment $\bar{\mu}^{(m)} = \frac{1}{2}\bar{r} \times e\bar{v}$, where $\bar{r}$ and $\bar{v}$ are the displacement and velocity vectors of a single positive charge. If we include both types of moment, we have

$$V(t) = -\bar{\mu}^{(e)} \cdot \bar{E} - \bar{\mu}^{(m)} \cdot \bar{B}. \tag{3.1.2}$$

At low intensities, the magnitudes of plane electric and magnetic fields are related by $B = E/c$, where c is the velocity of light. Because $\bar{\mu}^{(m)}$ is proportional to velocity v of the charge whereas $\bar{\mu}^{(e)}$ is not, the second term in Eq. (3.1.2) is almost always negligible compared to the first, by virtue of the factor $v/c << 1$. There are rare exceptions in dynamic systems where resonant enhancement of magnetic interactions takes place, but in subsequent chapters the interaction Hamiltonian will be taken to be

$$V(t) = -\bar{\mu}^{(e)} \cdot \bar{E}(t) = -e\bar{r} \cdot \bar{E}(t). \tag{3.1.3}$$

In this expression, although $\bar{\mu}^{(e)} = e\bar{r}$ is the electric dipole induced by a time-varying field and is therefore time-varying itself, it is a constant vector in the rotating frame of the optical field $E(t)$. Hence its dependence on time is dropped in Eq. (3.1.3). We shall see later in Section 7.5 that the situation is quite different for transverse magnetic moments created by intense light.

3.2 Perturbation theory

We now introduce an approximate method for calculating time development of a simple system in which the atomic properties are quantized but the radiation field is left in classical form (as a sinusoidal wave). This is called semiclassical perturbation theory. Results will be compared in Section 3.3 with an exact method, setting the stage for later combinations of exact and approximate techniques.

Consider an atom (Fig. 3.1) with only two levels $|1\rangle$ and $|2\rangle$ that is subjected to excitation by a standing wave:

$$\bar{E}(z,t) = \left\{ \begin{array}{ll} \hat{x}E_0(z)\cos\omega t, & t \geq 0 \\ 0, & t < 0 \end{array} \right\}. \tag{3.2.1}$$

Provided the light wave does not cause significant shifts in the energy levels of the atom, a solution to Eq. (3.2.1) can be written as a linear superposition of eigenfunctions
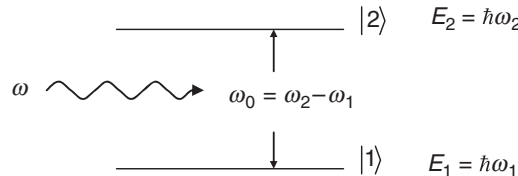

Figure 3.1 *Light of frequency ω interacting with a two-level atom which has a resonant frequency of ω_0.*

of H_0. We take the wavefunction to be

$$\psi\left(\bar{r}, t\right) = \sum_n C_n U_n\left(\bar{r}\right) \exp(-i\omega_n t), \tag{3.2.2}$$

where the basis functions U_n are eigenfunctions of H_0 determined by

$$H_0 U_n = E_n U_n \tag{3.2.3}$$

and eigenfrequencies ω_n are related to the energy eigenvalues according to

$$E_n = \hbar\,\omega_n. \tag{3.2.4}$$

Energies of the upper and lower levels are $\hbar\omega_2$ and $\hbar\omega_1$, respectively.

Assume that the light frequency ω is near the resonant transition frequency between levels 2 and 1, defined by

$$\omega_0 = \omega_2 - \omega_1, \tag{3.2.5}$$

so that $\omega \cong \omega_0$. Equation (3.2.2) can then be written out explicitly as

$$\psi\left(\bar{r}, t\right) = C_2\left(t\right) \exp(-i\omega_2 t) U_2\left(\bar{r}\right) + C_1\left(t\right) \exp(-i\omega_1 t) U_1\left(\bar{r}\right) \tag{3.2.6}$$

and substituted into Schrödinger's equation to find the temporal evolution of the system.

This procedure yields

$$i\hbar\frac{\partial}{\partial t}\sum_i C_i \exp(-i\omega_i t) U_i = (H_0 + V)\sum_i C_i \exp(-i\omega_i t) U_i$$

$$i\hbar\sum_i \left(\dot{C}_i - i\omega_i C_i\right) \exp(-i\omega_i t) U_i = \sum_i C_i \exp(-i\omega_i t)\left(E_i + V\right) U_i. \tag{3.2.7}$$

Multiplying from the left by U_j^* and integrating over all space, one obtains

$$i\hbar\left(\dot{C}_j - i\omega_j C_j\right) \exp(-i\omega_j t) = C_j \exp(-i\omega_j t) E_j + \sum_{i \neq j} V_{ji} C_i \exp(-i\omega_i t), \tag{3.2.8}$$

where the matrix elements V_{ji} are

$$V_{ji} = -e\bar{E} \cdot \int dV\,\psi_j^*(\bar{r},t)\bar{r}\psi_i(\bar{r},t) = \langle U_j| - e\bar{r} \cdot \bar{E}\,|U_i\rangle = -e\,\langle U_j|\,\bar{r}\,|U_i\rangle \cdot \bar{E}$$

$$= \left\{ \begin{array}{cc} -e\bar{r}_{ji} \cdot \bar{E}, & j \neq i \\ 0, & j = i \end{array} \right\}.$$

Equation (3.2.8) simplifies to

$$\dot{C}_j = \frac{1}{i\hbar}\sum_{i \neq j} V_{ji} C_i \exp[-i(\omega_i - \omega_j)t]. \tag{3.2.9}$$

In the present case, the sum over i runs over only the two values $i = 1, 2$ giving

$$\dot{C}_2 = \frac{1}{i\hbar} \exp[-i(\omega_1 - \omega_2)t] V_{21} C_1(t) \tag{3.2.10}$$

$$\dot{C}_1 = \frac{1}{i\hbar} \exp[-i(\omega_2 - \omega_1)t] V_{12} C_2(t) \tag{3.2.11}$$

and the off-diagonal, interaction matrix element is

$$V_{21} = -\bar{\mu}_{21} \cdot \bar{E}_0 \cos \omega t = -\frac{ex_{21}E_0}{2} \left[\exp(i\omega t) + \exp(-i\omega t)\right]. \tag{3.2.12}$$

Note that if the induced dipole moment is not parallel to $\bar{E}_0 = E_0 \hat{x}$ as assumed above, then the interaction strength is reduced by its projection on $\hat{x}$. This is one example of polarization effects to be covered later.

The time development of the atom is completely described by the two equations

$$\dot{C}_2 = \frac{i}{2} \frac{\bar{\mu}_{21} \cdot \bar{E}_0}{\hbar} \left\{\exp[i(\omega_0 + \omega)t] + \exp[i(\omega_0 - \omega)t]\right\} C_1 \tag{3.2.13}$$

and

$$\dot{C}_1 = \frac{i}{2} \frac{\bar{\mu}_{12} \cdot \bar{E}_0}{\hbar} \left\{\exp[-i(\omega_0 - \omega)t] + \exp[-i(\omega_0 + \omega)t]\right\} C_2. \tag{3.2.14}$$

All that remains is to solve these coupled partial differential equations.

Consider an iterative approach for a ground state atom that is weakly excited by light of frequency $\omega \neq \omega_0$, beginning at $t = 0$. The initial (zeroth order) conditions are $C_2^{(0)} = 0$ and $C_1^{(0)} = 1$. Substituting the initial C_2 and C_1 into Eq. (3.2.14), we obtain equations for changes of the coefficients at short times:

$$\dot{C}_2^{(1)} \cong \frac{i}{2} \frac{\bar{\mu}_{21} \cdot \bar{E}_0}{\hbar} \left(\exp[i(\omega_0 + \omega)t] + \exp[i(\omega_0 - \omega)t]\right), \tag{3.2.15a}$$

$$\dot{C}_1^{(1)} \cong 0. \tag{3.2.15b}$$

These first-order equations may be integrated directly. The results are

$$C_1^{(1)}(t) \cong C_1(0) = 1 \tag{3.2.16a}$$

and

$$C_2^{(1)}(t) \cong \frac{1}{2} \frac{\bar{\mu}_{21} \cdot \bar{E}_0}{\hbar} \left\{\frac{\exp[i(\omega_0 + \omega)t] - 1}{\omega_0 + \omega} + \frac{\exp[i(\omega_0 - \omega)t] - 1}{\omega_0 - \omega}\right\}. \tag{3.2.16b}$$

Since $\omega \sim 10^{15}$ rad/s at optical frequencies, it is an excellent approximation to drop the term proportional to $(\omega_0 + \omega)^{-1}$. This is called the rotating wave approximation (RWA). We retain only the term in which the atomic and field phasors rotate together, rather than in opposite senses. (A useful geometric model that pictures time development as rotation in a fictitious space is outlined in Section 3.8.) Hence,

the first-order predictions for the time dependence of the probability amplitudes in this problem are

$$C_1^{(1)}(t) \cong C_1(0) = 1 \tag{3.2.17}$$

and

$$C_2^{(1)}(t) \cong \frac{1}{2} \frac{\bar{\mu}_{21} \cdot \bar{E}_0}{\hbar} \left[\frac{\exp[i(\omega_0 - \omega)t] - 1}{(\omega_0 - \omega)} \right]. \tag{3.2.18}$$

Equation (3.2.18) can be rewritten as

$$C_2(t) = \frac{i}{2} \frac{\bar{\mu}_{21} \cdot \bar{E}_0}{\hbar} \exp[i(\omega_0 - \omega)t/2] \frac{\sin([\omega_0 - \omega]t/2)}{([\omega_0 - \omega]/2)}, \tag{3.2.19}$$

yielding a time-dependent probability of excitation to state 2 which is

$$|C_2(t)|^2 = \left(\frac{\bar{\mu}_{21} \cdot \bar{E}_0}{2\hbar} \right)^2 \frac{\sin^2([\omega_0 - \omega]t/2)}{([\omega_0 - \omega]/2)^2}. \tag{3.2.20}$$

Atomic states have a natural lifetime τ which is the inverse of the total decay rate γ out of that state. So far, we have ignored spontaneous decay of this kind in our analysis. In an attempt to include exponential relaxation processes like those depicted in Fig. 3.2, let us try augmenting the equations of motion (Eq. (3.2.9)) in an ad hoc manner to introduce decay:

$$\dot{C}_2 = -\frac{1}{2}\gamma_2 C_2 + \frac{i}{2} \frac{\bar{\mu}_{21} \cdot \bar{E}_0}{\hbar} \exp[i(\omega_0 - \omega)t]C_1, \tag{3.2.21}$$

$$\dot{C}_1 = -\frac{1}{2}\gamma_1 C_1 + \frac{i}{2} \frac{\bar{\mu}_{12} \cdot \bar{E}_0}{\hbar} \exp[-i(\omega_0 - \omega)t]C_2. \tag{3.2.22}$$

Note that these equations correctly predict exponential decay in the absence of light. That is, if we ignore the second term on the right of Eq. (3.2.21) by setting $C_1 = 0$ (or $E_0 = 0$) one can readily integrate the equation to find $C_2(t) = C_2(0) \exp(-\gamma_2 t/2)$. Thus spontaneous, exponential decay of the amplitude takes place at the expected rate. Moreover if we treat level 1 as the true ground state by choosing $\gamma_1 = -\gamma_2$, then
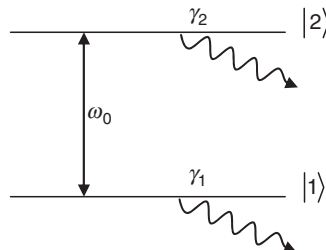

Figure 3.2 *Energy-level diagram of an atom with levels 2 and 1 undergoing decay at rates γ_2 and γ_1.*

in the absence of light note that occupation probability for the system as a whole should be conserved, since all the atoms that decay out of the excited state arrive in the ground state. The factor of $1/2$ in the first term on the right of both Eqs. (3.2.21) and (3.2.22) at least correctly accounts for the difference between probability amplitude and probability density.

Presuming the additions to Eqs. (3.2.21) and (3.2.22) are correct despite their ad hoc nature, a perturbative approach similar to that developed earlier could be used to solve them. For initial conditions $C_2(0) = 0$ and $C_1(0) = 1$, one finds

$$C_1(t) = C_1(0) \exp(-\gamma_1 t/2) = \exp(-\gamma_1 t/2). \tag{3.2.23}$$

Substituting Eq. (3.2.23) into Eq. (3.2.21) with an integrating factor of $\exp(\gamma_2 t/2)$, one finds

$$\frac{d}{dt} \exp(\gamma_2 t/2) C_2 = \frac{i}{2} \frac{\bar{\mu}_{21} \cdot \bar{E}_0}{\hbar} \exp[i(\omega_0 - \omega)t] \exp[(-\gamma_1 + \gamma_2)t/2].$$

Hence the perturbation theory solution is

$$C_2^{(1)}(t) = \exp(-\gamma_2 t/2) \left(\frac{i\Omega}{2} \right) \left[\frac{\exp[i(\omega_0 - \omega)t + (\gamma_2 - \gamma_1)t/2] - 1}{i(\omega_0 - \omega) + (\gamma_2 - \gamma_1)/2} \right], \tag{3.2.24}$$

where $\Omega \equiv \bar{\mu}_{21} \cdot \bar{E}_0/\hbar$. The probability of excitation to state 2 is therefore

$$|C_2(t)|^2 = \left(\frac{\Omega}{2} \right)^2 \left\{ \frac{\exp(-\gamma_1)t - 2\exp[-(\gamma_2 + \gamma_1)t/2]\cos\Delta t + \exp(-\gamma_2)t}{\Delta^2 + [(\gamma_2 - \gamma_1)/2]^2} \right\}, \tag{3.2.25}$$

where we have introduced the frequency detuning factor $\Delta \equiv \omega_0 - \omega$.

Exercise: Show that in this perturbative limit Eq. (3.2.25) reduces to a probability that is given at very short times ($t << \Delta^{-1}, \gamma_2^{-1}$) by

$$|C_2(t)|^2 \cong \left(\frac{\Omega t}{2} \right)^2 \frac{\sin^2(\Delta t / 2)}{[\Delta t / 2]^2}. \tag{3.2.26}$$

At short times we find the same transition probability as in Eq. (3.2.20). At first glance, the time dependence in Eq. (3.2.26) appears to be incompatible with a constant transition rate, which is the expected result. Despite the apparent quadratic dependence of the excitation probability on time t in the first factor on the right of Eq. (3.2.26), the transition rate is correctly predicted to be proportional to t itself however. This is due to the fact that the area under the $(\sin x/x)^2$ curve diminishes with time as $1/t$. Hence a perturbation calculation based on the squares of C coefficients seems to incorporate decay in a reasonable way. In Fig. 3.3, the perturbation result even gives qualitatively correct results beyond its range of applicability. Oscillations caused by competition between stimulated absorption and stimulated emission are found to gradually give way to a small but finite steady-state population in the upper state. (Transients of this kind are considered in more detail in Chapter 4) We shall see shortly, however, that there are serious problems with this description at anything
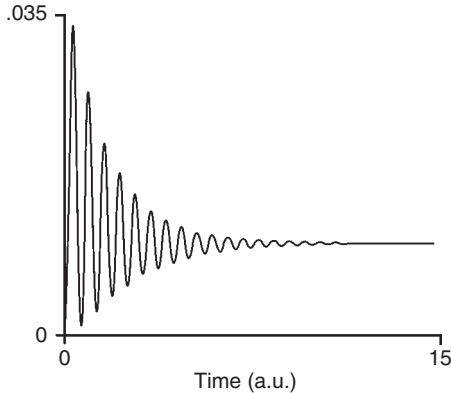
Figure 3.3 *Excited state occupation probability versus time for a two-level atom initially in the ground state, obtained from perturbation theory (plotted beyond its range of validity). This calculation (for Eq. (3.2.25) parameter values $\Delta = 10; \gamma_1 = 0; \gamma_2 = 1$) foreshadows the transient phenomenon of nutation (Chapter 4) even though a perturbation approach is not justified at long times.*

other than the very shortest timescales. Not only will this analytic approach be found to fail on resonance, but it also fails utterly off-resonance ($\omega \neq \omega_0$), where we *do expect* perturbation theory to work well.

3.3 Exact analysis

To gain perspective on the weaknesses and strengths of the perturbation approach above, we now reconsider Eq. (3.2.18) in the RWA using an exact approach developed by I. I. Rabi. The Rabi approach ignores decay, in favor of finding a solution for atomic dynamics in a strong field, to compare with perturbation results:

$$\dot{C}_2(t) = (i\Omega/2) \exp[i(\omega_0 - \omega)t]C_1, \tag{3.3.1}$$

$$\dot{C}_1(t) = (i\Omega^*/2) \exp[-i(\omega_0 - \omega)t]C_2. \tag{3.3.2}$$

Without losing generality, we shall assume that Ω is not complex and try a solution of the form

$$C_1(t) = \exp[i\mu t], \tag{3.3.3}$$

and substitute this into Eq. (3.3.2) to solve for C_2. This yields

$$C_2(t) = \frac{2\mu}{\Omega} \exp[i(\Delta + \mu)t]. \tag{3.3.4}$$

Using both Eqs. (3.3.3) and (3.3.4) in Eq. (3.3.2), we find that solutions only exist if

$$\mu_{1,2} = -\frac{1}{2}\Delta \pm \frac{1}{2}\left[\Delta^2 + \Omega^2\right]^{1/2}. \tag{3.3.5}$$

The most general solutions for C_2 and C_1 are therefore

$$C_1(t) = A\exp(i\mu_1 t) + B\exp(i\mu_2 t), \tag{3.3.6}$$

$$C_2(t) = (2/\Omega)\exp[i\Delta t]\left[A\mu_1\exp(i\mu_1 t) + B\mu_2\exp(i\mu_2 t)\right]. \tag{3.3.7}$$

Making use of initial conditions $C_2(0) = 0$ and $C_1(0) = 1$ to determine unknown coefficients A and B, we find

$$A = \left(\frac{\mu_2}{\mu_2 - \mu_1}\right)$$

and

$$B = \left(\frac{\mu_1}{\mu_1 - \mu_2}\right).$$

It is convenient to define the difference between the eigenfrequencies in Eq. (3.3.5) as the generalized Rabi flopping frequency:

$$\Omega_R \equiv \mu_1 - \mu_2 = \left[\Delta^2 + \Omega^2\right]^{1/2}. \tag{3.3.8}$$

The product of μ_1 and μ_2 is related to the resonant Rabi frequency $\Omega \equiv \mu E_0/\hbar$ by

$$\mu_1\mu_2 = -\left(\frac{\Omega}{2}\right)^2, \tag{3.3.9}$$

so we can write a solution for the coefficient $C_2(t)$ of the wavefunction which is

$$C_2(t) = i(\Omega/\Omega_R)\exp[i\Delta t/2]\sin(\Omega_R t/2), \tag{3.3.10}$$

with the result that the occupation probability becomes

$$|C_2(t)|^2 = \left(\frac{\Omega}{2}\right)^2\left[\frac{\sin(\Omega_R t/2)}{(\Omega_R/2)}\right]^2. \tag{3.3.11}$$

For large detuning (far-off resonance), we find

$$|C_2(t)|^2 = \left(\frac{\Omega}{2}\right)^2\left[\frac{\sin(\Delta t/2)}{\Delta/2}\right]^2 \tag{3.3.12}$$

in agreement with the result (Eq. (3.3.23)) from the perturbation theory, ignoring decay.

For zero detuning (on resonance) the exact procedure yields

$$|C_2(t)|^2 = \left(\frac{\Omega}{2}\right)^2\left[\frac{\sin(\Omega t/2)}{\Omega/2}\right]^2 = \sin^2(\Omega t/2). \tag{3.3.13}$$

The predicted dynamics for this case are illustrated in Fig. 3.4.

The predictions of Figs. 3.3 and 3.4 are obviously quite different. The perturbation approach considered in the last section therefore fails under conditions of resonant excitation – even if incident radiation is weak. The reason is that on resonance, the perturbation expansion no longer converges. High-order interactions become
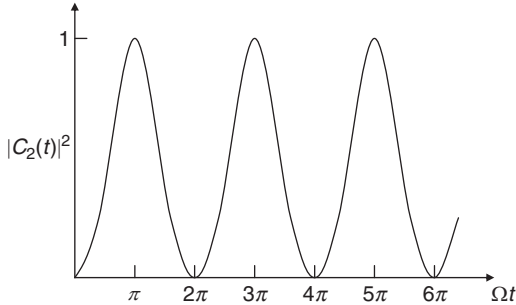
Figure 3.4 *Excited state occupation probability versus time at resonance* $(\Delta = 0)$.

important. Probability amplitudes like the second term in Eq. (3.2.16b) diverge. The exact solution plotted in Fig. 3.4 contains no such divergences, and indicates that on resonance undamped pulsations of the excited state population occur. The atom alternates regularly between the excited state and the ground state, undergoing a process known as Rabi flopping. Unlike the dynamics of Fig. 3.3, undamped oscillations can take place with resonant excitation and the ground state can be emptied periodically, giving rise to a transient population inversion.

3.4 Preliminary consideration of AC Stark or Rabi splitting

On resonance $(\omega = \omega_0)$, the eigenfrequencies in the Rabi solution reduce to

$$\mu_{1,2} = \pm \Omega/2,$$

where the subscripts 1, 2 refer to $+$ or $-$ solutions, respectively. The probability amplitudes for states a and b from Eqs. (3.3.6) and (3.3.7) in RWA are

$$C_2 = \frac{1}{2}\left[\exp(i\Omega t/2) - \exp(-i\Omega t/2)\right], \qquad (3.4.1)$$

and

$$C_1 = \frac{1}{2}\left(\exp(i\Omega t/2) + \exp(-i\Omega t/2)\right). \qquad (3.4.2)$$

Hence, on the basis of Eq. (3.2.2), the complete wavefunction should be

$$\psi = \frac{1}{2}\left\{ e^{-i(\omega_2 - \frac{\Omega}{2})t}\psi_2 - e^{-i(\omega_2 + \frac{\Omega}{2})t}\psi_2 + e^{-i(\omega_1 - \frac{\Omega}{2})t}\psi_1 + e^{-i(\omega_1 + \frac{\Omega}{2})t}\psi_1 \right\}. \qquad (3.4.3)$$

Notice that according to the expression above, the total wavefunction incorporates four oscillation frequencies. That is, Eq. (3.4.3) implies the existence of four distinct eigenfrequencies whereas there are only two eigenstates in the system. The energy-level structure suggested by this result is shown in Fig. 3.5. Because the number of eigenfrequencies exceeds the number of eigenstates, it is evident that a serious inconsistency has somehow entered into the calculation.
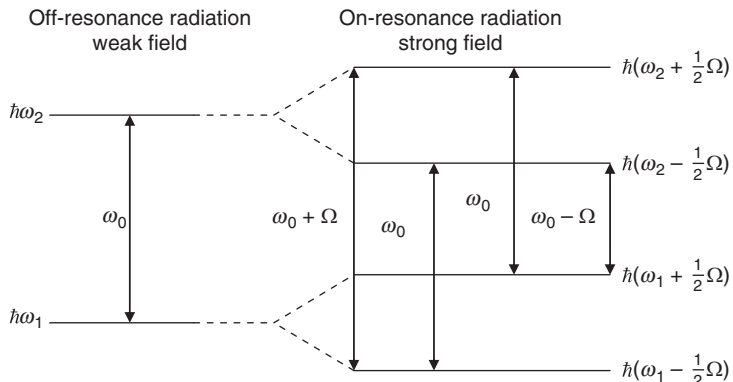
Figure 3.5 *A preliminary picture of strong field effects in a two-level atom.*
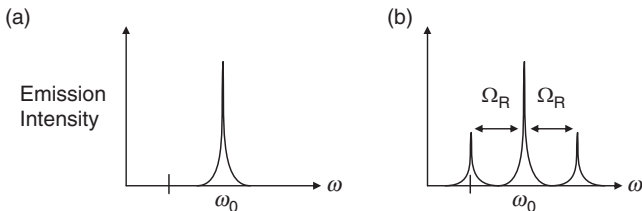
Figure 3.6 *Anticipated differences in the fluorescence spectrum of a two-level atom excited (a) off-resonance, and (b) on-resonance, based on Eq. (3.4.3) and Fig. 3.5.*

Ironically, the improper procedure used in arriving at Eq. (3.4.3) correctly foreshadows the response of a two-level atom driven by an optical field exactly on resonance, in which the atomic levels shift dynamically at the optical frequency through the Stark effect of the electric field. In this way, the atom undergoes what is known as AC Stark splitting or Rabi splitting (see Fig. 3.6). In later chapters, we shall approach time-dependent problems near resonances more cautiously, and not only resolve these discrepancies using strong-field analysis that incorporates decay consistently but achieve agreement with experiment [3.1, 3.2].

3.5   Transition rates

Common experience reveals three basic radiative processes: spontaneous decay (via emission) from a high-energy unstable state to a lower-energy stable state, and transitions induced by an external light field upward or downward between states. From analysis of Sections 3.2 and 3.3, we already know the probability of finding a two-level atom in state 2 is $|C_2(t)|^2$. Hence, if the atom is prepared in the lower state 1, the initial probability of atoms leaving state 1 (by absorption) is also given by

$$P = |C_2(t)|^2. \tag{3.5.1}$$

Consequently, the transition rate for absorption is

$$\frac{dP}{dt} = \frac{d}{dt} |C_2(t)|^2 . \tag{3.5.2}$$

For a two-level atom, which by assumption has no energy-level degeneracies, Eq. (3.5.2) also gives the rate of stimulated emission from state 2. To extend its applicability, we should account for the fact that both the incident light field and the resonant response of atoms have finite bandwidths. As a first step, let us ignore the atomic bandwidth, proportional to the spontaneous emission rate, and replace the radiation field factor E_0^2 in $|C_2(t)|^2$ by its spectral energy density $U(\omega)$. That is, we make the replacement

$$\frac{1}{2}\varepsilon_0 E_0^2(\omega) \, \delta(\omega - \omega_0) \Rightarrow U(\omega) \, d\omega. \tag{3.5.3}$$

The field E_0 might be that of a blackbody radiator or a single-mode laser field, with spectral densities that are very different, but the net probability P can always be found by using Eq. (3.5.3) to replace E_0 with $U(\omega)$ and integrating over frequency.

For example, what is the absorption rate in the case of broadband radiation? Using the expression (Eq. (3.3.11)) for $|C_2(t)|^2$, we find an absorption probability P_2 of

$$P_2 = \frac{1}{2} \left\langle \cos^2 \theta \right\rangle \frac{\mu_{21}{}^2}{\hbar^2 \varepsilon_0} \int d\omega t^2 U(\omega) \frac{\sin^2 \left[(\omega_0 - \omega) t / 2 \right]}{\left[(\omega_0 - \omega) t / 2 \right]^2},$$

where $\langle \cos^2 \theta \rangle$ is the average of the square of the geometric cosine factor from the inner product of $\bar{\mu}$ and $\bar{E}$. If the spectral density $U(\omega)$ varies slowly compared to the factor $\sin^2 x / x^2$ in the integral, we can approximate it with the resonance value $U(\omega_0)$. In this way, we find

$$P_2 = \left\langle \cos^2 \theta \right\rangle \frac{\mu_{21}{}^2}{\hbar^2 \varepsilon_0} U(\omega_0) \, t \int\limits_{-\infty}^{\infty} \frac{\sin^2 x}{x^2} \, dx = \left(\frac{\pi \mu_{21}{}^2}{\hbar^2 \varepsilon_0} \right) U(\omega_0) \, t \left\langle \cos^2 \theta \right\rangle . \tag{3.5.4}$$

For linearly polarized light, the angular average yields $\langle \cos^2 \theta \rangle = 1$. Hence

$$\frac{dP_2}{dt} = \pi \left(\frac{\mu_{21}{}^2}{\hbar^2 \varepsilon_0} \right) U(\omega_0) . \tag{3.5.5}$$

Exercise: Show that for monochromatic light with spectral density $U(\omega) = \frac{1}{2}\varepsilon_0 E_0^2 \delta(\omega - \omega_0)$ the transition rate given by Eq. (3.5.5) equals that from Fermi's golden rule (Appendix D) for a transition between discrete states at frequency ω_0. Assume the RWA applies, so that the interaction Hamiltonian can be written simply as $V_{21} = \frac{1}{2}(\mu_{21} \cdot E_0) \exp(i\omega t)$.

For unpolarized, isotropic radiation (like blackbody radiation) the orientational average yields $\langle \cos^2 \theta \rangle = 1/3$, and we instead find

$$\frac{dP_2}{dt} = \frac{\pi}{3} \left(\frac{\mu_{21}{}^2}{\hbar^2 \varepsilon_0} \right) U(\omega_0) . \tag{3.5.6}$$

The Einstein B coefficient for blackbody radiation can be obtained by comparing Eq. (3.5.6) with the defining relation for the stimulated emission rate, $dP_2/dt = BU(\omega_0)$, to obtain

$$B = \frac{\pi}{3}\left(\frac{\mu_{21}^2}{\hbar^2\varepsilon_0}\right). \tag{3.5.7}$$

To find A from B an assumption must be made regarding the spectral density. Blackbody sources have a spectral density function of the form derived by Planck:

$$U(\omega) = \frac{\hbar\omega^3 / \pi^2 c^3}{\exp(\hbar\omega / k_{\mathrm{b}}T) - 1}. \tag{3.5.8}$$

The spontaneous emission rate, the Einstein A coefficient, may then be obtained on the basis of "detailed balance" in the system. (i.e., "What goes up must come down!")

$$\dot{n}_2 = -An_2 - BU(\omega_0)(n_2 - n_1),$$
$$\dot{n}_1 = An_2 + BU(\omega_0)(n_2 - n_1).$$

In the steady state ($\dot{n} = 0$), both population equations above give the same result, namely Einstein's detailed balance relation:

$$[A + BU(\omega_0)]n_2 = BU(\omega_0)n_1. \tag{3.5.9}$$

In order for the populations to satisfy the Boltzmann distribution

$$n_2 = n_1\exp[-\hbar\omega / k_{\mathrm{B}}T],$$

the energy density must be given by Eq. (3.5.8), so the ratio of A and B must be

$$\frac{A}{B} = \frac{\hbar\omega^3}{\pi^2 c^3}. \tag{3.5.10}$$

Exercise: For a quasi two-level system with electronic degeneracies g_1 and g_2 in levels 1 and 2 respectively, find the A and B coefficients for all possible polarizations (as given in Table 3.1).

Table 3.1: *Two-level system transition rates.*

	Unpolarized isotropic	Linearly polarized	Circularly polarized
B_{21}	$\dfrac{\pi}{3}\dfrac{\mu_{21}^2}{\hbar^2\varepsilon_0}$	$\pi\dfrac{\mu_{21}^2}{\hbar^2\varepsilon_0}$	$\dfrac{\pi}{3}\dfrac{\mu_{21}^2}{\hbar^2\varepsilon_0}$
B_{12}	$\dfrac{g_2}{g_1}\cdot\dfrac{\pi}{3}\dfrac{\mu_{21}^2}{\hbar^2\varepsilon_0}$	$\dfrac{g_2}{g_1}\cdot\pi\dfrac{\mu_{21}^2}{\hbar^2\varepsilon_0}$	$\dfrac{g_2}{g_1}\cdot\dfrac{\pi}{3}\dfrac{\mu_{21}^2}{\hbar^2\varepsilon_0}$
A_{21}	$\dfrac{\pi}{3}\cdot\left(\dfrac{\hbar\omega^3}{\pi}c^3\right)^2\dfrac{\mu_{21}^2}{\hbar^2\varepsilon_0}$	$\pi\left(\dfrac{\hbar\omega^3}{\pi^2 c^3}\right)\dfrac{\mu_{21}^2}{\hbar^2\varepsilon_0}$	$\dfrac{\pi}{3}\cdot\left(\dfrac{\hbar\omega^3}{\pi^2 c^3}\right)\dfrac{\mu_{21}^2}{\hbar^2\varepsilon_0}$

Spontaneous transition probabilities (Einstein A coefficients) are tabulated for most atoms and ions in spectroscopic handbooks. From these tabulations, the dipole moments μ_{ab} may be readily calculated for simple systems, as shown by the correspondences in Table 3.1. However, the determination of matrix elements or transition rates that are optically induced via the interaction Hamiltonian $\bar{\mu} \cdot \bar{E}$ may involve more complicated geometric considerations. If the directions of $\bar{\mu}$ and $\bar{E}$ are fixed and known, as in the case of dopants or defects in crystals of high symmetry, then the calculation of $\langle \psi | \bar{\mu} \cdot \bar{E} | \psi \rangle$ is straightforward. More generally, however, this requires the use of the Wigner–Eckart theorem, as discussed in Chapter 4 in the context of Zeeman coherence and other phenomena.

3.6   The density matrix

Results for the probability of a transition or the value of some observable like an induced dipole moment are invariably expressed in terms of bilinear combinations of probability amplitudes like $C_2 C_2{}^*$ or $C_2 C_1{}^*$, as shown below. This is because the expectation value of any observable involves bilinear products of this type. As a consequence it is not surprising to find that, even in simple systems, one must carefully keep track of all possible bilinear combinations of probability amplitudes to describe dynamics consistently and accurately.

3.6.1   Electric dipole transition moments

The dipole moment in a two-level system has the following matrix elements:

$$e\bar{r}_{22} = \langle 2 \left| e\bar{r} \right| 2 \rangle = e \int d^3 r U_2^* (\bar{r}) \, \bar{r} U_2 (\bar{r}),$$

$$e\bar{r}_{21} = e\bar{r}_{12}^* = \langle 2 \left| e\bar{r} \right| 1 \rangle = e \int d^3 r U_2^* (\bar{r}) \, \bar{r} U_1 (\bar{r}),$$

$$e\bar{r}_{11} = \langle 1 \left| e\bar{r} \right| 1 \rangle = e \int d^3 r U_1^* (\bar{r}) \, \bar{r} U_1 (\bar{r}).$$

With a time-dependent state vector

$$|\psi (t)\rangle = C_2 \exp (-i\omega_2 t) |2\rangle + C_1 \exp (-i\omega_1 t) |1\rangle, \tag{3.6.1}$$

the expectation value of *any* operator O is

$$\langle O \rangle = \langle \psi \left| O \right| \psi \rangle = C_2 C_2^* O_{22} + C_1 C_1^* O_{11} + \{ C_2 C_1^* \exp [-i (\omega_2 - \omega_1) t] O_{12} + c.c. \} \tag{3.6.2}$$

according to Eq. (2.2.1). In a system with inversion symmetry, as we found in Section 2.2.3, all diagonal moments are 0 (i.e., $\langle 2|e\bar{r}|2\rangle = \langle 1|e\bar{r}|1\rangle = 0$). Hence the expectation value of the dipole moment operator for an electron is given by

$$\left\langle \bar{\mu}^{(e)} \right\rangle = \langle \psi \left| e\bar{r} \right| \psi \rangle = e C_2 C_1^* \exp [-i (\omega_2 - \omega_1) t] \bar{r}_{12} + c.c. \tag{3.6.3}$$

This highlights the importance of the off-diagonal bilinear combination $C_2 C_1^*$.

3.6.2   Pure case density matrix

One way of dealing systematically with the bilinear probability amplitudes like those in Eq. (3.6.3) is to organize them into a so-called density matrix ρ constructed from the expansion coefficients $c_2 = C_2 \exp(-i\omega_2 t)$ and $c_1 = C_1 \exp(-i\omega_1 t)$ using the matrix element definitions:

$$\rho_{22} \equiv c_2 c_2^*, \qquad\qquad \rho_{21} \equiv c_2 c_1^*,$$
$$\rho_{12} \equiv c_1 c_2^* = \rho_{21}^*, \qquad \rho_{11} \equiv c_1 c_1^*.$$

The explicit form of the density matrix is

$$\rho = \begin{pmatrix} c_2 c_2^* & c_2 c_1^* \\ c_1 c_2^* & c_1 c_1^* \end{pmatrix} = \begin{pmatrix} \rho_{22} & \rho_{21} \\ \rho_{12} & \rho_{11} \end{pmatrix}. \tag{3.6.4}$$

In terms of the two-level density matrix elements ρ_{ij}, the expectation value of an operator O can be expressed as

$$\langle O \rangle = (\rho_{22} O_{22} + \rho_{21} O_{12}) + (\rho_{12} O_{21} + \rho_{11} O_{11})$$
$$= \sum_i \sum_j \rho_{ij} O_{ji} = \sum_i (\rho O)_{ii}$$
$$= \text{Tr}(\rho O). \tag{3.6.5}$$

This trace of the product of the density matrix ρ and operator O, designated $\text{Tr}(\rho O)$, is the sum of diagonal matrix elements of ρO. Provided there are no diagonal (static) moments in the system, the expectation value of the electric dipole moment operator is

$$\langle e\bar{r} \rangle = \mu_{21} \rho_{12} + \mu_{12} \rho_{21}. \tag{3.6.6}$$

In virtually all atom–light interactions, we need to calculate system observables as a function of time. To follow temporal evolution, we therefore start by finding equations of motion for the amplitudes

$$c_1(t) = C_1(t) \exp(-i\omega_1 t),$$
$$c_2(t) = C_2(t) \exp(-i\omega_2 t),$$

and from these we find the equations for ρ_{ij}. In the Schrödinger picture, all the time dependence is associated with the state vector and the lower case c numbers incorporate all the time dependence, fast or slow. The wavefunction

$$\left| \psi(\bar{r}, t) \right\rangle = c_2(t) \left| U_2(\bar{r}) \right\rangle + c_1(t) \left| U_1(\bar{r}) \right\rangle \tag{3.6.7}$$

which must satisfy Schrödinger's equation

$$\frac{\partial}{\partial t} \left| \psi(t) \right\rangle = -\frac{i}{\hbar} H \left| \psi(t) \right\rangle. \tag{3.6.8}$$

From Eqs. (3.6.7) and (3.6.8) it is easily shown that

$$\dot{c}_2 = -i\omega_2 c_2 - \frac{i}{\hbar} V_{21} c_1, \tag{3.6.9}$$

$$\dot{c}_1 = -i\omega_1 c_1 - \frac{i}{\hbar} V_{12} c_2. \tag{3.6.10}$$

Hence equations of motions for individual elements of the density matrix are

$$\dot{\rho}_{22} = \dot{c}_2 c_2^* + c_2 \dot{c}_2^*$$

$$= \left(-i\omega_2 c_2 - \frac{i}{\hbar} V_{21} c_1 \right) c_2^* + c_2 \left(i\omega_2 c_2^* + \frac{i}{\hbar} V_{12} c_1^* \right)$$

$$= -\frac{i}{\hbar} V_{21} \rho_{12} + c.c., \tag{3.6.11}$$

$$\dot{\rho}_{11} = \frac{i}{\hbar} V_{21} \rho_{12} + c.c., \tag{3.6.12}$$

$$\dot{\rho}_{21} = \dot{c}_2 c_1^* + c_2 \dot{c}_1^*$$

$$= \left(-i\omega_2 c_2 - \frac{i}{\hbar} V_{21} c_1 \right) c_1^* + c_2 \left(i\omega_1 c_1^* + \frac{i}{\hbar} V_{21} c_2^* \right)$$

$$= -i\omega_0 \rho_{21} + \frac{i}{\hbar} V_{21} \left(\rho_{22} - \rho_{11} \right), \tag{3.6.13}$$

and

$$\dot{\rho}_{12} = \dot{\rho}_{21}^*, \tag{3.6.14}$$

where $\omega_0 \equiv \omega_2 - \omega_1$.

3.6.3   Mixed case density matrix

The pure case density matrix describes a single atom or molecule. However, in most real problems we have an ensemble of many similar systems to track. Typically, there are N identical systems all obeying the same equation of motion but exhibiting different phases or stages of evolution.

In the pure case we could have written

$$\rho = |\psi\rangle \langle \psi|, \tag{3.6.15}$$

since this operator expression projects out the right probability amplitudes to agree with our original definition (Eq. (3.6.4)) of ρ. By substituting Eq. (3.6.1) into Eq. (3.6.15) for example, the off-diagonal matrix element is found to be

$$\rho_{21} = \langle 2|\rho|1\rangle = \langle 2|\psi\rangle\langle\psi|1\rangle = c_2 c_1^*.$$

If only a certain fraction P_j of the atoms is in state ψ_j at time t, then for the entire ensemble we would write

$$\rho = \sum_{j=1}^{N} P_j \, |\psi_j\rangle \, \langle \psi_j| \, , \tag{3.6.16}$$

to describe a "mixed" case. That is, the system is in a mixture of pure case states. The summation can be either discrete or continuous. For example, the various ψ_j might differ only by a continuous distribution of phase angles developing in time (as in dephasing).

The important thing is that even after introducing this "statistical" aspect of an ensemble, expectation values and time dependence of the system can still be calculated the same way as before. In the case of the expectation value we find

$$\langle O \rangle = \sum_{j} P_j \, \langle \psi_j| \, O \, |\psi_j\rangle$$

$$= \sum_{j} P_j \sum_{k} \langle \psi_j| \, O \, |k\rangle \, \langle k \mid \Psi_j\rangle$$

$$= \sum_{k} \sum_{j} P_j \, \langle k \mid \Psi_j\rangle \, \langle \psi_j| \, O \, |k\rangle$$

$$= \sum_{k} \langle k| \sum_{j} P_j \, |\psi_j\rangle \, \langle \psi_j| \, O \, |k\rangle$$

$$= \sum_{k} (\rho O)_{kk} = Tr \, (\rho O). \tag{3.6.17}$$

Similarly, the equation of motion is

$$\dot{\rho} = \sum_{j} P_j \left\{ |\dot{\psi}_j\rangle\langle\psi_j| + |\psi_j\rangle\langle\dot{\psi}_j| \right\}$$

$$= -\frac{i}{\hbar} \sum_{j} P_j \left\{ H|\psi_j\rangle\langle\psi_j| - |\psi_j\rangle\langle\psi_j|H \right\}$$

$$= -\frac{i}{\hbar} \, [H, \rho] \, . \tag{3.6.18}$$

Individual matrix elements of the density matrix are therefore calculated from

$$\dot{\rho}_{ij} = -\frac{i}{\hbar} \langle i| H\rho - \rho H |j\rangle$$

$$= -\frac{i}{\hbar} \sum_{k} \left\{ \langle i \, |H| \, k\rangle \, \langle k \, |\rho| \, j\rangle - \langle i \, |\rho| \, k\rangle \, \langle k \, |H| \, j\rangle \right\}$$

$$= -\frac{i}{\hbar} \sum_{k} \left\{ H_{ik}\rho_{kj} - \rho_{ik} H_{kj} \right\}. \tag{3.6.19}$$

Since decay processes are not included in the Hamiltonian, Eq. (3.6.19) is the key formula for calculating $\rho_{ij}(t)$ to reveal population and polarization dynamics in the absence of losses. In the next section, relaxation terms are added to obtain a more general equation of motion. The significance of pure versus mixed cases is explored further in Problems in this chapter. Further discussion of the density matrix in the context of statistical mechanics may be found in Ref. [3.3].

3.7 Decay phenomena

Since the Hamiltonian in Eq. (3.6.19) is Hermitian, its eigenvalues are all real. Consequently, only lossless time-harmonic or constant temporal behavior can be described by Eq. (3.6.19). In real systems, daily experience teaches us that losses occur. To account for finite atomic lifetimes and other spontaneous relaxation processes in atoms that affect level populations we must add relaxation terms to Eq. (3.6.19), just as we did in Eqs. (3.2.21) and (3.2.22). Guided for the moment by the expectation that population of level i decays at a total rate γ_i which is twice the rate of decay of probability amplitude, we shall augment the density matrix equations to read

$$\dot{\rho}_{11} = -\gamma_1 \rho_{11} + \left[\frac{i}{\hbar} V_{21} \rho_{12} + c.c. \right], \tag{3.7.1}$$

$$\dot{\rho}_{22} = -\gamma_2 \rho_{22} - \left[\frac{i}{\hbar} V_{21} \rho_{12} + c.c. \right], \tag{3.7.2}$$

$$\dot{\rho}_{21} = -\frac{1}{2} (\gamma_2 + \gamma_1) \rho_{21} - i\omega_0 \rho_{21} + \frac{i}{\hbar} V_{21} (\rho_{22} - \rho_{11}). \tag{3.7.3}$$

This phenomenological approach to relaxation dynamics will be justified later in Sec. 6.4 on quantized reservoir theory. Eqs. (3.7.1–3.7.3) still do not account for all the interactions that strongly affect coherent optical dynamics, such as the effects of elastic collisions between atoms in a gas, or equivalently between atoms and phonons in solids. Collisions change the phase of individual probability amplitudes and therefore potentially affect diagonal and off-diagonal elements of the density matrix quite differently. This is easily confirmed by assigning time-dependent phase angles to the probability amplitudes $c_i \propto c_i(0) \exp(i\phi_i(t))$ and $c_j \propto c_j(0) \exp(i\phi_j(t))$. Then one can compare diagonal elements such as $\rho_{ii} = c_i c_i^* \propto |c_i(0)|^2$ with off-diagonal elements like $\rho_{ij} = c_i c_j* \propto c_i(0) c_j*(0) \exp(i(\phi_i(t) - \phi_j(t)))$ to recognize that a time-dependent phase term is retained only in the latter case. Since all elements of the density matrix correspond to measurable quantities, unlike the probability amplitudes themselves, phase evolution evidently plays a significant role in coherent dynamics.

To understand that the gradual loss of phase coherence between atoms (called dephasing) is a process distinct from population decay, one can consider the electromagnetic environment of Pr^{3+} ions in LaF_3 [3.4]. In isolation, these ions absorb light at a precise frequency ω_0, but in ensembles they experience random energy shifts due to crystal vibrations and other dynamic processes, such as nearby spin flips that modulate their instantaneous transition frequency (Fig. 3.7).
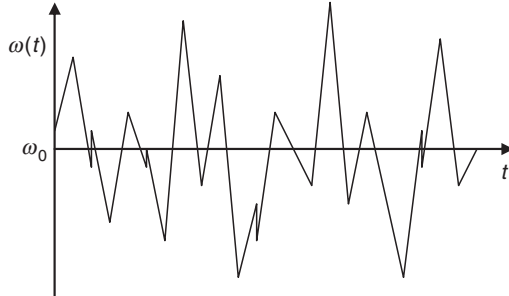
Figure 3.7 *Temporal fluctuations in the transition frequency of atoms due to dynamic changes in their environment.*

Let the time-varying transition frequency be $\omega(t)$ and its small, random frequency shift from the isolated resonance frequency be $\delta\omega(t)$. Ignoring other perturbations for the moment (i.e., setting $V_{21} = 0$ in Eq. (3.7.3)), we therefore write

$$\dot{\rho}_{21} = -\left[i\omega_0 + i\delta\omega(t) + \Gamma'_{21}\right]\rho_{21}, \tag{3.7.4}$$

where

$$\Gamma'_{21} = \frac{1}{2}(\gamma_2 + \gamma_1). \tag{3.7.5}$$

Formal integration of Eq. (3.7.4) yields

$$\rho_{21}(t) = \rho_{21}(0)\exp\left[-(i\omega_0 + \Gamma'_{21})t - i\int_0^t dt'\,\delta\omega(t')\right]. \tag{3.7.6}$$

Since all parameters except $\delta\omega(t)$ are fixed, an ensemble average only affects the final term in the argument of the exponential function in Eq. (3.7.6).

$$\left\langle \exp\left[-i\int_0^t \delta\omega(t')\,dt'\right]\right\rangle = \left\langle 1 - i\int_0^t dt_1\,\delta\omega(t_1) - \frac{1}{2}\int_0^t dt_1 \int dt_2\,\delta\omega(t_1)\,\delta\omega(t_2)\right.$$
$$\left. + \frac{(-i)^{2n}}{(2n)!}\int_0^t dt_1 \cdots \int_0^t dt_{2n}\,\delta\omega(t_1)\cdots\delta\omega(t_{2n}) + \dots\right\rangle. \tag{3.7.7}$$

Recognizing that

$$\langle\delta\omega(t)\rangle = 0, \tag{3.7.8}$$

and using a Markoff approximation for the pair correlation function, whereby frequency fluctuations at one time do not depend on prior dynamics, so that

$$\langle\delta\omega(t)\,\delta\omega(t')\rangle = 2\gamma_{\text{deph}}\delta(t - t'), \tag{3.7.9}$$

in agreement with the fluctuation–dissipation theorem, we obtain

$$\left\langle \exp\left[-i \int_0^t \delta\omega\,(t')\,dt'\right] \right\rangle = \exp\left(-\gamma_{\mathrm{deph}} t\right). \qquad (3.7.10)$$

Using Eq. (3.7.10) in Eq. (3.7.6), we find the result

$$\rho_{21}\,(t) = \rho_{21}\,(0)\exp\left[-\left(i\omega_0 + \Gamma'_{21} + \gamma_{\mathrm{deph}}\right) t\right]. \qquad (3.7.11)$$

By defining a total decay rate for dephasing according to

$$\Gamma \equiv \Gamma'_{21} + \gamma_{\mathrm{deph}} = \frac{1}{2}\left(\gamma_2 + \gamma_1\right) + \gamma_{\mathrm{deph}}, \qquad (3.7.12)$$

the equation of motion for the coherence becomes

$$\dot{\rho}_{21} = -\left(i\omega_0 + \Gamma\right)\rho_{21} + \frac{i}{\hbar}V_{21}\left(\rho_{22} - \rho_{11}\right). \qquad (3.7.13)$$

Exercise: Verify that a random frequency shift $\delta\omega << \omega$ has no effect on the level populations determined by ρ_{22} and ρ_{11}.

The phenomenological decay terms treated above include two types, differing by whether they affect the diagonal or off-diagonal elements of the density matrix. The two types are associated with population decay and polarization dephasing, respectively, and are important not only because they extend the applicability of our analysis, but together they provide overall conservation of occupation probabilities, unlike the squared amplitudes $|C_2|^2$ and $|C_1|^2$ alone. In Section 3.8 we develop a pictorial analogy, called the vector model, between the evolution of the populations and polarizations of a two-level atom and gyroscopic motion. It is useful not only for understanding all the aspects of dynamics covered so far – off-resonant excitation, Rabi flopping, population decay, and dephasing – but will later be used to picture the results of coherent interactions involving multiple pulses. The importance of even weak dephasing is illustrated by Problem 3.3.

3.8   Bloch equations

Having discussed a couple of important categories of relaxation process, and anticipating how to handle them, we now modify Eq. (3.6.19) using a phenomenological procedure that preserves the Hermitian character of H while adding decay terms to the equation of motion. The assumed form of radiative decay terms will be fully justified later in Chapter 6.

$$i\hbar\dot{\rho} = [H, \rho] + \text{relaxation terms}$$
$$= [H, \rho] \pm i\hbar\Lambda \pm i\hbar\gamma\rho - i\hbar\Gamma\rho \qquad (3.8.1)$$

In Eq. (3.8.1) we have divided relaxation terms into separate categories for incoherent pumping (Λ), radiative and non-radiative population relaxation (γ), and dephasing (Γ). Population changes due to incoherent pumping processes are particularly challenging to write down at this stage, even if energy pathways of the system are thought

to be fairly well understood. They may contribute population relaxation terms of the form $\dot{\rho}_{ii} \propto \pm i\hbar\Lambda$ in open systems where external mechanisms can add or remove population without preserving the optically excited number density. On the other hand, incoherent pumping may contribute terms of the form $\dot{\rho}_{ii} \propto \pm i\hbar\Lambda_{ij}\rho_{jj}$ in closed systems subject to thermal excitation from one level to another. Although relaxation has been introduced in a semiempirical way in Eq. (3.8.1), we shall make extensive use of this equation of motion in Chapters 4 and 5 to get started with the analysis of optical dynamics. Its form will be justified more rigorously later.

Under certain conditions, the density matrix equations of motion can be cast into a convenient form known as the optical Bloch equations, resembling equations for gyroscopic precession. The simplest version of these equations is called the vector model and illustrates that two-level atoms are analogous to spin 1/2 particles. This model provides a geometrical picture of the development of optical polarization in time, and simplifies calculations of coherent aspects of multiple pulse interactions. However, the Bloch equations originated from studies of spin magnetism and assume that diagonal and off-diagonal elements decay at similar rates. Hence, despite the visual "appeal" of the vector model, as described below, solutions of the Bloch equations should not be confused with full solutions of the density matrix.

Using the RWA, the atom–field interaction is

$$V_{21} = -\tfrac{1}{2}\mu_{21}E_0 e^{-i\omega t}, \tag{3.8.2}$$

and we introduce the slowly varying envelope approximation (SVEA) by writing

$$\rho_{21} = \tilde{\rho}_{21} e^{-i\omega t}, \tag{3.8.3}$$

where $\tilde{\rho}_{21}$ denotes the slowly varying amplitude of the matrix element ρ_{21} proportional to the amplitude of charge oscillation at the optical frequency. With the use of Eqs. (3.8.2) and (3.8.3), the equation of motion Eq. (3.7.3) becomes

$$\dot{\tilde{\rho}}_{21} = -\left[i\left(\omega_0 - \omega\right) + \Gamma\right]\tilde{\rho}_{21} - \frac{i}{2}\frac{\mu_{21}E_0}{\hbar}\left(\rho_{22} - \rho_{11}\right).$$

By defining $\Delta \equiv \omega_0 - \omega$ as the detuning of the optical frequency ω from the resonance at ω_0, one obtains

$$\left(\frac{d}{dt} + i\Delta + \Gamma\right)\tilde{\rho}_{21} = -\frac{i}{2}\Omega\left(\rho_{22} - \rho_{11}\right). \tag{3.8.4}$$

A simple, geometrical picture of system evolution emerges if we define components of a three-space vector by the real quantities

$$R_1 = \tilde{\rho}_{21} + \tilde{\rho}_{12}, \tag{3.8.5}$$

$$R_2 = -i\left(\tilde{\rho}_{21} - \tilde{\rho}_{12}\right), \tag{3.8.6}$$

$$R_3 = \rho_{22} - \rho_{11}. \tag{3.8.7}$$

These quantities vary slowly in an optical period, and because they are mutually independent can be viewed as components of the vector

$$\bar{R} = R_1 \hat{e}_1 + R_2 \hat{e}_2 + R_3 \hat{e}_3 \tag{3.8.8}$$

in a fictitious space spanned by the orthogonal basis set $(\hat{e}_1, \hat{e}_2, \hat{e}_3)$. The time development of each component is given by

$$\dot{R}_1 = \Delta R_2 - \Gamma R_1, \tag{3.8.9}$$

$$\dot{R}_2 = -\Delta R_1 - \Gamma R_2 - \Omega R_3, \tag{3.8.10}$$

$$\dot{R}_3 = -[\gamma_2 \rho_{22} - \gamma_1 \rho_{11}] + \Omega R_2. \tag{3.8.11}$$

The rate Γ is the reciprocal of the dephasing time T_2:

$$\Gamma = T_2^{-1}. \tag{3.8.12}$$

If we consider the limiting case $\Gamma = \gamma_2 = \gamma_1 = T_1^{-1} = T_2^{-1} = T^{-1}$ in Eqs. (3.8.9)–(3.8.11), we obtain

$$\dot{R}_1 = \Delta R_2 - \frac{1}{T} R_1, \tag{3.8.13}$$

$$\dot{R}_2 = -\Delta R_1 - \frac{1}{T} R_2 - \Omega R_3, \tag{3.8.14}$$

$$\dot{R}_3 = \Omega R_2 - \frac{1}{T} R_3. \tag{3.8.15}$$

Equations (3.8.13)–(3.8.15) are the optical Bloch equations. They can be written more compactly as

$$\dot{\bar{R}} = -\frac{1}{T} \bar{R} + \bar{\beta} \times \bar{R}, \tag{3.8.16}$$

where

$$\bar{\beta} = \Omega \hat{e}_1 - \Delta \hat{e}_3. \tag{3.8.17}$$

Because Eq. (3.8.16) is the equation of motion of a gyroscope, it shows that elements of the density matrix can be chosen (in the limiting case above) as components of a Bloch vector $\bar{R}$ which executes simple precession about an effective field $\bar{\beta}$ (Fig. 3.8). The length of $\bar{R}$ shrinks with time as $\exp[-t/T]$ due to decay processes.

Off-resonance, the effective field or torque vector $\bar{\beta}$ is a constant vector in the $\hat{e}_1 - \hat{e}_3$ plane in the absence of decay. In this case, a solution to Eq. (3.8.16) without the relaxation term is obtained by finding a unitary transformation which turns the Bloch vector into a constant vector. To freeze the action of the Bloch vector, we first rotate about $\hat{e}_2$ by angle α. Coordinates transform according to

$$\begin{pmatrix} x' \\ y' \\ z' \end{pmatrix} = \begin{pmatrix} \cos\alpha & 0 & \sin\alpha \\ 0 & 1 & 0 \\ -\sin\alpha & 0 & \cos\alpha \end{pmatrix} \begin{pmatrix} x \\ y \\ z \end{pmatrix},$$
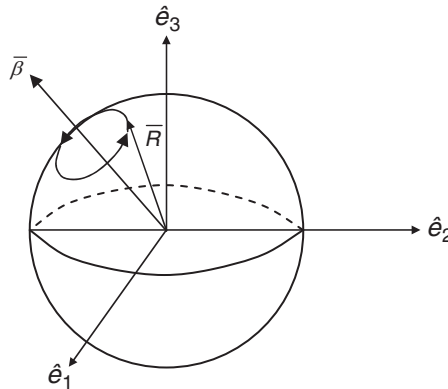
Figure 3.8 *Precessional motion of the Bloch vector $\bar{R}$ around the effective field $\bar{\beta}$. For the orientation of β that is shown, the detuning $\triangle$ is negative.*

so the Bloch vector transforms according to

$$
\begin{pmatrix} R_1 \\ R_2 \\ R_3 \end{pmatrix} = \begin{pmatrix} \cos\alpha & 0 & \sin\alpha \\ 0 & 1 & 0 \\ -\sin\alpha & 0 & \cos\alpha \end{pmatrix} \begin{pmatrix} R'_1 \\ R'_2 \\ R'_3 \end{pmatrix}. \tag{3.8.18}
$$

Exercise: Draw the direction of the effective field $\bar{\beta}$ (see Fig. 3.9) and sketch the motion of the Bloch vector $\bar{R}$ as a function of time, ignoring decay $(T = \infty)$. What is the significance of $\bar{R}$ passing periodically through the $\pm\hat{e}_3$ directions when $\Delta = 0$? What is the atomic state when $\bar{R}$ points along $\hat{e}_2$?

In this process, since the effective field $\bar{\beta}$ now lies along the new (primed) $\hat{e}_1$-axis, the Bloch vector merely executes a precession counter-clockwise about $\hat{e}'_1$. A second rotation about the $\hat{e}'_1$-axis therefore leads to a frame in which $\bar{R}$ is stationary. The
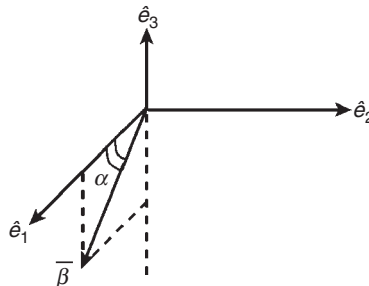
Figure 3.9 *The effective field $\bar{\beta}$ in the Bloch vector model. $\bar{\beta}$ makes an angle α with respect to the $\hat{e}_1$ -axis in the plane of basis vectors $\hat{e}_1, \hat{e}_2$ such that $\tan\alpha = \Delta/\Omega$ for positive detuning.*

rotation angle must be $\Omega_R(\Delta)t$.

$$
\begin{pmatrix} R'_1 \\ R'_2 \\ R'_3 \end{pmatrix} = \begin{pmatrix} 1 & 0 & 0 \\ 0 & \cos\Omega_R t & -\sin\Omega_R t \\ 0 & \sin\Omega_R t & \cos\Omega_R t \end{pmatrix} \begin{pmatrix} R''_1 \\ R''_2 \\ R''_3 \end{pmatrix} \tag{3.8.19}
$$

Now we can relate $\bar{R}(t)$ to $\bar{R}''$ at any time. But at $t = 0$, the Bloch vector $\bar{R}''$ is the same as the initial Bloch vector $\bar{R}(0)$ apart from a single coordinate rotation through angle α which we must "undo."

$$
\bar{R}'' = \begin{pmatrix} \cos\alpha & 0 & -\sin\alpha \\ 0 & 1 & 0 \\ \sin\alpha & 0 & \cos\alpha \end{pmatrix} \begin{pmatrix} R_1(0) \\ R_2(0) \\ R_3(0) \end{pmatrix}. \tag{3.8.20}
$$

Hence

$$
\bar{R} = \bar{\bar{U}}\bar{R}(0), \tag{3.8.21}
$$

where the evolution operator U is given by

$$
U = \begin{pmatrix} \cos\alpha & 0 & \sin\alpha \\ 0 & 1 & 0 \\ -\sin\alpha & 0 & \cos\alpha \end{pmatrix} \begin{pmatrix} 1 & 0 & 0 \\ 0 & \cos\Omega_R t & -\sin\Omega_R t \\ 0 & \sin\Omega_R t & \cos\Omega_R t \end{pmatrix} \begin{pmatrix} \cos\alpha & 0 & -\sin\alpha \\ 0 & 1 & 0 \\ \sin\alpha & 0 & \cos\alpha \end{pmatrix}.
$$

Making the assignments $\sin\alpha \equiv \Delta/\Omega_R$ and $\cos\alpha \equiv \Omega/\Omega_R$, based on the definitions $\Omega \equiv \mu E/\hbar$ and $\Omega_R \equiv \sqrt{\Delta^2 + \Omega^2}$, the final result is

$$
U = \begin{bmatrix} \dfrac{\Omega^2 + \Delta^2\cos\Omega_R t}{\Omega_R^2} & \dfrac{\Delta}{\Omega_R}\sin\Omega_R t & -\dfrac{\Delta\Omega}{\Omega_R^2}(1-\cos\Omega_R t) \\[3mm] -\dfrac{\Delta}{\Omega_R}\sin\Omega_R t & \cos\Omega_R t & -\dfrac{\Omega}{\Omega_R}\sin\Omega_R t \\[3mm] -\dfrac{\Delta\Omega}{\Omega_R^2}(1-\cos\Omega_R t) & \dfrac{\Omega}{\Omega_R}\sin\Omega_R t & \dfrac{\Delta^2 + \Omega^2\cos\Omega_R t}{\Omega_R^2} \end{bmatrix}. \tag{3.8.22}
$$

In the case of nuclear magnetic resonance, the spins precess in real space (with an $\hat{e}_3$-axis determined by the direction of the static field) about an effective magnetic field $\bar{\beta}$ consisting of the vector sum of applied static and oscillating magnetic fields. In the electric dipole or optical case considered here, there is no static field present, so the precession is not in real space. There is no fixed direction associated with the population difference $R_3 = \rho_{22} - \rho_{11}$. Nevertheless, there is a polarization axis, and in keeping with the spin analogy T_2 is called the "transverse" decay time since it

describes relaxation of transverse components of the Bloch vector. T_1 is called the "longitudinal" relaxation time since it applies to the $\hat{e}_3$ or $\hat{z}$ component.

3.9 Inhomogeneous broadening, polarization, and signal fields

The microscopic polarization induced by light in a medium is given by the expectation value of the atomic electric dipole moment in accord with Eq. (3.6.6):

$$< \mu >= \text{Tr}\,(\rho\mu) = \rho_{21}\mu_{12} + \rho_{12}\mu_{21}. \tag{3.9.1}$$

If we assume that atoms in a system are not identical, but have a distribution of resonant frequencies, due perhaps to a Maxwellian distribution of velocities or some other inhomogeneity in the system, then an ensemble average must be performed to account for this.

The resonant frequency of atom is shifted by motion according to the Doppler effect. This is a simple kinematic effect that may be readily understood in the following way. In Fig. 3.10, an atom of mass M in state E_1 moving at velocity $\bar{v}_1$ encounters a photon of momentum $\hbar\bar{k}$. After absorption of the photon, the atom is in a new internal energy state E_2 and has a new velocity $\bar{v}_2$. Conservation of energy and momentum for this interaction are described by the equations:

$$M\bar{v}_1 + \hbar\bar{k} = M\bar{v}_2, \tag{3.9.2}$$

$$E_1 + \frac{1}{2}Mv_1^2 + \hbar\omega = E_2 + \frac{1}{2}Mv_2^2. \tag{3.9.3}$$

According to Eq. (3.9.3), a stationary atom ($v_1 = 0$) absorbs very close to its resonance frequency

$$\omega_0 \equiv (E_2 - E_1)/\hbar, \tag{3.9.4}$$

because from Eq. (3.9.2) the recoil velocity v_2 of massive atoms is seen to be very small. For moving atoms however, we find upon substitution of Eqs. (3.9.4) and (3.9.2) into
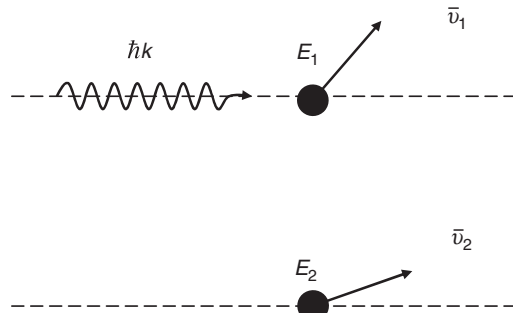

Figure 3.10 *Schematic diagram of an atom before (top) and after (bottom) interacting with a photon, illustrating the change in momentum of the atom that results from the inelastic scattering event.*

Eq. (3.9.3) that

$$\frac{1}{2}M\left(v_1^2 - v_2^2\right) + \hbar\omega = \hbar\omega_0. \tag{3.9.5}$$

If this expression is rewritten using Eq. (3.9.2) both as

$$Mv_1^2 + \hbar\bar{k}\cdot\bar{v}_1 = M\bar{v}_1\cdot\bar{v}_2, \tag{3.9.6}$$

and

$$Mv_2^2 = M\bar{v}_1\cdot\bar{v}_2 + \hbar\bar{k}\cdot\bar{v}_2, \tag{3.9.7}$$

then the energy conservation equation becomes

$$\hbar\omega_0 = \hbar\omega + \frac{1}{2}M(v_1^2 - v_2^2) = \hbar\omega + \frac{1}{2}(M\bar{v}_1\cdot\bar{v}_2 - \hbar\bar{k}\cdot\bar{v}_1) - \frac{1}{2}(M\bar{v}_1\cdot\bar{v}_2 + \hbar\bar{k}\cdot\bar{v}_2)$$

$$= \hbar\omega - \hbar\bar{v}_1\cdot\bar{k} - (\hbar^2 k^2/2M). \tag{3.9.8}$$

The second term on the right of Eq. (3.9.8) is the first-order Doppler shift, proportional to the projection of velocity on the line of sight. The third term gives the shift arising from recoil of the atom.

Taking only the Doppler shift from Eq. (3.9.8) into account, we find

$$<\mu> = \frac{1}{2}\mu_{12}<\tilde{\rho}_{21}>\exp[-i(\omega t - kz)] + c.c., \tag{3.9.9}$$

for example, where

$$<\tilde{\rho}_{21}> \equiv \frac{1}{kv\sqrt{\pi}}\int_{-\infty}^{\infty}\tilde{\rho}_{21}\exp[-(\Delta/kv)^2]d\Delta. \tag{3.9.10}$$

Here $<\tilde{\rho}_{21}>$ denotes an average over the Maxwellian molecular velocity distribution and v is the root-mean-square (rms) velocity. Hence the macroscopic polarization in a sample of molecular density N where each molecule develops an electric dipole moment $P \equiv <\mu>$ is

$$P(z,t) = Np = \frac{1}{2}N\mu_{12}<\tilde{\rho}_{21}>\exp[-i(\omega t - kz)] + c.c., \tag{3.9.11}$$

and $P(z,t)$ is the source of a signal field

$$E_s(z,t) = \frac{1}{2}E_{s0}(z,t)\exp[-i(\omega t - kz)] + c.c., \tag{3.9.12}$$

which must be calculated in a manner consistent with Maxwell's equations. That is, a signal wave emerges from the sample which must satisfy the wave equation

$$\bar{\nabla}\times\bar{\nabla}\times\bar{E} + \mu\sigma\frac{\partial\bar{E}}{\partial t} + \mu\varepsilon\frac{\partial^2\bar{E}}{\partial t^2} = -\mu\frac{\partial^2\bar{P}}{\partial t^2}. \tag{3.9.13}$$

A typical interaction problem begins by determining the atomic polarization using the Bloch or density matrix equations. Then the effects of medium polarization and propagation must be taken into account using Eq. (3.9.13). In this way, both microscopic

dynamics and macroscopic propagation effects are incorporated consistently through a coupled set of equations known as the Maxwell–Bloch equations.

As long as signal amplitude is much smaller than the incident laser field ($E_{so} << E_0$) we only need the lowest-order terms of the wave equation. In most dielectrics, $\bar{\nabla} \cdot \bar{P} = 0$, and so Eq. (3.9.13) reduces to

$$\frac{\partial^2 E}{\partial z^2} - \frac{1}{c^2}\frac{\partial^2 E}{\partial t^2} = \mu \frac{\partial^2 P}{\partial t^2}. \tag{3.9.14}$$

After substituting Eqs. (3.9.11) and (3.9.12) into this equation, using the RWA, and dropping second-order derivatives of slowly varying amplitudes, this yields

$$\left(\frac{1}{c}\frac{\partial}{\partial t} + \frac{\partial}{\partial z}\right) E_{so} = \frac{ik}{2\varepsilon} N\mu_{12} < \tilde{\rho}_{21} > . \tag{3.9.15}$$

Here, as before, it has been assumed that $\tilde{\rho}_{21}$ varies little within an optical period or an optical wavelength. This is consistent with the SVEA and (3.9.15) is the semiclassical equivalent of the classical expression (1.2.16). In the simplest case, for optically thin samples of length L, the signal field that emerges from the sample is obtained by direct integration of Eq. (3.9.15), yielding

$$E_{so} = \frac{ik}{2\varepsilon} NL\mu_{12} < \tilde{\rho}_{21} > . \tag{3.9.16}$$

In agreement with physical intuition, the signal field is proportional to sample length.

3.10 Homogeneous line-broadening through relaxation

The expression for the microscopic dipole moment on each atom is

$$p(t) = \rho_{12}\mu_{21} + \rho_{21}\mu_{12}, \tag{3.10.1}$$

and it may be compared term by term with the classical expression for the macroscopic polarization

$$P(t) = \tfrac{1}{2}\varepsilon_0 E_0 \left[\chi^{(e)}(\omega)\exp(-i\omega t) + \chi^{(e)}(-\omega)\exp(i\omega t)\right] \tag{3.10.2}$$

to relate the positive frequency component of electric susceptibility $\chi^{(e)}(\omega)$ to the off-diagonal density matrix element ρ_{21}. Since Eq. (1.2.17) shows that the atomic absorption coefficient $\alpha(\omega)$ can be found from the imaginary part of the susceptibility $\chi^{(e)}(\omega) = \chi_R(\omega) + i\chi_I(\omega)$ by $\alpha(\omega) = (\omega/c)\chi_I(\omega)$, the absorption spectrum for the case in which all the atoms are equivalent (homogeneous) can be predicted on the basis of solutions of the density matrix. According to Eq. (1.2.14) the frequency dependence of the dispersion (or refractive index) $n(\omega)$ can also be obtained from χ_R, but this is not of immediate interest here.

Let us proceed to calculate the absorption lineshape of a two-level system by solving for the off-diagonal density matrix elements and taking radiative damping, dephasing, and power broadening into account. To do this, we simply use Eq. (3.7.3) to solve for ρ_{21} which can then be substituted into Eq. (3.10.1). Having already discussed Doppler broadening, let us assume the atoms are at rest and solve the equation of motion to investigate some other spectral effects of relaxation processes.

Throughout Chapter 4 detailed solutions of the density matrix under various conditions are considered. Consequently, for the purpose of illustrating different broadening mechanisms, let us solve Eq. (3.7.3) for very short times only, by assuming that $\rho_{22} = 0$ and $\rho_{11} = 1$. One immediately obtains

$$\rho_{21} = \frac{1}{2}\Omega_{21}\exp(-i\omega t)\left\{\frac{(\omega_0 - \omega) + i\Gamma}{(\omega_0 - \omega)^2 + |\Omega_{21}|^2\,\Gamma/\gamma_2 + \Gamma^2}\right\}, \tag{3.10.3}$$

and the macroscopic susceptibility is

$$\chi^{(e)}(\omega) = \frac{N}{\varepsilon_0 \hbar}|\mu_{21}^2|\left\{\frac{(\omega_0 - \omega) + i\Gamma}{(\omega_0 - \omega)^2 + |\Omega_{21}|^2\,\Gamma/\gamma_2 + \Gamma^2}\right\}. \tag{3.10.4}$$

Notice the width of the resonance in the susceptibility in Eq. (3.10.4) is broadened by several factors. Power broadening or saturation broadening is caused by the term $\frac{\Gamma}{\gamma_2}|\frac{\bar{\mu}_{21}\cdot\bar{E}}{\hbar}|$ in the denominator, which depends on the incident field strength. The term Γ^2 describes broadening due to the total rate of dephasing. According to Eq. (3.7.12), this term therefore includes contributions due to population decay (called radiative or natural broadening) and contributions due to pure dephasing (arising from elastic collisions, phonon interactions, etc.). Power broadening, radiative decay, and pure dephasing are categorized as homogeneous broadening mechanisms, because on average each atom or optical center is affected in the same way.

The Doppler mechanism described in Section 3.9 has an effect that depends on a distinguishable property of each atom, namely its velocity. For this reason, Doppler broadening is referred to as inhomogeneous. Static crystal field broadening in solids is similar. The spectral shifts depend on "local" properties that vary from atom to atom, such as the resonant frequency. While the spectral shift arises from the atomic velocity in the case of Doppler broadening and from local variations in the internal electric field in solids, both situations cause inhomogeneous broadening.

Before leaving this topic, let us consider how a particular mechanism like Doppler broadening changes the spectral response of atoms mathematically. The Doppler effect arises when the component of velocity of an atom along the direction of propagation of light (v_z) results in a shift of its effective resonant frequency proportional to $\pm v_z/c$. The shifted resonance is at

$$\omega = \omega_0\left(1 \pm \frac{v_z}{c}\right), \tag{3.10.5}$$

where the lower (upper) signs correspond to motion parallel (antiparallel) to the wavevector of light propagating along z. To proceed we must assume a particular velocity distribution, say a Maxwellian velocity distribution, in order to determine the probability of finding an atom with absorption frequency between ω and $\omega + d\omega$. From statistical mechanics, this probability is known to be

$$\exp\left\{-Mc^2\left(\omega - \omega_0\right)^2/2\omega_0^2 k_{\mathrm{B}}T\right\}(c/\omega_0)d\omega, \tag{3.10.6}$$

where M is the mass of the atom, k_B is the Boltzmann's constant, and T is the temperature.

The inhomogeneous distribution described by Eq. (3.10.6) is Gaussian in form. This lineshape contribution will therefore be quite different from the Lorentzian one in Eq. (3.10.4), which described homogeneous broadening. In general, we can expect to encounter composite lineshapes which are convolutions of lineshapes due to several line-broadening mechanisms. For example, the composite lineshape $F(\omega)$ due to two line-broadening mechanisms described individually by $F_1(\omega)$ and $F_2(\omega)$, would be

$$F\left(\omega\right) = \int\limits_{-\infty}^{\infty} F_1\left(\nu\right)F_2\left(\omega + \omega_0 - \nu\right) d\nu. \qquad (3.10.7)$$

Any number of line-broadening mechanisms can be accounted for by repeated application of Eq. (3.10.7). The convolution of a Gaussian with a Lorentzian lineshape is called the Voigt profile (related to the error function), and unlike its two parent functions is unfortunately not integrable. Hence lineshape analysis can be quite complicated. It is for this reason that experimentalists have gone to great efforts to overcome the effects of broadening, by inventing techniques such as sub-Doppler linewidth spectroscopy. The extent of this inventiveness has been elegantly captured in Ref. [3.5].

3.11 Two-level atoms versus real atoms

Real atoms are not two-level atoms. Real atoms generally have many more energy levels than the two considered in Section 3.2. Yet, they are often remarkably well described by this simplest of all models.

The theory of absorption and dispersion based on classical harmonic oscillators for example accounts successfully for numerous optical phenomena, often by assuming the existence of a single resonance (analogous to a transition between two quantum levels). But how legitimate is such a simplified picture? Surely real atoms with complicated electronic structures need to be understood in great detail before there can be any hope of accounting for their "essential" features? This is a key concern in any new research project and an important theme of this book, which systematically steps through different aspects of optical interactions seeking to identify what approaches are indispensable in any given situation for predicting atomic and molecular dynamics when the wavefunction is not known. We therefore close this chapter by illustrating how *exact* correspondence can be achieved between experiments in a representative multilevel real atom and two-level theory of the optical interaction. This is done by considering how to convert a real sodium (Na) atom *experimentally* into a strictly two-level system (See also Ref. [3.6]).

Sodium is referred to as a "one-electron" atom, and yet it has a very complex energy level structure, as shown in Fig. 3.11. Each of its many electrons is characterized by several quantum numbers n, l, m_l and m_s. Electromagnetically inactive core electrons form "closed shells" with spectroscopic labels of the form $^{2S+1}L_J$ that specify the spin, orbit, and total angular momenta $S, L,$ and J. All these quantities are zero for electrons
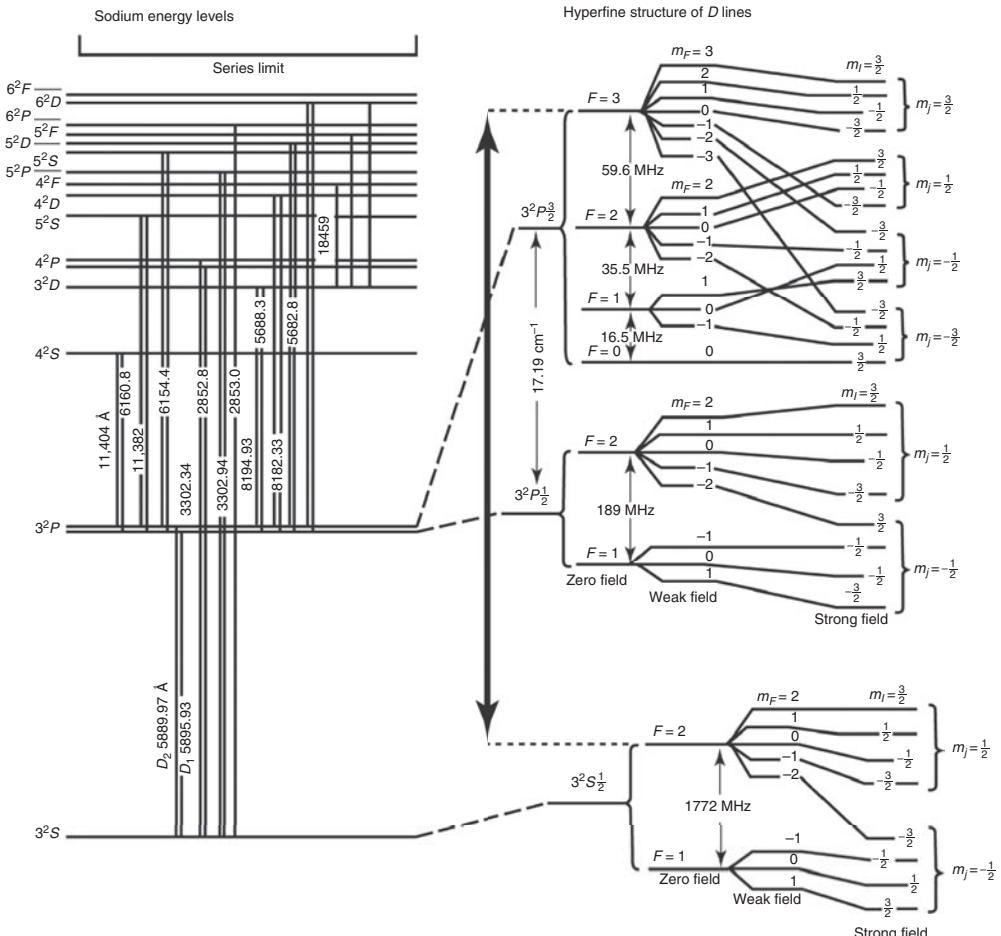
Figure 3.11 *Fine and hyperfine energy levels of the S, P, and D manifolds of Na, showing optical transitions to the left. The thick vertical arrow illustrates a transition which allows interaction of light with a closed, truly two-level system as described in the text. (After Ref. [3.7].)*

that form the closed shells. Electrons that are left over, called valence electrons, lie outside the closed shells and are responsible for electromagnetic transitions of Na in the optical range and its chemistry. So in addition to the closed shells, other states form by vector addition of the individual orbital and spin angular momenta (l_i and s_i) of valence electrons, yielding the key states for our purposes, of total angular momentum $\bar{J} = \bar{L} + \bar{S}$ in the weak-coupling, or Russell–Saunders, limit.

In Na, the closed shells comprise 10 electrons in a configuration written $1s^2 2s^2 2p^6$. The superscripts identify how many electrons occupy each nl state. In addition, there is one valence electron which occupies a $3s$ orbital in the ground state, but which may

Table 3.2: *Bandwidth associated with decay and line-broadening in Na atoms.*

Radiative lifetime

$\tau_{\mathrm{rad}}\left(^2P_{3/2}\right) = 16\,\mathrm{ns}$

$\partial\omega\,(\mathrm{FWHM}) = \frac{2}{\tau}$ (Homogeneous)

$\partial\lambda = \lambda(\partial\omega/\omega) \sim 10^{-3}\,\mathrm{nm}$

Collisional interval

$\tau_{\mathrm{coll}} \sim 10^{-7} - 10^{-8}\,\mathrm{s}$

$\partial\lambda \sim 10^{-3}\,\mathrm{nm}$ (Homogeneous)

Doppler broadening

$\partial\omega_{\mathrm{Doppler}}\,(\mathrm{FWHM}) = 2\omega\,(2\ln 2)^{1/2}\left(k_{\mathrm{B}}T/Mc^2\right)^{1/2}$ (Inhomogeneous)

$\partial\nu \sim 10\,\mathrm{GHz}\left(\sim 10^{10} - 10^{13}\,\mathrm{atoms/cm^3}\right)$

$\partial\lambda \sim 0.012\,\mathrm{nm}$

Transition interval

$\lambda_{D1} - \lambda_{D2} \sim 0.6\,\mathrm{nm}$

be promoted in principle to $4s$, $5s$, ... or $3p$, $4p$, ... or $3d$, $4d$, ... etc. by acquiring the appropriate energy. The electron spin may be "up" or "down," so the ground state has the spectroscopic designation $^2S_{1/2}$ (indicating $S = \frac{1}{2}, L = 0, J = \frac{1}{2}$). The first excited levels are $3p^2P_{3/2}$ and $3p^2P_{1/2}$, and the allowed electric dipole transitions between $3p^2P_{3/2} - 3s^2S_{1/2}$ and $3p^2P_{1/2} - 3S^2S_{1/2}$ are the Na D lines at 589.0 nm and 589.6 nm, respectively. The Na D lines are separated by 0.6 nm, but are not perfectly sharp. Collisions and the finite radiative lifetime of each level contribute to broadening. So one can ask whether it is possible to excite these transitions individually, even with perfectly monochromatic sources. That is, how do the linewidths and the separation of transitions affect experiments with real atoms? Is it possible to realize two-level atoms in practice by simply interrogating atoms with light of sufficiently narrow bandwidth that only one transition is excited, or by pulsing the light so the interaction is over before other levels can become involved?

Consider some of the characteristic timescales and bandwidths in Na vapor given in Table 3.2. From the entries in the table, it is evident that at ordinary temperatures coherent, quasi-monochromatic fields can indeed excite the D lines individually. We might be tempted to conclude that Na can therefore be treated as a two-level system. However, we have omitted important features of photon–atom interactions that invalidate this conclusion. Let us consider in more detail what is needed to make a two-level atom out of Na by accounting for spectral width of the light source (which may cause overlap of neighboring transitions) and also by recognizing that Na has additional (hyperfine) electronic structure.

Sodium has a nuclear spin of $I = 3/2$. The nuclear spin combines with each term of the total angular momentum J to produce additional levels labeled by quantum

number F which is the vector sum of J and I (hyperfine structure). Each hyperfine level is $(2F + 1)$-fold degenerate, as one can demonstrate by applying a magnetic field. Even in zero magnetic field, the width of optical excitation pulses must be carefully chosen if we are to think of Na as a two-level atom. For example, to excite only the $3P^2P_{3/2}(F = 2) \leftrightarrow 3s^2S_{1/2}(F = 1)$ transition, the spectral width of the optical pulse must not embrace the $3s^2S_{1/2}(F = 2)$ or $3p^2P_{3/2}(F = 1)$ levels. The pulsewidth must be less than 35.5 MHz ($\tau_p > 3 \times 10^{-8}$s). On the other hand, it seems that the pulse duration has to be less than the collision time ($\tau_{\text{coll}} \sim 10^{-7}$s) to avoid collisional redistribution of atoms to other states. So the required pulsewidth must lie in the range $3 \times 10^{-8}\,\text{s} < \tau_p < 10^{-7}\,\text{s}$, and even for pulse durations in this range the system could not remain a "two-level atom" for long.

Strictly speaking, even when excited with an appropriate pulsewidth on the $3P^2P_{3/2}(F = 2) \leftrightarrow 3s^2S_{1/2}(F = 1)$ transition, Na cannot be considered a two-level atom. The reason for this is that spontaneous decay is allowed from $3p^2P_{3/2}(F = 2)$ to $3s^2S_{1/2}(F = 2)$. This process cannot be avoided, and in this case removes atoms from the upper level and places them in a third state. Moreover, we still have not taken the M_F sublevels into account, which can influence the number of phased states participating in relaxation processes with or without applied magnetic fields in principle. This oversight might alter the outcome of coherent excitation of the atom, since the loss of phasing produces incoherent evolution.

In view of the discussion above, the objective to convert an atom like Na to a true two-level system would seem to be unattainable. Consider, however, what would happen if we worked instead on the transition $3^2S_{1/2}(F = 2) \leftrightarrow 3^2P_{3/2}(F = 3)$. This is the transition highlighted by the bold double-headed arrow in Fig. 3.11. In this case, spontaneous emission from the upper state is only allowed back to the same initial state ($\Delta F = 0, \pm 1$), and to no other. Consequently, our objective can be realized after all. This explains historically why this transition in Na vapor was used in successful observations of the resonance fluorescence spectrum of a truly two-level atom [3.1, 3.2]. We shall return to the analysis of this important problem in Chapter 6 when resonance fluorescence is considered in more detail.

Exercise: Is there another transition between the hyperfine manifolds of Na in Fig. 3.11 that can yield a closed two-level system?

Problems

3.1. Unpolarized radiation presents an electric field vector $\bar{E}$ whose orientation is random in time. If the transition dipole $\bar{\mu}$ driven by $\bar{E}$ has a fixed direction because the atom is situated in a crystal where the electric fields of nearby (stationary) atoms impose a fixed axis of quantization, all values of the angle θ between $\bar{E}$ and $\bar{\mu}$ are equally probable. On the other hand, for circularly polarized radiation, the argument of the $\cos\theta(t)$ factor in the scalar product $\bar{\mu} \cdot \bar{E}$ is $\theta(t) = \omega t$. Show that the first moment or average value of $\cos^2\theta$ in both cases is equal to $1/3$ in agreement with the transition rate prefactors in Table 3.1.

3.2. Just like the Hamiltonian operator of Problem 2.4, the density matrix operator for atoms in particular states may be represented by simply giving the entries for the matrix explicitly. For example, the ground state density matrix for a two-level atom is $\rho_g = \begin{bmatrix} 0 & 0 \\ 0 & 1 \end{bmatrix}$ and the excited state matrix is $\rho_e = \begin{bmatrix} 1 & 0 \\ 0 & 0 \end{bmatrix}$.

(a) Verify that these two representations are correct by calculating the occupation probabilities $\rho_{11} = \langle 1|\rho_g|1 \rangle$ and $\rho_{22} = \langle 2|\rho_e|2 \rangle$ for states 1 and 2. Thus, diagonal entries in ρ give occupation probabilities or populations of specific levels.

(b) Off-diagonal entries in ρ do not give populations. Show that $\rho_{12} = \langle 1|\psi\rangle\langle\psi|2\rangle = 0$, if $|\psi\rangle$ is an eigenstate and $\rho_{12} = \langle 1|\psi\rangle\langle\psi|2\rangle \neq 0$, if $|\psi\rangle$ is a superposition state like $|\psi\rangle = c_1|1\rangle + c_2|2\rangle$.

(c) To illustrate the difference between "pure" and "mixed" case density matrices, now consider both a single two-level atom in a superposition state described by

$$\rho_{\text{pure}} = \begin{bmatrix} \frac{1}{2} & \frac{1}{2} \\ \frac{1}{2} & \frac{1}{2} \end{bmatrix},$$
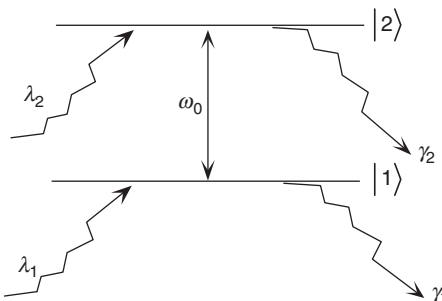
and an ensemble of such atoms at infinite temperature. Half the ensemble atoms are in the ground state and half are in the excited state, giving the matrix

$$\rho_{\text{mixed}} = \begin{bmatrix} \frac{1}{2} & 0 \\ 0 & \frac{1}{2} \end{bmatrix}.$$

Show that ρ_{pure} can be transformed using the rotation matrix $\begin{bmatrix} \cos\theta & \sin\theta \\ -\sin\theta & \cos\theta \end{bmatrix}$ to give ρ_g or ρ_e, but that it cannot be rotated to give ρ_{mixed} above. (This illustrates the fact that a single interaction with light – which causes rotations in the Hilbert space of the atom – cannot transform an entire system of independent atoms into the same state at the same time. Only operations on coherently prepared ensembles provide total system control.)

3.3. Consider a collection of N two-level atoms in which each atom is labeled by index j. The wavefunction of each atom j has a random phase factor ϕ_j, such that $y|\psi_j\rangle = C_1|1\rangle + \exp(i\phi_j)C_2|2\rangle$. The probability of atom j having any particular phase scales as $P_j = 1/N$ when ϕ_j is uniformly distributed between 0 and π.

(a) Show that $\rho_{12} = \{\sum_{j=1}^{N} P_j|\psi_j\rangle\langle\psi_j|\}_{12} = 0$ in the limit $N \to \infty$.

(b) Calculate the macroscopic polarization by inserting the atomic dipole operator into Eq. (3.6.17) to show that while a system may contain many oscillating dipoles, their relative phasing plays an important role in determining observable properties of an ensemble.

3.4. Consider a two-level atom, subjected to radiation near its resonant frequency ω_0, in which both levels undergo incoherent pumping and spontaneous decay.


(a) Write down the equations of motion for all elements of the density matrix in the Schrödinger representation.

(b) Now suppose that state $|1\rangle$ is the true ground state of the (closed) system and that state $|2\rangle$ has contributions to its population due to thermal and optical excitation from $|1\rangle$. Write down the equations of motion of ρ in this case ($\lambda_1 = 0$ and the magnitude of the thermal transition rate out of level 1 and into level 2 is $\lambda_2(\rho_{11} - \rho_{22})$.

(c) Use steady-state perturbation theory to solve the equations of part (b) for ρ_{11} and ρ_{22} to second order. What are the values of $\rho_{11} = \rho_{11}^{(0)} + \rho_{11}^{(1)} + \rho_{11}^{(2)}$ and $\rho_{22} = \rho_{22}^{(0)} + \rho_{22}^{(1)} + \rho_{22}^{(2)}$ at high intensities and do they make physical sense?

(d) Using the results of part (c), sketch absorption (proportional to the population difference) versus frequency at low intensity on an appropriate frequency scale, assuming collision broadening is negligible.
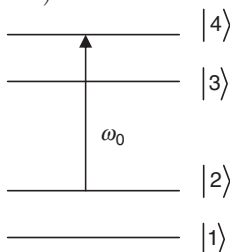
3.5. For a system with Hamiltonian $H = H_0 + V$, where V is a perturbation:

(a) Show the equations of motion of the density matrix in the Schrödinger, Interaction, and Heisenberg pictures are

$$i\hbar\dot{\rho}^{\mathrm{S}} = \left[H_0 + V, \rho^{\mathrm{S}}\right], \ \ i\hbar\dot{\rho}^{\mathrm{I}} = \left[V^{\mathrm{I}}, \rho^{\mathrm{I}}\right], \ \text{and} \ i\hbar\dot{\rho}^{\mathrm{H}} = 0.$$

(b) What can be said in general about eigenvalues and eigenfunctions of V if it is Hermitian?

(c) Not all interactions and perturbations are Hermitian. Write down the Schrödinger equation in matrix form for a four-level system subject to a Hermitian Hamiltonian H_0 and a perturbative, non-Hermitian interaction V which couples *only levels 3 and 4*. Find exact energy eigenvalues of the system in terms of matrix elements of H_0 and V using a diagonalization procedure, and compare their properties to eigenvalues of Hermitian operators.

3.6. Provide a proof that the largest magnitude to be expected for the off-diagonal density matrix element between two states is one-half.

3.7. Write down and solve (only) the equations of motion for *coherences* $\dot{\rho}_{ij}$ of a closed four-level system ($i, j = 1, 2, 3$, or 4) under steady-state conditions. The system is excited by a light field $E(t) = \frac{1}{2}E_0 \exp(i\omega t) + c.c.$ that couples only excited level $|2\rangle$ to level $|4\rangle$ via the dipole moment μ_{24} on the transition at frequency ω_0 (see figure). Assume that nonzero transition probabilities exist *between all levels* (no selection rules) and show explicitly from the equations of motion that all coherences other than that connecting levels 2 and 4 are 0 (using a method that is exact).

3.8. (*a*) Prove that in a closed two-level system, no 2×2 matrix Γ exists which correctly describes relaxation of the density matrix in the presence of dephasing and natural decay.

(*b*) Determine the nonzero elements of the four-index quantity $\Gamma_{\alpha\alpha'\beta\beta'}$ which does have sufficient dimensionality to describe these relaxation processes correctly:

$$i\hbar\dot{\rho}_{\alpha\alpha'} = [H, \rho]_{\alpha\alpha'} - i\hbar\sum_{\beta,\beta'}\Gamma_{\alpha\alpha'\beta\beta'}\rho_{\beta\beta'}.$$

The indices α, α', β, and β' can take on values 1 or 2, corresponding to the two levels of the system.
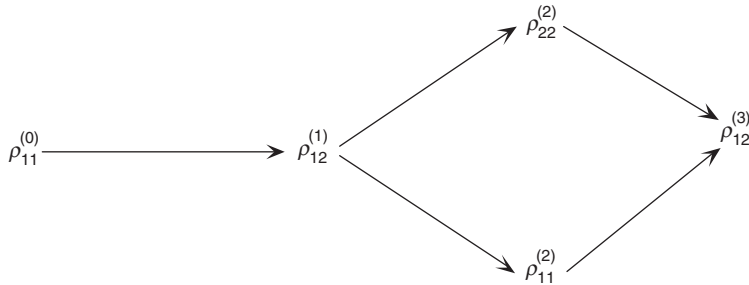
3.9. (*a*) Calculate general expressions for time-dependent elements of the density matrix ρ_{ij} of a two-level system in first-, second-, and third-order perturbation theory from the equation of motion

$$i\hbar\frac{d}{dt}\rho = [H_0, \rho] + [V, \rho] + i\hbar\left[\frac{d}{dt}\rho\right]_{\text{relaxation}}.$$

Assume V represents three weak applied light fields. In zeroth order, no light field is present, but V is distinct and nonzero for each successive order of perturbation. That is, $V^{(0)} = 0$, but $V^{(1)}, V^{(2)}, V^{(3)} \neq 0$.

(*b*) Solve these equations in the steady-state limit, assuming the system is initially in the ground state. Show that when a single field ($V = V^{(1)}$) acts on a two-levelsystem with one allowed transition ($\mu_{12} \neq 0$), new contributions to off-diagonal matrix elements ρ_{12} are generated only in odd orders of the perturbation sequence and diagonal matrix elements ρ_{11} and ρ_{22}

(populations) change only in even orders. The "perturbation chain" may therefore be pictured as
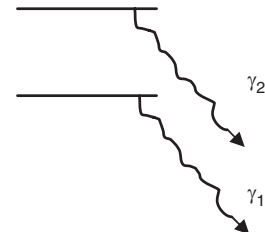

To do this, find $\rho_{12}^{(3)}$ and show that new contributions to coherence are generated in odd orders and population changes in even orders of perturbation. Note: This calculation provides valuable insight by showing that the response to a single light field proceeds first by the establishment of coherence, then a population correction which in turn modifies the coherence in third order, and so on. It tells us, for example, that to describe saturation effects (intensity-dependent absorption) we must include second-order effects. To describe intensity-dependent refractive index changes, we must go to third order since this involves a second-order effect acting on a third wave.

3.10. (*a*) Solve the damped equations of motion for an "open" two-level atom system in the interaction picture using the Rabi method and the following equations for the coefficients in the wavefunction expansion:

$$\dot{C}_2 = -\frac{1}{2}\gamma_2 C_2 + \frac{1}{2}i\Omega e^{i(\omega_0 - \omega)t}C_1$$

$$\dot{C}_1 = -\frac{1}{2}\gamma_1 C_1 + \frac{1}{2}i\Omega^* e^{-i(\omega_0 - \omega)t}C_2.$$

(*b*) Find $|C_1(t)y|^2$ and $|C_2(t)|^2$ for initial conditions $C_2(0) = 1$ and $C_1(0) = 0$ and comment on their sum (Do you find what you expect for an "open" system?).

3.11. Show that even if we consider a "closed" two-level system described by

$$\dot{C}_2 = -\frac{1}{2}\gamma_2 C_2 + \frac{1}{2}i\Omega e^{i(\omega_0 - \omega)t}C_1$$

$$\dot{C}_1 = +\frac{1}{2}\gamma_2 C_2 + \frac{1}{2}i\Omega^* e^{-i(\omega_0 - \omega)t}C_2$$

that the solution for $C_1(t)$ and $C_2(t)$ at arbitrary intensity, including the low intensity limit ($\Omega_R \to 0$), does not preserve trace. That is, despite the fact that

the initial rate of decay of state 2 equals the rate of growth of 1, we still do not obtain $|C_1(t)|^2 + |C_2(t)|^2 = 1$. (This failure of the rate equations is important motivation to retain bilinear coefficients like $C_2 C_1^*$ and $C_1 C_2^*$ in a density matrix description that does preserve trace in a consistent manner.)

3.12. To determine the spread expected in repeated measurements of the dipole moment $e\bar{r} = \mu \begin{bmatrix} 0 & 1 \\ 1 & 0 \end{bmatrix}$, one can calculate the root-mean-squared fluctuation given by $\sigma \equiv \sqrt{\langle (e\bar{r})^2 \rangle - \langle e\bar{r} \rangle^2}$.

Assuming μ is real, determine σ in terms of μ and elements of the density matrix for a two-level atom. (Hint: The angled brackets in the expression for σ indicate expectation values or means, calculated as traces of the operator with the density matrix.)

References

3.1. F. Schuda, C.R. Stroud, and M. Hercher, *J. Phys. B: Atom. Molec. Phys.* **7**, L198(1974).

3.2. R.E. Grove, F.Y. Wu, and S. Ezekiel, *Physical Review* **A 15**, 227(1977).

3.3. R. Kubo, *Statistical Mechanics*, North-Holland, London, 1965.

3.4. S.C. Rand, A. Wokaun, R.G. DeVoe, and R.G. Brewer, *Phys. Rev. Lett.* **43**, 1868(1979).

3.5. See, for example, M.D. Levenson and S. Kano, *Introduction to Nonlinear Laser Spectroscopy*, Academic Press, New York, 1988.

3.6. L. Allen and J.H. Eberly, *Optical Resonance and Two-Level Atoms*, Dover, New York, 1987.

3.7. F.J. Schuda, High Resolution Spectroscopy Using a CW Stabilized Dye Laser, PhD Dissertation, University of Rochester, 1974.

4

Transient Optical Response

Although the principal focus of subsequent chapters will be detailed calculations of steady-state response to light under various conditions, it is helpful to have a mental picture of how polarization grows, decays, and mediates transient interactions using the Bloch equations of Chapter 3. Among other things, this helps one develop a sense for what determines when dynamics should be considered "fast" or "slow." A key part of the successful analysis of dynamics in new systems lies in categorizing processes as "fast" or "slow" and deciding which quantities should be retained as time-dependent variables once the timescale of the analysis is specified.

This chapter also provides physical insight into the meaning of "dephasing" or "decoherence," and provides an easy way to introduce some surprisingly interesting coherent phenomena induced by repeated applications of pulsed applied fields. Interesting connections also exist between irreversible transient phenomena and frequency shifts, but these are deferred to a discussion in Appendix F. Finally, some limitations associated with the use of the simple Bloch vector model are noted at the end of the chapter, as a prelude to focusing on the full term-by-term density matrix treatment used in Chapters 5–7, which provides enough degrees of freedom for analytic solutions to all problems of interest.

4.1 Optical nutation

4.1.1 Optical nutation without damping

Consider what happens when atoms are suddenly exposed to light that is resonant with a ground state transition. This gives rise to a coherent transient phenomenon called nutation, which is the driven response of atoms to light illustrated in Fig. 4.1. Nutation describes the buildup of polarization caused by the application of an optical field.

Simple analytic solutions can be obtained, provided damping is ignored, even for atoms moving with a velocity v_z that modifies their detuning by the Doppler shift. The Bloch equations (Eqs. 3.8.13–3.8.15) describing evolution of the Bloch vector reduce to

$$\dot{R}_1 - \Delta R_2 = 0, \tag{4.1.1}$$

$$\dot{R}_2 + \Delta R_1 + \Omega R_3 = 0, \tag{4.1.2}$$

$$\dot{R}_3 - \Omega R_2 = 0. \tag{4.1.3}$$
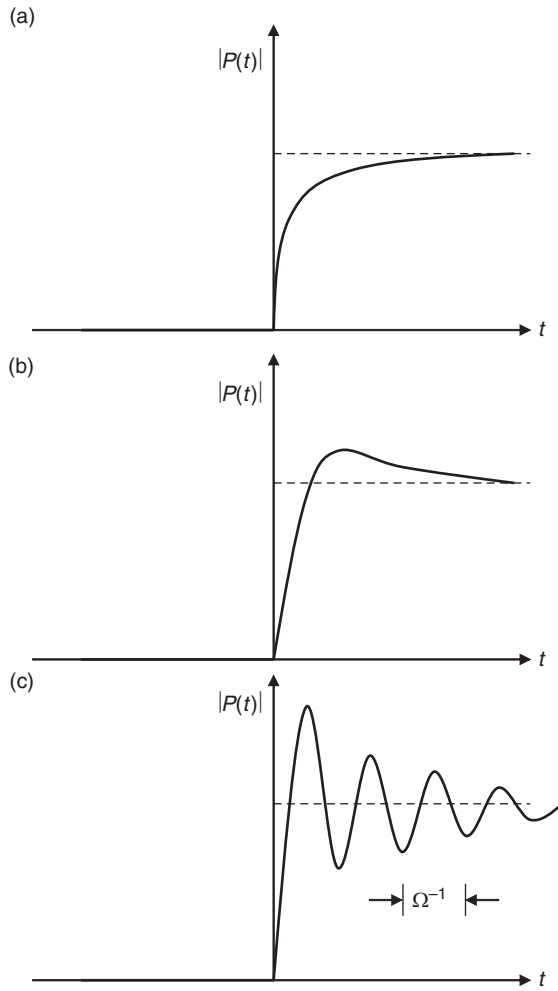
Figure 4.1 *Artist's concept of the onset of polarization due to nutation in (a) over-damped, (b) critically damped, and (c) under-damped conditions.*

For a system whose initial population distribution is described by $R_3(0)$, these equations are readily solved for $t > 0$, and give

$$R_1(t) = \frac{\Omega\Delta}{\Omega_R^2} R_3(0) \left[\cos \Omega_R t - 1\right], \tag{4.1.4}$$

$$R_2(t) = -\frac{\Omega}{\Omega_R} R_3(0) \sin \Omega_R t, \tag{4.1.5}$$

$$R_3(t) = R_3(0) \left[1 + \frac{\Omega^2}{\Omega_R^2} (\cos \Omega_R t - 1)\right], \tag{4.1.6}$$

where $\Omega_R^2 \equiv \Delta^2 + \Omega^2$, $\Delta \equiv \omega_0 - \omega - kv_z$, and $\Omega \equiv \mu_{21} E_{12}/\hbar$.

Exercise: Show that Eqs. (4.1.4)–(4.1.6) are reproduced by applying the evolution matrix in (Eq. (3.8.22)) to initial Bloch vector $\bar{R}(0) = (0, 0, R_3(0))$.

To calculate the signal field we need to evaluate the Doppler-averaged matrix element in Eq. (3.9.10)

$$
< \tilde{\rho}_{21} > = \frac{1}{kv\sqrt{\pi}} \int\limits_{-\infty}^{\infty} \frac{1}{2}(R_1 + iR_2)\exp(-[\Delta/kv]^2)d\Delta
$$

$$
= \frac{\Omega R_3(0)}{2kv\sqrt{\pi}} \int\limits_{-\infty}^{\infty} \left\{ \frac{\Delta}{\Omega_{\mathrm{R}}^2}[\cos\Omega_{\mathrm{R}}t - 1] + \frac{i}{\Omega_{\mathrm{R}}}\sin\Omega_{\mathrm{R}}t \right\} \exp(-[\Delta/kv]^2)d\Delta
$$

$$
= \frac{i\sqrt{\pi}}{2kv}\Omega R_3(0)\exp(-[\Delta_0/kv]^2)J_0(\Omega t), \tag{4.1.7}
$$

where we have assumed the excitation is tuned near (but not exactly to) the Doppler peak at $\Delta = \Delta_0$ with the consequence that the R_1 contribution is approximately zero. According to Eqs. 3.9.12 and 3.9.16, the signal field is

$$
E_{\mathrm{s}}(t) = \frac{-N\Omega L R_3(0)\sqrt{\pi}}{8\varepsilon v_0}\mu_{12}\exp(-[\Delta_0/kv]^2)J_0(\Omega t)e^{-i(\omega t - kz)} + c.c. \tag{4.1.8}
$$

The signal at the detector will exhibit a slow oscillation described by the zero-order Bessel function J_0 at frequency Ω in Eq. (4.1.8), as illustrated in Fig. 4.1c.

Notice that the amplitude of the Bloch vector given by Eqs. (4.1.4)–(4.1.6) is constant.

$$
\left|\bar{R}(t)\right| = (R_1^2(t) + R_2^2(t) + R_3^2(t))^{1/2} = R_3(0). \tag{4.1.9}
$$

Also, it precesses about the effective field vector $\bar{\beta}$ at the frequency

$$
\Omega_{\mathrm{R}} = (\Delta^2 + \Omega^2)^{1/2}. \tag{4.1.10}
$$

The motion of the Bloch vector is particularly easy to visualize for the case of exact resonance ($\Delta = 0$). The tip of the Bloch vector sweeps around a circle in the $\hat{e}_2, \hat{e}_3$ plane perpendicular to the effective field $\bar{\beta} = \Omega\hat{e}_1$. Hence, at one instant of time it points "up" along $+\hat{e}_3$ and a half period later it points "down" along $-\hat{e}_3$. This corresponds to "Rabi flopping" behavior in which a collection of atoms alternately occupies the excited state or the ground state under the influence of a resonant driving field.

The frequency of driven population oscillations is the Rabi frequency, and experimentally this may be verified by increasing or decreasing the input field as illustrated in Fig. 4.2a. When this is done, the Rabi oscillation frequency tracks the electric field linearly. On resonance, observations of the temporal oscillations (by any means that samples the excited versus ground state populations) provide a convenient way of measuring the transition dipole moment if the effective intensity of the wave is known [4.1]. With pulsed excitation, a precise number of Rabi oscillations may be induced by controlling the pulse area as illustrated in Fig. 4.2b. Measurement of the differential

(a)

(b)
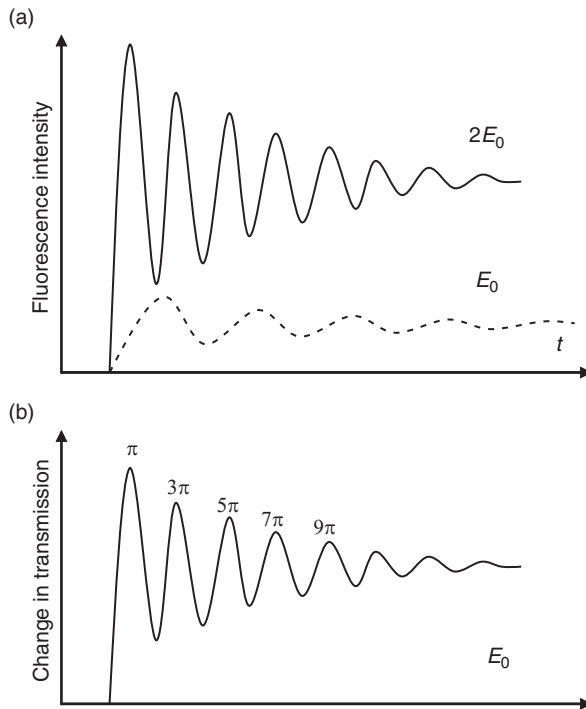
Figure 4.2 *Rabi oscillations in (a) transient fluorescence and (b) differential transmission experiments. The oscillation frequency in time-resolved experiments depends on the incident field strength. The oscillations versus power depend on the pulse area.*

transmission (described in more detail in Chapter 5) versus input power can also serve to determine the resonant Rabi frequency. This method is commonly applied in the characterization of semiconductor quantum wells and quantum dots [4.2, 4.3].

4.1.2 Optical nutation with damping

Throughout the algebraic treatment of nutation given above, population and polarization decay (T_1 and T_2 processes, respectively) were ignored. For interactions with light that are longer than the characteristic decay times, this omission is obviously unacceptable. However the Bloch equations do not yield to analysis when the decay terms are included, other than for a special case in which $T_1 = T_2$ [4.4]. This is due to the requirement that the Bloch model be based on the form of a simple gyroscopic equation of motion. Hence we shall await the density matrix methods of Chapters 5–7 which offer more degrees of freedom, and will not extend nutation analysis further here. Despite the limitations of the Bloch model, it works well for picturing the outcome of multiple pulse interactions in which the pulse durations are much shorter than the characteristic times T_1 and T_2. In Section 4.2 we shall also find that decay

processes that take place in the free precession periods between ultrafast pulses can be incorporated into this simplified analysis.

4.2 Free induction decay

Suppose a sample is resonantly excited by a laser beam until steady-state conditions are reached and then, at time $t = 0$, the excitation is suddenly switched off. After the switch, the polarization established in the sample prior to $t = 0$ continues to oscillate until contributions from different atoms get out of phase and the amplitude of the polarization drops to undetectable levels. During the time interval over which most of the atoms remain in phase with the excitation light (designated as the coherence time T_2 for historical reasons), an intense coherent beam is radiated in the forward direction. This is because the original excitation wave forced the array of atoms to oscillate in a fashion consistent with a forward-propagating beam. After the atoms lose coherence, they are said to have undergone "dephasing." The time dependence of this process is illustrated in Fig. 4.3.

Let us assume that the preparative stage ends by switching the transition frequency out of resonance with the laser frequency, in the manner of some of the earliest optical coherent transient experiments [4.5], and calculate the signal predicted by the Bloch equations. We can account for initial Boltzmann distributions of population by adding thermal source terms ρ_{11}^0 and ρ_{22}^0 to the Bloch equations of Chapter 3.

$$\dot{\rho}_{22} - \dot{\rho}_{11} = -(\rho_{22} - \rho_{11})/T_1 - i\Omega(\tilde{\rho}_{21} - \tilde{\rho}_{12}) + (\rho_{22}^0 - \rho_{11}^0)/T_1. \qquad (4.2.1)$$

In this way we obtain modified Bloch equations from Eqs. (3.8.13)–(3.8.15).

$$\dot{R}_1 = \Delta R_2 - R_1/T_2, \qquad (4.2.2)$$

$$\dot{R}_2 = -\Delta R_1 - R_2/T_2 - \Omega R_3, \qquad (4.2.3)$$

$$\dot{R}_3 = \Omega R_2 - (R_3 - R_3^0)/T_1, \qquad (4.2.4)$$

where $R_3^0 \equiv \rho_{22}^0 - \rho_{11}^0$. Since the atoms are prepared by steady-state irradiation prior to the free precession period, we require steady-state solutions of the nutation equations
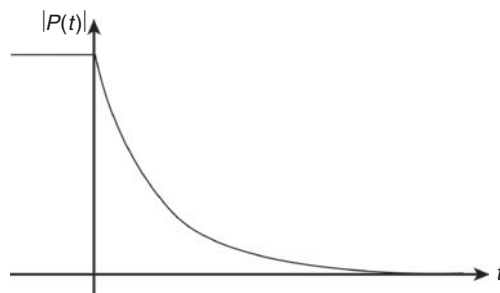
Figure 4.3 *Decay of the amplitude of optical polarization after the excitation is switched off at time $t = 0$.*

to determine the initial conditions for the free precession which begins at $t = 0$. These are found by setting time derivatives in Eqs. (4.2.2)–(4.2.4) equal to zero.

$$R_1(0) = -\Delta\Omega R_3^0 / \left(\Omega^2 T_1/T_2 + \Delta^2 + 1/T_2^2\right), \tag{4.2.5}$$

$$R_2(0) = -\left(\Omega R_3^0/T_2\right) / \left(\Omega^2 T_1/T_2 + \Delta^2 + 1/T_2^2\right), \tag{4.2.6}$$

$$R_3(0) = R_3^0 \left[(\Delta^2 + 1/T_2^2)/(\Omega^2 T_1/T_2 + \Delta^2 + 1/T_2^2)\right]. \tag{4.2.7}$$

At $t = 0$, the transition frequency is shifted instantaneously by a small amount $\delta\omega_{21}$. Hence the detuning changes to the new value,

$$\Delta' = \Delta + \delta\omega, \tag{4.2.8}$$

and the field is suddenly far out of resonance with the original set of atoms. This is equivalent to setting the field amplitude to zero. That is, $\Omega = 0$ for $t \geq 0$. The Bloch equations therefore assume the form

$$\dot{R}_1 - \Delta R_2 + R_1/T_2 = 0, \tag{4.2.9}$$

$$\dot{R}_2 + \Delta R_1 + R_2/T_2 = 0, \tag{4.2.10}$$

$$\dot{R}_3 + (R_3 - R_3^0)/T_1 = 0. \tag{4.2.11}$$

The solution of Eq. (4.2.11) may be guessed immediately.

$$R_3(t) = R_3^0 + \left[R_3(0) - R_3^0\right]\exp(-t/T_1). \tag{4.2.12}$$

Solutions of Eqs. (4.2.9) and (4.2.10) may be readily obtained by Laplace transform techniques.

$$R_2(t) = [-R_1(0)\sin\Delta t + R_2(0)\cos\Delta t]\exp(-t/T_2), \tag{4.2.13}$$

$$R_1(t) = [R_1(0)\cos\Delta t + R_2(0)\sin\Delta t]\exp(-t/T_2). \tag{4.2.14}$$

Equations (4.2.12)–(4.2.14) determine the motion of the Bloch vector $\bar{R}(t) = (R_1, R_2, R_3)$ in the absence of light, including "longitudinal" (population) and "transverse" (polarization) decay processes.

Exercise: Show that the evolution matrix for free precession that reproduces Eqs. (4.2.12)–(4.2.14) is

$$U_{\mathrm{FID}}(t) = \begin{bmatrix} \exp(-t/T_2)\cos\Delta t & \exp(-t/T_2)\sin\Delta t & 0 \\ -\exp(-t/T_2)\sin\Delta t & \exp(-t/T_2)\cos\Delta t & 0 \\ 0 & 0 & \exp(-t/T_1) \end{bmatrix}, \tag{4.2.15}$$

and that it is identical (apart from the decay factors) to that derivable from Eq. (3.8.22).

To find the sample polarization and signal field we next use Eqs. (3.9.11) and (3.9.16), respectively.

$$< \tilde{\rho}_{21} > = \frac{i\sqrt{\pi}}{2kv} \Omega R_3^0 \exp\left[-(\Delta_0/kv)^2\right] \left(\frac{1}{\sqrt{1+\Omega^2 T_1 T_2}} - 1\right)$$

$$\times \exp[i\delta\omega t] \exp\left[-\left(1 + \sqrt{1+\Omega^2 T_1 T_2}\right) t/T_2\right] \tag{4.2.16}$$

We have assumed that the excitation is centered at a detuning of $\Delta = \Delta_0$ near the Doppler peak and that the bandwidth of the excitation is narrow compared to the Doppler width $\sim kv$ so that the Gaussian factor may be removed from the integral. The amplitude of the signal field generated by this induced polarization is

$$E_{so} = (ik/2\varepsilon)NL\mu_{12} < \tilde{\rho}_{21} >, \tag{4.2.17}$$

provided the sample is "optically thin." For a sample to be optically thin, the length L traversed by the incident beam must be less than the inverse absorption length $(\alpha L < 1)$. The Doppler integral in (3.9.10) can also be evaluated exactly [4.6].

In the forward direction, the total field including the switched laser field is

$$E_{\mathrm{T}} = \frac{1}{2}(E_{so}\exp(-i[\omega t - kz]) + c.c.) + \frac{1}{2}E_0\exp(-i[\omega' t - kz])) + c.c. \tag{4.2.18}$$

The intensity, therefore, contains a cross term or beat signal contribution

$$|E_{\mathrm{T}}|_{\mathrm{beat}}^2 = \frac{1}{4}E_0^* E_{so}\exp(i\delta\omega t) + c.c., \tag{4.2.19}$$

where the signal field amplitude is

$$E_{so} = \frac{\sqrt{\pi}NL\mu_{12}^2 E_0 R_3^{(0)}}{4\varepsilon v\hbar} \left(\frac{1}{\sqrt{1+\Omega^2 T_1 T_2}} - 1\right) \exp[-(\Delta_0/kv)^2]$$

$$\times \exp\left[-\left(1 + \sqrt{1+\Omega^2 T_1 T_2}\right) t/T_2\right]. \tag{4.2.20}$$

The measured heterodyne signal intensity at the beat frequency is given by

$$I_s(t) \propto \mathrm{Re}\left\{|E_{\mathrm{T}}|_{\mathrm{beat}}^2\right\}, \tag{4.2.21}$$

and decays exponentially in time with an effective decay constant

$$\tau = T_2 \Big/ \left(1 + \sqrt{1+\Omega^2 T_1 T_2}\right). \tag{4.2.22}$$

Exercise: At what intensity does power-broadening result in effective decay constants of (a) $\tau = T_2/2$, and (b) $\tau = T_2/4$?

Apparatus suitable for observing coherent transients by fast frequency-switching of lasers is illustrated in Fig. 4.4. In the absence of power broadening, observations of free induction decay (FID) behavior furnish the homogeneous decay time T_2 and yield a measurement of the natural lifetime of the upper state in dielectric materials. In semiconductors, as a counterexample, the decay rate for recombination of electrons and holes is affected by the availability of final valence states, and consequently is
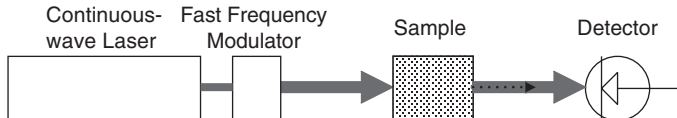
Figure 4.4 *A simple apparatus for coherent transient experimentation. The transmitted pump beam at the switched frequency (solid arrow) and the polarization established at the initial frequency prior to switching the frequency (dashed arrow) produce a heterodyne beat at the detector. The demodulated signal intensity is proportional to polarization amplitude.*

not purely a measure of an excited state property. Also, at intensities approaching saturation it is not precisely the homogeneous linewidth that is measured, but a power-broadened value. In the time domain, decay time measurements then determine the effective decay constant τ given by Eq. (4.2.22). Since Ω^2 is proportional to optical intensity, the pure dephasing time T_2 must in general be inferred from extrapolations of decay time measurements to zero intensity. If the preparatory pulse period is shorter than T_2, a distribution of atoms with Doppler shifts covering a bandwidth in excess of T_2^{-1} will also be excited. Consequently, the use of ultrashort preparation pulses results in apparent decay rates as high as $(T_2^*)^{-1}$, where $(T_2^*)^{-1}$ reflects the inhomogeneous rather than the homogeneous width of the transition.

A time-resolved FID signal observed by frequency switching [4.7] is illustrated in Fig. 4.5. The dephasing time T_2 is obtained by fitting the exponential decay of the envelope of polarization signal oscillations. The time it takes the signal intensity to fall to $1/e$ of its initial value yields a measurement of $T_2/2$ in heterodyne-detected
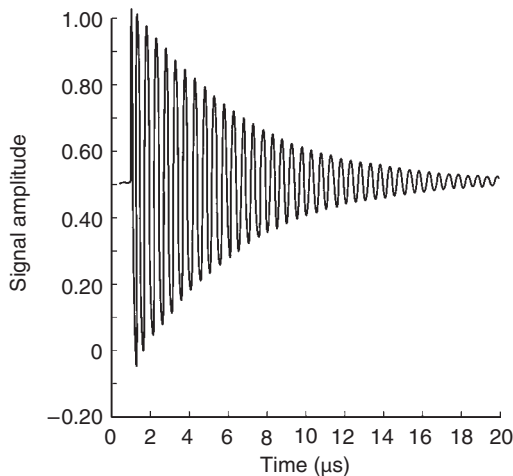
Figure 4.5 *An illustration of polarization decay observed in a heterodyne-detected free induction decay (FID) experiment in Pr^{3+} :LaF_3. The oscillations in the figure occur at the difference frequency $\nu_2 - \nu_1$ between the optical polarization established by the excitation laser (ν_2) prior to the frequency switch and the heterodyne reference frequency (ν_1). (After Ref. 4.7.)*
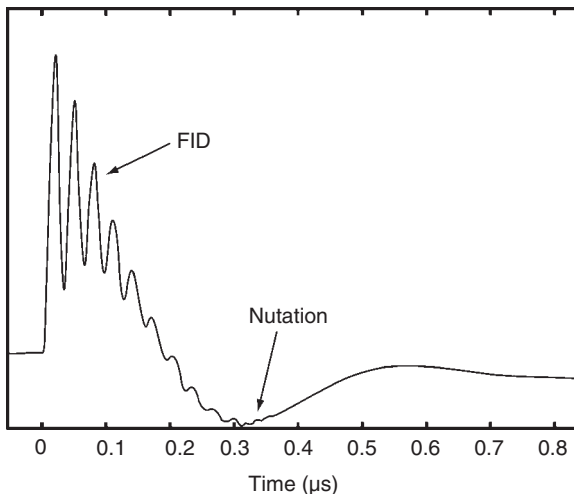
Figure 4.6 *Free induction decay (FID) and optical nutation signals observed simultaneously in iodine vapor by frequency switching. The FID oscillation frequency depends on the local oscillator frequency whereas the nutation oscillates at the resonant Rabi frequency which is intensity-dependent. (After Ref. 4.8.)*

experiments of this type, when the preparation time exceeds T_2. To avoid inaccuracies due to power broadening, the measurements must be extrapolated to zero power ($\Omega = 0$), according to Eq. (4.2.22).

When frequency switching is used to observe coherent transients, it sometimes happens that the frequency shift is insufficient to tune the laser completely off resonance during the free precession period. In this case, the laser shifts into resonance with a new packet of atoms that undergo nutation. Consequently, FID of one group and nutation of a second group of atoms may be observed simultaneously [4.8]. An example of this is shown in Fig. 4.6.

4.3   Photon echoes

Systems of atoms and molecules can be pulse-excited in at least three different ways. First, the amplitude of the excitation field can assume the form of pulses, as in the original experiments [4.9], or it can simply be switched on and off. Alternatively, the energy levels of the system may be shifted in and out of resonance with a fixed frequency field (e.g., by applying Stark switching pulses to the sample). Finally, the frequency of the excitation field can be switched in and out of resonance while the optical field amplitude and the sample resonant frequencies are held constant. The net effect is similar in all cases.

In Fig. 4.7, the optical intensity is assumed to be controlled with a fast modulator such as that shown in Fig. 4.4, or by some other means, so that the optical field is constant during the desired pulse periods and zero otherwise. For the two-pulse sequence shown in the figure, let us proceed to calculate Bloch vector dynamics during the
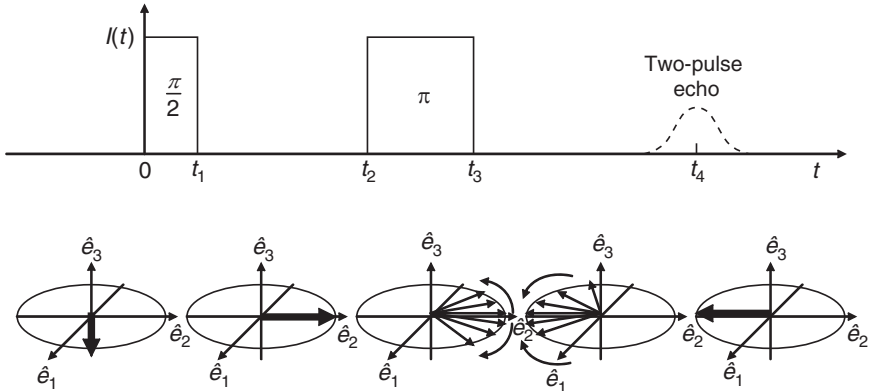
Figure 4.7 *Schematic diagram indicating how a photon echo polarization is formed. The echo results from rephasing of microscopic dipoles after a two-pulse sequence ($\pi/2 - \pi$) which reverses dephasing through a $180°$ rotation in spin space.*

various time periods when conditions are fixed. For purposes of illustration, this will be done using three different approaches: algebraic analysis, rotation matrix analysis, and a more formal density matrix operator method.

4.3.1   Algebraic echo analysis

$0 < t < t_1$

For sufficiently brief pulses ($t_1 << T_1, T_2$) no relaxation occurs during the applied pulse. As a consequence, relaxation terms in the optical Bloch equations may be dropped to obtain simplified equations during the first time period.

$$\dot{R}_1 - \Delta R_2 = 0, \tag{4.3.1}$$

$$\dot{R}_2 + \Delta R_1 + \Omega R_3 = 0, \tag{4.3.2}$$

$$\dot{R}_3 - \Omega R_2 = 0. \tag{4.3.3}$$

The solutions subject to the initial condition $R(0) = (0, 0, R_3(0))$ are

$$R_1(t_1) = \frac{\Delta \Omega R_3(0)}{\Omega_{\mathrm{R}}^2} \left(\cos \Omega_{\mathrm{R}} t_1 - 1 \right), \tag{4.3.4}$$

$$R_2(t_1) = -\frac{\Omega R_3(0)}{\Omega_{\mathrm{R}}} \sin \Omega_{\mathrm{R}} t_1, \tag{4.3.5}$$

$$R_3(t_1) = R_3(0) + \frac{\Omega^2 R_3(0)}{\Omega_{\mathrm{R}}^2} \left(\cos \Omega_{\mathrm{R}} t_1 - 1 \right). \tag{4.3.6}$$

Equations (4.3.4)–(4.3.6) are identical to the earlier results for nutation without damping.

$t_1 < t < t_2.$

Between pulses the field is off (Fig. 4.7). During this interval we set $\Omega = 0$ to solve the Bloch equations, simplified here by arbitrarily setting $R_3^0 = 0$. Note that if a different experimental approach is used, for example if the sample were switched sufficiently far out of resonance that the optical interaction stops during this period, one can still account for this using the same substitution $\Omega = 0$. The optical Bloch equations then reduce to

$$\dot{R}_1 - \Delta R_2 + R_1/T_2 = 0, \tag{4.3.7}$$

$$\dot{R}_2 + \Delta R_1 + R_2/T_2 = 0, \tag{4.3.8}$$

$$\dot{R}_3 + R_3/T_1 = 0. \tag{4.3.9}$$

The solutions to these equations are of course FID solutions given by Eqs. (4.2.12)–(4.2.14) with the time origin shifted to t_1.

$$R_1(t_2) = [R_1(t_1)\cos\Delta(t_2 - t_1) + R_2(t_1)\sin\Delta(t_2 - t_1)]\exp(-[t_2 - t_1]/T_2), \tag{4.3.10}$$

$$R_2(t_2) = [-R_1(t_1)\sin\Delta(t_2 - t_1) + R_2(t_1)\cos\Delta(t_2 - t_1)]\exp(-[t_2 - t_1]/T_2), \tag{4.3.11}$$

$$R_3(t_2) = R_3(t_1)\exp(-[t_2 - t_1]/T_1). \tag{4.3.12}$$

The appearance of t_1 as the time origin in these expressions is just the consequence of the new initial condition:

$$R(t_1) = (R_1(t_1), R_2(t_1), R_3(t_1)). \tag{4.3.13}$$

During the second pulse the solutions are again given by the solutions for nutation without damping. However, the initial condition is

$$R(t_2) = (R_1(t_2), R_2(t_2), R_3(t_2)). \tag{4.3.14}$$

Therefore at $t = t_3$ we find

$$R_1(t_3) = R_1(t_2) + \frac{\Delta R_2(t_2)}{\Omega_{\mathrm{R}}}\sin\Omega_{\mathrm{R}}(t_3 - t_2) + \frac{\Delta^2 R_1(t_2)}{\Omega_{\mathrm{R}}^2}[\cos\Omega_{\mathrm{R}}(t_3 - t_2) - 1]$$

$$+ \frac{\Delta\Omega R_3(t_2)}{\Omega_{\mathrm{R}}^2}[\cos\Omega_{\mathrm{R}}(t_3 - t_2) - 1], \tag{4.3.15}$$

$$R_2(t_3) = R_2(t_2)\cos\Omega_{\mathrm{R}}(t_3 - t_2) - [\Delta R_1(t_2) + \Omega R_3(t_2)]\frac{\sin\Omega_{\mathrm{R}}(t_3 - t_2)}{\Omega_{\mathrm{R}}}, \tag{4.3.16}$$

$$R_3(t_3) = R_3(t_2) + \Omega R_2(t_2)\frac{\sin\Omega_{\mathrm{R}}(t_3 - t_2)}{\Omega_{\mathrm{R}}}$$

$$+ [\Delta\Omega R_1(t_2) + \Omega^2 R_3(t_2)]\frac{\cos\Omega_{\mathrm{R}}(t_3 - t_2) - 1}{\Omega_{\mathrm{R}}^2}. \tag{4.3.17}$$

It is convenient to define a quantity at this point called the pulse "area," related to the time integral of the effective light field.

$$\theta(z) = \int\limits_{-\infty}^{\infty} \Omega_R(z,t)\,dt, \quad \Delta \neq 0$$

$$= \int\limits_{-\infty}^{\infty} \frac{\mu_{21} E_{12}(z,t)}{\hbar}\,dt, \quad \Delta = 0. \tag{4.3.18}$$

Adopting definitions of pulse areas for specific time intervals as

$$\theta_{10} = \sqrt{\Omega^2 + \Delta^2}\,(t_1 - t_0) = \Omega_R t_1, \tag{4.3.19}$$

$$\theta_{32} = \sqrt{\Omega^2 + \Delta^2}\,(t_3 - t_2) = \Omega_R\,(t_3 - t_2), \tag{4.3.20}$$

the algebraic solutions become

$$R_1\,(t_3) = R_1\,(t_2) + \frac{\Delta}{\Omega_R} R_2\,(t_2) \sin\theta_{32}$$

$$- \frac{2\Delta}{\Omega_R^2} \left[\Delta R_1\,(t_2) + \Omega R_3\,(t_2)\right] \sin^2\left(\frac{\theta_{32}}{2}\right), \tag{4.3.21}$$

$$R_2\,(t_3) = R_2\,(t_2) \cos\theta_{32} - \frac{1}{\Omega_R} \left[\Delta R_1\,(t_2) + \Omega R_3\,(t_2)\right] \sin\theta_{32}, \tag{4.3.22}$$

$$R_3\,(t_3) = R_3\,(t_2) + \frac{\Omega}{\Omega_R} R_2\,(t_2) \sin\theta_{32}$$

$$- \frac{2\Omega}{\Omega_R^2} \left[\Delta R_1\,(t_2) + \Omega R_3\,(t_2)\right] \sin^2\left(\frac{\theta_{32}}{2}\right), \tag{4.3.23}$$

by making use of the equality $(\cos\theta_{32} - 1) = -2\sin^2(\theta_{32}/2)$.

$\boxed{t \geq t_3}$

The period following application of the second pulse is described by FID solutions once again. The appropriate expressions are

$$R_1\,(t) = [R_1\,(t_3) \cos\Delta\,(t - t_3) + R_2\,(t_3) \sin\Delta\,(t - t_3)] \exp(-[t - t_3]/T_2), \tag{4.3.24}$$

$$R_2\,(t) = [-R_1\,(t_3) \sin\Delta\,(t - t_3) + R_2\,(t_3) \cos\Delta\,(t - t_3)] \exp(-[t - t_3]/T_2), \tag{4.3.25}$$

$$R_3\,(t) = R_3\,(t_3) \exp(-[t - t_3]/T_2). \tag{4.3.26}$$

By using the prior solutions for $R_1(t_3)$, $R_2(t_3)$, and $R_3(t_3)$ in Eqs. (4.3.24)–(4.3.26) we obtain the Bloch vector $R(t)$ for the time period $t > t_3$ after application of the

pulses, in terms of the initial conditions. To calculate the radiant polarization during this period, we need only the transverse components of the Bloch vector $R_1(t)$ and $R_2(t)$. They contain the factor

$$\cos \Delta (t - t_3) \cos \Delta (t_2 - t_1) \sin \Delta (t - t_3) \sin \Delta (t_2 - t_1) = \cos \Delta (t - 2\tau), \quad (4.3.27)$$

which is nonzero at time $t = 2\tau \equiv t_3 + t_2 - t_1$. These terms are responsible for the sudden appearance of radiative sample polarization at time $t = 2\tau$, since the Doppler phase vanishes. This rephasing of the polarizations of individual atoms at a time τ after the application of two pulses separated by an interval τ is called a photon echo. The polarization created by the first pulse is reestablished by the second pulse after a short delay equal to interval τ.

Other terms in the Bloch vector such as $\sin \Delta(t - 2\tau)$ are 0 at $t = 2\tau$ or do not rephase and need not be considered further. Echo terms in $R_1(t)$ are odd functions of Δ. Hence if we assume the optical excitation is tuned near the Doppler peak, which is represented by an even function of Δ, the Doppler-averaged R_1 component will be $< R_1(t) > \sim 0$. Consequently, the polarization reduces to

$$< \tilde{\rho}_{21}(t) > = \frac{i}{2} < R_2(t) >, \quad (4.3.28)$$

and the photon echo signal amplitude will be

$$E_{so}(L, t) = -kNL\mu_{21}R_2/4\varepsilon. \quad (4.3.29)$$

If the signal field is measured by heterodyne detection, as described in our earlier calculation of FID, the intensity contains a beat note.

$$|E_{\mathrm{T}}|^2_{\mathrm{beat}} = \frac{1}{4}E_0 E_{so}^* + c.c.$$

$$= \frac{\hbar kNL\Omega^4}{8\varepsilon\Omega_{\mathrm{R}}^3} R_3(0) e^{-t/T_2} \cos[\delta\omega (t - 2\tau)]$$

$$\times \left\langle \sin \theta_{10} \sin^2 \left(\frac{\theta_{32}}{2} \right) \cos[\Delta(t - 2\tau)] \right\rangle. \quad (4.3.30)$$

The signal reaches a maximum value at $t = 2\tau$ given by

$$|E_{\mathrm{T}}|^2_{\mathrm{beat}} = \frac{\hbar kNL\Omega^4}{8\varepsilon\Omega_{\mathrm{R}}^3} R_3(0) e^{-t/T_2} \left\langle \sin \theta_{10} \sin^2 \left(\frac{\theta_{32}}{2} \right) \right\rangle. \quad (4.3.31)$$

The echo envelope decays with a time constant T_2 and the signal will be largest for pulse areas $\theta_{10} = \pi/2$ and $\theta_{32} = \pi$. When optimized in this way, the input pulses are referred to as forming a $\frac{\pi}{2} - \pi$ sequence. An example of echo signals observed by heterodyne detection is given in Fig. 4.8 (see Ref. [4.10]).

Exercise: Calculate the envelope decay times for FID and the photon echo when the signals are detected directly as $|E_{so}|^2$ instead of by heterodyning as $E_0 E_{so}^* + c.c.$
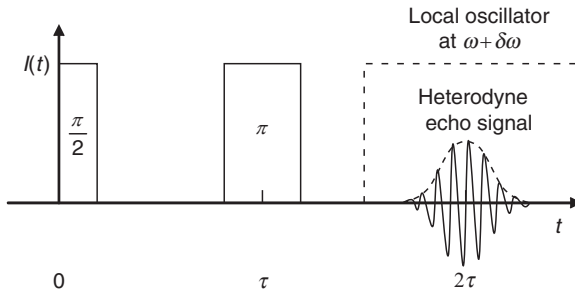
Figure 4.8 *Illustration of photon echoes detected by overlap of a local oscillator with the echo signal at the detector. The rapid oscillations within the echo pulse envelope reflect the heterodyne frequency difference between the oscillator ($\omega + \delta\omega$) and echo (ω) frequencies (see Ref. [4.10]).*

Photon echoes may also be excited using pulsed output obtained directly from appropriate laser sources. In this case, beam splitters and adjustable mechanical delay lines are typically used to provide the desired two-pulse sequence as shown schematically in Fig. 4.9. Pulse bandwidth may be sufficient to overlap more than one transition in such cases. The beating of multiple transitions then modulates the echo amplitude, furnishing a way to measure small differences in the transition frequencies. For example, by Fourier transforming the modulated echo envelope, energy-level spacings can be inferred for the emitting centers [4.11, 4.12]. Whenever echo experiments are performed with angled beams, the direction of propagation of the signal beam must be determined by considering conservation of linear momentum in the coherent interaction, in order to know exactly where to place the detector. This consideration relates to the need for "phase-matching" in photon echo observation, a topic considered in a little more detail in Section 5.4.1 on four-wave mixing in Chapter 5. Photon echoes are most commonly recorded as echo signal intensity versus inter-pulse delay. However if frequency-switching techniques are used, heterodyne detection can be applied to
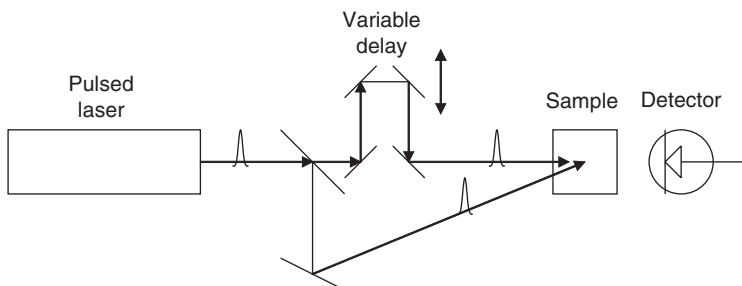
Figure 4.9 *Schematic diagram of a photon echo experiment based on a pulsed laser source. The detector is assumed to be placed in the direction of the phase-matched output determined by conservation of photon linear momentum.*

advantage by providing a reference field at the expected time of the echo, as depicted in Fig. 4.8.

4.3.2 Rotation matrix analysis

A rotation matrix approach to analyzing Bloch vector evolution was developed in Chapter 3. The general form for the overall rotation matrix applicable to a time interval characterized by constant (but arbitrary) conditions was given by Eq. (3.8.22). To describe multiple pulse excitation of a system, we now need to combine the two specific forms of the general rotation matrix U that apply to nutation and FID periods.

Exercise:

(a) By ignoring decay during pulses and assuming strong, nearly resonant excitation for which $(\Delta/\Omega_R) << 1$, show that the rotation matrices $U_{\text{pulse}}(t_1, t_0)$ and $U_{\text{FID}}(t_2, t_1)$ for nutation and FID respectively over the specific time intervals t_0 to t_1 and t_1 to t_2 are

$$U_{\text{pulse}}(t_1, t_0) = \begin{bmatrix} 1 & 0 & 0 \\ 0 & \cos[\Omega_R(t_1 - t_0)] & \sin[\Omega_R(t_1 - t_0)] \\ 0 & \sin[\Omega_R(t_1 - t_0)] & \cos[\Omega_R(t_1 - t_0)] \end{bmatrix}, \qquad (4.3.32)$$

$$U_{\text{FID}}(t_2, t_1) = \begin{bmatrix} \cos[\Delta(t_2 - t_1)] & -\sin[\Delta(t_2 - t_1)] & 0 \\ \sin[\Delta(t_2 - t_1)] & \cos[\Delta(t_2 - t_1)] & 0 \\ 0 & 0 & 1 \end{bmatrix}. \qquad (4.3.33)$$

(b) For a two-pulse sequence, show evolution of the Bloch vector is described by

$$\bar{R}(t) = U(t, t_0)\bar{R}(0) = U_{\text{FID}}(t, t_3)U_{\text{pulse}}(t_3, t_2)U_{\text{FID}}(t_2, t_1)U_{\text{pulse}}(t_1, t_0)\bar{R}(0), \qquad (4.3.34)$$

and show by matrix multiplication that the Bloch vector component $R_2(t)$, and consequently the echo polarization, exhibits the same dependence on pulse areas and inter-pulse delay as determined algebraically in Eq. (4.3.30).

In Fig. 4.10, the results from three different pulsed optical experiments in methyl fluoride are compared. The upper trace shows that, contrary to the calculation of Eq. (4.3.31), echo amplitude obtained using a Carr–Purcell [4.13–4.14] sequence of pulses $(\pi/2, \pi, \pi, \pi, \ldots)$ decays exponentially with a characteristic time that equals the population decay time T_1 rather than T_2. The results of delayed nutation shown in the same figure also have a characteristic time of T_1. In delayed nutation the recovery of probe absorption is monitored versus delay time, so that population decay is expected to govern this type of transient. However, the Carr–Purcell results present an unexpected example of how multiple-pulse sequences can measure decay processes other than pure dephasing. By repeatedly reversing the dephasing process using π-pulses, dephasing effects can be avoided altogether. This leaves only population decay to account for relaxation of the system. Further discussion of this point can be found
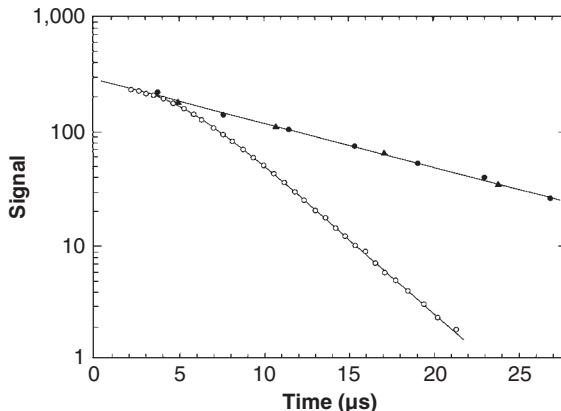
Figure 4.10 *Comparison of two-pulse echo signals with nutation and multiple-pulse (Carr–Purcell) echo results in* $^{13}CH_3F$. *Two-pulse echoes are sensitive to phase-changing collisions and measure* T_2. *Nutation and multiple-pulse sequences are limited by state-changing collisions, thereby reflecting population relaxation time* T_1. ● *Carr–Purcell echoes,* ▲ *Optical nutation, and* ○ *two-pulse echoes. (After Ref. [4.13]).*

in Ref. 4.15. Application of this principle to inhibit intramolecular and intermolecular energy transfer processes is discussed in Ref. [4.16].

The lowest trace in Fig. 4.10 gives the results of a simple two-pulse echo experiment, under conditions identical to those for the other two measurements. By its separation from the other curves however, the data of this experiment can clearly be seen to reflect a decay rate $(T_2)^{-1}$ that is faster than $(T_1)^{-1}$. At long times, the dephasing rate is governed by velocity-changing collisions that are elastic, and that lead only to phase changes of the excited atoms rather than abrupt changes of state (population decay). Thus, coherent optical transients are sensitive to mild dynamic perturbations in the vicinity of luminescent centers, making them exquisite tools for the observation (and control) of extremely weak interactions. An example of observation and decoupling of low energy nuclear spin interactions in optical spectroscopy is given in Ref. [4.17].

A simple experimental approach that may be applied to measure either T_1 or T_2 is provided by the stimulated echo, a three-pulse transient described in Ref. [4.18]. The dephasing and rephasing dynamics involved in this coherent transient are illustrated in Fig. 4.11. An example of the use of stimulated echoes to characterize luminescent centers in a solid may be found in Refs. [4.11] and [4.12].

4.3.3   Density matrix operator analysis

To conclude this chapter, a third approach to the calculation of echo signals in a two-level system is considered, as a prelude to choosing a methodology in Chapter 5 that will be applied throughout the remainder of the book. This one is based on formal integration of the equation of motion for the density matrix [4.19] and highlights
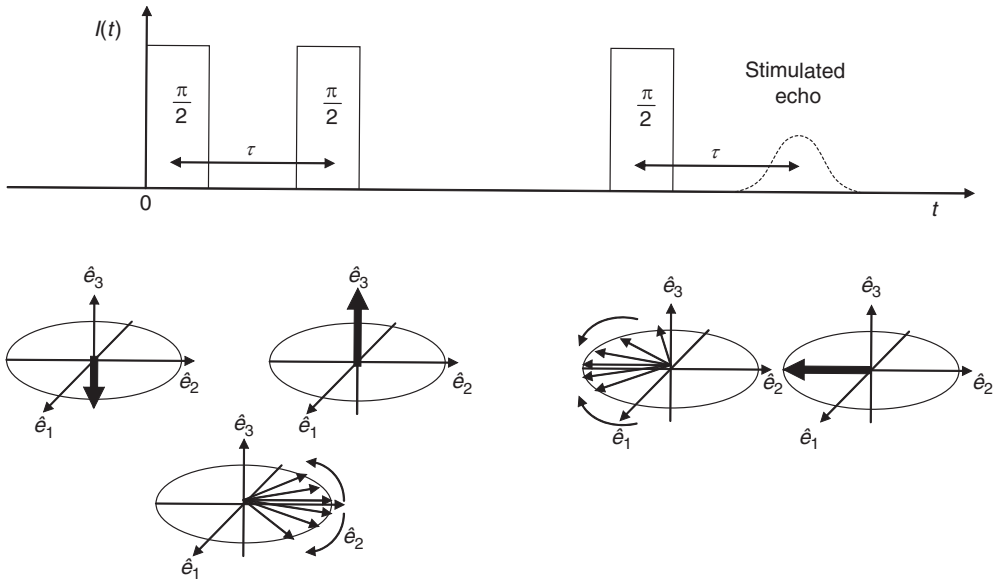
Figure 4.11 *Illustration of the pulse sequence and Bloch vector dynamics during three-pulse stimulated photon echoes.*

exponential forms of the evolution operators based on the angular momentum operator. In quantum mechanics, angular momentum operators are the generators of rotations (see Appendix H). So their appearance here cements the idea that coherent interactions between light and matter in nonlinear and quantum optics are unitary transformations in Hilbert space. This accounts for their prominence in coherent laser spectroscopies of many types [4.18], as well as in the fields of coherent control and quantum information science [4.20], where precise manipulation of populations and superposition states is critical to accuracy.

A few introductory remarks are needed, since multiple representations are used in this section. The interaction picture is used in addition to the Schrödinger representation for reasons that will shortly be made clear. In the Schrödinger picture, the density matrix satisfies the equation

$$i\hbar\frac{d\rho^{\mathrm{S}}}{dt} = [H, \rho^{\mathrm{S}}].\tag{4.3.35}$$

If H is time-independent ($H = H_0$), this equation has the particularly simple solution

$$\rho^{\mathrm{S}}(t - t_0) = U_0(t - t_0)\rho^{\mathrm{S}}(t_0)U_0^+(t - t_0),\tag{4.3.36}$$

where

$$U_0(t - t_0) = \exp[-i(t - t_0)H_0/\hbar].\tag{4.3.37}$$

Exercise: Verify that the transformed density matrix in Eq. (4.3.36) is a solution of the master Eq. (4.3.35) using direct differentiation of Eq. (4.3.37).

During periods when the Hamiltonian is not time-independent, for example during an optical pulse when $H(t) = H_0 + V(t)$, the density matrix Eq. (4.3.35) becomes difficult to solve. The two parts of the Hamiltonian cause essentially different dynamics. This is the motivation behind the interaction picture covered in Chapter 2, which removes the evolution of the state vector due solely to the static Hamiltonian (see Eq. (2.4.13)). The equation of motion for the density matrix in the interaction picture is

$$i\hbar \frac{d\rho^{\mathrm{I}}}{dt} = [V^{\mathrm{I}}, \rho^{\mathrm{I}}], \tag{4.3.38}$$

where $V^{\mathrm{I}}(t - t_0) = U_0^{+}(t - t_0) V U(t - t_0)$. This is often easier to solve than Eq. (4.3.35). The formal solution to Eq. (4.3.38) is

$$\rho^{\mathrm{I}}(t - t_0) = U_{\mathrm{I}}(t - t_0)\rho^{\mathrm{I}}(t_0)U_{\mathrm{I}}^{+}(t - t_0), \tag{4.3.39}$$

where

$$U_{\mathrm{I}}(t - t_0) = \exp[-\frac{i}{\hbar} \int_{t_0}^{t} V^{\mathrm{I}}(t')dt']. \tag{4.3.40}$$

The integral in the evolution operator above is readily evaluated in the interaction picture. This is due to the fact that the integrand consists of the slowly varying amplitude of the optical interaction $V^{\mathrm{I}} = \mu E_0 \sigma_1/2$ in the rotating wave approximation (RWA), not the rapidly varying interaction Hamiltonian of the lab frame. The operator $U_{\mathrm{I}}(t - t_0)$ describes the temporal evolution from t to t_0, but at the same time can be interpreted as a simple rotation through an angle θ about axis $\hat{n}$ in Hilbert space:

$$U_{\mathrm{I}}(\theta) = \exp[-i\sigma_1\theta/2] = \exp[-i\hat{n} \cdot \hat{S}_1\theta/\hbar], \tag{4.3.41}$$

A square pulse of duration ε and area $\theta(\varepsilon) = \mu E_0 \varepsilon/\hbar$ is assumed, and the spin angular momentum $\hat{n} \cdot \hat{S}_1 = \hbar\sigma_1/2$ has been introduced formally as the generator of rotations in two-level spin space. That the operator in Eq. (4.3.41) does indeed cause rotations like the matrices of the last section is justified more thoroughly in Ref. [4.21] and Appendix H.

We are now ready to write down the solution for the density matrix of a two-level system subjected to an arbitrary pulse sequence in terms of evolution operators. In principle, the temporal evolution is given by the appealingly simple expression

$$\rho(t) = U(t - t_0)\rho(t_0)U^{+}(t - t_0), \tag{4.3.42}$$

provided there is no dissipation in the system and we can determine the evolution operator $U(t - t_0)$. The initial matrix is assumed to correspond to an equilibrium state, with populations of ρ_{11} and ρ_{22} in the ground and excited states, respectively. Hence

$$\rho^{\mathrm{I}}(t_0) = \rho^{\mathrm{S}}(t_0) = \begin{bmatrix} \rho_{22} & 0 \\ 0 & \rho_{11} \end{bmatrix} = \frac{1}{2}(\sigma_0 - \sigma_3). \tag{4.3.43}$$

We consider the same sequence of two square pulses separated by the time interval τ that was analyzed in previous sections. The pulses are applied from $t = t_0$ to $t_1 = \varepsilon_1$

and from $t_1 = \varepsilon_1$ to $t_2 = \tau$. Each is followed by a free precession period, first from $t_1 = \varepsilon_1$ to $t_2 = \tau$ and then from $t_2 = \tau$ to $t_3 = \tau + \varepsilon_2$ as in Fig. 4.7. The system is strongly driven for brief moments and evolves freely at other times. The problem of determining the overall operator $U(t - t_0)$ is therefore rather complex, but can be subdivided conveniently on the basis of time periods when the Hamiltonian is H_0 versus when it is $H_0 + V(t)$. That is, the problem may be broken down into discrete periods during which the system is either perturbed or not.

During the free precession periods, evolution may be readily described in the Schrödinger picture using Eq. (4.3.36). During the pulses however, when the Hamiltonian is time-dependent, this expression is no longer valid. It is simpler to calculate the driven dynamics in the interaction picture and subsequently transform the result back to the Schrödinger lab frame to finish the calculation in a single frame. In this approach, time periods when radiation is present are handled in the interaction picture. Driven dynamics may be analyzed separately and then transformed to the Schrödinger picture using the result of the exercise below.

Exercise: Show directly from Eq. (2.4.13) that the density matrices in the Schrödinger and interaction pictures are related by

$$\rho^{\mathrm{S}}(t) = \exp[-iH_0 t/\hbar] \rho^{\mathrm{I}}(t) \exp[iH_0 t/\hbar]. \tag{4.3.44}$$

Following this strategy, a decomposition of the evolution operator is made into four time periods, and also into suitable representations. This gives the following result:

$$U(t - t_0) = U(t - t_3)U(t_3 - t_2)U(t_2 - t_1)U(t_1 - t_0)$$

$$= U_{\mathrm{S}}(t - t_3)\exp[-i\omega_0 t_3]U_{\mathrm{I}}(t_3 - t_2)U_{\mathrm{S}}(t_2 - t_1)\exp[-i\omega_0 t_1]U_{\mathrm{I}}(t_1 - t_0), \tag{4.3.45}$$

where

$$U_{\mathrm{I}}(t_1 - t_0) = \exp[-i\sigma_1 \theta_1/2], \tag{4.3.46}$$

$$U_{\mathrm{S}}(t_2 - t_1) = \exp[-(i/2)\omega_0(\tau - \varepsilon_1)\sigma_3], \tag{4.3.47}$$

$$U_{\mathrm{I}}(t_3 - t_2) = \exp[-i\sigma_1 \theta_2/2], \tag{4.3.48}$$

$$U_{\mathrm{S}}(t - t_3) = \exp[-(i/2)\omega_0(t - \tau - \varepsilon_2)\sigma_3]. \tag{4.3.49}$$

Substitution of Eqs. (4.3.46)–(4.3.49) into Eq. (4.3.45), followed by the combination of Eq. (4.3.45) with Eq. (4.3.42), yields an expression for the density matrix after the pulses have been applied.

$$\rho(t) = \exp\left[-\frac{i}{2}\omega_0(t - \tau)\sigma_3\right]\exp\left[-\frac{i}{2}\theta_2\sigma_1\right]\exp\left[-\frac{i}{2}\omega_0\tau\sigma_3\right]\exp\left[-\frac{i}{2}\theta_1\sigma_1\right]\rho(0) \cdot h.c. \tag{4.3.50}$$

Here *h.c.* stands for the Hermitian conjugate of the entire product of operators acting on $\rho(0)$ from the left.

To simplify Eq. (4.3.50) and compare it with earlier results, it is necessary to commute the second and third terms in $\rho(t)$. For this purpose, commutation relations of the Pauli matrices must be taken into account, and the identity in Problem 4.9 is helpful. Using the result

$$\exp\left[-\frac{i}{2}\theta_2\sigma_1\right]\exp\left[-\frac{i}{2}\omega_0\tau\sigma_3\right]$$

$$= -\cos\left(\frac{1}{2}\theta_2\right)\exp\left[-\frac{i}{2}\omega_0\tau\sigma_3\right] - i\sin\left(\frac{1}{2}\theta_2\right)\exp\left[\frac{i}{2}\omega_0\tau\sigma_3\right]$$

in Eq. (4.3.50), one finds

$$\rho(t) = -\left[\cos\left(\frac{1}{2}\theta_2\right)e^{-(i/2)\omega_0 t\sigma_3} + i\sigma_1\sin\left(\frac{1}{2}\theta_2\right)e^{-(i/2)\omega_0(t-2\tau)\sigma_3}\right]$$

$$\times \left[\cos\left(\frac{1}{2}\theta_1\right) - i\sigma_1\sin\left(\frac{1}{2}\theta_1\right)\right]\rho(0)\cdot h.c.$$

Only terms with the time argument $(t - 2\tau)$ can contribute to echo formation.

Consequently, the density matrix reduces to

$$\rho(t) = \sin^2\left(\frac{1}{2}\theta_2\right)\left\{e^{-(i/2)\omega_0(t-2\tau)\sigma_3}\left[\cos\left(\frac{1}{2}\theta_1\right) - i\sigma_1\sin\left(\frac{1}{2}\theta_1\right)\right]\sigma_1\rho(0)\cdot h.c.\right\}.$$

$$(4.3.51)$$

Now, only the σ_3 term in $\rho(0)$ leads to nonzero contributions to $\rho(t)$ in Eq. (4.3.51), since the unit matrix portion σ_0 allows conjugates to combine and cancel. Furthermore, terms containing $\sigma_1^2\rho(0)\sigma_1^2$ or $\sigma_1\rho(0)\sigma_1$ are proportional to σ_3. These terms are diagonal and cannot give rise to radiation. Diagonal terms of $\rho(t)$ do not appear in the calculation of polarization in Chapter 3. They do not correspond to oscillating dipole moments and cannot contribute to radiant emission by the sample.

Dropping the non-radiant terms, we therefore find

$$\rho(t) = \sin^2(\theta_2/2)$$

$$\times \left\{e^{-(i/2)\omega_0(t-2\tau)\sigma_3}\left[-\frac{i}{2}\cos(\theta_1/2)\sin(\theta_1/2)\right][\sigma_1,\sigma_3]e^{(i/2)\omega_0(t-2\tau)\sigma_3}\right\}$$

$$= -\frac{1}{2}\sin^2(\theta_2/2)\sin(\theta_1)\left\{e^{-(i/2)\omega_0(t-2\tau)\sigma_3}\sigma_2 e^{(i/2)\omega_0(t-2\tau)\sigma_3}\right\}. \qquad (4.3.52)$$

In this result for $\rho(t)$, which determines the signal field (see Eq. (3.9.16)), all the basic features of two pulse echoes established in earlier sections of this chapter are again evident. The echo appears at $t = 2\tau$ and the echo amplitude is maximum for pulse areas of $\theta_1 = \pi/2$ and $\theta_2 = \pi$.

Multiple pulse photon echoes like the stimulated echo illustrated in Fig. 4.11 provide a useful method of storing and retrieving information on demand and also of

processing information. For example, information in the form of amplitude modulation of the input light can be stored as an index or population grating in the medium and recalled at a later time (on demand) by the third pulse in a three-pulse echo sequence. High-fidelity applications of this kind have in fact been demonstrated by the retrieval of long pulse sequences constituting time-encoded bit strings [4.22]. High-speed, large bandwidth spectrum analysis can also be performed using coherent transients [4.23].

This subsection has presented yet another way to calculate the signal amplitude of photon echoes, adding to the methods covered in Sections 4.3.1 and 4.3.2. This third method was based on the formally concise expression (Eq. (4.3.42)), which yields the density matrix $\rho(t)$ directly. While appealingly simple at the outset, this formula contained an exponential form of the evolution operator and matrix representations of the SU(2) Pauli spin operators which introduced inconvenient limitations. Explicit use had to be made, for example of the SU(2) commutation relations, as well as expansions of the exponential functions in terms of the Pauli spin matrix operators.

A moment's pause makes one realize how awkward it would be to have to use complex functions of higher-order spinors, for example SU(n) spin matrices for an n-level system, to describe systems with more than two levels. Also, dissipation has been completely ignored in the treatment of this subsection. To include relaxation processes would greatly complicate the arguments of the temporal evolution operators even within a single time segment. This combination of drawbacks argues against adopting this approach as a general tool for analysis. Similar reservations can be leveled at the other approaches explored in Sections 4.3.1 and 4.3.2. Consequently, for the remainder of this book, we shall turn to solutions of the complete, differential master equation in component form. This will avoid restricting ourselves to a small number of energy levels or fields, and will include population and coherence decay processes which govern crucial aspects of the dynamics of real systems in a consistent manner.

Problems

4.1. Apply the evolution matrix $U(t)$ defined by $R(t) = U(t)R(0)$, where R is the Bloch vector, to find the radiant polarization P of a two-level system at an arbitrary time after applying a pulse as described below. Notice that the evolution period $R(t) = U(t)R(0)$ of interest consists of two parts, namely nutation and precession.

    (a) Assume the system is initially in the ground state and calculate the off-diagonal matrix element $<\tilde{\rho}_{12}>$ and the Doppler-averaged macroscopic polarization at times after the application of a single rectangular pulse that are short compared to T_2 in the limit of small detuning $((\Delta/\Omega_R) < 1$ and $(\Delta^2/\Omega_R^2) << 1)$. (Ignore population and polarization relaxation of the elements of R themselves.)

    (b) If the system is initially prepared in a state characterized by $R_1(0) = 1$, then what will the polarization be at short times after the pulse?

4.2. Using the evolution matrix approach, show that the application of a single resonant π-pulse to a ground state atom leaves the system in an inverted state, by removing all population from the initial state.

4.3. An atomic ensemble is subjected to a resonant $\pi/2$ pulse. Consider spatial phase in the derivation of the evolution matrix to decide if it is possible to irradiate the ensemble with a second $\pi/2$ pulse that may be co- or counter-propagating with respect to the first and to controllably direct the final population to either the ground state or the excited state.

4.4. The Maxwellian distribution of velocities of atoms in a gas gives rise to a Gaussian distribution of resonance frequencies $D(\omega)$ that Doppler-broadens the atomic transition linewidth.

   (a) Given the probability of finding atoms of resonant frequency ω in the interval $d\omega$ is $D(\omega) = C \exp\left\{-Mc^2(\omega_0 - \omega)^2/2\omega_0^2 k_B T\right\} d\omega$, find the full width at half maximum intensity (FWHM) of the Doppler-broadened line.

   (b) Collisions provide a second source of line-broadening on optical transitions that is inversely proportional to the time τ_0 between collisions. The full width at half maximum of the collisional contribution is just twice the collision rate given by

   $$\gamma_{\text{coll}} = \frac{1}{\tau_0} = \frac{4d^2 N}{V} \left(\frac{\pi k_B T}{M}\right)^{1/2}.$$
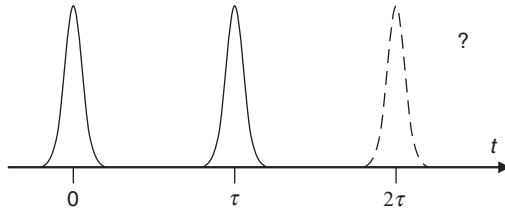
   Show that Doppler and collisional contributions to the transition linewidth are equal at a gas density for which the volume per atom is close to λd^2, where λ is the optical wavelength of the transition and d is the (average) distance between the atomic centers during collision.

4.5. A one-dimensional atomic medium consists of only four atoms located at irregular (non-periodic) positions $z = 0$, $3\lambda/5$, $8\lambda/9$, and $4\lambda/3$. A linearly polarized field $E(z, t) = \frac{1}{2}E_0\hat{x}\exp[i(\omega t - kz)] + c.c.$ is incident on the medium and excites a microscopic dipolar response $\bar{p} = \varepsilon_0\chi^{(e)}\bar{E}$ in each atom.

   (a) Calculate the net (macroscopic) polarization $\bar{P}(z, t) = \sum_{i=1}^{4} \bar{p}_i(z_i, t_i)$ of the system, being careful to account for the delay time associated with propagation of a fixed phase point of the driving field from one atom to the next, as well as their positions.

   (b) Compare the squared polarization $|\bar{P}|^2$, which is proportional to the intensity of scattered light from the system, to the value expected from four independent atoms. Show that the reemitted energy from the system has an intensity that is not linear in the number of emitters.
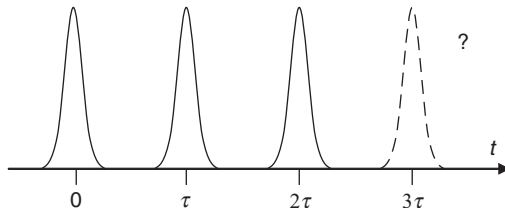
   (This problem illustrates the fact that the incident light can coherently phase randomly positioned atoms, and that phasing of constituent dipoles plays an important role in determining the strength of the resulting macroscopic polarization.)

4.6. A sequence of pulses is applied to a two-level, Doppler-broadened medium. Consider the pulses to be delta functions applied with an interval τ, as shown in

the accompanying figure. The pulse areas of the first and second pulses are θ_1 and θ_2, respectively.

(a) Write out a simplified evolution matrix for nutation of the Bloch vector $R(t)$ in the limit that $\Omega_R \gg \Delta$ (i.e. $\Omega_R \cong \Omega$).

(b) Solve for the complete Bloch vector at $t \geq \tau$ using the matrix evolution operator method. (Hint: Do not set $\Delta = 0$ during free precession periods or you lose track of when various potential signal contributions peak in time.) Ignore decay between pulses and do not assume any special values for θ_1 and θ_2.

(c) When the Doppler width is broad compared to the homogeneous linewidth, averaging over the distribution yields a simplified polarization $\bar{\bar{\rho}}_{12} \propto iR_2$. Then, only R_2 components contribute to the polarization. By examining your result for the final Bloch vector, determine whether an echo forms or not when $\theta_1 = \pi$ and $\theta_2 = \pi/2$. Justify.

(d) Is this pulse sequence equivalent to a stimulated echo sequence of three $\pi/2$ pulses? Draw Bloch *vector model pictures* to explain result (c) further and justify your conclusion.

(e) Finally, a third pulse of area $\theta_3 = \pi$ is applied at $t = 2\tau$ to complete a $\pi - \pi/2 - \pi$ sequence. Calculate the resulting behavior for $t \geq 2\tau$ and *explain* the result in words or pictures.

4.7. Assuming there is an allowed transition with a transition dipole moment μ between the two levels of a two-level system,

(a) Find the Bloch vector of a two-level system, initially in the ground state, that is irradiated by a resonant π-pulse of short duration $\tau_p (\tau_p \ll T_1, T_2)$. Take the time of observation to be $t = \tau$ (where $\tau_p \ll \tau < T_1, T_2$).

(b) Calculate and explain the value of polarization P observed at time $t = \tau$?

(c) Draw the Bloch vector in a suitable coordinate system at time $t = \tau$.

(d) What is the excited state population at $t = \tau$?

(e) What is the sign of the absorption at $t = \tau$? Would you expect a probe pulse to experience loss (positive absorption) or gain (negative absorption) at this time?

(f) If a second pulse, a $\pi/2$ pulse, is applied at time $t = \tau (\tau << T_1, \tau >> T_2)$, what is the polarization $P(t)$ at the end of the second pulse?

(g) Assuming the system is inhomogeneously broadened, would you expect an echo at time $t = 2\tau$? Why or why not?

4.8. Using Bloch vector diagrams similar to Fig. 4.5, give an argument explaining why the Carr–Purcell sequence of pulses, with areas and timing described by $\pi/2(t = 0), \pi(\tau), \pi(3\tau), \pi(5\tau), \ldots$, produces echoes at times $2\tau, 4\tau, 6\tau, \ldots$, whose envelope decays with a characteristic time T_1 instead of T_2.

4.9. By expanding the leftmost exponential function as an infinite sum, and using commutation properties of the Pauli matrices, show that

$$\exp\left[-\frac{i}{2}\theta_2\sigma_1\right]\exp\left[-\frac{i}{2}\omega_0\tau\sigma_3\right] = -\cos\left(\frac{1}{2}\theta_2\right)\exp\left[-\frac{i}{2}\omega_0\tau\sigma_3\right]$$

$$- i\sin\left(\frac{1}{2}\theta_2\right)\exp\left[\frac{i}{2}\omega_0\tau\sigma_3\right].$$

References

4.1. R.L. Shoemaker and E.W. Van Stryland, *J. Chem. Phys.* **64**, 1733 (1976).

4.2. D. Press, T.D. Ladd, B. Zhang, and Y. Yamamoto, *Nature* **456**, 218(2008).

4.3. T.H. Stievater, X. Li, D.G. Steel, D. Gammon, D.S. Katzer, D. Park, C. Piermarocchi, and L.J. Sham, *Phys. Rev. Lett.* **87**, 133603(2001).

4.4. F.A. Hopf, R.F. Shea, and M.O. Scully, *Phys. Rev.* **A7**, 2105(1973).

4.5. R.G. Brewer, Les Houches Lectures, Session XXVII, *Frontiers in Laser Spectroscopy Vol. 1*, Eds. R. Balian, S. Haroche, and S. Liberman, North-Holland Publishing Co., Amsterdam, 1977.

4.6. R.G. DeVoe and R.G. Brewer, *IBM J. Res. and Dev.*, **23**, 527 (1979).

4.7. R.G. DeVoe and R.G. Brewer, *Phys. Rev. Lett.* **50**, 1269(1983).

4.8. A.Z. Genack and R.G. Brewer, *Phys. Rev.* **A17**, 1463(1978).

4.9. I.D. Abella, N.A. Kurnit, and S.R. Hartmann, *Phys. Rev.* **141**, 391(1966).

4.10. R.M. Shelby and R.M. MacFarlane, *Phys. Rev. Lett.* **45**, 1098(1980).

4.11. Y.C. Chen, K. Chiang, and S.R. Hartmann, *Phys. Rev.* **B 21**, 40(1980).

4.12. A. Lenef, S.W. Brown, D.A. Redman, S.C. Rand, J. Shigley and E. Fritsch, *Phys. Rev.* **B53**, 15427(1996).

4.13. J. Schmidt, P. Berman, and R.G. Brewer, *Phys. Rev. Lett.* **31**, 1103(1973).

4.14. H.Y. Carr and E.M. Purcell, *Phys. Rev.* **94**, 630(1954).

4.15. For further discussion, see C.P. Slichter, Principles of Magnetic Resonance, Springer-Verlag, New York, 1980, pp. 252–254.

4.16. E.T. Sleva, M. Glasbeek, and A.H. Zewail, J. *Phys. Chem.* **90**, 1232(1986).

4.17. S.C. Rand, A. Wokaun, R.G. DeVoe, and R.G. Brewer, *Phys. Rev. Lett.* **43**, 1868(1979).

4.18. M.D. Levenson and S.S. Kano, *Introduction to Nonlinear Laser Spectroscopy*, Academic Press, New York, 1988.

4.19. L.G. Rowan, E.L. Hahn, and W.B. Mims, *Phys. Rev.* **137**, A61(1965).

4.20. M.A. Nielsen and I.L. Chuang, *Quantum Computation and Quantum Information*, Cambridge University Press, Cambridge, 2000.

4.21. E. Merzbacher, *Quantum Mechanics*, 2nd edition, J. Wiley & Sons, New York, 1970, pp. 266–274.

4.22. Y.S. Bai, W.R. Babbitt, and T.W. Mossberg, *Opt. Lett.* **11**, 724(1986).

4.23. V. Crozatier, G. Gorju, J.-L. LeGouet, F. Bretenaker, and I. Lorgere, *J. Lumin.* **127**, 104(2007).

5

Coherent Interactions of Fields and Atoms

In this chapter, the tools and perspectives developed earlier are applied to predict the dynamics of many different systems, starting from the simplest and progressing to more complicated ones. Systems in each successive subsection are representative of a class of problem, and only one change is introduced at each step. In this way a veritable catalog of possibilities is assembled, all described with the density matrix and the same interaction Hamiltonian using the semiclassical approach. The problems in which it becomes necessary to consider the quantum structure of the electromagnetic field itself are deferred to Chapter 6 on "Quantized Fields and Coherent States."

5.1 Stationary atoms

5.1.1 Stationary two-level atoms in a traveling wave

Consider a system of stationary two-level atoms as shown in Fig. 5.1, characterized by a single resonance frequency $\omega_0 \equiv \omega_2 - \omega_1$.

$$V(t) = -\frac{1}{2}\bar{\mu} \cdot \bar{E}_0 e^{i\omega t} + c.c. = -\frac{1}{2}\hbar\Omega e^{i\omega t} + c.c. \qquad (5.1.1)$$

According to Eqs. (3.6.19) and (3.8.1), the density matrix equations of motion are

$$i\hbar\dot{\rho}_{11} = V_{12}\rho_{21} - \rho_{12}V_{21} + i\hbar\gamma_{21}\rho_{22}, \qquad (5.1.2)$$

$$i\hbar\dot{\rho}_{22} = -V_{12}\rho_{21} + \rho_{12}V_{21} - i\hbar\gamma_{21}\rho_{22}, \qquad (5.1.3)$$

$$i\hbar\dot{\rho}_{12} = -\hbar\omega_0\rho_{12} + (V_{12}\rho_{22} - \rho_{11}V_{12}) - i\hbar\Gamma_{12}\rho_{12}, \qquad (5.1.4)$$

$$\rho_{21} = \rho_{12}^*. \qquad (5.1.5)$$

Note that either a plus or a minus sign may apply to the phenomenological population decay terms on the far right of Eqs. (5.1.2) and (5.1.3). The choice of sign must reflect whether the population is "arriving" (+) in a given level from more energetic states above it, or "leaving" (−). On the other hand, the sign for the decay of the off-diagonal
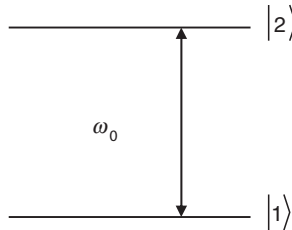
Figure 5.1 *Energy levels and resonant transition frequency in a two-level atom. The system is subjected to traveling plane wave excitation of the form.*

matrix element (the "coherence") in Eq. (5.1.4) is always negative, reflecting the fact that coherence of a system never spontaneously increases. When there is no driving field, it always decreases. In addition the dephasing rate constant is real, so that $\Gamma_{12} = \Gamma_{21}$. Although the subscripts on Γ_{12}, Γ_{21} seem unnecessary at this stage, they do indicate the levels connected by a particular coherence. Hence we shall retain them in anticipation of later situations in which there may be multiple coherences between more than two levels.

For steady-state behavior we assume that the response of the electron, described by off-diagonal element ρ_{12}, follows only one frequency component of the driving field, namely the positive one. This is called the rotating wave approximation (RWA). Rather than perform the time-integration of Eq. (5.1.4), which is necessary to find transient solutions, we begin by simply assuming the charge oscillation is at the optical frequency, so that the solution has the form

$$\rho_{12} = \tilde{\rho}_{12} e^{i\omega t}. \tag{5.1.6}$$

(This is justified by direct integration of the equation of motion for the off-diagonal density matrix element ρ_{12} in Appendix G.) Upon substitution of Eq. (5.1.6) into Eq. (5.1.4), one immediately finds

$$[\Gamma_{12} + i(\omega - \omega_0)]\tilde{\rho}_{12} + \dot{\tilde{\rho}}_{12} = i\Omega_{12}(\rho_{11} - \rho_{22})/2. \tag{5.1.7}$$

We now make the further assumption that $\tilde{\rho}_{12}$ varies much more slowly than the optical period. This corresponds to the assumption that $d\tilde{V}_{12}(t')/dt' \cong 0$ in Appendix G and is called the slowly varying envelope approximation (SVEA). It is implemented by setting $\dot{\tilde{\rho}}_{12} = 0$, which yields

$$\tilde{\rho}_{12} = \left[\frac{\Omega_{12}/2}{\Delta + i\Gamma}\right](\rho_{11} - \rho_{22}). \tag{5.1.8}$$

Note that we have dropped the subscripts on the dephasing rate for simplicity, since $\Gamma_{12} = \Gamma_{21} \equiv \Gamma$ is a real decay rate and there are only two energy levels in the system, so there is no possible ambiguity as to the polarization decay to which it refers. The steady-state solution for $\rho_{12}(t)$ is therefore

$$\rho_{12}(t) = \left(\frac{\Omega_{12}/2}{\Delta + i\Gamma}\right)(\rho_{11} - \rho_{22})e^{i\omega t}. \tag{5.1.9}$$

For systems in which emission and coherence properties are not of interest, often it is only the temporal development of populations that is needed to describe basic system dynamics. For this purpose, population equations that do not require knowledge of the off-diagonal elements of the density matrix suffice. For example, absorption of the system, which is proportional to the population difference $\rho_{11} - \rho_{22}$, can be predicted without knowing ρ_{12}. This can be demonstrated by substituting Eq. (5.1.9) and its conjugate into the density matrix equations for $\dot{\rho}_{11}$ and $\dot{\rho}_{22}$.

Exercise: Show that substitution of Eqs. (5.1.9) and (5.1.5) into Eqs. (5.1.2) and (5.1.3) results in the population rate equations:

$$\dot{\rho}_{11} = -\frac{\Gamma/2}{\Delta^2 + \Gamma^2} \, |\Omega_{12}|^2 \, (\rho_{11} - \rho_{22}) + \gamma_{21}\rho_{22}, \qquad (5.1.10)$$

$$\dot{\rho}_{22} = \frac{\Gamma/2}{\Delta^2 + \Gamma^2} \, |\Omega_{12}|^2 \, (\rho_{11} - \rho_{22}) - \gamma_{21}\rho_{22}. \qquad (5.1.11)$$

These are coupled equations for the populations in levels 1 and 2 that can be solved exactly and include intensity-dependent dynamics. Without having to evaluate ρ_{12} explicitly, they can be used to describe the bleaching of absorbing systems like colored filters by intense light beams.

The next step is to solve for the steady-state populations. Let us start with ρ_{22}, using Eq. (5.1.9) in Eq. (5.1.3). Setting $\dot{\rho}_{22} = 0$ for steady-state response, this procedure yields

$$\gamma_{21}\rho_{22} = \frac{i}{\hbar} \left(V_{12}\rho_{21} - \rho_{12}V_{21} \right)$$

$$= -(i\Omega_{12}\tilde{\rho}_{21} - i\Omega_{21}\tilde{\rho}_{12})/2$$

$$= |\Omega_{12}/2|^2 \, [L + L^*] \, (\rho_{11} - \rho_{22}) , \qquad (5.1.12)$$

where $L \equiv (i\Delta + \Gamma)^{-1}$. Solving for the excited state occupation in terms of that of the ground state, one finds

$$\rho_{22} = \left[\frac{(L + L^*) \, |\Omega_{12}/2|^2 \, /\gamma_{21}}{1 + (L + L^*) \, |\Omega_{12}/2|^2 \, /\gamma_{21}} \right] \rho_{11}. \qquad (5.1.13)$$

Since the total occupation probability must be unity $(\rho_{11} + \rho_{22} = 1)$, one also obtains

$$\rho_{11} = \left[\frac{1 + (L + L^*) \, |\Omega_{12}/2|^2 \, /\gamma_{21}}{1 + 2(L + L^*) \, |\Omega_{12}/2|^2 \, /\gamma_{21}} \right]. \qquad (5.1.14)$$

Exercise: Verify that ρ_{11}, ρ_{22} are purely real quantities that tend to appropriate limiting values as $\Omega \to \infty$ (i.e., at high intensity)

The absorption of light depends on the number of absorbers and their distribution among the available states. Hence it is proportional to $N(\rho_{11} - \rho_{22})$, where the population difference is given by Eqs. (5.1.13) and (5.1.14) as

$$\rho_{11} - \rho_{22} = \left[1 + 2(L + L^*) \left|\Omega/2\right|^2 / \gamma_{21}\right]^{-1}$$

$$= \left[1 + \frac{\Gamma \left|\Omega\right|^2}{(\Delta^2 + \Gamma^2)\gamma_{21}}\right]^{-1}. \tag{5.1.15}$$

Exercise: Find the limiting value of absorption as $\Omega \to \infty$ (high intensity limit)? Does the result in Eq. (5.1.15) make physical sense in this limit?

Equation (5.1.15) has the form $[1 + I/I_{\text{sat}}]^{-1}$, where the intensity I_{sat} at which absorption drops to half its maximum, a quantity known as the saturation intensity, is defined by

$$I_{\text{sat}} \equiv \hbar^2 \gamma_{21} \mu_0 c / (|\mu_{12}|^2 [L + L^*])$$

$$= \left[\frac{\hbar^2 \gamma_{21} \mu_0 c (\Delta^2 + \Gamma^2)}{|\mu_{12}|^2 \, 2\Gamma}\right] \tag{5.1.16}$$

Exercise: At a positive detuning from resonance equal to the linewidth (i.e., $\Delta = \Gamma$), does the intensity required to saturate the system increase or decrease, and by what factor? Does the saturation intensity depend on whether the detuning Δ is negative or positive?

5.1.2   Stationary three-level atoms in a traveling wave

We now consider the interaction of traveling wave excitation of the form in Eq. (5.1.1) with a system that has one additional level. Introduction of this one additional level can have significant implications for optical behavior. In the scheme of Fig. 5.2, it is implicitly assumed that ω is near or on-resonance for the $|1\rangle \leftrightarrow |2\rangle$ transition, but is far off-resonance for $|1\rangle \leftrightarrow |3\rangle$.
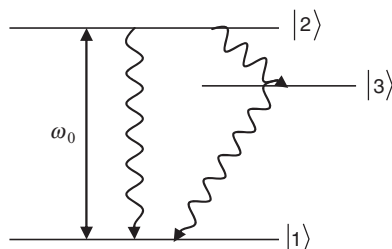
Figure 5.2 *Schematic of the excitation and relaxation processes of a three-level atom.*

The equations of motion are

$$\dot{\rho}_{11} = \frac{1}{i\hbar}\left(V_{12}\rho_{21} - \rho_{12}V_{21}\right) + \gamma_{21}\rho_{22} + \gamma_{31}\rho_{33}, \tag{5.1.17}$$

$$\dot{\rho}_{22} = -\frac{1}{i\hbar}\left(V_{12}\rho_{21} - \rho_{12}V_{21}\right) - \gamma_{21}\rho_{22} - \gamma_{23}\rho_{22}, \tag{5.1.18}$$

$$\dot{\rho}_{33} = \gamma_{23}\rho_{22} - \gamma_{31}\rho_{33}, \tag{5.1.19}$$

$$\dot{\rho}_{12} = i\omega_0\rho_{12} - \frac{1}{i\hbar}V_{12}\left(\rho_{11} - \rho_{22}\right) - \Gamma_{21}\rho_{12}, \tag{5.1.20}$$

$$\rho_{21} = \rho_{12}^*. \tag{5.1.21}$$

In writing Eqs. (5.1.17)–(5.1.21), a very important simplifying assumption has been made regarding driven processes. Since no light fields were intentionally applied to couple state $|1\rangle$ to $|3\rangle$ or $|2\rangle$ to $|3\rangle$ directly, equations for the other possible coherences ρ_{13} and ρ_{23} were dropped from all equations. In point of fact, coherences do develop between other pairs of states, but provided the optical frequency ω has a small detuning with respect to $\omega_0 = \omega_{12}$, and large detunings with respect to ω_{13} and ω_{23}, these coherences are extremely small due to the detuning dependence evident in the denominator of Eq. (5.1.9).

Spontaneous processes in three-level systems lead to population transfer among the states. Population can build up in state 3 if it is long lived, and significant changes in the distribution of population strongly alter the system saturation behavior. This can be shown starting from Eq. (5.1.19) by setting $\dot{\rho}_{33} = 0$ to examine steady-state behavior. We find

$$\rho_{33} = (\gamma_{23}/\gamma_{31})\rho_{22}. \tag{5.1.22}$$

To obtain ρ_{22}, we first need to determine ρ_{12} from Eq. (5.1.20). Using the same procedure as in the last subsection, we find

$$\rho_{12} = \left[\frac{\Omega_{12}/2}{\Delta + i\Gamma}\right](\rho_{11} - \rho_{22})\,e^{i\omega t}. \tag{5.1.23}$$

This is identical to Eq. (5.1.9) for two-level systems. Using this in Eq. (5.1.18), and setting $\dot{\rho}_{22} = 0$ for the steady-state solution, we find

$$\rho_{22} = \left[\frac{(L + L^*)\left|\Omega_{12}/2\right|^2/\gamma_2}{1 + (L + L^*)\left|\Omega_{12}/2\right|^2/\gamma_2}\right]\rho_{11}, \tag{5.1.24}$$

where $\gamma_2 = \gamma_{21} + \gamma_{23}$ is the total relaxation rate from level 2. From Eq. (5.1.22), we then find

$$\rho_{33} = \left[\frac{(L + L^*)\left|\Omega_{12}/2\right|^2\gamma_{23}/\gamma_{31}\gamma_2}{1 + (L + L^*)\left|\Omega_{12}/2\right|^2/\gamma_2}\right]\rho_{11}. \tag{5.1.25}$$

Now by using the closure relation for three levels, namely

$$\rho_{11} + \rho_{22} + \rho_{33} = 1, \tag{5.1.26}$$

we can determine ρ_{11} explicitly by substituting Eqs. (5.1.24) and (5.1.25) into Eq. (5.1.26). The result is

$$\rho_{11} = \left[\frac{1 + (L + L^*) \left| \Omega_{12}/2 \right|^2 / \gamma_2}{1 + (L + L^*)(2 + \gamma_{23}/\gamma_{31}) \left| \Omega_{12}/2 \right|^2 / \gamma_2} \right]. \tag{5.1.27}$$

Exercise: Do the solutions for ρ_{11}, ρ_{22}, ρ_{33} present sensible values in the high intensity limit $(|\Omega|^2 \to \infty)$? Do they agree with thermodynamic predictions for $T \to \infty$?

As before, absorption from the ground state is proportional to $\rho_{11} - \rho_{22}$. For the three-level system, we find

$$\rho_{11} - \rho_{22} = \left[1 + \frac{\left| \Omega_{12}/2 \right|^2}{\gamma_2} \left(2 + \frac{\gamma_{23}}{\gamma_{31}} \right) (L + L^*) \right]^{-1}. \tag{5.1.28}$$

This is of the form

$$\rho_{11} - \rho_{22} = \frac{1}{1 + I/I_{\text{sat}}}, \tag{5.1.29}$$

where

$$I_{\text{sat}} \equiv \frac{\hbar^2 \gamma_2 \mu_0 c}{|\mu_{12}|^2 \left(1 + \gamma_{23}/2\gamma_{31} \right)[L + L^*]} = \frac{\hbar^2 \gamma_2 \mu_0 c(\Delta^2 + \Gamma^2)}{2\Gamma |\mu_{12}|^2 \left(1 + \gamma_{23}/2\gamma_{31} \right)}. \tag{5.1.30}$$

Exercise: (*a*) If the rate of decay from level 2 to level 3 is much less than the rate from 2 to 1, the three-level system essentially reduces to a two-level system. Show that in this limit one obtains $I_{\text{sat}}(3 - levels) = I_{\text{sat}}(2 - levels)$. (*b*) Show by contrast that for finite γ_{23}, the three-level saturation intensity can be significantly lower than that of the corresponding two-level system if level $|3\rangle$ is metastable (very long-lived).

An important thing to note is that nonlinear behavior (i.e. saturable absorption) is more readily obtainable in three-level than two-level systems. However, one must tolerate the losses and reduced speed of dynamics caused by tuning near resonances.

5.1.3   Stationary two-level atoms in a standing wave

Consider the open system depicted in Fig. 5.3 of stationary, two-level atoms acted upon by a standing wave field. Incoherent pumping is assumed to occur to both levels from unobserved external sources with rates that do not depend on the state of the system. This pumping is balanced by spontaneous decay from both levels.

The interaction may be written as

$$V(t) = -\frac{1}{2}\mu E_0 e^{i(\omega t - kz)} + c.c. - \frac{1}{2}\mu E_0 e^{i(\omega t + kz)} + c.c. = -2\hbar\Omega \cos kz \cos \omega t, \tag{5.1.31}$$
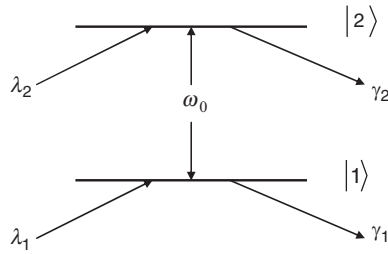
Figure 5.3 *Schematic diagram of a two-level atom interacting with a standing wave under conditions of incoherent pumping at rates λ_1 and λ.*

and the component equations of the density matrix are

$$\dot{\rho}_{11} = \lambda_1 - \gamma_1 \rho_{11} + 2i\Omega \cos kz \cos \omega t \left(\rho_{21} - \rho_{12} \right), \tag{5.1.32}$$

$$\dot{\rho}_{22} = \lambda_2 - \gamma_2 \rho_{22} - 2i\Omega \cos kz \cos \omega t \left(\rho_{21} - \rho_{12} \right), \tag{5.1.33}$$

$$\dot{\rho}_{21} = - \left(\Gamma_{21} + i\omega_0 \right) \rho_{21} - 2i\Omega \cos kz \cos \omega t \left(\rho_{22} - \rho_{11} \right), \tag{5.1.34}$$

$$\dot{\rho}_{21} = \dot{\rho}_{21}^*. \tag{5.1.35}$$

Letting

$$\rho_{12} = \tilde{\rho}_{12} e^{i\omega t} \tag{5.1.36}$$

as before, Eq. (5.1.34) yields

$$\dot{\tilde{\rho}}_{12} = - \left[\Gamma_{12} - i\Delta \right] \tilde{\rho}_{12} + 2i\Omega \cos kz \left(\rho_{22} - \rho_{11} \right). \tag{5.1.37}$$

In the steady state, this gives

$$\tilde{\rho}_{12} = \left[\frac{2\Omega \cos kz}{\Delta + i\Gamma_{12}} \right] \left(\rho_{11} - \rho_{22} \right). \tag{5.1.38}$$

Using the RWA, we can now evaluate the factor

$$\cos \omega t \left(\rho_{21} - \rho_{12} \right) = \frac{1}{2} \left(e^{i\omega t} + e^{-i\omega t} \right) \left(\tilde{\rho}_{21} e^{-i\omega t} - \tilde{\rho}_{12} e^{i\omega t} \right).$$

The result is

$$\cos \omega t (\rho_{21} - \rho_{12}) \cong \frac{1}{2} (\tilde{\rho}_{21} - \tilde{\rho}_{12}) = \frac{-i\Omega}{\Gamma_{21}} \cos kz \left(\rho_{22} - \rho_{11} \right) L(\Delta). \tag{5.1.39}$$

Returning now to Eqs. (5.1.32) and (5.1.33), we can write

$$\dot{\rho}_{11} = \lambda_1 - \gamma_1 \rho_{11} + \frac{2\Omega^2}{\Gamma_{21}} \cos^2 kz \left(\rho_{22} - \rho_{11} \right) L(\Delta), \tag{5.1.40}$$

$$\dot{\rho}_{22} = \lambda_2 - \gamma_2 \rho_{22} - \frac{2\Omega^2}{\Gamma_{21}} \cos^2 kz \left(\rho_{22} - \rho_{11} \right) L(\Delta). \tag{5.1.41}$$

The Lorentzian factor $L(\Delta)$ is defined by $L(\Delta) \equiv \Gamma_{12}^2/(\Delta^2 + \Gamma_{12}^2)$. Steady-state solutions are

$$\rho_{22} - \rho_{11} = \bar{N} \left/ \left[1 + \left(\frac{2(\gamma_1 + \gamma_2)}{\gamma_1 \gamma_2 \Gamma_{21}} \right) \Omega^2 L(\Delta) \cos^2 kz \right] \right. \tag{5.1.42}$$

$$\rho_{11} = \frac{\lambda_1}{\gamma_1} - \frac{2\Omega^2}{\gamma_1 \Gamma_{21}} L(\Delta) \cos^2 kz \cdot \bar{N} \left/ \left[1 + 2 \left(\frac{\gamma_1 + \gamma_2}{\gamma_1 \gamma_2 \Gamma_{21}} \right) \Omega^2 L(\Delta) \cos^2 kz \right] \right. \tag{5.1.43}$$

$$\rho_{22} = \frac{\lambda_2}{\gamma_2} + \frac{2\Omega^2}{\gamma_2 \Gamma_{21}} L(\Delta) \cos^2 kz \cdot \bar{N} \left/ \left[1 + 2 \left(\frac{\gamma_1 + \gamma_2}{\gamma_1 \gamma_2 \Gamma_{21}} \right) \Omega^2 L(\Delta) \cos^2 kz \right] \right. \tag{5.1.44}$$

In these expressions, following Ref. 5.1, we have introduced the average population difference

$$\bar{N} \equiv [\frac{\lambda_2}{\gamma_2} - \frac{\lambda_1}{\gamma_1}]$$

that exists in the absence of light. Notice that atoms saturate in a way that depends on their location z with respect to the standing wave pattern. This is reflected not only in the population difference $\rho_{22} - \rho_{11}$, but in the fact that the power-broadened transition linewidth varies from point to point see Fig. 5.4.

Exercise: Show explicitly that the population difference can be expressed in the form of a Lorentzian function of detuning Δ with a power-broadened linewidth of

$$\Gamma(z) = \Gamma_{21} \left[1 + \frac{2(\gamma_1 + \gamma_2)}{\gamma_1 \gamma_2 \Gamma_{21}} \Omega^2 \cos^2 kz \right]^{1/2}. \tag{5.1.45}$$

The off-diagonal density matrix element is found by using Eq. (5.1.42) in Eq. (5.1.38).

$$\tilde{\rho}_{12} = \left[\frac{i\Omega_{12} \cos kz}{\Gamma_{21} - i\Delta} \right] \bar{N} \left/ \left[1 + \left(\frac{2(\gamma_1 + \gamma_2)}{\gamma_1 \gamma_2 \Gamma_{21}} \right) \Omega^2 L(\Delta) \cos^2 kz \right] \right.$$

$$= \frac{2i\Omega_{12} \bar{N} \cos kz \, (\Gamma_{21} + i\Delta)}{\Delta^2 + \Gamma_{21}^2 \left[1 + \frac{8(\gamma_1 + \gamma_2)}{\gamma_1 \gamma_2 \Gamma_{21}} \Omega^2 \cos^2 kz \right]} \tag{5.1.46}$$
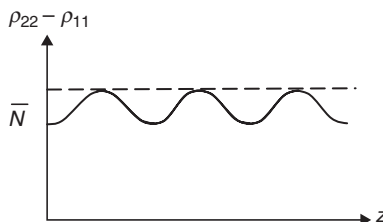
Figure 5.4 *Population difference versus position in a system of stationary two-level atoms subjected to standing wave excitation.*

The total polarization of the sample is found in the usual way from

$$P(z,t) = N_0 \langle \mu \rangle = N_0 (\mu_{12}\rho_{21} + \rho_{12}\mu_{21}). \tag{5.1.47}$$

In this instance however, a spatial average of Eq. (5.1.47) is needed to compute $P(z,t)$, since $\tilde{\rho}_{12}$ and $\tilde{\rho}_{21}$ depend on z. The atoms were assumed to be stationary, so they are distinguishable by position. The signal field radiated by the sample polarization must account for the spatial variations of polarization, requiring a less trivial integration of (3.9.15) than before.

Exercise: (*a*) Calculate the spatial average of $\tilde{\rho}_{12}$ given in Eq. (5.1.47). (*b*) If the atoms were moving with the usual Doppler distribution of frequencies, the frequency average would involve a Lorentzian lineshape and a Gaussian distribution function. What lineshape would result?

The modulation of $\rho_{22} - \rho_{11}$ as a function of z is referred to as *spatial hole-burning*. In the presence of hole-burning, the absorption shows dips or holes due to saturation. Holes may appear as a function of z as we have here, or as a function of frequency in inhomogeneously broadened systems. In the latter case, we speak of *frequency-domain hole-burning*, a phenomenon which may be exploited for high-resolution "saturation" spectroscopy [5.2]. This is discussed in the subsequent subsections.

Exercise: Can frequency-domain hole-burning occur on a homogeneously broadened optical transition?

5.2   Moving atoms

5.2.1   Moving atoms in a traveling wave

We now consider moving two-level atoms subjected to traveling wave excitation in the open system of the last section. The interaction is written

$$V(t) = -(\mu E_0/2\hbar)(\exp[i(\omega t - kz)] + c.c.) = -\frac{1}{2}\hbar\Omega \exp[i(\omega t - kz)] + c.c. \tag{5.2.1}$$

Due to the atomic motion at velocity $\overline{V}$, the full-time derivative of ρ consists of its explicit time dependence plus a velocity-dependent contribution from the time dependence of the atomic position $z(t)$. The quantum mechanical transport equation is therefore modified to

$$i\hbar \left(\frac{\partial}{\partial t} + \bar{v} \cdot \bar{\nabla} \right) \rho = [H, \rho] + \frac{d\rho}{dt}\bigg|_{\text{relax}}, \tag{5.2.2}$$

$$\left(\frac{\partial}{\partial t} + v_z \frac{\partial}{\partial z} \right) \rho_{11} + \gamma_1 \rho_{11} = \lambda_1 - i\Omega \cos(kz - \omega t)(\rho_{12} - \rho_{21}), \tag{5.2.3}$$

$$\left(\frac{\partial}{\partial t} + v_z \frac{\partial}{\partial t} \right) \rho_{22} + \gamma_2 \rho_{22} = \lambda_2 + i\Omega \cos(kz - \omega t)(\rho_{12} - \rho_{21}), \tag{5.2.4}$$

$$\left(\frac{\partial}{\partial t} + v_z \frac{\partial}{\partial z} - i\omega_0 \right) \rho_{12} + \Gamma_{12} \rho_{12} = i\Omega \cos\left(kz - \omega t\right) \left(\rho_{22} - \rho_{11}\right). \qquad (5.2.5)$$

As usual we set

$$\rho_{12} = \tilde{\rho}_{12} \exp[i(\omega t - kz)], \qquad (5.2.6)$$

and solve for $\tilde{\rho}_{12}$ in steady state. If $\tilde{\rho}_{12}$ is sufficiently slowly varying in space and time, then the derivatives on the left side yield

$$\frac{d\rho_{12}}{dt} = \left(\frac{\partial}{\partial t} + v \frac{\partial}{\partial z} \right) \rho_{12} = i\left(\omega - kv\right) \rho_{12}, \qquad (5.2.7)$$

where the subscript z on velocity has been dropped. Then

$$\tilde{\rho}_{12} = i \left[\frac{(\Omega/2)}{\Gamma_{21} - i\left(\Delta + kv\right)} \right] (\rho_{22} - \rho_{11}) \qquad (5.2.8)$$

and

$$\rho_{22} - \rho_{11} = \bar{N}\left(v\right) \Big/ \left[1 + \frac{2(\Omega/2)^2 \left[\gamma_1 + \gamma_2\right]}{\Gamma_{21}\gamma_1\gamma_2} L(\Delta + kv) \right], \qquad (5.2.9)$$

where the equilibrium occupation versus frequency,

$$\bar{N}(v) \equiv \left(\frac{\lambda_2(v)}{\gamma_2} - \frac{\lambda_1(v)}{\gamma_1} \right),$$

reflects the lineshape of the inhomogeneous velocity distribution. For a gas, this is given by the distribution of Doppler-shifted atomic resonance frequencies. $L(\Delta + kv)$ in Eq. (5.2.9) is the real Lorentzian factor defined in Eq. (5.1.39). The behavior of the population difference in Eq. (5.2.9) is illustrated in Fig. 5.5.

Equation (5.2.9) can also be written as

$$\rho_{22} - \rho_{11} = \bar{N}\left(v\right) \left[1 - \frac{2I\eta\Gamma_{21}^2}{\left(\Delta + kv\right)^2 + \Gamma_{21}^2 \left(1 + 2I\eta\right)} \right], \qquad (5.2.10)$$
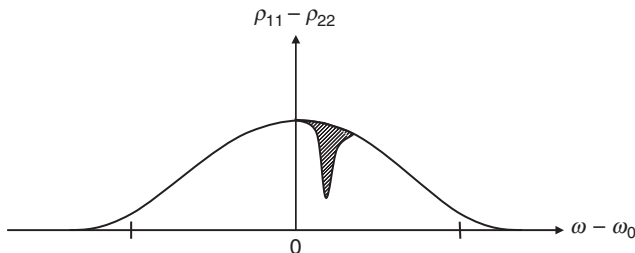
Figure 5.5 *Spectral hole-burning in an inhomogeneously broadened system of two-level atoms subjected to a single traveling wave. The shaded region shows the spectral hole that is burnt into the equilibrium distribution of atoms versus frequency (for negative $\bar{N}$).*
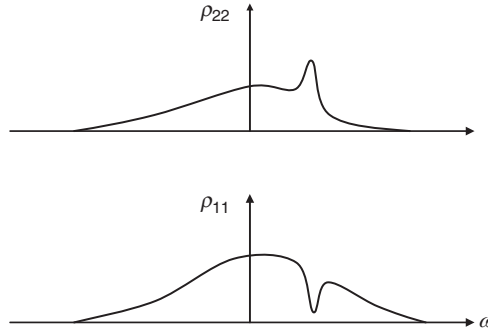
Figure 5.6 *Nonequilibrium features in the individual population distributions of states 1 and 2 of a system of moving two-level atoms subjected to traveling wave excitation.*

where $I \equiv 2(\Omega/2)^2/\gamma_1\gamma_2$ and $\eta \equiv (\gamma_1 + \gamma_2)/2\Gamma_{12}$. From this expression, it is more obvious that the deviation from the unperturbed value $-\bar{N}(v)$ is a power-broadened Lorentzian of width

$$\Gamma = \Gamma_{12} \left(1 + 2I\eta\right)^{1/2}. \tag{5.2.11}$$

Thus, the atom–field interaction burns a hole in the population difference $\rho_{11} - \rho_{22}$. Figure 5.6 illustrates the population changes induced by the field in the individual states 1 and 2.

$$\rho_{11}(v) = \frac{\lambda_1(v)}{\gamma_1} + \bar{N}(v) \frac{I\gamma_1\Gamma_{21}}{(\Delta + kv)^2 + \Gamma_{21}^2 (1 + 2I\eta)}, \tag{5.2.12}$$

$$\rho_{22}(v) = \frac{\lambda_2(v)}{\gamma_2} - \bar{N}(v) \frac{I\gamma_2\Gamma_{21}}{(\Delta + kv)^2 + \Gamma_{21}^2 (1 + 2I\eta)}. \tag{5.2.13}$$

Previously, we obtained the response of the whole medium (the total polarization P in Eq. 3.9.11) by calculating an average microscopic dipole and simply multiplying by N, the number of absorbers per unit volume. Here, the weighting function for atoms of a particular velocity is already included in the expression for ρ_{21} through the normalized occupation factor $\bar{N}(v)$. In the present situation, we must integrate over velocity in addition to multiplying by N.

$$P(z, t) = N \int_{-\infty}^{\infty} (\mu_{12}\rho_{21} + \mu_{21}\rho_{12}) \, dv. \tag{5.2.14}$$

By comparing this with Eq. (3.10.2), which defines susceptibilities according to

$$P(z, t) = \frac{1}{2}\varepsilon_0 \mathrm{E}_0 \left\{ \chi(\omega) e^{-i(\omega t - kz)} + \chi(-\omega) e^{i(\omega t - kz)} \right\}, \tag{5.2.15}$$

we can look at the in-phase and out-of-phase response by evaluating real and imaginary parts of the linear susceptibility (quantities related by the Kramers-Kronig relations):

$$\chi = \chi' + i\chi''. \tag{5.2.16}$$

$$\chi(\omega) = \frac{N\mu}{\varepsilon_0 E_0} \int_{-\infty}^{\infty} \tilde{\rho}_{21}(v)\, dv = -i \frac{N\mu^2}{\varepsilon_0 \hbar} \int_{-\infty}^{\infty} \left[\frac{\Gamma_{21} - i(\Delta + kv)}{(\Delta + kv)^2 + \Gamma_{21}^2(1 + 2I\eta)} \right] \bar{N}(v)\, dv.$$

$$\tag{5.2.17}$$

We assume $\bar{N}(v)$ has the form

$$\bar{N}(v) = \frac{\Lambda_0}{\sqrt{\pi} v_0} \exp\left(-v^2/v_0^2\right), \tag{5.2.18}$$

where v_0 is the $1/e$ width of the velocity distribution, and evaluate real and imaginary parts of Eq. (5.2.17) corresponding to dispersion and absorption of the sample, respectively. The imaginary or absorptive part is

$$\chi'' = \frac{N\Lambda_0\mu^2}{\sqrt{\pi}\varepsilon_0\hbar} \int_{-\infty}^{\infty} \left[\frac{\Gamma_{12}}{(\Delta + kv)^2 + \Gamma_{21}^2(1 + 2I\eta)} \right] \frac{\exp(-v^2/v_0^2)}{\sqrt{\pi} v_0}\, dv. \tag{5.2.19}$$

The integral in Eq. (5.2.19) is the convolution of a Gaussian and a Lorentzian. This is the plasma dispersion function for which tables and asymptotic forms are available in mathematical handbooks.

When the linewidth kv_0 of the Doppler distribution greatly exceeds the homogeneous width Γ_{12} the plasma dispersion function has a simple asymptotic form, and

$$\chi'' = \frac{N\Lambda_0\mu^2 e^{-\Delta^2/k^2 v_0^2}}{\sqrt{\pi}\varepsilon_0\hbar k v_0 (1 + 2I\eta)^{1/2}} \int_{-\infty}^{\infty} \frac{\Gamma_p}{x^2 + \Gamma_p^2}\, dx = \frac{\sqrt{\pi} N\Lambda_0\mu^2 e^{-\Delta^2/k^2 v_0^2}}{\varepsilon_0\hbar k v_0 (1 + 2I\eta)^{1/2}}. \tag{5.2.20}$$

This limit, in which $kv_0 \gg \Gamma_p \equiv (1 + 2I\eta)^{1/2}\Gamma_{12}$, is known as the Doppler limit and also permits asymptotic evaluation of the dispersion.

$$\chi' = -\frac{N\Lambda_0\mu^2}{\sqrt{\pi}\varepsilon_0\hbar v_0} \int_{-\infty}^{\infty} \frac{(\Delta + kv)\, e^{-v^2/v_0^2}}{(\Delta + kv)^2 + \Gamma_p^2}\, dv$$

$$= -\frac{N\Lambda_0\mu^2}{\sqrt{\pi}\varepsilon_0\hbar v_0} \int_{-\infty}^{\infty} e^{-(x-\Delta)^2/k^2 v_0^2} \frac{x\, dx}{x^2 + \Gamma_p^2}$$

$$= -\frac{N\Lambda_0\mu^2}{\sqrt{\pi}\varepsilon_0\hbar v_0} e^{-\Delta^2/k^2 v_0^2} \int_{-\infty}^{\infty} \frac{e^{2\Delta x/k^2 v_0^2} x e^{-x^2/k^2 v_0^2}}{x^2 + \Gamma_p^2}\, dx$$

$$= -\frac{2\Delta N \Lambda_0 \mu^2}{\sqrt{\pi}\varepsilon_0 \hbar k^3 v_0^3} e^{-\Delta^2/k^2 v_0^2} \int\limits_{-\infty}^{\infty} \frac{x^2}{x^2 + \Gamma_p^2} e^{-x^2/k^2 v_0^2} dx$$

$$= -\frac{2\Delta N \Lambda_0 \mu^2}{\varepsilon_0 \hbar (kv_0)^2} e^{-\Delta^2/k^2 v_0^2}. \tag{5.2.21}$$

Notice that in the low intensity limit $I \to 0$ both χ' and χ'' are constants, so that we recover the usual relationship $P = \varepsilon_0 \chi E$ for linear response with χ a constant. On the other hand, for high intensities $I \gg 1$, the absorption becomes nonlinear and $\chi'' \propto 1/\sqrt{I}$ in this inhomogeneously broadened system according to Eq. (5.2.20). This behavior is quite distinct from the absorption saturation in homogeneously broadened systems, as described by Eq. (5.1.15) for example (see Refs. [5.3] and [5.14]). There $\chi'' \propto 1/I$ for $I \gg 1$. Finally, notice that the dispersion, by which we mean χ', does not saturate. Physically, this is because all atoms contribute to the dispersion, even in the low intensity limit.

5.2.2 Moving atoms in a standing wave

We consider the same standing wave interaction introduced previously in Eq. (5.1.29).

$$V(t) = -2\hbar\Omega \cos kz \cos \omega t. \tag{5.2.22}$$

For moving atoms, Eqs. (5.1.30)–(5.1.33) become

$$\left(\frac{\partial}{\partial t} + v\frac{\partial}{\partial z}\right)\rho_{11} = \lambda_1 - \gamma_1\rho_{11} + 2i\Omega \cos kz \cos \omega t \left(\rho_{21} - \rho_{12}\right), \tag{5.2.23}$$

$$\left(\frac{\partial}{\partial t} + v\frac{\partial}{\partial z}\right)\rho_{22} = \lambda_2 - \gamma_2\rho_{22} - 2i\Omega \cos kz \cos \omega t \left(\rho_{21} - \rho_{12}\right), \tag{5.2.24}$$

$$\left(\frac{\partial}{\partial t} + v\frac{\partial}{\partial z}\right)\rho_{21} = -\left(\Gamma_{21} + i\omega_0\right)\rho_{21} - 2i\Omega \cos kz \cos \omega t \left(\rho_{22} - \rho_{11}\right), \tag{5.2.25}$$

$$\dot{\rho}_{12} = \dot{\rho}_{21}^*. \tag{5.2.26}$$

Since the standing wave corresponds to two oppositely directed traveling waves, we expect off-diagonal density matrix elements of the form

$$\rho_{21} = e^{-i\omega t}\left(\rho_+ e^{ikz} + \rho_- e^{-ikz}\right). \tag{5.2.27}$$

Populations will also display spatial variation, changing sinusoidally at twice the periodicity of either traveling wave. This is the same behavior we calculated earlier for stationary atoms in a standing wave field. Hence we expect populations of the form

$$\rho_{11} = \bar{\rho}_{11} + \left[\rho_1 e^{2ikz} + \rho_1^* e^{-2ikz}\right], \tag{5.2.28}$$

$$\rho_{22} = \bar{\rho}_{22} + \left[\rho_2 e^{2ikz} + \rho_2^* e^{-2ikz}\right], \tag{5.2.29}$$

where $\bar{\rho}_{11}$, $\bar{\rho}_{22}$ are constant, spatially averaged values of the populations.

Using the RWA, we find

$$\cos kz \cos \omega t \,(\rho_{21} - \rho_{12}) = \frac{1}{4} \left\{ (\rho_+ - \rho_-^*) \left[e^{2ikz} + 1 \right] - (\rho_+^* - \rho_-) \left[e^{-2ikz} + 1 \right] \right\},$$
(5.2.30)

$$\cos kz \cos \omega t \,(\rho_{22} - \rho_{11}) = \frac{1}{4} \left\{ (\bar{\rho}_{22} - \bar{\rho}_{11}) \left[e^{-i(\omega t + kz)} + e^{-i(\omega t - kz)} \right] \right.$$
$$\left. + (\rho_2 - \rho_1) \, e^{-i(\omega t - kz)} + (\rho_2^* - \rho_1^*) \, e^{-i(\omega t + kz)} \right\}. \quad (5.2.31)$$

Substitution of Eqs. (5.2.28)–(5.2.31) into our starting equations gives us the main working equations of this subsection.

$$(-i\omega + ikv)\rho_+ e^{-i(\omega t - kz)} + (-i\omega - ikv)\rho_- e^{-i(\omega t + kz)}$$
$$= -(\Gamma_{21} + i\omega_0) \left[\rho_+ e^{-i(\omega t - kz)} + \rho_- e^{-i(\omega t + kz)} \right] - i(\Omega/2)(\bar{\rho}_{22} - \bar{\rho}_{11}) e^{-i(\omega t + kz)}$$
$$+ \left[-i(\Omega/2)(\bar{\rho}_{22} - \bar{\rho}_{11}) + -i(\Omega/2)(\rho_2 - \rho_1) \right] e^{-i(\omega t - kz)}$$
$$- i(\Omega/2)(\rho_2^* - \rho_1^*) e^{-i(\omega t + kz)} \dots$$
(5.2.32)

$$(\gamma_1 + 2ikv)\,\rho_1 e^{2ikz} + (\gamma_1 - 2ikv)\,\rho_1^* e^{-2ikz} = \lambda_1 - \gamma_1 \bar{\rho}_{11}$$
$$+ \frac{i\Omega}{4} \left\{ \rho_+ \left[e^{2ikz} + 1 \right] + \rho_- \left[e^{-2ikz} + 1 \right] - \rho_+^* \left[e^{-2ikz} + 1 \right] - \rho_-^* \left[e^{2ikz} + 1 \right] \right\}$$
(5.2.33)

$$(\gamma_2 + 2ikv)\,\rho_2 e^{2ikz} + (\gamma_2 - 2ikv)\,\rho_2^* e^{-2ikz} = \lambda_2 - \gamma_2 \bar{\rho}_{22}$$
$$- \frac{i\Omega}{4} \left\{ \rho_+ \left[e^{2ikz} + 1 \right] + \rho_- \left[e^{-2ikz} + 1 \right] - \rho_+^* \left[e^{-2ikz} + 1 \right] - \rho_-^* \left[e^{2ikz} + 1 \right] \right\}$$
(5.2.34)

Solution of these equations yields

$$\rho_2 - \rho_1 = -\frac{i\Omega}{4} \left[\frac{1}{\gamma_1 + 2ikv} + \frac{1}{\gamma_2 + 2ikv} \right] (\rho_+ - \rho_-^*), \quad (5.2.35)$$

$$\bar{\rho}_{22} - \bar{\rho}_{11} = \bar{N} - \frac{i\Omega}{4} \left(\rho_+ + \rho_- - \rho_+^* - \rho_-^* \right) \left[\frac{1}{\gamma_1} + \frac{1}{\gamma_2} \right]. \quad (5.2.36)$$

Use of these two relations in Eq. (5.2.32), together with the complex conjugate of Eq. (5.2.32), permits an explicit solution for $(\rho_+ - \rho_-^*)$. One finds

$$(\rho_+ - \rho_-^*)$$
$$= -i\Omega(L_+ + L_-^*)\bar{N} / \left[1 + \frac{\Omega^2}{4} \left(\frac{1}{\gamma_1} + \frac{1}{\gamma_2} + \frac{1}{\gamma_1 + 2ikv} + \frac{1}{\gamma_2 + 2ikv} \right) (L_+ + L_-^*) \right],$$
(5.2.37)

where

$$L_+ \equiv \frac{1}{i\left(\Delta + kv\right) + \Gamma_{21}}, L_- \equiv \frac{1}{i\left(\Delta - kv\right) + \Gamma_{21}}. \tag{5.2.38}$$

Substitution of Eq. (5.2.37) into Eq. (5.2.36) then yields the main result, namely an explicit expression for the average population difference in states 1 and 2 in the presence of light.

$$\bar{\rho}_{22} - \bar{\rho}_{11} = \bar{N} \left\{ 1 - \frac{\Omega^2}{4} \left(\frac{1}{\gamma_1} + \frac{1}{\gamma_2} \right) \right.$$

$$\times \left[\left((L_+ + L_-^*)^{-1} + \frac{\Omega^2}{4} \left(\frac{1}{\gamma_1} + \frac{1}{\gamma_2} + \frac{1}{\gamma_1 + 2ikv} + \frac{1}{\gamma_2 + 2ikv} \right) \right)^{-1} + c.c. \right] \right\} \tag{5.2.39}$$

Now let us examine this result in two special cases to understand its meaning:

(a) First, in the limit of no atomic motion ($v \to 0$), evaluation of Eq. (5.2.39) simply gives

$$\bar{\rho}_{22} - \bar{\rho}_{11} = \bar{N}, \tag{5.2.40}$$

and

$$\rho_{22} - \rho_{11} = \bar{N} \left\{ 1 - \frac{\Omega^2}{\Gamma} \left[\frac{(L_+ + L_-^*)}{1 + \Omega^2(L_+ + L_-^*)/\Gamma} \right] \cos 2kz \right\}, \tag{5.2.41}$$

where we have taken $\gamma_1 = \gamma_2 = \Gamma$ for simplicity. Notice we recover the simple spatial hole-burning dependence of the population difference of Eq. (5.1.40) in this limit.

(b) Second, we can specialize to a closed two-level system by taking the following values for key rates in the system:

$$\lambda_2 = 0; \lambda_1 = \gamma_1 W\left(v\right); \gamma_1 = \gamma_2 = \Gamma; \Gamma_{21} = \Gamma/2.$$

The quantity $W(v)$ normalizes the population at velocity v according to

$$\rho_{11}(v) + \rho_{22}(v) = W\left(v\right) \tag{5.2.42}$$

and is therefore also given by the relation

$$W\left(v\right) = -\bar{N}(v) = \frac{\lambda_1(v)}{\Gamma(v)}, \tag{5.2.43}$$

when there is no pumping into level 2. These substitutions ensure that no time-dependent accumulation of probability takes place in the analysis. The ground state population of the ground state is constant in the absence of light. In this instance, the population difference in Eq. (5.2.36) is

$$\bar{\rho}_{22} - \bar{\rho}_{11} = \bar{N} - \frac{i\Omega}{2\Gamma} \left(\rho_+ + \rho_- - \rho_+^* - \rho_-^* \right). \tag{5.2.44}$$

By combining Eqs. (5.2.37) and (5.2.35) with Eqs. (5.2.30) and (5.2.31), we can obtain an expression for $(\rho_+ - \rho_-^*)$ in terms of $(\bar{\rho}_{22} - \bar{\rho}_{11})$ which is particularly amenable to analysis, showing that saturation of moving atoms exhibits features which are quite different from that of stationary atoms. The result is

$$\rho_+ - \rho_-^* = -i\Omega(L_+ + L_-^*)(\bar{\rho}_{22} - \bar{\rho}_{11}) / \left[1 + 2(\Omega/2)^2(L_+ + L_-^*)/(\Gamma + 2ikv)\right]. \tag{5.2.45}$$

The difference between this quantity and its conjugate is what is needed to evaluate Eq. (5.2.44).

$$(\rho_+ - \rho_-^*) - (\rho_+^* - \rho_-) = \left\{ \frac{-i\Omega(L_+ + L_-^*)(\bar{\rho}_{22} - \bar{\rho}_{11})}{1 + 2(\Omega/2)^2(L_+ + L_-^*)/(\Gamma + 2ikv)} + c.c. \right\}. \tag{5.2.46}$$

Now we can make use of Eq. (5.2.46) in Eq. (5.2.44) to determine the average population difference in the presence of light. This yields

$$\bar{\rho}_{22} - \bar{\rho}_{11} = \bar{N} - \frac{\Omega^2}{2\Gamma} \left\{ \frac{(\bar{\rho}_{22} - \bar{\rho}_{11})}{(L_+ + L_-^*)^{-1} + 2(\Omega/2)^2/(\Gamma + 2ikv)} + c.c. \right\}$$

$$= \bar{N} - \frac{\Omega^2}{2\Gamma} \left\{ \frac{(\Gamma + 2ikv)(\bar{\rho}_{22} - \bar{\rho}_{11})}{\Delta^2 - k^2v^2 + i\Gamma kv + (\Gamma/2)^2 + 2(\Omega/2)^2} + c.c. \right\}. \tag{5.2.47}$$

The final result is

$$\bar{\rho}_{11} - \bar{\rho}_{22} = \frac{W(v)}{1 + 2(\Omega/2\Gamma)^2 \left[L(kv + \Omega') + L(kv - \Omega')\right]}, \tag{5.2.48}$$

where

$$\Omega' \equiv \left[\Delta^2 + (\Omega/2)^2/2\right]^{1/2}, \tag{5.2.49}$$

and

$$L(x) \equiv (\Gamma/2)^2 / [(\Gamma/2)^2 + x^2], x \equiv kv \pm \Omega'. \tag{5.2.50}$$

Notice in Fig. 5.7 that two Lorentzian-shaped holes are burned in the population difference $\rho_{11} - \rho_{22}$ plotted as a function of velocity. These are frequency-domain holes since velocity is proportional to frequency shift across the Doppler-broadened lineshape. This makes obvious sense because the standing wave is composed of two traveling waves each of which burns its own hole.

Two remarkable consequences of the atomic motion under saturation conditions are contained in the population difference expression given by Eq. (5.2.48). First, the spectral holes generated by incident light are not located at the Doppler-shifted detuning values $kv = \pm\Delta$. Instead holes are burned at slightly different values, given by

$$kv = \pm\Omega' \cong \pm(\Delta + \Omega^2/16\Delta + \ldots). \tag{5.2.51}$$

This may be interpreted to mean that there is a light-induced shift of the atomic resonance (called the *light shift*) which is proportional to intensity. The magnitude of
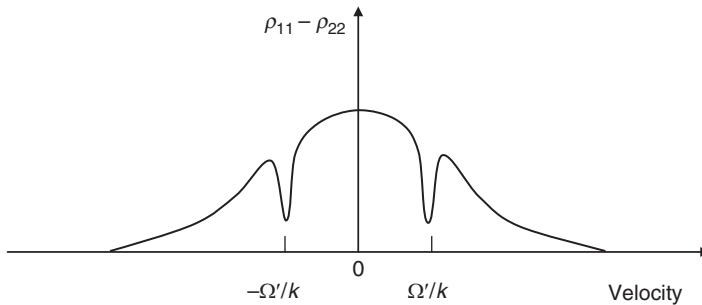
Figure 5.7 *Spectral hole-burning in a system of moving atoms subjected to standing wave excitation. In multi-level systems, hole-burning can be used for precision spectroscopy of energy level separations [5.2].*

this quadratic shift versus field amplitude is

$$\Delta\omega \cong \Omega^2/16\Delta. \tag{5.2.52}$$

The interaction between one of the waves and an atom is altered by the presence of the second wave in an unanticipated way. A second, related consequence is that if the pump frequency is tuned to exact resonance the absorption spectrum still appears to contain two features. The resonant hole-burning spectrum is a doublet. According to Eq. (5.2.48), when $\Delta = 0$, we still have two Lorentzians superimposed on the velocity distribution, centered at

$$kv = \pm\Omega/2\sqrt{2}. \tag{5.2.53}$$

The doublet predicted for zero detuning in Fig. 5.8 is a reflection of AC Stark or Rabi splitting under resonant pumping conditions. However, while the analysis presented here anticipates Rabi splitting and the light shift effect, it is not strictly valid when $\Delta = 0$, since we assumed $\Delta >> \Gamma$ in the derivation. A proper analysis of strong field effects on resonance will again have to await the analytic approaches of Chapter 6. Additional reading on the light shift may be found in Refs. 5.4 and 5.5.
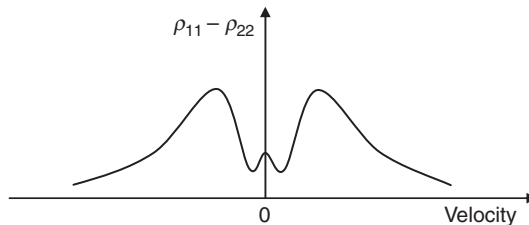
Figure 5.8 *Spectral hole-burning in a system of moving atoms subjected to standing wave excitation. The spectrum reveals that even at zero detuning ($\Delta = 0$) saturation produces a doublet due to the "light shift" effect.*

5.3   Tri-level coherence

5.3.1   Two-photon coherence

We now turn to interactions involving two fields and three or more energy levels. Figure 5.9 shows three basic types of three-level systems. In discussing coherence involving three levels, we shall focus on only one of these, the cascade configuration, since only slight modifications of the analysis are needed to describe V- and Λ-configurations. An important working assumption is that level 1 is optically connected to 2 ($\mu_{12} \neq 0$), level 2 is connected to 3 ($\mu_{23} \neq 0$), but that level 1 is not connected to level 3 ($\mu_{13} = 0$). These properties are of course determined by the symmetry character of the eigenstates. We shall also assume that the frequencies of two incident light fields E_1 and E_2 are close enough to their intended transitions that they do not induce any unintended transitions at other detunings.

$$E_1(z, t) = E_1 \cos(\omega_1 t + k_1 z), \tag{5.3.1}$$

$$E_2(z, t) = E_2 \cos(\omega_2 t + k_2 z). \tag{5.3.2}$$

Since we now have more than one transition to consider, the resonance Rabi frequency acquires a subscript to label the relevant transition, according to

$$\Omega_i \equiv \mu_i E_i / \hbar, \tag{5.3.3}$$

where $i = 1, 2$ and μ_i is the dipole moment associated with field amplitude E_i.

The density matrix equation may then be written out in two groups as populations:

$$\dot{\rho}_{11} = \lambda_1 - \gamma_1 \rho_{11} + i\Omega_1 \cos(\omega_1 t + k_1 z)(\rho_{21} - \rho_{12}),$$

$$\dot{\rho}_{22} = -\gamma_2 \rho_{22} - i\Omega_1 \cos(\omega_1 t + k_1 z)(\rho_{21} - \rho_{12}) + i\Omega_2 \cos(\omega_2 t + k_2 z)(\rho_{32} - \rho_{23}),$$

$$\dot{\rho}_{33} = -\gamma_3 \rho_{33} - i\Omega_2 \cos(\omega_2 t + k_2 z)(\rho_{32} - \rho_{23}), \tag{5.3.4}$$

and coherences:

$$\dot{\rho}_{21} = -(\Gamma_{21} + i\omega_{21})\rho_{21} - i\Omega_1 \cos(\omega_1 t + k_1 z)(\rho_{22} - \rho_{11}) + i\Omega_2 \cos(\omega_2 t + k_2 z)\rho_{31},$$

$$\dot{\rho}_{31} = -(\Gamma_{31} + i\omega_{31})\rho_{31} - i\Omega_1 \cos(\omega_1 t + k_1 z)\rho_{32} + i\Omega_2 \cos(\omega_2 t + k_2 z)\rho_{21},$$
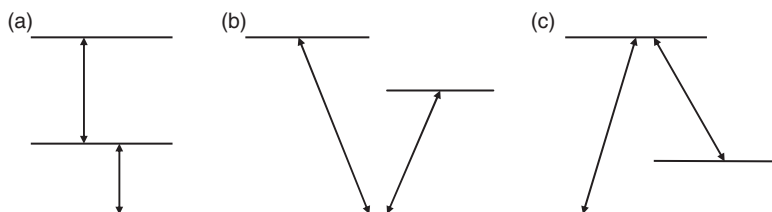
Figure 5.9 *Basic configurations of energy levels and allowed transitions in three-level systems.* (a) *Cascade,* (b) *V-configuration, and* (c) *Λ- or inverted V-configuration.*

$$\dot{\rho}_{32} = -\left(\Gamma_{32} + i\omega_{32}\right)\rho_{32} - i\Omega_2 \cos\left(\omega_2 t + k_2 z\right)\left(\rho_{33} - \rho_{22}\right) + -i\Omega_1 \cos\left(\omega_1 t + k_1 z\right)\rho_{31}.$$
$$(5.3.5)$$

Since several resonant frequencies appear in Eq. (5.3.5), the subscripts indicating the levels involved have been retained. For example ω_{21} is the positive frequency difference between levels 1 and 2. To illustrate how various factors control coherences in this system, consider a simplified approach to solving these equations. In Section 5.2, we considered values of the incoherent pumping rates that effectively closed the system. If we again assume there is no pumping except to the lowest level, we have

$$\bar{N} = -\lambda_1/\gamma_1. \tag{5.3.6}$$

Now the RWA may be applied by writing

$$\rho_{21} = \tilde{\rho}_{21} \exp[-i(\omega_1 t + k_1 z)],$$

$$\rho_{32} = \tilde{\rho}_{32} \exp[-i(\omega_2 t + k_2 z)],$$

$$\rho_{31} = \tilde{\rho}_{31} \exp[-i(\omega_1 + \omega_2)t - i(k_1 + k_2)z], \tag{5.3.7}$$

and using a perturbation approach in which we set $E_2 = 0$ in first order and $E_1 = 0$ in second order. We shall use the superscript 1 to indicate the presence of field E_1 rather than the order of perturbation in the first step. The solutions are

$$\rho_{11}^{(1)} = -\bar{N} \left[\frac{1 + \dfrac{\Omega_1^2}{4\gamma_2}\left(L_1 + L_1^*\right)}{1 + \dfrac{\Omega_1^2}{4}\left(\dfrac{1}{\gamma_1} + \dfrac{1}{\gamma_2}\right)\left(L_1 + L_1^*\right)} \right], \tag{5.3.8}$$

$$\rho_{22}^{(1)} = -\bar{N} \left[\frac{\dfrac{\Omega_1^2}{4\gamma_2}\left(L_1 + L_1^*\right)}{1 + \dfrac{\Omega_1^2}{4}\left(\dfrac{1}{\gamma_1} + \dfrac{1}{\gamma_2}\right)\left(L_1 + L_1^*\right)} \right], \tag{5.3.9}$$

$$\tilde{\rho}_{21}^{(1)} = -\bar{N} \left[\frac{i\Omega_1 L_1}{1 + \dfrac{\Omega_1^2}{4}\left(\dfrac{1}{\gamma_1} + \dfrac{1}{\gamma_2}\right)\left(L_1 + L_1^*\right)} \right], \tag{5.3.10}$$

where $L_1 \equiv \left[i\left(\Delta_1 - k_1 v\right) + \Gamma_{21}\right]^{-1}$ and $\Delta_1 \equiv \omega_{21} - \omega_1$. Now let us calculate coherences involving level 3 by turning on field E_2. We work only with the last two equations of Eq. (5.3.5). With the substitutions of Eq. (5.3.7), these relations yield

$$\tilde{\rho}_{31}^{(2)} = -\left(\frac{i\Omega_1}{2}\right)L_{12}^*\tilde{\rho}_{32}^{(2)} + \left(\frac{i\Omega_2}{2}\right)L_{12}^*\tilde{\rho}_{21}^{(1)}, \tag{5.3.11}$$

$$\tilde{\rho}_{32}^{(2)} = i\Omega_2 L_2^*\rho_{22}^{(1)} - \left(\frac{i\Omega_1}{2}\right)L_2^*\tilde{\rho}_{31}^{(2)}, \tag{5.3.12}$$

where we have defined additional resonant denominators $L_2 \equiv [i\,(\Delta_2 - k_2 v) + \Gamma_{21}]^{-1}$ and $L_{12} \equiv [[i\,(\Delta_1 + \Delta_2) - v\,(k_1 + k_2)] + \Gamma_{31}]^{-1}$ with $\Delta_2 \equiv \omega_{32} - \omega_2$.

Solution of the coupled equations (5.3.8)–(5.3.12) now yields

$$\tilde{\rho}_{32}^{(2)} = \left[\frac{i\Omega_2 L_2^* \rho_{22}^{(1)} + \left(\dfrac{\Omega_1 \Omega_2}{4}\right) L_2^* L_{12}^* \tilde{\rho}_{21}^{(1)}}{1 + \left(\dfrac{\Omega_1}{2}\right)^2 L_2^* L_{12}^*} \right], \tag{5.3.13}$$

$$\tilde{\rho}_{31}^{(2)} = \left[\frac{\left(\dfrac{i\Omega_2}{2}\right) L_{12}^* - \left(\dfrac{i\Omega_1^2 \Omega_2}{8}\right) L_2^* (L_{12}^*)^2}{1 + \left(\dfrac{\Omega_1}{2}\right)^2 L_2^* L_{12}^*} \right] \tilde{\rho}_{21}^{(1)} + \left[\frac{\left(\dfrac{\Omega_1 \Omega_2}{2}\right) L_2^*}{1 + \left(\dfrac{\Omega_1}{2}\right)^2 L_{2^*} L_{12}^*} \right] \rho_{22}^{(1)}. $$

$$\tag{5.3.14}$$

Notice that there are two contributions to both the tri-level coherences $\tilde{\rho}_{31}^{(2)}$ and $\tilde{\rho}_{32}^{(2)}$. One is proportional to the population change in level 2, namely to $\rho_{22}^{(1)}$, and the other depends on the induced coherence $\tilde{\rho}_{21}^{(1)}$. A fundamental difference therefore emerges between $\tilde{\rho}_{31}^{(2)}$ and $\tilde{\rho}_{32}^{(2)}$. The coherence between levels 2 and 3 leads to radiation, whereas that between levels 1 and 3 does not. This is because the polarization in the former case, developed on the 3↔2 transition, is

$$P(\omega_2) = (\mu_{32}\rho_{23} + \mu_{23}\rho_{32}) \neq 0.$$

Both the dipole moment μ_{32} and the coherence $\tilde{\rho}_{32}^{(2)}$ itself are nonzero. By contrast, the coherence between levels 1 and 3 does not radiate because

$$P(\omega_1 + \omega_2) = (\mu_{31}\rho_{13} + \mu_{13}\rho_{31}) = 0.$$

The excitation $\tilde{\rho}_{31}^{(2)}$ is therefore an example of a non-radiative, two-photon coherence.

5.3.2   Zeeman coherence

We now consider another kind of tri-level coherence, involving magnetic sublevels of a nominally two-level system. So far, we have considered the light to be an essentially scalar field E, albeit one that is polarized in some particular direction. We have ignored the possibility that the field conveys angular momentum to the atoms or carries it away. It was assumed that the medium responds merely by charge motion along the polarization direction. Consequently, we reduced the vector interaction $V = -\bar{\mu} \cdot \bar{E}$ to the scalar quantity μE_0. However, this is not always appropriate. Strictly speaking, the field $\bar{E}$ is vectorial and is capable of changing the angular momentum state of atoms, or the magnetic aspects of the wavefunction, when its axial rather than polar components exert themselves.
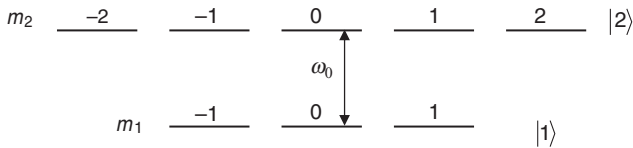
Figure 5.10 *Magnetic sublevels of a quasi-two-level system with* $J = 1$ *ground state and a* $J = 2$ *excited state. Sublevels are distinguished by* m_j, *the quantum number specifying projections of* J *on the quantization axis for each state.*

To investigate the coherences which can be established between selected magnetic sublevels using circularly polarized light, we shall apply second-order perturbation theory to the density matrix and use the Wigner–Eckart (W–E) theorem (Appendix H) to keep track of vector properties of V. As usual we need to determine matrix elements $V_{ij} = \langle i|V|j \rangle$ of the atom–field interaction. Consider a two-level system with magnetic degeneracy like that in Fig. 5.10. We write the field in irreducible form as

$$\bar{E}(z, t) = -\frac{1}{2}\left\{E_+\hat{\varepsilon}_- e^{-i(\omega t - kz)} + E_-\hat{\varepsilon}_+ e^{-i(\omega t - kz)}\right\} + c.c., \qquad (5.3.15)$$

where

$$\hat{\varepsilon}_\pm = \mp(\hat{x} \pm i\hat{y})\big/\sqrt{2}, \qquad (5.3.16)$$

are the transverse basis states of the rank one spherical tensor. By writing the field–atom interaction as an irreducible tensor (see Appendix H), we can make use of the W–E theorem to assist with the evaluation of its matrix elements.

If $T_q^{(k)}$ is an irreducible spherical tensor operator, then according to the W–E theorem (Appendix H), its matrix element can be decomposed as follows:

$$\langle \alpha j m| T_q^{(k)} |\alpha' j' m' \rangle = (-1)^{j-m}\langle \alpha j \| T^{(k)} \| \alpha' j' \rangle \begin{pmatrix} -j & k & j' \\ -m & q & m' \end{pmatrix}, \qquad (5.3.17)$$

where $\langle \alpha j \| T^{(k)} \| \alpha' j' \rangle$ is called the reduced matrix element, and $\begin{pmatrix} -j & k & j' \\ -m & q & m' \end{pmatrix}$ is a Wigner 3-j symbol.

The importance of the W–E theorem is that it separates the matrix element into two distinct parts. The 3-j symbol contains all the geometrical aspects of the problem and is tabulated in many references [5.6]. The so-called reduced matrix element $\langle \|T\| \rangle$ is the "real" multipole transition moment, a quantity that is independent of coordinate system or geometry, which otherwise would be a rather ill-defined (origin-dependent) quantity in complex vector spaces.

The first step in applying Eq. (5.3.17) to the problem at hand is to write the interaction Hamiltonian V itself as an irreducible tensor. $V = -\bar{\mu} \cdot \bar{E}$ is a scalar

product of the field vector and the dipole moment given by

$$\bar{\mu} = e\bar{r} = e\left[x\hat{x} + y\hat{y} + z\hat{z}\right]$$

$$= \frac{1}{2}er\left[(\hat{x} - i\hat{y})\exp i\phi + (\hat{x} + i\hat{y})\exp(-i\phi)\right] + \hat{z}er\cos\theta$$

$$= er\left[\sum_{q=-1}^{1}(-1)^q C_q^{(1)}\hat{\varepsilon}_{-q}\right]. \tag{5.3.18}$$

Here we have introduced the quantity $C_q^{(\ell)}$, which is the Racah tensor of rank l, related to the spherical harmonics by $C_q^{(\ell)} \equiv \left(\frac{4\pi}{2\ell+1}\right)^{1/2} Y_q^{(\ell)}$. On the basis of Eq. (5.3.18), we see that the general dipole moment μ has three irreducible tensor components.

$$\mu_{\pm} = -erC_{\pm 1}^{(1)},$$

$$\mu_0 = erC_0^{(1)}.$$

The field $\bar{E}$ in Eq. (5.3.15) is already in irreducible tensor form, since $\hat{\varepsilon}_{\pm}$ are basis vectors of the rank one spherical tensor. Ignoring time dependence, the interaction is therefore

$$V = -\bar{\mu}\cdot\bar{E} = -\sum_q (-1)^q \mu_q E_{-q}$$

$$= +er\left\{\sum_q (-1)^q C_q^{(\ell)} E_{-q}\right\}$$

$$= -\frac{1}{2}\{\mu_+ E_- + \mu_- E_+\}. \tag{5.3.19}$$

We need matrix elements of V starting from state j and ending up in state i. Adopting the notation $|j\rangle = |\alpha'j'm'\rangle$ and $|i\rangle = |\alpha j m\rangle$ for initial and final states, we find

$$\langle V_{ij}\rangle_{E_-} = \langle i|V_-|j\rangle = \frac{1}{2}\langle \alpha j m|\mu_+ E_-|\alpha'j'm'\rangle = \frac{1}{2}eE_-\langle \alpha j m|rC_+^{(1)}|\alpha'j'm'\rangle,$$

$$\langle i|V_-|j\rangle = \frac{eE_-}{2}\langle \alpha j \|rC^{(1)}\|\alpha'j'\rangle (-1)^{j-m}\begin{pmatrix} j & l & j' \\ -m & l & m' \end{pmatrix}, \tag{5.3.20}$$

by using the W–E theorem.

$\begin{pmatrix} j & l & j' \\ -m & l & m' \end{pmatrix}$ is a Wigner 3-j symbol that renders the matrix element V_{ij} zero unless

$$\Delta j = j - j' = 0, \pm 1$$

$$\Delta m = m - m' = +1$$

$$j = 0 \longleftrightarrow\!\!\!\times\!\!\!\longrightarrow j' = 0. \tag{5.3.21}$$
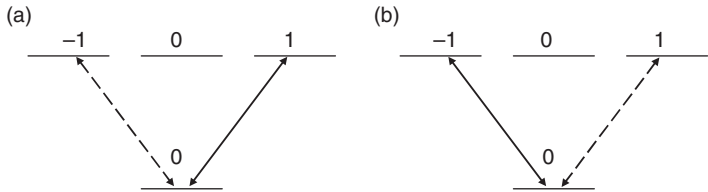
Figure 5.11 *Allowed absorption transitions (solid arrows) induced to different magnetic sublevels by circularly polarized light with* (a) *positive helicity ($\Delta m = +1$) and* (b) *negative helicity ($\Delta m = -1$). Forbidden transitions are dashed.*

These selection rules show that to first order in the perturbation, positive helicity light ($\bar{E}_- \propto E_-\hat{\varepsilon}_+$) excites only absorptive transitions in which m increases by one unit to $m = m' + 1$. That is, light with a positive projection of angular momentum on $\hat{z}$ adds one unit of momentum to the atom per absorbed quantum. Conversely in emission it carries away one unit of angular momentum. This behavior is illustrated in Fig. 5.11 on a $J = 0 \rightarrow J = 1$ transition of a system that is initially in the ground state and is subjected to circularly polarized light of positive or negative helicity. Only one transition takes place, with an attendant change in the magnetic quantum number of the occupied state.

Now consider what happens in a second-order interaction with a single circularly polarized field using perturbation theory (Appendix D).

$$i\hbar\dot{\rho}^{(2)} = \left[H_0, \rho^{(2)}\right] + \left[V^{(1)}, \rho^{(1)}\right] - i\hbar(\partial\rho^{(2)}/\partial t). \tag{5.3.22}$$

With the rotating wave approximation, the interaction matrix elements have the form

$$V_{m_{j2}m_{j1}} = -\frac{1}{2}\left\{\mu_-^{(m)} E_+ \exp(ikz) + \mu_+^{(m)} E_- \exp(ikz)\right\} \exp(-iwt), \tag{5.3.23}$$

and

$$V_{m_{j1}m_{j2}} = -\frac{1}{2}\left\{\mu_-^{(m)} E_+ \exp(ikz) + \mu_+^{(m)} E_- \exp(ikz)\right\}^* \exp(iwt). \tag{5.3.24}$$

For stationary two-level atoms we readily find the off-diagonal component

$$-iw\rho^{(1)}_{m_2m_1} = -iw_0\rho_{m_2m_1} - (i/\hbar)V_{m_2m_1}(\rho^{(0)}_{m_1m_1} - \rho^{(0)}_{m_2m_2}) - \Gamma_{m_2m_1}\rho^{(1)}_{m_2m_1}, \tag{5.3.25}$$

$$\tilde{\rho}^{(1)}_{m_2m_1} = \frac{\tilde{V}_{m_2m_1}}{\hbar[\Delta - i\Gamma_{m_2m_1}]}(\rho^{(0)}_{m_1m_1} - \rho^{(0)}_{m_2m_2}). \tag{5.3.26}$$

In second order, the populations of states 1 and 2 change. Since there are sub-states within state 2, coherent relationships may arise between sub-state populations.

Hence we encounter density matrix elements such as

$$\rho_{m'_2 m_2}^{(2)} = -(i/\hbar\gamma_{m_2}) \left[\tilde{V}_{m'_2 m_1} \tilde{\rho}_{m_1 m_2}^{(1)} - \tilde{\rho}_{m_2 m_1}^{(1)} \tilde{V}_{m_1 m'_2} \right]$$

$$= \frac{-2\Gamma_{m_2 m_1}}{\hbar^2 \gamma_{m_2}} \left[\frac{\tilde{V}_{m'_2 m_1} \tilde{V}_{m_2 m_1}^*}{\Delta^2 + (\Gamma_{m_2 m_1})^2} \right] (\rho_{m_2 m_2}^{(0)} - \rho_{m_1 m_1}^{(0)}). \tag{5.3.27}$$

Upon substitution of the irreducible forms of the interaction given by Eqs. (5.3.23) and (5.3.24), the excited state population reduces to

$$\rho_{m'_2 m_2}^{(2)} = \frac{\Gamma}{2\hbar^2 \gamma_{m_2} [\Delta^2 + (\Gamma_{m_2 m_1})^2]} \left[\{ <\mu_+^*> E_-^* <\mu_+> E_- \} \right.$$

$$+ <\mu_+^*> E_-^* <\mu_-> E_+ + <\mu_-^*> E_+^* <\mu_+> E_-$$

$$+ \left\{ <\mu_-^*> E_+^* <\mu_-> E_+ \} \right] \left(\rho_{m_1 m_1}^{(0)} - \rho_{m_2 m_2}^{(0)} \right). \tag{5.3.28}$$

The first and last terms in Eq. (5.3.28), the ones in curly brackets, involve a sequence of two transitions that individually obey opposite selection rules. However, they are similar overall, because they involve the field combinations $E_-^* E_-$ and $E_+^* E_+$, and mediate two-photon transitions that result in no net angular momentum exchange with the atom. This process merely returns population to its original state as shown in Fig. 5.12, while modifying the occupation probability. This is the origin of common saturation which is an example of nonlinear susceptibility to the driving fields. In this case, the overall selection rule on the initial and final magnetic quantum numbers is

$$m_2 - m'_2 = 0. \tag{5.3.30}$$

The other two terms in Eq. (5.3.28) are driven by the field combinations $E_-^* E_+$ and $E_+^* E_-$. These again mediate sequences of two transitions, but in this case there is an overall exchange of angular momentum. These two-photon transitions obey the selection rule

$$m_2 - m'_2 = \pm 2. \tag{5.3.31}$$
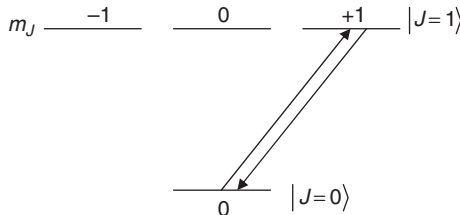
Figure 5.12 *A two-photon transition stimulated by circularly polarized light in a two-level system with magnetically degenerate level 2. The energy states are labeled by their total angular momentum quantum numbers* J = 1 *and* J = 0 *and their projections* m_J *on the quantization axis.*
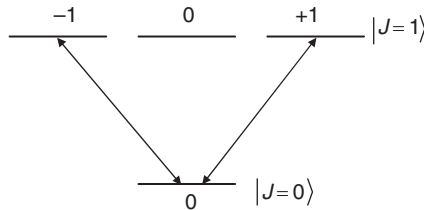
Figure 5.13 *A pair of allowed electric dipole transitions that connects two magnetic sublevels of the same state to establish Zeeman coherence via a two-photon process.*

There is an important difference between the two types of two-photon transition present in the second-order perturbation calculation. The first type connects only two sublevels, whereas the latter connects three. This introduces a new degree of freedom in off-diagonal coherence terms $\rho^{(2)}_{m'_2 m_2}$ established by interactions like $E^*_- E_-$ and $E^*_+ E_+$ that makes them different from an ordinary saturation process. Figure 5.13 makes it clear that it is possible to create phased charge oscillation between sublevels of the *same* state via the polarization of the medium induced by the two-photon transition. This is called a Zeeman coherence.

Zeeman coherences first appear in second order, because the field must act at least twice to return the atom to a different sublevel of the original degenerate manifold. However, they are not diagonal population terms. $\rho_{m'_1 m_1}$ is a diagonal element of the density matrix only if $m'_j = m_j$. If $m'_j \neq m_j$, the initial and final quantum numbers are different and the matrix element is off-diagonal. Interestingly, because there is no energy difference between the two levels between which this coherence has been established, it is non-radiative. In Chapter 7, important applications of non-radiative or "dark" coherences will be covered.

The calculation of the Zeeman coherence for a case like the system shown in Fig. 5.13 can be completed by setting $\rho^{(0)}_{22} \cong 0$ and assuming that thermal equilibrium among sublevels makes their populations equal. Then each of these sublevel populations has a value $\approx \rho^{(0)}_{11}/3$. Consequently, the Zeeman coherence terms alone give the result

$$\rho^{(2)}_{1,-1} = \frac{\Gamma_{12}\rho^{(0)}_{11}}{6\hbar^2\gamma_2(\Delta^2 + \Gamma^2_{12})}$$

$$\times \left\{ \left(E^*_- E_+ \right) \langle 1,-1 | \mu^*_+ \mu_- | 11 \rangle + \left(E^*_+ E_- \right) \langle 11 | \mu^*_- \mu_+ | 1,-1 \rangle \right\}. \qquad (5.3.32)$$

That this two-photon coherence is nonzero may readily be verified by including intermediate states in the two-photon matrix elements of Eq. (5.3.32). Angular momentum is conserved since the $\pm 2\hbar$ furnished by the field is acquired in two allowed steps during the atomic transitions:

$$\langle 11 | \mu^*_- | 00 \rangle \langle 00 | \mu_+ | 1,-1 \rangle \neq 0, \quad (\Delta m = +2), \qquad (5.3.33)$$

or

$$\langle 1, -1 \, | \mu_+^* | \, 00 \rangle \, \langle 00 \, | \mu_- | \, 11 \rangle \neq 0, \qquad (\Delta m = -2) \,. \tag{5.3.34}$$

5.4 Coherent multiple field interactions

5.4.1 Four-wave mixing

Consider a three-level system with three collinear waves E_f, E_b, and E_p incident on it, as shown in Fig. 5.14. Using perturbation theory, we wish to show in a simple way that a coherence appears *in third order* which radiates a phase conjugate, time-reversed replica of an input probe wave E_p. We can also show that by tuning the probe frequency, information on relaxation processes in the system can be obtained [5.2] which might otherwise be unmeasurable (Fig. 5.15).

$$i\hbar\dot{\rho}_{11} = (V_{12}\rho_{21} - \rho_{12}V_{21}) + i\hbar\gamma_{31}\rho_{33} + i\hbar\gamma_{21}\rho_{22}, \tag{5.4.1}$$

$$i\hbar\dot{\rho}_{22} = -\,(V_{12}\rho_{21} - \rho_{12}V_{21}) - i\hbar\,(\gamma_{21} + \gamma_{23})\,\rho_{22}, \tag{5.4.2}$$

$$i\hbar\dot{\rho}_{33} = i\hbar\gamma_{23}\rho_{22} - i\hbar\gamma_{31}\rho_{33}, \tag{5.4.3}$$

$$i\hbar\dot{\rho}_{12} = -\hbar\omega_0\rho_{12} + (V_{12}\rho_{22} - \rho_{11}V_{12}) - i\hbar\Gamma_{21}\rho_{12}, \tag{5.4.4}$$

$$\rho_{21} = \rho_{12}^*. \tag{5.4.5}$$
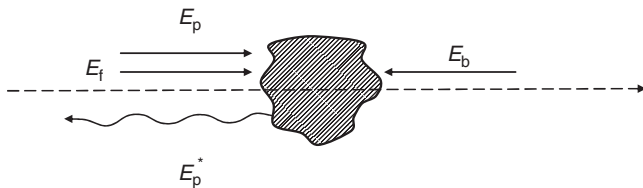
Figure 5.14 *Three incident fields impinging on a sample (shaded) and giving rise to a fourth wave, the output signal wave, via a third-order process called four-wave mixing.*
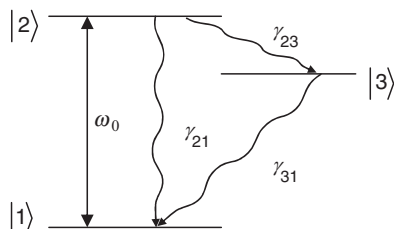
Figure 5.15 *Radiative and non-radiative transitions in a three-level system undergoing nearly degenerate four-wave mixing on the $1 \leftrightarrow 2$ transition.*

The three perturbing waves yield traveling wave interactions given by

$$(V_{12})_j = -\frac{1}{2}\big[\mu_{12}E_j \exp\big[i(\omega_j t - k_j z)\big] + c.c.\big], \tag{5.4.6}$$

where the subscript j= f, b, p denotes the forward pump, backward pump, and probe waves, respectively. Because there are multiple incident waves, we also apply the subscript j to earlier notations for the Rabi frequency, phase, and detuning.

$$\Omega_j \equiv \mu_{12}E_j/2\hbar$$

$$\Phi_j \equiv \omega_j t - k_j z$$

$$\Delta_j \equiv \omega_0 - \omega_j.$$

Now according to Eqs. (5.4.1–5.4.5), a third order off-diagonal matrix element $\rho_{12}^{(3)}$ can only be obtained from second-order population elements $\rho_{22}^{(2)}$ and $\rho_{11}^{(2)}$ which are in turn derived from a first-order element $\rho_{12}^{(1)}$. This perturbation chain is illustrated in Fig. 5.16.

From Eq. (5.4.4), we can solve directly to find

$$\left(\rho_{12}^{(1)}\right)_j = \left[\frac{\Omega_j}{\Delta_j + i\Gamma_{21}}\right] e^{i\phi_j} \rho_{11}^{(0)}. \tag{5.4.7}$$

Since we are interested in tuning the frequency of the probe wave E_{p}, we need to anticipate that population pulsations may appear in the solutions. First we write

$$i\hbar\dot{\rho}_{22}^{(2)} = -\hbar \sum_{j,k} \Omega_j^* e^{-i\phi_j} e^{i\phi_k} \left(\frac{\Omega_k}{\Delta_k + i\Gamma_{21}}\right) \rho_{11}^{(0)}$$

$$+ \hbar \sum_{j,k} \Omega_j e^{-i\phi_k} e^{i\phi_j} \left(\frac{\Omega_k^*}{\Delta_k - i\Gamma_{21}}\right) \rho_{11}^{(0)} - i\hbar\left(\gamma_{21} + \gamma_{23}\right) \rho_{22}^{(2)}. \tag{5.4.8}$$

Then, set $\gamma_2 \equiv \gamma_{21} + \gamma_{23}$ and retain only phase-matched terms containing Ω_{p}^*. This means we shall ultimately ignore terms in which the spatial phase factor, or linear momentum, of the signal wave is different from the net phase factor or momentum of
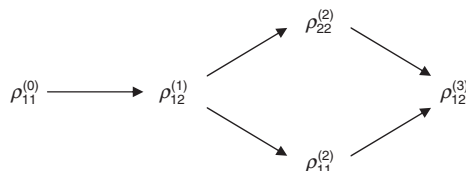
Figure 5.16 *Illustration of the perturbation changes expected when one field acts on a single transition in each new order.*

the three input waves.

$$i\hbar \left(\dot{\rho}_{22}^{(2)} + \gamma_2 \rho_{22}^{(2)} \right) = \rho_{11}^{(0)} \left[\Omega_{\mathrm{p}}^* \Omega_{\mathrm{f}} e^{-i(\phi_{\mathrm{p}} - \phi_{\mathrm{f}})} \left(\frac{1}{\Delta_{\mathrm{p}} - i\Gamma_{21}} - \frac{1}{\Delta_{\mathrm{f}} + i\Gamma_{21}} \right) \right.$$

$$\left. + \Omega_{\mathrm{p}}^* \Omega_{\mathrm{b}} e^{-i(\phi_{\mathrm{p}} - \phi_{\mathrm{b}})} \left(\frac{1}{\Delta_{\mathrm{p}} - i\Gamma_{21}} - \frac{1}{\Delta_{\mathrm{b}} + i\Gamma_{21}} \right) \right]. \quad (5.4.9)$$

Now we see that with a detuned probe frequency $\omega_{\mathrm{p}} = \omega + \delta$, the terms on the right side oscillate as $\exp(-i\delta t)$. Hence, we use the substitution

$$\rho_{22} = \tilde{\rho}_{22} \exp(-i\delta t), \quad (5.4.10)$$

and find the following expression for $\tilde{\rho}_{22}$.

$$\tilde{\rho}_{22}^{(2)} = \frac{\rho_{11}^{(0)}}{\delta + i\gamma_2} \left[\Omega_{\mathrm{p}}^* \Omega_{\mathrm{f}} \left(\frac{1}{\Delta_{\mathrm{p}} - i\Gamma_{21}} - \frac{1}{\Delta_{\mathrm{f}} + i\Gamma_{21}} \right) \right.$$

$$\left. + \Omega_{\mathrm{p}}^* \Omega_{\mathrm{b}} \left(\frac{1}{\Delta_{\mathrm{p}} - i\Gamma_{21}} - \frac{1}{\Delta_{\mathrm{b}} + i\Gamma_{21}} \right) \right]. \quad (5.4.11)$$

Similarly from Eq. (5.4.3) we may find ρ_{33},

$$\tilde{\rho}_{33} = \left(\frac{\gamma_{23}}{-i\delta + \gamma_2} \right) \tilde{\rho}_{22}, \quad (5.4.12)$$

and substitution in Eq. (5.4.1) gives the second-order ground state population.

$$\tilde{\rho}_{11}^{(2)} = \frac{-\rho_{11}^{(0)}}{\gamma_2 - \gamma_{31}} \left(\frac{\gamma_{23}}{\delta + i\gamma_{31}} + \frac{\gamma_{21} - \gamma_{31}}{\delta + i\gamma_2} \right) \left[\Omega_{\mathrm{p}}^* \Omega_{\mathrm{f}} \left(\frac{1}{\Delta_{\mathrm{p}} - i\Gamma_{21}} - \frac{1}{\Delta_{\mathrm{f}} + i\Gamma_{21}} \right) \right.$$

$$\left. + \Omega_{\mathrm{p}}^* \Omega_{\mathrm{b}} \left(\frac{1}{\Delta_{\mathrm{p}} - i\Gamma_{21}} - \frac{1}{\Delta_{\mathrm{b}} + i\Gamma_{21}} \right) \right]. \quad (5.4.13)$$

Notice that a resonant denominator $(\delta + i\gamma_{31})^{-1}$ appears in the ground state element $\rho_{11}^{(2)}$, but does not appear in $\rho_{22}^{(2)}$. Finally, with Eqs. (5.4.11) and (5.4.13) in Eq. (5.4.4), we find

$$\rho_{12}^{(3)} = \rho_{11}^{(0)} \left[\left(1 + \frac{\gamma_{21} - \gamma_{31}}{\gamma_2 - \gamma_{31}} \right) \left(\frac{1}{\delta + i\gamma_2} \right) + \left(\frac{1}{\gamma_2 - \gamma_{31}} \right) \left(\frac{1}{\delta + i\gamma_{31}} \right) \right]$$

$$\times \left[\frac{\Omega_{\mathrm{p}}^* \Omega_{\mathrm{f}} \Omega_{\mathrm{b}}}{(\Delta_{\mathrm{b}} + \delta + i\Gamma_{21})} e^{i(\omega - \delta)t + ikz} \left(\frac{1}{\Delta_{\mathrm{p}} - i\Gamma_{21}} - \frac{1}{\Delta_{\mathrm{f}} + i\Gamma_{21}} \right) \right.$$

$$\left. + \frac{\Omega_{\mathrm{p}}^* \Omega_{\mathrm{b}} \Omega_{\mathrm{f}}}{(-\Delta_{\mathrm{f}} + \delta + i\Gamma_{21})} e^{i(\omega - \delta)t + ikz} \left(\frac{1}{\Delta_{\mathrm{p}} - i\Gamma_{21}} - \frac{1}{\Delta_{\mathrm{b}} + i\Gamma_{21}} \right) \right]. \quad (5.4.14)$$

This third-order coherence between states $|1\rangle$ and $|2\rangle$ is radiative because $\mu_{12} \neq 0$. It gives rise to a time-reversed replica of the probe wave proportional to E_{p}^*. In this geometry, the fourth wave in the phase-matched interaction is thus a phase conjugate
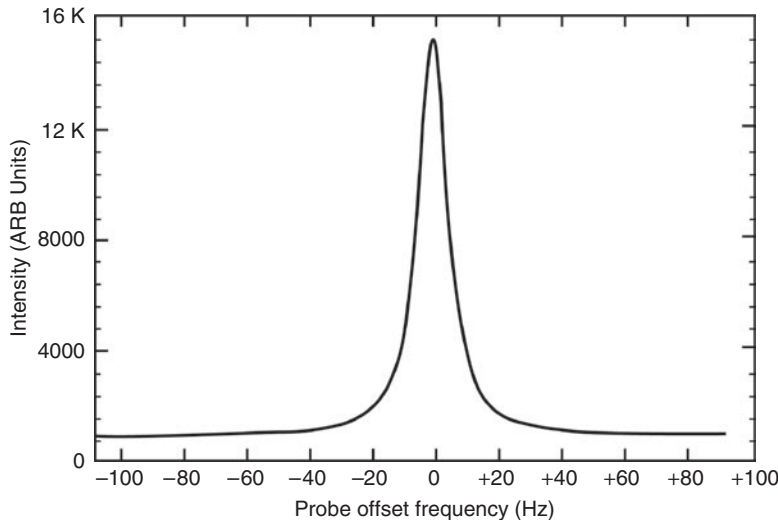
Figure 5.17 *The nearly degenerate four-wave mixing spectrum of three-level Cr^{3+} ions in sapphire, showing the Lorentzian-shaped resonance whose width is given by the slow decay rate γ_{31} from the metastable third level (after Ref. [5.3]). Underlying the main resonance in the figure is a second, much broader resonance with a width reflecting the decay rate γ_{21} of the second excited state in the system.*

signal wave and its spectrum (Fig. 5.17) versus detuning exhibits resonances whose widths reflect the rates of various decay processes possible within the atom.

In this derivation it was implicitly assumed that the sample was optically thin, since field amplitudes throughout the sample were taken to be constant. On the basis of Eq. (5.4.14) it is clear that on resonance ($\Delta \sim 0$), a system with large homogeneous broadening ($\Gamma_2 >> \gamma_{31}, \delta$) and a metastable third state ($\gamma_{31} << \gamma_{21}, \gamma_{23}$) exhibits a four-wave mixing spectrum which is just a single Lorentzian peak with a full width at half maximum (FWHM) equal to γ_{31}. Thus, an ultranarrow resonance appears because of ground state saturation due to slow decay from level $|3\rangle$, as indicated in Fig. 5.17. The simplicity of this result is a useful feature of nearly degenerate four-wave mixing (NDFWM). Probably the most remarkable aspect of it is that the decay time of the long-lived level can be measured accurately by optical means even if its decay to the ground state is completely non-radiative.

The phase conjugate character of the coherence in Eq. (5.4.14) is of great interest in its own right. Significant applications of phase conjugation exist in adaptive optics, imaging through obscuring media and laster technology. The reader is directed to Ref. 5.7 for further discussion of this topic.

Variations of this nonlinear approach to laser spectroscopy are useful for extremely precise measurements of relative splittings in optical spectra. For example, sub-kilohertz resolution is readily obtained in measurements of hyperfine-split transitions of dopant ions in solids [5.8]. An extension of the theoretical treatment of nearly degenerate four-wave mixing to the regime of strong pump fields also reveals a spectrum with new features in it that are not present in Eq. (5.4.14). AC Stark resonances,

with detunings determined by the transition dipole moment (and the optical field), appear when transition $1 \rightarrow 2$ saturates. This analysis is presented in the next section.

5.4.2 Pump-probe experiments

Third-order interactions are by no means restricted to the specialized geometry of NDFWM analyzed in the previous section. In fact, third-order interactions may take place when only one or two beams are incident on a sample. Hence they are more common than might be expected, and researchers using optical characterization techniques not only need to be able to anticipate when saturation effects need to be taken into account, but also be aware of simple two-beam measurements in which the third-order susceptibility $\chi^{(3)}$ dominates the analysis, such as pump-probe experiments.

To illustrate this, let us now discuss the *pump-probe* scenario of Fig. 5.18. It is common practice to saturate systems with a strong pump wave and then monitor bleaching or recovery dynamics with a probe wave. The objective is usually to obtain information about time-dependent processes in completely unknown systems by forcing it slightly away from equilibrium. There are two basic approaches. The probe may be delayed in time or detuned in frequency. The first technique measures the dynamics directly in the temporal domain. The second measures dynamics in the corresponding Fourier space by frequency-domain spectroscopy.

What is not so obvious at first is that both types of experiment involve a third-order interaction. In this section, we address the equations governing this general class of measurement and then analyze the frequency-domain spectrum in detail, to show that indeed three input fields determine the response just as in four-wave mixing [5.9]. To broaden the applicability of the analysis, we extend it to three-level systems however using an approach that combines exact and perturbative analysis. At the end, we shall point out that pump-probe experiments measure the same basic quantities as NDFWM spectroscopy of the last section.

In a typical pump-probe experiment, a strong (saturating) pump wave and a weak probe wave intersect at a small angle within the sample. To investigate the probe transmission spectrum versus pump-probe detuning, we ignore the directions of the two input waves. This means that we ignore phase-matching, and simply find the changes induced by the pump wave in the real and imaginary parts of the refractive
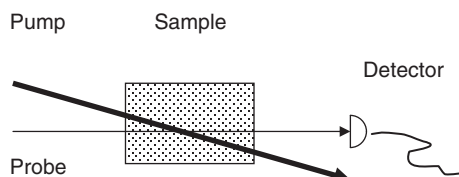
Figure 5.18 *Typical geometry of a pump-probe experiment in which a strong wave (dark arrow) partially saturates an absorptive transition or induces a parametric change in the birefringence or dispersion of a sample. The transmission of a probe wave is monitored with a detector.*
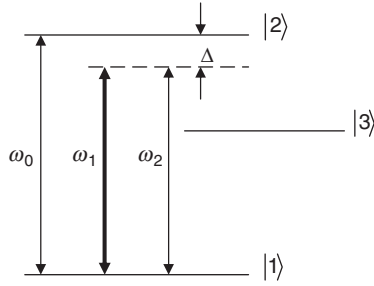
Figure 5.19 *Energy levels and detunings of a three-level system driven by two optical waves of similar frequency.*

index of the sample. These changes may be probed from any angle and depend on the relaxation rates among various levels in the system, so it may not seem too surprising that the resulting probe spectrum contains the same basic information about the atomic system that was provided by NDFWM spectroscopy. However, the analysis of the last section was strictly perturbative, whereas in this section the pump wave is considered intense enough that an exact treatment that includes saturation effects is desired [5.10]. One consequence of this is that new high field features appear (Rabi sidebands).

The component equations of the density matrix corresponding to the three-level system in Fig. 5.19 are

$$\dot{\rho}_{11} = -(i/\hbar)(V_{12}\rho_{21} - \rho_{12}V_{21}) + \gamma_{31}\rho_{33} + \gamma_{21}\rho_{22}, \tag{5.4.15}$$

$$\dot{\rho}_{22} = +(i/\hbar)(V_{12}\rho_{21} - \rho_{12}V_{21}) - (\gamma_{21} + \gamma_{23})\rho_{22}, \tag{5.4.16}$$

$$\dot{\rho}_{33} = -\gamma_{31}\rho_{33} + \gamma_{23}\rho_{22}, \tag{5.4.17}$$

$$\dot{\rho}_{12} = -(i/\hbar)V_{12}(\rho_{22} - \rho_{11}) - (i/\hbar)(H_{11}\rho_{12} - \rho_{12}H_{22}) - \Gamma\rho_{12}, \tag{5.4.18}$$

$$\rho_{21} = \rho_{12}^*. \tag{5.4.19}$$

In this problem, the optical interaction is separated into two parts. The first is due to a strong pump wave E_1 and the second is due to a weak probe wave E_2. The pump wave is a traveling wave of the usual form

$$E_1(t) = \frac{1}{2}E_{10}\exp(i\omega_1 t) + c.c, \tag{5.4.20}$$

and the probe is similar,

$$E_2(t) = \frac{1}{2}E_{20}\exp(i\omega_2 t) + c.c., \tag{5.4.21}$$

except that $E_{20} << E_{10}$.

The interaction Hamiltonian is written as the sum of a zeroth-order pump interaction and a first-order probe interaction. That is,

$$V = V^{(0)} + V^{(1)}, \tag{5.4.22}$$

where

$$V^{(0)} = -\frac{1}{2}\hbar\Omega_1 \exp(i\omega_1 t) + c.c., \tag{5.4.23}$$

$$V^{(1)} = -\frac{1}{2}\hbar\Omega_2 \exp(i\omega_2 t) + c.c., \tag{5.4.24}$$

and $\Omega_1 \equiv \mu E_{10}/\hbar$ and $\Omega_2 \equiv \mu E_{20}/\hbar$.

The effect of $V^{(0)}$ may be taken into account exactly, by the same procedure as in Section 5.1.2. This yields the results

$$\tilde{\rho}_{12}^{(0)} = \frac{(\Omega_1/2)}{\Delta + i\Gamma}(\rho_{11}^{(0)} - \rho_{22}^{(0)}), \tag{5.4.25}$$

$$\rho_{11}^{(0)} = \frac{1 + \Gamma[2\gamma_2(\Delta^2 + \Gamma^2)]^{-1}|\Omega_1|^2}{1 + \Gamma[2\gamma_2(\Delta^2 + \Gamma^2)]^{-1}(2 + \gamma_{23}/\gamma_{31})|\Omega_1|^2}, \tag{5.4.26}$$

$$\rho_{22}^{(0)} = \frac{\Gamma[2\gamma_2(\Delta^2 + \Gamma^2)]^{-1}|\Omega_1|^2}{1 + \Gamma[2\gamma_2(\Delta^2 + \Gamma^2)]^{-1}(2 + \gamma_{23}/\gamma_{31})|\Omega_1|^2}. \tag{5.4.27}$$

Although the population expressions in Eqs. (5.4.26) and (5.4.27) are exact, in the next step of the calculation they are taken as the zeroth-order solutions in a perturbation expansion (see Appendix D). The first-order equation of motion that includes the effect of the weak probe wave has the form

$$i\hbar\dot{\rho}^{(1)} = [H_0, \rho^{(1)}] + [V^{(0)}, \rho^{(1)}] + [V^{(1)}, \rho^{(0)}] + i\hbar\dot{\rho}_{\text{relax}}^{(1)}. \tag{5.4.28}$$

The various components are

$$\dot{\rho}_{11}^{(1)} = i(\Omega_1/2)\tilde{\rho}_{12}^{*(1)} + c.c. + i(\Omega_2/2)\tilde{\rho}_{12}^{*(0)} + c.c. + \gamma_{21}\rho_{22}^{(1)} + \gamma_{31}\rho_{33}^{(1)}, \tag{5.4.29}$$

$$\dot{\rho}_{22}^{(1)} = -i(\Omega_1/2)\tilde{\rho}_{12}^{*(1)} + c.c. - i(\Omega_2/2)\tilde{\rho}_{12}^{*(0)} + c.c. - (\gamma_{21} + \gamma_{23})\rho_{22}^{(1)}, \tag{5.4.30}$$

$$\dot{\rho}_{33}^{(1)} = \gamma_{31}\rho_{33}^{(1)} + \gamma_{32}\rho_{22}^{(1)}, \tag{5.4.31}$$

$$\dot{\rho}_{12}^{(1)} = i(\Omega_1/2)\exp(i\omega_1 t)(\rho_{22}^{(1)} - \rho_{11}^{(1)})$$

$$+ i(\Omega_2/2)\exp(i\omega_2 t)(\rho_{22}^{(0)} - \rho_{11}^{(0)}) + i\omega_0\rho_{12}^{(1)} - \Gamma\rho_{12}^{(1)}. \tag{5.4.32}$$

Because the pump and probe waves are detuned, their combined driving effect can produce pulsations in population and coherence at frequency $\pm\delta$. Consequently, the solutions acquire additional time dependences and are assumed to have the

forms

$$\rho_{11} = \rho_{11}^{(0)} + \rho_{11}^{(1)} = \rho_{11}^{(0)} + \rho_{11}^{(+)} \exp(i\delta t) + \rho_{11}^{(-)} \exp(-i\delta t), \qquad (5.4.33)$$

$$\rho_{22} = \rho_{22}^{(0)} + \rho_{22}^{(1)} = \rho_{22}^{(0)} + \rho_{22}^{(+)} \exp(i\delta t) + \rho_{22}^{(-)} \exp(-i\delta t), \qquad (5.4.34)$$

$$\rho_{33} = \rho_{33}^{(0)} + \rho_{33}^{(1)} = \rho_{33}^{(0)} + \rho_{33}^{(+)} \exp(i\delta t) + \rho_{33}^{(-)} \exp(-i\delta t), \qquad (5.4.35)$$

$$\tilde{\rho}_{12} = \tilde{\rho}_{12}^{(0)} + \tilde{\rho}_{12}^{(1)} = \tilde{\rho}_{12}^{(0)} + \tilde{\rho}_{12}^{(+)} \exp(i\delta t) + \tilde{\rho}_{12}^{(-)} \exp(-i\delta t). \qquad (5.4.36)$$

The time derivatives on the left side of Eqs. (5.4.29)–(5.4.32) acquire new "beat" terms, even if we restrict our solutions to steady-state conditions by assuming that

$$\dot{\rho}_{11}^{(+)} = \dot{\rho}_{11}^{(-)} = \dot{\rho}_{22}^{(+)} = \dot{\rho}_{22}^{(-)} = \dot{\rho}_{33}^{(+)} = \dot{\rho}_{33}^{(-)} = 0, \qquad (5.4.37)$$

and

$$\dot{\tilde{\rho}}_{12}^{(+)} = \dot{\tilde{\rho}}_{12}^{(-)} = 0. \qquad (5.4.38)$$

For example, by substituting Eqs. (5.4.34) and (5.4.35) into Eq. (5.4.31) and setting the coefficients of individual frequency components equal to zero, we find

$$\rho_{33}^{(0)} = (\gamma_{23}/\gamma_{31})\rho_{22}^{(0)}, \qquad (5.4.39)$$

$$\rho_{33}^{(+)} = [\gamma_{23}/(\gamma_{31} + i\delta)]\rho_{22}^{(+)}, \qquad (5.4.40)$$

$$\rho_{33}^{(-)} = [\gamma_{23}/(\gamma_{31} - i\delta)]\rho_{22}^{(-)}. \qquad (5.4.41)$$

Now, using the results for $\rho_{33}^{(\pm)}$ given in Eqs. (5.4.40) and (5.4.41), together with the first-order closure relation

$$\rho_{11}^{(1)} + \rho_{22}^{(1)} + \rho_{33}^{(1)} = 0, \qquad (5.4.42)$$

one finds

$$\rho_{11}^{(+)} = -\left\{1 + \left(\frac{\gamma_{23}}{\gamma_{31} + i\delta}\right)\right\}\rho_{22}^{(+)}, \qquad (5.4.43)$$

$$\rho_{11}^{(-)} = -\left\{1 + \left(\frac{\gamma_{23}}{\gamma_{31} - i\delta}\right)\right\}\rho_{22}^{(-)}. \qquad (5.4.44)$$

After substitution of these results in Eq. (5.4.29), expressions for the first-order excited state amplitudes are obtained.

$$\rho_{22}^{(+)} = i(\gamma_2 + i\delta)^{-1}\left\{(\Omega_1^*/2)\tilde{\rho}_{12}^{(+)} - (\Omega_1/2)\tilde{\rho}_{12}^{*(-)} - (\Omega_2/2)\tilde{\rho}_{12}^{*(0)}\right\}, \qquad (5.4.45)$$

$$\rho_{22}^{(-)} = \rho_{22}^{(+)*}. \qquad (5.4.46)$$

Next, by substituting Eq. (5.4.36) into Eq. (5.4.32), one can also find the coherence amplitudes

$$\tilde{\rho}_{12}^{(+)} = i[(\Delta - \delta) + i\Gamma][(\Omega_1/2)(\rho_{11}^{(+)} - \rho_{22}^{(+)}) + (\Omega_2/2)(\rho_{11}^{(0)} - \rho_{22}^{(0)})], \quad (5.4.47)$$

$$\tilde{\rho}_{12}^{(-)} = [(\Delta + \delta) + i\Gamma]^{-1}[(\Omega_1/2)(\rho_{11}^{(-)} - \rho_{22}^{(-)})]. \tag{5.4.48}$$

Finally, substitution of these last two relations in Eq. (5.4.45) yields a general expression for $\rho_{22}^{(+)}$, from which all other quantities may be determined using Eqs. (5.4.43)–(5.4.48).

$$\rho_{22}^{(+)} = \frac{(\delta - 2i\Gamma)(\Omega_1^* \Omega_2/4)(\rho_{11}^{(0)} - \rho_{22}^{(0)})}{(\delta - i\gamma_2)[(\Delta + \delta) - i\Gamma][(\Delta - \delta) + i\Gamma] + 2[2 + \gamma_{23}/(\gamma_{31} + i\delta)][\delta - i\Gamma]\,|\Omega_1/2|^2}. \tag{5.4.49}$$

With this result in hand, the coherence in Eq. (5.4.36) is fully determined to first order. The probe polarization and susceptibility can therefore be determined for any value of the pump intensity, resonance detuning Δ, and pump-probe detuning δ from the polarization $P(\omega + \delta) = \mu_{12}\rho_{21}(\omega + \delta) + \mu_{21}\rho_{12}(\omega + \delta)$.

Results are shown in Fig. 5.20a–c for the absorption spectrum of the probe at low, moderate, and high pump intensities, respectively. The pump detuning and decay parameters were identical for these comparisons. At low intensities, weak dispersive beam coupling is seen at zero detuning and an absorption peak is present at a pump-probe detuning of $\delta/\Gamma = 10$. Just above saturation, the dispersive feature at zero detuning reveals two resonances, one for each decay process from the excited states, and the absorption peak at $\delta/\Gamma = 10$ decreases in strength. At twenty-times saturation $(\Omega/\Gamma = 20)$, power-broadening smears out the narrowest central resonance and two Rabi sidebands appear at the generalized Rabi frequency splitting of $\delta/\Gamma = \pm 22.3$ in Fig. 5.20c. The central dispersive feature in each spectrum is a weak field response present at intensities below the saturation intensity. When magnified, the central feature shows two overlapping resonances whose widths are determined by the decay rates of levels 2 and 3. Consequently, experimental measurements of their widths provide direct determinations of the excited state decay rates, just as in NDFWM spectroscopy described in the previous section. Power broadening can obscure the central feature, as shown in Fig. 5.20c where the second resonance disappears at high intensity.

Pump-probe spectroscopy is frequently performed with short pulses to monitor changes in sample transmission versus time. System dynamics are then revealed in the time domain as "differential transmission" instead of in the frequency domain as calculated here and portrayed in Fig. 5.20. Experimentally, measurements may be made by delaying the probe pulse with respect to the pump pulse using a mechanical delay line [5.11, 5.12, 5.13]. Theoretically, analysis requires direct integration of the time-dependent density matrix Eqs. (5.4.29)–(5.4.32). The outcome of analyzing the temporal profile of the transient transmission spectrum is however analogous to frequency-domain measurements. The results reflect the decay rates of dynamic processes in excited states of the system.
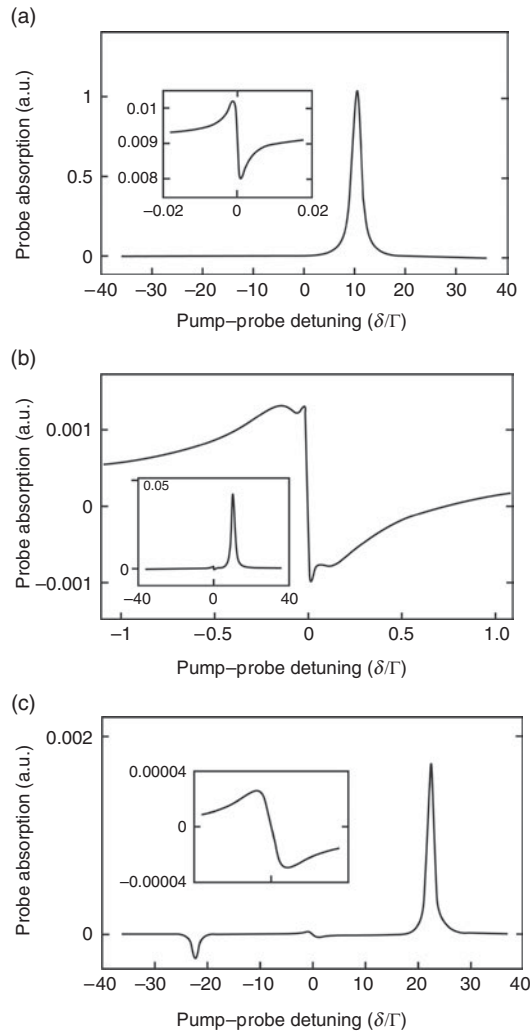
Figure 5.20 *Nearly degenerate pump-probe transmission spectra of three-level atoms with* $\gamma_{31} = 0.0001$, $\gamma_2 = 0.1$, *and* $\gamma_{23} = 0.05$ *at* (a) *low intensity* $(\Omega/\Gamma = 0.1)$, (b) *moderate intensity* $(\Omega/\Gamma = 3.0)$, *and* (c) *high intensity* $(\Omega/\Gamma = 20)$. *The insets show enlargements of the central detuning region in each case.* (*After Ref.* [5.10].)

5.4.3 Higher-order interactions and Feynman diagrams

In Section 5.4.1, a four-wave mixing interaction with counter-propagating pump waves was analyzed to illustrate the appearance of coherence with phase-conjugate properties. In the last section, beam coupling calculations revealed numerous resonances in the frequency domain spectrum. When as many as three input waves interact, there are of course many combinations of field amplitudes, when positive

and negative frequencies are taken into account. All contribute to the total medium response. In Section 4.5, we simplified the analysis greatly by dropping all terms which did not contribute to the phase-matched interaction of interest. Similarly in the last section we simplified the mathematical treatment by ignoring the spatial phases of interacting fields. Often these simplifications are difficult to foresee in new problems, and a diagrammatic approach can be helpful. The problem of writing down the appropriate density matrix elements or susceptibilities for a particular four-wave mixing interaction using perturbation theory is in itself not an easy task. This is obvious by simply evaluating the total number of terms possible in four-wave mixing: $\chi_{ijke}^{(3)}$ gives rise to $4 \cdot 3 \cdot 2 \cdot 1 = 24$ terms when fields are real or $24 \times 2 = 48$ terms when fields are taken to be complex (negative frequencies or phase conjugate amplitudes are included). To be useful a diagrammatic technique should therefore provide a simple picture of the dynamics and immediately yield the corresponding mathematical expression.

We proceed by drawing a "timeline" for temporal development of a system. With respect to its initial value, the density matrix can be written in terms of an evolution operator $U(t)$ as

$$\rho = |\psi\rangle \langle\psi| = U(t) |\psi_0\rangle \langle\psi_0| U^+(t). \tag{5.4.14}$$

Hence to write down coherences like $\rho^{(n)} = P^{(n)}/\langle\mu\rangle$ which may be driven by positive or negative frequency components of incident fields, or susceptibilities such as $\chi_{ijk}^{(n)} = P^{(n)}/E_i E_j E_k$ which depend on multiple field amplitudes and detunings, we shall need a double-sided Feynman diagram. In such a diagram, one side takes care of ket evolution $U(t)|\psi_0\rangle$ and the other follows bra development $\langle\psi_0|U(t)^+$. Each side of the diagram keeps track of one part of the system development in time, either the left (positive) or right (negative) side with the initial time and state of the system at the bottom and the final time and state of the top. The system moves from bottom to top by single photon interactions at each vertex and propagation from one vertex to the next.

Consider the simplest possible interaction namely absorption of a single photon by a system initially in its ground state $\rho^0 = |g\rangle\langle g|$. Analytic results for first-order perturbation in a two-level system are

$$\rho_{eg}^{(1)} = -\frac{i}{2\hbar} \left[\frac{\mu_{eg} E}{i(\omega - \omega_{eg}) + \Gamma_{eg}} \right] \rho_{gg}^{(0)} e^{i\omega t} - \frac{i}{2\hbar} \left[\frac{\mu_{eg}^* E^*}{-i(\omega + \omega_{eg}) + \Gamma_{eg}} \right] \rho_{gg}^{(0)} e^{-i\omega t},$$

$$\tag{5.4.15}$$

$$\chi_{ij}^{(1)} = \frac{P_i^{(1)}(\omega)}{E_j(\omega)} = \frac{1}{\hbar} \left[\frac{(\mu_j)_{eg} (\mu_i)_{eg}}{(\omega - \omega_{eg}) + i\Gamma_{eg}} \right] \rho_{gg}^{(0)} + \frac{1}{\hbar} \left[\frac{(\mu_j)_{ge} (\mu_i)_{ge}}{(\omega + \omega_{ge}) + i\Gamma_{ge}} \right] \rho_{gg}^{(0)}. \tag{5.4.16}$$

Based on the expression above, there should be two diagrams to describe the full susceptibility, corresponding to the rotating wave term and the counter-rotating wave term. In Fig. 5.21, the diagram on the left shows a positive frequency absorptive interaction by the ket. The diagram on the right indicates absorption of a negative frequency (conjugate) field by the bra. Together, these diagrams comprise a diagrammatic
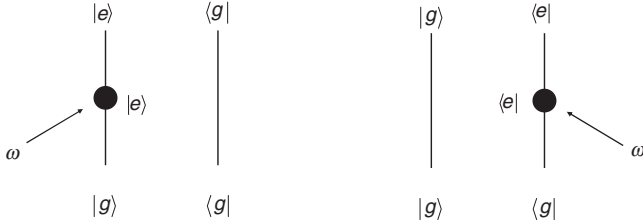
Figure 5.21 *Illustration of the two simplest double-sided Feynman diagrams representing evolution of the ket* (left) *and bra* (right) *components of the density matrix.*

equivalent to the two analytic terms in the first-order perturbation theory expression for $\rho_{eg}^{(1)}$ given in Eq. (5.4.15). In first order, the final state of the system is $|e\rangle\langle g|$. Both the analytic expression and the diagram show this. To obtain the mathematical expression from the structure of the diagram, we choose to associate the matrix element with the vertex and the resonant denominator with propagation between vertices. Specifically, the interactions

$$I_j^{\mathrm{L}} = \frac{1}{\hbar} (\mu_j)_{eg} E_j e^{i\omega_j t} \leftrightarrow \text{ left vertex,}$$

$$I_j^{\mathrm{R}} = \frac{1}{\hbar} (\mu_j)_{eg}^* E_j^* e^{-i\omega_j t} \leftrightarrow \text{ right vertex}$$

are vertex contributions and

$$\Pi_j^{\mathrm{L}} = [\omega_{eg} - \omega + i\Gamma_{eg}]^{-1} \leftrightarrow \text{ propagation from } |g\rangle \text{ to } |e\rangle \text{ on the left,}$$

$$\Pi_j^{\mathrm{R}} = [\omega_{eg} + \omega + i\Gamma_{eg}]^{-1} \leftrightarrow \text{ propagation from } \langle g| \text{ to } \langle e| \text{ on the right}$$

are the propagators. With these substitutions, we can write the density matrix as

$$\rho_{eg}^{(1)} = \frac{1}{2} \left[\Pi_j^{\mathrm{L}} I_j^{\mathrm{L}} + \Pi_j^{\mathrm{R}} I_j^{\mathrm{R}} \right] \rho_{gg}^{(0)}, \qquad (5.4.17)$$

or we could write the susceptibility as

$$\chi_{ij}^{(1)}(\omega) = \frac{1}{2} \left[\Pi_j^{\mathrm{L}} I_j \frac{(\mu_i)_{eg}}{E_j} + \Pi_j^{\mathrm{R}} I_j^{\mathrm{R}} \frac{(\mu_i)_{eg}^*}{E_j^*} \right] \rho_{gg}^{(0)}. \qquad (5.4.18)$$

If the system has many levels, the net susceptibility $\chi^{(1)}$ taking contributions from all states into account requires summation over possible initial and final states g, e.

$$\chi_{ij}^{(1)}(\omega) = \frac{1}{2} \sum_{g,e} \left[\Pi_j^{\mathrm{L}} I_j^{\mathrm{L}} \frac{(\mu_i)_{eg}}{E_j} + \Pi_j^{\mathrm{R}} I_j^{\mathrm{L}} \frac{(\mu_i)_{eg}^*}{E_j^*} \right] \rho_{gg}^{(0)}. \qquad (5.4.19)$$

Notice that to calculate the correct density matrix elements from diagrams, we multiply the vertex and propagator contributions and sum over states. For the correct susceptibility, we have in addition to multiply by the dipole moment $(\mu_i)_{eg}$ between
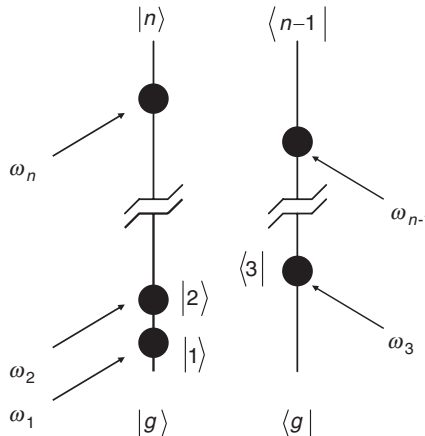
Figure 5.22 *Double-sided Feynman diagram illustrating a sequence of* n *optical interactions affecting the evolution of the ket and bra of the density matrix.*

initial and final states before summing, because the diagrams strictly show only development of ρ.

For higher-order processes (Fig. 5.22), there are more numerous permutations of the diagrams. These involve reordering of the vertices vertically, and all left–right permutations to include conjugate processes, but the procedure is a straightforward extension of the above. Spontaneous emission and other incoherent decay and nonparametric processes are omitted. We have the following rules:

1. Draw all possible diagrams, corresponding to all permutations of vertices ordered in time and distributed between the bra and ket lines.
2. For the jth vertex connecting state $|n\rangle$ to $|n'\rangle$, assign the following interaction factors:

$$I_j = \frac{1}{\hbar} (\mu_j)_{n'n} E_j e^{i\omega_j t} \quad \leftrightarrow \quad \text{absorption on the left,}$$

$$I_j = \frac{1}{\hbar} (\mu_j)_{n'n} E_j e^{i\omega_j t} \quad \leftrightarrow \quad \text{emission on the right,}$$

$$I_j = \frac{1}{\hbar} (\mu_j)^*_{n'n} E_j^* e^{-i\omega_j t} \quad \leftrightarrow \quad \text{absorption on the right,}$$

$$I_j = \frac{1}{\hbar} (\mu_j)^*_{n'n} E_j^* e^{-i\omega_j t} \quad \leftrightarrow \quad \text{emission on the left.}$$

3. Propagation from the jth to the $(j+1)$th vertex along ket–bra double timelines $|l\rangle\langle k|$ is described by propagator $\Pi_j = [\omega_{lk} + i\Gamma_{lk} \mp \sum_{i=1}^{j} \omega_i]^{-1}$. The summation contains all frequencies up to and including ω_j, and each ω_i may be positive or negative depending on whether the corresponding ith vertex shows absorption on the left or the right, respectively. If the ith vertex indicates emission, the signs are reversed for a vertex on the right and left, respectively.

4. Multiply all factors describing evolution from $|g\rangle\langle g|$ to $|n'\rangle\langle n|$ and sum over all possible states.
5. To find the contribution of one diagram to the nth-order density matrix $\rho^{(n)}$, the nth-order density matrix $\rho^{(n)}$ is the sum of all such diagrams.

The contribution to $\rho^{(n)}$ from the diagram above may be written down directly as

$$
\sum_{g1...n} \frac{1}{(2\hbar)^n} \left\{ \frac{|n\rangle\, \mu_{(n)(n-1)} \cdots \mu_{1g}\rho_{gg}^{(0)}\mu_{g3} \cdots \mu_{(n-1)(n-2)}\, \langle n-1|}{\Pi_n^{-1}\Pi_{n-1}^{-1} \cdots (\omega_{2g} - (\omega_2 + \omega_1) + i\Gamma_{2g})(\omega_{1g} - \omega_1 + i\Gamma_{1g})} \right\}.
$$

$$
E_1 E_2 E_3^* \cdots E_{n-1}^* E_n \exp(\omega_1 + \omega_2 - \omega_3 \ldots - \omega_{n-1} + \omega_n)t \qquad (5.4.20)
$$

It must be borne in mind that the diagrammatic technique illustrated here ignores all incoherent driving terms and assumes that population changes are negligible (all detunings are finite). That is, only terms driven by external fields are taken into account. This approach cannot be used to formulate solutions to problems in which dark (non-radiative) processes play an important role.

Problems

5.1. The initial state of a pair of identical two-level atoms A and B located at the origin is

$$
\psi = \frac{|1\rangle|0\rangle + |0\rangle|1\rangle}{\sqrt{2}},
$$

where the ket products denote the products of the wavefunctions for atoms A and B in the order $|A\rangle|B\rangle$. A, B may be 0 or 1. This state is the result of excitation by a single photon capable of providing enough energy to excite atom A or atom B of the pair but not both.

(a) Show that ensemble average measurements of the probability for finding the atoms in particular combination states, as given by the pair density matrix elements $\langle\psi|\rho_{AB}|\psi\rangle$ where $\rho_{AB} = |A\rangle|B\rangle\langle B|\langle A|$, confirm that half the time one finds atom A excited and half the time one finds B excited (i.e., find ρ_{01} and ρ_{10}).

(b) Next, separate the two atoms *of a single pair* by a distance on the order of a meter in the laboratory, without causing any phase or state change and make a sequential determination of the states of each separate atom. Because the pair is initially in a superposition state (and given the fundamental postulate of quantum mechanics) the state of atom A is unknowable until a measurement is made. Similarly, the state of atom B is indeterminate until measured. Find the probability amplitude for ψ to yield each possible product state of A and B by projecting ψ directly onto each of the four possible eigenstate products in turn.

(c) In part (b), compare the probabilities of finding B in state 0 or 1 after A is found in 0. Suggest a resolution of the surprising fact that B seems to "know" the measured state of atom A and always conserves energy even

though it has an overall 50% probability of being found in either state and is measured at a different location.

5.2. Assume that, in the case of resonant optical excitation of a closed two-level system, steady-state, oscillatory solutions for the level populations exist, of the form

$$\rho_{11} = \tilde{\rho}_{11}(1 - \cos \xi t),$$

$$\rho_{22} = \tilde{\rho}_{22}(1 + \cos \xi t).$$

(a) Use closure to find consistent (time-independent) values for $\tilde{\rho}_{11}$ and $\tilde{\rho}_{22}$.

(b) Find the slowly varying amplitude $\tilde{\rho}_{12}$ of the polarization $\rho_{12} = \tilde{\rho}_{12}e^{i\omega t}$ using the results of part (a).

(c) Based merely on what you know about resonant excitation, what would you expect the value of ξ to be?

(d) What is the physical reason accounting for the time-dependence of $\tilde{\rho}_{12}$?

(e) The absorption of the system is proportional to $\rho_{11} - \rho_{22}$. Does it ever go to 0? Show and explain.

5.3. A short pulse of central frequency ω is incident on a closed two-level system at time $t = t_0$. The impulsive light–atom interaction is of the form

$$V(t) = V_0\delta(t - t_0)e^{i\omega t} + c.c.$$

Assume that although the interaction is represented mathematically by a delta function, it occurs over a time that is actually long compared to the optical period. Thus, SVEA is still valid.

Solve for the density matrix elements, starting with ρ_{12}. Find the time-dependent solutions for the occupations of the two states of the system for times $t > t_0$. Ignore all considerations related to Fourier components of the pulse or pulse bandwidth.

5.4. In a two-level gas, the polarization is proportional to the Doppler-averaged matrix element

$$\overline{\tilde{\rho}_{12}(t)} = \frac{1}{u\sqrt{\pi}} \int\limits_{-\infty}^{\infty} \tilde{\rho}_{12}e^{-\left(\frac{v_z}{u}\right)^2} dv_z.$$

In frequency-switched observations of free induction decay one has

$$\tilde{\rho}_{12} = \frac{i\Omega}{2} R_3(0)e^{-t/T_2}e^{i\delta\omega t}e^{i\Delta t}\left(\frac{i\Delta + \Gamma'}{\Delta^2 + \Gamma^2}\right),$$

where $\Gamma' \equiv \frac{1}{T_2}, \Gamma^2 \equiv \frac{1}{(T_2)^2} + \Omega^2\frac{T_1}{T_2}, \Delta \equiv \omega_0 - \omega - kv_z$, and the frequency shift $\delta\omega$ is independent of Δ.

(a) Show that the integral above can be expressed analytically in terms of the error function $W(z)$ of complex argument, with different forms for cases $t < 2\Gamma/(ku)^2$ and $t > 2\Gamma/(ku)^2$.

(b) Show that for long times (greater than the inverse Doppler width) the result for $\overline{\tilde{\rho}}_{12}$ is the same as that obtained in lecture notes when one ignores a small imaginary component in the expression for the beat signal.

5.5. Verify that components $V_q^{(k)}$ of an irreducible spherical tensor operator of rank $k = 1$ are related to the rank one Cartesian components V_j of vector operator V by

$$V_1^{(1)} = -\frac{V_x + iV_y}{\sqrt{2}},$$

$$V_0^{(1)} = V_z,$$

$$V_{-1}^{(1)} = \frac{V_x - iV_y}{\sqrt{2}}.$$

Hint: One way to show this is to demonstrate that the given expressions satisfy the commutation relations of a rank $k = 1$ tensor.
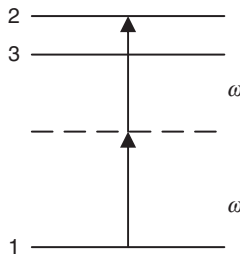
5.6. By examining the conditions required for the Clebsch–Gordan coefficient or the 3-j symbol to be nonzero (see Appendix H), show that the trace of any irreducible spherical tensor operator vanishes, except for rank $k = 0$ (scalar operators).

5.7. Prove that a state with angular momentum $J < k/2$ does not have a static 2^k-pole moment. For example, a state with $J = 1$ cannot have a 2^2-pole (quadrupole) moment. (Consider the expectation value of the tensor $\langle T_q^{(k)} \rangle \equiv \langle r^{(k)} Y_q^{(k)} \rangle$ and apply the W–E theorem or use tensor commutation relations of $T_q^{(k)}$ with the angular momentum operator to find any general restriction on q associated with static moments and to show that the 2^k-pole moment is 0 for $J < k/2$.)

5.8. Clebsch–Gordon coefficients are related to 3-j symbols according to the formula

$$(j_i J; m_i m | j_i J j_f; m_f) = (-)^{-j_i + J - m_f} \sqrt{2j_f + 1} \begin{pmatrix} j_i & J & j_f \\ m_i & m & -m_f \end{pmatrix},$$

where j_i and j_f are the initial and final j values of the atomic transition and J is the angular momentum of the interaction. Their squares are proportional to the probabilities of transitions between states (Appendix H).

(a) Use a property of the 3-j symbols to show that only initial and final sublevels differing in magnetic quantum number m by 0 or ± 1 have finite probabilities for electric dipole transitions.

(b) Calculate all seven of the Clebsch–Gordon coefficients for a transition from initial state $|j_i m_i\rangle$ with $j_i = 1$ to final state $|j_f m_f\rangle$ with $j_f = 1$ via the rank one electric dipole operator ($J = 1; m = 0, \pm 1$). Are any of the transitions forbidden?

(c) Repeat the calculation for all nine coefficients on a $j_i = 1$ to $j_f = 1$ transition. Are any of the transitions forbidden in this case?

5.9. A three-level atom initially occupies the ground state. It undergoes resonant two-photon absorption to state 2, driven by an incident field at frequency ω as indicated in the accompanying diagram. Level 3 is very far off-resonance for either one-photon or two- photon excitation, and the only nonzero transition dipole moments are μ_{13} and μ_{23}.

(a) Write down the density matrix equation of motion for the coherence ρ_{13}, omitting all decay terms. Assume the Hamiltonian is $H = H_0 + V$ and express your answer in terms of explicit matrix elements. (Do not solve the equation as yet.)

(b) At what frequencies do coherences ρ_{13} and ρ_{12} oscillate?

(c) *Without making any rotating wave approximation*, solve for a steady-state solution of ρ_{13} assuming that the perturbation
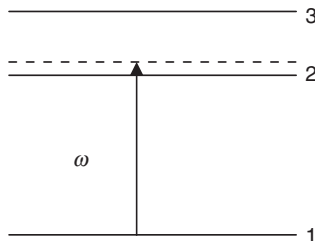
$$V = -\frac{1}{2}\mu_{13}Ee^{i\omega t} + c.c. - \frac{1}{2}\mu_{23}^*E^*e^{-i\omega t} + c.c.$$

does not cause a large change in ground state population. Leave your answer in terms of the slowly varying amplitude $\tilde{\rho}_{12}$(i.e., it is not necessary to complete the problem by solving for the steady-state value of ρ_{12}).

5.10. In the three-level system shown in the figure, an incident light field composed of counter-propagating waves of the same frequency ω is tuned *between* the two closely spaced levels $|2\rangle$ and $|3\rangle$. These levels are close enough so that polarizations ρ_{21} and ρ_{31} can be created on both the $1 \to 2$ and $1 \to 3$ transitions of the moving atoms. Transitions to both excited states are dipole-allowed and the Doppler-broadened linewidths of these transitions overlap. When effects of second order and higher are taken into account, one finds the resonance factor

$$\rho_{21} \propto \frac{1}{[i(\Delta_{21} + kv) + \Gamma_{21}][-i(\Delta_{31} - kv) + \Gamma_{31}]}$$

in the expression for the polarization, where $\Delta_{21} \equiv \omega_{21} - \omega$, $\Delta_{31} \equiv \omega_{31} - \omega$, and v is the velocity.

(a) Ignoring decay factors Γ (i.e., setting $\Gamma_{21} = \Gamma_{31} = 0$), identify a Doppler frequency shift kv at which resonant response is obtained that is *higher than first order*. (Because there are two free variables ω and v, proceed by eliminating ω to find kv.)

(b) Explain the physical origin of this "crossover" resonance by considering the Doppler shift from part (a) at which it occurs. (Note: ρ_{31} has a similar factor in it but need not be considered explicitly.)

(c) What is the macroscopic radiant polarization of the atoms, if indeed there is any? (Find the *general* expression and make appropriate substitutions to decide.)

5.11. Prove that the general form of $\rho_{12}(t)$ *cannot be real*. (Hint: Instead of using Eq. (G.1), assume $\rho_{12}(t)$ is given by a real expression such as $\rho_{12}(t) = \frac{1}{2}\tilde{\rho}_{12}\exp(i\omega t) + c.c.$ Substitute this into the equation of motion (G.4). By equating coefficients for positive and negative frequency terms to separate Eq. (G.4) into one equation for the amplitude $\tilde{\rho}_{12}$ and one for $\tilde{\rho}_{12}^*$, show that steady-state solutions yield the result $\tilde{\rho}_{12}^* \neq (\tilde{\rho}_{12})^*$. Since $\tilde{\rho}_{12}^* \neq (\tilde{\rho}_{12})^*$ is necessary for the density matrix to provide consistent solutions of the equation of motion, this is sufficient to establish the fact that $\rho_{12}(t)$ is always complex.)

5.12. (a) Sketch all the double-sided Feynman diagrams for the state of a system undergoing two-photon emission from an initial state $|e\rangle\langle e|$.

(b) In how many ways can this occur in principle?

(c) Consider a multilevel system and give an argument as to whether the diagrams of part (a) correspond to physically independent processes or not.

(d) In a single diagram of your choice from (a), label all states and frequencies and write down the perturbation expression for its contribution to the second-order density matrix element $\rho^{(2)}$.

References

5.1. S. Stenholm, *Foundations of Laser Spectroscopy*, J. Wiley and Sons, New York, 1984.

5.2. See for example, R.M. Macfarlane and R.M. Shelby, *Opt. Lett.* **6**, 96(1981).

5.3. S.C. Rand, in *Laser Spectroscopy and New Ideas*, Springer Series in Optical Sciences, Vol. 54, Springer-Verlag, New York, 1987.

5.4. S.H. Autler and C.H. Townes, *Phys. Rev.* **100**, 703(1955).

5.5. P. Avan and C. Cohen-Tannoudji, *J. Phys. B: At. Mol. Phys.* **10**, 155(1977).

5.6. See for example, I.I. Sobelman, *Atomic Spectra and Radiative Transitions*, Springer-Verlag Series in Chemical Physics, Springer-Verlag, New York (1979).

5.7. R.W. Fisher, Optical Phase Conjugation, Academic Press, New York, 1983.

5.8. Y.S. Bai and R. Kachru, *Phys. Rev. Lett.* **67**, 1859(1991).

5.9. R.W. Boyd, M.G. Raymer, P. Narum, and D.J. Harter, *Phys. Rev.* A**24**, 411(1981).

5.10. Q. Shu, *Cooperative Optical Nonlinearities in Tm:LiYF$_4$*, Ph.D. Dissertation, University of Michigan, 1996, pp. 29–37.

5.11. R. Levy, B. Honerlage, and J.B. Grun, *Phys. Rev.* B**19**, 2326(1979).

5.12. Y. Aoyagi, Y. Segawa, and S. Namba, *Semiconductors Probed by Ultrafast Laser Spectroscopy*, ed. R.R. Alfano, Vol. 1, Academic Press, 1984, pp. 329–49.

5.13. T.S. Sosnowski, T.B. Norris, H. Jiang, J. Singh, K. Kamath, and P. Bhattacharya, *Phys. Rev.* B**57**, R9423(1991).

5.14. P.G. Pappas, M.M. Burns, D.D. Hirshelwood, M.S. Feld, and D.E. Murnick, *Phys. Rev.* A**21**, 1955(1980).

6

Quantized Fields and Coherent States

When optical fields are weak, spontaneous processes and statistical fluctuations that we have not yet considered assume greater importance. Additionally, interactions of light with atoms exactly on resonance alter the static part of the Hamiltonian significantly in a dynamic way, even while transitions between the "renormalized" and shifted energy levels are taking place. In these limits, new phenomena emerge that require careful attention to the "quantized" or particle-like nature of the electromagnetic field as well as strong coupling of light and matter. Hence, this chapter begins with the formal quantization of the electromagnetic field interaction – introduction of a particle-like description of light – and then uses it to cover subjects where quantum optics provides insights and sometimes unique agreement with experimentally measured dynamics.

6.1 Quantization of the electromagnetic field

The classical description of fields is best formulated in terms of a vector potential $\bar{A}$ and a scalar potential φ that simplify the relationship between fields and sources. By imposing constraints on the potentials, one can guarantee that the fields $\bar{E}$ and $\bar{B}$ determined by them always satisfy Maxwell's equations (see Appendix C). Since Maxwell's equations represent the distillation of all that was known about electromagnetic phenomena before the advent of quantum mechanics, the quantum mechanical version of electrodynamics should also satisfy Maxwell's equations.

In developing quantum electrodynamics, we therefore begin with Eqs. (C.3) and (C.7), by writing

$$\bar{B} = \bar{\nabla} \times \bar{A}, \tag{6.1.1}$$

$$\bar{E} = -\frac{\partial \bar{A}}{\partial t} - \bar{\nabla}\varphi. \tag{6.1.2}$$

In vacuum $\bar{B} = \mu_0 \bar{H}$ and $\bar{D} = \varepsilon_0 \bar{E}$. Use of these expressions in the cross-substituted curl equations of classical electrodynamics (Chapter 1) then yields a wave equation for the vector potential.

$$\nabla^2 \bar{A} - \mu_0 \varepsilon_0 \frac{\partial^2 \bar{A}}{\partial t^2} - \bar{\nabla}\left(\bar{\nabla} \cdot \bar{A}\right) = -\mu_0 \bar{J} + \mu_0 \varepsilon_0 \bar{\nabla}\frac{\partial \varphi}{\partial t}. \tag{6.1.3}$$

Some arbitrariness is associated with the definition of the potentials. This is evident from the fact that the fields are not altered if one makes the gauge transformations

$$\bar{A}' = \bar{A} + \bar{\nabla}\Phi, \tag{6.1.4}$$

$$\varphi' = \varphi - \frac{\partial\Phi}{\partial t}, \tag{6.1.5}$$

where Φ is an arbitrary scalar function. Hence the selection of gauge is arbitrary, and for convenience we can choose the so-called Coulomb gauge in which $\bar{\nabla} \cdot \bar{A} = 0$. In this gauge, the vector potential becomes solenoidal or "transverse" like the magnetic field ($\bar{\nabla} \cdot \bar{B} = 0$), and the scalar potential φ is directly related to any static charge distribution in the region of interest ($\nabla^2\varphi = -\bar{\nabla} \cdot \bar{E} = -\rho_V/\varepsilon_0$). This shows that the volumetric charge density ρ_V determines both the scalar potential and any static component of the electric field $\bar{E}$. Since φ is not time-varying, Eq. (6.1.3) reduces to

$$\left(\nabla^2 - \frac{1}{c^2}\frac{\partial^2}{\partial t^2}\right)\bar{A} = -\mu_0\bar{J}. \tag{6.1.6}$$

This equation shows that the current $\bar{J}$ determines both the magnitude and direction of the vector potential and the magnetic flux density $\bar{B} = \bar{\nabla} \times \bar{A}$ (Fig. 6.1).
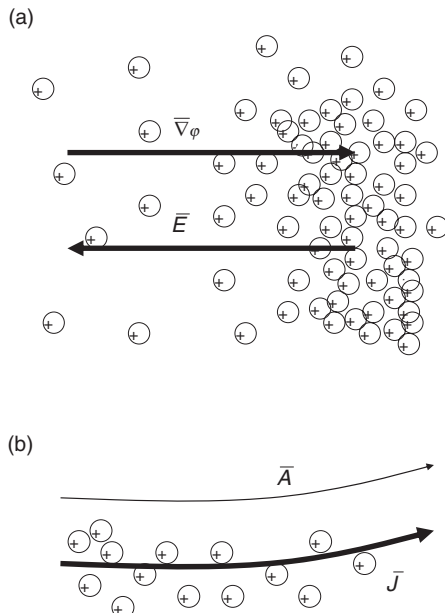
Figure 6.1 *Illustrations of the vectorial relationships between (a) a static charge distribution that generates a potential gradient and consequently an electric field $\bar{E} = -\bar{\nabla}\varphi$, and (b) a flow of charges that produces a vector potential and an associated magnetic flux density $\bar{B} = \bar{\nabla} \times \bar{A}$.*

The scalar and vector potentials are related to charge and current distributions at the (primed) source coordinates:

$$\varphi(\bar{r}) = (4\pi\varepsilon_0)^{-1} \int \frac{\rho_V(\bar{r}')dV'}{|\bar{r} - \bar{r}'|} \tag{6.1.7}$$

$$\bar{A}(\bar{r}, t) = (\mu_0/4\pi) \int \frac{\bar{J}(\bar{r}')dV'}{|\bar{r} - \bar{r}'|}. \tag{6.1.8}$$

Due to its transverse character, the electric field may be divided into two parts (transverse and longitudinal),

$$\bar{E} = \bar{E}_\perp + \bar{E}_\|, \tag{6.1.9}$$

with the properties

$$\bar{\nabla} \cdot \bar{E}_\perp = 0, \tag{6.1.10}$$

$$\bar{\nabla} \times \bar{E}_\| = 0. \tag{6.1.11}$$

Then from Eq. (6.1.2) we obtain the relations between these field components and the potentials:

$$\bar{E}_\perp = -\frac{\partial \bar{A}}{\partial t}, \tag{6.1.12}$$

$$\bar{E}_\| = -\bar{\nabla}\varphi. \tag{6.1.13}$$

$\bar{E}_\|$ is a longitudinal electric field which reflects Coulomb interactions between charges. This term is of no interest in far-field radiation problems. Therefore, we turn to the problem of quantizing the energy of the transverse field by focusing on $\bar{A}$, $\bar{E}_\perp$, and $\bar{B}$.

A charged particle in the electromagnetic field has a Hamiltonian given by the sum of its kinetic and potential energies, with the kinetic term expressed in terms of the canonical momentum.

$$H = \frac{1}{2m} \left(\bar{p} - q\bar{A}\right)^2 + q\varphi. \tag{6.1.14}$$

In Hamilton's formulation, the equations of motion are

$$\dot{\bar{r}} = \frac{\partial H}{\partial \bar{p}} = \frac{\bar{p} - q\bar{A}}{m} = \bar{v}, \tag{6.1.15}$$

$$\dot{\bar{p}} = -\bar{\nabla}H. \tag{6.1.16}$$

Together with Eq. (6.1.14), Eq. (6.1.16) yields the Lorentz force law

$$\dot{\bar{v}} = \frac{1}{m} \left[\dot{\bar{p}} - q\frac{\partial}{\partial t}\bar{A} - q\left(\bar{v} \cdot \bar{\nabla}\right)\bar{A}\right]$$

$$= -\frac{q}{m} \left[\bar{\nabla}\varphi + \frac{\partial}{\partial t}\bar{A} - \bar{\nabla}\left(\bar{v} \cdot \bar{A}\right) + \left(\bar{v} + \bar{\nabla}\right)\bar{A}\right]$$

$$= \frac{q}{m} \left[\bar{E} + \bar{v} \times \bar{B}\right]. \tag{6.1.17}$$

The process of quantization of conjugate pairs of variables like $(\bar{r}, \bar{p})$ proceeds with the introduction of a commutator consistent with their equation of motion. Consequently, the electromagnetic fields $\bar{E}$ and $\bar{B}$ that exert forces on charges will be quantized in a way which satisfies Eq. (6.1.17). Instead of working directly with Eq. (6.1.17) however, we shall make use of an expression for the energy density of electromagnetic fields (derivable from Maxwell's equations) together with the force law.

To do this, we first expand $\bar{A}$ in terms of the modes of a cavity of volume V. Instead of using standing waves for the expansion, we introduce running waves that are subject to periodic boundary conditions:

$$\bar{A}(\bar{r}, t) = \frac{-i}{\sqrt{\varepsilon_0 V}} \sum_{k,\lambda} \bar{c}_{k\lambda}(t) \exp(i\bar{k} \cdot \bar{r}) + c.c. \tag{6.1.18}$$

Here $\bar{k}$ is the wave vector and $\lambda = 1, 2$ is an index for polarization of the field. The initial phase factor of $-i$ in Eq. (6.1.18) is arbitrary, but ensures convenient forms of the electric and magnetic fields. For the running waves in Eq. (6.1.18) to be solutions of the wave equation in free space, they must be transverse in character. Hence the condition may be imposed that $\bar{\nabla} \cdot \bar{A} = 0$, or

$$\bar{k} \cdot \bar{c}_{k\lambda} = 0. \tag{6.1.19}$$

The wave amplitude $\bar{c}_{k\lambda}$ must be perpendicular to $\bar{k}$, so there can be only two independent polarizations $\hat{e}_{k\lambda}$ for each $\bar{k}$. It follows from Eq. (6.1.6) that the amplitudes of right-going wave solutions must have the form

$$\bar{c}_{k\lambda}(t) = \hat{e}_{k\lambda} c_{k\lambda}(0) \exp(-i\omega_k t). \tag{6.1.20}$$

The dispersion relation $\omega_k = ck$ of Section 1.2 has also been assumed.

On the basis of Eqs. (6.1.12) and (6.1.20), the transverse (radiation zone) electric field is

$$\bar{E}_\perp = \frac{1}{\sqrt{\varepsilon_0 V}} \sum_{k,\lambda} \left[\omega_k \bar{c}_{k\lambda}(t) \exp(i\bar{k} \cdot \bar{r}) + c.c. \right]. \tag{6.1.21}$$

The magnetic flux density may similarly be found from Eq. (6.1.1).

$$\bar{B} = \bar{\nabla} \times \bar{A}(\bar{r}, t) = \frac{\bar{k}}{\sqrt{\varepsilon_0 V}} \times \sum_{k,\lambda} \left[\bar{c}_{k\lambda}(t) \exp(i\bar{k} \cdot \bar{r}) + c.c. \right]. \tag{6.1.22}$$

Since the energy density of the radiation field is

$$U_{\text{rad}} = \left(\varepsilon_0 E_\perp^2 + B^2/\mu_0 \right)/2, \tag{6.1.23}$$

the next step of the quantization procedure is to substitute Eqs. (6.1.21) and (6.1.22) into the energy density of Eq. (6.1.23) and to find the total energy for the cavity volume V. Upon substitution, the Dirac delta function

$$\frac{1}{V} \int dV \exp\left(i \left[\bar{k} - \bar{k}' \right] \cdot \bar{r} \right) = \delta \left(\bar{k} - \bar{k}' \right), \tag{6.1.24}$$

may be recognized and used to simplify the vector product

$$\sum_{k',\lambda'} \left(\bar{k} \times \bar{c}_{k\lambda}\right) \cdot \left(\bar{k}' \times \bar{c}_{k'\lambda'}^*\right) \delta(\bar{k} - \bar{k}') = k^2 \left|c_{k\lambda}\right|^2, \qquad (6.1.25)$$

that appears in the volume integral of the energy density of the radiation field. One finds

$$U_{\text{field}} = \frac{1}{2} \int dV \left(\varepsilon_0 E_\perp^2 + B^2/\mu_0\right) = 2 \sum_{k,\lambda} \omega_k^2 \left|c_{k\lambda}\right|^2. \qquad (6.1.26)$$

Now, to quantize the energy in Eq. (6.1.26), scalar variables $Q_{k\lambda}$ and $P_{k\lambda}$ are introduced using the definition

$$\bar{c}_{k\lambda} = \frac{1}{2} \left(Q_{k\lambda} + \frac{iP_{k\lambda}}{\omega_k}\right) \hat{\varepsilon}_{k\lambda}, \qquad (6.1.27)$$

where $\hat{\varepsilon}_{k\lambda}$ represent the circular polarization basis vectors of Eq. (1.2.24) with the property

$$\hat{\varepsilon}_{k\lambda} \cdot \hat{\varepsilon}_{k\lambda'} = \delta_{\lambda\lambda'}. \qquad (6.1.28)$$

The change of variables in Eq. (6.1.27) is useful because U_{field} can then be written in a form recognizable as a sum of simple harmonic oscillator Hamiltonians (compare Eq. (2.2.19)).

$$U_{\text{field}} = \sum_{k,\lambda} \frac{1}{2} \left[P_{k\lambda}^2 + \omega_k^2 Q_{k\lambda}^2\right] \equiv \sum_{k,\lambda} H_{k\lambda}. \qquad (6.1.29)$$

Using Eq. (6.1.20), it can readily be shown that $Q_{k\lambda}$ and $P_{k\lambda}$ also obey Hamilton's equations of motion.

$$\dot{Q}_{k\lambda} = P_{k\lambda} = \frac{\partial H_{k\lambda}}{\partial P_{k\lambda}}, \qquad (6.1.30)$$

$$\dot{P}_{k\lambda} = -\omega_k^2 Q_{k\lambda} = -\frac{\partial H_{k\lambda}}{\partial Q_{k\lambda}}. \qquad (6.1.31)$$

This demonstrates that not only can U_{field} be reduced to a sum of Hamiltonians of harmonic oscillator form, but $P_{k\lambda}$ and $Q_{k\lambda}$ are the canonical variables of the "oscillators." Hence, $P_{k\lambda}$ and $Q_{k\lambda}$ are the natural variables to use in quantizing our field theory, and their indices tell us that the oscillators in question correspond to the modes of free space. We next postulate the commutator for the corresponding operators to be

$$\left[\hat{Q}_{k\lambda}, \hat{P}_{k'\lambda'}\right] = i\hbar \delta_{kk'} \delta_{\lambda\lambda'}, \qquad (6.1.32)$$

and introduce some operators that are convenient for exploring the energy structure

of the electromagnetic field, namely

$$\hat{a}_{k\lambda}^- = \sqrt{\frac{\omega_k}{2\hbar}} \left(Q_{k\lambda} + i\frac{P_{k\lambda}}{\omega_k} \right), \tag{6.1.33}$$

$$\hat{a}_{k\lambda}^+ = \sqrt{\frac{\omega_k}{2\hbar}} \left(\hat{Q}_{k\lambda} - i\frac{\hat{P}_{k\lambda}}{\omega_k} \right). \tag{6.1.34}$$

Exercise: Verify using Eq. (6.1.32) that the operators $\hat{a}^-, \hat{a}^+$ satisfy the commutation relation

$$\left[\hat{a}_{k\lambda}^-, \hat{a}_{k\lambda'}^+ \right] = \delta_{kk'}\delta_{\lambda\lambda'}, \tag{6.1.35}$$

and confirm the following quantum mechanical expressions for electromagnetic field quantities:

$$A(\bar{r},t) = -i\sum_{k,\lambda} \sqrt{\frac{\hbar}{2\varepsilon_0\omega_k V}} \left[\hat{a}_{k\lambda}^-(t)\hat{\varepsilon}_{k\lambda}^- \exp(i\bar{k}\cdot\bar{r}) - \hat{a}_{k\lambda}^+(t)\hat{\varepsilon}_{k\lambda}^+ \exp(-i\bar{k}\cdot\bar{r}) \right] \tag{6.1.36}$$

$$E_\perp(\bar{r},t) = \sum_{k,\lambda} \sqrt{\frac{\hbar\omega_k}{2\varepsilon_0 V}} \left[\hat{a}_{k\lambda}^-(t)\hat{\varepsilon}_{k\lambda}^- \exp(i\bar{k}\cdot\bar{r}) + \hat{a}_{k\lambda}^+(t)\hat{\varepsilon}_{k\lambda}^+ \exp(-i\bar{k}\cdot\bar{r}) \right] \tag{6.1.37}$$

$$B(\bar{r},t) = \sum_{k,\lambda} \sqrt{\frac{\hbar}{2\varepsilon_0\omega_k V}} \left[\hat{a}_{k\lambda}^-(t)\left(\bar{k}\times\hat{\varepsilon}_{k\lambda}^- \right)\exp(i\bar{k}\cdot\bar{r}) + \hat{a}_{k\lambda}^+(t)\left(\bar{k}\times\hat{\varepsilon}_{k\lambda}^+ \right)\exp(-i\bar{k}\cdot\bar{r}) \right]$$

$$\tag{6.1.38}$$

$$U_{\text{field}} \equiv \hat{H}_{\text{field}} = \sum_{k,\lambda} \hat{H}_{k\lambda} = \sum_{k,\lambda} \hbar\omega_k \left(\hat{a}_{k\lambda}^+\hat{a}_{k\lambda}^- + \frac{1}{2} \right). \tag{6.1.39}$$

Exercise: Introduce vacuum impedance $\eta_0 \equiv \sqrt{\mu_0/\varepsilon_0}$ and show that in free space Eq. (6.1.38) is equivalent to

$$B(\bar{r},t) = -i\sum_{k,\lambda} \sqrt{\frac{\eta_0\hbar\omega_k}{2V}} \left[\hat{a}_{k\lambda}^-(t)\hat{\varepsilon}_{k\lambda}^+ \exp(i\bar{k}\cdot\bar{r}) - \hat{a}_{k\lambda}^+(t)\hat{\varepsilon}_{k\lambda}^- \exp(-i\bar{k}\cdot\bar{r}) \right]. \tag{6.1.40}$$

Using the operators of Eqs. (6.1.33 and 6.1.34), the Hamiltonian operator for the field assumes a particularly compact form:

$$\hat{H}_{\text{field}} = \sum_{k,\lambda} \hbar\omega_k \left(\hat{a}_{k\lambda}^+\hat{a}_{k\lambda}^- + \frac{1}{2} \right). \tag{6.1.41}$$

Using Eqs. (6.1.35) and (6.1.41), we can find the additional commutation relations

$$\left[\hat{H}, \hat{a}^- \right] = -\hbar\omega\hat{a}^-, \tag{6.1.42}$$

$$\left[\hat{H}, \hat{a}^+ \right] = \hbar\omega\hat{a}^+, \tag{6.1.43}$$

applicable to a particular single mode of the field, and the eigenvalues and eigenstates of the quantized electromagnetic field can be determined.

Let the eigenstates be $|n\rangle$ and the corresponding eigenvalues be E_n, so that

$$\hat{H} |n\rangle = E_n |n\rangle . \tag{6.1.44}$$

The energy of the field state $\hat{a}^- |n\rangle$ is different from E_n, and may be found by substituting Eq. (6.1.42) into Eq. (6.1.44).

$$\hat{H}\hat{a}^- |n\rangle = (\hat{a}^- \hat{H} - \hbar\omega\hat{a}^-)|n\rangle$$

$$= (E_n - \hbar\omega)\hat{a}^- |n\rangle. \tag{6.1.45}$$

The action of $\hat{H}$ on state $\hat{a}^- |n\rangle$ reveals that its eigenvalue is $E_n - \hbar\omega$. Evidently, the operator $\hat{a}^-$ reduces the energy eigenvalue of the field by an amount $\hbar\omega$, making it an energy "lowering" or "annihilation" operator. Repeated application of this operator therefore produces eigenstates with progressively smaller eigenvalues until the state of lowest energy is reached.

The lowest eigenvalue is positive. This is readily confirmed by examining the expectation value of the Hamiltonian for an arbitrary state $|\psi\rangle$.

$$\left\langle \psi \left| \hbar\omega \left(\hat{a}^+\hat{a}^- + \frac{1}{2} \right) \right| \psi \right\rangle = \hbar\omega \langle\psi| \hat{a}^+\hat{a}^- |\psi\rangle + \frac{1}{2}\hbar\omega. \tag{6.1.46}$$

The expectation value $\langle\psi|\hat{a}^+\hat{a}^-|\psi\rangle$ can be interpreted as the probability $\langle\psi'|\psi'\rangle$ of being in the state $|\psi'\rangle = \hat{a}^-|\psi\rangle$. All state occupation probabilities are positive definite. Since ω is also positive, the entire right side of Eq. (6.1.46) must be positive. The eigenvalue E_n is therefore positive.

Now consider the lowest energy eigenstate of the field $|\psi_0\rangle = |0\rangle$, where the notation simply labels the state by its quantum number n. The lowest energy state has $n = 0$. Action of $\hat{a}^-$ on $|0\rangle$ must yield 0, since otherwise $|0\rangle$ would not be the state of lowest energy.

$$\hat{a}^- |0\rangle = 0. \tag{6.1.47}$$

The lowest possible energy in each mode of the field can now be calculated, with the result

$$\left\langle 0 \left| \hbar\omega \left(\hat{a}^+\hat{a}^- + \frac{1}{2} \right) \right| 0 \right\rangle = \hbar\omega \langle 0| \hat{a}^+\hat{a}^- |0\rangle + \frac{1}{2}\hbar\omega = \frac{1}{2}\hbar\omega. \tag{6.1.48}$$

Hence the energy of the zero state is

$$E_0 \equiv \langle 0| \hat{H}_{\text{field}} |0\rangle = \frac{1}{2}\hbar\omega. \tag{6.1.49}$$

Application of the commutation relation Eq. (6.1.43) can now be used to generate

all states of higher energy, together with their eigenvalues. For example, the $n = 1$ state is

$$\hat{H}\,|1\rangle = \hat{H}\hat{a}^+\,|0\rangle = \left(\hat{a}^+\hat{H} + \hbar\omega\hat{a}^+\right)|0\rangle$$

$$= \left(\frac{1}{2}\hbar\omega\hat{a}^+ + \hbar\omega\hat{a}^+\right)|0\rangle$$

$$= \frac{3}{2}\hbar\omega\hat{a}^+\,|0\rangle. \tag{6.1.50}$$

Repeating this procedure n times yields

$$\hat{H}\,|n\rangle = \hat{H}\left(\hat{a}^+\right)^n |0\rangle = \left(n + \frac{1}{2}\right)\hbar\omega\left(\hat{a}^+\right)^n |0\rangle. \tag{6.1.51}$$

The eigenvalues of the field are therefore

$$E_n = \left(n + \frac{1}{2}\right)\hbar\omega. \tag{6.1.52}$$

According to Eq. (6.1.45), the state $\hat{a}^-|n\rangle$ is an eigenstate of the Hamiltonian. If such a state is to be consistently normalized, we need to find a scalar s_n such that

$$\hat{a}^-\,|n\rangle = s_n\,|n-1\rangle. \tag{6.1.53}$$

From Eq. (6.1.51) we see that

$$\left(\hat{a}^+\hat{a}^- + \frac{1}{2}\right)\hbar\omega\,|n\rangle = \left(n + \frac{1}{2}\right)\hbar\omega\,|n\rangle,$$

or

$$\langle n|\,\hat{a}^+\hat{a}^-\,|n\rangle = n\,\langle n|\,n\rangle = n. \tag{6.1.54}$$

Multiplying Eq. (6.1.53) by its adjoint we find

$$s_n^2\,\langle n-1|\,n-1\rangle = \langle n|\,\hat{a}^+\hat{a}^-\,|n\rangle = n, \tag{6.1.55}$$

or

$$s_n = \sqrt{n}. \tag{6.1.56}$$

The result is

$$\hat{a}^-\,|n\rangle = \sqrt{n}\,|n-1\rangle. \tag{6.1.57}$$

By analyzing the effect of the adjoint operator $\hat{a}^+\,|n\rangle = s_{n+1}\,|n+1\rangle$, one finds

$$s_{n+1}^2\,\langle n+1|\,n+1\rangle = \langle n|\,\hat{a}^-\hat{a}^+\,|n\rangle = \langle n|\,(\hat{a}^+\hat{a}^- + 1)\,|n\rangle = (n+1). \tag{6.1.58}$$

Therefore, we also find

$$s_{n+1} = \sqrt{n+1}, \tag{6.1.59}$$

$$\hat{a}^+\,|n\rangle = \sqrt{n+1}\,|n+1\rangle. \tag{6.1.60}$$
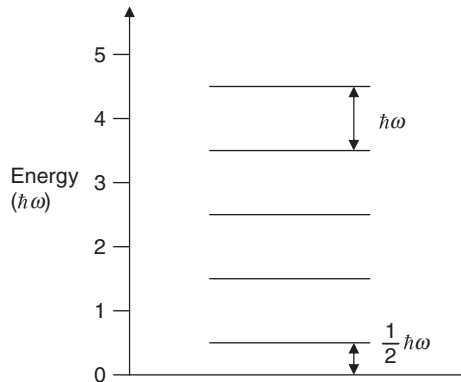
Figure 6.2 *Energy structure of the quantized electromagnetic field for a single mode, showing equally spaced levels above the zero-point energy of $\frac{1}{2}\hbar\omega$, the energy of the vacuum field.*

When written in terms of the "creation" or "raising" operator $\hat{a}^{+}$, the normalized eigenstates are therefore

$$|n\rangle = \frac{1}{\sqrt{n!}} \left(\hat{a}^{+}\right)^{n} |0\rangle, \tag{6.1.61}$$

and may be thought of as states with n quanta of energy $\hbar\omega$ in the mode. Such states are called photon number or Fock states. Although the allowed energy eigenvalues for each mode are now discrete as shown in Fig. 6.2, the energy expectation values for multimode fields can take on essentially any value if they consist of superpositions of a great many photon number eigenstates. Also the lowest energy state does not correspond to occupation of the mode by one quantum, since its energy is only half the requisite energy per photon. This is the zero-point energy of the field.

In the treatment above, the Pauli exclusion principle is ignored. This is because the field states are equally spaced, making them bosonic in character. More than one quantum of excitation may exist per mode. In half-integer spin systems the statistics are different. Only one excitation per available state is permitted. Hence, in Fermionic systems great care must be exercised in the construction of appropriate energy states (see Appendix E).

Exercise:

(a) Show that the expectation value of the electric field in a Fock state is 0. That is, show that

$$\left\langle n \left| \hat{E} \right| n \right\rangle = 0. \tag{6.1.62}$$

(b) Show that the expectation of the square of the electric field in a number state is not zero. This result indicates that the energy density is not zero, and there are field fluctuations even in the lowest energy state of the field, although it is unoccupied. These are known as vacuum field fluctuations.

$$\left\langle n \left| \hat{E}^{2} \right| n \right\rangle \neq 0. \tag{6.1.63}$$

6.2   Spontaneous emission

In this section, a single-mode calculation of light emission induced by the quantized electromagnetic field is presented. Even when the radiation field contains no photons, emission is found to be induced by vacuum field fluctuations. This explains the origin of spontaneous emission but fails to give a proper account of the decay behavior of real atoms, because a single-mode treatment also introduces spontaneous absorption, which is not observed in nature. This shortcoming is remedied (in Section 6.3) by taking into account the many modes of space available for spontaneous emission that are not available in the absorption process.

   With both quantized atomic states $|\psi_{\text{atom}}\rangle = |\psi_m\rangle$ and quantized field states $|\psi_{\text{field}}\rangle = \sum_n c_n |n\rangle$ in hand, the construction of completely quantized state vectors for the system consisting of atom plus field is straightforward. We begin by writing down an expansion in terms of atom–field product states

$$|\psi> = \sum_{m,n} c_{mn} |\psi_m\rangle |n\rangle, \tag{6.2.1}$$

and consider an atom with two states labeled 1 and 2. The system Hamiltonian is

$$\hat{H} = \hat{H}_{\text{atom}} + \hat{H}_{\text{field}} + \hat{H}_{\text{int}}. \tag{6.2.2}$$

For interaction of the atom with a single-mode field, the first two components of $\hat{H}$ are simply

$$\hat{H}_{\text{atom}} = \hbar \begin{pmatrix} \omega_2 & 0 \\ 0 & \omega_1 \end{pmatrix}, \tag{6.2.3}$$

$$\hat{H}_{\text{field}} = \hbar\omega \left(\hat{a}^+ \hat{a}^- + \frac{1}{2} \right). \tag{6.2.4}$$

As in Eq. (2.3.8), the dipole moment operator is $\hat{\mu} = \mu(\hat{\sigma}^+ + \hat{\sigma}^-)$. Since the interaction of light with the atom takes place at the origin in the point dipole approximation, the electric field operator Eq. (6.1.35) reduces to $\hat{E} = \sum_{k,\lambda} \sqrt{\hbar\omega_k/2\varepsilon_0 V}[\hat{a}_{k\lambda}^- + \hat{a}_{k\lambda}^+]\hat{e}_{k\lambda}$ for linear (real) polarization in the direction $\hat{e}_{k\lambda}$, so for this case the last component of the total Hamiltonian can simply be written

$$\hat{H}_{\text{int}} = -\mu\xi \left(\hat{\sigma}^- + \hat{\sigma}^+ \right) \left(\hat{a}^-(t) + \hat{a}^+(t) \right) \hat{\mu} \cdot \hat{e}, \tag{6.2.5}$$

where $\xi \equiv \sqrt{\hbar\omega/2\varepsilon_0 V}$ is the electric field per photon and μ is the electric dipole matrix element. In many materials the induced dipole is parallel to the field direction. Under these circumstances one has the additional simplification that $\hat{\mu} \cdot \hat{e} = 1$. However, in crystals the induced dipole may not be parallel to the field, in which case this simplification is unacceptable.

Eq. (6.2.5) is the coupling Hamiltonian for an atom interacting with a single-mode field polarized along the direction $\hat{e}$. In it appear the combinations of Pauli spin matrices $\hat{\sigma}^+$ and $\hat{\sigma}^-$ encountered in Chapter 2:

$$\hat{\sigma}^- = \frac{1}{2}(\hat{\sigma}_x - i\hat{\sigma}_y) = \begin{pmatrix} 0 & 0 \\ 1 & 0 \end{pmatrix}, \qquad (6.2.6)$$

$$\hat{\sigma}^+ = \frac{1}{2}(\hat{\sigma}_x + i\hat{\sigma}_y) = \begin{pmatrix} 0 & 1 \\ 0 & 0 \end{pmatrix}. \qquad (6.2.7)$$

$\hat{\sigma}^+$ and $\hat{\sigma}^-$ change the occupation of states of the atom in the same way that $\hat{a}^+, \hat{a}^-$ change the occupation number of states of the electromagnetic field. This was confirmed in Eqs. (2.3.6) and (2.3.7):

$$\hat{\sigma}^- \begin{pmatrix} 1 \\ 0 \end{pmatrix} = \begin{pmatrix} 0 \\ 1 \end{pmatrix}; \quad \hat{\sigma}^+ \begin{pmatrix} 0 \\ 1 \end{pmatrix} = \begin{pmatrix} 1 \\ 0 \end{pmatrix}. \qquad (6.2.8)$$

Note however that atomic operators only act on atomic states. They do not have any effect on states of the field. Similarly, field operators do not change the state of the atom, only the state of the field.

In the interaction representation, the interaction Hamiltonian becomes

$$\hat{H}_{\text{int}}^{\text{I}} = \hbar g \left\{ \hat{a}^- \hat{\sigma}^+ \exp[-i(\omega - \omega_0)t] + h.c. + \hat{a}^- \hat{\sigma}^- \exp[-i(\omega + \omega_0)t] + h.c. \right\}, \qquad (6.2.9)$$

where $g \equiv -(\mu\xi/\hbar)$. Utilizing the RWA, this simplifies to

$$\hat{H}_{\text{int}}^{\text{I}} = \hbar g \left\{ \hat{a}^- \hat{\sigma}^+ \exp[-i(\omega - \omega_0)t] + h.c. \right\}. \qquad (6.2.10)$$

The omitted terms are called non-secular because they do not conserve energy. The final Hamiltonian in Eq. (6.2.10) only causes transitions between the states $|2\rangle|n\rangle$ and $|1\rangle|n+1\rangle$, where a photon is added to the field as the atom makes a downward transition, thus conserving energy. States $|2\rangle|n+1\rangle$ and $|1\rangle|n\rangle$ can therefore be ignored and Eq. (6.2.1) becomes

$$\left|\psi^{\text{I}}\right\rangle = c_{2,n}|2n\rangle + c_{1,n+1}|1, n+1\rangle. \qquad (6.2.11)$$

In the interaction picture, the Schrodinger equation is

$$\frac{d}{dt}|\psi^{\text{I}}\rangle = -\frac{i}{\hbar}\hat{H}_{\text{int}}^{\text{I}}|\psi^{\text{I}}\rangle. \qquad (6.2.12)$$

Substitution of Eqs. (6.2.10) and (6.2.11) into (6.2.12) yields

$$\frac{d}{dt}|\psi^{\text{I}}\rangle = -ig\left[\hat{a}^- \hat{\sigma}^+ \exp[-i(\omega - \omega_0)t] + h.c.\right]\left\{c_{2,n}|2n\rangle + c_{1,n+1}|1, n+1\rangle\right\}. \qquad (6.2.13)$$
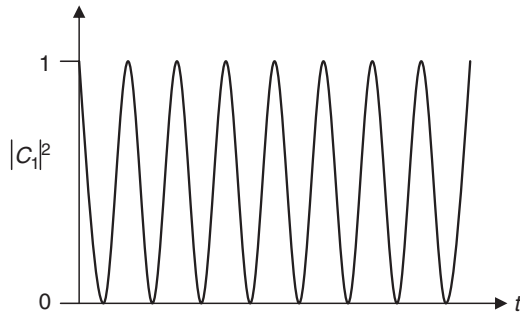
Figure 6.3 *Qualitative behavior of spontaneous absorption predicted by an exact Rabi treatment of a two-level atom interacting with a single mode of the electromagnetic field.*

From Eq. (6.2.11) we can also write

$$\frac{d}{dt}\left|\psi^{\mathrm{I}}\right\rangle = \dot{c}_{2,n}\left|2n\right\rangle + \dot{c}_{1,n+1}\left|1, n+1\right\rangle. \tag{6.2.14}$$

Projecting both Eqs. (6.2.13) and (6.2.14) onto $\langle 2n|$ now gives the coefficient

$$\dot{c}_{2,n} = -igc_{1,n+1}\sqrt{n+1}\exp[-i(\omega - \omega_0)t]. \tag{6.2.15}$$

Similarly, projection onto $\langle 1, n+1|$ yields the coefficient

$$\dot{c}_{1,n+1} = -igc_{2,n}\sqrt{n+1}\exp[i(\omega - \omega_0)t]. \tag{6.2.16}$$

First-order perturbation solutions of Eqs. (6.2.15) and (6.2.16) for an atom initially in the excited state give the emission probability. At short times this is the same as the probability of finding the atom in the lower state. Hence it is equal to

$$|c_{1,n+1}|^2 \doteq g^2\left(n+1\right)t^2\left[\frac{\sin^2\left(\omega - \omega_0\right)t/2}{\left[\left(\omega - \omega_0\right)t/2\right]^2}\right]. \tag{6.2.17}$$

Notice that even with no photons present ($n = 0$), there is some probability of finding that the atom has decayed. Since there is no external field present, this accounts for the well-known phenomenon of spontaneous emission. Unfortunately the theory is flawed, because the absorption probability for an atom initially in the ground state is also nonzero. This would cause spontaneous absorption (Fig. 6.3), which is not observed in nature. That is, we would calculate

$$|c_{2,n}|^2 \doteq g^2\left(n+1\right)t^2\left[\frac{\sin^2\left(\omega - \omega_0\right)t/2}{\left[\left(\omega - \omega_0\right)t/2\right]^2}\right]. \tag{6.2.18}$$

This flaw in the theory is not due to the perturbation approach we chose. The exact Rabi solution predicts the same (unphysical) behavior. In emission, the Rabi results are

$$c_{2,n} = \cos\left(g\sqrt{(n+1)}t\right), \tag{6.2.19}$$

$$c_{1,n+1} = -i\sin\left(g\sqrt{(n+1)}t\right), \tag{6.2.20}$$

and in absorption one finds

$$c_{2,n} = -i\sin\left(g\sqrt{(n+1)}t\right), \tag{6.2.21}$$

$$c_{1,n+1} = \cos\left(g\sqrt{(n+1)}t\right). \tag{6.2.22}$$

The theory obviously needs refinement. An atom cannot absorb a quantum spontaneously from the vacuum state without producing a state of the field with one less photon. Such a state would necessarily be of lower energy than the vacuum state, but $|0\rangle$ is already defined to be the lowest energy eigenstate of the field. Hence, this violates a key premise, and we need to pursue a remedy of this problem in the next section by investigating a multimode version of this analysis.

6.3 Weisskopf–Wigner theory

So far, our theory of transition rates and decay involves only a single mode of the field, and emission is assumed to be perfectly monochromatic. However, to be in accord with the Heisenberg uncertainty principle, there must be a spread in emitted frequencies for any process that takes place over a finite interval. That is, the emission spectrum must have a finite bandwidth, something that can only be included through a multimode treatment.

To extend the treatment to more than one mode, the Hamiltonian must be written as a summation over all possible modes s. The wavefunction must also be written as a summation over all possible states of the atom m and mode occupation numbers n_s.

$$\hat{H}_{\text{int}}^{\text{I}} = \sum_s \hbar g_s \left[\hat{\sigma}^+ \hat{a}_s \exp[-i(\omega_s - \omega_0)t] + h.c.\right], \tag{6.3.1}$$

$$|\psi^{\text{I}}\rangle = \sum_\alpha \sum_{n_1} \sum_{n_2} \cdots \sum_{n_s} \cdots C_{\alpha;n_1,n_2\dots n_s\dots} |\alpha; n_1, n_2, \dots n_s, \dots\rangle. \tag{6.3.2}$$

In Eq. (6.3.2), the sum over energy states includes $\alpha = 1, 2$ and the sum over photon occupation runs over the values $n_s = 0, 1, 2, 3 \dots \infty$. The field operators $\hat{a}_s^-, \hat{a}_s^+$ for

mode s affect only the occupation of the individual mode s. So, for example

$$\hat{a}_s^- |\alpha; n_1 n_2 \ldots n_s \ldots\rangle = \hat{a}_s^- |\alpha\rangle |n_1\rangle |n_2\rangle \ldots |n_s\rangle \ldots$$

$$= |\alpha\rangle |n_1\rangle |n_2\rangle \ldots \hat{a}_s^- |n_s\rangle \ldots$$

$$= \sqrt{n_s} |\alpha; n_1, n_2 \ldots (n_s - 1) \ldots\rangle . \qquad (6.3.3)$$

As before, transition probability amplitudes are calculated according to

$$\dot{C}_{\alpha; n_1 n_2 \ldots n_s \ldots} = -\frac{i}{\hbar} \sum_{\beta} \sum_{m_1, m_2, \ldots m_s \ldots}$$

$$\langle \alpha; n_1, n_2, \ldots n_s \ldots | \sum_s (\hat{H}_{int}^{I})_s |\beta; m_1, m_2 \ldots m_s \ldots\rangle C_{\beta; m_1, m_2 \ldots m_s \ldots}.$$

$$(6.3.4)$$

The interaction matrix element can be simplified:

$$\langle \alpha; n_1, n_2 \ldots n_s \ldots | \sum_r (\hat{H}_{int}^{I}) |\beta; m_1, m_2 \ldots m_r \ldots\rangle$$

$$= \sum_r \langle n_r | \langle \alpha | \left(\hat{H}_{int}^{I} \right)_r |\beta\rangle |m_r\rangle \langle n_1, n_2 \cdots n_{r-1}, n_{r+1} \cdots |m_1, m_2 \cdots m_{r-1}, m_{r+1} \cdots\rangle$$

$$= \sum_r \langle \alpha; n_r | \left(\hat{H}_{int}^{I} \right)_r |\beta; m_r\rangle \delta_{n_1 m_1} \delta_{n_2 m_2} \cdots \delta_{n_{r-1} m_{r-1}} \delta_{n_{r+1} m_{r+1}} \cdots \qquad (6.3.5)$$

so that

$$\dot{C}_{\alpha; n_1, n_2 \ldots n_s \ldots} = -\frac{i}{\hbar} \sum_{\beta} \sum_r \sum_{m_r} \langle \alpha; n_r | (H_{int}^{I})_r |\beta; m_r\rangle C_{\beta; n_1, n_2 \ldots m_r \ldots}. \qquad (6.3.6)$$

Note that the interaction matrix element is zero if H_{int} has the form in Eq. (6.3.1) and the atomic state remains unchanged ($\alpha = \beta$). So the final equations of motion in this case are

$$\dot{C}_{2; n_1, n_2 \ldots n_s \ldots} = -i \sum_r g_r \sqrt{n_r + 1} \exp[-i(\omega_r - \omega_0)t] C_{1; n_1, n_2 \ldots (n_r + 1) \ldots} \qquad (6.3.7)$$

$$\dot{C}_{1, n_1, n_2 \ldots n_s \ldots} = -i \sum_r g_r \sqrt{n_r} \exp[i(\omega_r - \omega_0)t] C_{2, n_1 \ldots (n_r - 1) \ldots} \qquad (6.3.8)$$

Now, returning to the emission problem, assume that initially there are no photons in any mode, and that the system is in the upper state $|2\rangle$. Then the initial condition and equations of motion are

$$C_{2, \{0\}} (0) = 1, \qquad (6.3.9)$$

$$\dot{C}_{2, \{0\}} = -i \sum_r g_r \exp[-i(\omega_r - \omega_0)t] C_{1, \{1_r\}}, \qquad (6.3.10)$$

$$\dot{C}_{1, \{1_s\}} = -i g_s \exp[i(\omega_s - \omega_0)t] C_{2, \{0\}}, \qquad (6.3.11)$$

where $\omega_0 = \omega_2 - \omega_1$. The formal solution of Eq. (6.3.11), namely

$$C_{1,\{1_r\}}(t) = -ig_r \int_0^t \exp[i(\omega_r - \omega_0)t']C_{2,\{0\}}(t')\,dt', \tag{6.3.12}$$

may be used in Eq. (6.3.10) to find

$$\dot{C}_{2,\{0\}} = -\sum_r g_r^2 \int_0^t \exp\left[-i(\omega_r - \omega_0)(t - t')\right]C_{2,\{0\}}(t')\,dt'. \tag{6.3.13}$$

The summation over r accounts for all the modes into which emission may occur. We assume the modes are closely spaced in frequency, and replace the summation over r by integration over frequency ω'. That is, we make the replacement

$$\sum_r \rightarrow \int D(\omega')d\omega', \tag{6.3.14}$$

where $D(\omega)$, the number of final radiation states per unit frequency interval in a volume V, is called the density of states or the density of modes:

$$D(\omega) = \frac{V\omega^2}{\pi^2 c^3}. \tag{6.3.15}$$

With these changes, Eq. (6.3.13) becomes

$$\dot{C}_{2,\{0\}}(t) = -\int d\omega' g^2(\omega')\,D(\omega') \int_0^t \exp[-i(\omega' - \omega_0)(t - t')]C_{2,\{0\}}(t')\,dt. \tag{6.3.16}$$

We now assume that $g^2(\omega')$ and $D(\omega')$ vary slowly with frequency. These quantities can then be removed from inside the integral in Eq. (6.3.16).

$$\dot{C}_{2,\{0\}} = -g^2(\omega)D(\omega) \int d\omega' \int_0^t \exp[-i(\omega' - \omega)(t - t')]C_{2,\{0\}}(t')dt'. \tag{6.3.17}$$

For a given mode frequency ω', the final integral is dominated by contributions at $t = t'$. Hence

$$\int d\omega' \int_0^t \exp[-i(\omega' - \omega)(t - t')]C_{2,\{0\}}(t')dt' \tag{6.3.18}$$

$$= C_{2,\{0\}}(t)\left\{\pi\delta(\omega' - \omega_0) - iP\left(\frac{1}{\omega' - \omega_0}\right)\right\}. \tag{6.3.19}$$

In Eq. (6.3.19), P denotes the principal part of the integral. This equation reveals that

the relaxation process has real and imaginary parts given by

$$\text{Re}\left\{\dot{C}_{2,\{0\}}(t)\right\} = -\pi g^2(\omega) D(\omega) C_{2,\{0\}}(t) \tag{6.3.20}$$

$$\text{Im}\left\{\dot{C}_{2,\{0\}}(t)\right\} = g^2(\omega) D(\omega) P\left(\frac{1}{\omega' - \omega}\right) C_{2,\{0\}}(t) \tag{6.3.21}$$

The real part of $\dot{C}_{2,\{0\}}$ describes spontaneous relaxation of the system. Eq. (6.3.20) has the form

$$\dot{C}_{2,\{0\}}(t) = -\frac{1}{2}\gamma C_{2,\{0\}}(t), \tag{6.3.22}$$

where the decay rate is given by

$$\gamma \equiv 2\pi g^2(\omega) D(\omega) = \frac{\mu^2 \omega^3}{\varepsilon_0 \pi \hbar c^3}. \tag{6.3.23}$$

The interaction constant g^2 in Eq. (6.3.23) depends on the square of the scalar product between the field and induced dipole direction as indicated in Eq. (6.2.5). This contributes a factor of $\cos^2\theta$ to the decay rate which must be averaged over θ. Since the vacuum field is unpolarized the result is $<\cos^2\theta> = 1/3$, so the spontaneous emission rate is $\gamma_{sp} = \gamma/3$. Solution of Eq. (6.3.22) then yields exponential decay of the occupation probability itself:

$$\left|C_{2,\{0\}}(t)\right|^2 = \exp(-\gamma_{sp}t). \tag{6.3.24}$$

This justifies our earlier assumption that upper state probability decays with a lifetime $\tau = 1/\gamma_{sp}$. Additional details may be found in Ref. [6.1]. The imaginary part of $\dot{C}_{2,\{0\}}$ in Eq. (6.3.21) yields a shift of the energy level. For more discussion of driven and undriven dissipation processes and associated frequency shifts (the AC Stark shift and Lamb shift respectively) see Appendix F and Refs. [6.2 and 6.3].

Exercise: Show that spontaneous absorption no longer occurs with a multimode treatment, by calculating $\dot{C}_2(0)$ for the initial condition $C_1(0) = 1$.

6.4   Coherent states

In previous sections we found that annihilation and creation operators $\hat{a}^-$, $\hat{a}^+$ changed the occupation of number states used to describe the field. Now we construct states of the field which "cohere" when acted upon by the non-Hermitian operator $\hat{a}^-$. These new states are normalized eigenstates of the operator $\hat{a}^-$ that remain essentially unchanged as they propagate in space and time. Because they retain their basic form, they are said to be coherent and closely describe the properties of laser beams for example.

A coherent state $|\alpha\rangle$ is defined to be an eigenstate of the annihilation operator. It maintains its essential character despite changes in the number of photons of which it is composed. Thus,

$$\hat{a}^-|\alpha\rangle = \alpha|\alpha\rangle. \tag{6.4.1}$$

Eigenstates of field operators must be based on the operator $\hat{a}^-$ because $\hat{a}^+$ does not have eigenstates. A discussion of this point may be found in Ref. [6.4] and it means the action of the creation operator on a coherent state can only be defined when it acts to the left, since this is the conjugate of Eq. (6.4.1).

$$\langle\alpha|\, a^+ = \langle\alpha|\, \alpha^* \tag{6.4.2}$$

We shall insist that $|\alpha\rangle$ be normalized:

$$\langle\alpha|\, \alpha\rangle = 1. \tag{6.4.3}$$

However, because they are eigenstates of a non-Hermitian operator, different coherent states $|\alpha\rangle$ and $|\alpha'\rangle$ are not orthogonal, although they do form a complete set. Here we merely seek the relationship between $|\alpha\rangle$ and our earlier number states $|n\rangle$.

$$|\alpha\rangle = \sum_{n=0}^{\infty} |n\rangle\langle n|\alpha\rangle \tag{6.4.4}$$

$$\hat{a}^-|\alpha\rangle = \sum_{n=0}^{\infty} \hat{a}^-|n\rangle\langle n|\alpha\rangle. \tag{6.4.5}$$

Insertion of the earlier result from Eq. (6.1.54) yields

$$\hat{a}^-|\alpha\rangle = \sum_{n=1}^{\infty} \langle n|\alpha\rangle\sqrt{n}|n-1\rangle. \tag{6.4.6}$$

By replacing n with $n+1$, the sum can be rewritten as

$$\hat{a}^-|\alpha\rangle = \sum_{n=0}^{\infty} \langle n+1|\alpha\rangle\sqrt{n+1}|n\rangle. \tag{6.4.7}$$

Combining Eqs. (6.4.5) and (6.4.7) we obtain

$$\sum_{n=0}^{\infty} \sqrt{n+1}|n\rangle\langle n+1|\alpha\rangle = \sum_{n=0}^{\infty} \hat{a}^-|n\rangle\langle n|\alpha\rangle = \alpha|\alpha\rangle. \tag{6.4.8}$$

Multiplying through by $\langle m|$ and using the orthogonality of the number states ($\langle m|n\rangle = \delta_{mn}$), one finds

$$\langle n+1|\, \alpha\rangle = \frac{\langle n|\, \alpha\rangle}{\sqrt{n+1}}\alpha. \tag{6.4.9}$$

All the coefficients $\langle n|\alpha\rangle$ for the expansion in Eq. (6.4.4) can be found by using Eq. (6.4.9) as a recursion relation to build up subsequent coefficients from the first one, which is $\langle 0|\alpha\rangle$.

$$\langle n\,|\alpha\rangle = \frac{\alpha^n}{\sqrt{n!}}\,\langle 0\,|\alpha\rangle\,. \tag{6.4.10}$$

Substituting Eq. (6.4.10) in Eq. (6.4.4) we find

$$|\alpha\rangle = c_0 \sum_{n=0}^{\infty} \frac{\alpha^n}{\sqrt{n!}} |n\rangle, \tag{6.4.11}$$

where $c_0 \equiv <0|\alpha>$. But what is c_0? To find this coefficient explicitly, we make use of the normalization condition $\langle\alpha|\alpha\rangle = 1$.

$$\langle\alpha|\,\alpha\rangle = |c_0|^2 \sum_{m,n} \frac{(\alpha^*)^m \, \alpha^n}{\sqrt{m!n!}} < m|n >$$

$$= |c_0|^2 \sum_n \frac{|\alpha|^{2n}}{n!} = |c_0|^2 \exp(|\alpha|^2). \tag{6.4.12}$$

Setting Eq. (6.4.12) equal to 1, the coefficient is found to be

$$c_0 = \exp\left(-\frac{1}{2}|\alpha|^2\right). \tag{6.4.13}$$

Consequently the normalized form of the coherent state is

$$|\alpha\rangle = \exp\left(-\frac{1}{2}|\alpha|^2\right) \sum_n \frac{\alpha^n}{\sqrt{n!}} |n\rangle, \tag{6.4.14}$$

or

$$|\alpha\rangle = \hat{D}(\alpha)|0\rangle = e^{-\frac{1}{2}|\alpha|^2 + \alpha a^+} |0\rangle. \tag{6.4.15}$$

Exercise: Using the Campbell–Baker–Haussdorf or Weyl formula (see Problem 6.1)

$$\exp\left(\hat{c} + \hat{d} + \frac{1}{2}\left[\hat{c},\hat{d}\right]\right) = \exp(\hat{c})\exp(\hat{d}), \tag{6.4.16}$$

and commutation relations of the raising and lowering operators, show that Eq. (6.4.15) can also be expressed in the form

$$|\alpha\rangle = e^{\alpha a^+ - \alpha^* a^-} |0\rangle. \tag{6.4.17}$$

Now consider some of the properties of coherent states, as defined by Eq. (6.4.14). The proportion of a coherent state that consists of some particular number state is given by the projection (or inner product) of the one on the other.

$$\langle n|\,\alpha\rangle = \exp\left(-|\alpha|^2/2\right) \frac{\alpha^n}{\sqrt{n!}}. \tag{6.4.18}$$

Hence

$$|\langle n|\,\alpha\rangle|^2 = \exp\left(-|\alpha|^2/2\right) \frac{|\alpha|^{2n}}{n!}. \tag{6.4.19}$$

The quantity $|\langle n|\alpha\rangle|^2$ is also the probability of finding n photons in the state $|\alpha\rangle$. The probability distribution of a coherent state, given by Eq. (6.4.19), is Poissonian rather than Gaussian in form.

Let us examine more closely how the state $|\alpha\rangle$ evolves in time. By making use of what we have learned about the way the ladder operators $\hat{a}$ and $\hat{a}^+$ act on number states, we find

$$|\alpha(t)\rangle = \exp(-iHt/\hbar)\,|\alpha(0)\rangle$$

$$= \exp[-i\hbar\omega(\hat{a}^+\hat{a}^-)t/\hbar]\left\{\exp\left(-\frac{1}{2}|\alpha|^2\right)\sum_n\frac{\alpha^n}{\sqrt{n!}}\,|n\rangle\right\}$$

$$= \sum_n\frac{[\alpha\exp(-i\omega t)]^n}{\sqrt{n!}}\exp\left(-\frac{1}{2}|\alpha|^2\right)|n\rangle$$

$$= |\alpha\exp(-i\omega t)\rangle. \tag{6.4.20}$$

As time progresses, the eigenvalue of state $|\alpha\rangle$ merely acquires a phase factor. That is, it evolves coherently. A more complete proof that $|\alpha\rangle$ evolves coherently in time, in which H is the general Hamiltonian of a forced harmonic oscillator, may be found in Ref. [6.5].

An interesting point is that expectation values for the electric field and the field fluctuations in a coherent state both differ from those of an electric field that is a number state.

$$\langle\alpha|\,\hat{E}\,|\alpha\rangle = \xi\hat{\varepsilon}\left[\langle\alpha|\,\hat{a}^-\,|\alpha\rangle + \langle\alpha|\,\hat{a}^+\,|\alpha\rangle\right] = \xi\hat{\varepsilon}(\alpha+\alpha^*) \neq 0. \tag{6.4.21}$$

The amplitude of the field in Eq. (6.4.21) depends on the complex quantity α. The phase of the field is the phase of α and the magnitude depends on $|\alpha|$, which is proportional to the square root of the number of photons.

Exercise: Show that

$$\langle\alpha|\,E^2\,|\alpha\rangle = \frac{\hbar\omega}{2\varepsilon_0 V}\left(1 - [\alpha-\alpha^*]^2\right). \tag{6.4.22}$$

Use this result to show that the mean square fluctuation of the field is

$$\left\langle\Delta E^2\right\rangle \equiv \langle\alpha|\,E^2\,|\alpha\rangle - (\langle\alpha|\,E\,|\alpha\rangle)^2 = \frac{\hbar\omega}{2\varepsilon_0 V}. \tag{6.4.23}$$

Eq. (6.4.23) is an important result which differs from our earlier one for photon number states where the mean square fluctuation tended to infinity as the photon number n increased. Here we find that quantum fluctuations in a coherent state are just zero-point fluctuations of the vacuum which exhibit no dependence on E or α.

Notice that the expectation value of the field in a coherent state, given by Eq. (6.4.21) for a single mode, returns the form of a classical plane wave. Hence, there must be a very close correspondence between a single mode coherent field and a classical plane wave. Multimode coherent states correspond to superpositions of plane waves. Moreover, the relative fluctuations in the field diminish as the mean number of photons in the coherent state increases, as indicated in Fig. 6.4. Coherent states therefore resemble well-defined classical fields more and more as their amplitude increases.
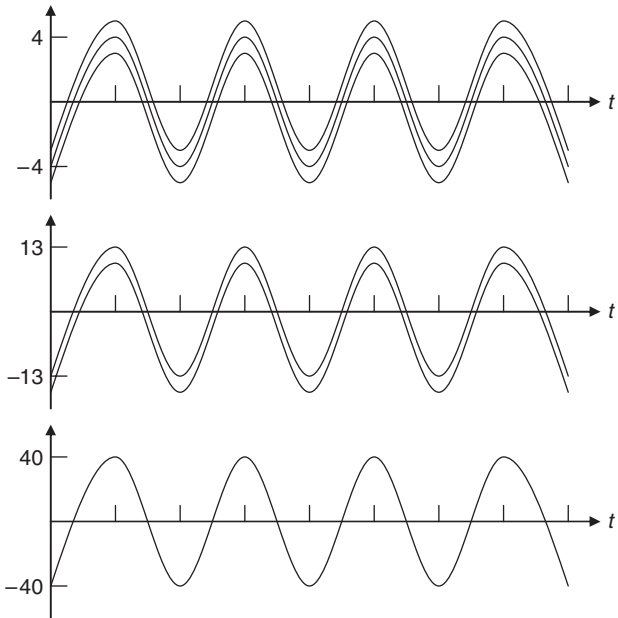
Figure 6.4 *A schematic illustration of the relative reduction of noise in a coherent state that accompanies an increase of the strength of the field. From top to bottom, the mean photon number $|\alpha|^2$ is 4, 40, and 400, respectively. The vertical width of the traces reflects the uncertainty in the field value, and includes both the amplitude uncertainty due to Δn and the phase uncertainty. (After Ref. [6.6].)*

Now let us examine uncertainties of the conjugate variables Q, P defined by Eqs. (6.1.30) and (6.1.31), which characterize the electromagnetic field in photon number and coherent states. The inverses of Eqs. (6.1.33) and (6.1.34) yield

$$\hat{Q} = \sqrt{\frac{\hbar}{2\omega}} \left(\hat{a}^- + \hat{a}^+ \right) \tag{6.4.24}$$

$$\hat{P} = -i\sqrt{\frac{\hbar\omega}{2}} \left(\hat{a}^- - \hat{a}^+ \right). \tag{6.4.25}$$

Exercise: It can readily be shown that for a field in a number state $|n\rangle$ the fluctuations of $< \hat{P} >$ and $< \hat{Q} >$ have the following properties:

$$(\Delta Q)_n^2 \equiv \langle n| \hat{Q}^2 |n\rangle - \langle n| \hat{Q} |n\rangle^2 = \frac{\hbar}{2\omega} (2n + 1) \tag{6.4.26}$$

$$(\Delta P)_n^2 \equiv \langle n| \hat{P}^2 |n\rangle - \langle n| \hat{P} |n\rangle^2 = \frac{\hbar\omega}{2} (2n + 1) \tag{6.4.27}$$

$$(\Delta Q \Delta P)_n = \frac{\hbar}{2} (2n + 1). \tag{6.4.28}$$

The product of uncertainties ΔP and ΔQ obeys an uncertainty principle, since for all values of n we find $(\Delta Q \Delta P) \geq \hbar/2$. However, only for the vacuum state do we find the minimum uncertainty condition $(\Delta Q \Delta P) = \hbar/2$ via Eq. (6.4.28).

With Eqs. (6.4.24) and (6.4.25) it can be shown that for a coherent state we have slightly different relations:

$$\langle \alpha | \hat{Q} | \alpha \rangle = \left(\frac{\hbar}{2\omega} \right)^{1/2} (\alpha^* + \alpha) \tag{6.4.29}$$

$$\langle \alpha | \hat{Q}^2 | \alpha \rangle = \frac{\hbar}{2\omega} \left([\alpha + \alpha^*]^2 + 1 \right) \tag{6.4.30}$$

$$\langle \alpha | \hat{P} | \alpha \rangle = i \left(\frac{\hbar}{2\omega} \right)^{1/2} (\alpha^* + \alpha) \tag{6.4.31}$$

$$\langle \alpha | \hat{P}^2 | \alpha \rangle = \frac{\hbar\omega}{2} \left([\alpha - \alpha^*]^2 - 1 \right) \tag{6.4.32}$$

$$(\Delta Q)_c^2 = \langle \alpha | \hat{Q}^2 | \alpha \rangle - \langle \alpha | \hat{Q} | \alpha \rangle^2 = \frac{\hbar}{2\omega} \tag{6.4.33}$$

$$(\Delta P)_c^2 = < \alpha \left| \hat{P}^2 \right| \alpha > - < \alpha \left| \hat{P} \right| \alpha >^2 = \frac{\hbar\omega}{2} \tag{6.4.34}$$

$$(\Delta Q \Delta P)_c = \frac{\hbar}{2}. \tag{6.4.35}$$

Notice that according to Eq. (6.4.35) a coherent state is always a minimum uncertainty state, whereas among the number states only the vacuum state had minimum uncertainty.

Since each mode of the radiation field has a complex amplitude, there must be two "quadrature" components associated with real and imaginary parts of the field operators $\hat{a}^-, \hat{a}^+$. This realization leads to an interesting discovery. So let us now write

$$\hat{a}^- = \frac{1}{\sqrt{2}} (\hat{a}_1 + i\hat{a}_2); \quad \hat{a}^+ = \frac{1}{\sqrt{2}} (\hat{a}_1 - i\hat{a}_2) \tag{6.4.36}$$

$$\hat{a}_1 = \frac{1}{\sqrt{2}} (\hat{a}^+ + \hat{a}^-); \quad \hat{a}_2 = \frac{i}{\sqrt{2}} (\hat{a}^+ - \hat{a}^-) \tag{6.4.37}$$

where subscripts refer to the two quadratures. With these definitions we find

$$\hat{Q} = \sqrt{\frac{\hbar}{2\omega}} (\hat{a}^+ + \hat{a}^-) = \sqrt{\frac{\hbar}{\omega}} \hat{a}_1, \tag{6.4.38}$$

$$\hat{P} = i\sqrt{\frac{\hbar\omega}{2}} (\hat{a}^+ - \hat{a}^-) = \sqrt{\hbar\omega} \hat{a}_2. \tag{6.4.39}$$

We can show explicitly that $\hat{a}_1$ and $\hat{a}_2$ correspond to orthogonal degrees of freedom in complex space by writing down the electric field operator in terms of these quadrature

components.

$$\hat{E}\,(\bar{r}, t) = \sqrt{\frac{\hbar\omega}{2\varepsilon_0 V}}\hat{\varepsilon}\,\left[\hat{a}^-\exp[-i(\omega t - \bar{k}\cdot\bar{r})] + \hat{a}^+\exp[i(\omega t - \bar{k}\cdot\bar{r})]\right]$$

$$= \sqrt{\frac{\hbar\omega}{\varepsilon_0 V}}\hat{\varepsilon}\,[\hat{a}_1\cos\phi + \hat{a}_2\sin\phi], \qquad (6.4.40)$$

where $\phi = \omega t - \bar{k}\cdot\bar{r}$.

It is interesting to compare the variances exhibited in the two quadratures of photon number representations of coherent states (Fig. 6.5). Since we already know that $[\hat{a}^-, \hat{a}^+] = 1$, it is straightforward to show that

$$[\hat{a}_1, \hat{a}_2] = i. \qquad (6.4.41)$$

Exercise: Show that if two variables A, B obey a commutator relation of the form $[A, B] = ic$, where c is a constant, the product of their uncertainties is given by

$$\Delta A \Delta B \geq c/2. \qquad (6.4.42)$$

On the basis of Eqs. (6.4.41) and (6.4.42), a photon number state $|n\rangle$ has fluctuations of the quadrature components that obey the uncertainty relation

$$(\Delta a_1 \Delta a_2)_n \geq 1/2. \qquad (6.4.43)$$

For a coherent state, the uncertainty product assumes the minimum value. This means

$$(\Delta a_1 \Delta a_2)_c = 1/2. \qquad (6.4.44)$$

Ordinarily the variances in a_1 and a_2 are equal. However, the implication of Eq. (6.4.44) is that in a broad class of coherent states called "squeezed states," which may be generated by creating correlations between the quadratures, the fluctuations in one quadrature may be reduced below the noise level of an ordinary (minimum uncertainty) coherent state. The noise in the second quadrature correspondingly must increase above the minimum level to maintain agreement with Eq. (6.4.44),
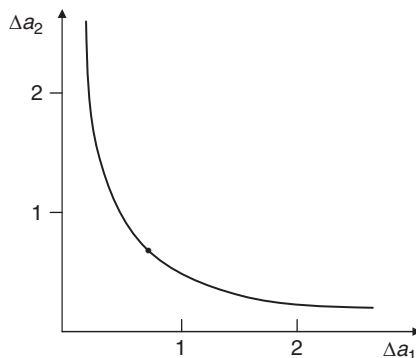
Figure 6.5 *The relationship between variances of the two quadratures of generalized coherent states. The dot corresponds to a coherent state with equal variances. All other points on the curve correspond to squeezed coherent states.*
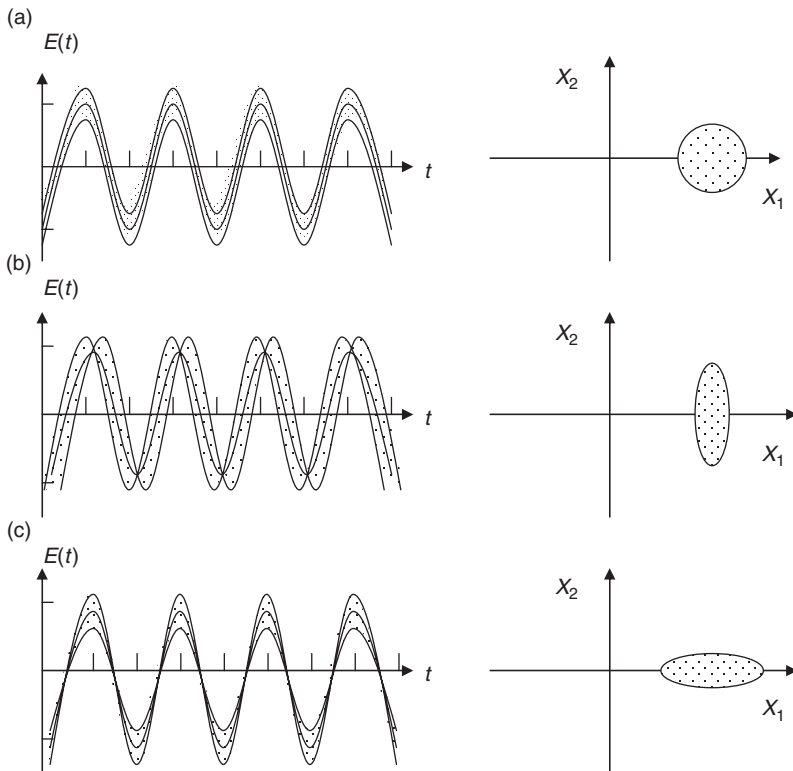
Figure 6.6 *Left: Plots of the electric field of an electromagnetic wave versus time of (a) an ordinary coherent state, (b) a coherent state with squeezed amplitude fluctuations, and (c) a coherent state with squeezed phase fluctuations. (After Ref. [6.6].) Right: Loci of the tip of the electric field vector at a single point in time, corresponding to the peak of E(t) for each case.*

as illustrated in Fig. 6.5. This provides a way of "beating" the uncertainty principle in at least one quadrature.

The quadrature operators $\hat{a}_1$ and $\hat{a}_2$ that exhibit correlated noise properties can refer not only to the amplitude of the electromagnetic field, but also to its phase in principle. Hence a generalized coherent state of the field may have phase noise or amplitude noise that descends below the shot-noise limit in one quadrature, as illustrated in Fig. 6.6.

Methods for controlling amplitude or phase fluctuations of "squeezed" light are discussed further in Chapter 7. These methods are based on nonlinear optical interactions that go beyond the intended scope of this book, so the interested reader should consult the references at the end of Chapter 7. Experimental realization of squeezed states of light has been the basis for efforts to send information from one point to another below the standard noise limits of communication systems. By reducing the noise in isolated quadratures below the shot-noise limit, squeezing also offers potential improvements in the precision of optical measurements based on interferometry Ref. [6.7], where the

objective is invariably to measure the positions or shifts of optical interference fringes with the best possible signal-to-noise ratio.

6.5   Statistics

6.5.1   Classical statistics of light

Statistical properties of light are determined by correlations between electric field amplitudes at different locations or times. They vary greatly from one light source to another and can be compared by calculating the first-order correlation function of the field,

$$< E^* (t) E (t + \tau) >= \frac{1}{T} \int_0^T E^* (t) E (t + \tau) \, dt, \tag{6.5.1}$$

or its normalized counterpart called the degree of first-order temporal coherence:

$$g^{(1)} (\tau) >= \frac{< E^* (t) E (t + \tau) >}{< E^* (t) E (t) >}. \tag{6.5.2}$$

$g^{(1)} (\tau)$ should not be confused with the coupling term in earlier expressions of the interaction Hamiltonian Eq. (6.2.9) or (6.3.1). The quantity $g^{(1)}(\tau)$ is intimately related (by the Wiener–Khintchine theorem) to the power spectrum of the light $F(\omega)$:

$$F (\omega) = \frac{|E (\omega)|^2}{\int_{-\infty}^{+\infty} |E (\omega)|^2 \, d\omega} = \frac{1/4\pi^2 \int_0^T \int_{-\infty}^{+\infty} E^* (t) E (t + \tau) \exp(i\omega\tau) dt d\tau}{(T/2\pi) < E^* (t) E (t) >}$$

$$= \frac{(T/4\pi^2) \int_{-\infty}^{+\infty} < E^* (t) E (t + \tau) > \exp(i\omega\tau) d\tau}{(T/2\pi) < E^* (t) E (t) >}$$

$$= \frac{1}{2\pi} \int_{-\infty}^{+\infty} g^{(1)} (\tau) \exp(i\omega\tau) d\tau. \tag{6.5.3}$$

Here the period T over which time-averaging is performed is assumed to be longer than both the optical period and the coherence or correlation time τ_c, the characteristic time of decay of field correlations due to random phase disruptions or fluctuations at the source.

Consider some of the basic characteristics of a classical light source. The source could be a star with an emission spectrum, centered at frequency ω_0, which is broadened by the effects of interatomic collisions. From moment to moment, the phase of the electric field experiences random jumps due to the chaotic conditions within the source.

Hence, the first-order correlation of the total field emitted by N identical atoms is

$$< E^* (t) E (t + \tau) > = E_0^2 \exp(-i\omega_0\tau)$$

$$< \left\{ e^{-i\phi_1(t)} + \cdots + e^{-i\phi_N(t)} \right\} \left\{ e^{i\phi_1(t+\tau)} + \cdots + e^{i\phi_N(t+\tau)} \right\} >$$

$$= E_0^2 \exp(-i\omega_0\tau) \sum_{i=1}^{N} < \exp\left[i \left\{ \phi_i(t+\tau) - \phi_i(t) \right\} \right] > . \qquad (6.5.4)$$

Once any atom jumps to a new phase of its oscillation, it ceases to contribute to the phase correlation. Hence for delays exceeding the period over which atom i evolves harmonically, that is for $\tau_i << \tau$, one finds $< \exp\left[i \left\{ \phi_i(t+\tau) - \phi_i(t) \right\} \right] >= 0$. In the opposite limit, when $\tau_i >> \tau$, atom i maintains the same phase as τ is varied, and the result is $< \exp\left[i \left\{ \phi_i(t+\tau) - \phi_i(t) \right\} \right] >= 1$. In reality there is a distribution $p(\tau_i)$ of the constant phase periods for each atom, so the phase correlation function in Eq. (6.5.4) is proportional to the probability that the atom does not undergo a phase jump.

We shall assume that the phase jump process is Markoffian. Then, the probability that the atom maintains constant phase for a period of time τ_i decreases exponentially with time according to

$$p(\tau_i) = \exp(-\tau_i/\tau_c). \qquad (6.5.5)$$

In this expression, τ_c is the average interval over which atoms emit with constant phase or the optical coherence time. The phase correlation function for atom i may then be written as

$$< \exp\left[i \left\{ \phi_i(t+\tau_c) - \phi_i(t) \right\} \right] >= \frac{1}{\tau_c} \int_{\tau}^{\infty} p(\tau_i) d\tau_i. \qquad (6.5.6)$$

For N atoms, Eq. (6.5.4) then yields

$$< E^* (t) E (t + \tau) > = N E_0^2 \exp\left\{ -i\omega_0\tau - (\tau/\tau_c) \right\}, \qquad (6.5.7)$$

or

$$g^{(1)}(\tau) = \exp\left\{ -i\omega_0\tau - (\tau/\tau_c) \right\}. \qquad (6.5.8)$$

This is the first-order correlation of light from a source in which the probability that phase remains constant decreases exponentially with the length of the constant phase period. The magnitude of this function is plotted in Fig. 6.7.

Statistical properties of light can be investigated through field measurements at different locations in either time or space. It is therefore useful to generalize the concept of first-order degree of coherence to include correlations between fields measured at different space–time points (r_1, t_1) and (r_2, t_2).

$$g^{(1)}(r_1, t_1; r_2, t_2) = \frac{< E^* (r_1, t_1) E (r_2, t_2) >}{< |E(r_1, t_1)|^2 |E(r_2, t_2)|^2 >^{1/2}}. \qquad (6.5.9)$$

(a)

(b)
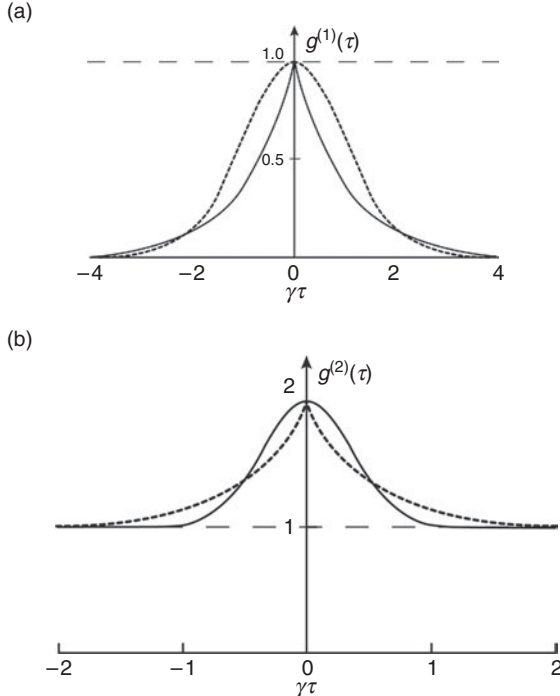
Figure 6.7 *(a) Illustrations of the first-order correlation function of light from sources with Lorentzian (solid curve) and Gaussian (dashed) phase distributions. (b) The second-order correlation functions of Lorentzian (dashed curve) and Gaussian (solid) light sources. The scaling factor on the horizontal axis is the dephasing rate $\gamma \equiv 1/\tau_c$. (Adapted from Ref. [6.9]).*

Now if a light field consists of contributions from two sources,

$$E(r,t) = u_1 E(r_1, t_1) + u_2 E(r_2, t_2), \tag{6.5.10}$$

as in a Young's interference experiment, the intensity of light at an arbitrary field point (r, t) averaged over a single period would be

$$I(r,t) = \frac{1}{2}\varepsilon_0 c |E(r,t)|^2$$

$$= \frac{1}{2}\varepsilon_0 c \left\{ |u_1|^2 |E(r_1, t_1)|^2 + |u_2|^2 |E(r_2, t_2)|^2 + 2u_1^* u_2 \operatorname{Re}\left[E^*(r_1, t_1)E(r_2, t_2)\right] \right\}. \tag{6.5.11}$$

Averaged over times long compared to the coherence time τ_c, the intensity is

$$\langle I(r_1, t_1)\rangle = \frac{1}{2}\varepsilon_0 c \left\{ \langle |u_1|^2 |E(r_1, t_1)|^2\rangle + \langle |u_2|^2 |E(r_2, t_2)|^2\rangle \right.$$

$$\left. + 2u_1^* u_2 \operatorname{Re}\langle E^*(r_1, t_1)E(r_2, t_2)\rangle \right\}. \tag{6.5.12}$$

Notice that the first-order coherence contributes explicitly to the last term in the ensemble average and governs the formation of fringes in classical interference experiments. Conversely Young's interference patterns determine the degree of first-order field coherence.

Intensity correlations yield what is known as the second-order coherence function.

$$g^{(2)}\left(r_1, t_1; r_2, t_2; r_2, t_2; r_1, t_1\right) = \frac{<E^*\left(r_1, t_1\right) E^*\left(r_2, t_2\right) E\left(r_2, t_2\right) E\left(r_1, t_1\right)>}{<\left|E\left(r_1, t_1\right)\right|^2><\left|E\left(r_2, t_2\right)^2\right|>}$$

(6.5.13)

or

$$g^{(2)} = \frac{<\bar{I}\left(r_1, t_1\right)\bar{I}\left(r_2, t_2\right)>}{<\bar{I}\left(r_1, t_1\right)><\bar{I}\left(r_2, t_2\right)>}.$$

(6.5.14)

Historically, the measurement of $g^{(2)}$ by the intensity correlation technique of Hanbury, Brown, and Twiss [6.8] made it possible to obtain statistical information on field correlations without the need for interferometric stability. However $g^{(2)}$ only contains information about energy dynamics of the field (photon arrival times) and unlike $g^{(1)}$ yields no information about phase fluctuations.

Before turning to statistics of quantized fields, let us consider the limiting values for $g^{(1)}$ and $g^{(2)}$ for classical (unquantized) light sources. First we reiterate the earlier point that fields that maintain their phase for an average time of τ_c are completely correlated at short delay times ($\tau << \tau_c$) and are completely uncorrelated at long delay times ($\tau >> \tau_c$). Hence $g^{(1)}$ takes on the limiting values

$$g^{(1)}\left(\tau\right) \to 0, \text{ when } \tau >> \tau_c,$$

(6.5.15)

$$g^{(1)}\left(\tau\right) \to 1, \text{ when } \tau << \tau_c.$$

(6.5.16)

and its range is

$$0 \le g^{(1)} \le 1.$$

(6.5.17)

To establish the allowed range for $g^{(2)}$, we note that by applying the Cauchy-Schwartz inequality to intensity measurements at times t_1 and t_2, we find the inequality

$$\bar{I}^2\left(t_1\right) + \bar{I}^2\left(t_2\right) \ge 2\bar{I}\left(t_1\right)\bar{I}\left(t_2\right).$$

(6.5.18)

For N pairs of intensity measurements, the statistical averages of the left and right sides of Eq. (6.5.18) yield the inequality

$$\left\langle \bar{I}^2\left(t\right)\right\rangle \ge \left\langle \bar{I}\left(t\right)\right\rangle^2.$$

(6.5.19)

Thus, we are assured that the numerator in Eq. (6.5.14) always equals or exceeds the denominator. Consequently, the range of $g^{(2)}$ is

$$g^{(2)}(0) \ge 1.$$

(6.5.20)

Because intensity is positive definite and there is no upper limit for $g^{(2)}$, its range is

$$1 \le g^{(2)}\left(\tau\right) \le \infty.$$

(6.5.21)

Two examples of the second-order correlation function of classical sources are shown in Fig. 6.7b. We shall see that quite different shapes and limits are predicted by quantum theory for the second-order coherence of quantum sources in the next section.

6.5.2   Quantum statistics of light

Since the electric field is real, the electric field operator is a sum of Hermitian conjugates.

$$\hat{E}(r,t) = \hat{E}^+(r,t) + \hat{E}^-(r,t), \tag{6.5.22}$$

where

$$\hat{E}^+(r,t) = \sum_k (\hbar\omega_k/2\varepsilon_0 V)^{1/2} \, \hat{\varepsilon}_k \hat{a}_k \exp\left(-i\omega_k t + i\bar{k}\cdot\bar{r}\right) \tag{6.5.23}$$

and

$$\hat{E}^-(r,t) = \sum_k (\hbar\omega_k/2\varepsilon_0 V)^{1/2} \, \hat{\varepsilon}_k^+ \hat{a}_k^+ \exp\left(i\omega_k t + i\bar{k}\cdot\bar{r}\right). \tag{6.5.24}$$

To analyze the quantum degree of coherence in Young's interference experiment, we introduce the field operators

$$\hat{E}^\pm(r,t) = u_1 \hat{E}^\pm(r_1,t_1) + u_2 \hat{E}^\pm(r_2,t_2) \tag{6.5.25}$$

in place of Eq. (6.5.10) and calculate the expectation value of the intensity operator quantum mechanically.

$$\begin{aligned}
< \hat{I}(r,t) > \equiv < \hat{E}^-\hat{E}^+ > \; = 2\varepsilon_0 c \Big\{ &|u_1|^2 < \hat{E}^-(r_1,t_1)\hat{E}^+(r_1,t_1) > \\
&+ |u_2|^2 < \hat{E}^-(r_2,t_2)\hat{E}^+(r_2,t_2) > \\
&+ u_1^* u_2 < \hat{E}^-(r_1,t_1)\hat{E}^+(r_2,t_2) > \\
&+ u_1 u_2^* < \hat{E}^-(r_2,t_2)\hat{E}^+(r_1,t_1) > \Big\}
\end{aligned} \tag{6.5.26}$$

To find the correlation in terms of field operators, we turn to the density matrix and follow Eq. (3.6.17) by calculating $< \hat{E}^-\hat{E}^+ >= Tr[\hat{\rho}\hat{I}]$, where $\hat{I}$ is the intensity operator.

In the case of the Young's interference experiment, wave amplitudes emanating from two closely spaced slits are assumed to have the same magnitude but different phase. Hence, the last two terms in $<\hat{I}>$ are complex conjugates, and we can write

$$\begin{aligned}
< \hat{I}(r,t) > \; = 2\varepsilon_0 c \Big\{ &|u_1|^2 < \hat{E}^-(r_1,t_1)\hat{E}^+(r_1,t_1) > \\
&+ |u_2|^2 < \hat{E}^-(r_2,t_2)\hat{E}^+(r_2,t_2) > \\
&+ 2u_1^* u_2 \, \text{Re} < \hat{E}^-(r_1,t_1)\hat{E}^+(r_2,t_2) > \Big\}.
\end{aligned} \tag{6.5.27}$$

The two pinholes create or annihilate photons in the cavity formed by the lens and the aperture plane of the double-slit experiment. For a given detector position, two modes contribute to the signal:

$$\hat{a}^+ = \left(\hat{a}_1^+ + \hat{a}_2^+\right)/\sqrt{2}, \tag{6.5.28}$$

$$\hat{a} = \left(\hat{a}_1 + \hat{a}_2\right)/\sqrt{2}. \tag{6.5.29}$$

Hence the field operator contains two contributions:

$$\hat{E}^+\left(r, t\right) \propto u_1 \hat{a}_1 \exp(iks_1) + u_2 \hat{a}_2 \exp(iks_2), \tag{6.5.30}$$

where s_1 and s_2 are the distances of slit 1 and 2 from the detector. Correspondingly, the propagation times from slits 1 and 2 to the detector are

$$t_1 = t - \left(s_1/c\right), \tag{6.5.31}$$

$$t_2 = t - \left(s_2/c\right). \tag{6.5.32}$$

Thus, for an incident beam with n photons, the intensity of the interference pattern is

$$< \hat{I}\left(r, t\right) > \propto |u_1|^2 \left\langle n \left|\hat{a}_1^+ \hat{a}_1\right| n\right\rangle + |u_2|^2 \left\langle n \left|\hat{a}_2^+ \hat{a}_2\right| n\right\rangle$$

$$+ 2u_1^* u_2 \cos\left\{k\left(s_1 - s_2\right)\right\} \left\langle n \left|\hat{a}_1^+ \hat{a}_2\right| n\right\rangle$$

$$\propto n \left\{\frac{1}{2}\left(|u_1|^2 + |u_2|^2\right) + u_1^* u_2 \cos k\left(s_1 - s_2\right)\right\}. \tag{6.5.33}$$

Notice that as $n \to 0$, the interference effect remains unchanged. This indicates that even if there is only a single photon in the apparatus, interference is still observed.

The quantum degree of first-order coherence is

$$g^{(1)}\left(r_1, t_1; r_2, t_2\right) = \frac{< \hat{E}^-\left(r_1, t_1\right) \hat{E}^+\left(r_2, t_2\right) >}{\left[< \hat{E}^-\left(r_1, t_1\right) \hat{E}^+\left(r_1, t_1\right) >< \hat{E}^-\left(r_2, t_2\right) \hat{E}^+\left(r_2, t_2\right) >\right]^{1/2}}, \tag{6.5.34}$$

and its range is the same as the classical $g^{(1)}$. The quantum degree of second-order coherence is

$$g^{(2)}\left(r_1, t_1; r_2, t_2; r_2, t_2; r_1, t_1\right) = \frac{< \hat{E}^-\left(r_1, t_1\right) \hat{E}^-\left(r_2, t_2\right) \hat{E}^+\left(r_2, t_2\right) \hat{E}^+\left(r_1, t_1\right) >}{< \hat{E}^-\left(r_1, t_1\right) \hat{E}^+\left(r_1, t_1\right) >< \hat{E}^-\left(r_2, t_2\right) \hat{E}^+\left(r_2, t_2\right) >}. \tag{6.5.35}$$

Notice that the second-order coherence $g^{(2)}$ contains only products of field operators and their Hermitian conjugates. As a result, $g^{(2)}$ must be positive definite. That is,

$$0 \le g^{(2)}\left(\tau\right) \le \infty. \tag{6.5.36}$$
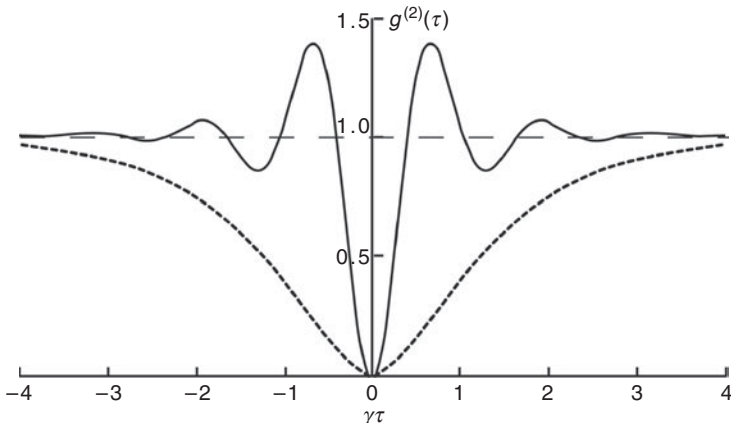
Figure 6.8 *Quantum second-order correlation functions for nonclassical light $(g^{(2)} < 1)$ such as that from an atom that is weakly excited (dashed curve; $\Omega << \gamma$) or strongly driven (solid curve; $\Omega = 5\gamma$). There is no collisional dephasing; so $\gamma = 1/\tau_{sp}$ is determined solely by the radiative decay rate. (Adapted from figures in Ref. [6.9].)*

Even for zero time delay $(\tau = 0)$ it is not possible to prove $g^{(2)}(\tau) \geq 1$ as in the classical case. Consequently, light which exhibits second-order coherence in the range

$$0 \leq g^{(2)}(\tau) \leq 1, \tag{6.5.37}$$

is deemed "nonclassical" light. Figure 6.8 shows some examples of non-classical correlations.

What light sources actually exhibit values in the range $0 \leq g^{(2)}(\tau) \leq 1$? Do sources of "nonclassical" light exist? Consider a single mode Fock state in which the number of photons is determined by $< \hat{n} >=< \hat{a}^+ \hat{a} >$. Its second-order coherence function is

$$g^{(2)}(\tau) = \frac{< \hat{a}^+ \hat{a}^+ \hat{a} \hat{a} >}{< \hat{a}^+ \hat{a} >^2}. \tag{6.5.38}$$

By calculating Eq. (6.5.35) explicitly it is easy to show that the Fock state $|n\rangle$ has a second-order correlation function given by

$$g^{(2)}(\tau) = \begin{cases} (n-1)/n, & n \geq 2 \\ 0 & n = 0, 1 \end{cases} . \tag{6.5.39}$$

This value for $g^{(2)}(\tau)$ is always less than unity, showing that a photon number state exemplifies one characteristic of nonclassical light. Even at zero time delay, correlations lie in the range $0 \leq g^{(2)}(\tau) \leq 1$ which is less than the uncorrelated light value $g^{(2)}(0) = 1$. This is because the arrival times of photons from nonclassical light sources are not clustered together. They are said to be "anti-bunched." That is, a

second photon cannot emerge from such a source immediately after emission of a first photon.

A concrete example of a nonclassical source of light is an atom. Atoms cannot emit a second photon immediately after a first because each radiative event requires decay to a lower energy state. Decay takes time and further emission cannot take place until the atom returns to the ground state and is re-excited. The quantum degree of second-order correlation corresponding to this behavior is illustrated in Fig. 6.8. Only individual luminescent centers that obey anti-bunching photon statistics exhibit a correlation function that is zero at zero delay, like that in Fig. 6.8. The fluorescence of an ensemble of atoms is the incoherent sum of emission events that are uncorrelated. Hence large ensembles yield $g^{(2)}(\tau) = 1$, for all τ. Even for an ensemble of just two atoms, $g^{(2)}(0)$ never drops to a value much below one half.

6.6 Quantized reservoir theory

6.6.1 The reduced density matrix

It often happens that we regard one component of a system as more "interesting" than other parts, or one part of a problem more important than another. We may wish to follow the behavior of one part while ignoring the rest of the system – possibly a large reservoir – or we may wish to examine the interaction of the system with a reservoir without solving for any reservoir dynamics. Fortunately this is always possible using the "reduced" density matrix. In this section, we introduce reduced density matrices and then utilize them in examining the very important problem of a two-level atom interacting with a simple, quantized reservoir. This problem serves as a model for others.

Consider a system AB with two components A and B which do not interact (Fig. 6.9). The components A and B occupy two independent mathematical spaces, and the state of the combined system $|\varphi_{ab}\rangle$ is just the uncorrelated product of component wave functions,

$$|\varphi_{ab}\rangle = |\varphi_a\rangle |\varphi_b\rangle. \tag{6.6.1}$$

Hence the systems A, B and AB are pure states.

$$\rho(A) = |\varphi_a\rangle \langle \varphi_a| \tag{6.6.2}$$

$$\rho(B) = |\varphi_b\rangle \langle \varphi_b| \tag{6.6.3}$$

$$\rho(AB) = |\varphi_{ab}\rangle \langle \varphi_{ab}|. \tag{6.6.4}$$

We now show that the expectation of any operator $O(A)$ which acts only on wave functions in subsystem A can be calculated from a reduced density matrix for A

which does not depend on reservoir variables.

$$\langle 0(A) \rangle = \mathrm{Tr}\, \{O(A)\rho(AB)\}$$

$$= \sum_{ab} \langle \varphi_{ab} | O(A)\rho(AB) | \varphi_{ab} \rangle$$

$$= \sum_{aba'b'} \langle \varphi_{ab} | O(A) | \varphi_{a'b'} \rangle \langle \varphi_{a'b'} | \rho(AB) | \varphi_{ab} \rangle$$

$$= \sum_{aba'} \langle \varphi_{ab} | O(A) | \varphi_{a'} \rangle \sum_{b'} \delta_{bb'} \langle \varphi_{a'} | \langle \varphi_{b'} | \rho(AB) | \varphi_{b'} \rangle | \varphi_a \rangle$$

$$= \sum_{aa'} \langle \varphi_a | O(A) | \varphi_{a'} \rangle \sum_b \langle \varphi_{a'} | \langle \varphi_b | \rho(AB) | \varphi_b \rangle | \varphi_a \rangle$$

$$= \sum_a \langle \varphi_a | O(A) \mathrm{Tr}_B \rho(AB) | \varphi_{a'} \rangle \tag{6.6.5}$$

where we have used $\mathrm{Tr}_B \rho(AB) \equiv \sum_b \langle \varphi_b | \rho(AB) | \varphi_b \rangle$. Notice that this result has the form

$$\langle O(A) \rangle \equiv \sum_a \langle \varphi_a | O(A) \rho(A) | \varphi_a \rangle, \tag{6.6.6}$$

if we define a reduced density matrix $\rho(A)$ for subsystem A by the relation

$$\rho(A) \equiv \mathrm{Tr}_B \rho(AB). \tag{6.6.7}$$

Similarly, it is easy to show that

$$\langle O(B) \rangle \equiv \sum_b \langle \varphi_b | O(B) \rho(B) | \varphi_b \rangle, \tag{6.6.8}$$

where

$$\rho(B) \equiv \mathrm{Tr}_A \rho(AB). \tag{6.6.9}$$

The derivation of results Eqs. (6.6.7) and (6.6.9) for systems in which the subsystems A and B interact is more cumbersome, but the results are the same [6.10]. Reduced density matrices are still found to be adequate for calculating variables of the subsystems alone (such as $<O(A)>$, $<O(B)>$). The importance of this is that the time development of reduced density operators can be obtained without calculating reservoir variables. Thus, we can choose theoretically to include or ignore dynamic processes of a host medium B in which an optical center A is located in the same way that the strength of the optical interaction between light and center A can be adjusted experimentally by changing the detunings with respect to resonances in subsystems A and B. This idea is depicted schematically in Fig. 6.9.
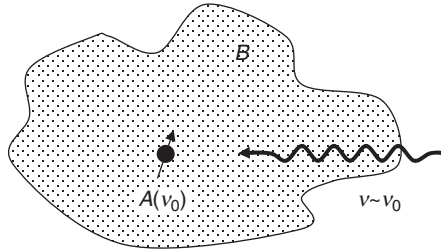
Figure 6.9 *A schematic drawing of a compound system comprised of an optical center A with a resonance at frequency ν_0 in a host medium B, called the reservoir. Experimentally, the optical interaction can be targeted to A by tuning the light frequency near ν_0. Theoretically, the operators describing the dynamics of A can be determined while ignoring dynamics of B by tracing over the reservoir states.*

Take the compound system Hamiltonian to be

$$H_{AB} = H_A + H_B + V, \tag{6.6.10}$$

where V represents an interaction between systems A and B. The equation of motion is

$$i\hbar\dot{\rho}_{AB}(t) = [H_{AB}, \rho_{AB}(t)]. \tag{6.6.11}$$

However for the subsystem A we can write

$$i\hbar\dot{\rho}_A(t) = i\hbar\text{Tr}_B\dot{\rho}_{AB}(t)$$

$$= \text{Tr}_B\left[(H_A + H_B + V), \rho_{AB}(t)\right]. \tag{6.6.12}$$

Making use of the results

$$\text{Tr}_B\left[H_A, \rho_{AB}(t)\right] = [H_A, \text{Tr}_B\rho_{AB}(t)] = [H_A, \rho_A(t)] \tag{6.6.13}$$

$$\text{Tr}_B\left[H_B, \rho_{AB}(t)\right] = \sum_B \left[< \varphi_B |H_B\rho_{AB}(t)| \varphi_B > - < \varphi_B |\rho_{AB}(t)H_B| \varphi_B >\right]$$

$$= \sum_B \left[E_B < \varphi_B |\rho_{AB}(t)| \varphi_B > - < \varphi_B |\rho_{AB}(t)| \varphi_B > E_B\right] = 0, \tag{6.6.14}$$

one obtains dynamic equations for the subsystems. In the Schrodinger representation

$$i\hbar\dot{\rho}_A(t) = [H_A, \rho_A] + \text{Tr}_B\left[V, \rho_{AB}(t)\right], \tag{6.6.15}$$

$$i\hbar\dot{\rho}_B(t) = [H_B, \rho_B] + \text{Tr}_A\left[V, \rho_{AB}(t)\right]. \tag{6.6.16}$$

In the interaction picture

$$i\hbar\dot{\rho}_A(t) = \text{Tr}_B\left[V(t), \rho_{AB}(t)\right], \tag{6.6.17}$$

$$i\hbar\dot{\rho}_B(t) = \text{Tr}_A\left[V(t), \rho_{AB}(t)\right]. \tag{6.6.18}$$

To solve for $\rho_A(t)$ and $\rho_B(t)$ when $V \neq 0$, that is when the subsystems are correlated by virtue of an interaction V, we can imagine a perturbative approach which assumes the coupling makes only a small addition to the density matrix of the uncoupled subsystems.

$$\rho_{AB}(t) = \rho_A(t)\rho_B(t) + \rho_C(t) \tag{6.6.19}$$

The idea behind Eq. (6.6.19) is that $\rho_C(t)$ represents a weak correlation which develops in time between subsystems A and B because of their interaction.

$$
\begin{aligned}
\text{Tr}_B\left[V(t), \rho_{AB}(t)\right] &= \text{Tr}_B\left[V(t), \rho_A(t)\rho_B(t)\right] + \text{Tr}_B\left[V(t), \rho_C(t)\right] \\
&= \text{Tr}_B\left[V(t), \rho_B(t)\right]\rho_A(t) + \text{Tr}_B\left[\rho_B(t)V(t), \rho_A(t)\right] \\
&\quad + \text{Tr}_B\left[V(t), \rho_C(t)\right] \\
&= \text{Tr}_B\left[V(t)\rho_B(t), \rho_A(t)\right] + \text{Tr}_B\left[V(t), \rho_C(t)\right] \\
&= \left[V_A(t), \rho_A(t)\right] + \text{Tr}_B\left[V(t), \rho_C(t)\right] \tag{6.6.20}
\end{aligned}
$$

In obtaining Eq. (6.6.20) we have used the fact that operators commute under a trace, and have also defined

$$V_A(t) \equiv \text{Tr}_B\left[V(t), \rho_B(t)\right]. \tag{6.6.21}$$

$V_A(t)$ is a self-consistent correction to the energy of subsystem A. We finally obtain

$$i\hbar\dot{\rho}_A(t) = \left[V_A(t), \rho_A(t)\right] + \text{Tr}_B\left[V(t), \rho_C(t)\right], \tag{6.6.22}$$

$$i\hbar\dot{\rho}_B(t) = \left[V_B(t), \rho_B(t)\right] + \text{Tr}_A\left[V(t), \rho_C(t)\right]. \tag{6.6.23}$$

To solve these equations we need an equation for the correlation operator ρ_C. This is found by differentiating its defining relation.

$$
\begin{aligned}
i\hbar\dot{\rho}_C(t) &= i\hbar\left[\dot{\rho}_{AB}(t) - \dot{\rho}_A\rho_B - \rho_A\dot{\rho}_B\right] \\
&= \left[V, \rho_A\rho_B + \rho_C\right] - \left[V_A, \rho_A\right]\rho_B - \text{Tr}_B\left[V, \rho_C\right]\rho_B \\
&\quad -\rho_A\left[V_B, \rho_B\right] - \rho_A\text{Tr}_A\left[V, \rho_C\right]. \tag{6.6.24}
\end{aligned}
$$

By restricting ourselves to two-level atoms or simple harmonic oscillators (SHOs) interacting with a reservoir of SHOs we can set

$$V_A = V_B = 0. \tag{6.6.25}$$

We shall neglect higher-order terms involving the commutator $[V, \rho_C]$ and may assume that B is a reservoir which is too large to undergo significant change upon energy input from A, so that

$$\dot{\rho}_B(t) \approx 0. \tag{6.6.26}$$

Hence Eq. (6.6.24) simplifies to

$$i\hbar\dot{\rho}_C(t) = \left[V(t), \rho_A(t)\rho_B(t)\right]. \tag{6.6.27}$$

If systems A and B are initially uncorrelated ($\rho_C(t_0) = 0$), the formal solution of Eq. (6.6.27) is

$$\rho_C(t) = -\frac{i}{\hbar} \int_{t_0}^{t} dt' \left[V(t'), \rho_A(t')\rho_B(t') \right].$$

(6.6.28)

This solution provides a starting point for iterative solutions of ρ_C in terms of ρ_A, ρ_B when A and B are on an equal footing, or for simplified solutions when one subsystem is a large reservoir.

$$\rho_C(t) \doteq -\frac{i}{\hbar} \int_{t_0}^{t} dt' \left[V(t'), \rho_A(t')\rho_B(t_0) \right].$$

(6.6.29)

Eq. (6.6.26) is called the "reservoir assumption." Notice that it has been used to write Eq. (6.6.29). Together with Eq. (6.6.28) it allows us to write the decay law for subsystem A simply as

$$\dot{\rho}_A(t) = -\frac{i}{\hbar} \int_{t_0}^{t} dt' \mathrm{Tr}_B \left[V(t), [V(t'), \rho_A(t')\rho_B(t_0)] \right].$$

(6.6.30)

Eq. (6.6.30) is a key result of this section that can be used to evaluate decay of a radiation field or atom interacting with an ensemble of oscillators. The ensemble may be a reservoir of phonons, photons, or cavity modes. As an example of its use we now treat the problem of a two-level atom coupled to modes of an unstructured vacuum, re-deriving the Weisskopf–Wigner result for spontaneous emission.

6.6.2   Application of the reduced density matrix

Quantum mechanically, an atom makes transitions described by creation and annihilation operators $\hat{\sigma}^+$ and $\hat{\sigma}^-$ when its excitation frequency is close to the atomic resonant frequency ω_0. The simple harmonic oscillators of the reservoir in which it is embedded are similarly described by creation and annihilation operators $\hat{b}_k^+$ and $\hat{b}_k^-$, where k is the mode index, and they have corresponding excitation frequencies designated by ω_k. Multi-component systems like this must conserve energy as they undergo internal changes. Hence the excitation of the atom must be accompanied by an energy-conserving de-excitation of an oscillator, and vice versa. To simplify notation we dispense with carets over operators.

In the rotating wave approximation, the coupling Hamiltonian in the interaction picture is

$$V = \sum_k \hbar g_k \left[\sigma^- b_k^+ \exp[-i(\omega_0 - \omega_k)t] + h.c. \right].$$

(6.6.31)

We assume that the reservoir consists of a thermal equilibrium distribution of vacuum modes. The density operator for a single mode k of thermal radiation is

$$\rho_{kk} = \frac{\exp\left(-\hbar\omega_k b_k^+ b_k / k_B T\right)}{Tr\left\{\exp\left(-\hbar\omega_k b_k^+ b_k / k_B T\right)\right\}}$$

$$= \exp\left(-\hbar\omega_k b_k^+ b_k / k_B T\right)\left[1 - \exp\left(-\hbar\omega_k / k_B T\right)\right], \qquad (6.6.32)$$

where the second line makes use of the binomial expansion. Hence for all modes

$$\rho_B = \prod_k \exp\left(-\hbar\omega_k b_k^+ b_k / k_B T\right)\left[1 - \exp\left(-\hbar\omega_k / k_B T\right)\right]. \qquad (6.6.33)$$

To work out, say, the first term for $\dot{\rho}_A(t)$ in Eq. (6.6.30) we need to evaluate the following trace.

$$\mathrm{Tr}_B\left\{V(t)V(t')\rho_A(t')\rho_B(t_0)\right\}$$

$$= \hbar^2 \sum_B \langle\psi_B| \left\{ \sum_{j\ell} g_\ell g_j \sigma b_\ell^+ \ \sigma b_j^+ \exp(-2i\omega_0 t + i\omega_l t + i\omega_l t')\rho_A(t')\rho_B \right.$$

$$+ \sum_{j\ell} g_\ell g_j \left[\sigma b_\ell^+ \sigma^+ b_j \exp[-i(\omega_0 - \omega_l)t + i(\omega_0 - \omega_j)t']\rho_A(t')\rho_B + h.c.\right]$$

$$+ \left. \sum_{j\ell} g_\ell g_j \sigma^+ b_\ell \sigma^+ b_j \exp(2i\omega_0 t - i\omega_l t - i\omega_l t')\rho_A(t')\rho_B \right\} |\psi_B\rangle$$

$$= \hbar^2 \sum_B \langle\psi_B| \sum_{j\ell} g_\ell g_j \left[\sigma b_\ell^+ \sigma^+ b_j \exp[-i(\omega_0 - \omega_l)t + i(\omega_0 - \omega_j)t']\rho_A(t')\rho_B\right.$$

$$+ h.c.]|\psi_B\rangle$$

$$= \hbar^2 \sum_{j\ell} g_\ell g_j \sigma\sigma^+ Tr_B\left(b_\ell^+ b_j \rho_B\right)\rho_A(t')\exp[-i(\omega_0 - \omega_l)t + i(\omega_0 - \omega_j)t'] + h.c.$$

$$(6.6.34)$$

In obtaining Eq. (6.6.34), the high-frequency contributions have been dropped, consistent with the rotating wave approximation.

Exercise: Show the following results, where $\bar{n}_k$ is the average occupation of reservoir mode k.

$$\mathrm{Tr}_B[b_j^+ b_k \rho_B] = \bar{n}_k \delta_{jk} \qquad (6.6.35)$$

$$\mathrm{Tr}_B[b_j b_k^+ \rho_B] = (\bar{n}_k + 1)\delta_{jk} \qquad (6.6.36)$$

$$\mathrm{Tr}_B[b_j b_k \rho_B] = \ <b_j b_k>_B = 0 \qquad (6.6.37)$$

$$\mathrm{Tr}_B[b_j^+ b_k^+] = \ <b_j^+ b_k^+>_B = 0 \qquad (6.6.38)$$

Making use of the results of the exercise above, Eq. (6.6.34) can be simplified further.

$$\text{Tr}_B \left[V(t) V(t') \rho_A(t') \rho_B(t_0) \right]$$
$$= \hbar^2 \sum_k g_k^2 \left\{ \left[\sigma^+ \sigma \rho_A(t') (\bar{n}_k + 1) \exp[i(\omega_0 - \omega_k)(t - t')] + \right. \right.$$
$$+ \sigma \sigma^+ \rho_A(t') \bar{n}_k \exp[-i(\omega_0 - \omega_k)(t - t')]] + h.c. \bigg\} . \tag{6.6.39}$$

Substituting this expression and similar terms for the remaining commutator contributions into the equation for $\rho_A(t)$, we find

$$\dot{\rho}_A(t) = -\int_{t_0}^t dt' \sum_k g_k^2 \left\{ \sigma^+ \ \sigma \rho_A(t') (\bar{n}_k + 1) \exp[i(\omega_0 - \omega_k)(t - t')] \right.$$

$$+ \sigma \sigma^+ \rho_A(t') \bar{n}_k \exp[-i(\omega_0 - \omega_k)(t - t')]$$

$$- \sigma^+ \rho_A(t') \sigma (\bar{n}_k + 1) \exp[i(\omega_0 - \omega_k)(t - t')]$$

$$+ \sigma \rho_A(t') \sigma^+ \bar{n}_k \exp[-i(\omega_0 - \omega_k)(t - t')] \bigg\} + h.c. \tag{6.6.40}$$

We proceed by noting that the summation over boson states can be converted in the usual way to an integration over frequency by introducing the density of reservoir oscillator states $D(\omega)$.

$$\sum_k \rightarrow \int d\omega D(\omega). \tag{6.6.41}$$

We assume that the density of states $D(\omega)$, the coupling strength $g(\omega)$, and the mode occupation probability $\bar{n}(\omega)$ all change little over the frequency range of the atomic resonance. These factors may then be treated as having the constant value

$$D(\omega)\bar{n}(\omega)g^2(\omega) = D(\omega_0)\bar{n}(\omega_0)g^2(\omega_0), \tag{6.6.42}$$

and may be factored from the integral. Additionally, the integrand is dominated by contributions to the exponential factors at times $t' \approx t$. Consequently we may set $\rho_A(t') = \rho_A(t)$, which is equivalent to the Markoff approximation made in our earlier analysis of dephasing (Section 3.7). Finally we note

$$\int_{t_0}^t dt' \exp[\pm i(\omega_0 - \omega)(t - t')] = \pi \delta(\omega_0 - \omega). \tag{6.6.43}$$

Therefore,

$$\dot{\rho}_A(t) = -\pi D(\omega_0) g^2(\omega_0) \left\{ \bar{n} \left[\sigma \sigma^+ \rho_A(t) - \sigma^+ \rho_A(t)\sigma \right] \right.$$
$$+ (\bar{n} + 1) \left[\sigma^+ \sigma \rho_A(t) - \sigma \rho_A(t)\sigma^+ \right] \bigg\} + h.c. \tag{6.6.44}$$

By identifying the decay constant for the transition at frequency ω_0 as

$$\gamma \equiv 2\pi D(\omega_0) g^2(\omega_0), \tag{6.6.45}$$

we obtain a key result of this section:

$$\dot{\rho}_A(t) = -\frac{1}{2}\gamma \left\{ \bar{n} \left[\sigma\sigma^+ \rho_A(t) - \sigma^+ \rho_A(t)\sigma \right] + \left\{ (\bar{n}+1) \left[\sigma^+ \sigma\rho_A(t) - \sigma\rho_A(t)\sigma^+ \right] + h.c. \right\} \right. . \tag{6.6.46}$$

Notice that for a reservoir with no excitations ($\bar{n} = 0$), an initially excited atom will decay from its upper state 2 according to the law

$$\dot{\rho}_{22}^A(t) = -\frac{1}{2}\gamma \left\langle 2 \left| \sigma^+ \sigma\rho_A(t) - \sigma\rho_A(t)\sigma^+ \right| 2 \right\rangle + h.c.$$

$$= -\frac{1}{2}\gamma \left\langle 2 \left| \sigma^+ \sigma\rho_A(t) \right| 2 \right\rangle - \frac{1}{2}\gamma \left\langle 2 \left| \rho_A^+(t)\sigma^+ \sigma \right| 2 \right\rangle . \tag{6.6.47}$$

Recall that $\rho = \rho^+$ for diagonal matrix elements like the one above. So Eq. (6.6.47) yields

$$\dot{\rho}_{22}^A(t) = -\gamma \rho_{22}^A(t). \tag{6.6.48}$$

Eq. (6.6.48) shows that quantized reservoir theory based on the reduced density matrix reproduces the Wigner–Weisskopf spontaneous emission decay law derived earlier. As illustrated in Fig. 6.10, it demonstrates that the decay of an atom (A) takes place via coupling with available modes of the reservoir (modes of space B) whose dynamics can be ignored. If all modes of space are available, the decay proceeds exponentially at the natural decay rate γ. However, by placing the atom near one or more conducting surfaces, the decay rate can be altered significantly. As suggested by the diagram in Fig. 6.10*b*, the presence of a cavity diminishes the density of states $D(\omega)$ available for the emission process if the separation of the plates is less than half the emission
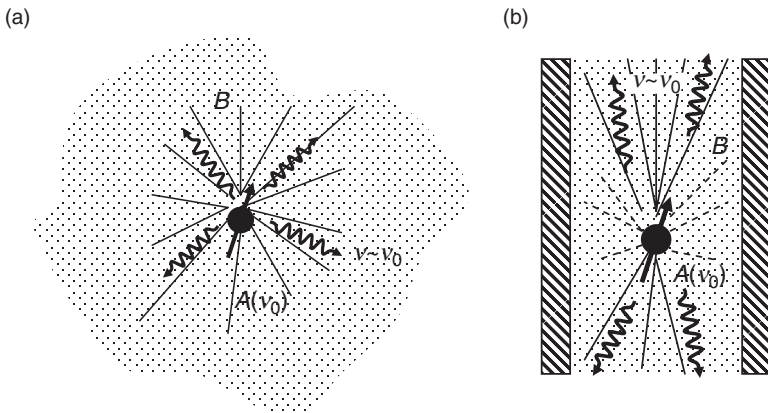
Figure 6.10 *(a) Radiative coupling of an excited atom to all modes of space. (b) Radiative coupling of an atom to modes of space restricted by the presence of conducting surfaces.*

wavelength [6.11]. Thus spontaneous emission is inhibited. On the other hand, for large spacings, resonant cavity modes can enhance the decay rate, yielding a decay rate proportional to the cavity Q factor [6.12].

Using the formalism of quantum relaxation theory one can account for the prevalence of exponential decay processes in nature. The formulation above is applicable to any situation in which two-level systems are coupled to a reservoir of simple harmonic oscillators, or vice versa. Although the development of this section has focused on the implications of atom–reservoir coupling for decay, a broader discussion brings to light four fundamental phenomena underlying such coupling. Appendix F presents the close links between spontaneous decay, stimulated emission, the Lamb shift, and the AC Stark shift.

6.7 Resonance fluorescence

When an atom is excited exactly on resonance, the conditions needed to apply perturbation theory are not met, and its predictions fail. The need for a different approach is illustrated in this section, where the resonance fluorescence spectrum is found to differ significantly from the predictions of perturbation theory, because resonant light dynamically alters the eigenfunctions and eigenenergies of the atom. The original work was done by Mollow [6.13] but the development presented here follows Ref. [6.14] and shows that strong field fluorescence from a two-level system consists of three lines (the Mollow triplet), as indicated in Fig. 6.11. It provides useful perspective on what went right and what went wrong in our preliminary discussion of strong field effects in Section 3.4, based on perturbation theory. The experiments [6.15, 6.16, 6.17] in which the resonance fluorescence spectrum was first observed also illustrate the fact that multilevel atoms like sodium can indeed be converted into true two-level systems by carefully restricting the accessible optical transitions to just one, as described in Section 3.11. For sodium, the transition $3^2S_{1/2}(F = 2) \leftrightarrow 3^2P_{3/2}(F = 3)$ was selected, since excitation to $F = 3$ can only be followed by emission back to the initial state $F = 2$ according to the selection rule for one-photon transitions among hyperfine states ($\Delta F = 0, \pm 1$).

6.7.1 Fluorescence of strongly driven atoms

Fluorescence spectra are frequency–domain versions (Fourier transforms) of the power delivered to, or taken away from, the optical field by various modes in real time. Hence we begin with an expression for the rate of change of energy in each mode and polarization state, labelled by k and λ respectively, versus time. According to Eq. (6.1.38) the total emitted power can be written as

$$P(t) = \frac{\partial}{\partial t} \sum_{k,\lambda} \hbar\omega_k \left\langle \hat{a}_{k\lambda}^+(t)\hat{a}_{k\lambda}^-(t) \right\rangle . \tag{6.7.1}$$

To evaluate $P(t)$, we first need to find the equation of motion for $\langle \hat{a}^+(t)\hat{a}^-(t) \rangle$. For this we require the system Hamiltonian comprised of the field, atom, and interaction energies. We can drop the zero-point energy of the field since it does not contribute to
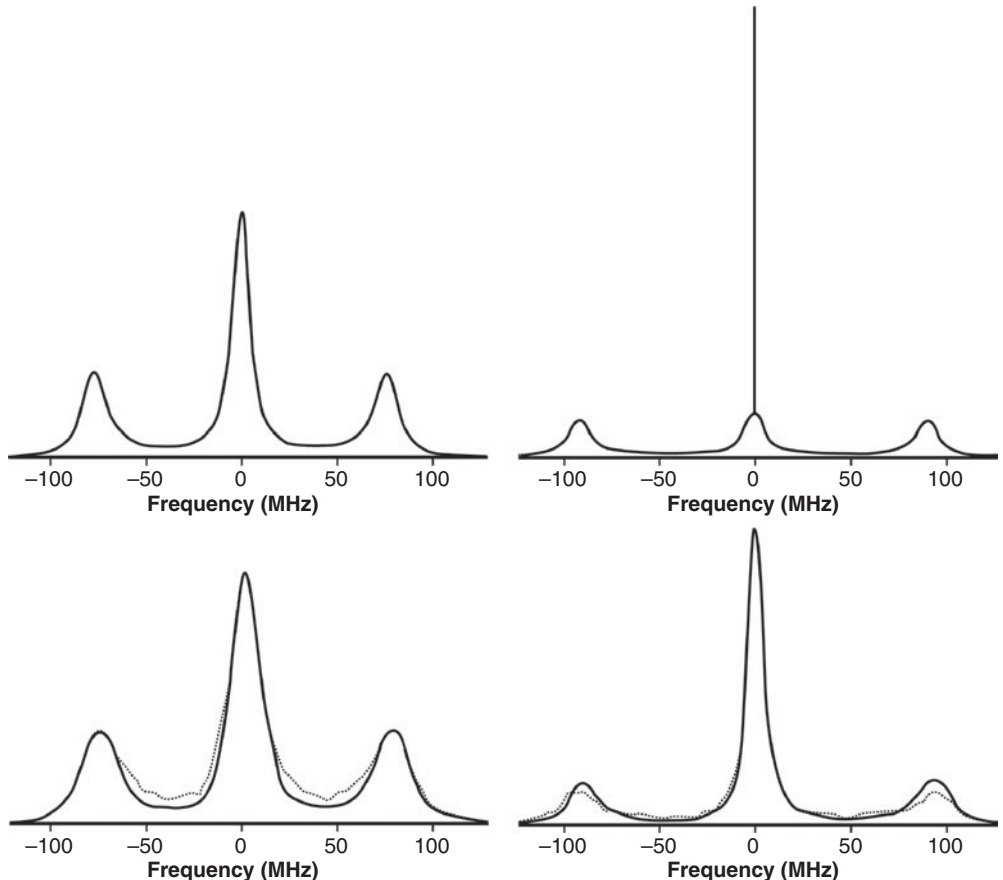
Figure 6.11 *Calculated (top) and observed (bottom) resonance fluorescence spectra of sodium atoms. The solid curves in the experimental traces are best fits to data taken exactly on resonance ($\Omega_R = \Omega$ at left) and at a finite detuning off resonance ($\Omega_R = 7.8\Omega$ at right). (Illustration adapted from Refs. [6.20, 6.21, 6.22] (theory) and Refs. [6.15, 6.16, 6.17] (experiment)).*

the equations of motion, and choose the zero of energy for the atom midway between its two states. Thus we find

$$H = \sum_{k,\lambda} \hbar\omega_k \hat{a}^+_{k\lambda}\hat{a}_{k\lambda} + \frac{1}{2}\hbar\omega_0\hat{\sigma}_3 + \hbar\sum_{k\lambda} g_{k\lambda}\left(\hat{\sigma}^+\hat{a}^-_{k\lambda} + \hat{\sigma}^-\hat{a}^+_{k\lambda}\right), \tag{6.7.2}$$

following replacement of the interaction with $-\bar{\mu}\cdot\bar{E}(t) = \hbar g_0\mu_0(\sigma^+ + \sigma^-)(a^- + a^+)\hat{\mu}\cdot\hat{\varepsilon}$, using

$$g_{k\lambda} = -(\mu_0 g_0\hat{\mu}\cdot\hat{\varepsilon})_{k\lambda} = -\mu\left(\frac{\omega_k}{2\hbar\varepsilon_0 V}\right)^{1/2}\hat{\mu}\cdot\hat{\varepsilon}_{k\lambda}. \tag{6.7.3}$$

The rotating wave approximation has been assumed in Eq. (6.7.2).

Exercise: Using Eq. (2.4.24) and the commutation properties of operators that do not commute, verify that the equations of motion in the Heisenberg picture describing the interplay of field, atomic polarization, and population in resonance fluorescence are given by

$$\dot{\hat{a}}_{k\lambda}^{-} = -i\omega_k \hat{a}_{k\lambda}^{-} - ig_{k\lambda}\hat{\sigma}^{-} \tag{6.7.4}$$

$$\dot{\hat{\sigma}}^{-} = -i\omega_0\hat{\sigma}^{-} + i\sum_{k,\lambda} g_{k\lambda}\hat{\sigma}_3\hat{a}_{k\lambda}^{-} \tag{6.7.5}$$

$$\dot{\hat{\sigma}}_3 = 2i\sum_{k,\lambda} g_{k\lambda}\left(\hat{\sigma}^{-}\hat{a}_{k\lambda}^{+} - \hat{\sigma}^{+}\hat{a}_{k\lambda}^{-}\right). \tag{6.7.6}$$

The conjugate equations for the field and atom lowering operators are

$$\dot{\hat{a}}_{k\lambda}^{+} = i\omega_k\hat{a}_{k\lambda}^{+} + ig_{k\lambda}\hat{\sigma}^{+}, \tag{6.7.7}$$

$$\dot{\hat{\sigma}}^{+} = i\omega_0\hat{\sigma}^{+} - i\sum_{k,\lambda} g_{k\lambda}\hat{\sigma}_3\hat{a}_{k\lambda}^{+}. \tag{6.7.8}$$

Note that Eqs. (6.7.4)–(6.7.6) consist of three coupled equations in the operators $\hat{a}^{-}$, $\hat{\sigma}^{-}$, and $\hat{\sigma}_3$ that represent the three physical parts of the system. Not surprisingly, as we proceed to solve these equations, we shall encounter three coupled equations involving three related correlation functions.

   The next step is to proceed with formal integration of Eq. (6.7.4). To simplify notation we dispense with operator carets and introduce the slowly varying quantities $\tilde{a}_{k\lambda}^{-}(t) = a_{k\lambda}^{-}\exp[i\omega_k t]$, $\tilde{a}_{k\lambda}^{+}(t) = a_{k\lambda}^{+}\exp[-i\omega_k t]$, $\tilde{\sigma}^{-}(t) = \sigma^{-}\exp[i\omega_k t]$, and $\tilde{\sigma}^{+}(t) = \sigma^{+}(t)\exp[-i\omega_k t]$. Steady-state conditions are not assumed as yet, so that Eq. (6.7.4) becomes

$$\dot{\tilde{a}}_{k\lambda}^{-}(t') = -ig_{k\lambda}\tilde{\sigma}^{-}(t'). \tag{6.7.9}$$

Upon integration between the limits 0 and t, this yields

$$\tilde{a}_{k\lambda}^{-}(t) = \tilde{a}_{k\lambda}^{-}(0) - ig_{k\lambda}\int_0^t dt'\tilde{\sigma}^{-}(t'). \tag{6.7.10}$$

Multiplying through by $\exp(-i\omega_k t)$, one finds

$$a_{k\lambda}^{-}(t) = a_{k\lambda}^{-}(0)\exp(-i\omega_k t) - ig_{k\lambda}\int_0^t dt'\tilde{\sigma}^{-}(t')\exp(-i\omega_k t)$$

$$= a_{k\lambda}^{-}(0)\exp(-i\omega_k t) - ig_{k\lambda}\int_0^t dt'\sigma^{-}(t')\exp[-i\omega_k(t-t')]. \tag{6.7.11}$$

The Hermitian conjugate operator is

$$a_{k\lambda}^{+}(t) = a_{k\lambda}^{+}(0)\exp(i\omega_k t) + ig_{k\lambda}\int_0^t dt'\sigma^{+}(t')\exp[i\omega_k(t-t')]. \tag{6.7.12}$$

Next, we describe the evolution of the atomic operators in terms of slowly varying amplitudes referenced to the resonance frequency of the atom ω_0. This is a matter of convenience that is intended to make it easier to interpret the final results.

$$s^-(t) = \sigma^- \exp[i\omega_k t] \exp[i\Delta' t], \tag{6.7.13}$$

$$s^+(t') = \sigma^+(t') \exp[-i\omega_k t'] \exp[-i\Delta' t']. \tag{6.7.14}$$

Here $\Delta' = \omega - \omega_k$. In terms of the slowly varying amplitudes s^- and s^+, the radiated power obtained by substituting Eqs. (6.7.11) and (6.7.12) and Eqs. (6.7.4) and (6.7.5) into Eq. (6.7.1) is

$$P(t) = \sum_{k,\lambda} \hbar\omega_k \left\langle \dot{a}^+_{k\lambda}(t) a^-_{k\lambda}(t) + a^+_{k\lambda}(t) \dot{a}^-_{k\lambda}(t) \right\rangle$$

$$= -\sum_{k\lambda} ig_{k\lambda}\hbar\omega_k \left[\left\langle a^+_{k\lambda}(0)\sigma^-(t) \right\rangle e^{i\omega_k t} - \left\langle \sigma^+(t) a^-_{k\lambda}(0) \right\rangle e^{-i\omega_k t} \right]$$

$$+ 2\mathrm{Re} \sum_{k\lambda} g^2_{k\lambda}\hbar\omega_k \int_0^t dt' \left\langle s^+(t')s^-(t) \right\rangle e^{i\Delta'(t-t')}. \tag{6.7.15}$$

The first two terms on the right side of Eq. (6.7.15) give the rate of change of field energy due to stimulated emission and absorption. The last term involves only atomic operators and represents power scattered quasi-elastically out of the incident beam as resonance fluorescence. It is this term that is of most interest here. Making use of the density of modes to replace the sum over k, λ by an integral, one finds that the fluorescence is determined entirely by a polarization correlation function.

$$P_s(t) = 2\mathrm{Re} \sum_{k\lambda} g^2_{k\lambda}\hbar\omega_k \int_0^t dt' \left\langle s^+(t')s^-(t) \right\rangle e^{i\Delta'(t-t')}$$

$$= \frac{1}{4\pi\varepsilon_0} \frac{4\mu^2}{3c^3} \mathrm{Re} \int_0^\infty d\omega'' \, (\omega'')^4 \int_0^t dt' \left\langle s^+(t')s^-(t) \right\rangle e^{i\Delta''(t-t')}. \tag{6.7.16}$$

Here ω'' is a representative mode frequency near that of the driving field. The detuning has been redefined accordingly as $\Delta'' \equiv \omega - \omega''$. Since we expect the spectrum to be dominated by quasi-elastic frequencies $\omega \cong \omega''$, the frequency factor $(\omega'')^4$ in Eq. (6.7.16) is well approximated by ω_0^4, and may be removed from the integral, with the result

$$P_s(t) \cong \frac{\mu_{12}^2 \omega_0^4}{3\pi\varepsilon_0 c^3} \mathrm{Re} \int_0^\infty d\omega'' \int_0^t dt' \left\langle s^+(t')s^-(t) \right\rangle \exp[i(\omega - \omega'')(t-t')]. \tag{6.7.17}$$

In the stationary regime ($t \to \infty$), the two-time correlation function $\left\langle s^+(t')s^-(t) \right\rangle$ only depends on the difference between t and t'. Hence we define $\tau = t - t'$ and re-express the steady-state power as

$$P_s(\infty) \cong \frac{\mu_{12}^2 \omega_0^4}{3\pi\varepsilon_0 c^3} \mathrm{Re} \int_0^\infty d\omega \int_0^\infty d\tau \left\langle s^+(t_0)s^-(t_0 + \tau) \right\rangle \exp[i(\omega - \omega_0)\tau], \tag{6.7.18}$$

where t_0 is any time in the stationary regime. In this limit, the power spectrum is

$$P(\omega) \propto 2\mathrm{Re} \int_0^\infty d\tau \, \langle s^+(t_0)s^-(t_0 + \tau)\rangle \exp[i(\omega - \omega'')\tau]$$

$$= 2\mathrm{Re} \int_0^\infty d\tau g(\tau) \exp[i(\omega - \omega'')\tau], \tag{6.7.19}$$

and is entirely determined by the Fourier transform of the first-order correlation function $g(\tau)$ of the atomic operator. This result reflects a fundamental relationship between time–domain fluctuations and frequency–domain power spectra, known as the Wiener–Khintchine theorem [6.18]. To calculate the resonance fluorescence spectrum we therefore need to determine

$$g(\tau) \equiv \langle s^+(t_0)s^-(t_0 + \tau)\rangle. \tag{6.7.20}$$

This is the heart of the resonance fluorescence problem and requires solution of Eqs. (6.7.4)–(6.7.6) as an interdependent set of equations, with all modes participating.

Rewriting Eqs. (6.7.5) and (6.7.6) using the earlier solution for $a_{k\lambda}^-$ from Eq. (6.7.11) one finds

$$\dot{\sigma}^-(t) = -i\omega_0\sigma^-(t) - \frac{i}{\hbar}\mu \cdot \sigma_3(t)E^+(t), \tag{6.7.21}$$

$$\dot{\sigma}_3(t) = (2i/\hbar)\mu \cdot \left[E^+(t)\sigma^+(t) - E^-(t)\sigma^-(t)\right], \tag{6.7.22}$$

where

$$E^+(t_0) = \sum_{k\lambda} \left(\frac{\hbar\omega_k}{2\varepsilon_0 V}\right)^{1/2} a_{k\lambda}^-(t)\hat{\varepsilon}_{k\lambda}, \tag{6.7.23}$$

and

$$E^-(t) = \left[E^+(t)\right]^+. \tag{6.7.24}$$

Now notice that the electric field operator $E^+(t)$ in Eq. (6.7.23) consists of two parts, since $a_{k\lambda}^-(t)$ consists of the two parts given in Eq. (6.7.11). Consequently

$$E^+(t) = \sum_{k\lambda} \left(\frac{\hbar\omega_k}{2\varepsilon_0 V}\right)^{1/2} a_{k\lambda}^-(0) \exp(-i\omega_k t)\hat{\varepsilon}_{k\lambda} -$$

$$-i\sum_{k\lambda} \left(\frac{\hbar\omega_k}{2\varepsilon_0 V}\right)^{1/2} \hat{\varepsilon}_{k\lambda}g_{k\lambda} \int_0^t dt'\sigma^-(t') \exp[-i\omega_k(t - t')]$$

$$\equiv E_0^+(t) + E_{RR}^+(t). \tag{6.7.25}$$

The first term in this result, $E_0^+(t)$, is the solution of the homogeneous Maxwell equation. That is, it is the field without any modification due to the atom. The second term is the modification due to the presence of the atom, called the radiation reaction field E_{RR}^+. This is clear from the absence of field operators in the second integral.

In classical electrodynamics, the reaction of an atom to its own radiation can be estimated from Newton's Third Law stating that for every action there is an equal and opposite reaction. Even though we have undertaken to calculate the emission spectrum in a fully quantum mechanical manner, we are guided by correspondence with classical concepts. Hence in the point dipole approximation, we assume the radiation reaction field is given by the operator for the corresponding classical field expression [6.17]:

$$E_{RR}(t) = E_{RR}^+(t) + E_{RR}^-(t) = \frac{1}{4\pi\varepsilon_0} \left[\frac{2}{3c^3}\dddot{\sigma}_x - \frac{4K_c}{3\pi c^2}\ddot{\sigma}_x \right] \mu \tag{6.7.26}$$

K_c is a high-frequency cut-off from the non-relativistic theory of point dipoles [6.19]. By assuming harmonic oscillation of $\sigma^-(t)$ and $\sigma^+(t)$ at frequency ω_0 and rewriting the Pauli matrix as $\sigma_x \mu = [\sigma^- + \sigma^+]\mu$, Eq. (6.7.26) can be re-expressed as

$$E_{RR}(t) \doteq \frac{i\omega_0^3}{6\pi\varepsilon_0 c^3} \left[\sigma^-(t) - \sigma^+(t) \right] \mu^2 + \frac{K_c\omega_0^2}{3\pi^2\varepsilon_0 c^2} \left[\sigma^-(t) - \sigma^+(t) \right] \mu^2. \tag{6.7.27}$$

With this result in hand, we can write

$$\mu \cdot E_{RR}^+(t) \cong (i\beta + \gamma)\,\hbar\sigma^-(t), \tag{6.7.28}$$

where $\beta \equiv \mu^2\omega_0^3/6\pi\varepsilon_0\hbar c^3 = \gamma_{sp}/2$ and $\gamma \equiv K_c\mu^2\omega_0^2/3\pi^2\varepsilon_0\hbar c^2$. Use of Eq. (6.7.28) in Eq. (6.7.21) now gives an equation for the transition operator of the atom that includes radiation reaction.

$$\dot{\sigma}^-(t) = -i\omega_0\sigma^-(t) + i\,(i\beta + \gamma)\,\sigma^-(t) - \frac{i}{\hbar}\mu \cdot \sigma_3(t)E_0^+(t) \tag{6.7.29}$$

The result $\sigma_3\sigma^- = -\sigma^-$ has been used to simplify Eq. (6.7.29). Eqs. (6.7.21) and (6.7.22) can now be written in a simple form.

$$\dot{\sigma}^-(t) = -i\,(\omega_0 - \gamma - i\beta)\,\sigma^-(t) - \frac{i}{\hbar}\mu \cdot \sigma_3(t)E_0^+(t) \tag{6.7.30}$$

$$\dot{\sigma}_3(t) = -2\beta\,(1 + \sigma_3(t)) - \frac{2i}{\hbar}\mu \cdot \left[E^-(t)\sigma^-(t) - \sigma^+(t)E^+(t) \right]. \tag{6.7.31}$$

Let us return to the problem of calculating $g(\tau)$, for which we need to work with expressions written in terms of slowly varying operators $s^\pm = \sigma^\pm \exp(\mp i\omega t)$. Eqs. (6.7.30) and (6.7.31) become

$$\dot{s}^-(t) = -i\,(\omega_0 - \omega - i\beta)\,s^-(t) - \frac{i}{\hbar}\mu \cdot \sigma_3(t)E^+(t)\exp(i\omega t) \tag{6.7.32}$$

$$\dot{\sigma}_3(t) = -2\beta\,(1 + \langle\sigma_3(t)\rangle)$$

$$+\frac{2i}{\hbar}\mu \cdot \left[s^+(t)E_0^+(t)\exp(i\omega t) - E_0^-(t)s^-\exp(-i\omega t) \right]. \tag{6.7.33}$$

In order for the expectation value of $E_0^+(t)$ in the equation above to correctly yield the amplitude of a coherent state of the form $< E_0(t) >= E_0\sin\omega t$, we assume that

$$E_0^+(t)\,|\psi\rangle = \frac{i}{2}E_0\exp(-i\omega t)\,|\psi\rangle. \tag{6.7.34}$$

Then the equation of motion for $g(\tau)$ becomes

$$\frac{\partial}{\partial \tau} g(\tau) = -i(\omega_0 - \omega - i\beta)g(\tau) - \frac{\mu E_0}{2\hbar}\left\langle s^+(t_0)\sigma_3(t+\tau)\right\rangle$$

$$= -i(\omega_0 - \omega - i\beta)g(\tau) + \frac{\Omega_R}{2}h(\tau), \tag{6.7.35}$$

where we have defined

$$h(\tau) \equiv \left\langle s^+(t_0)\sigma_3(t_0 + \tau)\right\rangle. \tag{6.7.36}$$

From Eq. (6.7.31) we can also work out an equation of motion for $h(\tau)$, the second correlation function to appear in our expressions:

$$\frac{\partial}{\partial \tau} h(\tau) = -2\beta\left\langle s^-(t_0)\right\rangle - \Omega_R\left\langle s^+(t_0)s^+(t_0+\tau)\right\rangle +$$

$$-(2i\mu/\hbar)\left\langle s^+(t_0)E_0^-(t_0+\tau)s^-(t_0+\tau)\right\rangle \exp[-i\omega(t_0+\tau)]. \tag{6.7.37}$$

It can be shown [6.8] that the commutator of atom and field operators in Eq. (6.7.37) is zero for delay times $\tau >> \omega_0^{-1}$. That is, $[s^+(t_0), E_0^-(t_0+\tau)] \approx 0$. So the last term in Eq. (6.7.37) simplifies to

$$-\Omega_R\left\langle s^+(t_0)s^-(t_0+\tau)\right\rangle = -\Omega_R g(\tau). \tag{6.7.38}$$

Hence the equation for the second of our correlation functions, $h(\tau)$, becomes

$$\frac{\partial}{\partial \tau} h(\tau) = -2\beta h(\tau) - 2\beta\left\langle s^+(t_0)\right\rangle - \Omega_R\left\langle s^+(t_0)s^+(t+\tau)\right\rangle - \Omega_R g(\tau)$$

$$= -2\beta h(\tau) - 2\beta\left\langle s^+(t_0)\right\rangle - \Omega_R f(\tau) - \Omega_R g(\tau). \tag{6.7.39}$$

In Eq. (6.7.39) we encounter a third and final correlation function, defined by

$$f(\tau) \equiv \left\langle s^+(t_0)s^+(t_0+\tau)\right\rangle. \tag{6.7.40}$$

The equation of motion for $f(\tau)$, the last needed to solve the resonance fluorescence problem, is obtained from Eq. (6.7.32).

$$\frac{\partial}{\partial \tau} f(\tau) = i(\omega_0 - \omega + i\beta)f(\tau) + i(\mu/\hbar)\left\langle s^+(t_0)E_0^-(t_0+\tau)\right\rangle \exp[-i\omega(t_0+\tau)]$$

$$= i(\omega_0 - \omega + i\beta)f(\tau) + (\Omega_R/2)h(\tau). \tag{6.7.41}$$

Finally, with Eqs. (6.7.35), (6.7.39), and (6.7.41), we have a closed set of equations for the correlation functions $g(\tau)$, $h(\tau)$, $f(\tau)$ which collectively determine the

emission spectrum. Gathering them together, we have

$$\left[\frac{\partial}{\partial\tau} + i\left(\Delta - i\beta\right)\right]g(\tau) = \frac{\Omega_R}{2}h(\tau) \tag{6.7.42}$$

$$\left[\frac{\partial}{\partial\tau} + 2\beta\right]h(\tau) = 2\beta\left\langle s^+\left(t_0\right)\right\rangle - \Omega_R g(\tau) - \Omega_R f(\tau) \tag{6.7.43}$$

$$\left[\frac{\partial}{\partial\tau} - i\left(\Delta + i\beta\right)\right]f(\tau) = \frac{\Omega_R}{2}h(\tau) \tag{6.7.44}$$

where $\Delta \equiv \omega_0 - \omega$. We must solve these equations subject to the initial conditions

$$g(0) = \left\langle s^+(t_0)s^-(t_0)\right\rangle, \tag{6.7.45}$$

$$h(0) = \left\langle s^+(t_0)\sigma_3(t_0)\right\rangle, \tag{6.7.46}$$

$$f(0) = \left\langle s^+(t_0)s^+(t_0)\right\rangle = 0. \tag{6.7.47}$$

Values of the initial correlations $g(0) = \langle s^+ s^- \rangle = \frac{1}{2}(1 + \langle \sigma_3(t_0)\rangle)$ and $h(0) = \langle s^+\sigma_3 \rangle = \langle s^+(t_0)\rangle$ can be found using the algebra of the Pauli spin operators. It is also easy to work out $\langle s^+(t_0)\rangle$ and $\langle \sigma_3(t_0)\rangle$ from Eqs. (6.7.32) and (6.7.33), by taking expectation values of each equation and setting the time derivatives equal to 0 for steady-state solutions. This yields the results

$$g(0) = \Omega_R^2/4[\Delta^2 + \frac{1}{2}\beta^2\Omega_R^2], \tag{6.7.48}$$

$$h(0) = \Omega_R(\beta + i\Delta)/2[\Delta^2 + \beta^2 + (\Omega_R^2/2)]. \tag{6.7.49}$$

On Resonance: For $\Delta = 0$ at high intensities ($\Omega_R >> \beta$), the solution of Eq. (6.7.42) that takes into account the condition in Eq. (6.7.45) is

$$g(\tau) \cong \frac{1}{2}\left[\exp(-\beta\tau) + \exp(-3\beta\tau/2)\cos\Omega_R\tau\right] + (\beta/\Omega_R)^2. \tag{6.7.50}$$

The power spectrum of resonance fluorescence is obtained from the Fourier transform of the first-order correlation function as expressed by Eq. (6.7.19):

$$P(\omega) = \frac{3\beta/8}{\left(\omega - \omega_L - \Omega_R\right)^2 + 9\beta^2/4} + \frac{\beta/2}{\left(\omega - \omega_L\right)^2 + \beta^2} + \frac{3\beta/8}{\left(\omega - \omega_L + \Omega_R\right)^2 + 9\beta^2/4}$$

$$+ 2\pi\left(\beta/\Omega_R\right)^2\delta\left(\omega - \omega_L\right). \tag{6.7.51}$$

This is the exact expression for the spectrum of resonance fluorescence. In it, the frequency of the laser used to excite the atom has been relabeled $\omega_L = \omega''$. At high fields ($\Omega >> \beta$) the spectrum consists of a delta function plus a three-component spectrum shown in the plots of Fig. 6.11. At low fields ($\Omega << \beta$) it consists of the delta function alone, as discussed by Heitler [6.23]. While the three-line, resonance fluorescence spectrum was first observed over thirty years ago [6.15, 6.16, 6.17], it is only recently that these features have been reported in the resonance fluorescence of individual molecules [6.24].
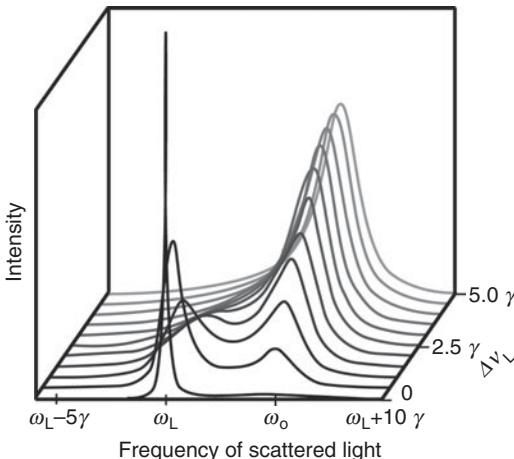
Figure 6.12 *Near resonance fluorescence spectrum at low intensity as a function of the bandwidth $\Delta\nu_L$ of incident light. The frequency of the incident light is detuned from resonance by five natural linewidths ($\Delta = \omega_0 - \omega = 5\gamma$). The triplet spectrum is absent. (Illustration adapted from [6.25].)*

Off resonance: If incident light is detuned from resonance, the scattered light spectrum has a significant dependence on bandwidth. When the resonance is displaced beyond the weak tail of the incident light spectral distribution, scattering only takes place at the incident frequency. In Fig. 6.12, this results in an intense narrow peak at the laser frequency ω_L. In the foreground of the figure, the laser is assumed to have negligible bandwidth compared to the atomic linewidth and it is detuned by five times the transition linewidth. In traces that move progressively toward the back of the figure, the bandwidth of the incident light increases. Because the excitation begins to overlap the resonance frequency more and more as its bandwidth grows, the fluorescent emission that follows absorption by the atom grows in intensity. The atomic emission is broadened by the radiative lifetime and centered on the resonant frequency ω_0.

6.7.2   Coherence of strongly driven two-level atoms

The general solution for the first-order correlation function $g^{(1)}(\tau)$ in Eq. (6.7.50) provides the quantum degree of first-order coherence of two-level atoms driven strongly on resonance. This function was plotted earlier as the solid curve in Fig. 6.7. The calculation of intensity correlations which yield the second-order correlation function $g^{(2)}(\tau)$ of driven atoms, requires additional considerations.

Resonance fluorescence is radiation from electric dipole oscillations of driven atoms. Hence it is determined by correlation properties of the atomic transition operators $\hat{\sigma}^\pm$, not the field operators $\hat{E}^\pm$. Since the atomic operators are already normalized, the quantum degree of second-order coherence is simply

$$g^{(2)}(\tau) = \left\langle \hat{\sigma}^+(t_0)\hat{\sigma}^+(t_0 + \tau)\hat{\sigma}^-(t_0 + \tau)\hat{\sigma}^-(t_0) \right\rangle$$

$$= \left\langle s^+(t_0)s^+(t_0 + \tau)s^-(t_0 + \tau)s^-(t_0) \right\rangle. \tag{6.7.52}$$

This expression may be reduced, using properties of the Pauli matrices:

$$s^+(t_0 + \tau)s^-(t_0 + \tau) = \sigma^+(t_0 + \tau)\sigma^-(t_0 + \tau)$$

$$= \frac{1}{2} + \sigma_z(t_0 + \tau). \tag{6.7.53}$$

Substitution of Eq. (6.7.53) into Eq. (6.7.52) then results in the expression

$$g^{(2)}(\tau) = \frac{1}{2}g^{(1)}(0) + \frac{1}{2}G(\tau), \tag{6.7.54}$$

where $g^{(1)}(0)$ is given by Eq. (6.7.50) and the remaining correlation function

$$G(\tau) \equiv \langle s^+(t_0)\sigma_z(t_0 + \tau)s^-(t_0)\rangle, \tag{6.7.55}$$

is still to be determined.

Just as in Section 6.7.1, where a set of differential equations for three related correlation functions was solved to obtain $g(\tau)$, the solution for $g^{(2)}(\tau)$ can be found by solving a set of equations for the three interrelated correlation functions

$$F(\tau) \equiv \langle s^+(t_0)s^+(t_0 + \tau)s^-(t_0)\rangle, \tag{6.7.56}$$

$$G(\tau) \equiv \langle s^+(t_0)\sigma_z(t_0 + \tau)s^-(t_0)\rangle, \tag{6.7.57}$$

$$H(\tau) \equiv \langle s^+(t_0)s^-(t_0 + \tau)s^-(t_0)\rangle, \tag{6.7.58}$$

that are determined by the operators s^+, s^-, and σ_z. From the Heisenberg equations of motion for the various atomic operators, it can be shown that

$$\frac{\partial F(\tau)}{\partial \tau} = i(\Delta + i\beta)F(\tau) + (\Omega_R/2)G(\tau), \tag{6.7.59}$$

$$\frac{\partial G(\tau)}{\partial \tau} = -2\beta g(0) - 2\beta G(\tau) - \Omega_R(F(\tau) + H(\tau)), \tag{6.7.60}$$

$$\frac{\partial H(\tau)}{\partial \tau} = -i(\Delta - i\beta)F(\tau) + (\Omega_R/2)G(\tau). \tag{6.7.61}$$

These equations may be solved [6.26] using the initial conditions

$$F(0) = \langle s^+(t_0)s^+(t_0)s^-(t_0)\rangle = 0, \tag{6.7.62}$$

$$G(0) = \langle s^+(t_0)\sigma_z(t_0)s^-(t_0)\rangle = -\langle s^+(t_0)s^-(t_0)\rangle = -g(0), \tag{6.7.63}$$

$$H(0) = \langle s^+(t_0)s^-(t_0)s^-(t_0)\rangle = 0, \tag{6.7.64}$$

to find an exact solution for $g^{(2)}(\tau)$. At resonance ($\Delta = 0$), the result is

$$g^{(2)}(\tau) = g(0)^2 \left[1 - \exp\left(\frac{-3\beta\tau}{2}\right)\left(\cos(\Omega''\tau) + \frac{\beta}{\Omega''}\sin(\Omega''\tau)\right)\right] \tag{6.7.65}$$

where

$$\Omega'' \equiv \sqrt{\Omega_R^2 - (\beta^2/4)}. \tag{6.7.66}$$

For $\tau = 0$, the quantum degree of second-order coherence $g^{(2)}(0)$ clearly takes on nonclassical values, since $g^{(2)}(0) = 0$. This quantum effect was evident in the earlier plot of this function for a single atom presented in Fig. 6.8. There is an "anti-bunching" effect in the emission rate of fluorescence photons from single atoms. The photon statistics of driven atoms reflects their internal quantum structure and their inability to emit a second photon immediately after a first. A finite time is required for re-excitation of an atom before it can emit again, automatically making it a "nonclassical" source of light.

6.8 Dressed atoms

6.8.1 Strong coupling of atoms to the electromagnetic field

An elegant approach to the analysis of resonance fluorescence that is quite a bit simpler than that presented in Section 6.7 is possible by diagonalizing the complete Hamiltonian, including the light field [6.26]. This method is referred to as dressed atom theory.

Consider a quantum system consisting of a two-level atom in a near-resonant radiation field. Initially we neglect the interaction between the two parts of the system, and identify the "bare" states of the uncoupled system. Written as the product of atomic and number states, these are

$$|1, n\rangle = |1\rangle |n\rangle \tag{6.8.1}$$

and

$$|2, n - 1\rangle = |2\rangle |n - 1\rangle. \tag{6.8.2}$$

These states are eigenstates of the atom-plus-field Hamiltonian $H_{\text{atom}} + H_{\text{field}}$ with eigenenergies

$$E_{1,n} = -\frac{\hbar\omega_0}{2} + n\hbar\omega, \tag{6.8.3}$$

$$E_{2,n-1} = \frac{\hbar\omega_0}{2} + (n - 1)\hbar\omega, \tag{6.8.4}$$

and a transition energy of

$$E_{2,n-1} - E_{1,n} = \hbar(\omega_0 - \omega) = \hbar\Delta. \tag{6.8.5}$$

The two uncoupled states have the same energy. That is, they are degenerate when $\Delta = 0$.

Next we introduce the interaction between the field and atom, and attempt to find an exact description of the system in terms of coupled states, one which takes the atom–field interaction into account. These states must be constructed to be eigenstates of the entire Hamiltonian

$$H = H_{\text{atom}} + H_{\text{field}} + H_{\text{int}}. \tag{6.8.6}$$

The photons may be pictured as "dressing" the atom, and near resonance or at very high intensities it is impossible to distinguish which photons interact with the atom,

or how many interactions take place. The available states are different from those of the bare atom by virtue of the strong interaction H_{int}. The task is therefore to find new coupled or dressed states $|D\rangle$ of the system,

$$|D\rangle = c_1 |1, n\rangle + c_2 |2, n - 1\rangle, \tag{6.8.7}$$

which satisfy the energy equation

$$H |D\rangle = (H_{\text{atom}} + H_{\text{field}} + H_{\text{int}}) |D\rangle = E_D |D\rangle. \tag{6.8.8}$$

Now $|1, n\rangle$ and $|2, n - 1\rangle$ are orthonormal, so upon substitution of Eq. (6.8.7) into Eq. (6.8.8) we immediately obtain

$$c_1 \langle 1, n | H | 1, n\rangle + c_2 \langle 1, n | H | 2, n - 1\rangle = E_D c_1, \tag{6.8.9}$$

$$c_1 \langle 2, n - 1 | H | 1, n\rangle + c_2 \langle 2, n - 1 | H | 2, n - 1\rangle = E_D c_2. \tag{6.8.10}$$

By explicit evaluation of the matrix element using the Hamiltonian of Eq. (6.2.10) with $\Delta = 0$, we find

$$\langle 2, n - 1 | H | 1, n\rangle = \hbar \langle 2, n - 1 | g\hat{a}\hat{\sigma}^+ + g^*\hat{a}^+\hat{\sigma}^- | 1, n\rangle = \hbar g \sqrt{n}, \tag{6.8.11}$$

and the two Eqs. (6.8.9) and (6.8.10) simplify to

$$c_1 (E_1 - E_D) + c_2 \hbar g^* \sqrt{n} = 0, \tag{6.8.12}$$

$$c_1 \hbar g \sqrt{n} + c_2 (E_2 - E_D) = 0. \tag{6.8.13}$$

The solution of the secular equation for coupled Eqs. (6.8.12) and (6.8.13) then indicates that the energy levels are shifted by the light [7.14] in accord with

$$
\begin{aligned}
E_D &= \frac{1}{2} (E_1 + E_2) \pm \frac{1}{2} \sqrt{(E_1 + E_2)^2 - 4 \left(E_1 E_2 - \hbar^2 |g|^2 n \right)} \\
&= \left(n - \frac{1}{2} \right) \hbar\omega \pm \frac{1}{2} \hbar \sqrt{\Delta^2 + 4 |g|^2 n} \\
&= \left(n - \frac{1}{2} \right) \hbar\omega \pm \frac{1}{2} \hbar\Omega_R,
\end{aligned}
\tag{6.8.14}
$$

where $\Omega_R \equiv \sqrt{\Delta^2 + 4|g|^2 n}$ is the generalized Rabi frequency. The quantities E_D are the eigenvalues of the dressed states depicted in Fig. 6.13. To find the corresponding eigenstates $|D\rangle$, it is convenient to define

$$\sin 2\theta = \frac{2 |g| \sqrt{n}}{\Omega_R} \equiv \frac{\Omega}{\Omega_R}, \tag{6.8.15}$$

$$\cos 2\theta \equiv \frac{\Delta}{\Omega_R}. \tag{6.8.16}$$
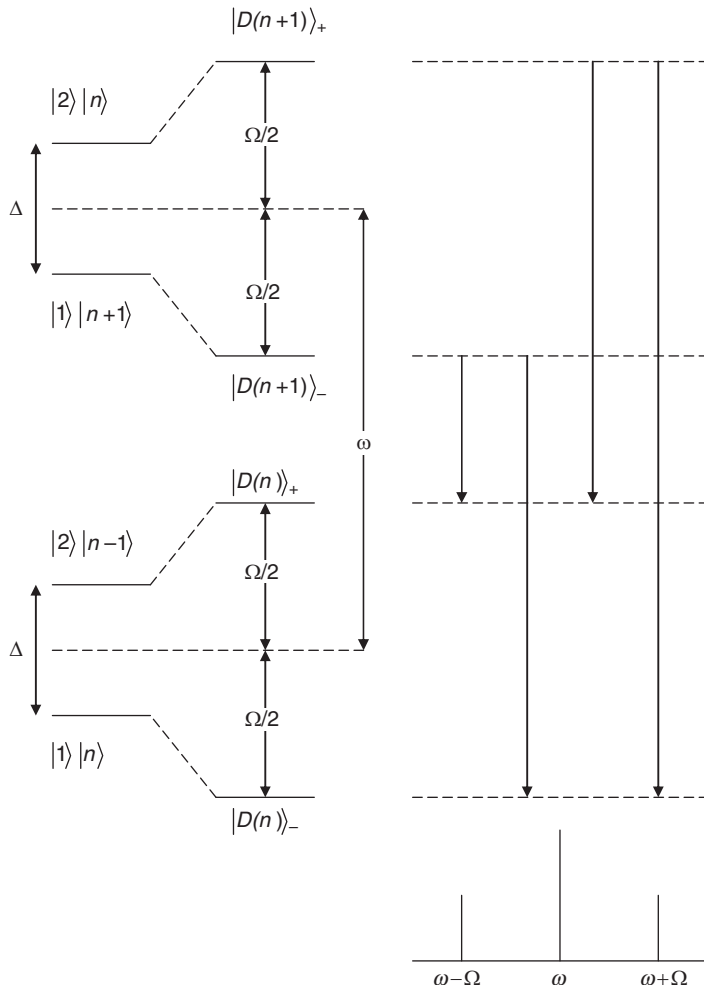
Figure 6.13 *Schematic depiction of dressed atom energy levels and the transitions between them. The resonance fluorescence spectrum predicted by the model is shown in the lower right, directly beneath the transitions giving rise to it. (After Ref. [6.10].)*

With $E_D = E_+(n)$, we proceed to solve for the coefficients c_1 and c_2, obtaining

$$\frac{1}{2} c_1 \left(\Delta + \Omega_R \right) = c_2 g^* \sqrt{n}, \tag{6.8.17}$$

$$\frac{1}{4} \left| c_1 \right|^2 \left(\Delta + \Omega_R \right)^2 = \left| c_2 \right|^2 \left| g \right|^2 n. \tag{6.8.18}$$

Exercise: Show that by imposing the normalization condition $|c_1|^2 + |c_2|^2 = 1$, Eq. (6.8.18) can be solved to yield the following expressions for the coefficients:

$$|c_1|^2 = \sin^2 \theta, \tag{6.8.19}$$

$$|c_2|^2 = \cos^2 \theta, \tag{6.8.20}$$

and that these expressions are consistent with Eqs. (6.8.15) and (6.8.16).

Given the results in Eq. (6.8.19) and Eq. (6.8.20), the first dressed state can be written as

$$|D(n)\rangle_+ = \sin \theta \, |1, n\rangle + \cos \theta \, |2, n - 1\rangle. \tag{6.8.21}$$

With $E_D = E_-(n)$, we find a second solution.

$$|c_1|^2 = \cos^2 \theta \tag{6.8.22}$$

$$|c_2|^2 = \sin^2 \theta \tag{6.8.23}$$

In order for $|D(n)\rangle_-$ to be orthogonal to $|D(n)\rangle_+$, the signs of the coefficients must be chosen such that

$$|D(n)\rangle_- = \cos \theta \, |1, n\rangle - \sin \theta \, |2, n - 1\rangle. \tag{6.8.24}$$

Notice that the dressed states $|D\rangle_+$, $|D\rangle_-$ are not degenerate on resonance, the way the uncoupled states were. For $\Delta = 0$, we now find $\Omega_R = \Omega$ $(2\theta = \pi/2)$ and

$$E_+(n) - E_-(n) = \hbar\Omega, \tag{6.8.25}$$

$$|D(n)\rangle_\pm = \frac{1}{\sqrt{2}} \left[|1, n\rangle \pm |2, n - 1\rangle \right]. \tag{6.8.26}$$

Based on Eq. (6.8.26), a complex picture of the states and energies of the atom + field system now emerges. To begin with, there is an infinite ladder of dressed states. To see this, consider two bare states that are slightly different from the initial basis states taken above. If we had started with states

$$|1, n + 1\rangle = |1\rangle \, |n + 1\rangle, \tag{6.8.27}$$

$$|2, n\rangle = |2\rangle \, |n\rangle, \tag{6.8.28}$$

differing from our original bare states by the presence of an added photon in the particular mode of interest of the radiation field, we would have found dressed states $|D(n + 1)\rangle_+$, $|D(n + 1)\rangle_-$ with energies

$$E_\pm(n + 1) = \left[(n + 1) - \frac{1}{2} \right] \hbar\omega \pm \frac{1}{2}\hbar\Omega_R. \tag{6.8.29}$$

Because there are infinitely many possible n values, there are infinitely many dressed states. These states may be thought of as excited states of the dressed atom, and discrete transitions can take place between these levels, as shown in Figs. 6.13 and 6.14. The predicted resonance fluorescence spectrum is shown at lower right in Fig. 6.13, and is a triplet in agreement with results of the last section.
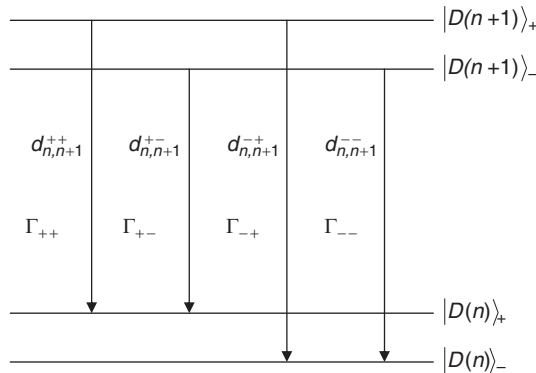
Figure 6.14 *Nomenclature of dipole moments d and transition rates Γ connecting specific adjacent pairs of dressed states during fluorescent transitions.*

6.8.2 Dressed state population dynamics

Using the dressed state formalism we can readily check that the transitions between dressed states depicted in Fig. 6.13 have nonzero transition moments and do indeed produce electric dipole radiation that accounts for the Mollow triplet spectrum. Recalling that the atomic dipole operator $\hat{\mu} = \hat{\sigma}^+ + \hat{\sigma}^-$ only acts on the atomic part of the atom–field product states, the moment between the upper states of two adjacent dressed state manifolds may be calculated as follows for example.

$$
\begin{aligned}
[\langle D_+(n)\,|e\hat{r}|\,D_+(n+1)\rangle &= \mu\left\{[\langle 1,n|\sin\theta + \langle 2,n-1|\cos\theta]\;(\sigma+\sigma^+)\,[\sin\theta\,|1,n+1\rangle\right. \\
&\quad \left. +\;\cos\theta\,|2,n\rangle]\}] \right. \\
&= \mu\left\{\langle n|\,\langle 1|\,(\sin\theta)\sigma^-(\cos\theta)\,|2\rangle\,|n\rangle\right\} \\
&= \frac{1}{2}\mu\sin 2\theta \neq 0.
\end{aligned}
\tag{6.8.30}
$$

Transitions are possible in the dressed state system whenever the dipole moment is nonzero. Since the field has already been incorporated into the electronic structure of the system, radiative transitions take place at a rate Γ_{ij} that is simply proportional to the square of the matrix element of the electric dipole moment between initial and final dressed states D_i and D_j (following Fermi's Golden Rule):

$$
\Gamma_{ij} = |\langle D(n_j)|\,e\hat{r}\,|D(n_i)\rangle|^2\,.
\tag{6.8.31}
$$

To analyze the transition rates among the dressed states shown in Fig. 6.14, which in turn determine the intensities of features in the resonance fluorescence spectrum, all four matrix elements $d_{ij}^{\pm} = \langle D_\pm(n_j)|\,e\hat{r}\,|D_\pm(n_i)\rangle$ are needed. We calculate them explicitly below and then proceed to develop rate equations based on knowledge of the relative rates Γ_{ij}.

Exercise: Show that the expected dipole moment $d_{fi}^{\pm\pm} = \langle D_\pm(n_f)|e\hat{r}|D_\pm(n_i)\rangle$ between initial and final states $|D(n+1)\rangle_+$ and $|D(n)\rangle_+$ differs from that between $|D(n+1)\rangle_+$

and $|D(n)\rangle_-$, and that both have the nonzero values given below.

$$d^{++}_{n,n+1} = \mu \left\{ \langle 1, n| \sin\theta + \langle 2, n-1| \cos\theta \right\} \left(\sigma + \sigma^+ \right) \left\{ \sin\theta\, |1, n+1\rangle + \cos\theta\, |2, n\rangle \right\}$$
$$= \mu \sin\theta \cos\theta, \tag{6.8.32}$$

$$d^{-+}_{n,n+1} = \mu \left\{ \langle 1, n| \cos\theta - \langle 2, n-1| \sin\theta \right\} \left(\sigma + \sigma^+ \right) \left\{ \sin\theta\, |1, n+1\rangle + \cos\theta\, |2, n\rangle \right\}$$
$$= \mu \cos^2\theta. \tag{6.8.33}$$

Exercise: Show that the remaining two transition dipole moments between states $|D(n+1)\rangle_-$ and $|D(n)\rangle_+$ and between $|D(n+1)\rangle_-$ and $|D(n)\rangle_-$ are:

$$d^{+-}_{n,n+1} = -\mu \sin^2\theta. \tag{6.8.34}$$

$$d^{--}_{n,n+1} = -\mu \sin\theta \cos\theta, \tag{6.8.35}$$

The populations in various dressed states can be assessed by calculating diagonal elements of the density matrix $\rho = |D\rangle\langle D|$ and solving rate equations similar to Eqs. (5.1.10) and (5.1.11). Populations of the various dressed states will be denoted by

$$\pi_\pm(n) = \langle D_\pm(n)| \rho |D_\pm(n)\rangle. \tag{6.8.34}$$

Changes in the population of a particular dressed state via one-photon transitions can occur in two ways. Relaxation into a given level involves two transitions down from the upper neighboring manifold and relaxation out of the level takes place by two transitions down to the next neighboring manifold. Hence the population rate equations are very simple:

$$\dot\pi_-(n) = -\left(\Gamma_{--} + \Gamma_{+-}\right)\pi_-(n) + \Gamma_{--}\pi_-(n+1) + \Gamma_{-+}\pi_+(n+1) \tag{6.8.35}$$

$$\dot\pi_+(n) = -\left(\Gamma_{-+} + \Gamma_{++}\right)\pi_+(n) + \Gamma_{++}\pi_+(n+1) + \Gamma_{+-}\pi_-(n+1) \tag{6.8.36}$$

If we assume the illumination is intense, there is little difference between occupation values of number states labelled with $n-1$, n or $n+1$. Hence the same may be said of neighboring dressed state manifolds, and we can write $\pi_\pm(n+1) \cong \pi_\pm(n) = p_0(n)\pi_\pm$, where $p_0(n)$ is the distribution of photons among the available modes. Adjacent dressed states connected by one-photon transitions then all obey the same equations.

$$\dot\pi_- = -\Gamma_{+-}\pi_- + \Gamma_{-+}\pi_+, \tag{6.8.37}$$

$$\dot\pi_+ = -\Gamma_{-+}0_+ + \Gamma_{+-}\pi_-. \tag{6.8.38}$$

In steady state, we can solve for the populations themselves by setting $\dot\pi = 0$ in Eqs. (6.8.37) and (6.8.38) and making use of the condition

$$\Gamma_{+-}\pi_-(\infty) = \Gamma_{-+}\pi_+(\infty), \tag{6.8.39}$$

together with the closure relation

$$\pi_-(\infty) + \pi_+(\infty) = 1. \tag{6.8.40}$$

(a)

(b)
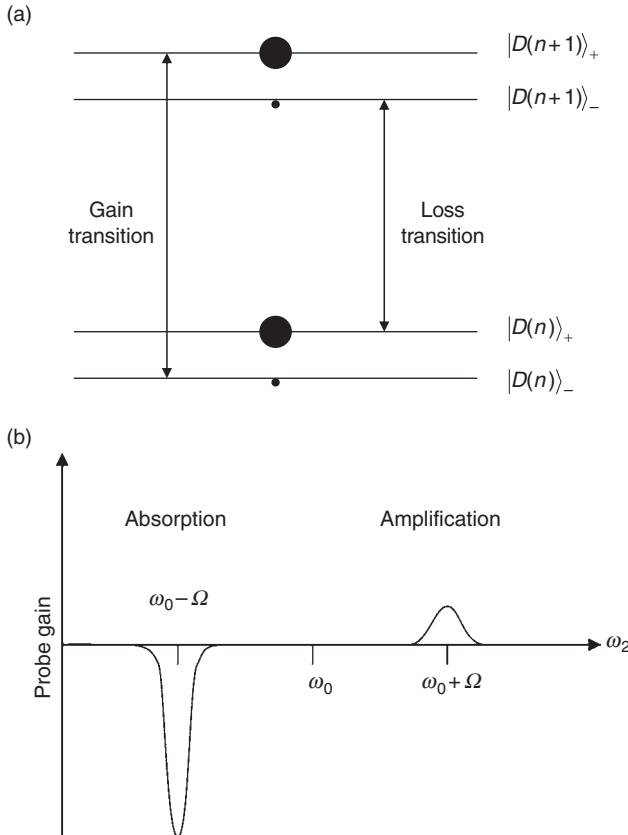
Figure 6.15 *(a) Population differences among dressed states at finite detunings of the pump wave. The size of the filled black circle indicates the relative size of the population. (b) Schematic illustration of the absorption spectrum of a near-resonant probe versus frequency ω_2 of the coupling laser. (After Ref. [6.27].)*

The results are

$$\pi_+ (\infty) = \frac{\Gamma_{+-}}{\Gamma_{-+} + \Gamma_{+-}} = \frac{\sin^4 \theta}{\sin^4 \theta + \cos^4 \theta}, \tag{6.8.41}$$

$$\pi_- (\infty) = \frac{\Gamma_{-+}}{\Gamma_{-+} + \Gamma_{+-}} = \frac{\cos^4 \theta}{\sin^4 \theta + \cos^4 \theta}. \tag{6.8.42}$$

Exactly on resonance ($\theta = \pi/4$) the populations of the upper ($+$) and lower ($-$) dressed states are equal. However, for finite detuning of the pump wave the populations may differ (Fig. 6.15a).

In particular, at detunings equal to plus or minus the Rabi frequency, the population difference may be positive or negative. The result is that continuous gain or loss may be experienced by a probe wave passing through the pumped region of a nominally

two-level system (Fig. 6.15b). Because this is a steady-state result, it appears to violate the prescription of thermodynamics that in steady state the excited state population of a two-level system can never exceed that of the ground state. The resolution of this dilemma is that with near-resonant excitation the dressed state model no longer consists of just two atom–field levels. It becomes a multilevel system.

Since n is not a good quantum number of the dressed states, the number of photons n in the field is indeterminate. Similarly, it is not known whether the atom is in bare state $|1\rangle$ or $|2\rangle$ at any time, because these states are no longer eigenstates of the coupled system. Field and atom cannot be considered separate entities near resonance. Transitions of the driven system would normally proceed by stimulated emission and absorption processes, but we have integrated the field with the atom so intimately that we may speak of resonance fluorescence as being the spontaneous emission of dressed atoms.

In summary, near-resonant electromagnetic fields act to couple or "dress" the uncoupled or "bare" states of the atom and field, and effect a significant change in its eigenstates and eigenenergies. The modification of the atomic electronic structure by light is important enough that neither the state of the field (specified purely by the number of photons) nor the state of the atom (specifying which of the original states of the atom is occupied) is any longer well defined. The coupled atom–field system can exhibit optical gain, despite the fact that sustained population inversions of true two-level systems are thermodynamically impossible.

Problems

6.1. In formal solutions of the Schrodinger equation one sometimes encounters functions of operators that do not commute. Then, identities such as the Weyl relation are useful.

(a) Show that

$$\exp(\hat{c} + \hat{d} + \frac{1}{2}\left[\hat{c}, \hat{d}\right]) = \exp(\hat{c})\exp(\hat{d})$$

is valid for any pair of operators $\hat{c}$ and $\hat{d}$ which commute with their own commutator according to

$$\left[\hat{c}, \left[\hat{c}, \hat{d}\right]\right] = \left[\hat{d}, \left[\hat{c}, \hat{d}\right]\right] = 0.$$

(b) Use the result above to show that coherent states can be written in the compact form

$$|\alpha\rangle = \hat{\alpha}|0\rangle,$$

where $\hat{\alpha} \equiv \exp(\alpha\hat{a}^{+} - \alpha^{*}\hat{a})$ transforms the ground state into state $|\alpha\rangle$.

(c) Show that $\hat{\alpha}$ is in fact a displacement operator with the property that

$$\hat{\alpha}^{+}\hat{a}\hat{\alpha} = \hat{a} + \alpha$$

using the result of part (a) and the commutation relation for field operators $\hat{a}$ and $\hat{a}^{+}$.

6.2. This problem shows that when an external force acts on a quantized simple harmonic oscillator initially in the ground state, the system can be left in an excited state, with energy determined by the Fourier component $g(\omega)$ of the driving force that is in resonance with the unforced or "free" oscillator. This state that is excited in this way is a minimum uncertainty state of constant width that oscillates harmonically in coordinate and momentum space.

The Hamiltonian of a forced linear harmonic oscillator

$$H = \frac{p^2}{2\mu} + \frac{1}{2}\mu\omega^2 q^2 - qF(t) - \rho G(t)$$

can be written in the form

$$H = \hbar\omega\left(a^+ a + \frac{1}{2}\right) + f(t)a + f^*(t)a^+,$$

provided we define a complex-valued forcing function

$$f(t) = -\sqrt{\frac{\hbar}{2\mu\omega}}F(t) + i\sqrt{\frac{\hbar\mu\omega}{2}}G(t).$$

(a) Show that the equation of motion for $a(t)$ in the Heisenberg representation is

$$\frac{da(t)}{dt} + i\omega a(t) = -\frac{i}{\hbar}f^*(t).$$

(Changes in the excitation level of the oscillator depend on $f^*(t)$.)

(b) Use a Green's function approach to solve the equation of motion of part (a) for $a(t)$ by adding the appropriate particular solution

$$a_p(t) = -\frac{i}{\hbar}\int_{-\infty}^{\infty} G(t - t')f^*(t')dt'$$

to first one and then the other of the two homogeneous solutions $a_<(t)$ and $a_>(t)$ corresponding to $t < t'$ and $t > t'$ respectively. Write down the two resulting general solutions for $a(t)$, only formal expressions in terms of $a_<(t)$ and $a_>(t)$ are needed. Note that $G(t - t')$ is proportional to $e^{-i\omega(t-t')}$ when $t \neq t'$, but at $t = t'$ integration of the Green's function equation over an interval including t' shows that it must satisfy the condition:

$$\lim_{\varepsilon \to 0} [G(+\varepsilon) - G(-\varepsilon)] = 1,$$

where $\varepsilon \equiv t - t'$. Hence suitable representations for the Green's functions are given by

$$G_<(t - t') = \eta(t - t')e^{-i\omega(t-t')}$$

$$G_>(t - t') = -\eta(t' - t)e^{-i\omega(t-t')}$$

where η is a step function:

$$\eta(x) \equiv \int\limits_{-\infty}^{x} \delta(x')dx' = \begin{cases} 0, & x < 0 \\ 1, & x > 0 \end{cases}.$$

(c) Equating the two solutions from part (b), show that

$$a_>(t) = a_<(t) - \frac{i}{\hbar}g^*(\omega),$$

where

$$g^*(\omega) \equiv \int\limits_{-\infty}^{\infty} e^{-i\omega(t-t')}f^*(t')dt'.$$

(d) Assume that the action of the displacement operator $\hat{\alpha}$ in problem 6.1 is such that it transforms the field annihilation operator in time according to $a_>(t) = \hat{\alpha}^+ a_< \hat{\alpha}$. Then determine the actual value of the eigenvalue α of the coherent state, to reveal its relationship with the Fourier spectrum of the forcing function.

(e) Show that the number of quanta at frequency ω is 0 before the forcing function $f(t)$ is applied, but is proportional to the square of its Fourier component $g(\omega)$ for $t > 0$. To do this, evaluate $\langle 0|\hat{a}_<^+ \hat{a}_< |0\rangle$ and $\langle 0|\hat{a}_>^+ \hat{a}_> |0\rangle$.

6.3. Show that the variables P and Q introduced simply as linear combinations of field amplitudes are indeed the conjugate variables needed for quantum field theory by showing that they obey Hamilton's equations $\dot{Q}_{k\sigma} = \dfrac{\partial H}{\partial P_{k\sigma}}$ and $\dot{P}_{k\sigma} = -\dfrac{\partial H}{\partial Q_{k\sigma}}$, where H is expressed explicitly in terms of P and Q.

6.4. Show that unlike the situation for the annihilation operator on which the development of coherent states rests, no eigenstate of the field creation operator exists.

6.5. The momentum density of an electromagnetic field is given by the Poynting vector divided by c^2 (see, e.g., Stratton, "Electromagnetic Theory"). Classically, this means the total momentum of the field associated with a volume V in space can be written

$$\bar{G} = \frac{1}{c^2} \int (\bar{E} \times \bar{H})d^3r$$

Show that quantization of the fields in this expression reveals that the momentum of each plane wave is quantized in units of $\hbar\bar{k}$.

6.6. Thermal radiation is quite different from single-mode laser fields, due to dependence of the occupation probability of a state with n photons of frequency ω on the thermodynamic temperature T of the medium (governed by Boltzmann statistics).

(*a*) From the expression

$$\hat{\rho} = \sum_{\psi} P_{\psi} |\psi >< \psi|,$$

and the value of P_{ψ} from statistical mechanics for the probability that n photons occupy a mode, show that the radiative density operator for thermal radiation at frequency ω is

$$\hat{\rho} = \left[1 - \exp\left(\frac{-\hbar\omega}{k_B T}\right)\right] \sum_{n} \exp\left(\frac{-n\hbar\omega}{k_B T}\right) |n >< n|$$

(*b*) Use the relation

$$\bar{n} = \langle \hat{n} \rangle = Tr\left(\rho a^+ a\right)$$

and the result of part (*a*) to show that the density operator can be expressed as

$$\hat{\rho} = \sum_{n} \frac{(\bar{n})^n}{(1 + \bar{n})^{1+n}} |n >< n|.$$

(*c*) Also show that the density operator for single-mode thermal radiation can be written in the equivalent form

$$\hat{\rho} = \left\{1 - \exp\left(\frac{-\hbar\omega}{k_B T}\right)\right\} \exp\left(\frac{-\hbar\omega \hat{a}^+ \hat{a}}{k_B T}\right),$$

where the exponential is defined by its usual power-series expansion.

Additional discussion of density operators for different types of radiation field can be found in Ref. [6.9].

6.7. The one-photon coherent state $|\alpha\rangle$ is an eigenstate of the annihilation operator $\hat{a}$. Hence $\hat{a}|\alpha\rangle = \alpha|\alpha\rangle$. Use this information and the definition of the photon number operator $\hat{n} \equiv \hat{a}^+ \hat{a}$ to find

(*a*) the second-order degree of correlation $g^{(2)}(\tau) = \langle \hat{a}^+ \hat{a}^+ \hat{a} \hat{a} \rangle / \langle \hat{a}^+ \hat{a} \rangle^2$ of the coherent state $|\alpha\rangle$, and the root mean square fluctuation $\Delta n_{\mathrm{rms}} \equiv (\langle (n - \langle n \rangle)^2 \rangle)^{1/2} = (\langle n^2 \rangle - \langle n \rangle^2)^{1/2}$ of the number of photons. Express your answer in terms of $\langle n \rangle$ and note the form of Δn_{rms} that is characteristic of a Poisson process.

(*b*) Calculate $g^{(2)}(\tau)$ and Δn_{rms} for the Fock state $|n\rangle$. Compare with part (*a*) to decide which state, $|\alpha\rangle$ or $|n\rangle$, is *noisier*.

6.8. A single-mode number (Fock) state contains exactly n photons.

(*a*) Calculate the first- and second-order coherence functions, $g^{(1)}$ and $g^{(2)}$ of the state.

(*b*) As a function of τ, how does each function from part (*a*) compare with coherences of classical and nonclassical sources? (Consider an atom, a thermal source, a "coherent" state $|\alpha\rangle$, and squeezed light in addition to

the Fock state. You can simply look up correlation plots for most of these other cases* and present comparisons in the form of sketches.)

(*c*) Which of these sources are nonclassical?

(*See, e.g., Refs. [6.9] and [6.20].)

6.9. (*a*) Calculate the magnitude of the quantum degree of first-order coherence $|g^{(1)}|$ of the single-mode coherent state $|\alpha\rangle$ given by

$$|\alpha\rangle = \exp(-|\alpha|^2/2) \sum_{n=0}^{\infty} \frac{\alpha^n}{(n!)^{1/2}} |n\rangle$$

where $|n\rangle$ denotes the single-mode Fock state.

(*b*) Calculate the root mean square fluctuation $\Delta E = [<\hat{E}^2> - <\hat{E}>^2]^{1/2}$ of the electric field operator $\hat{E} = E_0(\hat{a}^- + \hat{a}^+)\sin kz$ for the state

$$|\psi\rangle = \frac{1}{\sqrt{2}} \left[|n\rangle + e^{-i\Omega t} |n+1\rangle \right].$$

6.10. Calculate the root mean square fluctuation $\Delta E = [<\hat{E}^2> - <\hat{E}>^2]^{1/2}$ of the vacuum field.

6.11. Solve Eq. (6.7.42) in the low intensity limit for the first-order quantum coherence $g^{(1)}(\tau)$ of resonance fluorescence.

6.12. "Quantum beats" may be observed in the luminescence of three-level atoms prepared in a coherent superposition state that decays spontaneously. The beats consist of a modulation in the envelope of luminescent decay. In a semiclassical picture, the total emission intensity is simply proportional to the square of the total field radiated by two dipole polarizations comprising the initial tri-level coherence:

$$|E_{\text{TOT}}|^2 = \left| E_1 e^{i\omega_1 t} + E_2 e^{i\omega_2 t} \right|^2 \propto E_1 E_2^* e^{i(\omega_1 - \omega_2)t} + c.c.$$

The signal intensity should therefore contain a signal at beat frequency $\Delta\omega = \omega_1 - \omega_2$. This seems to provide a convenient method of measuring the level splitting $\Delta\omega$ regardless of whether the splitting is between excited states or ground states ("*V*-type" or "Λ-type" atoms respectively – see Figs. 1 and 2).

(*a*) For a *V*-type atom (Fig. 1), write down the semiclassical density matrix equation of motion for $\dot{\rho}_{12}^{(3)}$ to show that there is indeed a radiant polarization on the 1↔2 transition that originates from any coherence $\rho_{32}^{(2)}$ existing between levels 2 and 3. The only nonvanishing matrix elements for the *V*-type system are $\mu_{12} = e\langle 1|r|2\rangle$ and $\mu_{13} = e\langle 1|r|3\rangle$.

(*b*) According to quantum electrodynamics, quantum beats in luminescence arise from tri-level coherence that radiates spontaneously with a signal amplitude of $E_S \propto \langle\psi(t)|E_1^-(t)E_2^+(t)|\psi(t)\rangle$, where $E_1(t) = E_1^+(t) + E_1^-(t)$ is the field at ω_1 and $E_2(t) = E_2^+(t) + E_2^-(t)$ is the field at ω_2. Note that $E_k^{(+)}(r,t) \equiv |E_k|a_k e^{-i\omega_k t}U_k(r)$ and its adjoint are field annihilation and
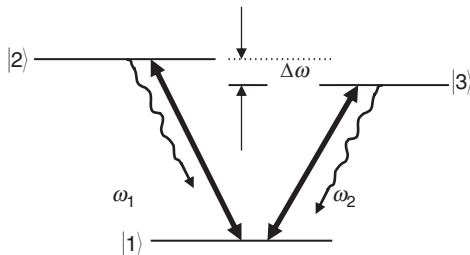
Figure 1. *A V-type energy level scheme. Applied fields at frequencies ν_1 and ν_2 that create the initial coherent superposition state of the atom are shown as bold arrows. Spontaneous decay is indicated by wiggly arrows.*
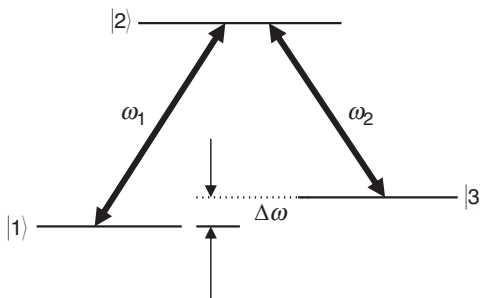
Figure 2. *A Λ-type energy level scheme. The nonvanishing matrix elements in this case are $\mu_{12} = e\langle 1|r|2\rangle$ and $\mu_{23} = e\langle 2|r|3\rangle$. Again the bold arrows indicate the applied fields that create the initial coherent superposition state of the atom.*

creation operators respectively. Calculate E_S for V-type atoms using the system wavefunction that comprises the initial superposition state plus states reached by spontaneous emission, namely:

$$|\psi\rangle = |i\rangle\,|n(\omega_1)\rangle\,|n(\omega_2)\rangle = \sum_i [a_i\,|i\rangle\,|0\rangle\,|0\rangle + b_i\,|1\rangle\,|1\rangle\,|0\rangle + c_i\,|1\rangle\,|0\rangle\,|1\rangle].$$

The factors a_i, b_i, and c_i are occupation probability amplitudes associated with atomic levels $i = 1, 2$, or 3.

(c) Does the QED signal polarization contain the expected beats?

(d) Recalculate E_S for the Λ-type atom depicted below, again using a wavefunction which is the initial superposition state plus the states accessed by spontaneous emission, namely $|\psi\rangle = \sum_i [a_i|i\rangle|0\rangle|0\rangle + b_i|1\rangle|1\rangle|0\rangle + c_i|3\rangle|0\rangle|1\rangle]$.

(e) Describe the QED results of parts (b) and (c) in a few words and compare them with the expectation of the semiclassical argument presented at the beginning of this problem.
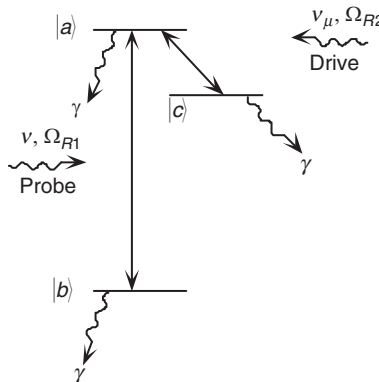
6.13. In a system (depicted below) consisting of three-level atoms in a Λ-configuration, an initial state $|\psi(0)\rangle = C_a(0)|a\rangle + C_b(0)|b\rangle + C_c(0)|c\rangle$ evolves in time under the influence of two driving fields to the exact state $|\psi(t)\rangle = C_a(t)|a\rangle + C_b(t)|b\rangle + C_c(t)|c\rangle$, where

$$C_a(t) = \left[C_a(0)\cos(\Omega t/2) - iC_b(0)\frac{\Omega_{R1}}{\Omega}\sin(\Omega t/2) - iC_c(0)\frac{\Omega_{R2}}{\Omega}\sin(\Omega t/2 \right]e^{-\gamma t/2},$$

$$C_b(t) = \left\{ -iC_a(0)\frac{\Omega_{R1}}{\Omega}\sin(\Omega t/2) + C_b(0)\left[\frac{\Omega_{R2}^2}{\Omega^2} + \frac{\Omega_{R1}^2}{\Omega^2}\cos(\Omega t/2)\right] \right.$$

$$\left. + C_c(0)\left[\frac{-\Omega_{R1}\Omega_{R2}}{\Omega^2} + \frac{\Omega_{R1}\Omega_{R2}}{\Omega^2}\cos(\Omega t/2)\right] \right\}e^{-\gamma t/2},$$

$$C_c(t) = \left\{ -iC_a(0)\frac{\Omega_{R2}}{\Omega}\sin(\Omega t/2) + C_b(0)\left[-\frac{\Omega_{R1}\Omega_{R2}}{\Omega^2} + \frac{\Omega_{R1}\Omega_{R2}}{\Omega^2}\cos(\Omega t/2)\right] \right.$$

$$\left. + C_c(0)\left[\frac{\Omega_{R1}^2}{\Omega^2} + \frac{\Omega_{R2}^2}{\Omega^2}\cos(\Omega t/2)\right] \right\}e^{-\gamma t/2},$$

Here Ω_{R1} and Ω_{R2} are the Rabi frequencies associated with the resonant fields driving the $|a\rangle \to |b\rangle$ and $|a\rangle \to |c\rangle$ transitions, respectively, and $\Omega = \sqrt{\Omega_{R1}^2 + \Omega_{R2}^2}$.

(a) State the main characteristic of a "dark" state.

(b) Assuming $\gamma = 0$, show that atoms prepared in the initial state

$$|\psi(0)\rangle = \frac{\Omega_{R2}}{\Omega}|b\rangle - \frac{\Omega_{R1}}{\Omega}|c\rangle$$

are in a trapped or "uncoupled" state.

(c) Assuming $\gamma = 0$ and that atoms are prepared initially in the ground state, find the probability of absorbing a probe laser photon (HINT: probability of the atom evolving from $|\psi(0)\rangle$ to $|a\rangle$).

(d) What is the condition under which the probability of absorption from the ground state on the $|b>\rightarrow|a>$ transition vanishes, giving electromagnetically induced transparency? (HINT: Use a projection technique to follow the development of excited state probability amplitude.)

6.14. This problem makes use of the expressions for amplitudes $C_a(t), C_b(t)$, and $C_c(t)$ in problem 6.13 above and assumes the initial state of the atom is $|\psi(0)\rangle = |a\rangle$. By simply taking this initial condition into account, and calculating density matrix elements as explicit bilinear products of state amplitudes:

(a) Find the polarization $P(t)$ on the $|a\rangle \leftrightarrow |b\rangle$ transition.

(b) Identify the amplitude of the component $P^+(\omega)$ in the macroscopic polarization $P(t) = P(-\omega)e^{i\omega t} + P(\omega)e^{-i\omega t}$ and, for the stated initial condition, calculate the time t_1 at which the gain factor $\Gamma = Im\{P(\omega)\}$ first reaches a maximum.

(c) Find the occupation probabilities of states $|a\rangle$ and $|b\rangle$ and show that at time t_1 (when the gain is maximum) the population in the system is inverted (meaning there is more population in the upper state than in the lower).

(d) Give the time interval, if there is one, over which there exists gain but there is no inversion.

6.15. A two-level atom system is subjected to a strong nearly resonant light field. Verify that the dressed states $|D(n)_+\rangle$ and $|D(n)_-\rangle$ form an orthogonal basis, like the uncoupled product states.

6.16. Using expressions from the dressed state theory of resonance fluorescence for level populations $\pi^\pm(\infty)$ and transition rates per atom $\Gamma = |<d>|^2$ between dressed states:

(a) Prove that *at exact resonance* the intensity of the central fluorescence component of the Mollow triplet is twice that of either sideband.

(b) "Stimulated" emission rates depend on the difference between initial and final state populations rather than the population of the initial state alone. Show that the rates of stimulated emission and stimulated absorption for one-photon transitions of the dressed atom are different and find their dependence on the mixing angle θ.

(c) Using the result of part (b), consider the gain–loss spectrum that would be measured by a tunable probe wave passing through the dressed atom sample. How many peaks are expected in the spectrum versus detuning, and are they positive peaks or negative?

(d) At exact resonance compare the rates of "stimulated" emission (from part (b)) and "spontaneous" emission (from part (a)) and comment on whether resonance fluorescence should be regarded as the stimulated or spontaneous emission of dressed atoms.

References

6.1. M. Sargent, M.O. Scully, and W.E. Lamb, *Laser Physics*, Addison-Wesley, Reading, MA, 1974, pp. 236–40.

6.2. J.J. Sakurai, *Advanced Quantum Mechanics*, Benjamin-Cummings Publ. Co., Menlo Park, CA, 1967, Sects. 2–8.

6.3. S. Stenholm, *Foundations of Laser Spectroscopy*, J. Wiley & Sons, New York, 1984.

6.4. A.S. Davydov, *Quantum Mechanics*, 2nd edition, Pergamon Press, Oxford and New York, 1976, pp.134–5.

6.5. R.J. Glauber, Phys. Lett. **21**, 650(1966).

6.6. C. Caves, Phys. Rev. D **23**, 1693(1981).

6.7. See special issue: Squeezed States of the Electromagnetic Field, J.O.S.A. **B4**, (1987).

6.8. R. Hanbury-Brown and R.Q. Twiss, Nature **127**, 27(1956).

6.9. R. Loudon, *The Quantum Theory of Light*, 2nd edition, Oxford University Press, London, 1983; also 3rd edition, Oxford University Press, London, 2000.

6.10. M. Weissbluth, *Photon–Atom Interactions*, Academic Press, Boston, MA, 1989.

6.11. D. Kleppner, Phys. Rev. Lett. **47**, 233(1981).

6.12. E.M. Purcell, Phys. Rev. **69**, 681(1946).

6.13. B.R. Mollow, Phys. Rev. **188**, 1969(1969).

6.14. P.L. Knight and P.W. Milonni, Phys. Rep. **66**, 21–107(1980).

6.15. R.E. Grove, F.Y. Wu, and S. Ezekiel, Phys. Rev. Lett. **35**, 1426(1975). (Check author list.)

6.16. F. Schuda, C.R. Stroud, and M. Hercher, J. Phys. B: Atom. Molec. Phys. **7**, L198(1975).

6.17. W. Hartig, W. Rasmussen, R. Scheider, and H. Walther, Z. Phyzik A **278**, 205(1976).

6.18. Further discussion can be found in M. Born and E. Wolf, *Principles of Optics*, 7th edition, Cambridge University Press, Cambridge, 1999, pp. 566–9.

6.19. See, for example, A.D. Jackson, *Classical Electrodynamics*, 2nd edition, Wiley, New York, 1975, pp. 780–6.

6.20. B.R. Mollow, Phys. Rev. **188**, 1969(1969).

6.21. A.L. Newstein, Phys. Rev. **167**, 89(1968).

6.22. A.L. Burshtein, Sov. Phys. JETP **22**, 939(1966).

6.23. W. Heitler, *Quantum Theory of Radiation*, 3rd edition, Oxford University Press, London, 1954.

6.24. G. Wrigge, I. Gerhardt, J. Hwang, G. Zumofen, and V. Sandoghar, Nat. Phys. **4**, 60(2008).

6.25. P.L. Knight, W.A. Molander, and C.R. Stroud, Phys. Rev. A**17**, 1547(1978).

6.26. C. Cohen-Tannoudji and S. Reynaud, Dressed Atom approach to resonance fluorescence, in *Multiphoton Processes*, eds. J.H. Eberly and P. Lambropoulos, J. Wiley & Sons, New York, 1977, pp. 103–18.

6.27. F.Y. Wu, S. Ezekiel, M. Ducloy, and B.R. Mollow, Phys. Rev. Lett. **38**, 1077(1977).

6.28. P. Meystre and M. Sargent, *Elements of Quantum Optics*, 3rd edition, Springer-Verlag, New York, 1999.

7
Selected Topics and Applications

In this chapter, the tools developed in earlier chapters are applied to analyze a limited number of selected topics. They are neither comprehensive nor in any sense the "most important" examples of what has been learned so far. However, they do describe surprising results that are close enough to the "research front" that readers can begin to see how problems from many disciplines can be attacked with the basic tool in hand. This chapter is intended to demonstrate that techniques from earlier chapters can be used in familiar ways on challenging new problems. The chosen topics have the merit of illustrating a few more pedagogically important principles while demonstrating a wide range of applications for which light is a suitable probe or means of control and density matrix analysis is tractable.

7.1   Mechanical effects of light and laser cooling

Light can do more than most of us imagine. It can transfer linear momentum, angular momentum, or energy to material systems. Thus, it can slow down, twist, or pull on matter as well as initiate dynamics and chemistry. All that is required is that the light is tuned near an optical transition that satisfies appropriate selection rules. In this section, several surprising mechanical effects of light are described, beginning within physical forces that arise from optical energy gradients in laser beams. Slowing and cooling of atoms as the result of near resonant interactions with light will be discussed in Sections 7.1.2–7.1.4.

7.1.1   Radiation pressure, dipole forces, and "optical tweezers"

After observing that comet tails always point away from the sun, Kepler suggested that light fields exert pressure on matter. Since that time it has been shown that a wave of intensity I produce a force per unit area (or pressure) that is given in classical terms by

$$\frac{F}{A} = \frac{I}{c}. \tag{7.1.1}$$

In all earlier sections, we ignored center-of-mass motion of atoms interacting with light, as well as spatial variations in the light distribution itself. Although mechanical forces of light are weak, there are micro-mechanical devices in which they nevertheless lead to important applications [7.1]. To analyze in detail how light can push or pull directly on atoms, we need to account for both these aspects of the problem. This is

readily done by including the center-of-mass (kinetic) contribution to the energy in the Hamiltonian of the (two-level) atom,

$$H = \frac{p^2}{2M} + \frac{1}{2}\hbar\omega_0\sigma_z, \tag{7.1.2}$$

and recognizing that both the amplitude and the phase of an inhomogeneous light wave vary in space by writing the interaction Hamiltonian as

$$V(\bar{r}) = -\frac{1}{2}\hbar\Omega(\bar{r})\exp[i(\omega t + \varphi(\bar{r}))]\,|1\rangle\langle 2| + h.c. \tag{7.1.3}$$

The force $\overline{F}$ exerted by light is best calculated using the Heisenberg equation of motion since it is a property of the field operator itself that is of interest. Bearing in mind that linear momentum operator $\bar{p}$ commutes with the Hamiltonian H above, and that in the coordinate representation $\bar{p} = -i\hbar\overline{\nabla}$, we find

$$\overline{F} = \frac{d\bar{p}}{dt} = \frac{i}{\hbar}[(H+V),\bar{p}] = -\overline{\nabla}V(\bar{r}). \tag{7.1.4}$$

Exercise: Show that upon substitution of Eq. (7.1.3) into Eq. (7.1.4), the force operator for the positive frequency component in the rotating wave approximation (RWA) becomes

$$F = \frac{1}{2}\hbar\Omega(\bar{r})\exp[-i(\omega t + \varphi(\bar{r}))]\,\{\alpha(\bar{r}) - i\beta(\bar{r})\}, \tag{7.1.5}$$

where the real and imaginary parts are given by

$$\overline{\alpha}(\bar{r}) \equiv \frac{\overline{\nabla}\Omega(\bar{r})}{\Omega(\bar{r})} \text{ and } \overline{\beta}(\bar{r}) \equiv \overline{\nabla}\phi(\bar{r}). \tag{7.1.6}$$

The expectation value of the force F is given by its trace with the density matrix:

$$\langle F\rangle = \mathrm{Tr}\,\{F,\rho\} = \frac{1}{2}\hbar\Omega(\bar{r})\,\{\overline{\alpha}(\bar{r})(\tilde{\rho}_{12} + \tilde{\rho}_{21}) + i\overline{\beta}(\bar{r})(\tilde{\rho}_{21} - \tilde{\rho}_{12})\}$$

$$= \frac{1}{2}\hbar\Omega\,\{R_1\overline{\alpha} + R_2\overline{\beta}\}. \tag{7.1.7}$$

The first term on the right is purely real and gives the dipole force $\langle F_{\mathrm{dip}}\rangle$. Note that it is proportional to the component R_1 of the Bloch vector given by Eq. (3.85). The second term is purely imaginary and produces a dissipative force $\langle F_{\mathrm{diss}}\rangle$. It is proportional to R_2 of the Bloch vector specified by Eq. (3.86). Together these two forces comprise the total force exerted by light on the atom:

$$\langle F\rangle = \langle F_{\mathrm{dip}}\rangle + \langle F_{\mathrm{diss}}\rangle. \tag{7.1.8}$$

If we make use of the steady-state solution (Eq. (5.1.8)) for the off-diagonal density matrix elements of atoms at rest, the expression for the dipole force term in Eq. (7.1.7) reduces to

$$\langle F_{\mathrm{dip}}\rangle = \frac{\hbar}{4}\left(\frac{\Delta}{\Delta^2 + \Gamma^2}\right)\overline{\nabla}\Omega^2(\bar{r})[\rho_{11} - \rho_{22}], \tag{7.1.9}$$

since $\Omega\overline{\nabla}\Omega = \overline{\nabla}\Omega^2/2$.
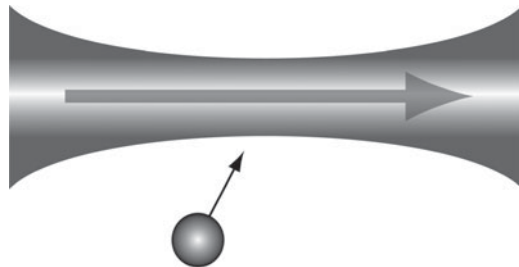
Figure 7.1 *Illustration of a two-level atom being attracted to the high intensity at the focus of a light beam propagating to the right. The light is detuned to the red side of the atomic resonant frequency.*

The population difference in Eq. (7.1.9) plays no role far off-resonance where this force is commonly applied, since then $\rho_{11} - \rho_{22} \sim 1$. Note too that the dipole force is zero unless the gradient of optical intensity is nonzero. Evidently, it is significant only in inhomogeneous fields such as the focal regions of laser beams (see Fig. 7.1). Plane waves do not exert a dipole force, since $\overline{\alpha} = \overline{\nabla}\Omega/\Omega = 0$. Moreover, the force is "strong-field seeking" for red detunings, since then the force points in the direction of highest intensity. For blue detunings, the opposite is true. The force is repulsive or "weak-field seeking." The result in Eq. (7.1.9) therefore indicates that a strongly focused, red-detuned laser beam can attract atoms or transparent objects to its center as indicated in Fig. 7.1. This is the basis for the manipulation of small particles with laser beams [7.2, 7.3] that led to the introduction of "optical tweezers" for biological research [7.4]. Figure 7.2 is intended to illustrate two laser beams trapping particles attached to a molecule in the viewing plane of a microscope.

As mentioned earlier, a dissipative force accompanies the dipole force. In fact, dissipation is present for every plane wave component of the incident beam, because it does not require a field gradient, only a phase gradient. It originates from the second term in Eq. (7.1.7). Upon evaluation for stationary atoms in a plane wave (i.e., $\overline{\nabla}E_0 = 0$ and $\overline{\nabla}\phi = -k\hat{z}$), the dissipative force yields

$$\langle \overline{F}_{\text{diss}}(v = 0)\rangle = \frac{\hbar\Omega\overline{\beta}}{2}\frac{(-\Gamma\Omega)}{(\Delta^2 + \Gamma^2)}(\rho_{11} - \rho_{22}) = \frac{\hbar}{2}\frac{k\Gamma\Omega^2\hat{z}}{(\Delta^2 + \Gamma^2)}(\rho_{11} - \rho_{22}). \quad (7.1.10)$$

This force is directed along the propagation axis of the wave.

Additional discussion of tweezers can be found in Ref. [7.5]. Trapping with the dipole force using inhomogeneous waves is described further in Refs. [7.6, 7.7]. Use of the dissipative force in Eq. (7.1.10) to cool gases is described next. Approaches to laser cooling based upon alternative concepts are considered in Sections 7.1.3 and 7.2.

7.1.2 Laser cooling via the Doppler shift

Although the dipole force described in the last section can be used for manipulating or trapping atoms and particles using high power focused lasers tuned far to the red side of resonances (in regions of spectral transparency), interactions closer to resonance
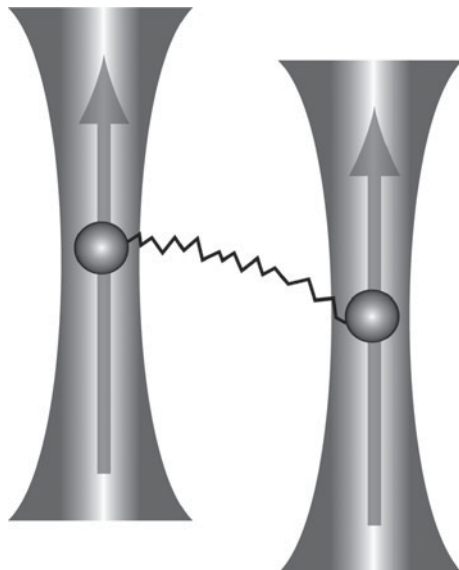
Figure 7.2 *Schematic drawing of two focused laser beams holding silica beads attached to either end of a macromolecule, permitting it to be moved or straightened for study. By moving the beams individually or in tandem, "optical tweezers" can manipulate the molecule. The beads experience a force that keeps them at the beam foci, as described in the text.*

can be effective at more modest powers. The technique described in this section relies on the Doppler effect (Section 3.9) near resonances [7.8] to cool the system, and is usually called Doppler cooling.

In Fig. 7.3, a two-level atom is pictured moving at a velocity v opposite to that of the light beam, in the $-\hat{z}$-direction. Because of the first-order Doppler shift (Section 3.9), the atom is not in resonance if the light frequency ω is tuned to the resonant frequency ω_0 itself. However, photons will be resonantly absorbed if the Doppler shift is compensated by detuning to a lower frequency namely $\omega = \omega_0 - kv$. For each absorbed photon, the atom then acquires linear momentum by an amount $\hbar k$, opposing its initial momentum. Following absorption, light is reemitted as spontaneous emission in a random direction that on average carries away no momentum. Hence as the result of absorbing a photon the atom is slowed by an average amount $\Delta v = \hbar k / M$.

The average emission frequency of the atom is ω_0, since even the Doppler-broadened emission spectrum of an ensemble is centered on the rest frame resonance frequency. Consequently, the average atom radiates more energy than it absorbs after absorbing a photon on the "red" side of resonance. In fact, energy and momentum decrease simultaneously and the atom cools. This is the basis for Doppler laser cooling of gases [7.9] and "anti-Stokes" cooling of solids [7.10].

This argument can be made quantitative by simply extending the result of the last section for dissipative forces on stationary atoms to the case of moving atoms. Consider an atom with positive velocity v that is situated in a wave traveling in the $\hat{z}$ direction.
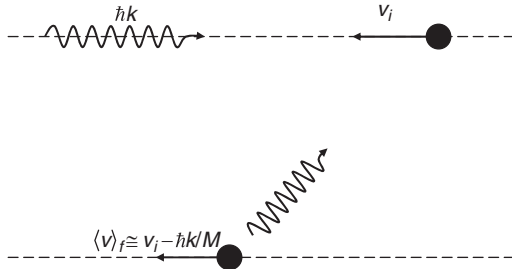
Figure 7.3 (Top) *An atom of velocity v travels in a direction opposite to that of an incident beam.* (Middle) *Following absorption of a photon, it* (bottom) *reradiates the energy, resulting on average in a slower final velocity, since the emitted photon emerges in a random direction and therefore carries away an average momentum of 0.*

According to Eq. (5.2.8), the off-diagonal element is then

$$\tilde{\rho}_{21} = \left[\frac{i(\Omega/2)}{\Gamma + i(\Delta - kv)}\right](\rho_{11} - \rho_{22}). \tag{7.1.11}$$

The Doppler shift is small compared to typical linewidths (and optimal detunings as we shall see). That is, $kv << \Gamma, \Delta$. Hence it plays little role in the magnitude of the denominator in Eq. (7.1.11). We find qualitatively new contributions to the force on the atom however by expanding this expression to first order in the shift.

$$\tilde{\rho}_{21} = \frac{i(\Omega/2)}{(\Gamma + i\Delta)}\left(\frac{1}{1 - ikv/[\Gamma + i\Delta]}\right)(\rho_{11} - \rho_{22})$$

$$\cong \frac{i(\Omega/2)(\Gamma - i\Delta)}{\Gamma^2 + \Delta^2}\left\{1 + i\left(\frac{\Gamma - i\Delta}{\Gamma^2 + \Delta^2}\right)kv\right\}(\rho_{11} - \rho_{22}). \tag{7.1.12}$$

For the plane wave under consideration, there is no transverse intensity gradient. Hence $\overline{\alpha} = 0$ and $\overline{\beta} = -k\hat{z}$. The force in Eq. (7.1.7) is therefore simply

$$\langle F \rangle = -\frac{1}{2}\hbar\Omega R_2 k\hat{z}, \tag{7.1.13}$$

where R_2 is the second component of the Bloch vector defined in Eq. (3.8.6) in Chapter 3.

From Eq. (7.1.12), we can identify R_2 directly as

$$R_2 = -\left\{\frac{\Omega\Gamma}{\Delta^2 + \Gamma^2} + \frac{2\Omega\Gamma\Delta kv}{(\Delta^2 + \Gamma^2)^2}\right\}(\rho_{11} - \rho_{22}),$$

and so the expression for the force becomes

$$\langle F \rangle = \langle F_{\text{diss}}(v = 0)\rangle + \frac{\hbar k^2\Omega^2\Gamma\Delta}{(\Delta^2 + \Gamma^2)^2}(\rho_{11} - \rho_{22})v\hat{z}. \tag{7.1.14}$$

In this form, it is obvious that the dissipative force on the atom points in the direction of propagation of the light field, regardless of whether the atom is moving or not.

The first term on the right side of Eq. (7.1.14) reproduces the result for stationary atoms given by Eq. (7.1.10). The second term is a velocity-dependent force whose sign depends on detuning Δ. For positive ("red") detuning, it accelerates atoms traveling in the $(+\hat{z})$-direction and decelerates atoms traveling in the $(-\hat{z})$-direction. However for any given velocity v, if the detuning is fixed at $\Delta = k\,|v|$, we see that the force is far more effective at deceleration than at acceleration. This is because an atom co-propagating with the light at velocity v sees a detuning of $\Delta = -2k\,|v|$ due to the Doppler effect. As the result of this detuning, it experiences a greatly reduced force compared to the atom propagating toward the light source, which is in exact resonance.

For negative ("blue") detuning, the forces reverse. Therefore, there is great potential for detailed control of the motion of atoms with mechanical forces exerted by light. Red-detuned light is particularly effective however, as discussed in the introduction of this section, at reducing the energy and momentum of moving atoms simultaneously. This principle is utilized for fast, efficient Doppler cooling in magneto-optic traps, to be described next. In solids, because there is no obvious way to implement the complete Doppler cooling strategy based on moving atoms, optical refrigeration techniques developed to date are less efficient [7.11].

7.1.3 Magneto-optic trapping

To cool atoms effectively using the Doppler effect, net cooling must be achieved for atoms traveling in either direction along any Cartesian axis. For this purpose, beams along all three axes are needed. Counter-propagating pairs of red-detuned waves can interact with atoms traveling in positive or negative direction along any given axis. In addition, a central region must be provided where cold atoms can collect. Atoms away from center should experience Doppler cooling and a net force driving them to the origin.

The apparatus depicted in Fig. 7.4 uses a combination of magnetic and optical trapping to trap and cool atoms in this manner [7.12]. A key ingredient is the introduction of a pair of coils carrying opposing currents as shown in Fig. 7.4b. This coil configuration gives rise to a magnetic field that increases linearly from the origin. Due to linear Zeeman splitting, states with opposite magnetic projections on either side of the origin experience a magnetic restoring force that points to the center of the trap (see Fig. 7.4a). However, the restoring force only acts on atoms that reach the excited state through interaction with one of the red-detuned beams and thereby develop a magnetic moment. Hence when atoms are slowed and cooled by the standing wave along each axis, it is possible for them to fall into the capture range of the magnetic trap, whereupon they accumulate at the origin if their velocity is low enough.

The detuning that results in an extremum of the cooling rate by the Doppler method may be readily calculated from Eq. (7.1.14). The stopping force will have a maximum when $\partial \langle F \rangle / \partial \Delta = 0$. The population difference $(\rho_{11} - \rho_{22})$ contains some detuning dependence of its own, particularly as one approaches resonance, but we can estimate

(a)

(b)

(b)
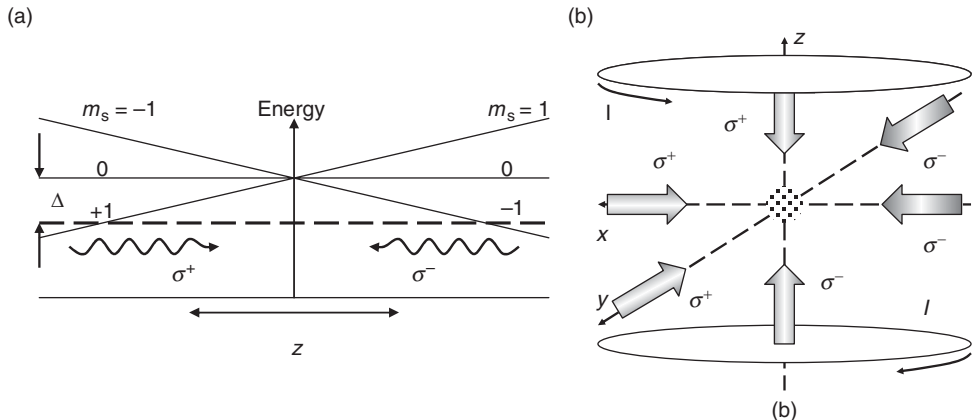
Figure 7.4 *Magneto-optic trap combining Doppler cooling with a magnetic restoring force centered on the origin. (a) For a hypothetical atom with an $S = 0$ ground state and $S = 1$ excited state, the excited substates split as shown in an anti-Helmholtz field. Angular momentum selection rules then stipulate positive (negative) helicity light incident from the left (right) to achieve resonance with left-(right-)going atoms attempting to leave the trap. Hence atoms that would otherwise be lost from the trap are cooled further and may remain trapped. (b) The overall trap geometry showing the coils at top and bottom, and six beams of appropriate polarization to provide cooling on the hypothetical $S = 0 \rightarrow S = 1$ transition. (After [7.12].)*

the optimal detuning for cooling by setting

$$\frac{\partial}{\partial \Delta} \left(\frac{\Delta}{(\Gamma^2 + \Delta^2)^2} \right) = 0. \tag{7.1.15}$$

The result is

$$\Delta = (\Gamma/\sqrt{3}) \approx \Gamma/2. \tag{7.1.16}$$

This relation suggests that the temperature limit of the Doppler cooling method is set by the energy balance between cooling and heating at the detuning specified by Eq. (7.1.16). The lowest temperature achievable by the Doppler cooling method should therefore be

$$k_B T_D = \frac{1}{2} \hbar \Gamma. \tag{7.1.17}$$

Still lower temperatures can be reached using polarization gradient cooling and trapping, described next.

7.1.4   Laser cooling below the Doppler limit

To cool matter below the Doppler limit of Eq. (7.1.17), new principles must be utilized to improve the cooling rate for slow atoms. An important advance historically was the idea of using polarization gradients in the force law expressed by Eq. (7.1.4) to reach a temperature corresponding to the recoil limit [7.13, 7.14].

The recoil limit is determined by the energy imparted by a single absorbed photon of wavenumber k to an atom of mass M (see Section 3.9). This energy equals $\hbar^2 k^2/2M$, and so the recoil-limited temperature is

$$k_{\rm B} T_{\rm R} = \hbar^2 k^2/2M. \tag{7.1.18}$$

Understandably, to reach temperatures lower than the Doppler limit, cooling and trapping mechanisms that do not rely on the Doppler effect and yet still exert viscous damping and cooling must be utilized. Here, we shall consider only one polarization gradient technique that provides a higher rate of cooling than Doppler cooling for very slowly moving atoms.

In the previous three sections, we analyzed forces arising from spatial gradients associated with Doppler shifts in the light–matter interaction or inhomogeneous light fields. Spatial variations of the optical polarization can also produce strong forces on atoms, as we now show. First, we specialize to an atom with the level structure shown in Fig. 7.5.

Consider two counter-propagating plane waves with orthogonal linear polarizations (often referred to as the lin $\perp$ lin configuration of a one-dimensional "optical molasses").

Exercise: Show that the total field in a lin $\perp$ lin configuration can be written in the form

$$\overline{E} = \frac{1}{2} E_0 \exp[-i(\omega t - kz)] \{\hat{x} + \hat{y} \exp(-2ikz)\} + c.c.$$
$$= E(z) \exp[-i\omega t] + c.c., \tag{7.1.19}$$

where the amplitude of the positive frequency component is

$$E(z) = \frac{1}{2} E_0 (\hat{x} + \hat{y}) \cos kz + \frac{1}{2} i E_0 (\hat{x} - \hat{y}) \sin kz, \tag{7.1.20}$$

and that its ellipticity evolves along z as shown in Fig. 7.6.

The optical interaction in a lin $\perp$ lin field configuration is found by substituting Eq. (7.1.20) for the field into Eq. (5.3.19) and taking the electric dipole moment of the
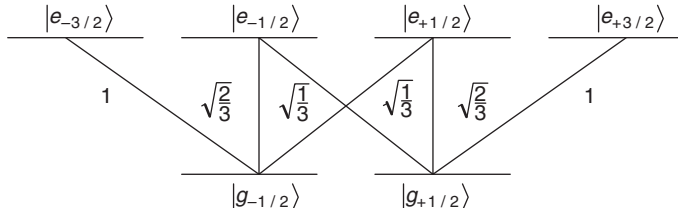
Figure 7.5 *Atomic levels and Clebsch–Gordan (C–G) coefficients for a $J_g = 1/2 \leftrightarrow J_e = 3/2$ transition. Transition probabilities are proportional to the square of the C–G coefficients. See Appendix H.*
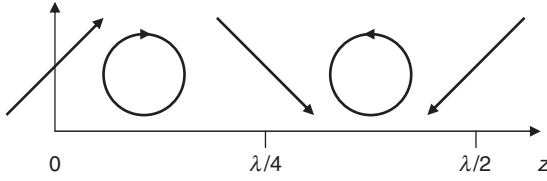
Figure 7.6 *Polarization states of the total optical field in the lin $\perp$ lin configuration.*

transition with a Clebsch–Gordan (C–G) coefficient of unity to be μ_0. Then, we have

$$
V(z,t) = -\frac{1}{\sqrt{2}}\hbar\Omega \sin kz \left[|e_{3/2}\rangle \langle g_{1/2}| + \sqrt{\frac{1}{3}}\, |e_{1/2}\rangle \langle g_{-1/2}| \right] \exp(-i\omega t) + h.c.
$$

$$
-\frac{1}{\sqrt{2}}\hbar\Omega \cos kz \left[|e_{-3/2}\rangle \langle g_{-1/2}| + \sqrt{\frac{1}{3}}\, |e_{-1/2}\rangle \langle g_{1/2}| \right] \exp(-i\omega t) + h.c.,
$$

$$(7.1.21)$$

where $\Omega = \mu_0 E_0/\hbar$, and a shift of origin along z by $\lambda/8$ has been applied to simplify the result. The factor of $\sqrt{2}$ that appears in Eq. (7.1.21) is discussed in Section 7.3.

As before, the average force acting on the atom is given by

$$
\langle F \rangle = \text{Tr}\{F,\rho\} = \text{Tr}\{\overline{\nabla}V,\rho\}
$$

$$
= \frac{\hbar k\Omega}{\sqrt{2}}\cos kz \left[\langle g_{1/2}|\,\tilde{\rho}\,|e_{3/2}\rangle + \sqrt{\frac{1}{3}}\,\langle g_{-1/2}|\,\tilde{\rho}\,|e_{1/2}\rangle + c.c. \right]
$$

$$
-\frac{\hbar k\Omega}{\sqrt{2}}\sin kz \left[\langle g_{-1/2}|\,\tilde{\rho}\,|e_{-3/2}\rangle + \sqrt{\frac{1}{3}}\,\langle g_{1/2}|\,\tilde{\rho}\,|e_{-1/2}\rangle + c.c. \right]. \quad (7.1.22)
$$

If we assume that atomic motion is slow enough not to mix ground state populations established by optical pumping in different locations of the polarization field (Fig. 7.6), we can drop the velocity-dependent term in the transport equations for system coherences. The equations for coherences appearing in Eq. (7.1.22) may then be written as

$$
i\hbar \langle g_{1/2}|\,\dot{\rho}\,|e_{3/2}\rangle = -\hbar(\omega_0 + i\Gamma)\langle g_{1/2}|\,\rho\,|e_{3/2}\rangle + \langle g_{1/2}|\,(V\rho - \rho V)\,|e_{3/2}\rangle, \quad (7.1.23)
$$

$$
i\hbar \langle g_{-1/2}|\,\dot{\rho}\,|e_{1/2}\rangle = -\hbar(\omega_0 + i\Gamma)\langle g_{-1/2}|\,\rho\,|e_{1/2}\rangle + \langle g_{-1/2}|\,(V\rho - \rho V)\,|e_{1/2}\rangle,
$$

$$(7.1.24)$$

$$
i\hbar \langle g_{-1/2}|\,\dot{\rho}\,|e_{-3/2}\rangle = -\hbar(\omega_0 + i\Gamma)\langle g_{-1/2}|\,\rho\,|e_{-3/2}\rangle + \langle g_{-1/2}|\,(V\rho - \rho V)\,|e_{-3/2}\rangle,
$$

$$(7.1.25)$$

$$
i\hbar \langle g_{1/2}|\,\dot{\rho}\,|e_{-1/2}\rangle = -\hbar(\omega_0 + i\Gamma)\langle g_{1/2}|\,\rho\,|e_{-1/2}\rangle + \langle g_{1/2}|\,(V\rho - \rho V)\,|e_{-1/2}\rangle.
$$

$$(7.1.26)$$

Making use of the slowly varying envelope approximation (SVEA), Eqs. (7.1.23)–(7.1.26) become

$$i\hbar\left(\langle g_{1/2}|\,\dot{\tilde{\rho}} - i(\Delta + i\Gamma)\tilde{\rho}\,|e_{3/2}\rangle\right) = -\frac{\hbar\Omega}{\sqrt{2}}\sin kz\,[\langle e_{3/2}|\,\rho\,|e_{3/2}\rangle$$

$$-\langle g_{1/2}|\,\rho\,|g_{1/2}\rangle]$$

$$-\frac{\hbar\Omega}{\sqrt{2}}\cos kz\sqrt{\frac{1}{3}}\,\langle e_{-1/2}|\,\rho\,|e_{3/2}\rangle, \quad (7.1.27)$$

$$i\hbar\left(\langle g_{-1/2}|\,\dot{\tilde{\rho}} - i(\Delta + i\Gamma)\tilde{\rho}\,|e_{1/2}\rangle\right) = -\frac{\hbar\Omega}{\sqrt{2}}\sin kz\sqrt{\frac{1}{3}}\,[\langle e_{1/2}|\,\rho\,|e_{1/2}\rangle$$

$$-\langle g_{-1/2}|\,\rho\,|g_{-1/2}\rangle]$$

$$-\frac{\hbar\Omega}{\sqrt{2}}\cos kz\,\langle e_{-1/2}|\,\rho\,|e_{-3/2}\rangle, \quad (7.1.28)$$

$$i\hbar\left(\langle g_{-1/2}|\,\dot{\tilde{\rho}} - i(\Delta + i\Gamma)\tilde{\rho}\,|e_{-3/2}\rangle\right) = -\frac{\hbar\Omega}{\sqrt{2}}\cos kz\,[\langle e_{-3/2}|\,\rho\,|e_{-3/2}\rangle$$

$$-\langle g_{-1/2}|\,\rho\,|g_{-1/2}\rangle]$$

$$-\frac{\hbar\Omega}{\sqrt{2}}\sin kz\sqrt{\frac{1}{3}}\,\langle e_{-1/2}|\,\rho\,|e_{-3/2}\rangle, \quad (7.1.29)$$

$$i\hbar\left(\langle g_{1/2}|\,\dot{\tilde{\rho}} - i(\Delta + i\Gamma)\tilde{\rho}\,|e_{-1/2}\rangle\right) = -\frac{\hbar\Omega}{\sqrt{2}}\cos kz\sqrt{\frac{1}{3}}\,[\langle e_{-1/2}|\,\rho\,|e_{-1/2}\rangle$$

$$-\langle g_{1/2}|\,\rho\,|g_{1/2}\rangle]$$

$$-\frac{\hbar\Omega}{\sqrt{2}}\sin kz\,\langle e_{3/2}|\,\rho\,|e_{-1/2}\rangle. \quad (7.1.30)$$

Steady-state solutions may be found by setting $\dot{\tilde{\rho}} = 0$. In the low intensity limit (characterized by negligible excited state populations and coherences), one finds

$$\langle g_{1/2}|\,\tilde{\rho}\,|e_{3/2}\rangle = \frac{\Omega}{\sqrt{2}}\frac{1}{\Delta + i\Gamma}\sin kz\,\langle g_{1/2}|\,\rho\,|g_{1/2}\rangle, \quad (7.1.31)$$

$$\langle g_{-1/2}|\,\tilde{\rho}\,|e_{1/2}\rangle = \frac{\Omega}{\sqrt{6}}\frac{1}{\Delta + i\Gamma}\sin kz\,\langle g_{-1/2}|\,\rho\,|g_{-1/2}\rangle, \quad (7.1.32)$$

$$\langle g_{-1/2}|\,\tilde{\rho}\,|e_{-3/2}\rangle = \frac{\Omega}{\sqrt{2}}\frac{1}{\Delta + i\Gamma}\cos kz\,\langle g_{-1/2}|\,\rho\,|g_{-1/2}\rangle, \quad (7.1.33)$$

$$\langle g_{1/2}|\,\tilde{\rho}\,|e_{-1/2}\rangle = \frac{\Omega}{\sqrt{6}}\frac{1}{\Delta + i\Gamma}\cos kz\,\langle g_{1/2}|\,\rho\,|g_{1/2}\rangle. \quad (7.1.34)$$

Substitution of these results into Eq. (7.1.22) for the force leads to

$$\langle F \rangle = \frac{1}{3} \left(\frac{\Omega^2}{\Delta^2 + \Gamma^2} \right) \Delta \hbar k \sin 2kz \left[\langle g_{1/2} | \rho | g_{1/2} \rangle - \langle g_{-1/2} | \rho | g_{-1/2} \rangle \right]. \tag{7.1.35}$$

To complete the evaluation of the force exerted on atoms in this light trap, according to Eq. (7.1.35) we must solve for the (position-dependent) population difference of the two ground state levels. With the compact notation

$$\pi^{(g)}_{\pm 1/2} \equiv \langle g_{\pm 1/2} | \rho | g_{\pm 1/2} \rangle, \tag{7.1.36}$$

$$\pi^{(e)}_{\pm 3/2} \equiv \langle g_{\pm 3/2} | \rho | g_{\pm 3/2} \rangle, \tag{7.1.37}$$

$$\pi^{(e)}_{\pm 1/2} \equiv \langle g_{\pm 1/2} | \rho | g_{\pm 1/2} \rangle, \tag{7.1.38}$$

the ground state population equations may be written as

$$\dot{\pi}^{(g)}_{\pm 1/2} = 2\Gamma \left[\pi^{(e)}_{\pm 3/2} + \frac{2}{3} \pi^{(e)}_{\pm 1/2} + \frac{1}{3} \pi^{(e)}_{\mp 1/2} \right] + \left[\frac{i\Omega}{\sqrt{2}} \sin kz \, \langle e_{\pm 3/2} | \tilde{\rho} | g_{\pm 1/2} \rangle \right.$$

$$\left. + \frac{i\Omega}{\sqrt{6}} \cos kz \, \langle e_{\mp 1/2} | \tilde{\rho} | g_{\pm 1/2} \rangle + c.c. \right]. \tag{7.1.39}$$

This equation makes it evident that the task still remains of determining excited state populations $\pi^{(e)}$. Steady-state values of $\pi^{(e)}_i$ are readily calculated however from the corresponding transport equations:

$$\dot{\pi}^{(e)}_{3/2} = -2\Gamma \pi^{(e)}_{3/2} + \frac{\Omega}{\sqrt{2}} \sin kz \left[i \langle g_{1/2} | \tilde{\rho} | e_{3/2} \rangle + c.c. \right], \tag{7.1.40}$$

$$\dot{\pi}^{(e)}_{1/2} = -2\Gamma \pi^{(e)}_{1/2} + \frac{\Omega}{\sqrt{2}} \sin kz \left[i \sqrt{\frac{1}{3}} \langle g_{-1/2} | \tilde{\rho} | e_{1/2} \rangle + c.c. \right], \tag{7.1.41}$$

$$\dot{\pi}^{(e)}_{-1/2} = -2\Gamma \pi^{(e)}_{-1/2} + \frac{\Omega}{\sqrt{2}} \cos kz \left[i \sqrt{\frac{1}{3}} \langle g_{1/2} | \tilde{\rho} | e_{-1/2} \rangle + c.c. \right], \tag{7.1.42}$$

$$\dot{\pi}^{(e)}_{-3/2} = -2\Gamma \pi^{(e)}_{-3/2} + \frac{\Omega}{\sqrt{2}} \cos kz \left[i \langle g_{-1/2} | \tilde{\rho} | e_{-3/2} \rangle + c.c. \right]. \tag{7.1.43}$$

By inserting the earlier expressions for coherences given by Eqs. (7.1.31)–(7.1.34) into Eqs. (7.1.40)–(7.1.43), the steady-state populations are found to be

$$\pi^{(e)}_{3/2} = \frac{(\Omega^2/2)}{\Delta^2 + \Gamma^2} \pi^{(g)}_{1/2} \sin^2 kz, \tag{7.1.44}$$

$$\pi^{(e)}_{1/2} = \frac{1}{3} \frac{(\Omega^2/2)}{\Delta^2 + \Gamma^2} \pi^{(g)}_{-1/2} \sin^2 kz, \tag{7.1.45}$$

$$\pi^{(e)}_{-1/2} = \frac{1}{3} \frac{(\Omega^2/2)}{\Delta^2 + \Gamma^2} \pi^{(g)}_{1/2} \cos^2 kz, \tag{7.1.46}$$

$$\pi^{(e)}_{-3/2} = \frac{(\Omega^2/2)}{\Delta^2 + \Gamma^2} \pi^{(g)}_{-1/2} \cos^2 kz. \tag{7.1.47}$$
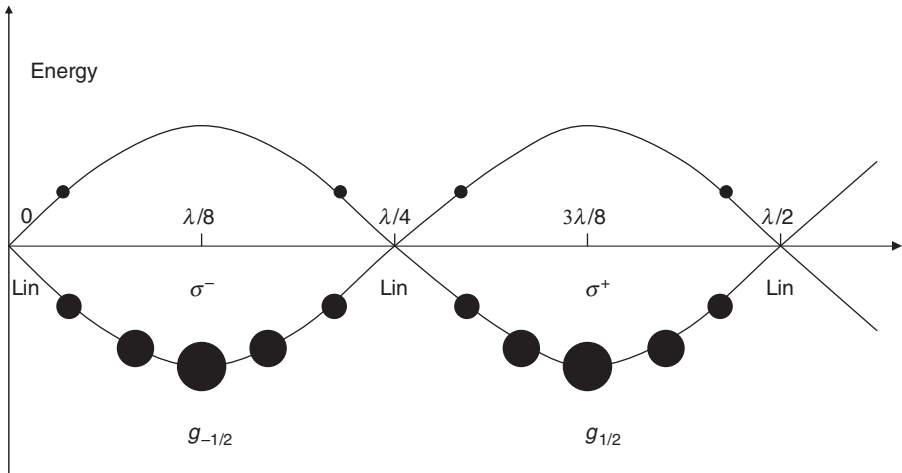
Figure 7.7 *Light-shifted energy levels and steady-state populations (represented by the size of filled circles) in the optical potential of the lin $\perp$ lin configuration for positive detuning Δ. (After [7.13].)*

Finally, by inserting Eqs. (7.1.44)–(7.1.47) and (7.1.31)–(7.1.34) into Eq. (7.1.39), we find

$$\dot{\pi}_{1/2}^{(g)} = -\frac{2\Gamma}{9} \left(\frac{(\Omega^2/2)}{\Delta^2 + \Gamma^2} \right) \left[\pi_{1/2}^{(g)} \cos^2 kz - \pi_{-1/2}^{(g)} \sin^2 kz \right]. \tag{7.1.48}$$

Stationary solutions of Eq. (7.1.48) are

$$\pi_{1/2}^{\text{st}}(z) = \sin^2 kz, \tag{7.1.49}$$

$$\pi_{-1/2}^{\text{st}}(z) = \cos^2 kz, \tag{7.1.50}$$

as shown in Fig. 7.7.

When Eqs. (7.1.49) and (7.1.50) are substituted into Eq. (7.1.35), the force on atoms takes the form

$$\langle F \rangle = \frac{1}{3} \left(\frac{\Omega^2}{\Delta^2 + \Gamma^2} \right) \Delta \hbar k \sin 2kz \left[\sin^2 kz - \cos^2 kz \right], \tag{7.1.51}$$

which averages to zero over a wavelength. However, slowly moving atoms (for which the Doppler shift kv is much smaller than the rate constant

$$\Gamma' = \tau_p^{-1} \equiv \frac{2\Gamma}{9} \frac{(\Omega^2/2)}{\Delta^2 + \Gamma^2}, \tag{7.1.52}$$

in Eq. (7.1.48) alter the populations from the stationary distribution in an important way that yields a large force with a small capture range. As the result of atomic motion over an average (optical pumping) time of τ_p, the population distribution in either ground state decreases by an amount given approximately by

$$\pi_i(z, v) = \pi_i^{\text{st}}(z) - v\tau_p \frac{d}{dz} \pi_i^{\text{st}} + \ldots \tag{7.1.53}$$

This adds a velocity-dependent term to the force, namely

$$\langle F \rangle = -\frac{4}{3} \left(\frac{(\Omega^2/2)}{\Delta^2 + \Gamma^2} \right) \Delta \hbar k^2 v \tau_p \left\langle \sin^2 2kz \right\rangle_\lambda = - \left(3\hbar k^2 \frac{\Delta}{\Gamma} \right) v, \qquad (7.1.54)$$

which damps atomic motion at a rate that is independent of laser power. The lack of a dependence on power clearly distinguishes this (Sisyphus) laser cooling mechanism from Doppler cooling. Other forms of polarization gradient are discussed in Refs. [7.13, 7.14].

7.2 Dark states and population trapping

States that do not interact with light at all often have surprisingly important applications. In the next two subsections, "dark" states are introduced and their central role in yet another approach to laser cooling is investigated.

7.2.1 Velocity-selective coherent population trapping

The creation of coherent superpositions of states can substantially alter the interactions of atoms with light. In this section, it is shown that atoms can exist in states that are deliberately decoupled from electromagnetic fields, where they can neither absorb nor emit radiation but are simply "trapped". Imagine a three-level system in which circularly polarized light establishes a Λ-configuration, as shown in Fig. 7.8. This could be ^{4}He vapor, for example, where $g_\pm$ represents the two Zeeman $m = \pm 1$ sublevels of the 2^3S_1 state and e_0 is the $m = 0$ sublevel of 2^3P_1.

In ^{4}He there is of course another ground state sublevel g_0 with $m = 0$, but the transition to the excited state $2^3P_1(m = 0)$ is forbidden from this sublevel. Its 3-j symbol is zero. Hence, it can be ignored, permitting us to focus on the "family" of states shown in Fig. 7.9.

Exercise: Calculate all the 3-j symbols for transitions shown in Fig. 7.8. Show that the transition $|g_0\rangle \leftrightarrow |e_0\rangle$ has zero transition probability. (See Appendix H.)

We shall refer to this family of three states coupled by absorption and emission as

$$\mathcal{F}(p) = \{|e_0, p\rangle, |g_-, p - \hbar k\rangle, |g_+, p + \hbar k\rangle\}. \qquad (7.2.1)$$
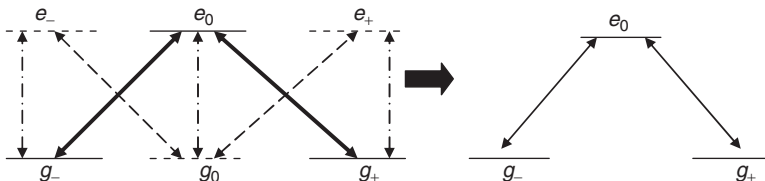
Figure 7.8 *Transitions of a $J = 1 \leftrightarrow J = 1$ system interacting with circularly polarized light beams. The two dashed transitions form a V-system which is not coupled to the Λ-configuration (solid arrows), except through spontaneous emission (dash–dot arrows). Atoms that undergo spontaneous emission contribute to optical pumping, eventually causing all atoms to join the Λ-system.*
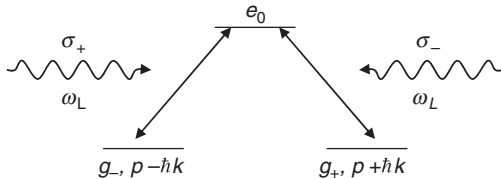
Figure 7.9 *Simplified three-state system that forms a closed family of states interacting only among themselves by absorption and emission processes.*

As long as spontaneous emission and changes of linear momentum are ignored, this is a closed family of states coupled by circularly polarized light. Atoms in the system are taken to be sufficiently cold that the spread in their linear momentum Δp may be much less than the photon momentum $(\Delta p << \hbar k)$. This causes the atoms to become delocalized since the uncertainty in atomic position obeys a relation of the form $\Delta x \geq \hbar/\Delta p$. The atoms cease to be point-like and it is necessary to consider position z to be an operator $(\hat{z})$, whose expectation values will be governed by the de Broglie wave. Under these conditions the displacement operator $\hat{p} = \exp(\pm ik\hat{z})$ for the atomic momentum, which is conjugate to $\hat{z}$, becomes a function of the $\hat{z}$ operator and restricts changes in momentum to units of $\hbar k$.

The structure of the optical field is unimportant for the topic of velocity-selective population trapping. Hence the laser field will be taken to be classical. As usual, the Hamiltonian is considered to be the sum of two parts:

$$H = H_0 + V, \tag{7.2.2}$$

$$H_0 = \frac{p^2}{2m} + \hbar\omega_0 \left|e_0\right\rangle \left\langle e_0\right|. \tag{7.2.3}$$

The ground states $\left|g_+\right\rangle$ and $\left|g_-\right\rangle$ are taken to have the same energy (0), and the field and the interaction to have the forms given previously by Eqs. (5.3.15) and (5.1.1).

Making use of the scalar definitions

$$\Omega_\pm \equiv \frac{\mu_\pm E_\mp}{\hbar}, \tag{7.2.4}$$

$$\mu_\pm = erC_\pm^{(1)}, \tag{7.2.5}$$

and the selection rules

$$\left\langle e_0 \left|\mu_+\right| g_+\right\rangle = \left\langle e_0 \left|\mu_-\right| g_-\right\rangle = 0, \tag{7.2.6}$$

we can write the perturbation as

$$V = -\frac{1}{2} \left[\hbar\Omega_+ \left|e_0\right\rangle \left\langle g_-\right| \exp(ikz) + \hbar\Omega_- \left|e_0\right\rangle \left\langle g_+\right| \exp(-ikz)\right] \exp(-i\omega t) + h.c. \tag{7.2.7}$$

It is important to note that although we shall omit the caret on z, it is to be treated as an *operator* not a continuous variable in Eq. (7.2.7). Hence, $\exp(\pm ikz)$ is a momentum

displacement operator, which can be represented by

$$\exp(\pm ikz) = \sum_p |p\rangle \langle p \mp \hbar k|. \tag{7.2.8}$$

$$V = -\sum_p \frac{1}{2} \left[\hbar\Omega_+ |e_0, p\rangle \langle g_-, p - \hbar k| \right.$$

$$\left. + \hbar\Omega_- |e_0, p\rangle \langle g_+, p + \hbar k| \right] \exp(-i\omega t) + h.c. \tag{7.2.9}$$

From this expression for the interaction Hamiltonian, it is immediately apparent that $|e\rangle \equiv |e_0 p\rangle$ is coupled only to $|g_-, p - \hbar k\rangle$ and $|g_+, p + \hbar k\rangle$ optically. Hence, this interaction can only induce transitions within the family $\mathcal{F}(p)$. For a fixed value of p, the dynamics are fully describable by a closed set of nine equations.

To write out the evolution equations of the set, we make use of the transformations

$$\tilde{\rho}_{e\pm}(p) = \rho_{e\pm} \exp(i\omega t), \tag{7.2.10}$$

$$\tilde{\rho}_{+-}(p) = \rho_{+-}(p), \tag{7.2.11}$$

$$\tilde{\rho}_{ii}(p) = \rho_{ii}(p). \tag{7.2.12}$$

In Eq. (7.2.12) the index i takes on only the values $i = +, -, e$ designating members of the family. Then, the dynamics are completely described by

$$\frac{d}{dt}\tilde{\rho}_{--}(p) = i\frac{\Omega_+^*}{2}\tilde{\rho}_{e-}(p) + c.c., \tag{7.2.13}$$

$$\frac{d}{dt}\tilde{\rho}_{++}(p) = i\frac{\Omega_-^*}{2}\tilde{\rho}_{e+}(p) + c.c., \tag{7.2.14}$$

$$\frac{d}{dt}\tilde{\rho}_{ee}(p) = -\left[i\frac{\Omega_+^*}{2}\tilde{\rho}_{e-}(p) + i\frac{\Omega_-^*}{2}\tilde{\rho}_{e+}(p) \right] + c.c., \tag{7.2.15}$$

$$\frac{d}{dt}\tilde{\rho}_{e+}(p) = i\left(-\Delta - k\frac{p}{M} + \omega_r \right)\tilde{\rho}_{e+}(p)$$

$$+ i\frac{\Omega_+}{2}\left[\tilde{\rho}_{++}(p) - \tilde{\rho}_{ee}(p) \right] + i\frac{\Omega_-}{2}\tilde{\rho}_{-+}(p), \tag{7.2.16}$$

$$\frac{d}{dt}\tilde{\rho}_{e-}(p) = i\left(-\Delta + k\frac{p}{M} + \omega_r \right)\tilde{\rho}_{e-}(p)$$

$$+ i\frac{\Omega_-}{2}\left[\tilde{\rho}_{--}(p) - \tilde{\rho}_{ee}(p) \right] + i\frac{\Omega_+}{2}\tilde{\rho}_{-+}^*(p), \tag{7.2.17}$$

$$\frac{d}{dt}\tilde{\rho}_{-+}(p) = +i\frac{\Omega_-^*}{2}\tilde{\rho}_{e+}(p) - i\frac{\Omega_+}{2}\tilde{\rho}_{e-}^*(p) - 2ik\frac{p}{M}\tilde{\rho}_{-+}(p), \tag{7.2.18}$$

together with three complex-conjugate equations for the remaining off-diagonal elements $\tilde{\rho}_{+e} = \tilde{\rho}_{e+}^*$, $\tilde{\rho}_{-e} = \tilde{\rho}_{e-}^*$, and $\tilde{\rho}_{+-} = \tilde{\rho}_{-+}^*$. In Eqs. (7.2.16) and (7.2.17), we have introduced a "recoil" frequency shift $\omega_r \equiv \hbar k^2/2M$ together with the optical wavevector $k = 2\pi/\lambda$. The shift ω_r is relatively unimportant unless $\Delta p << \hbar k$, which is exactly the range of interest for matter wave mechanics and laser cooling.

The importance of the evolution equations above is that they permit us to analyze how velocity selection can arise during population trapping. For this purpose, consider two special linear combinations of the ground states $|g_+, p + \hbar k\rangle$ and $|g_-, p - \hbar k\rangle$ designated by $|\psi_{\text{NC}}(p)\rangle$ and $|\psi_{\text{C}}(p)\rangle$.

$$|\psi_{\text{NC}}(p)\rangle = \frac{\Omega_-}{\left(|\Omega_+|^2 + |\Omega_-|^2\right)^{1/2}} |g_-, p - \hbar k\rangle$$

$$-\frac{\Omega_+}{\left(|\Omega_+|^2 + |\Omega_-|^2\right)^{1/2}} |g_+, p + \hbar k\rangle \quad (7.2.19)$$

$$|\psi_{\text{C}}(p)\rangle = \frac{\Omega_+^*}{\left(|\Omega_+|^2 + |\Omega_-|^2\right)^{1/2}} |g_-, p - \hbar k\rangle$$

$$+\frac{\Omega_-^*}{\left(|\Omega_+|^2 + |\Omega_-|^2\right)^{1/2}} |g_+, p + \hbar k\rangle . \quad (7.2.20)$$

The first state $|\psi_{\text{NC}}(p)\rangle$ is not coupled radiatively to the excited state $|e_0, p\rangle$ whereas the second state $|\psi_{\text{C}}(p)\rangle$ is.

Exercise: Show that the interaction matrix element of the "non-coupled" state $|\psi_{\text{NC}}\rangle$ vanishes.

$$\langle e_0, p| V |\psi_{\text{NC}}(p)\rangle = 0. \quad (7.2.21)$$

An atom in the non-coupled state $|\psi_{\text{NC}}(p)\rangle$ therefore cannot absorb light and cannot be excited to $|e_0, p\rangle$. On the other hand, the coupled state, represented by $|\psi_{\text{C}}\rangle$, is radiatively coupled to the excited state.

Exercise: Show that the interaction matrix element of the coupled state is nonzero:

$$\langle e_0, p| V |\psi_{\text{C}}(p)\rangle = (\hbar/2) \left(|\Omega_+|^2 + |\Omega_-|^2\right)^{1/2} \exp(-i\omega t). \quad (7.2.22)$$

Of main interest to us here is the evolution of population among the available states. To examine trapping dynamics, we next examine the rate of change of population in the non-coupled state. To do this, the time rate of change of the diagonal density matrix element can be evaluated, giving

$$\frac{d}{dt} \langle \psi_{\text{NC}}(p)| \rho |\psi_{\text{NC}}(p)\rangle = ik\frac{p}{M}\frac{2\Omega_+\Omega_-}{|\Omega_+|^2 + |\Omega_-|^2} \langle \psi_{\text{NC}}(p)| \rho |\psi_{\text{C}}(p)\rangle + c.c. \quad (7.2.23)$$

This result shows that the population in $|\psi_{\text{NC}}(p)\rangle$ changes only if the atoms are moving. If $p = 0$, the right-hand side of the equation above, which is proportional to p, vanishes. So an atom prepared in $|\psi_{\text{NC}}(0)\rangle$ cannot leave this state by free evolution or by the absorption of a photon. Though we have not explicitly considered population change due to spontaneous emission, it is also clear that the atom cannot leave $|\psi_{\text{NC}}(0)\rangle$ by

this process, since $|\psi_{\mathrm{NC}}(0)\rangle$ is a linear combination of two radiatively stable ground states.

Consequently, this situation provides velocity-selective coherent population trapping (VSCPT). If $p \neq 0$, there is a (coherent but non-radiative) coupling proportional to kp/M between $|\psi_{\mathrm{NC}}(p)\rangle$ and $|e_0(p)\rangle$. Although the state $|\psi_{\mathrm{NC}}(p)\rangle$ cannot evolve radiatively by coupling to the excited state, it also cannot be considered a perfect trap when $p \neq 0$. Excitation by the laser can then still take place after an intermediate transition to $|\psi_{\mathrm{C}}(p)\rangle$. The factor p/M on the right side of Eq. (7.2.23) is the atomic velocity in the excited state for the family $\mathcal{F}(p)$. Hence we note that coherent population trapping in $|\psi_{\mathrm{NC}}(p)\rangle$ is velocity-selective, since it happens only for $p = 0$.

Exercise: Calculate the matrix element appearing on the right side of Eq. (7.2.23) to show explicitly that when $p \neq 0$ an intermediate transition takes place from $|\psi_{\mathrm{NC}}(p)\rangle$ to $|\psi_{\mathrm{C}}(p)\rangle$ and leads indirectly to coupling of the "non-coupled" state with the excited state $|e_0(p)\rangle$.

7.2.2   Laser cooling via VSCPT

Dark states and VSCPT can be exploited for laser cooling of atoms by adding two essential ingredients to the discussion of Section 7.2.1. First, a mechanism must exist to couple atoms in families with differing linear momenta (to allow $\mathcal{F}(p) \to \mathcal{F}(0)$). Second, it must be possible to establish the coherent superposition of $|g_+, +\hbar k\rangle$ and $|g_-, -\hbar k\rangle$ that is needed from the outset. That is, a method of producing the non-coupled state $|\psi_{\mathrm{NC}}(0)\rangle$ is needed. Fortunately, these two ingredients are provided by spontaneous emission and optical pumping, respectively.

Consider an atom in the excited state $|e_0(p)\rangle$ of the family $\mathcal{F}(p)$. Such an atom can emit a fluorescence photon in any direction, as indicated in Fig. 7.10. Suppose that the fluorescence photon has a linear momentum u along $\hat{z}$, where u may have a value between $-\hbar k$ and $+\hbar k$. Due to conservation of momentum, the atomic momentum changes by $-u$. Consequently, it makes a transition from $|e_0(p)\rangle$ to either $|g_+, p - u\rangle$ or $|g_-, p - u\rangle$, or a superposition of these two states. Notice that $|g_+, p - u\rangle$ belongs to the family of states $\mathcal{F}(p - u - \hbar k)$, whereas $|g_-, p - u\rangle$ belongs to $\mathcal{F}(p - u + \hbar k)$.
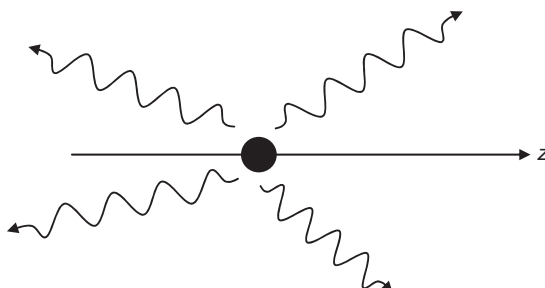
Figure 7.10 *Emission by an atom in the excited state $|e_0(p)\rangle$. The emitted photon directions are arbitrary, so the projection of photon momentum along z has a continuous range between $-\hbar k$ and $+\hbar k$.*
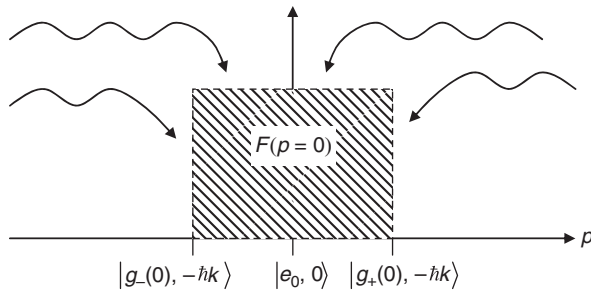
Figure 7.11 *Schematic illustration of the redistribution of atoms among families with different values of linear momentum p, leading to accumulation of low velocity atoms in the $\mathcal{F}(p=0)$ family that occupies the shaded region of the diagram.*

Spontaneous emission therefore provides a mechanism for atoms of one family to be redistributed to another, according to

$$\mathcal{F}(p) \rightarrow \mathcal{F}(p'), \qquad (7.2.24)$$

where

$$p - 2\hbar k \leq p' \leq p + 2\hbar k. \qquad (7.2.25)$$

Notice that the gradual redistribution or "diffusion" of atoms can cause accumulation of atoms in the $\mathcal{F}(p=0)$ family as depicted schematically in Fig. 7.11, provided some of the atoms end up in the $|\psi_{\mathrm{NC}}(0)\rangle$ state.

Notice however that $|\psi_{\mathrm{NC}}(0)\rangle$ is a coherent superposition state. How can such a state be the result of processes involving incoherent dynamics, like spontaneous emission? The answer is that $|\psi_{\mathrm{NC}}(0)\rangle$ is the result of a combination of spontaneous emission followed by a selective filtering process. This process is outlined next.

While atoms that diffuse into ground state $|g_+, \hbar k\rangle$ or $|g_-, -\hbar k\rangle$ are in the $\mathcal{F}(p=0)$ family, they are not yet in the trapping state $|\psi_{\mathrm{NC}}(0)\rangle$. However, the ground state components contain amplitudes from both $|\psi_{\mathrm{NC}}(0)\rangle$ and $|\psi_{\mathrm{C}}(0)\rangle$.

Exercise: Show explicitly that one can write

$$|g_\pm, \pm\hbar k\rangle = \mp\frac{1}{\sqrt{2}}\left[|\psi_{\mathrm{NC}}(0)\rangle \mp |\psi_{\mathrm{C}}(0)\rangle\right]. \qquad (7.2.26)$$

Consequently, in the presence of light, the $|\psi_{\mathrm{C}}(0)\rangle$ component of both $|g_+, \hbar k\rangle$ and $|g_-, -\hbar k\rangle$ becomes involved in new fluorescence cycles, whereas the $|\psi_{\mathrm{NC}}(0)\rangle$ component is stable and does not lead to system excitation. Light actively filters the atomic state in favor of the dark, uncoupled state $|\psi_{\mathrm{NC}}(0)\rangle$.

In summary, "diffusion" of atoms in momentum space causes rapid redistribution of atoms among the available momentum families, including $\mathcal{F}(p=0)$. Once in the $\mathcal{F}(p=0)$ family, atoms undergo a self-filtering process driven by the applied light field that generates a dark state. Cold atoms then remain cold, while others join $\mathcal{F}(p=0)$. Curiously, although the atoms are left in a state in which the average momentum is
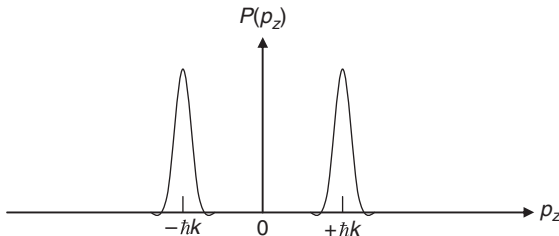
Figure 7.12 *Schematic diagram of the probability distribution of linear momentum mea-surements in a sample of atoms cooled by VSCPT below the recoil limit. (After Ref. [7.54].)*

much less than $\hbar k$, the result of a measurement of p can only be $\pm\hbar k$, since the act of measuring p produces an eigenstate of the linear momentum operator. Since $|\psi_{\mathrm{NC}}(p)\rangle$ is not an eigenstate of operator $\hat{p}$, the result of many measurements of its momentum yields a distribution like that in Fig. 7.12 when the effective temperature descends below the recoil limit.

VSCPT is an effective method for cooling gas samples below the recoil limit. Additional reading can be found in Refs. [7.9, 7.15, 7.54]. The development of such techniques was an important step on the road to achieving Bose–Einstein condensation of neutral atoms [7.16]–[7.18].

7.3   Coherent population transfer

Next we examine the application of three-level coherence to population transfer in a system driven by two fields. The solution to the problem of transferring pop-ulation in the most efficient way from state $|1\rangle$ to $|3\rangle$ of the system depicted in Fig. 7.13 proves to be interesting, because it prescribes a counterintuitive procedure that utilizes adiabatic passage, a process of fundamental importance in quantum mechanics. It also generalizes the concept of coherent population trapping to the case of time-varying fields, since the incident light in this case is a two-color pulsed field.

In this application, a coherent two-photon method is sought to transfer population between levels 1 and 3. There are many reasons why population transfer of this type might be useful. A few are mentioned at the end of the section. The symmetry of the states is assumed to be such that electric dipole transitions are allowed between 1↔2 and 2↔3, but not between 1↔3. That is, $\mu_{13} = 0$. This is essential if the population is to remain in level 3 for any significant period of time after its transfer.

The two applied light fields are assumed to have frequencies close to the transition frequencies ω_{12} and ω_{23}. They are detuned by small amounts (Δ_{12} and Δ_{23}) from their respective one-photon transitions to minimize spontaneous emission losses as shown in Fig. 7.13. An effective Hamiltonian H_{eff} that incorporates both fields using the RWA can be constructed to simplify the search for eigenstates of this problem [7.19]–[7.22]. Here, however we shall proceed by first writing out the exact equations of motion for $\rho(t)$ in terms of the full interaction Hamiltonian $H(t)$ and then proceeding
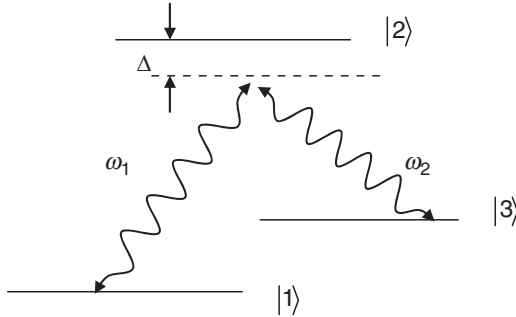
Figure 7.13 *Three-level model for the analysis of coherent population transfer by adiabatic passage.*

to identify a simplified matrix $H_{\text{eff}}(t)$ that reproduces the equations for the slowly varying amplitudes, according to

$$i\hbar\dot{\tilde{\rho}} = [H_{\text{eff}}(t), \tilde{\rho}]. \tag{7.3.1}$$

This procedure will identify the effective Hamiltonian as having the matrix form

$$H_{\text{eff}} = -\frac{1}{2}\hbar \begin{bmatrix} 0 & \Omega_1(t) & 0 \\ \Omega_1(t) & 2\Delta(t) & \Omega_2(t) \\ 0 & \Omega_2(t) & 0 \end{bmatrix}, \tag{7.3.2}$$

where $\Delta(t)$ is the one-photon detuning and $\Omega_n(t) = \mu_n E_n(t)/\hbar$ are the resonant Rabi frequencies of the two fields $(n = 1, 2)$.

The interaction is of the form

$$V(t) = -\frac{1}{2}\left[\mu_{12}E_1 \exp(i\omega_1 t) + c.c.\right] - \frac{1}{2}\left[\mu_{23}E_2 \exp(i\omega_2 t) + c.c.\right] \tag{7.3.3}$$

$$= -\frac{1}{2}\left[\hbar\Omega_1(t) \exp(i\omega_1 t) + c.c.\right] - \frac{1}{2}\left[\hbar\Omega_2(t) \exp(i\omega_2 t) + c.c.\right], \tag{7.3.4}$$

where $\Omega_1(t) \equiv \mu_{12}E_1(t)/\hbar$ and $\Omega_2(t) \equiv \mu_{23}E_2(t)/\hbar$. The equations of motion are therefore

$$i\hbar\dot{\rho}_{11} = -\frac{1}{2}\hbar\Omega_1(t) \exp(i\omega_1 t)\rho_{21} + \frac{1}{2}\rho_{12}\hbar\Omega_1^*(t) \exp(-i\omega_1 t), \tag{7.3.5}$$

$$i\hbar\dot{\rho}_{22} = -\frac{1}{2}\hbar\Omega_1^*(t) \exp(-i\omega_1 t)\rho_{12} + \frac{1}{2}\rho_{21}\hbar\Omega_1(t) \exp(i\omega_1 t)$$

$$= -\frac{1}{2}\hbar\Omega_2(t) \exp(-i\omega_2 t)\rho_{32} + \frac{1}{2}\rho_{23}\hbar\Omega_2^*(t) \exp(i\omega_2 t), \tag{7.3.6}$$

$$i\hbar\dot{\rho}_{33} = -\frac{1}{2}\hbar\Omega_2^*(t) \exp(i\omega_2 t)\rho_{23} + \frac{1}{2}\rho_{32}\hbar\Omega_2(t) \exp(-i\omega_2 t), \tag{7.3.7}$$

$$i\hbar\dot{\rho}_{12} = -\hbar\omega_{12}\rho_{12} - \frac{1}{2}\hbar\Omega_1(t) \exp(i\omega_1 t) (\rho_{22} - \rho_{11}) + \rho_{13}\frac{1}{2}\hbar\Omega_2^*(t) \exp(i\omega_2 t),$$

$$\tag{7.3.8}$$

$$i\hbar\dot\rho_{23} = \hbar\omega_{23}\rho_{23} - \frac{1}{2}\hbar\Omega_{2`}(t)\exp(-i\omega_2 t)(\rho_{33} - \rho_{22}) - \frac{1}{2}\hbar\Omega_{1`}^*(t)\exp(-i\omega_1 t)\rho_{13},$$

$$(7.3.9)$$

$$i\hbar\dot\rho_{13} = -\hbar\omega_{13}\rho_{13} - \frac{1}{2}\hbar\Omega_{1`}\exp(i\omega_1 t)\rho_{23} + \rho_{12}\frac{1}{2}\hbar\Omega_{2`}(t)\exp(-i\omega_2 t). \qquad (7.3.10)$$

These six equations are augmented by three for the remaining (conjugate) coherences $\rho_{21} = \rho_{12}^*$, $\rho_{31} = \rho_{13}^*$, and $\rho_{32} = \rho_{23}^*$. Since the total population may be assumed to be constant, the closure condition $\rho_{11} + \rho_{22} + \rho_{33} = 1$ can be used to reduce the number of independent elements of the density matrix from nine (in a three-level system) to eight. (For an interesting discussion of the relationship between these eight density matrix elements and Gell-Mann's SU(3) generators, isospin, and hypercharge of particle physics, see Ref. [7.23].)

We begin by solving Eqs. (7.3.8–7.3.10) for the steady-state system coherences. Using the SVEA, one can anticipate solutions based on the substitutions

$$\rho_{12} = \tilde\rho_{12}\exp(i\omega_1 t) \rightarrow \dot\rho_{12} = \dot{\tilde\rho}_{12}\exp(i\omega_1 t) + i\omega_1\tilde\rho_{12}\exp(i\omega_1 t), \qquad (7.3.11)$$

$$\rho_{13} = \tilde\rho_{13}\exp(i\omega_{13}t) \rightarrow \dot\rho_{13} = \dot{\tilde\rho}_{13}\exp(i\omega_{13}t) + i\omega_{13}\tilde\rho_{13}\exp(i\omega_{13}t), \qquad (7.3.12)$$

$$\rho_{23} = \tilde\rho_{23}\exp(-i\omega_2 t) \rightarrow \dot\rho_{23} = \dot{\tilde\rho}_{23}\exp(-i\omega_2 t) - i\omega_2\tilde\rho_{23}\exp(-i\omega_2 t), \quad (7.3.13)$$

where $\omega_{13} \equiv \omega_{12} - \omega_{23}$ (and equals $\omega_1 - \omega_2$ at two-photon resonance). Starting with Eq. (7.3.11), this yields

$$i\hbar\left[\dot{\tilde\rho}_{12}\exp(i\omega_1 t) + i\omega_1\tilde\rho_{12}\exp(i\omega_1 t)\right] = -\hbar\omega_{12}\tilde\rho_{12}\exp(i\omega_1 t) +$$

$$-\frac{1}{2}\hbar\Omega_1(t)\exp(i\omega_2 t)\left(\rho_{22}^0 - \rho_{11}^0\right) + \frac{1}{2}\hbar\Omega_2^*(t)\exp(i\omega_2 t)\tilde\rho_{23}\exp(i\omega_{23}t)$$

$$= -\hbar\omega_{12}\tilde\rho_{12}\exp(i\omega_1 t) +$$

$$-\frac{1}{2}\hbar\Omega_1(t)\exp(i\omega_1 t)\left(\rho_{22}^0 - \rho_{11}^0\right) + \frac{1}{2}\hbar\Omega_2^*(t)\tilde\rho_{13}\exp(i\omega_1 t). \qquad (7.3.14)$$

By introducing the definitions

$$\Delta_{12} \equiv \omega_{12} - \omega_1, \qquad (7.3.15)$$

$$\Delta_{23} \equiv \omega_{23} - \omega_2, \qquad (7.3.16)$$

this and subsequent equations of motion for the coherences can be simplified by assuming that the two-photon resonance condition $(\Delta = -\Delta_{12} = \Delta_{23})$ is met.

$$i\hbar\dot{\tilde\rho}_{12} = \hbar\Delta\tilde\rho_{12} - \frac{1}{2}\hbar\Omega_1(t)\left[\rho_{22}^0 - \rho_{11}^0\right] + \frac{1}{2}\hbar\Omega_2^*(t)\tilde\rho_{13},$$

$$\dot{\tilde\rho}_{12} = -i\Delta\tilde\rho_{12} + \frac{1}{2}\Omega_1(t)\left[\rho_{22}^0 - \rho_{11}^0\right] - \frac{1}{2}\hbar\Omega_2^*(t)\tilde\rho_{13}, \qquad (7.3.17)$$

$$i\hbar\left[\dot{\tilde\rho}_{23}\exp(-i\omega_2 t) - i\omega_2\tilde\rho_{23}\exp(-i\omega_2 t)\right] = \hbar\omega_{23}\tilde\rho_{23}\exp(-i\omega_2 t) +$$

$$-\frac{1}{2}\hbar\Omega_2(t)\exp(-i\omega_2 t)\left[\rho_{33}^0 - \rho_{22}^0\right] - \frac{1}{2}\hbar\Omega_1^*(t)\exp(-i\omega_1 t)\tilde{\rho}_{13}\exp(i\omega_{13} t),$$

$$\dot{\tilde{\rho}}_{23} = -i\Delta\tilde{\rho}_{23} + \frac{i}{2}\Omega_2(t)\left[\rho_{33}^0 - \rho_{22}^0\right] + \frac{i}{2}\Omega_1^*(t)\tilde{\rho}_{13}, \tag{7.3.18}$$

$$i\hbar\left[\dot{\tilde{\rho}}_{13}\exp(i\omega_{13} t) + i\omega_{13}\tilde{\rho}_{13}\exp(i\omega_{13} t)\right] = -\hbar\omega_{13}\tilde{\rho}_{13}\exp(i\omega_{13} t) +$$

$$-\frac{1}{2}\hbar\Omega_1(t)\exp(i\omega_1 t)\tilde{\rho}_{23}\exp(-i\omega_2 t) + \frac{1}{2}\hbar\Omega_2(t)\tilde{\rho}_{12}\exp(-i\omega_2 t)\exp(i\omega_1 t),$$

$$\dot{\tilde{\rho}}_{13} = \frac{i}{2}\Omega_1(t)\tilde{\rho}_{23} - \frac{i}{2}\Omega_2(t)\tilde{\rho}_{12}. \tag{7.3.19}$$

Exercise: Show that Eqs. (7.3.5)–(7.3.7) and Eqs. (7.3.17)–(7.3.19) are reproduced by the matrix equation of motion for $\tilde{\rho}$ in terms of the effective Hamiltonian. That is, show that in agreement with Eqs. (7.3.1) and (7.3.2),

$$i\hbar\dot{\tilde{\rho}} = -\frac{\hbar}{2}\begin{bmatrix} 0 & \Omega_1 & 0 \\ \Omega_1 & 2\Delta & \Omega_2 \\ 0 & \Omega_2 & 0 \end{bmatrix}\begin{bmatrix} \rho_{11} & \tilde{\rho}_{12} & \tilde{\rho}_{13} \\ \tilde{\rho}_{21} & \rho_{22} & \tilde{\rho}_{23} \\ \tilde{\rho}_{31} & \tilde{\rho}_{32} & \rho_{33} \end{bmatrix} + \frac{\hbar}{2}\begin{bmatrix} \rho_{11} & \tilde{\rho}_{12} & \tilde{\rho}_{13} \\ \tilde{\rho}_{21} & \rho_{22} & \tilde{\rho}_{23} \\ \tilde{\rho}_{31} & \tilde{\rho}_{32} & \rho_{33} \end{bmatrix}\begin{bmatrix} 0 & \Omega_1 & 0 \\ \Omega_1 & 2\Delta & \Omega_2 \\ 0 & \Omega_2 & 0 \end{bmatrix}.$$

$$\tag{7.3.20}$$

Once the effective Hamiltonian has been identified in appropriate matrix form (see Appendix I for more discussion), it is straightforward to solve for its eigenvalues λ_i and eigenvectors $\overline{W}_i$ by examining the secular equation

$$\left[H_{\text{eff}} - \lambda\overline{\overline{U}}\right]\overline{W} = 0. \tag{7.3.21}$$

In Eq. (7.3.21), the quantity $\overline{\overline{U}}$ is the unit matrix.

Exercise: Show that the three eigenvalues of Eq. (7.3.21) are given by

$$\lambda_1 = 0, \tag{7.3.22}$$

$$\lambda_\pm = \Delta(t) \pm \sqrt{\Delta^2 + \Omega_1^2 + \Omega_2^2}. \tag{7.3.23}$$

By introducing a "mixing" angle defined by

$$\tan\theta(t) \equiv \Omega_1(t)/\Omega_2(t), \tag{7.3.24}$$

it may easily be verified that the eigenvector corresponding to the first eigenvalue in Eq. (7.3.22) is given by

$$|W_1(t)\rangle = \cos\theta(t)\,|1\rangle - \sin\theta(t)\,|3\rangle, \tag{7.3.25}$$

independent of Δ. This particular state vector does not evolve temporally on the timescale set by our choice of interaction reference frame, because its eigenvalue is zero.

Notice that as the ratio of the field amplitudes is varied, the mixing angle $\theta(t)$ changes. $\theta(t)$ goes to the limiting value in which complete transfer of population

occurs from state $|1\rangle$ to state $|3\rangle$ provided the ratio of pulse amplitudes follows the prescription:

$$[\Omega_1(t)/\Omega_2(t)]_{t=-\infty} \to 0, \tag{7.3.26}$$

and

$$[\Omega_1(t)/\Omega_2(t)]_{t=+\infty} \to \infty. \tag{7.3.27}$$

The first limit ensures that the system starts in state $|1\rangle$, since $|\langle 1| \, W_1(t)\rangle|^2_{t=-\infty} = 1$. The second limit ensures that the final state is $|3\rangle$, since $|\langle 3| \, W_1(t)\rangle|^2_{t=+\infty} = 1$. Notice that the limiting values of the mixing angles that are required for complete transfer of population require the second transition to precede the first. Hence, the optimal pulse interaction corresponds to the counterintuitive sequence of pulses illustrated in Fig. 7.14. The prescription for optimal transfer of population seems nonintuitive only because there is initially no population in state 3 to respond in the usual way to the pulse at ω_2. Nevertheless, the system does respond by establishing a coherence at this frequency – a charge oscillation that is not accompanied by an atomic transition – that can mediate a two-photon transition if ground state atoms are excited within the dephasing time of the ω_2 transition.

It is easy to see now that $|W_1(t)\rangle$ is a coherently trapped state even when θ is time-dependent. This stems from the fact that

$$H_{\text{eff}} \, |W_1(t)\rangle = 0, \tag{7.3.28}$$

regardless of the values of t, $\Omega_1(t)$, $\Omega_2(t)$, and $\Delta(t)$. On the basis of the Schrödinger equation, Eq. (7.3.28) can obviously also be written in the form

$$i\hbar \frac{\partial}{\partial t} \, |W_1(t)\rangle = 0, \tag{7.3.29}$$

showing explicitly that, contrary to the notation, the state $|W_1(t)\rangle$ is actually independent of time. The probability amplitude $|W_1\rangle$ is constant.

Moreover, any component of a more general state of the system $\psi(t)$ that has the form of $|W_1(t)\rangle$ is trapped. This is easily shown by projecting the Schrödinger equation
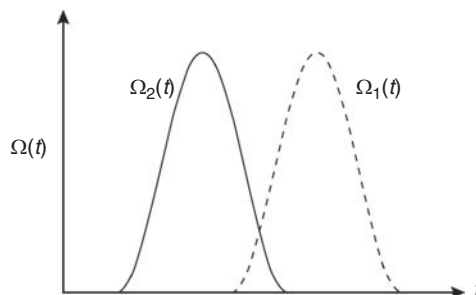
Figure 7.14 *Illustration of a suitable pulse sequence for adiabatic transfer of population from level 1 to 3. Notice that pulse 2 is applied before pulse 1.*

onto state $\langle W_1(t)|$. This procedure yields

$$\langle W_1(t)| \, i\hbar\frac{\partial}{\partial t} \, |\psi(t)\rangle = \langle W_1(t)| \, H_{\text{eff}}(t) \, |\psi(t)\rangle . \qquad (7.3.30)$$

Because $\langle W_1(t)| \, H_{\text{eff}} = 0$, and $|W_1(t)\rangle$ is time-independent according to Eq. (7.3.29), the left side of Eq. (7.3.30) can be written as $i\hbar\partial/\partial t \, \langle W_1(0) \mid \psi(t)\rangle$, and we find

$$\frac{\partial}{\partial t} \, \langle W_1(0) \mid \psi(t)\rangle = 0, \qquad (7.3.31)$$

$$\langle W_1(0) \mid \psi(t)\rangle = \text{constant.} \qquad (7.3.32)$$

To conclude this section, we mention a few applications. Using coherent population transfer, a population inversion of level 3 with respect to level 1 could be produced. If level 3 were a metastable level with no electric dipole moment for transitions to the ground state, this method of transfer would produce optical gain at frequency ω_{13} with minimal losses associated with spontaneous decay of atoms in excited state 2. Also, one can imagine storing a bit of information in the quantum bit (qubit) comprised of the "upper" and "lower" states (states 3 and 1, respectively) of the system. Coherent population transfer is also useful in chemistry in state-selective reactions (see for example Ref. [7.24]). For further discussion of adiabatic passage, see Ref. [7.22].

7.4   Coherent transverse optical magnetism

In other parts of this book, the optical magnetic field was assumed to play a negligible role in light–matter interactions. This may be attributed to the fact that the Lorentz force due to the optical B field is much smaller than the force of E on any charge moving at sub-relativistic speeds ($v << c$, where c is the speed of light in vacuum). For a plane wave in free space this is implied by the small ratio of optical field amplitudes $B/E = 1/c$. Nevertheless, strong magnetic interactions can be induced by light in nominally "nonmagnetic" materials [7.25] at intensities far below the relativistic intensity threshold ($<< 10^{18}\,\text{W/cm}^2$). An example of elastic scattering of intense magnetic dipole radiation at $90°$ from a light beam is shown in Fig. 7.15. In this section, we explore the basis for strong optically induced magnetization that arises from magnetic displacement currents in insulators at moderate intensities.

Transverse optical magnetization relies on a phenomenon known as parametric resonance [7.26], which provides a very effective means of exciting underdamped harmonic oscillators in analytical mechanics. If any parameter determining a parametric resonance is modulated at twice the natural oscillation frequency, it results in large amplitude motion. Moreover as the strength of the driving field is increased, the tuning requirements on the modulation frequency become progressively more and more relaxed. This particular aspect of parametric resonances makes the phenomenon seem very different from ordinary resonances, where an exact tuning requirement must be fulfilled before large amplitude motion will take place. Numerous examples of parametric resonance are known to exist [7.27], even some in mechanical systems
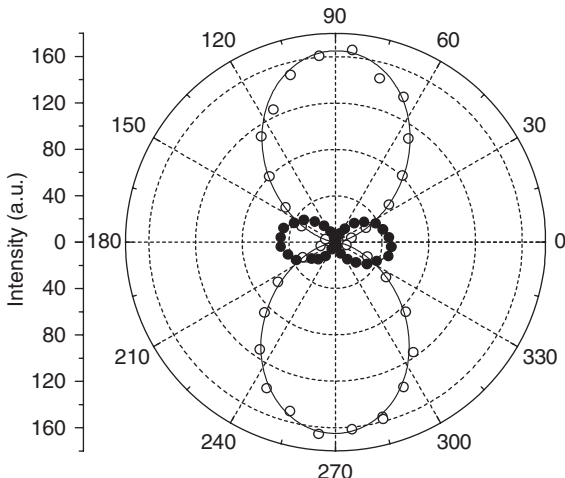
Figure 7.15 *Radiation patterns of scattered light intensity observed in liquid* CCl_4 *[7.25]. Open circles were measured for linear input polarization with the analyzer parallel to the incident electric field at* $10^8 \, W/cm^2$, *whereas filled circles are for an analyzer orientation perpendicular to the electric field. Both sets of data were recorded at a scattering angle of* $90°$.

where the weak forces of light pressure play a role [7.28]. In this section, we show that a more dramatic interplay between electric and magnetic oscillations driven by a magneto-electric coherence can not only induce transverse magnetization at optical frequencies but can do so at relatively modest intensities. In dielectrics, an oscillatory magnetic dipole moment can develop that is as large as the static magnetization in many common ferromagnets.

To analyze the effect of the combined forces of E and B on a charge, consider a two-level system. As usual, the system Hamiltonian $H = H_0 + V(t)$ is assumed to consist of a static part $H_0 = \hbar\omega_1 |1\rangle \langle 1| + \hbar\omega_2 |2\rangle \langle 2|$ which describes the unperturbed eigenstates and an optical interaction $V(t)$ of the form $V(t) = -\overline{\mu}^{(e)} \cdot \overline{E}(t) - \overline{\mu}^{(m)}(t) \cdot \overline{B}(t)$, which allows for dynamic magnetic dipole interactions. The irreducible representations of the (polar) electric and (axial) magnetic components of the optical wave are

$$\overline{E}(t) = -\frac{1}{2}[E_+\hat{\varepsilon}_- + E_-\hat{\varepsilon}_+]e^{i\phi} + c.c., \tag{7.4.1}$$

$$\overline{B}(t) = -\frac{i}{2}[B_+\hat{\varepsilon}_- - B_-\hat{\varepsilon}_+]e^{i\phi} + c.c. \tag{7.4.2}$$

For an introduction to irreducible tensors, which provide a symmetry-based approach to analyzing new problems systematically, see Appendix H. In the expressions above, $\phi \equiv \omega t - kz$ is the optical phase and the circular basis vectors $\hat{\varepsilon}_0 = \hat{z}$ and $\hat{\varepsilon}_\pm = -(\hat{x} \pm i\hat{y})/\sqrt{2}$ are components of the rank one spherical tensor. Linear polarization along $\hat{x}$ corresponds to the choice $E_+ = E_- = E_0/\sqrt{2}$, assuming both circular components contribute to the field interaction.

The irreducible electric and magnetic dipole moments induced by the field have magnitudes and directions given by

$$\overline{\mu}^{(e)} = -(\mu_-^{(e)}\hat{\varepsilon}_+ + \mu_+^{(e)}\hat{\varepsilon}_-), \tag{7.4.3}$$

and

$$\overline{\mu}^{(m)} = -i(\mu_+^{(m)}\hat{\varepsilon}_- - \mu_-^{(m)}\hat{\varepsilon}_+), \tag{7.4.4}$$

respectively. The electric dipole (ED) and magnetic dipole (MD) moments induced by light polarized along $\hat{x}$ have magnitudes $\mu_0^{(e)} = \sqrt{2}\mu_\pm^{(e)}$ and $\mu_0^{(m)} = \sqrt{2}\mu_\pm^{(m)}$, respectively. If we adopt primed coordinates (r', θ', φ') centered on the atom, the vector moments are given explicitly by

$$\langle \overline{\mu}^{(e)}(t) \rangle_{12} = \int dV' \psi_1^*(r', \theta', \varphi', t) e\overline{r}' \psi_2(r', \theta', \varphi', t) + c.c.$$

$$= \hat{r} \langle 1| \mu^{(e)} |2\rangle \rho_{21}(t) + c.c. \tag{7.4.5}$$

and

$$\langle \overline{\mu}^{(m)}(t) \rangle_{12} = (e/2m) \int dV' \psi_1^*(r', \theta', \varphi', t) \overline{r}' \times \overline{p}' \psi_2(r', \theta', \varphi', t) + c.c.$$

$$= (e/2m) \int dV' c_1^*(t) \psi_1^*(r', \theta', \varphi') \overline{L} c_2(t) \psi_2(r', \theta', \varphi') + c.c.. \tag{7.4.6}$$

At low intensities the magnetic moment in Eq. (7.4.6) is negligible for linear polarization, because the linear momentum $\overline{p}'$ of the electron is parallel to its displacement $\overline{r}'$. The cross product in the integrand of Eq. (7.4.6) therefore vanishes, and the magnetic moment is zero. In the case of circular polarization, the electron follows the electric field adiabatically, circulating around the propagation axis in such a way that it induces a magnetic moment oriented along the z-axis (the angular momentum is $\overline{L} = \overline{r}' \times \overline{p}' \neq 0$). Consequently, in one-photon, electric field-mediated interactions, angular momentum carried by the field $E(z, t)$ can be transferred to the atom. The initial and final states $|1\rangle$ and $|2\rangle$ must differ in magnetic quantum number m accordingly ($m_2 = m_1 \pm 1$) to conserve momentum.

In the case of an interaction mediated jointly by the optical E and B fields, the orientation of the magnetic moment is along the y-axis and its calculation is complicated by the presence of two driving forces that contribute to the motion. In this case, the Lorentz force due to the optical B field causes the induced momentum to acquire a component that is azimuthal with respect to the B field. That is, angular momentum develops around the axis of B. Ignoring motion that is not driven by either E or B, we begin by writing the linear momentum operator as $\overline{p}' = \hat{r}'p_{r'} + \hat{\varphi}'p_{\varphi'}$, where the spherical source coordinates r', θ' and φ' are referenced to a polar axis parallel to B ($\hat{z}' = \hat{y}$). The x'-direction is chosen to point along the E field, but the azimuthal angle φ' is measured with respect to $\hat{y}' = -\hat{z}$ rather than $\hat{x}'$. The expression for the

magnetic moment in Eq. (7.4.6) then simplifies to

$$\langle \overline{\mu}^{(m)} \rangle_{12} = (e/2m) \int dV' \psi_1^*(r', \varphi', t) \overline{r}'(t) \times [\overline{p}_{r'} + \overline{p}_{\varphi'}] \psi_2(r', \varphi', t) + c.c.$$

$$= -(e/2m)\hat{y} \int dV' \psi_1^*(r', \theta', \varphi', t) r' p_{\varphi'} \psi_2(r', \theta', \varphi', t) + c.c. \qquad (7.4.7)$$

Under the action of the orthogonal forces due to E and B, the time dependence of radial ($\hat{r}$) and azimuthal ($\hat{\varphi}$) motions may differ. Hence by assuming that the wavefunction is separable, we can introduce expansion coefficients for the radial and angular parts of the wavefunction as follows: $\psi(r', t) = c^{(e)}(t)\psi(r')$ and $\psi(\theta', \varphi', t) = c^{(m)}(t)\psi(\theta', \varphi')$. Correspondingly, we define electric and magnetic density sub-matrices by $\rho_{ij}^{(e)} = c_j^{*(e)} c_i^{(e)}$ and $\rho_{ij}^{(m)} = c_j^{*(m)} c_i^{(m)}$, whereupon the transverse magnetic moment becomes

$$< \overline{\mu}^{(m)} > = -\hat{y}'(e/2m) \langle 1| r' p_{\varphi'} |2 \rangle \rho_{21}^{(m)}(t) \tilde{\rho}_{21}^{(e)} + c.c. \qquad (7.4.8)$$

Accordingly, the expectation value for the transverse magnetic moment is given by

$$< \mu^{(m)} > = \text{Tr} \left\{ \mu^{(m)}, \rho^{(m)}(t) \tilde{\rho}^{(e)} \right\}, \qquad (7.4.9)$$

in the rotating frame. The sub-matrices $\rho^{(m)}(t)$ and $\rho^{(e)}(t)$ are designated as magnetic and electric using superscripts m and e since they describe motions that are azimuthal (with respect to B) and radial (parallel to E), respectively. The full density matrix is just their product. In the lab frame, this is

$$\rho(t) = |\psi\rangle \langle\psi| = |\psi(r)\rangle |\psi(\theta, \varphi, t)\rangle \langle\psi(\theta, \varphi, t)| \langle\psi(r)| = \rho^{(m)}(t)\rho^{(e)}. \qquad (7.4.10)$$

Hence $\rho^{(m)}(t)$ and $\rho^{(e)}(t)$ describe kinematically distinct degrees of freedom in the motion driven by the two applied fields E and B. To calculate the optically induced magnetization, these sub-matrices can be evaluated separately and then combined using Eq. (7.4.10) to find $\rho(t)$.

Calculation of the time dependence of transverse magnetization is challenging. The electric dipole interaction is normally written as $-\overline{\mu}^{(e)} \cdot \overline{E}(t)$, where only $\overline{E}(t)$ depends explicitly on time. This is due to the fact that the induced electric dipole moment is constant in the frame rotating with the electric field. For the magnetic interaction however, the induced charge oscillation along z varies as $\sim e^{2i\omega t}$ in the lab frame and as $\sim e^{i\omega t}$ in the rotating frame. Applying the RWA for the electric interaction, we therefore write $V(t)$ including the magnetic interaction as

$$V(t) = -\frac{\hbar}{2} \left[(\Omega_+^{*(m)} + \Omega_-^{*(m)}) + (\Omega_+^{(e)} + \Omega_+^{(m)} e^{i\varphi})e^{i\varphi} + (\Omega_-^{(e)} + \Omega_-^{(m)} e^{-i\varphi})e^{-i\varphi} \right] + c.c.. \qquad (7.4.11)$$

Here $\Omega_\pm^{(e)} \equiv \mu_\mp^{(e)} E_\pm / \hbar$ and $\Omega_\pm^{(m)} \equiv \mu_\mp^{(m)} B_\pm / \hbar$ are electric and magnetic interaction terms for positive or negative ($\pm$) helicity.

The time dependence of the purely magnetic interaction either adds to or subtracts from that of the purely electric interaction when E and B jointly determine the

dynamics. Consequently, the combined action of E and B produces driving forces at frequencies of $0, \pm 2\omega$. On this basis the off-diagonal element of the full density matrix will have the form

$$\rho_{12}(t) = \tilde{\rho}_{12}^{(m)*}\tilde{\rho}_{12}^{(e)} + \tilde{\rho}_{12}^{(m)}\tilde{\rho}_{12}^{(e)}e^{2i\omega t}. \tag{7.4.12}$$

Once the form and time dependence of the density matrix is established, steady-state solutions for the sub-matrices may be found in the usual way by writing out the two-level system equations of motion, grouping terms with the same frequency dependence, and setting $\dot{\tilde{\rho}}_{12}^{(e)} = \dot{\tilde{\rho}}_{12}^{(m)} = 0$. To include strong field effects in the analysis, the electric field interaction alone is applied in zeroth order, and then both the magnetic and electric interactions are applied as additional perturbations in first order. The results are

$$\rho_{12}^{(e)} = \frac{1}{2}\left\{\frac{[\Omega_+^{(e)} + \Omega_-^{*(e)}]_{12}}{(\Delta_1 + i\Gamma_{12})}e^{i\omega t}\right\}(\rho_{11} - \rho_{22}), \tag{7.4.13}$$

$$\rho_{12}^{(m)} = \frac{1}{2}\left\{\frac{[\Omega_+^{\prime(m)} + \Omega_-^{\prime(m)}]_{12}}{(\omega_0 + i\Gamma_{12}^{(m)})}e^{-i\omega t} + \frac{[\Omega_+^{(m)} + \Omega_-^{*(m)}]_{12}}{(\Delta_2 + i\Gamma_{12}^{(m)})}e^{i\omega t}\right\}\left(\rho_{11}^{(0)} - \rho_{22}^{(0)}\right). \tag{7.4.14}$$

Note that the product $\rho_{12}^{(m)}\rho_{12}^{(e)}$ obtained using the results of Eqs. (7.4.13)–(7.4.14) does have the form anticipated by Eq. (7.4.12). The counter-rotating magnetic amplitudes that give rise to the first term on the right side of (7.4.14) are defined by $\Omega_\pm^{\prime(m)} \equiv \mu_\mp^{(m)}B_\pm^*/\hbar$ and the detuning parameters are $\Delta_1 \equiv \omega_0 - \omega$ and $\Delta_2 \equiv \omega_0 - 2\omega$.

As stated above, the magnetic interaction has been treated as a perturbation to obtain Eq. (7.4.14). Consequently, the population difference equals its initial value, denoted by the superscript 0, and the substitution $\rho_{11}^{(0)} - \rho_{22}^{(0)} \cong 1$ can be made. Population saturation effects due to the electric interaction are nevertheless taken into account through the second application of the electric dipole interaction in first order. The population difference $(\rho_{11} - \rho_{22})$ that appears in Eq. (7.4.14) is then given by

$$\rho_{11} - \rho_{22} = \left[1 + \frac{\Gamma_{12}^{(e)}\left|\Omega_+^{(e)} + \Omega_-^{*(e)}\right|^2}{\gamma_{22}(\Delta_1^2 + \Gamma_{12}^{(e)2})}\right]^{-1}. \tag{7.4.15}$$

The radiant magnetization is found by calculating the trace of the magnetic dipole operator with the full density matrix. In the lab frame, where $\mu_{21}^{(m)} \propto e^{-i\omega t}$, this yields

$$\overline{M} = N\mathrm{Tr}\left\{\overline{\mu}^{(m)}(t), \rho^{(m)}(t)\rho^{(e)}(t)\right\}$$

$$= -(Ne/2m)\hat{y}[\langle 2|\overline{L}_y|1\rangle\,\tilde{\rho}_{12}^{(m)}\tilde{\rho}_{12}^{(e)}e^{i\omega t} + c.c.]. \tag{7.4.16}$$
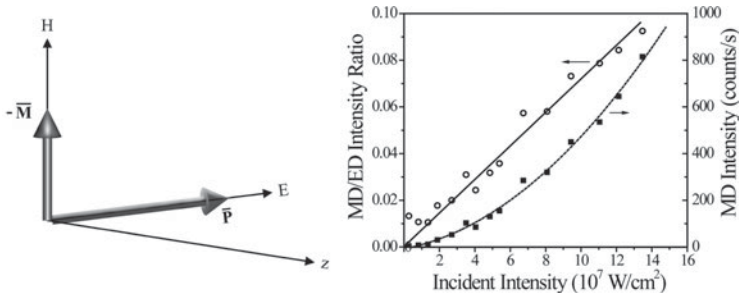
Figure 7.16 *(Left) Directional relationships between the coherent transverse magnetization M and optical polarization P produced by an intense plane wave propagating along the z-axis in a bound electron system. (Right) The intensity of scattered magnetic dipole radiation versus incident intensity in CCl_4 [7.25], together with its ratio with respect to electric dipole scattering.*

According to this result, the magnetic moment induced by light is antiparallel to the optical magnetic field and depends quadratically on the input field amplitudes, as indicated in Fig. 7.16. Notice that although the process giving rise to this magnetization is second order in the field, the magnetic dipole oscillates in the lab frame of reference at the optical frequency ω, not at 2ω.

The magnetization in (7.4.16) is of the form

$$\overline{M} = \frac{1}{2}\tilde{M}e^{i\phi} + h.c., \tag{7.4.17}$$

where the slowly varying amplitude is given by

$$\tilde{M} = -\hat{y}\left(\frac{Ne}{m}\right)\frac{1}{2}\left[\frac{\langle 2|\,L_y\,|1\rangle\,[\Omega_0^{(e)}]_{12}[\Omega_0^{(m)}]_{12}}{(\Delta_1 + i\Gamma_{12}^{(e)})(\Delta_2 + i\Gamma_{12}^{(m)})}\right.$$

$$\left. + \frac{\langle 2|\,L_y\,|1\rangle^*\,[\Omega_0^{*(e)}]_{12}[\Omega_0''^{(m)*}]_{12}}{(\omega_0 - i\Gamma_{12}^{(e)})(\Delta_2 - i\Gamma_{12}^{(m)})}\right](\rho_{11} - \rho_{22}). \tag{7.4.18}$$

This result has been specialized to the case of linear polarization. The field factors are $\Omega_0''^{(m)} = \mu_0^{(m)}B_0^*/\hbar$, $\Omega_0^{(m)} = \mu_0^{(m)}B_0/\hbar$, and $\Omega_0^{(e)} = \mu_0^{(e)}E_0/\hbar$. In the rotating frame, only one circular component of the electric field interaction contributes to $\overline{M}(t)$, whereas both circular components of the magnetic interaction participate. Hence the specific replacement $\Omega_0^{(m)} = [\Omega_+^{(m)} + \Omega_-^{*(m)}]$ has been made for the magnetic term, and $\Omega_0^{(e)} = \frac{1}{2}[\Omega_+^{(e)} + \Omega_-^{*(e)}]$ for the electric term.

The result in Eq. (7.4.18) is not yet consistent with the fact that of all the electrons that can be set in motion by the electric field within a given volume, at most half can contribute to a magnetic moment in the same volume [7.25]. Consequently, the amplitude of the oscillatory magnetization must be corrected by a factor of two with the substitution $L_y \to 2L_y$ before $\tilde{M}$ can be compared directly with the amplitude of electric polarization $\tilde{P}$. Dropping the counter-rotating term of Eq. (7.4.18) which is

small, the final expression for the induced transverse magnetization is

$$\tilde{M} = -\hat{y} \left(\frac{Ne}{m} \right) \left[\frac{\langle 2| L_y |1\rangle [\Omega_0^{(e)}]_{12}[\Omega_0^{(m)}]_{12}}{(\Delta_1 + i\Gamma_{12}^{(e)})(\Delta_2 + i\Gamma_{12}^{(m)})} \right] (\rho_{11} - \rho_{22}). \tag{7.4.19}$$

The induced MD and ED moments therefore have the dimensionless ratio

$$R = \left| \frac{\tilde{M}}{c\tilde{P}} \right| = \left| \left(\frac{e}{mc} \right) \frac{\langle 2| L_y |1\rangle \, \tilde{\rho}_{12}^{(e)} \, \tilde{\rho}_{12}^{(m)}}{\langle 2| ex |1\rangle \, \tilde{\rho}_{12}^{(e)}} \right| = \left| \left(\frac{\langle 2| x(p_z/mc) |1\rangle}{\langle 2| x |1\rangle} \right) \tilde{\rho}_{12}^{(m)} \right|. \tag{7.4.20}$$

The momentum $\langle p_z \rangle$ of charge motion along the z-axis cannot exceed $\langle p_z \rangle = mc$. Consequently, the ratio of matrix elements in parentheses on the right side of Eq. (7.4.20) cannot exceed unity. In addition, the maximum value of the off-diagonal matrix element $\tilde{\rho}_{12}^{(m)}$ is $1/2$ (see Problem 3.6). So the ratio R, which is also the ratio of radiant magnetic and electric susceptibilities, has a maximum value of

$$R_{\max} = 1/2. \tag{7.4.21}$$

On the basis of Eqs. (7.4.16), (7.4.20), and (7.4.21), the radiant magnetic emission *intensity* is predicted to be quadratic with respect to the input intensity, it may be enhanced electronically and parametrically by resonant denominators containing Δ_1 and Δ_2, and it can grow to a value of at most one fourth ($R_{\max}^2 = 1/4$) the electric dipole emission intensity. The quadratic nature of this nonlinear process and the upper limit on magnetic intensity have been verified experimentally [7.25]. Note that to reach the limit of magnetic dipole intensity predicted in Eq. (7.4.21), the momentum of the electron must effectively reach the relativistic limit of $\langle p_z \rangle = mc$ without the benefit of relativistic optical field strengths that can accelerate electrons to the speed of light during each half-cycle. The phenomenon of parametric resonance makes this possible [7.26, 7.27].

For an isolated atom in space, the flux density of the driving field is $B = \mu_0 H$, so the macroscopic magnetic susceptibility may simply be written as N times the free space result.

$$\chi^{(m)} = \frac{\tilde{M}}{H_0} = \left(\frac{-Ne}{2mH_0} \right) \frac{1}{2} \left[\frac{\langle 2| L_y |1\rangle \, \hbar\Omega_0^{(e)} \hbar\Omega_0^{(m)}}{\hbar^2(\Delta_1 + i\Gamma_{12}^{(e)})(\Delta_2 + i\Gamma_{12}^{(m)})} \right] (\rho_{11} - \rho_{22})$$

$$= \left(\frac{-N\mu_0 e^3}{4m^2\hbar^2} \right) \left[\frac{|\langle 2| L_y |1\rangle|^2 \langle 1| x |2\rangle}{(\Delta_1 + i\Gamma_{12}^{(e)})(\Delta_2 + i\Gamma_{12}^{(m)})} \right] (\rho_{11} - \rho_{22}) E_0. \tag{7.4.22}$$

The ratio of magnetic and electric susceptibilities is negative, emphasizing the diamagnetic character of transverse optical magnetization.

$$\frac{\chi^{(m)}(\omega)}{\chi^{(e)}(\omega)} = -\left(\frac{\mu_0 \varepsilon_0 e}{4m^2\hbar} \right) \frac{|\langle 2| L_y |1\rangle|^2 E_0}{\langle 2| x |1\rangle (\Delta_2 + i\Gamma_{12}^{(m)})} = \frac{-1}{\hbar c^2} \frac{|\langle 2| \mu^{(m)} |1\rangle|^2}{\langle 2| ex |1\rangle} \frac{E_0 e^{-i\varphi_{\mathrm{P}}}}{\sqrt{\Delta_2^2 + \Gamma_{12}^{2(m)}}}.$$

$$\tag{7.4.23}$$
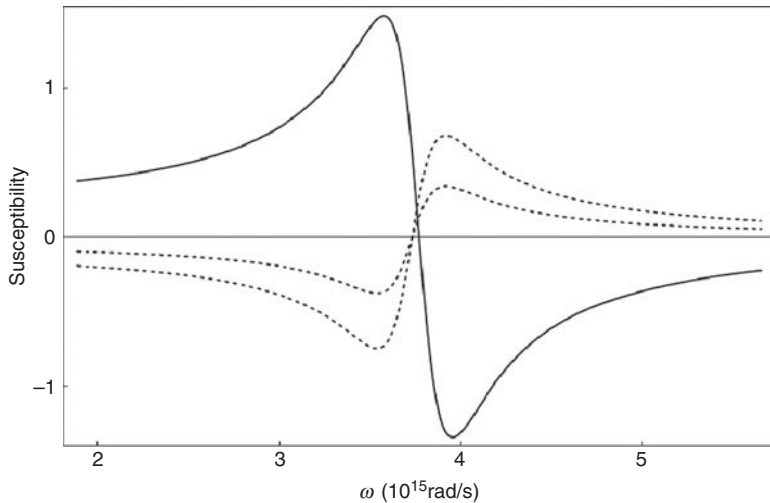
Figure 7.17 *Dispersion of the electric (solid curve) and magnetic (dashed) susceptibilities in the vicinity of a resonance centered at $\lambda_0 = 500$ nm. The parametric linewidth to frequency ratio is assumed to be $\Gamma_{12}^{(m)}/\omega_0 = 0.1$ and the plasma frequency is 2×10^{15} rad/s [7.32].*

The phase angle $\varphi_p \equiv \tan^{-1}(\Gamma_{12}^{(m)}/\Delta_2)$ is very small and cannot lead to an overall sign change in Eq. (7.4.23). Near an electronic resonance, the linewidth $\Gamma_{12}^{(m)}$ of the parametric resonance is much less than the detuning $\Delta_2 = \omega_0 - 2\omega \cong -\omega_0$, so $\varphi_p << \pi/2$. As a result, the susceptibilities $\chi^{(e)}$ and $\chi^{(m)}$ have the general appearance shown in Fig. 7.17. The refractive index $n = \sqrt{(1 + \chi^{(e)})(1 + \chi^{(m)})}$ can be reduced substantially in the vicinity of the resonance region. Modified index materials are of great interest, for applications such as sub-wavelength imaging [7.29] and transformation optics [7.30].

The appearance of the matrix element $\langle 2| L_y |1 \rangle$ in the magnetic susceptibility of Eq. (7.4.22) reflects its transformation as a rotation. However, the magnetic response is also proportional to $\langle 1| x |2 \rangle$. Hence both these matrix elements must be nonzero and the field amplitude in Eq. (7.4.23) large, if the ratio of magnetic to electric susceptibility in Eq. (7.4.23) is to approach unity at sub-relativistic intensities ($<< 10^{18}$ W/cm^2). For this to happen, energy from the motion induced by the electric field along x must be transferred to momentum p_ϕ that is azimuthal with respect to B, via parametric resonance [7.26, 7.27].

A more formal consideration of the role of symmetry in optical magnetism may be based on the Wigner–Eckart theorem. Explicit evaluation of magnetic matrix elements between states of well-defined total initial and final angular momentum l_1 and l_2 yields

$$\left\langle 2 \left| V_{\pm}^{(m)} \right| 1 \right\rangle = (-)^{l_2 - m_2} \frac{1}{2} \left\{ B_{\mp} \left\langle \alpha_2 l_2 m_2 \left\| \mu_{\pm}^{(m)} \right\| \alpha_1 l_1 m_1 \right\rangle + c.c. \right\} \begin{pmatrix} l_2 & 1 & l_1 \\ -m_2 & q & m_1 \end{pmatrix}.$$

$$(7.4.24)$$

MD and ED interaction matrix elements are proportional to the same 3-j symbol that appears on the right side of Eq. (7.4.24). This 3-j symbol describes spin angular momentum that may be contributed by the light field by virtue of its polarization. (Light can also carry orbital angular momentum. See Ref. [7.31], for example.) This 3-j symbol accounts for angular momentum that is quantized along the propagation axis, and is unrelated to the transverse magnetic moment. The induced transverse moment described here oscillates at the optical frequency and always has a value of zero, averaged over times longer than the optical period, for linear polarization ($q = 0$). Both the electric and magnetic dipole transitions then carry no angular momentum with respect to the quantization axis along z. The reduced matrix elements for the MD and ED still differ however, since they transform as rotations and translations, respectively. For simultaneous transitions of both types using linear polarization, the matrix elements of $R(y)$ and x must simultaneously be nonzero. This dictates that $\Delta l = \pm 1$ and $\Delta m = m_2 - m_1 = 0$.

The magneto-electric coherence in Eq. (7.4.12) supports two other novel interactions, in addition to optical magnetization. Both of these additional effects are dipole interactions that emerge from evaluations of *longitudinal* electric polarization contributions.

$$\overline{P}(t) = N\hat{z}(\mu_{21}^{(e)}(t)\rho_{12}^{(m)}(t)\rho_{12}^{(e)} + c.c.). \qquad (7.4.25)$$

The charge oscillations along z take place at a doubled frequency 2ω in the lab frame. Consequently, the electric dipole operator in Eq. (7.4.25) has a time dependence of $\mu_{21}^{(e)}(t) \propto e^{-2i\omega t}$. When combined with the time dependence of the coherence $\rho^{(m)}\rho^{(e)}$, the polarization calculation shows that parametric resonance mediates longitudinal charge separation and z-polarized second harmonic radiation in addition to transverse magnetization.

The combined selection rules associated with the reduced matrix elements of transverse magnetization in Eq. (7.4.20) are satisfied in many point symmetry groups. Hence transverse optical magnetism driven by a combination of the E and B fields of light provides a widely applicable mechanism for altering the constitutive parameter $\mu^{(m)}$ of optical materials as indicated in Fig. 7.17. It also introduces the possibility of nonlinear beam–beam interactions in right-angle geometries that may enable new methods of ultrafast switching. Effective fields of $\approx$1–10 Tesla can be induced in dielectrics and semiconductors (below the bandgap), so it is potentially useful for preserving spin orientation in regions illuminated with light [7.32]. Finally, there are proposals [7.33] to use finely spaced magnetization structures to induce negative refractive index behavior in the propagation of de Broglie waves for atom optics. Coherent optical magnetization clearly provides a novel way of realizing spatially varying magnetism for many applications without permanent magnets or coils.

7.5   Electromagnetically induced transparency

An important manifestation of tri-level coherence is electromagnetically induced transparency (EIT). This phenomenon [7.34, 7.35] provides a way of making opaque
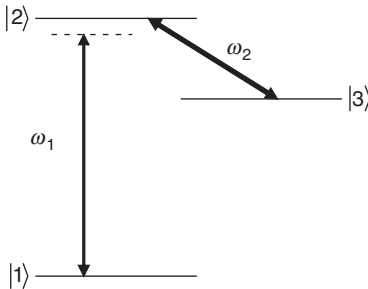
Figure 7.18 *Three-level system subjected to a strong pump wave at $\omega_2 = \omega_{23}$ and probed for absorption at frequency ω_1 in the vicinity of the ground state resonance at frequency ω_{12}.*

media transparent at the very center of an absorption transition where the losses would ordinarily be at their peak. It provides a means of altering the refractive index of optical media and for this reason is of use in nonlinear optics where the objective is generally to arrange for waves of different frequencies to propagate at the same speed so that they can interact coherently and produce waves at new frequencies. Because the transparency in EIT is achieved on resonance, this process also enables maximization of the resonant enhancement of wave-mixing processes, for which it was developed. References to these and other applications are mentioned at the end of this section.

EIT is based on the application of a strong driving field that is transmitted by the material and serves to modulate the energy of the final state of the ground state transition so effectively that absorption of a probe at the original resonant frequency becomes negligible (Fig. 7.18). As usual, we begin by writing down a system Hamiltonian consisting of terms for the unperturbed atom and the optical interaction.

$$H = H_0 + V, \tag{7.5.1}$$

$$H_0 = \hbar\omega_2 \left|2\right\rangle \left\langle2\right| + \hbar\omega_1 \left|1\right\rangle \left\langle1\right| + \hbar\omega_3 \left|3\right\rangle \left\langle3\right|, \tag{7.5.2}$$

$$V = -(\hbar/2)\left[\Omega_1 \exp(i\omega_1 t)\left|2\right\rangle\left\langle1\right| + \Omega_2 \exp(i\omega_2 t)\left|2\right\rangle\left\langle3\right|\right] + h.c.. \tag{7.5.3}$$

The equations of motion for the off-diagonal matrix elements are given by

$$\dot{\rho}_{21} = -(i\omega_{21} + \Gamma_{21})\rho_{21} + \frac{i}{2}\Omega_1^* \exp(-i\omega_1 t)(\rho_{11} - \rho_{22}) + \frac{i}{2}\Omega_2^* \exp(-i\omega_2 t)\rho_{31}, \tag{7.5.4}$$

$$\dot{\rho}_{31} = -(i\omega_{31} + \Gamma_{31})\rho_{31} + \frac{i}{2}\Omega_1^* \exp(-i\omega_1 t)\rho_{32} + \frac{i}{2}\Omega_2 \exp(i\omega_2 t)\rho_{21}, \tag{7.5.5}$$

$$\dot{\rho}_{23} = -(i\omega_{23} + \Gamma_{23})\rho_{23} + \frac{i}{2}\Omega_2^* \exp(-i\omega_2 t)(\rho_{33} - \rho_{22}) + \frac{i}{2}\Omega_1^* \exp(-i\omega_1 t)\rho_{13}. \tag{7.5.6}$$

Because the coherent driving field that couples $|2\rangle$ and $|3\rangle$ is presumed to be both intense and resonant ($\omega_2 = \omega_{23}$), we adopt a procedure which treats the Ω_2 interaction exactly and the Ω_1 interaction as a perturbation. This is similar to the procedure we adopted to analyze optical magnetism in the last section. It focuses on two key coherences, namely ρ_{21} and ρ_{31}, by dropping the second term on the right of Eq. (7.5.5). Since the weak probe wave cannot generate significant coherence between states 1 and 3 before wave 2 acts, this term which provides the only coupling to ρ_{23} may conveniently be ignored.

The initial conditions are assumed to be that the atom resides in the ground state and there is no pre-established coherence in the system:

$$\rho_{11}^{(0)} = 1, \tag{7.5.7}$$

$$\rho_{22}^{(0)} = \rho_{33}^{(0)} = \rho_{32}^{(0)} = 0. \tag{7.5.8}$$

With these assumptions and the substitutions

$$\rho_{21} = \tilde{\rho}_{21} \exp(-i\omega_1 t), \tag{7.5.9}$$

$$\rho_{31} = \tilde{\rho}_{31} \exp[-i(\omega_1 - \omega_2)t], \tag{7.5.10}$$

one finds that the three equations above for coherences in the system reduce to just two:

$$\dot{\tilde{\rho}}_{21} = -\left(\Gamma_{21} + i\Delta\right)\tilde{\rho}_{21} + \frac{i}{2}\Omega_1^* + \frac{i}{2}\Omega_2^*\tilde{\rho}_{31}, \tag{7.5.11}$$

$$\dot{\tilde{\rho}}_{31} = -\left(\Gamma_{31} + i\Delta\right)\tilde{\rho}_{31} + \frac{i}{2}\Omega_2\tilde{\rho}_{21}, \tag{7.5.12}$$

where $\Delta = \omega_{21} - \omega_1$.

Equations (7.5.11) and (7.5.12) may be readily solved in steady state, by setting $\dot{\tilde{\rho}}_{21} = \dot{\tilde{\rho}}_{31} = 0$ as in earlier chapters. The microscopic polarization at the probe frequency is found to be

$$\rho_{21} = \frac{(i\Omega_1^*/2)(\Gamma_{31} + i\Delta)}{\left[(\Gamma_{21} + i\Delta)(\Gamma_{31} + i\Delta) + |\Omega_2|^2/4\right]} \exp(-i\omega_1 t). \tag{7.5.13}$$

For a sample of atomic density N, the macroscopic polarization P is given by

$$P = N\left(\mu_{21}\rho_{12} + \mu_{12}\rho_{21}\right)$$

$$= \frac{(Ni\Omega_1^*/2)(\Gamma_{31} + i\Delta)}{\left[(\Gamma_{21} + i\Delta)(\Gamma_{31} + i\Delta) + |\Omega_2|^2/4\right]} \exp(-i\omega_1 t) + c.c. \tag{7.5.14}$$

P may also be written in terms of the electric susceptibility $\chi = \chi' + i\chi''$ as

$$P = \frac{1}{2}\varepsilon_0 E_1\left[\chi(\omega)e^{-i\omega t} + \chi(-\omega)e^{i\omega t}\right]. \tag{7.5.15}$$

(a)

(b)
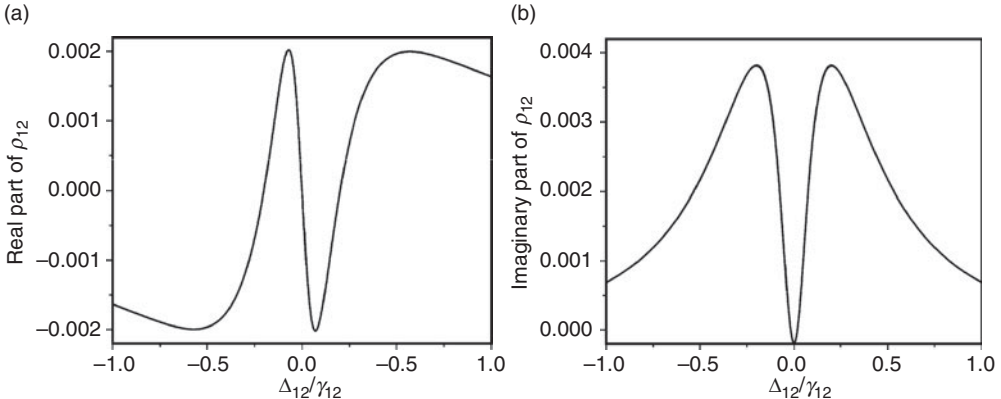
Figure 7.19 *Plots of* (a) *the real part and* (b) *the imaginary part of the polarization versus detuning at probe frequency* ω_1 *in a* Λ-*system that is strongly driven on the second transition at frequency* ω_2. *These curves correspond to the dispersive and absorptive components of the polarization and curve* (b) *shows the induced transparency on resonance.*

To determine the real and imaginary components of the susceptibility, Eqs. (7.4.14) and (7.5.15) must be compared term by term. The results are

$$\chi' = \left(\frac{N |\mu_{21}|^2}{\varepsilon_0 \hbar} \right) \frac{\Delta \left[\Gamma_{31}(\Gamma_{21} + \Gamma_{31}) + (\Delta^2 - \Gamma_{21}\Gamma_{31} - |\Omega_2|^2/4) \right]}{\left(\Delta^2 - \Gamma_{21}\Gamma_{31} - |\Omega_2|^2/4 \right)^2 + \Delta^2 (\Gamma_{21} + \Gamma_{31})^2}, \qquad (7.5.16)$$

$$\chi'' = \left(\frac{N |\mu_{21}|^2}{\varepsilon_0 \hbar} \right) \frac{\left[\Delta^2 (\Gamma_{21} + \Gamma_{31}) - \Gamma_{31} \left(\Delta^2 - \Gamma_{21}\Gamma_{31} - |\Omega_2|^2/4 \right) \right]}{\left(\Delta^2 - \Gamma_{21}\Gamma_{31} - |\Omega_2|^2/4 \right)^2 + \Delta^2 (\Gamma_{21} + \Gamma_{31})^2}. \qquad (7.5.17)$$

A plot of χ'' (see Fig. 7.19) versus detuning reveals that as the result of strong pumping at ω_2 where the sample is always transparent, absorption at the *probe* frequency develops a local minimum at line center ($\Delta = 0$). The residual absorption on resonance is determined by

$$\chi'' = \left(\frac{N |\mu_{21}|^2}{\varepsilon_0 \hbar} \right) \left[\frac{\Gamma_{31}}{\Gamma_{21}\Gamma_{31} + |\Omega_2|^2/4} \right], \qquad (7.5.18)$$

and approaches zero asymptotically when the Rabi frequency Ω_2 exceeds the decay rate $\Gamma_{23} = \sqrt{\Gamma_{21}\Gamma_{31}}$ on the pump transition.

EIT may be understood on the basis of a simple physical picture, presented in Fig. 7.20. The intense coupling laser at frequency ω_2 modulates energy levels 2 and 3, even if there is no population in these levels. Both levels undergo Rabi splitting as shown in the figure. Consequently, the upper level of the probe transition is displaced from its original position. The resonance frequency is displaced, and the absorption at the probe center frequency is greatly reduced. The surprising result is therefore that
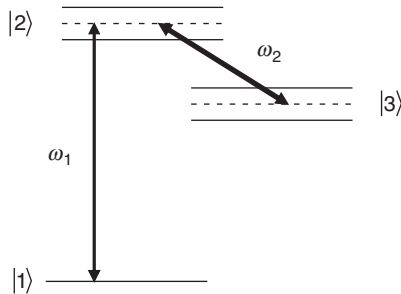
Figure 7.20 *Physical picture of the EIT phenomenon due to Rabi splitting on the strongly driven coupling transition at ω_2.*

both the coupling and probe beams can propagate essentially losslessly through the medium exactly on resonance.

Notice in Fig. 7.19 that the slope of the index profile is very steep at the resonant frequency under EIT conditions. The large dispersion near resonance is useful for changing the speed at which light propagates through the system, in addition to altering its losses. In particular, light can be slowed, stopped, or stored using EIT [7.36]. Usually, we think of the speed of light in a medium as a fixed property which exhibits only small variations with wavelength. For example the group velocity, which is the speed at which information travels through a medium, is completely determined by refractive index properties. It is defined by $v_\mathrm{g} \equiv \partial\omega/\partial k$ and is equal to

$$v_\mathrm{g} = c/(n(\omega) + \omega[\partial n(\omega)/\partial\omega]), \qquad (7.5.19)$$

where c is the speed of light in vacuum. However, in the presence of EIT, for $n > 1$ and $\omega[\partial n(\omega)/\partial\omega] >> 1$, the group velocity is reduced to much less than c. This reduction has now been confirmed in many published experiments and is useful for delay lines in signal processing [7.37].

In avalanche upconversion systems, the dispersion $\partial n/\partial\omega$ of the EIT feature can be reversed [7.38] compared to that in Fig. 7.19a (where, $\partial n/\partial\omega > 0$). Hence so-called superluminal velocities may also be reached through the use of EIT. However, the bandwidth of such effects is so limited as to pertain only to the phase velocity, which is well known to be highly variable. EIT does provide a method for transmitting light through highly absorbing media [7.34], slowing and storing light [7.39], enhancing nonlinear optical interactions [7.35, 7.40], producing low-loss media with high refractive indices [7.41] and enabling lasing without inversion [7.42]. Some of these applications of EIT are discussed in Ref. [7.43]. For electromagnetically induced absorption, see Ref. [7.44].

7.6   Squeezed light

In Chapter 6, the concept of squeezed states was introduced and some of the properties of these special coherent states were examined. Here, the challenge of finding a way to create a squeezed state of an electromagnetic wave is considered, together with possible applications.

To get started, a squeezing operator $\hat{S}$ is identified that can mathematically modify the statistics of the field operators $\hat{a}, \hat{a}^+$ in just the right way to generate a squeezed state of the light field, instead of an ordinary coherent state. After confirming that the squeezing operator works, we shall try to interpret it to identify experimental processes that allow manipulation of light fields in the same way as the squeezing operator.

The squeezing operation affects the noise properties of a system. So it can be anticipated that the operator $\hat{S}$ involves changes in occupation of the modes contributing to the field. Moreover, it should be a nonlinear function of the field creation and annihilation operators, because as we have seen noise is redistributed between quadratures of each cycle of light at the fundamental frequency. To have low losses, the operator should also be unitary.

Consider the operator

$$\hat{S}(z) = \exp\left[\left(z\,\hat{a}^2 - z^*\hat{a}^{+2}\right)/2\right], \tag{7.6.1}$$

where $z = r\exp(-i\theta)$ is referred to as the complex squeeze parameter. Equation (7.6.1) has the form $\hat{S}(z) = \exp(\hat{A})$, where the argument

$$\hat{A} = \left(z\,\hat{a}^2 - z^*\hat{a}^{+2}\right)/2 \tag{7.6.2}$$

is Hermitian. $\hat{S}(z)$ is therefore unitary.

$$\hat{S}^+(z) = \hat{S}^{-1}(z). \tag{7.6.3}$$

The electromagnetic field consists of an expansion in terms of the creation and annihilation operators. If we consider just a single mode, the transformed annihilation operator is

$$\hat{t} \equiv \hat{S}(z)\hat{a}\hat{S}^+(z) = \exp(\hat{A})\hat{a}\exp(-\hat{A})$$

$$= \hat{a} + \left[\hat{A}, \hat{a}\right] + \frac{1}{2!}\left[\hat{A}\left[\hat{A}, \hat{a}\right]\right] + \frac{1}{3!}\left[\hat{A}\left[\hat{A}\left[\hat{A}, \hat{a}\right]\right]\right] + \dots. \tag{7.6.4}$$

Since $[\hat{a}, \hat{a}^+] = 1$, this can rewritten as

$$\hat{t} = \hat{a} + z^*\hat{a}^+ \frac{1}{2!}|z|^2\,\hat{a} + \frac{1}{3!}|z|^2\,z^*\hat{a}^+ + \frac{1}{4!}|z|^4\,\hat{a} + \dots$$

$$= \hat{a}\left(1 + \frac{1}{2!}r^2 + \frac{1}{4!}r^4 + \dots\right) + \hat{a}^+\exp(i\theta)\left(r + \frac{1}{3!}r^3 + \frac{1}{5!}r^5 + \dots\right)$$

$$= \hat{a}\cosh(r) + \hat{a}^+\exp(i\theta)\sinh(r), \tag{7.6.5}$$

$$\hat{t}^+ = \hat{a}^+\cosh(r) + \hat{a}\exp(-i\theta)\sinh(r). \tag{7.6.6}$$

By introducing definitions

$$\mu \equiv \cosh(r), \tag{7.6.7}$$

$$\nu \equiv \exp(i\theta)\sinh(r), \tag{7.6.8}$$

the transformed annihilation operator for a single mode can be written

$$\hat{t} = \mu^*\hat{a} - \nu\hat{a}^+, \tag{7.6.9}$$

where

$$|\mu|^2 - |\nu|^2 = 1. \tag{7.6.10}$$

This operator can be decomposed into quadrature components

$$\hat{t}_1 = \frac{i}{\sqrt{2}} \left(\hat{t}^+ + \hat{t} \right) = \hat{a}_1 \exp(r) \tag{7.6.11}$$

and

$$\hat{t}_2 = \frac{i}{\sqrt{2}} \left(\hat{t}^+ - \hat{t} \right) = \hat{a}_2 \exp(-r). \tag{7.6.12}$$

Exercise: Show that the quadrature operators in Eqs. (7.6.11) and (7.6.12) have a commutator given by

$$[\hat{t}_1, \hat{t}_2] = i/2. \tag{7.6.13}$$

Based on Eqs. (B.19) and (7.6.13), the uncertainty product associated with the quadrature operators $\hat{t}_1$ and $\hat{t}_2$ is

$$\left\langle (\Delta t_1)^2 \right\rangle^{1/2} \left\langle (\Delta t_2)^2 \right\rangle^{1/2} = 1/2. \tag{7.6.14}$$

Any operator for which the standard (root-mean-square) deviation is below the minimum for an ordinary coherent state, namely

$$\left\langle (\Delta t_i)^2 \right\rangle < 1/2, (i = 1, 2) \tag{7.6.15}$$

can generate a squeezed state. Consequently it should be possible for either quadrature $\hat{t}_1$ or $\hat{t}_2$ in Eq. (7.6.14) to exhibit squeezing.

How can light with the squeezed property (Eq. (7.6.14)) be produced experimentally? For guidance on this question, note that application of the squeeze operator $\hat{S}$ to the optical field operator $\hat{a}$ generates a squeezed coherent state operator $\hat{t}$. This suggests that we compare the form of $\hat{S}$ with the interaction Hamiltonians V for various possible optical interactions, particularly nonlinear parametric processes involving the simultaneous creation or annihilation of pairs of photons. The reason for this is that Eq. (7.6.2) contains nonlinear combinations of the field operators not found in the simple one-photon interaction Hamiltonian (Eq. (6.2.10)). So it is natural to search for quadratic processes (or higher-order processes) that have a form like the quadratic operator terms that appear in the argument A of the squeezing operator in Eq. (7.6.2).

A suitable Hamiltonian in this regard is the one for parametric down conversion involving three modes. In this process, an intense pump wave (mode 3) splits into signal and idler waves (modes 1 and 2) via the nonlinear susceptibility $\chi^{(2)}(\omega_3 = \omega_1 + \omega_2)$ of the medium. The interaction destroys one pump photon and creates one photon in each of the modes 1 and 2. The inverse (Hermitian conjugate) process also takes place, giving rise to second harmonic generation. The interaction energy can therefore be written as

$$\hat{V} = - \left[\varepsilon_0 \chi^{(2)} \hat{E}_1^- \hat{E}_2^- \right] \cdot \hat{E}_3^+ + h.c. \tag{7.6.16}$$

For high conversion efficiency, the pump wave is normally intense. Hence it can be treated as a classical wave of amplitude $E_0(Z)$, but moreover we shall assume the undepleted pump approximation [7.45] so that the pump intensity is simply constant. When the parametric process is degenerate ($a_1 = a_2$), and the substitution $f \equiv (-\varepsilon_0 \chi^{(2)}/2V)\sqrt{\omega_1 \omega_2/\varepsilon_1 \varepsilon_2} E_0$ is made to correspond to high pump intensity, Eq. (7.6.16) reduces to

$$\hat{V} = \hbar f[(\hat{a}^+)^2 + (\hat{a})^2]. \tag{7.6.17}$$

Notice that this has the same form as the operator $\hat{A}$ in Eq. (7.6.2) for which squeezed states are the eigenstates. Both parametric down conversion and second harmonic generation can therefore be used to generate squeezed states of light.

Squeezed light offers the means of communicating securely and improving optical interferometry [7.46]. The "quiet" quadrature of squeezed light can be used for example to transmit information at levels below the usual shot-noise limits in communication channels. The precision of interferometric measurements can also be improved when squeezed light is used because noise invariably limits the precision with which fringe positions can be determined. In general, the inherent uncertainty of measurements made using squeezed light can be made less than that of the "unsqueezed" world in which we live. Methods for the production and use of squeezed states of light for applications of various kinds are described or referenced by Mandel and Wolf [7.47].
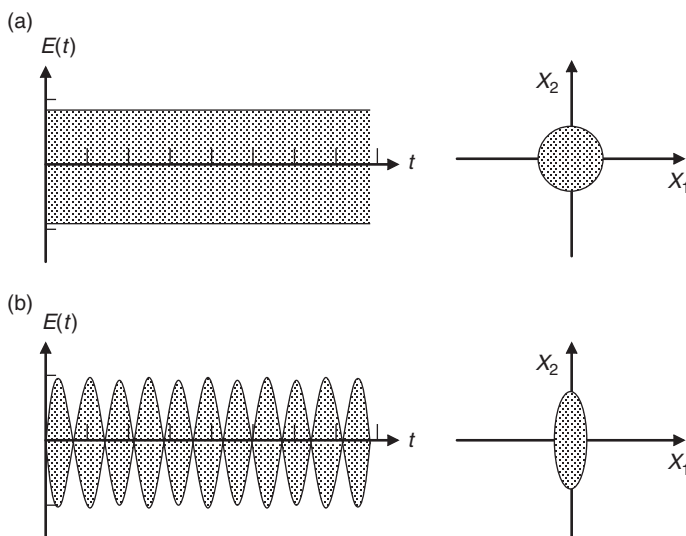
Figure 7.21 *Illustration of the fluctuations of the electric field $E(t)$ of vacuum. (Left) Time dependence of the fluctuations in a single mode of (a) unsqueezed vacuum, and (b) amplitude-squeezed vacuum. (Right) Loci of the tip of the electric field vector at a single point in time for the corresponding cases.*

Finally, we note that squeezing is not limited to states of light. The currents in common electronic components like resistors can be squeezed. Squeezing can also be applied to matter waves – the de Broglie waves associated with particles. Even the fluctuations of modes of the vacuum field can be squeezed as illustrated in Fig. 7.21.

Exercise: Evaluate the squeezed number operator $\hat{t}^{+}\hat{t}$ in the vacuum state $10 >$. (a) Show that $\langle 0| \hat{t}^{+}\hat{t} |0\rangle = \sinh^{2} r$. (b) Is it possible for the squeezed, single-mode vacuum state to contain an average of one photon or more?

7.7   Cavity quantum electrodynamics (QED)

An important example of the quantized reservoir theory of Section 6.3 is provided by the damping of a light field by atoms passing through a single-mode field region in an optical cavity. A reservoir of excitable atoms can damp the field intensity exponentially in the same way that spontaneous emission damps an excited state population. In the three subsections that follow this problem is analyzed first by ignoring spontaneous emission effects, then by including natural decay in the weak atom–field coupling limit, and finally by treating the interesting case of strong atom–field coupling and its effect on spontaneous decay, which is the realm of cavity QED.

7.7.1   Damping of an optical field by two-level atoms

Consider a lossless linear optical cavity, as shown in Fig. 7.22. In the figure, two-level atoms pass through a light field confined to a single cavity mode $|n\rangle$.
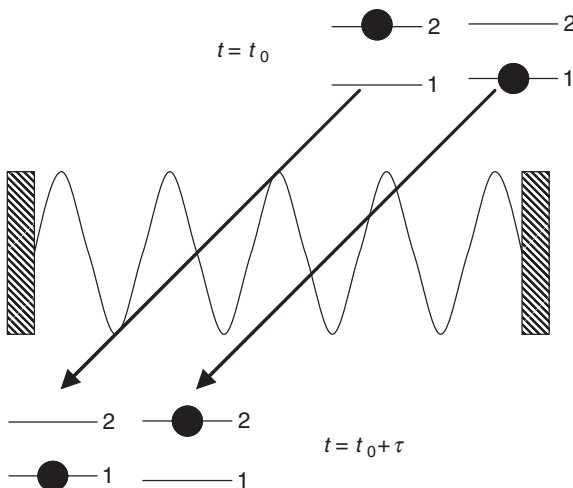
Figure 7.22 *An atomic beam of two-level atoms passing through a single-mode cavity, acting as a reservoir for decay of the optical simple harmonic oscillator.*

They interact with the field through absorption and stimulated emission for a time τ. Spontaneous emission is ignored. The state of the atom will be described by

$$\rho_A = \begin{bmatrix} \rho_{22} & 0 \\ 0 & \rho_{11} \end{bmatrix} \tag{7.7.1}$$

and the state of the field has a density operator

$$\rho_B = |n\rangle \langle n| . \tag{7.7.2}$$

The interaction between the atoms and the field is given by

$$V = \hbar g \begin{bmatrix} 0 & \sigma^+ a^- \exp[-i(\Omega - \omega_0)t] \\ \sigma^- a^+ \exp[+i(\Omega - \omega_0)t] & 0 \end{bmatrix} . \tag{7.7.3}$$

Using the equations of motion derived earlier for the temporal evolution of subsystems A and B, only with A and B interchanged, we write

$$\dot{\rho}_B(t) = -\frac{1}{\hbar^2} \int_{t_0}^{t} dt' \mathrm{Tr}_A [V(t)V(t')\rho_B(t')\rho_A(t_0) - V(t)\rho_B(t')\rho_A(t_0)V(t')] + h.c.$$

$$= -\frac{1}{\hbar^2} \int_{t_0}^{t} dt' \{\exp[-i(\Omega - \omega_0)(t - t')][V_{12}V_{21}\rho_{11}(t_0)\rho_B(t') - V_{12}\rho_{22}(t_0)\rho_B(t')V_{21}]\}$$

$$-\frac{1}{\hbar^2} \int_{t_0}^{t} dt' \{\exp[i(\Omega - \omega_0)(t - t')][V_{12}V_{21}\rho_{22}(t_0)\rho_B(t')$$

$$-V_{12}\rho_{11}(t_0)\rho_B(t')V_{21}]\} + h.c. \tag{7.7.4}$$

On resonance $(\Omega = \omega_0)$ the argument of the exponential function is 0, so that if we ignore the small change that takes place in ρ_B during the short transit time $\tau = t - t_0$ of each atom traveling through the beam, the integration yields

$$\dot{\rho}_B(t) = -g^2\tau[(a^+a\rho_B - a\rho_B a^+)\rho_{11} + (\rho_B aa^+ - a^+\rho_B a)\rho_{22}] + h.c. \tag{7.7.5}$$

If atoms pass through the beam at a rate r, the number of atoms in the beam at any time is $r\tau$. By identifying the absorption and emission rates per photon as $R_1 = 2r\tau^2 g^2 \rho_{11}$ and $R_2 = 2r\tau^2 g^2 \rho_{22}$, respectively, the equation of motion for decay of the intensity in the cavity mode becomes

$$\dot{\rho}_B(t) = -\frac{R_1}{2}[a^+a\rho_B(t) - a\rho_B(t)a^+] - \frac{R_2}{2}[\rho_B(t)aa^+ - a^+\rho_B(t)a] + h.c. \tag{7.7.6}$$

This result has the same form as the equation for atomic decay through coupling to a reservoir of simple harmonic oscillators. Hence it is not surprising that when one evaluates the rate of change of the probability that the mode contains n photons, we

find a similar result:

$$\langle n| \dot{\rho}_B(t) |n\rangle = -\frac{R_1}{2}[\langle n| a^+ a \rho_B(t) |n\rangle - \langle n| a\rho_B(t)a^+ |n\rangle]$$

$$-\frac{R_2}{2}[\langle n| \rho_B(t)aa^+ |n\rangle - \langle n| a^+ \rho_B(t)a |n\rangle] + h.c.$$

$$= -\frac{R_1}{2}[n \langle n| \rho_B |n\rangle - (n+1) \langle n+1| \rho_B |n+1\rangle]$$

$$-\frac{R_2}{2}[(n+1) \langle n+1| \rho_B |n+1\rangle - n \langle n| \rho_B |n\rangle] + h.c.$$

$$= -R_1[n \langle n| \rho_B |n\rangle - (n+1) \langle n+1| \rho_B |n+1\rangle]$$

$$-R_2[(n+1) \langle n+1| \rho_B |n+1\rangle - n \langle n| \rho_B |n\rangle]. \qquad (7.7.7)$$

The occupation of the cavity mode evidently depends on the balance between absorption of cavity photons by ground state atoms and stimulated emission into the cavity mode by excited atoms passing through the beam. For example, if there are no excited atoms passing through the beam ($R_2 = 0$), then exponential decay of the intensity will ensue. This can be seen by substituting $\rho_B = |n\rangle \langle n|$ in the equation above, whereupon one finds that the total number of photons in the beam is governed by the equation $\dot{n}(t) = (-R_1 + R_2)n(t)$ with the solution

$$n(t) = n(0) \exp[(-R_1 + R_2)t]. \qquad (7.7.8)$$

7.7.2   Weak coupling regime

Real atom–cavity interactions must take into account losses from spontaneous emission by atoms in the cavity, and loss of photons from the cavity mode through scattering or finite reflectivity of the mirrors, as well as the strength g of atom–cavity coupling (Fig. 7.23). Here we consider both types of loss explicitly in the weak coupling limit.

First, recall that in the presence of dissipation (through coupling of the system to a reservoir) the equation of motion separates into a Hermitian portion that depends on the Hamiltonian and a non-Hermitian part $L(\rho)$ that describes the relaxation. The
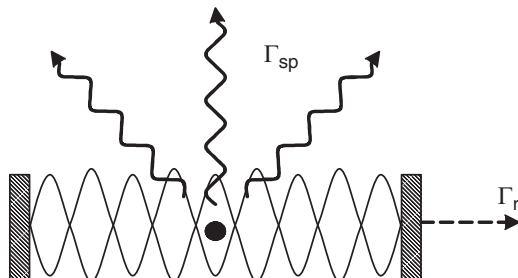
Figure 7.23 *A stationary atom interacting with photons in a cavity. Losses due to spontaneous emission and finite mirror transmission occur with loss rates of* Γ_{sp} *and* Γ_r, *respectively.*

quantum relaxation term was considered in Section 6.6, and must be of the so-called Lindblad form

$$L(\rho) = -\frac{1}{2}\sum_i (\hat{A}_i^+ \hat{A}_i \rho + \rho \hat{A}_i^+ \hat{A}_i) + \sum_i \hat{A}_i \rho \hat{A}_i^+, \tag{7.7.9}$$

if the description is to preserve trace ($\mathrm{Tr}(\rho) = 1$). The last term in $L(\rho)$, called the quantum jump Liouvillian, is discussed further at the end of this section.

In a coupled atom–cavity system, there are two additive sources of loss. We treat both as couplings to thermal reservoirs, modeled as before as continua of simple harmonic oscillators. Using the Markoff approximation, the equation of motion for the reduced matrix element of the atom–cavity system becomes

$$\dot{\rho} = -\frac{i}{\hbar}[H_0, \rho] - \frac{i}{\hbar}[V, \rho] - \frac{1}{2}\hbar\Gamma_{sp}[(\sigma^+\sigma^-\rho - \sigma^-\rho\sigma^+) + h.c.]$$
$$-\frac{1}{2}\hbar\Gamma_r[(a^+a^-\rho - a^-\rho a^+) + h.c.] \tag{7.7.10}$$

The interaction Hamiltonian is given by

$$V = \hbar g[a^+\sigma^- \exp(i\Omega_c t) + h.c.], \tag{7.7.11}$$

where Ω_c is the cavity mode resonant frequency. Now, we choose a particularly simple set of states with which to explore the dynamics.

If there is initially only one excitation in the system, there are exactly three states to consider. Two of the available $|atom, field\rangle$ product states are the "one-quantum" states $|2\rangle \equiv |2, 0\rangle$ and $|1\rangle \equiv |1, 1\rangle$ that are directly coupled by the driving field interaction. The third state $|0\rangle \equiv |1, 0\rangle$ results from the irreversible loss of a photon through the mirror, and is coupled to $|1\rangle \equiv |1, 1\rangle$ by loss of cavity photons through the mirrors and to $|2\rangle \equiv |2, 0\rangle$ by spontaneous emission.

Exercise: Show from Eq. (7.7.10) that the equations of motion are

$$i\hbar\dot{\rho}_{00} = i\hbar\Gamma_r\rho_{11} + i\hbar\Gamma_{sp}\rho_{22} \tag{7.7.12}$$

$$i\hbar\dot{\rho}_{11} = V_{12}\rho_{21} - \rho_{12}V_{21} - i\hbar\Gamma_r\rho_{11}, \tag{7.7.13}$$

$$i\hbar\dot{\rho}_{22} = -V_{12}\rho_{21} + \rho_{12}V_{21} - i\hbar\Gamma_{sp}\rho_{22}, \tag{7.7.14}$$

$$i\hbar\dot{\rho}_{12} = -\hbar\omega_0\rho_{12} + V_{12}(\rho_{22} - \rho_{11}) - (i\hbar/2)(\Gamma_{sp} + \Gamma_r)\rho_{12}. \tag{7.7.15}$$

We proceed to solve these equations by choosing the coherence judiciously to be

$$\rho_{12}(t) = \tilde{\rho}_{12} \exp(i\Omega_c t), \tag{7.7.16}$$

whereupon the time derivative becomes

$$\dot{\rho}_{12}(t) = \dot{\tilde{\rho}}_{12} \exp(i\Omega_c t) + i\Omega_c\tilde{\rho}_{12} \exp(i\Omega_c t). \tag{7.7.17}$$

Substituting Eq. (7.7.17) into Eq. (7.7.15), one finds

$$i\hbar\dot{\tilde{\rho}}_{12} = -\hbar\Delta\tilde{\rho}_{12} + \tilde{V}_{12}(\rho_{22} - \rho_{11}) - (i\hbar/2)(\Gamma_{sp} + \Gamma_r)\tilde{\rho}_{12}, \tag{7.7.18}$$

where $\Delta \equiv \omega_0 - \Omega_c$. In order to integrate (7.7.18) it is helpful to introduce an integrating factor via the substitution $\tilde{\rho}_{12} = \rho'_{12} \exp(i\Delta - \Gamma_\phi)t$, where $\Gamma_\varphi \equiv (\Gamma_{sp} + \Gamma_r)/2$. Eq. (7.7.18) then becomes

$$\dot{\rho}'_{12} \exp(i\Delta - \Gamma_\phi)t = -ig(\rho_{22} - \rho_{11}), \tag{7.7.19}$$

since $\tilde{V}_{12} = \hbar g$. Formal integration yeilds

$$\rho'_{12}(t) = -ig \int_0^t [\rho_{22}(t') - \rho_{11}(t')] \exp\left[-(i\Delta' - \Gamma_\phi)t'\right] dt'. \tag{7.7.20}$$

Next consider the "bad" cavity limit of Eq. (7.7.20) in which $\Gamma_r \gg g, \Gamma_{sp}$. Assume that the populations are slowly-varying for times $t \gg \Gamma_r^{-1}$, and that the ground state population remains low because of rapid decay to the reservoir. Then the population difference can be removed from the integral.

$$\rho'_{12}(t) = -ig \left(\rho_{22}(t) - \rho_{11}(t)\right) \int_0^t \exp\left[-\left(i\Delta - \frac{1}{2}\Gamma_r\right)t'\right] dt' \tag{7.7.21}$$

Then, for times longer than the inverse cavity loss rate ($t \gg \Gamma_r^{-1}$) the integral can easily be evaluated.

$$\rho'_{12}(t) = \left(\frac{g}{\Delta + i\Gamma_r/2}\right) \left(\rho_{22}(t) - \rho_{11}(t)\right). \tag{7.7.22}$$

Equations for the populations can be obtained by substituting Eq. (7.7.22) into Eqs. (7.7.13) and (7.7.14). The substitution yields

$$\dot{\rho}_{11} = g^2 \left[\frac{1}{-i\Delta + \Gamma_r/2} + c.c.\right] (\rho_{11} - \rho_{22}) - \Gamma_r \rho_{11}, \tag{7.7.23}$$

$$\dot{\rho}_{22} = -g^2 \left[\frac{1}{-i\Delta + \Gamma_r/2} + c.c.\right] (\rho_{11} - \rho_{22}) - \Gamma_{sp} \rho_{22}. \tag{7.7.24}$$

We now assume there are solutions of the form

$$\rho_{22}(t) = \rho_2(0) \exp\left[(\alpha + \alpha^*)t\right], \tag{7.7.25}$$

and

$$\rho_{11}(t) = \rho_1(0) \exp\left[(\beta + \beta^*)t\right], \tag{7.7.26}$$

in view of the presence of complex conjugates in the equations of motion for ρ_{11} and ρ_{22}.

Finally, substitution of Eqs. (7.7.25) and (7.7.26) into (7.7.24) immediately furnishes an expression for the decay constant of the excited state.

$$\alpha = -\frac{g^2(i\Delta + \Gamma_r/2)}{\Delta^2 + (\Gamma_r/2)^2} - \Gamma_{sp}. \tag{7.7.27}$$

So the excited state of the atom decays exponentially, according to

$$\rho_{22}(t) = \exp[(\alpha + \alpha^*)t], \tag{7.7.28}$$

with a decay rate modified by the properties of the cavity as specified by Eq. (7.7.27). This solution corresponds to the weak coupling limit in which the cavity modifies the decay rate, but does not qualitatively change the dynamics, because it has a low quality factor. When the atom–field coupling increases, the dynamics do change qualitatively however, as shown in the next section.

7.7.3 Strong coupling regime

Equation (7.7.27) is not the most general solution to the equation of motion of the coupled atom-field problem. In the earlier treatment of weak coupling, the population in the lower state was assumed to decay rapidly to the reservoir, so that ρ_{11} played little role in the solution of Eq.(7.7.20). An exact approach must recognize that strong atom-cavity interaction leads to strong coupling of the ground and excited state that manifests itself as a splitting of modes at resonance, in a manner reminiscent of the Rabi splitting of atomic emission in resonance fluorescence. This is the strong coupling regime of cavity QED [7.48].

Unlike the situation in the "bad" cavity limit of the last section, the ground state plays an important role when $g \gg \Gamma_r, \Gamma_{sp}$. Then, according to Eqs. (7.7.13) and (7.7.14), both $\rho_{11}(t)$ and $\rho_{22}(t)$ are dominated by the coherences $\rho_{12} = c_1^* c_2$ and $\rho_{21} = c_1 c_2^*$. Since a photon is present only when the atom is in the ground state, we anticipate that only two complex frequencies α_+ and α_- will determine the time development of the system. Combination frequencies $\alpha_+^* + \alpha_-$ and $\alpha_+ + \alpha_-^*$ will govern the evolution of $\rho_{12} = c_1^* c_2$ and $\rho_{12} = c_1^* c_2$ and thereby contribute to the evolution of diagonal elements of the density matrix. As a consequence, the general form of the populations become

$$\rho_{22}(t) = \rho_{2a} e^{(\alpha_+ + \alpha_+^*)t} + \rho_{2b} e^{(\alpha_+ + \alpha_-^*)t} + \rho_{2b}^* e^{(\alpha_+^* + \alpha_-)t} + \rho_{2c} e^{(\alpha_- + \alpha_-^*)t}, \tag{7.7.29}$$

$$\rho_{11}(t) = \rho_{1a} e^{(\alpha_+ + \alpha_+^*)t} + \rho_{1b} e^{(\alpha_+ + \alpha_-^*)t} + \rho_{1b}^* e^{(\alpha_+^* + \alpha_-)t} + \rho_{1c} e^{(\alpha_- + \alpha_-^*)t}. \tag{7.7.30}$$

In principle, we could proceed to analyze strong coupling by finding ρ_{12}' with the use of an exact evaluation of Eq. (7.7.20), rather than the earlier approximation. This can be done by inserting (7.7.29) and (7.7.30) into Eq. (7.7.20) prior to performing the integration. However this approach leads to cubic equations for the exponents. So it is preferable to proceed in a much simpler way by solving the equations of motion for the probability amplitudes themselves that compose the density matrix elements. These equations are

$$\dot{C}_2(t) = -(\Gamma_{sp}/2)C_2(t) - igC_1(t), \tag{7.7.31}$$

$$\dot{C}_1(t) = (i\Delta - \Gamma_r/2)C_1(t) - igC_2(t). \tag{7.7.32}$$

Just like the populations, the amplitudes $C_2(t)$ and $C_1(t)$ will evolve with two complex frequencies α_+ and α_-. Hence they are assumed to have the forms

$$C_2(t) = C_{2+} \exp(\alpha_+ t) + C_{2-} \exp(\alpha_- t), \tag{7.7.33}$$

and

$$C_1(t) = C_{1+} \exp(\alpha_+ t) + C_{1-} \exp(\alpha_- t). \tag{7.7.34}$$

Upon substitution of (7.7.33) and (7.7.34) into Eqs. (7.7.31) and (7.7.32) and the collection of terms in $\exp(\alpha_+ t)$ or $\exp(\alpha_- t)$, the differential equations for the amplitudes reduce to coupled algebraic equations.

$$[\alpha_\pm + (\Gamma_{sp}/2)]C_{2\pm} = -igC_{1\pm}, \tag{7.7.35}$$

$$[\alpha_\pm - i\Delta + (\Gamma_r/2)]C_{1\pm} = -igC_{2\pm}. \tag{7.7.36}$$

These are readily solved to give

$$\alpha_\pm = -\frac{1}{2}(\Gamma_\phi - i\Delta) \pm \frac{1}{2}\sqrt{(\Gamma_\phi - i\Delta)^2 - 4(g^2 - \frac{1}{2}i\Delta\Gamma_{sp} + \frac{1}{4}\Gamma_r\Gamma_{sp})}. \tag{7.7.37}$$

Applying the conditions of the strong coupling limit $(g >> \Gamma_r, \Gamma_{sp})$ this result reduces to

$$\alpha_\pm = -\frac{1}{2}(\Gamma_\phi - i\Delta) \pm ig. \tag{7.7.38}$$

In the strong coupling regime the decay of the atom develops Rabi-like oscillations. Any photon emitted into the cavity mode in this "good" cavity limit is likely to be reabsorbed by the atom before exiting the cavity. The atom is therefore driven by its own emission in this limit, and exhibits the behavior shown in Fig.7.24, referred to as vacuum Rabi oscillations. The absorption of a probe wave shows only two transitions however, split by the vacuum Rabi frequency 2g. The three distinguishable transition frequencies of our earlier dressed atom picture of the resonance fluorescence of atoms are not observed, because in the present case only the ground state has a photon present that can dress the atom.

As the cavity is tuned through resonance, the Rabi sidebands in a probe absorption spectrum exchange intensity. First one and then principally the other transition is excited (Fig. 7.25). For large positive detunings, the symmetric dressed state has the character of bare state $|1,1\rangle$ and an energy like that of the bare excited atom. Hence it is "atom-like". The character of the anti-symmetric state is primarily that of $|2,0\rangle$ and it has an energy determined by the cavity frequency. It is therefore deemed "cavity-like". As the detuning is varied from positive to negative, these states evolve from mostly atom-like to mostly cavity-like, and vice versa, as one can show with dressed state analysis. At zero detuning, where the atom-field interaction is strongest because of cavity enhancement, the transitions have mixed character and undergo an avoided crossing. The intensity exchange through the avoided crossing region is a signature of the strong coupling regime of cavity QED.

Superposition states, including those of cavity QED, are important in the field of quantum information science. They are the basis for quantum computational speedup proposals, quantum encryption, and secure quantum communication [7.48]. When it is possible to separate the components of superposition states physically
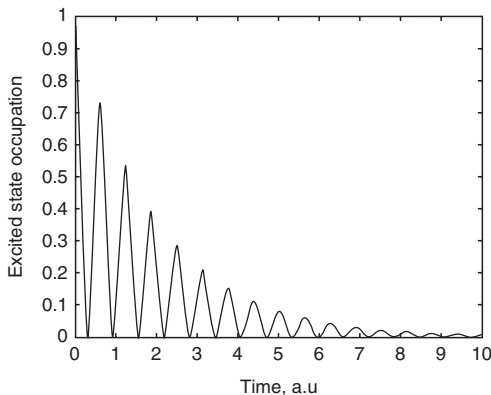
Figure 7.24 *Oscillations in the excited state population decay of an atom interacting with a resonant cavity in the strong coupling regime. Since electric field fluctuations of the vacuum induce spontaneous emission, these are called vacuum Rabi oscillations. The envelope of these oscillations corresponds to the exponential decay encountered in the weak coupling regime. Parameter values are:* $\Gamma_\phi = 0.25, g = 5,$ *and* $\Delta = 0$.
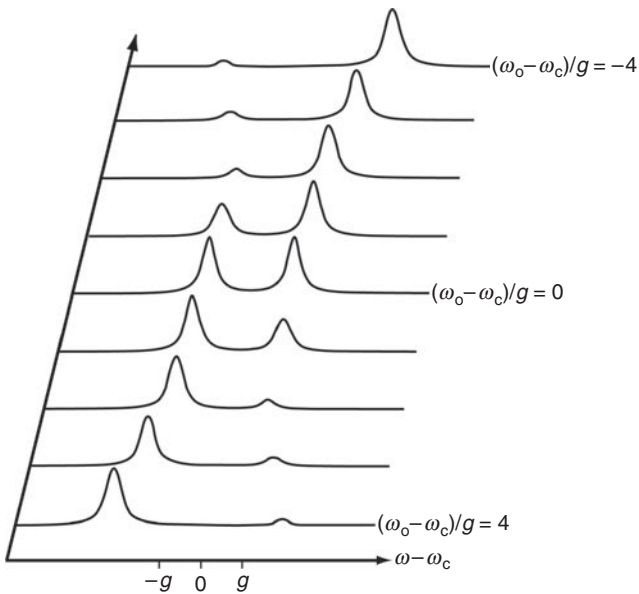
Figure 7.25 *Illustration of the intensity exchange between features at the avoided crossing that characterizes the probe absorption spectrum of strongly coupled cavity QED.*

while still retaining the coherent phase information, they are said to be *entangled*. Transport of quantum state information to remote locations then becomes possible. The strongly coupled field–atom system of this section is an example of an entangled system that is potentially suitable for such applications, since the atom and light propagate in different directions following their interaction (see Ref. [7.50] for an experimental realization). While cavity enhancement and entanglement are important ingredients in some quantum information applications, neither is essential however [7.51]. Ongoing experimental research is investigating many other approaches to the creation, transport, and manipulation of entangled states [7.52]. This topic is explored in Problems 5.1 and 7.5.

This section has analyzed the interaction of atoms with light for atom–field couplings that are sufficiently enhanced by a cavity so that the Rabi frequency exceeds the decoherence time. That is, the strong coupling regime corresponds to the condition $\Gamma << \Omega_R$. Generally, the optical carrier frequency greatly exceeds the Rabi frequency ($\Omega_R << \omega$). However, one can imagine even stronger coupling, characterized by $\Omega_R \approx \omega$, in which photon exchange occurs on the timescale of the optical period itself. Under such extreme conditions the RWA would break down, and interactions become nonadiabatic. Efforts to extend strong cavity QED to this regime of ultra-strong light–matter interactions have been undertaken in experiments based on intersubband cavity polaritons [7.53].

Problems

7.1. Verify the values of the Clebsch–Gordan coefficients shown in Fig. 7.5 for a $J_g = 1/2 \leftrightarrow J_e = 3/2$ transition.

7.2. Calculate the seven Clebsch–Gordan coefficients for a $J_g = 1 \leftrightarrow J_e = 1$ transition.

7.3. Calculate the fifteen Clebsch–Gordan coefficients and relative transition probabilities between hyperfine levels of Sodium on the $F = 2 \rightarrow F' = 3$ transition used in the first experimental observations of the Mollow triplet.

7.4. *Statistics of squeezed states*

(a) Using the squeezed field operator $\hat{t} \equiv \hat{S}\hat{a}\hat{S}^+ = \hat{a}^- \cosh r + \hat{a}^+ e^{i\theta} \sinh r$, show that the mean square of the number of photons in a squeezed, single-mode vacuum state $|0\rangle$ is $\langle 0| \hat{t}^+\hat{t}^+\hat{t}\hat{t} |0\rangle = 3 \sinh^4 r + \sinh^2 r$.
(Note: $\hat{S}^+\hat{S} = 1$, and r and θ are the magnitude and phase of the complex squeeze parameter $z = re^{i\theta}$. For large $|z|$, there is strong squeezing and for $|z| = 0$ or $r = 0$ there is no squeezing at all).

(b) Use the result of part (a) and the exercise in Section 7.6 to show that for a squeezed single-mode vacuum state

$$g^{(2)}(0) = \frac{\langle a^+ a^+ \hat{a}\hat{a}\rangle}{\langle \hat{a}^+\hat{a}^-\rangle^2} = 3 + \frac{1}{\langle n\rangle}.$$

Squeezed vacuum is bunched rather than anti-bunched.

7.5. In this problem, the practical issue of preserving entanglement and the need to avoid spontaneous emission are explored.

Consider a two-level atom that is coupled to a single-mode field in a cavity. The atom may be in state $|\uparrow\rangle$ or $|\downarrow\rangle$, while the field is in $|+\rangle$ or $|-\rangle$, depending on whether the atom has added a photon to the field by undergoing a transition $|\uparrow\rangle \rightarrow |\downarrow\rangle$ or has removed a photon by absorption. The only other process possible is that the atom spontaneously decays to the ground state without adding a photon to the mode (the emitted photon escapes from the cavity). There are thus three states in the product basis: $|\uparrow\rangle |-\rangle$, $|\downarrow\rangle |+\rangle$, and $|\downarrow\rangle |-\rangle$, and the full density matrix is 3×3 instead of 2×2. That is,

$$\tilde{\rho} = \begin{bmatrix} \rho_{\uparrow-,\uparrow-} & \rho_{\uparrow-,\downarrow+} & \rho_{\uparrow-,\downarrow-} \\ \rho_{\downarrow+,\uparrow-} & \rho_{\downarrow+,\downarrow+} & \rho_{\downarrow+,\downarrow-} \\ \rho_{\downarrow-,\uparrow-} & \rho_{\downarrow-,\downarrow+} & \rho_{\downarrow-,\downarrow-} \end{bmatrix}.$$

Note, however, that if spontaneous emission is absent, the density matrix elements in the 2×2 sub-matrix

$$\tilde{\rho}_{\text{sub}} = \begin{bmatrix} \rho_{\uparrow-,\uparrow-} & \rho_{\uparrow-,\downarrow+} \\ \rho_{\downarrow+,\uparrow-} & \rho_{\downarrow+,\downarrow+} \end{bmatrix}$$

fully describe the system. On resonance, elements of $\tilde{\rho}_{\text{sub}}$ can be found from the Bloch vector $\overline{R}(t)$:

$$\overline{R}(t) = \begin{bmatrix} V(t) \\ W(t) \end{bmatrix} = \overleftrightarrow{M} \overline{R}_i(0) = \begin{bmatrix} \cos\theta & -\sin\theta \\ \sin\theta & \cos\theta \end{bmatrix} \begin{bmatrix} V(0) \\ W(0) \end{bmatrix},$$

using standard relations $\tilde{\rho}_{\uparrow-,\downarrow+} = -iV/2$, $\tilde{\rho}_{\downarrow+,\uparrow-} = \tilde{\rho}*_{\uparrow-,\downarrow+}$ and $W = \rho_{\uparrow-,\uparrow-} - \rho_{\downarrow+,\downarrow+}$. In the absence of spontaneous emission, one also has $\rho_{\uparrow-,\uparrow-} + \rho_{\downarrow+,\downarrow+} = 1$. Also, without spontaneous emission the remaining elements of $\tilde{\rho}$ are 0 since they do not conserve energy in the coupled atom–cavity system.

(a) A fully entangled "initial" state is produced in the 2×2 subspace of $\tilde{\rho}_{\text{sub}}$ by applying an ultrashort $\pi/2$ pulse to the $|\downarrow\rangle |+\rangle$ state. The initial Bloch vector after pulse 1 is

$$\overline{R}(t_1 = 0) = \begin{bmatrix} 1 \\ 0 \end{bmatrix}.$$

Calculate the Bloch vectors $\overline{R}(t_2)$ and $\overline{R}(t_3)$, following a second $\pi/2$ pulse at time t_2 that converts the excitation to a pure excited state population, and a third pulse of arbitrary area θ at time t_3, respectively. Omit precession and dephasing between the pulses.

(b) Determine all elements of the 3×3 density matrix after the third pulse (in the *absence* of spontaneous emission).

(c) Show that the probabilities of finding the system in states $|\uparrow\rangle |-\rangle$ and $|\downarrow\rangle |+\rangle$ are exactly anti-correlated for arbitrary θ by calculating the expectation

values of $\tilde{\rho}$ for these states. Show that when one is maximum, the other is always minimum.

(d) Calculate the "fidelity (F)" of entanglement in the final state when $\theta = -\pi/2$. (Fidelity $F = \sqrt{\langle\psi_1(0)|\,\tilde{\rho}_{\text{final}}(t)\,|\psi_1(0)\rangle}$ measures the degree of overlap with the initial reference state $\psi_1(0) = \frac{1}{\sqrt{2}}\begin{bmatrix}1\\1\end{bmatrix}$ to see how much of the original entanglement is recovered after transformation.) To find F, a rotation must be applied independently to the off-diagonal terms of $\tilde{\rho}_{\text{sub}}(\theta = -\pi/2)$ according to the prescription $\tilde{\rho}_{\text{final}} = \tilde{\rho}'_{\text{sub}}\left(-\frac{\pi}{2}, \varphi\right) = \begin{bmatrix} \rho_{\uparrow-,\uparrow-} & \rho_{\uparrow-,\downarrow+}(e^{i\varphi}) \\ \rho_{\downarrow+,\uparrow-}(e^{-i\varphi}) & \rho_{\downarrow+,\downarrow+} \end{bmatrix}$.

Simply multiply your off-diagonal entries by $e^{\pm i\phi}$ as indicated, evaluate F and give its value for $\phi = \pi/2$.

(Note: In practice the phase angle ϕ is varied to map out the magnitude of residual polarization terms, converting coherences to populations so that they can be measured.)

(e) Suppose that between pulses 2 and 3, a spontaneous emission event occurs and the atom drifts into a null of the standing wave in the cavity. Write down the full density matrix just prior to pulse 3 and determine the fidelity of entanglement as before, following the $\theta = -\pi/2$ pulse. Compare with the result of part (d).

7.6. (a) In laser cooling, position z must be considered an operator instead of a scalar under certain circumstances. Why is this so and what is the implication for the eigenvalues of z when the spread in linear momentum Δp of the atoms becomes less than the photon momentum $\hbar k$?

(b) Using the expressions for the interaction V of ^{4}He atoms with circularly polarized light on the $2^3S_1(\text{m} = \pm 1)$-$2^3P_1(\text{m} = 0)$ transitions, consider the coherent superposition states $|\psi_{\text{NC}}(p)\rangle$ and $|\psi_{\text{C}}(p)\rangle$, and show explicitly that the NC state does not couple to the excited state whereas the C state does.

7.7. (a) Calculate the root-mean-square fluctuations of the electric field operator $E = \frac{1}{\sqrt{2}}(a + a^+)\sin(kz - \omega t)$ in the following two distinct states:

$$|\psi_1\rangle = |n\rangle \text{ and } |\psi_2\rangle = e^{i(kz-\omega t)}|n-3\rangle + |n-2\rangle + e^{i(kz-\omega t)}|n+2\rangle + |n+3\rangle.$$

(b) Show that in state $|\psi_1\rangle$, noise is a minimum only at times when the amplitude of the field goes to 0 as the result of its sinusoidal motion (i.e., when $kz = \omega t$). This shows that individual photon number states exhibit noise that is proportional to the instantaneous field amplitude.

(c) Show that for the simple superposition state $|\psi_2\rangle$, the noise can be 0 at another time during each period by finding a *nonzero* phase angle $\phi = kz - \omega t$ for which the root-mean-square field is 0. Assume n is large.

Note: This property vanishes if $|\psi_2\rangle$ is properly normalized. Only more complicated superpositions of number states (coherent states) can exhibit amplitude squeezing when properly normalized.

7.8. On resonance ($\Delta = 0$),

$$g_{atom}^{(2)}(\tau) = \left[1 - \exp\left(\frac{-3\beta\tau}{2} \right) \left(\cos(\Omega''\tau) + \frac{\beta}{\Omega''} \sin(\Omega''\tau) \right) \right],$$

where $\Omega'' \equiv \sqrt{\Omega^2 - (\beta^2/4)}$, $\Omega \equiv \mu E/\hbar$ and $\beta \equiv \gamma_{sp}/2$.

(a) What specific value of $g^{(2)}(\tau)$ is *uniquely* characteristic of emission from a quantum light source consisting of *a single atom?* Give a one sentence explanation of the mechanism that allows an atom to exhibit this special value.

(b) Suppose that $g^{(2)}(\tau)$ is measured for an ensemble of *two uncorrelated atoms*. Each atom emits individually in accord with $g_{atom}^{(2)}$ above. However when a measurement of $g^{(2)}(\tau)$ is made based on the total intensity from both atoms, one atom may emit at a time when the other cannot, thereby altering the value of $g_{ensemble}^{(2)}$ with respect to $g_{atom}^{(2)}$. Estimate $g_{ensemble}^2(0)$ for the two-atom ensemble in the *weak field limit* by approximating it with $g^{(2)}(\tau)$ for one atom at a delay τ equal to its most probable time of emission.

References

7.1. T. Carmon, H. Rokhsari, L. Yang, T.J. Kippenberg, and K.J. Vahala, *Phys. Rev. Lett.* **94**, 223902(2005).

7.2. J.P. Gordon and A. Ashkin, *Phys. Rev.* **A21**, 1606(1980).

7.3. A. Ashkin, J.M. Dziedzic, J.E. Bjorkholm, and S. Chu, *Opt. Lett.* **11**, 288(1986).

7.4. A. Ashkin and J.M. Dziedzic, *Science* **235**, 1517(1987).

7.5. S. Chu, *Reviews of Modern Physics* **70**(3)(1998).

7.6. J. Dalibard and C. Cohen-Tannoudji, *J.O.S.A.* **B2**, 1707(1985).

7.7. S. Chu, J.E. Bjorkholm, A. Ashkin, and A. Cable, *Phys. Rev. Lett.* **57**, 314(1986).

7.8. T. Hansch and A.L. Schawlow, *Opt. Commun.* **13**, 68–71(1975).

7.9. See, for example, H. Metcalf and P. van der Straten, *Laser Cooling and Trapping*, Springer-Verlag, New York, 1999.

7.10. R.I. Epstein, M.I. Buchwals, B.C. Edwards, T.R. Gosnell, and C.E. Mungan, *Nature* (London) **377**, 500(1995).

7.11. J. Thiede, J. Distel, S.R. Greenfield, and R.I. Epstein, *Appl. Phys. Lett.* **86**, 154107(2005).

7.12. E.L. Raab, M. Prentiss, A. Cable, S. Chu, and D.E. Pritchard, *Phys. Rev. Lett.* **59**, 2631(1987).

7.13. J. Dalibard and C. Cohen-Tannoudji, *J.O.S.A.* **B6**, 2023(1989).

7.14. P.J. Ungar, D.S. Weiss, E. Riis, and S. Chu, *J.O.S.A.* **B6**, 2058(1989).

7.15. M. Kasevich and S. Chu, Phys. *Rev. Lett.* **69**, 1741(1992).

7.16. M.H. Anderson, J.R. Ensher, M.R. Matthews, C.E. Wieman, and E.A. Cornell, *Science* **269**, 198–201(1995).

7.17. L. Pitaevskii and S. Stringari, *Bose–Einstein Condensation*, Clarendon Press, Oxford, 2003.

7.18. C.A. Regal, M. Geiner, and D.S. Lin, *Phys. Rev. Lett.* **92**, 040403(2004).

7.19. B.W. Shore, *The Theory of Atomic Excitation*, J. Wiley & Sons, New York, 1990.

7.20. J. Oreg, G. Hazak, and J.H. Eberly, *Phys. Rev.* A **32**, 2776(1985).

7.21. J.R. Kuklinski, U. Gaubatz, F.T. Hioe, and K. Bergmann, *Phys. Rev.* A **40**, 6741(1989).

7.22. M.P. Fewell, B.W. Shore, and K. Bergmann, *Austr. J. Phys.* **50**, 281(1997).

7.23. F. Hioe, *Physical Review* **A28**, 879(1983).

7.24. J. Gong and S.A. Rice, J. Chem. Phys. *120*, 5117(2004).

7.25. S.C. Rand, W.M. Fisher, and S.L. Oliveira, *J.O.S.A.* **B25**, 1106(2008).

7.26. B. Ya. Zeldovich, *Physics – Uspekhi* **51** (5), 465–84(2008).

7.27. See for example A.H. Nayfeh, *Perturbation Methods*, J. Wiley & Sons, New York, 1973.

7.28. R. Di Leonardo, G. Ruocco, J. Leach, M.J. Padgett, A.J. Wright, J.M. Girkin, D.R. Burnham, and D. McGloin, *Phys. Rev. Lett.* 99, 010601(2007).

7.29. J. Pendry, *Phys. Rev. Lett.* **85**, 3966(2000).

7.30. J.B. Pendry, D. Schurig, and D.R. Smith, *Science* **312**, 1780(2006).

7.31. S. Barreiro and J.W.R. Tabosa, *Phys. Rev. Lett.* **90**, 133001(2003).

7.32. S.C. Rand, Quantum Theory of Coherent Transverse Optical Magnetism, *J.O.S.A.* B *26*, B120(2009).

7.33. J. Baudon, M. Hamamda, J. Grucker, M. Boustimi, F. Perales, G. Dutier, and M. Ducloy, Phys. Rev. Lett. *102*, 140403(2009).

7.34. K.-J. Boller, A. Imamoglu, and S.E. Harris, *Phys. Rev. Lett.* **66**, 2593(1991).

7.35. K. Hakuta, L. Marmet, and B.P. Stoicheff, *Phys. Rev. Lett.* **66**, 596(1991).

7.36. L.V. Hau, S.E. Harris, and Z. Dutton, *Nature* **397**, 594(1999).

7.37. M.F. Yanik and S. Fan, *Nature Physics* **3**, 372(2007); Z. Shi, R.W. Boyd, R.M. Camacho, P.V. Vudyasetu, and J.C. Howell, *Phys. Rev. Lett.* **99**, 240801 (2007).

7.38. Q. Shu and S.C. Rand, Phys. Rev. B *55*, 8776(1997).

7.39. A.S. Zibrov, A.B. Matsko, O. Kocharovskaya, Y.V. Rostovtsev, G.R. Welch, and M.O. Scully, *Phys. Rev. Lett.* **88**, 103601(2002).

7.40. K. Hakuta, M. Suzuki, M. Katsuragawa, and J.Z. Li, *Phys. Rev. Lett.* **79**, 209(1997).

7.41. M.O. Scully, *Phys. Rev. Lett.* **67**, 1855(1991); M. Fleischauer, C.H. Kreitel, M.O. Scully, C. Su, B.T. Ulrich, and S.-Y. Zhu, *Phys. Rev.* A**46**, 1468(1992).

7.42. A. Nottlemann, C. Peters, and W. Lange, *Phys. Rev. Lett.* **70**, 1783(1993); E.S. Fry, X. Li, D. Nikonov, G.G. Padmabandu, M.O. Scully, A.V. Smith, F.K. Tittel, C. Wang, S.R. Wilkinson, and S.-Y. Zhu, *Phys. Rev. Lett.* **70**, 3235(1993); W.E. van der Veer, R.J.J. van Diest, A. Donszelmann, H.B. van Linden, and van den Heuvell, *Phys. Rev. Lett.* **70**, 3243(1993).

7.43. M. O. Scully and M. S. Zubairy, *Quantum Optics*, Cambridge University Press, Cambridge, 1997.

7.44. A. Lezama, S. Barreiro, and A.A. Akulshin, *Phys. Rev.* A**59**, 4732(1999).

7.45. A. Yariv, *Quantum Electronics*, J. Wiley & Sons, 3rd edition, New York, 2003.

7.46. H.P. Yuen and J.H. Shapiro, *IEEE Trans. Inf. Theor.* **26**, 78(1980).

7.47. L. Mandel and E. Wolf, *Optical Coherence and Quantum Optics*, Cambridge University Press, Cambridge, 1995.

7.48. P. Berman, ed., *Cavity Quantum Electrodynamics*, Academic Press, Inc., New York, 1994.

7.49. M.A. Nielson, and I.L. Chuang, *Quantum Computation and Quantum Information*, Cambridge University Press, Cambridge, 2000.

7.50. Q.A. Turchette, C.J. Hood, W. Lange, H. Mabuchi, and H.J. Kimble, *Phys. Rev. Lett.* **75**, 4710(1995).

7.51. P. Knight, *Science* **287**, 441(2000).

7.52. Supplementary reading on advanced quantum information experimentation using single atoms, quantum dots, ions, color centers, and nuclear spins may be found in: B.B. Blinov, D.L. Moehring, L.-M. Duan, and C. Monroe, *Nature* **428**, 153(2004); X. Li, Y. Wu, D.G. Steel, D. Gammon, T.H. Stievater, D.S. Katzer, D. Park, C. Piermarocchi, and L.J. Sham, *Science* **301**, 809(2003); R.G. Brewer, R.G. DeVoe, and R. Kallenbach, *Phys. Rev.* A**46**, R6781(1992); F. Jelezko, T. Gaebel, I. Popa, M. Domhan, A. Gruber, and J. Wrachtrup, *Phys. Rev. Lett.* **93**, 130501(2004); I.L. Chuang, N. Gershenfeld, and M.G. Kubinec, *Phys. Rev. Lett.* **18**, 3408(1998).

7.53. C. Ciuti, G. Bastard, and I. Carusotto, *Phys. Rev.* **B72**, 115303(2005); A.A. Anappara, S. De Liberato, A. Tredicucci, C. Ciuti, G. Biasiol, L. Sorba, and F. Beltram, *Phys. Rev.* **B79**, R201303(2009); G. Gunter, A.A. Anappara, J. Hees, A. Sell, G. Biasial, L. Sorba, S. De Liberato, C. Ciuti, A. Tredicucci, A. Leitenstorfer, and R. Huber, *Nature* **458**, 178(2009).

7.54. A. Aspect, E. Arimondo, R. Kaiser, N. Vansteenkiste, and C. Cohen-Tannoudji, *J.O.S.A.* **B6**, 2112(1989).

Appendices

Appendix A

Expectation Values

In quantum mechanics, operators appear in place of the continuous variables from classical mechanics and their commutation properties must be taken into account when predicting the outcome of measurements. For an operator $\hat{O}$ that in general does not commute with wavefunction ψ, the average value of $\hat{O}$ expected in a series of measurements could in principle be defined in two ways:

$$\left\langle \hat{O} \right\rangle = \int \hat{O} \psi^* \psi d^3 r, \tag{A.1}$$

or

$$\left\langle \hat{O} \right\rangle = \int \psi^* \hat{O} \psi d^3 r. \tag{A.2}$$

We can judge whether Eq. (A.1) or Eq. (A.2) is correct by testing the outcome of each expression against Schrödinger's wave equation (Eq. (1.3.5)). As an example, consider the Hamiltonian operator $\hat{H}$. If we ignore operator commutation rules we can imagine two possible expressions for the first moment, namely

$$\left\langle \hat{H} \right\rangle = i\hbar \int \frac{\partial}{\partial t} (\psi^* \psi) d^3 r, \tag{A.3}$$

$$\left\langle \hat{H} \right\rangle = i\hbar \int \psi^* \frac{\partial}{\partial t} \psi dx. \tag{A.4}$$

The correct expression for $\left\langle \hat{H} \right\rangle$ must however be fully consistent with Eq. (1.3.5). If we multiply through $\hat{H}\psi = i\hbar \frac{\partial \psi}{\partial t}$ by ψ^* and integrate over volume, we find

$$\left\langle \hat{H} \right\rangle = \int \psi^* \hat{H} \psi d^3 r = i\hbar \int \psi^* \frac{\partial \psi}{\partial t} d^3 r, \tag{A.5}$$

in agreement with definition Eqs. (A.2) and (1.3.11). If instead we operate with $\hat{H}$ on $\psi^* \psi$, we find

$$\int \hat{H} \psi^* \psi d^3 r = i\hbar \int \frac{\partial}{\partial t} (\psi^* \psi) d^3 r = i\hbar \int \left(\psi^* \frac{\partial}{\partial t} \psi + \psi \frac{\partial}{\partial t} \psi^* \right) d^3 r. \tag{A.6}$$

Evaluation of the last integral for the simplest case in which ψ is an eigenstate with eigenvalue E yields $2E$. The outcome $2E$ clearly contradicts the starting assumption and is therefore inconsistent with Schrödinger's equation. Only the second definition yields the correct result, uniquely establishing Eq. (A.2) as the definition of the expectation value. Overall, this illustrates the importance of commutation properties of operator expressions in quantum mechanics.

Appendix B

The Heisenberg Uncertainty Principle

To derive the Heisenberg uncertainty principle analytically for specific operators such as x and p_x, the following argument can be used. The squared standard deviations of position and momentum observables are

$$\langle \Delta x^2 \rangle = \int \psi^* \left(x - x < x > \right)^2 \psi \, dV, \tag{B.1}$$

$$\langle \Delta p_x^2 \rangle = \int \psi^* \left(-i\hbar \frac{\partial}{\partial x} - \langle p_x \rangle \right)^2 \psi \, dV. \tag{B.2}$$

Taking the average values to be 0, ($\langle x \rangle = \langle p_x \rangle = 0$), we find

$$\langle \Delta p_x^2 \rangle \langle \Delta x^2 \rangle = \int \psi^* \left(-\hbar^2 \frac{\partial^2}{\partial x^2} \right) \psi \, dr \int \psi^* x^2 \psi \, dV. \tag{B.3}$$

Integration by parts permits us to write

$$\int \psi^* \frac{\partial^2 \psi}{\partial x^2} \, dV = - \int \frac{\partial \psi^*}{\partial x} \frac{\partial \psi}{\partial x} \, dV, \tag{B.4}$$

$$\langle \Delta p_x^2 \rangle \langle \Delta x^2 \rangle = \hbar^2 \int \frac{\partial \psi^*}{\partial x} \frac{\partial \psi}{\partial x} \, dV \int \psi^* x^2 \psi \, dV. \tag{B.5}$$

Now, using the Schwartz inequality, we obtain

$$\int ff^* dV \int g^* g \, dV \geq \left[\frac{1}{2} \left(\int fg^* \, dV + \int gf^* \, dV \right) \right]^2. \tag{B.6}$$

Setting $f \equiv \partial \psi / \partial x$ and $g \equiv x\psi$ in this expression, one finds

$$\langle \Delta p_x^2 \rangle \langle \Delta x^2 \rangle \geq \frac{\hbar^2}{4} \left(\int \frac{\partial \psi}{\partial x} x \psi^* \, dV + \int x\psi \frac{\partial \psi^*}{\partial x} \, dV \right)^2$$

$$\geq \frac{\hbar^2}{4} \left(\int x \frac{\partial}{\partial x} (\psi \psi^*) \, dV \right)^2 = \frac{\hbar^2}{4}$$

$$\geq \frac{\hbar^2}{4}. \tag{B.7}$$

The final integral above is again evaluated by parts and is equal to -1. Defining the uncertainties in momentum and position as $\Delta p_x \equiv \langle \Delta p_x^2 \rangle^{1/2}$ and $\Delta x \equiv \langle \Delta x^2 \rangle^{1/2}$, we obtain

$$\Delta p_x \Delta x \geq \frac{\hbar}{2}. \tag{B.8}$$

The operators x and p_x provide one example of two Hermitian operators $\hat{A}$ and $\hat{B}$ with a commutator that is Hermitian and nonzero. Note that this results in an uncertainty principle between $\hat{A}$ and $\hat{B}$. Next, this result is extended to the general case.

Consider two Hermitian operators $\hat{A}$ and $\hat{B}$ with a Hermitian commutator

$$\left[\hat{A}, \hat{B} \right] = i\hat{C}. \tag{B.9}$$

It is shown below that the standard deviations ΔA and ΔB have the product

$$\Delta A \Delta B \geq \frac{1}{2} |\langle C \rangle|. \tag{B.10}$$

The standard deviations (uncertainties) in $\hat{A}$ and $\hat{B}$ are defined as

$$\Delta A \equiv \hat{A} - \langle A \rangle, \tag{B.11}$$

$$\Delta B \equiv \hat{B} - \langle B \rangle, \tag{B.12}$$

hence observed values of their squares are

$$\langle (\Delta A)^2 \rangle = \langle \psi \Delta A | \Delta A \psi \rangle = \|\Delta A \psi\|^2 \tag{B.13}$$

and

$$\langle (\Delta B)^2 \rangle = \langle \psi \Delta B | \Delta B \psi \rangle = \|\Delta B \psi\|^2. \tag{B.14}$$

The Schwartz inequality is equivalent to the inequality expressing the fact that the inner product of two vector operators, namely $\langle \psi \Delta A | \Delta B \psi \rangle$, is less than the product of their lengths, given by $\|\Delta A \psi\| \|\Delta B \psi\|$. That is,

$$\|\Delta A \psi\|^2 \|\Delta B \psi\|^2 \geq |\langle \psi \Delta A | \Delta B \psi \rangle|^2, \tag{B.15}$$

or

$$(\Delta A)^2 (\Delta B)^2 \geq |\langle \psi \Delta A | \Delta B \psi \rangle|^2 = |\langle \psi | \Delta A \Delta B | \psi \rangle|^2. \tag{B.16}$$

The last step above is due to the Hermiticity of ΔA. The product $\Delta A \Delta B$ on the right hand side of this result can be reexpressed in terms of the commutator of $\hat{A}$ and $\hat{B}$, because any operator can be written as a linear combination of two Hermitian

operators:

$$\Delta A \Delta B = \frac{1}{2}(\Delta A \Delta B + \Delta B \Delta A) + \frac{1}{2}[\Delta A, \Delta B]$$

$$= \frac{1}{2}(\Delta A \Delta B + \Delta B \Delta A) + \frac{1}{2}[A, B]$$

$$= \hat{D} + \frac{i}{2}\hat{C}. \tag{B.17}$$

Hence,

$$(\Delta A)^2 (\Delta B)^2 \geq \left| \left\langle \psi \left| \hat{D} + \frac{i}{2}\hat{C} \right| \psi \right\rangle \right|^2 = \left| \langle D \rangle + \frac{i}{2}\langle C \rangle \right|^2. \tag{B.18}$$

Because $\hat{D}$ and $\hat{C}$ are Hermitian, their expectation values are real. Consequently, the squared expression on the right above is simply

$$(\Delta A)^2 (\Delta B)^2 \geq |\langle D \rangle|^2 + \frac{1}{4}|\langle C \rangle|^2 \geq \frac{1}{4}|\langle C \rangle|^2. \tag{B.19}$$

The uncertainties in A and B therefore satisfy the general relation

$$(\Delta A)(\Delta B) \geq \frac{1}{2}|\langle C \rangle|. \tag{B.20}$$

Appendix C

The Classical Hamiltonian of Electromagnetic Interactions

The nonrelativistic force on a charged particle of velocity $\bar{v}$ is the Lorentz force

$$\bar{F} = q\left[\bar{E} + (\bar{v} \times \bar{B})\right]. \tag{C.1}$$

On the basis of the vector identity

$$\bar{\nabla} \cdot (\bar{\nabla} \times \bar{A}) = 0, \tag{C.2}$$

where $\bar{A}$ is an arbitrary vector potential, we conclude from the Maxwell equation $\bar{\nabla} \cdot \bar{B} = 0$ that $\bar{B}$ can always be written in the form

$$\bar{B} = \bar{\nabla} \times \bar{A}, \tag{C.3}$$

where $\bar{A}$ is a vector potential.

Similarly, applying Eq. (C.3) in the Maxwell equation $\bar{\nabla} \times \bar{E} = -\dfrac{\partial \bar{B}}{\partial t}$, we see that it can be written as

$$\bar{\nabla} \times \bar{E} + \frac{\partial}{\partial t}(\bar{\nabla} \times \bar{A}) = 0, \tag{C.4}$$

or by reversing the order of derivatives, as

$$\bar{\nabla} \times \left(\bar{E} + \frac{\partial \bar{A}}{\partial t}\right) = 0. \tag{C.5}$$

Making use of a second vector identity, namely

$$\bar{\nabla} \times \bar{\nabla}\phi = 0, \tag{C.6}$$

where ϕ is a scalar potential, the electric field can clearly always be written as

$$\bar{E} = -\bar{\nabla}\phi - \frac{\partial \bar{A}}{\partial t}. \tag{C.7}$$

The expression for the Lorentz force becomes

$$\bar{F} = q\left[-\bar{\nabla}\phi - \frac{\partial \bar{A}}{\partial t} + \left(\bar{v} \times \left[\bar{\nabla} \times \bar{A}\right]\right)\right]. \tag{C.8}$$

Using the replacements $\dfrac{d\bar{A}}{dt} = \dfrac{\partial \bar{A}}{\partial t} + (\bar{v} \cdot \bar{\nabla})\bar{A}$ and $\bar{v} \times (\bar{\nabla} \times \bar{A}) = \bar{\nabla}(\bar{v} \cdot \bar{A}) - (\bar{v} \cdot \bar{\nabla})\bar{A}$, we find

$$\bar{F} = q\left[-\bar{\nabla}\phi + \bar{\nabla}\left(\bar{v} \cdot \bar{A}\right) - \frac{\partial \bar{A}}{\partial t} - \left(\bar{v} \cdot \bar{\nabla}\right)\bar{A}\right]$$

$$= q\left[-\bar{\nabla}\left(\phi - \bar{v} \cdot \bar{A}\right) - \frac{d\bar{A}}{dt}\right]$$

$$= q\left[-\bar{\nabla}\left(\phi - \bar{v} \cdot \bar{A}\right) - \frac{d}{dt}\bar{\nabla}_v\left(\bar{v} \cdot \bar{A}\right)\right]. \tag{C.9}$$

Since the scalar potential ϕ does not depend on velocity, the ith component of the force on a particle may be written as

$$F_i = q\left[-\frac{\partial U}{\partial x_i} - \frac{d}{dt}\frac{\partial U}{\partial v_i}\right], \tag{C.10}$$

where $i = x, y, z$ and $U \equiv q(\phi - \bar{A} \cdot \bar{v})$. Here U is a generalized potential function from which we obtain the Lagrangian in traditional, nonrelativistic mechanics:

$$L = T - U = \frac{mv^2}{2} - q\phi + q\bar{A} \cdot \bar{v}. \tag{C.11}$$

The Lagrangian in turn furnishes the Hamiltonian

$$H = \sum_i \dot{x}_i \frac{\partial L}{\partial \dot{x}_i} - L = \frac{1}{2}mv^2 + q\phi, \tag{C.12}$$

which, when expressed in terms of the canonical momentum $p_i = \partial L/\partial \dot{x}_i = mv_i + qA_i$, yields

$$H = \frac{1}{2m}\left(\bar{p} - q\bar{A}\right) \cdot \left(\bar{p} - q\bar{A}\right) + q\phi. \tag{C.13}$$

The Hamiltonian in Eq. (C.13) can be converted to a form that is much more convenient for describing the system in terms of the applied fields E and B, to separate out multipole contributions, and for eventual quantization [C.1]. To make the conversion,

we note that Eqs. (C.3) and (C.7) can be satisfied if $\phi(\bar{r}, t)$ and $\bar{A}(\bar{r}, t)$ are expanded in Taylor's series representations as

$$\phi(\bar{r}, t) = -\bar{r} \cdot \bar{E}(0, t) - \frac{1}{2}\bar{r}\bar{r} : (\bar{\nabla}\bar{E}(0, t)) + \dots, \qquad (C.14)$$

and

$$\bar{A}(\bar{r}, t) = \frac{1}{2}\bar{B}(r) \times \bar{r} + \frac{1}{3}\bar{r} \cdot \bar{\nabla}\bar{B}(0, t) \times \bar{r} + \dots . \qquad (C.15)$$

These expansions constitute a specific choice of gauge consistent with Taylor expansions of the fields themselves:

$$\bar{E}(\bar{r}, t) = \bar{E}(0, t) + \bar{r} \cdot (\bar{\nabla}\bar{E}(0, t) + \dots, \qquad (C.16)$$

$$\bar{B}(\bar{r}, t) = \bar{B}(0, t) + \bar{r} \cdot (\bar{\nabla}\bar{B}(0, t) + \dots . \qquad (C.17)$$

By substituting Eqs. (C.14) and (C.15) into Eq. (C.13), one finds that the interaction Hamiltonian assumes the form

$$H = -\bar{\mu}^{(e)} \cdot \bar{E} - \bar{\mu}^{(m)} \cdot \bar{B} \qquad (C.18)$$

if we retain only the leading electric and magnetic dipole terms, with moments $\bar{\mu}^{(e)} = e\bar{r}$ (pointing from the negative to the positive charge) and $\bar{\mu}^{(m)} = \frac{1}{2}e\bar{r} \times \bar{v}$.

References

C.1 L.D. Barron and C.G. Gray, *J. Phys. A: Math., Nucl. Gen.*, **6**, 59(1973).

Appendix D

Stationary and Time-dependent Perturbation Theory

A. Stationary perturbation theory

Assume that the system Hamiltonian can be written as the sum of two parts, one of which is the unperturbed part ($\hat{H}_0$) and the second of which is an interaction $\hat{V}$.

$$\hat{H} = \hat{H}_0 + \lambda\hat{V}, \qquad (D.1)$$

λ is a perturbation parameter that merely keeps track of the presence and order of perturbation. When $\lambda = 0$ the perturbation is removed, and $\hat{H} = \hat{H}_0$. When $\lambda = 1$ the perturbation is present, and $\hat{H} = \hat{H}_0 + \hat{V}$.

Eigenvalues and eigenfunctions of the unperturbed system may be found by solving the energy equation $\hat{H}_0\phi_n = E_n^0\phi_n$. When the interaction is included, this requires solution of the equation

$$\left(\hat{H}_0 + \lambda\hat{V}\right)\psi = E\psi. \qquad (D.2)$$

Solutions can readily be found when there is no degeneracy, that is when all energy levels are widely separated, by using an approximate method. For this purpose, an

expansion based on the complete set of eigenfunctions ϕ_n of the unperturbed problem may be used.

$$\psi = \sum_n a_n \phi_n. \tag{D.3}$$

Inserting this expansion into Eq. (D.2), one obtains

$$\left(E - E_m^0\right) a_n = \lambda \sum_n V_{mn} a_n, \tag{D.4}$$

where $V_{mn} \equiv \langle \phi_m | \hat{V} | \phi_n \rangle$.

Because of the perturbation, the energies and eigenfunctions of the system change. To determine the corrections to the energy and eigenfunction of the lth stationary state, a scheme of successive approximations for E_l and a_n is used.

$$E_l = E_l^{(0)} + \lambda E_l^{(1)} + \lambda^2 E_l^{(2)} + \dots, \tag{D.5}$$

$$a_m = a_m^{(0)} + \lambda a_m^{(1)} + \lambda^2 a_m^{(2)} + \dots. \tag{D.6}$$

If we assume the system starts in state l, we have $a_m^{(0)} = \delta_{ml}$, so that

$$a_m = \delta_{ml} + \lambda a_m^{(1)} + \lambda^2 a_m^{(2)} + \dots. \tag{D.7}$$

Substituting Eqs. (D.7) and (D.5) into Eq. (D.4), one finds

$$\left[E_l^0 - E_m^0 + \lambda E_l^{(1)} + \lambda^2 E_l^{(2)} + \dots \right] \left[\delta_{ml} + \lambda a_m^{(1)} + \lambda^2 a_m^{(2)} + \dots \right]$$

$$= \lambda \sum_n V_{mn} \left[\delta_{nl} + \lambda a_n^{(1)} + \dots \right]. \tag{D.8}$$

If $m = l$, then comparison of terms of the same order in λ yields

$$E_l^{(1)} = V_{ll},$$

$$E_l^{(2)} + E_l^{(1)} a_l^{(1)} = \sum_n V_{\ln} a_n^{(1)} \dots. \tag{D.9}$$

If $m \neq l$ the result is

$$a_m^{(1)} \left(E_l^0 - E_m^0 \right) = V_{ml},$$

$$E_l^{(1)} a_m^{(1)} + \left(E_l^0 - E_m^0 \right) a_m^{(2)} = \sum_n V_{mn} a_n^{(1)} \dots. \tag{D.10}$$

By setting $\lambda = 1$, the first-order approximation for the energy of the perturbed state l is found to be

$$E_l = E_l^0 + \lambda E_l^{(1)} = E_l^0 + V_{ll}. \tag{D.11}$$

Then, using Eqs. (D.9) and (D.10) in Eq. (D.3), the first-order wavefunction becomes

$$\psi_l = \phi_l + \lambda a_l^{(1)} \phi_l + \sum_{m \neq l} \frac{V_{ml}}{E_l^0 - E_m^0} \phi_m. \tag{D.12}$$

In order that this expression yields the initial condition $\psi_l = \phi_l$ when $V_{m\ell} = 0$ after setting $\lambda = 1$, the coefficient in Eq. (D.12) must have the value $a_l^{(1)} = 0$. Hence,

$$\psi_l = \phi_l + \sum_{m \neq l} \frac{V_{ml}}{E_l^0 - E_m^0} \phi_m. \tag{D.13}$$

In second order we find

$$E_l^{(2)} = \sum_{m \neq l} \frac{V_{l,n} V_{nl}}{E_l^0 - E_n^0} \phi_m, \tag{D.14}$$

and

$$E_l = E_l^0 + V_{ll} + \sum_{n \neq l} \frac{|V_{l,n}|^2}{E_l^0 - E_n^0} \phi_m. \tag{D.15}$$

From this expression it follows that the second-order correction to the ground state energy of any system is *always negative* (when $E_\ell^0 < E_n^0$).

Perturbation theory is only valid if the expansion series converges. For this to take place, each correction must be smaller than the preceding one. That is, the condition

$$|H_{l,n}| = |V_{l,n}| << |E_l^0 - E_n^0| \tag{D.16}$$

must be fulfilled for all $m \neq l$.

Hence a necessary condition for validity of the perturbation method is that the distance between any given level and all other levels of the unperturbed problem must be large compared to the magnitude of the change in energy caused by the perturbation. Naturally this entails that the level ℓ cannot be degenerate, since otherwise the energy difference in the unperturbed problem would vanish.

Perturbation theory is also valid only if both the eigenfunctions and eigenvalues of $\hat{H}$ change continuously into those of the operator H_0 as $\lambda \to 0$. Sometimes this requirement is not satisfied when the character of the solution changes as the perturbation parameter vanishes. An example is provided by the evolution of a system from one with a discrete spectrum into one with a continuous spectrum. Consider a Hamiltonian with potential energy

$$U(x) = \frac{1}{2} \mu^2 \omega^2 x^2 + \lambda x^3. \tag{D.17}$$

For $\lambda = 0$, this is a harmonic oscillator with a discrete spectrum $E_n^0 (n + \frac{1}{2}) \hbar \omega$, as is well known. If λ is not 0 however, we find that the condition

$$\lambda \left| \langle m \left| x^3 n \right| \rangle \right| << \left| E_m^0 - E_n^0 \right| = \hbar \omega \left| m - n \right| \tag{D.18}$$

is always satisfied. For any nonvanishing value of λ, the spectrum of the perturbed Hamitonian is then continuous! For large, negative values of x, the potential energy

becomes lower than the total energy of the particle, so it can pass through the potential barrier in the direction of $x = -\infty$ and not return. This means that while the condition $|V_{lm}| << |E_l^0 - E_m^0|$ is necessary for perturbation theory to be applicable, it is not sufficient in itself to guarantee validity of the result.

B. Time-dependent perturbation theory

In time-dependent perturbation theory, the eigenstates of H_0 are taken to be the basis states of the problem, and the task of calculating the wavefunction simplifies to one of determining the time-varying superposition of these states caused by the interaction $V(t)$. This approach ignores the possibility that the basis states themselves are altered by the "perturbing" interaction $V(t)$, but for weak, nonresonant interactions this is acceptable. A perturbation parameter λ is used to keep track of the order in which each successive contribution to the approximate description arises.

$$H = H_0 + \lambda V(t), \tag{D.19}$$

$$\psi(\bar{r}, t) = \sum_n \left[C_n^{(0)} + \lambda C_n^{(1)} + \lambda^2 C_n^{(2)} + \ldots \right] U_n(\bar{r}) \exp(-i\omega_n t). \tag{D.20}$$

These expansions may be substituted into the Schrödinger equation $i\hbar \frac{\partial \psi}{\partial t} = H\psi$ to obtain

$$i\hbar \frac{\partial}{\partial t} \sum_n \left[C_n^{(0)}(t) + \lambda C_n^{(1)}(t) + \ldots \right] U_n(\bar{r}) \exp(-i\omega_n t)$$

$$= H_0 \sum_n \left[C_n^{(0)}(t) + \lambda C_n^{(1)}(t) + \ldots \right] U_n(\bar{r}) \exp(-i\omega_n t)$$

$$+ \lambda V \sum_n \left[C_n^{(0)}(t) + \lambda C_n^{(1)}(t) + \ldots \right] U_n(\bar{r}) \exp(-i\omega_n t), \tag{D.21}$$

$$i\hbar \sum_n \left[\dot{C}_n^{(0)}(t) + \lambda \dot{C}_n^{(1)}(t) + \ldots \right] U_n(\bar{r}) \exp(-i\omega_n t) + \hbar\omega_n \psi$$

$$= H_0 \psi + \lambda V \sum_n \left[C_n^{(0)}(t) + \lambda C_n^{(1)}(t) + \ldots \right] U_n(\bar{r}) \exp(-i\omega_n t). \tag{D.22}$$

Note that $H_0\psi = \hbar\omega_n\psi$. Hence, after multiplying both sides by $U_n(\bar{r}) * \exp(i\omega_n t)$, integrating over all space, and making use of the orthonormal properties of the eigenstates, one finds

$$i\hbar \left[\dot{C}_k^{(0)}(t) + \lambda \dot{C}_k^{(1)}(t) + \ldots \right]$$

$$= \sum_n \langle k| V |n\rangle [\lambda C_n^{(0)}(t) + \lambda^2 C_n^{(1)}(t) + \ldots] \exp(-i[\omega_n - \omega_k]t). \tag{D.23}$$

This yields

$$\left[\dot{C}_k^{(0)} + \lambda \dot{C}_k^{(1)} + \ldots \right] = \sum_n \frac{V_{kn}}{i\hbar} \left[\lambda C_n^{(0)} + \lambda^2 C_n^{(1)} + \ldots \right] \exp(-i[\omega_n - \omega_k]t). \tag{D.24}$$

Equating coefficients of various powers of λ:

$$\lambda^{(0)} : \dot{C}_k^{(0)} = 0, \tag{D.25}$$

$$\lambda^{(1)} : \dot{C}_k^{(1)} = \frac{V_{kn}}{i\hbar} \dot{C}_n^{(0)} \exp(-i[\omega_n - \omega_k]t), \tag{D.26}$$

$$\lambda^{(2)} : \dot{C}_k^{(2)} = \frac{V_{kn}}{i\hbar} \dot{C}_n^{(1)} \exp(-i[\omega_n - \omega_k]t). \tag{D.27}$$

By solving the equations for each order, an expression for the wavefunction valid to any desired degree of approximation may be obtained.

By solving the first-order equations for a sinusoidal perturbation, such as an optical field, an expression known as Fermi's golden rule can be derived for the transition rate between states that is valid for short times. Equation (D.25) shows that the zero-order coefficients $C_k^{(0)}$ are constant in time. We assume that all zero-order coefficients are 0 except one with $k = m$, so that prior to the onset of the perturbation the system is in an eigenstate of the unperturbed Hamiltonian. Integration of Eq. (D.25) then yields

$$C_k^{(1)}(t) = \frac{1}{i\hbar} \int\limits_{-\infty}^{t} V_{km}(t') \exp(-i[\omega_m - \omega_k]t')dt'. \tag{D.28}$$

The constant of integration has been set equal to 0 so that $C_k^{(1)}$ itself is 0 at $t = -\infty$. Note that if V is of finite duration, the probability amplitude of state $k(k \neq m)$ following the perturbation is proportional to the Fourier component of the perturbation between state k and m (see also Problem 6.2).

Next, we assume the perturbation is harmonic in time and is turned on at $t = 0$ and off at $t = t_0$. Thus

$$V_{km}(t') = 2V_{km} \cos(\omega t') \tag{D.29}$$

and

$$C_k^{(1)}(t \geq t_0) = -\frac{V_{km}}{\hbar} \left\{ \frac{\exp(i[\omega_{km} + \omega]t_0) - 1}{\omega_{km} + \omega} + \frac{\exp(i[\omega_{km} - \omega]t_0)}{\omega_{km} - \omega} \right\}. \tag{D.30}$$

Close to optical resonances, where $\omega_{km} - \omega \approx 0$, the second term in Eq. (D.30) is dominant. Hence one can simplify the calculation by making what is known as the rotating wave approximation (RWA) in which the first term is ignored. Then,

$$\left| C_k^{(1)}(t \geq t_0) \right|^2 = \left| \frac{V_{km}}{\hbar} \right|^2 t_0^2 \frac{\sin^2 \left[\frac{1}{2}(\omega_{km} - \omega)t_0 \right]}{\left[\frac{1}{2}(\omega_{km} - \omega)t_0 \right]^2}. \tag{D.31}$$

The factor of 2 inserted into Eq. (D.29) ensures that in the RWA the physically relevant matrix element is V_{km} rather than $V_{km}/2$ (see Ref. [D.1]). If we denote the transition probability per unit time as rate Γ_{km}, we now find

$$\Gamma_{km} = \frac{1}{t_0} \int \left| C_k^{(1)}(t \geq t_0) \right|^2 \rho(\omega_k)d\omega_k, \tag{D.32}$$

where $\rho(\omega_k)d\omega_k$ is the number of final states with frequencies between ω_k and $\omega_k + d\omega_k$. $\rho(\omega_k)$ is referred to as the density of final frequency states. If we change variables to $x \equiv \frac{1}{2}(\omega_{km} - \omega)t_0$, the integration is readily performed and yields

$$\Gamma_{km} = (2\pi/\hbar^2)\,|V_{km}|^2\,\rho(\omega_k). \tag{D.33}$$

For a monochromatic field, the perturbation is $V = V(\omega_0)$. Assuming the transition is between discrete states, whereupon the density of final states can be written as $\rho(\omega) = \delta(\omega - \omega_0)$, Eq. (D.33) simplifies to the expression

$$\Gamma(\omega) = (2\pi/\hbar^2)\,|V(\omega_0)|^2\,\delta(\omega - \omega_0) \tag{D.34}$$

for the transition rate. Calculations of transition rates based on Fermi's golden rule in Eq. (D.34) give results in agreement with those of Section 3.5 upon specification of the corresponding spectral density of the optical field.

C. Perturbation theory with the density matrix

The approach outlined in Section B of this Appendix can also be applied to time-dependent perturbation analysis of the density matrix. In this case, the expressions for the density matrix and the interaction are written

$$\rho = \rho^{(0)} + \lambda\rho^{(1)} + \lambda^2\rho^{(2)} + \lambda^3\rho^{(3)} + \dots, \tag{D.35}$$

$$V = V^{(0)} + \lambda V^{(1)} + \lambda^2 V^{(2)} + \lambda^3 V^{(3)} + \dots, \tag{D.36}$$

and upon substitution into the equation of motion

$$i\hbar\frac{\partial\rho}{\partial t} = [H_0, \rho] + [V, \rho] + i\hbar\frac{\partial\rho}{\partial t}\,|_{\text{relax}}, \tag{D.37}$$

one obtains

$$i\hbar\frac{\partial}{\partial t}\left(\rho^{(0)} + \lambda\rho^{(1)} + \lambda^2\rho^{(2)} + \lambda^3\rho^{(3)} + \dots\right)$$
$$= \left[H_0, \rho^{(0)} + \lambda\rho^{(1)} + \lambda^2\rho^{(2)} + \lambda^3\rho^{(3)} + \dots\right]$$
$$+ \left[V^{(0)} + \lambda V^{(1)} + \lambda^2 V^{(2)} + \lambda^3 V^{(3)} + \dots, \rho^{(0)} + \lambda\rho^{(1)} + \lambda^2\rho^{(2)} + \lambda^3\rho^{(3)} + \dots\right]. \tag{D.38}$$

Equating coefficients of corresponding orders of λ on the left and right side of Eq. (D.38), one finds

Zeroth-order $\lambda^{(0)}$:

$$i\hbar\frac{\partial}{\partial t}\rho^{(0)} = \left[H_0, \rho^{(0)}\right] + \left[V^{(0)}, \rho^{(0)}\right] + i\hbar\frac{\partial}{\partial t}\rho^{(0)}\bigg|_{\text{relax}}, \tag{D.39}$$

First-order $\lambda^{(1)}$:

$$i\hbar\frac{\partial}{\partial t}\rho^{(1)} = \left[H_0, \rho^{(1)}\right] + \left[V^{(0)}, \rho^{(1)}\right] + \left[V^{(1)}, \rho^{(0)}\right] + i\hbar\frac{\partial}{\partial t}\rho^{(1)}\bigg|_{\text{relax}}, \tag{D.40}$$

Second-order λ^2:

$$i\hbar\frac{\partial}{\partial t}\rho^{(2)} = \left[H_0, \rho^{(2)}\right] + \left[V^{(0)}, \rho^{(2)}\right] + \left[V^{(1)}, \rho^{(1)}\right] + \left[V^{(2)}, \rho^{(0)}\right] + i\hbar\frac{\partial}{\partial t}\rho^{(2)}\bigg|_{\text{relax}},$$

$$(D.41)$$

Third-order λ^3:

$$i\hbar\frac{\partial}{\partial t}\rho^{(3)} = \left[H_0, \rho^{(3)}\right] + \left[V^{(0)}, \rho^{(3)}\right] + \left[V^{(1)}, \rho^{(2)}\right] + \left[V^{(2)}, \rho^{(1)}\right]$$

$$+ \left[V^{(3)}, \rho^{(0)}\right] + i\hbar\frac{\partial}{\partial t}\rho^{(3)}\bigg|_{\text{relax}}, \qquad (D.42)$$

and so on for higher orders.

In practice, one finds that matrix elements for populations are 0 in odd orders and nonzero in even orders of perturbation. This corresponds to the simple physical fact that interactions begin with populations in eigenstates and coherence can only be established by the action of an applied field. Thus one order of perturbation is required to establish polarization. Only after a superposition state has been established that includes a new state can the distribution of population change. Consequently, population change appears in the next order of perturbation. The procedure for solving the equations of motion (Eqs. (D.39)–(D.41)) begins with the determination of first-order coherences – the off-diagonal elements of the density matrix – and then proceeds to populations. Note that once the contributions $\rho^{(0)}, \rho^{(1)}, \rho^{(2)}, \rho^{(3)}, \ldots$ to the desired order are determined, they must be added according to Eq. (D.35) to find $\rho(t)$ itself to that order, after setting $\lambda = 1$.

References

D.1. L.I. Schiff, *Quantum Mechanics*, 3rd edition, McGraw-Hill, New York, 1968, p. 283.

D.2. A.S. Davydov, *Quantum Mechanics*, 2nd edition, Pergamon Press, Oxford, 1976, p. 189.

Appendix E

Second Quantization of Fermions

With few exceptions, the systems considered in examples and problems of this book are assumed to be bosonic in character. That is, they are assumed not to have occupation probabilities dominated by spin-related considerations. Their spectra generally have large numbers of energy levels and their statistics are governed by the Bose–Einstein distribution, unlike fermionic systems that have a very small number of energy levels and obey Fermi–Dirac statistics (to describe the latter we shall follow the discussion in Ref. [E.1]). This of course ignores the important role played by the Pauli exclusion principle in many systems of practical importance, such as semiconductors, as well as the possibility of converting bosonic systems into fermionic systems and vice versa by altering experimental conditions. At the end of Chapter 3, an example of the conversion of a multilevel atom into a two-level atom was considered, and other examples can be

found in the literature on Bose–Einstein condensates near Feshbach resonances [E.2]. Here we briefly consider some of the implications of the exclusion principle that were omitted in earlier discussions.

Fermions obey population statistics that are different from those of bosons, and this difference is reflected in the commutation relations for fermionic operators. Fermionic operators *anti-commute*. For example, the annihilation and creation operators of a fermionic state labelled with index k, namely $\hat{\alpha}_k$ and $\hat{\alpha}_k^+$, obey the commutation rules:

$$[\hat{\alpha}_k, \hat{\alpha}_\ell]_+ = [\hat{\alpha}_k^+, \hat{\alpha}_\ell^+]_+ = 0,$$

$$[\hat{\alpha}_k, \hat{\alpha}_\ell^+]_+ = \delta_{k\ell}, \tag{E.1}$$

where the symbol $[\ldots]_+$ implies the sum $[\hat{\alpha}, \hat{\beta}]_+ \equiv \hat{\alpha}\hat{\beta} + \hat{\beta}\hat{\alpha}$.

Other than electrons, what systems are fermionic, and do they exhibit familiar features? On the basis of Eq. (E.1) and our earlier representation of two-level atoms by anti-commuting Pauli matrices, we may infer that two-level atoms are fermionic as one example. On the other hand, electromagnetic fields and simple harmonic oscillators, both of which are characterized by an infinite number of equally spaced energy levels, are bosonic. In this Appendix we discuss differences in the way wave functions are constructed for fermionic and bosonic systems, while emphasizing that their system energies share a simple feature in the limit of weak interactions.

Define a fermionic number operator $\hat{N}_k = \hat{\alpha}_k^+ \hat{\alpha}_k$ and note that according to Eq. (E.1)

$$\hat{N}_k^2 = \hat{\alpha}_k^+ \hat{\alpha}_k \hat{\alpha}_k^+ \hat{\alpha}_k = \hat{\alpha}_k^+ \left(1 - \hat{\alpha}_k^+ \hat{\alpha}_k\right) \hat{\alpha}_k = \hat{\alpha}_k^+ \hat{\alpha}_k = \hat{N}_k. \tag{E.2}$$

If $\hat{N}_k$ has eigenvalues n_k, then obviously

$$n_k^2 = n_k \rightarrow n_k = 0, 1. \tag{E.3}$$

For a given state k, the operator $\hat{N}$ can be represented by the diagonal matrix

$$\hat{N} = \begin{bmatrix} 0 & 0 \\ 0 & 1 \end{bmatrix}, \tag{E.4}$$

when there is no energy level degeneracy.

Suitable matrices for $\hat{\alpha}, \hat{\alpha}^+$ which are consistent with the commutation relations are

$$\hat{\alpha} = \begin{bmatrix} 0 & 1 \\ 0 & 0 \end{bmatrix},$$

$$\hat{\alpha}^+ = \begin{bmatrix} 0 & 0 \\ 1 & 0 \end{bmatrix}. \tag{E.5}$$

The two possible states of the system are

$$|0\rangle = \begin{bmatrix} 1 \\ 0 \end{bmatrix},$$

$$|1\rangle = \begin{bmatrix} 0 \\ 1 \end{bmatrix}, \tag{E.6}$$

and it is easily verified that $\hat{\alpha}$ and $\hat{\alpha}^+$ play the roles of destruction and creation operators, respectively. That is,

$$\hat{\alpha}|n> = n|1-n>; \quad \hat{\alpha}^+|n> = (1-n)|1-n>, \tag{E.7}$$

where $n = 0, 1$.

To describe a complete system of fermions, we must introduce the exclusion principle by permitting the sign of the wavefunction to be altered by the action of $\hat{\alpha}, \hat{\alpha}^+$. Order the states of the system in an arbitrary but definite way, for example $1, 2 \ldots k \ldots$. Then permit $\hat{\alpha}_k, \hat{\alpha}_k^+$ to act as before, except that the sign will be determined by whether the kth state is preceded in the assumed order by an even or odd number of occupied states.

$$\hat{\alpha}_k|n_1, \cdots n_k, \cdots> = \theta_k n_k|n_1, \cdots 1 - n_k, \cdots>,$$

$$\hat{\alpha}_k^+|n_1, \cdots n_k, \cdots> = \theta_k (1 - n_k)|n_1, \cdots 1 - n_k, \cdots>, \tag{E.8}$$

$$\theta_k \equiv (-)^{\nu_k}; \nu_k \equiv \sum_{j=1}^{k-1} n_j.$$

ν_k is the number of states, preceding state k, which are occupied. For a particular single particle state k of the system, it is easy to show that

$$\hat{\alpha}_k \hat{\alpha}_k^+|\cdots n_k \cdots> = (1 - n_k)^2 \theta_k^2|\cdots n_k \cdots>$$

$$= (1 - n_k)|\cdots n_k \cdots>,$$

$$\hat{\alpha}_k^+ \hat{\alpha}_k|\cdots n_k \cdots> = n_k|\cdots n_k \cdots>,$$

$$\hat{\alpha}_k \hat{\alpha}_k|\cdots n_k \cdots> = n_k (1 - n_k)|\cdots n_k \cdots> = 0, \tag{E.9}$$

$$\hat{\alpha}_k^+ \hat{\alpha}_k^+|\cdots n_k \cdots> = \hat{\alpha}_k^+ \theta (1 - n_k)|\cdot (1 - n_k) \cdots>$$

$$= \theta^2 (1 - n_k) n_k|\cdots n_k \cdots>$$

$$= 0,$$

From these relations it is easily seen that the commutation relations given by Eqs. (E.1) are satisfied for $k = \ell$. For example,

$$\left[\hat{\alpha}_k, \hat{\alpha}_k^+\right] = 1 - n_k + n_k = 1. \tag{E.10}$$

For $k \neq \ell \, (k > \ell)$,

$$\hat{\alpha}_\ell \hat{\alpha}_k|\cdots n_\ell \cdots n_k \cdots> = \theta_k n_k \hat{\alpha}_\ell|\cdots n_\ell \cdots|1 - n_k \cdots>$$

$$= \theta_k \theta_\ell n_k n_\ell|\cdots 1 - n_\ell \cdots 1 - n_k \cdots>,$$

$$\hat{\alpha}_k \hat{\alpha}_\ell|\cdots n_\ell \cdots n_k \cdots> = \theta_\ell n_\ell \hat{\alpha}_k|\cdots 1 - n_\ell \cdots n_k \cdots> \tag{E.11}$$

$$= \theta_{k-1} \theta_\ell n_\ell n_k|\cdots 1 - n_\ell \cdots 1 - n_\ell \cdots 1 - n_k \cdots>.$$

Hence, $\hat{\alpha}_\ell \hat{\alpha}_k + \hat{\alpha}_k \hat{\alpha}_\ell \Rightarrow (-1)^{k+\ell} n_k n_\ell + (-)^{k+\ell-1} n_k n_\ell = 0$. Remaining commutation relations are satisfied in the same way.

Notice from this that the result of applying Fermi operators $\hat{\alpha}_k \hat{\alpha}_k^+$ depends not only on occupation number k but also on the occupation numbers of all preceding states. Thus α_k and α_ℓ are not entirely independent. This means that the order of processes in fermionic systems is even more important to the outcome of interactions than it is for bosonic systems.

In the configuration representation we would write the total system Hamiltonian as

$$\hat{H}\left(\xi, \xi_2, \ldots, \xi_n\right) = \sum_{i=1}^{N} \hat{H}\left(\xi_i\right), \tag{E.12}$$

where ξ_i gives the spatial and spin coordinates of each of the N fermions. Here $\hat{H}(\xi_i)$ is the single particle Hamiltonian for the particle specified by ξ_i. Single particle states $\phi_s(\xi_i)$ and their eigenvalues ε_s are determined by

$$\left[\hat{H}\left(\xi\right) - \varepsilon_s\right] \phi_s\left(\xi\right) = 0. \tag{E.13}$$

To see what the form of the total system Hamiltonian is in the occupation number representation, we introduce field operators $\hat{\psi}$ defined by

$$\psi\left(\xi, t\right) = \sum_s \hat{\alpha}_s \phi_s\left(\xi\right) \exp(-i\omega_s t), \tag{E.14}$$

where $\omega_s \equiv \varepsilon_s / \hbar$ and write the total Hamiltonian in the form

$$\hat{H} = \int \hat{\psi}^+\left(\xi\right) \hat{H}\left(\xi\right) \hat{\psi}\left(\xi\right) d\left(\xi\right), \tag{E.15}$$

where the integration includes a sum over spin variables σ. At a fixed time t we can show that

$$\left[\hat{\psi}\left(\xi'\right), \psi^+\left(\xi\right)\right] = \sum \phi_s\left(\xi'\right) \phi_\ell^*\left(\xi\right) \left[\hat{\alpha}_s, \hat{\alpha}_\ell^+\right]_+ = \delta\left(\xi' - \xi\right), \tag{E.16}$$

where

$$\delta\left(\xi' - \xi\right) = \delta_{\sigma\sigma'} \delta\left(\vec{r}' - \vec{r}\right). \tag{E.17}$$

Similarly,

$$\left[\hat{\psi}\left(\xi'\right), \hat{\psi}\left(\xi\right)\right]_+ = \left[\hat{\psi}^+\left(\xi'\right), \psi^+\left(\xi\right)\right]_+ = 0. \tag{E.18}$$

Substituting these expressions into the integral representation of the Hamiltonian operator, we find

$$\hat{H} = \sum_s \varepsilon_s \hat{\alpha}_s^+ \hat{\alpha}_s = \sum_s \hat{n}_s \varepsilon_s. \tag{E.19}$$

This result shows that the energy of a system of non-interacting fermions is just the sum of the individual particle energies, a familiar result that holds for purely bosonic systems also. In interacting systems of fermions, a similar decomposition of the system

into a simple sum of (renormalized) individual particle energies can only be performed for extremely weak interactions that can be taken into account via an effective field. For this to be true, the fermions have to be widely spaced. For close particles and strong interactions, the concept of single particle states and single particle energies breaks down completely. Equations (E.12) and (E.19) are no longer valid in this limit. In order to ensure that no two fermions have the same wavefunction (occupy the same state), many body techniques are required for analysis.

References

E.1. A.S. Davydov, *Quantum Mechanics*, 2nd edition, Pergamon Press, Oxford, 1976, p. 362.

E.2. See, for example, C.A. Regal, M. Geiner, and D.S. Lin, Phys. Rev. Lett. **92**, 040403(2004).

Appendix F

Frequency Shifts and Decay due to Reservoir Coupling

A single parameter such as the decay constant γ introduced in Chapter 3 is typically thought to account for a single process, such as the rate of population decay in two-level atoms. However, here we show on the basis of perturbation theory that as many as four fundamentally different physical processes are linked to the decay constants in our description of atomic dynamics.

In Section 6.3 an exponential form was derived for the population decay of a two-level system via spontaneous emission. This justified the assumed form of phenomenological decay terms in Chapter 3, where perturbation theory was used to solve for the probability amplitudes of a two-level system undergoing radiative decay after being prepared in the excited state.

$$C_2^{(1)}(t) = \exp(-\gamma_2 t/2), \tag{F.1}$$

for times short compared to lifetime γ_1^{-1} but long compared to field periods. The process of emission from $|2\rangle$ to $|1\rangle$ also excites one of many radiation modes of the electromagnetic field. These modes are labeled by index λ. Then, setting $(\Omega_{21})_\lambda \equiv \mu_{21}E_\lambda/\hbar$ in the rate equations of Chapter 3, one finds

$$(\dot{C}_1)_\lambda = \sum_\lambda \frac{i}{2}(\Omega_{21})_\lambda \exp(-i[\omega_0 - \omega_\lambda]t)(C_2)_\lambda, \tag{F.2}$$

$$(\dot{C}_2)_\lambda = \sum_\lambda \frac{i}{2}(\Omega_{12})_\lambda \exp(i[\omega_0 - \omega_\lambda]t)(C_1)_\lambda \tag{F.3}$$

by ignoring the effect of decay at short times. Substitution of Eq. (F.1) into Eq. (F.2) then yields

$$(\dot{C}_1)_\lambda = \sum_\lambda \frac{i}{2}(\Omega_{21})_\lambda \exp(-i[\omega_0 - \omega_\lambda]t - \gamma_2 t/2). \tag{F.4}$$

This is easily solved to give

$$\left(C_1^{(1)}\right)_\lambda (t) = \sum_\lambda \frac{i}{2}(\Omega_{21})_\lambda \left[\frac{\exp(-i[\omega_0 - \omega_\lambda]t - \gamma_2 t/2) - 1}{-i[\omega_0 - \omega_\lambda] - \frac{1}{2}(\gamma_2 - \gamma_1)}\right]. \tag{F.5}$$

Now we use the first order perturbation results to extract a general form of γ_2. Upon substitution of Eqs. (F.1) and (F.5) into Eq. (F.3), we find

$$-\frac{\gamma_2}{2}\exp(-\gamma_2 t/2) = \sum_\lambda \left(\frac{i}{2}\right)^2 |(\Omega_{12})_\lambda|^2 \left[\frac{\exp(-\gamma_2 t/2) - \exp(i[\omega_0 - \omega_\lambda]t)}{-i[\omega_0 - \omega_\lambda] - \frac{1}{2}(\gamma_2 - \gamma_1)}\right]$$

or

$$\gamma_2 = \frac{1}{2}\sum_\lambda |(\Omega_{12})_\lambda|^2 \left[\frac{1 - \exp(i[\omega_0 - \omega_\lambda]t + \gamma_2 t/2)}{-i[\omega_0 - \omega_\lambda] - \frac{1}{2}(\gamma_2 - \gamma_1)}\right]. \tag{F.6}$$

Replacing the summation over modes with an integral over the density of modes $D(\omega) = V\omega^2/\pi^2 c^3$ available per unit frequency interval according to

$$\sum_\lambda \rightarrow \int V\rho(\omega)d\omega, \tag{F.7}$$

Eq. (F.6) becomes

$$\gamma_2 = \frac{1}{2}\int |\Omega_{12}(\omega)|^2 \left[\frac{1 - \exp(i[\omega_0 - \omega]t + \gamma_2 t/2)}{-i[\omega_0 - \omega] - \frac{1}{2}(\gamma_2 - \gamma_1)}\right] D(\omega)d\omega. \tag{F.8}$$

For convenience we define the factor

$$f(\omega) \equiv \frac{1}{2}|\Omega_{12}(\omega)|^2 D(\omega), \tag{F.9}$$

in terms of which our general expression for γ_2 becomes

$$\gamma_2 = i\int_\omega f(\omega) \left[\frac{1 - \exp(i[\omega_0 - \omega]t + \gamma_2 t/2)}{[\omega_0 - \omega] - \frac{i}{2}(\gamma_2 - \gamma_1)}\right] d\omega. \tag{F.10}$$

If $(\gamma_2 - \gamma_1) << \omega$ the denominator in Eq. (F.10) simplifies to $\sim [\omega_0 - \omega]^{-1}$, and at short times the portion of the integrand in square brackets simplifies to

$$Lim_{t\rightarrow\infty} \left[\frac{1 - \exp(i[\omega_0 - \omega]t + \gamma_2 t/2)}{[\omega_0 - \omega] - \frac{i}{2}(\gamma_2 - \gamma_1)}\right] \approx \left[\frac{1 - \cos(\omega_0 - \omega)t}{(\omega_0 - \omega)}\right] + i\left[\frac{\sin(\omega_0 - \omega)t}{(\omega_0 - \omega)}\right]$$

$$= \boldsymbol{P}\left\{\frac{1}{(\omega_0 - \omega)}\right\} + i\pi\delta(\omega_0 - \omega), \quad \text{(F.11)}$$

where $\boldsymbol{P}$ denotes the principal part. With this simplification, Eq. (F.10) becomes

$$\gamma_2 \propto \int_\omega \left\{i\boldsymbol{P}\left[\frac{1}{\omega_0 - \omega}\right] - \pi\delta(\omega_0 - \omega)\right\} f(\omega)d\omega. \tag{F.12}$$

This development shows (with only first-order perturbation theory) that finite lifetime, and the coupling to radiation modes that causes it, leads to a separation of γ_b into real and imaginary parts. Thus,

$$\gamma_2 = \gamma_r + i\gamma_{im}, \tag{F.13}$$

where the associated expressions are given by

$$\gamma_{im} \propto \frac{1}{2}\boldsymbol{P}\left\{\int \frac{|\Omega_{12}(\omega)|^2}{\omega_0 - \omega} D(\omega)d\omega\right\}, \tag{F.14}$$

$$\gamma_r \propto -\frac{\pi}{2}D(\omega_0)\left|\Omega_{12}(\omega_0)\right|^2. \tag{F.15}$$

The decay processes in Eqs. (F.14) and (F.15) are both induced by real optical fields, as is apparent by their mutual dependencies on $|\Omega_{12}|^2$. Now we are in a position to gain some perspective on the purely quantum mechanical effects that result from quantization of the radiation field by taking into account that the total electric field includes the vacuum state which does not depend on mode occupation number n_λ, and a part which does depend on n_λ. By recognizing that according to Sections 6.2 and 6.3 fluctuations of the vacuum field can induce spontaneous decay in much the same manner that the photon field induces stimulated relaxation, we see that the imaginary and real rate constants above split into two additional parts corresponding to spontaneous and stimulated processes. That is,

$$\gamma_2 = \gamma_r^{(\text{spont})} + \gamma_r^{(\text{induced})} + i\gamma_{im}^{(\text{spont})} + i\gamma_{sm}^{(\text{induced})}. \tag{F.16}$$

The physical effects of relaxation are reflected in the frequency and time dependence of the emitted radiation. That is, the field leaving the atom has the form

$$E \propto \exp(-i\omega_0 t)\cdot\exp(-\gamma_2 t)$$
$$= \exp\left[-i\left(\omega_0 + \gamma_{im}^{(\text{spont})} + \gamma_{im}^{(\text{induced})}\right)\right]\cdot\exp\left[-\left(\gamma_r^{(\text{spont})} + \gamma_r^{(\text{induced})}\right)t\right]. \tag{F.17}$$

As a result of atom–field coupling four important processes take place, namely spontaneous decay, stimulated decay, the Lamb shift, and the AC Stark shift. This is illustrated in Fig. F.1.
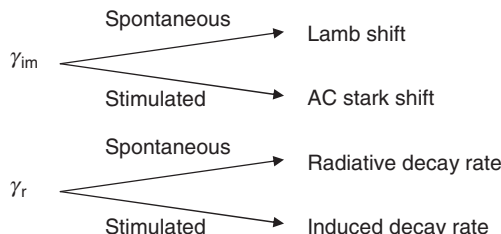
Figure F.1 *Four fundamental, distinguishable physical processes that are intimately linked to field-driven decay of atoms*

Appendix G

Solving for Off-diagonal Density Matrix Elements

Off-diagonal elements of the density matrix describe charge oscillations initiated by applied fields. Hence, the full temporal evolution of their amplitudes reflects transient buildup (or decay) of an oscillation prior to the establishment of any steady-state amplitude. The frequency of the oscillation is ω, as determined by the driving field. Hence the general form of the solution is

$$\rho_{ij}(t) = \tilde{\rho}_{ij}(t)\exp(i\omega t), \tag{G.1}$$

where i, j specify the initial and final states of the transition closest in frequency to ω and $\tilde{\rho}_{ij}$ is the slowly varying amplitude of the polarization.

The time derivative of ρ_{ij} is

$$\dot{\rho}_{ij} = \dot{\tilde{\rho}}_{ij}\exp(i\omega t) + i\omega\tilde{\rho}_{ij}\exp(i\omega t). \tag{G.2}$$

If the assumption is made that $\dot{\tilde{\rho}}_{ij} = 0$, then substitution of Eq. (G.2) into the equation of motion yields an algebraic equation that may be readily solved to find the steady-state solution. More generally $\dot{\tilde{\rho}}_{ij} \neq 0$, and the equation of motion must be integrated to find a solution, as follows.

Take the interaction to be

$$V_{ij}(t) = \frac{1}{2}\left[\tilde{V}_{ij}(t)\exp(i\omega t) + \tilde{V}_{ij}^{*}(t)\exp(-i\omega t)\right]. \tag{G.3}$$

Substituting Eqs. (G.3) and (G.2) into the equation of motion for a two-level system, as an example, one finds

$$\dot{\tilde{\rho}}_{12} = i\Delta\tilde{\rho}_{12} + (\tilde{V}_{12}/2i\hbar)(\rho_{22} - \rho_{11}) - \Gamma_{12}\tilde{\rho}_{12}, \tag{G.4}$$

where $\Delta \equiv \omega_0 - \omega$. Next, use is made of an integrating factor through the substitution of

$$\tilde{\rho}_{12} = \tilde{\rho}_{12}'\exp[(i\Delta - \Gamma)t]. \tag{G.5}$$

This yields

$$\dot{\tilde{\rho}}_{12}'\exp[(i\Delta - \Gamma)t] + (i\Delta - \Gamma)\tilde{\rho}_{12}'\exp[(i\Delta - \Gamma)t]$$
$$= (i\Delta - \Gamma)\tilde{\rho}_{12}'\exp[(i\Delta - \Gamma)t] + (\tilde{V}_{12}/2i\hbar)(\rho_{22} - \rho_{11}),$$

or

$$\dot{\tilde{\rho}}_{12}' = (\tilde{V}_{12}/2i\hbar)(\rho_{22} - \rho_{11})\exp[-(i\Delta - \Gamma)t]. \tag{G.6}$$

The next step is to integrate over time between appropriate limits, for example 0 and t. One finds

$$\tilde{\rho}_{12}' = \frac{-i}{2\hbar}\int_0^t \tilde{V}_{12}(t')(\rho_{22}(t') - \rho_{11}(t'))\exp[-(i\Delta - \Gamma)t']dt'. \tag{G.7}$$

If the interaction starts at time zero, as assumed in Eq. (G.7), then the integral must be performed by taking the transient buildup of the envelope function $\tilde{V}_{12}(t')$ into account.

Since $\tilde{V}_{12}(t')$ itself cannot be approximated by a constant over the interval of integration, it cannot be removed from the integral. The steady-state solution, identical to that obtained by solving Eq. (G.4) algebraically with the assumption $\dot{\tilde{\rho}}_{12} = 0$, may be found directly after setting the lower limit of integration equal to $t' = -\infty$ and integrating by parts.

$$\int_{-\infty}^{t} \tilde{V}_{12}(t')(\rho_{22}(t') - \rho_{11}(t')) \exp[-(i\Delta - \Gamma)t']dt'$$

$$= \left[\frac{\tilde{V}_{12}(t')(\rho_{22}(t') - \rho_{11}(t')) \exp[-(i\Delta - \Gamma)t']}{-(i\Delta - \Gamma)} \right]_{-\infty}^{t} +$$

$$- \int_{-\infty}^{t} \left(\frac{d}{dt'} \tilde{V}_{12}(t')(\rho_{22}(t') - \rho_{11}(t')) \right) \frac{\exp[-(i\Delta - \Gamma)t']}{-(i\Delta - \Gamma)} dt'. \quad (G.8)$$

Under steady-state conditions ($\dot{\rho}_{11} = \dot{\rho}_{22} = 0$), assuming the interaction is turned on adiabatically at early times so that $d\tilde{V}_{12}(t')/dt' \cong 0$, the second integral on the right is zero. One therefore finds the result

$$\frac{-i}{2\hbar} \int_{-\infty}^{t} \tilde{V}_{12}(t')(\rho_{22}(t') - \rho_{11}(t')) \exp[-(i\Delta - \Gamma)t']dt'$$

$$= \frac{i}{2\hbar} \left[\frac{\tilde{V}_{12}(t) \exp[-(i\Delta - \Gamma)t]}{(-i\Delta + \Gamma)} \right] (\rho_{11}(t) - \rho_{22}(t)), \quad (G.9)$$

and

$$\tilde{\rho}'_{12}(t) = \frac{i\tilde{V}_{12}(t)}{2\hbar(-i\Delta + \Gamma)} (\rho_{11}(t) - \rho_{22}(t)) \exp[-(i\Delta - \Gamma)t]. \quad (G.10)$$

Using Eq. (G.10) in Eq. (G.5), the steady-state value for the slowly varying polarization amplitude is found to be

$$\tilde{\rho}_{12} = \frac{-\tilde{V}_{12}}{2\hbar(\Delta + i\Gamma)} (\rho_{11} - \rho_{22}) = \frac{(\Omega_{12}/2)}{(\Delta + i\Gamma)} (\rho_{11} - \rho_{22}), \quad (G.11)$$

and the final result for the off-diagonal coherence (polarization) is therefore

$$\rho_{12}(t) = \left(\frac{\Omega_{12}/2}{\Delta + i\Gamma} \right) (\rho_{11}(t) - \rho_{22}(t)) \exp(i\omega t). \quad (G.12)$$

This result is the same as that obtained by substituting Eq. (G.2) into the equation of motion for ρ_{12} after setting $\dot{\tilde{\rho}}_{12} = 0$. Determinations of ρ_{12} that include transient behavior associated with a rapid onset of the interaction must include an evaluation of the second term on the right of Eq. (G.8), since then $d\tilde{V}_{12}(t')/dt' \neq 0$. Similarly, population oscillations or rapid population dynamics require a full evaluation of Eq. (G.8). A useful alternative is to assume the interaction appears instantaneously ("sudden" approximation) at $t = 0$, and to evaluate the integral using (G.7). However, for steady-state conditions, we note that the result in Eq. (G.12) agrees with the result obtained in Chapter 5 using the simple substitutions $\rho_{12}(t) = \tilde{\rho}_{12} \exp(i\omega t)$ and $\dot{\tilde{\rho}}_{12} = 0$.

Appendix H

Irreducible Spherical Tensor Operators and the Wigner–Eckart (W–E) Theorem

In our introductions to various sciences, most of us encounter problems that seem to have a set of "natural" coordinates associated with them. By choosing "natural" coordinates one can simplify the mathematical analysis. Good choices correspond to descriptions that mimic one or more symmetry elements of the problem. "Unnatural" coordinates give rise to unwieldy expressions that are unnecessarily complicated. Consequently, an entire subject is devoted to identification and exploitation of the simplest mathematical formalism to use in analyzing any problem, namely group theory. Because group theory is an important subject that transcends the limited objectives of this book, and can be a very powerful companion in the analysis of optical problems we shall not diminish it by attempting to introduce it here. However, some exposure to key results that can be explained succinctly is beneficial for application to the advanced topics considered in Chapters 6 and 7 of this book. Consequently, this appendix covers the essentials of tensor analysis to explain what is known as the "irreducible" representation of physical problems.

A pure rotation R transforms a state vector ψ into ψ' via a unitary transformation U_R that acts on each component in the same way that spatial coordinates transform.

$$\psi' = U_R \psi. \tag{H.1}$$

In an analogous fashion, operators V_i $(i = 1, 2, 3)$ are said to form the Cartesian components of a vector operator V, if under every rotation their expectation values transform like components of a vector. Thus a vector operator is required to have expectation values that transform according to the equation

$$\langle \psi \, |V_i| \, \psi \rangle' = \sum_{j=1}^{3} R_{ij} \langle \psi \, |V_j| \, \psi \rangle , (i, j = 1, 2, 3). \tag{H.2}$$

The entries in the rotation matrix $R_{ij} = \partial x'_i / \partial x_j$ are cosines of the angles between the rotated positive x'_i-axis and the positive x_j-axis prior to rotation [H.1] describing the transformation of the coordinates.

Substitution of Eq. (H.1) into Eq. (H.2) yields

$$\langle \psi \,|U_R^+ \, VU_R| \, \psi \rangle = \sum_{j=1}^{3} R_{ij} \, \langle \psi \,|V_j| \, \psi \rangle \,,$$

$$V_i' = U_R^+ \, VU_R = \sum_{j=1}^{3} R_{ij} V_j, \tag{H.3}$$

since the relation should hold for arbitrary ψ.

We now proceed to generalize Eq. (H.3) to operators of higher rank than vectors. Vectors are tensors of rank one ($k = 1$) that have three spatial components related to x, y, and z. Tensors of rank two ($k = 2$) can be thought of as the most general product of two vector operators $\bar{V}_{1m}$ and $\bar{V}_{2n}$. They therefore consist of the set of all nine products of the vector components (i.e., $V_{1m}V_{2n}$ for $m, n = x, y, z$). Irreducible spherical tensors are constructed in a basis that reflects the rotational symmetry of a sphere. So, a spherical tensor operator of arbitrary rank k will be defined more generally as a set of quantities $[T^{(k)}]_j$ which obey a transformation law similar to Eq. (H.3), except that we shall assume it is of covariant form, which transforms as the inverse of Eq. (H.3), and write it in a basis that distinguishes clockwise from counterclockwise rotations.

As a first step in determining the conventional expression for the tensor transformation law, consider extending Eq. (H.3) to the case of a second rank tensor with all Cartesian indices written out explicitly. The required transformation has the form

$$(T)'_{ij} = \sum_{k,l} \frac{\partial x_k}{\partial x_i'} \frac{\partial x_l}{\partial x_j'} T_{kl} = \sum_{k,l} D_{klij} T_{kl}, \tag{H.4}$$

where the transformation coefficients are $D_{klij} = \frac{\partial x_k}{\partial x_i'} \frac{\partial x_l}{\partial x_j'}$. Now, the notation applicable to tensors of all ranks uses an index q (where $q = \{-k, -k+1, -k+2, \ldots +k\}$) to replace multiple Cartesian subscripts referring to individual components of the tensor. In addition, we note a distinction is introduced between D and R. We shall insist that D be the simplest possible representation of rotations, or in other words that it be "irreducible" in addition to producing the desired transformation for rank k tensors. Irreducible tensors consist of the minimum number of independent elements that span a given space, formed into linear combinations of Cartesian components that present the least mathematical complexity, and they mimic the properties and dynamics of objects and processes in the real world with which we are familiar.

Thus the tensor transformation law is a notationally simplified version of Eq. (H.4) that uses the index q and coefficients $D_{q'q}^{(k)}$ from a unitary rotation based on the angular momentum operator.

$$(T_q^{(k)})' = \sum_{q'=-k}^{k} T_{q'}^{(k)} D_{q'q}^{(k)}(R). \tag{H.5}$$

A direct comparison with vector transformation components is possible after inversion of Eq. (H.3).

$$(V_j)' = \sum_{i=1}^{3} V_i R_{ij}. \tag{H.6}$$

Notice the summation in Eq. (H.6) is over the first subscript of R, just as the summation in Eq. (H.5) is over the first subscript of $D_{q'q}^{(k)}$.

Equation (H.5) now defines tensor operator components that transform like irreducible components of vectors. This equation can be used to test whether quantities of interest have the tensor properties required to provide the simplest mathematical description of system states, energies, and dynamics. It can also be used to determine explicit components of tensors in terms of vector Cartesian components. For example we make use of Eq. (H.5) below to determine the components of a rank one tensor $T^{(1)}$. However, it proves to be more convenient to work with commutation relations that are equivalent to the transformation rules than to use Eq. (H.5) itself.

To find the commutation relations of interest, we proceed by substituting the irreducible form for infinitesimal rotations into Eq. (H.5). The axis and magnitude of the rotation are specified by axial vector $\bar{\varepsilon}$, and only terms up to first order will be considered. Borrowing expressions for the lowest order terms of the Wigner D coefficients that represent three-dimensional irreducible rotations (see, for example, Eq. (16.54) of Ref. [H.2]), we have

$$D_{m'm}^{(i)}(\bar{\varepsilon}) = \delta_{m'm} - \frac{i\varepsilon_x + \varepsilon_y}{2}\sqrt{(j-m)(j+m+1)}\delta_{m',m+1}$$

$$- \frac{i\varepsilon_x - \varepsilon_y}{2}\sqrt{(j+m)(j-m+1)}\delta_{m',m+1} - i\varepsilon_z m\delta_{m'm}. \tag{H.7}$$

The transformation rule Eq. (H.5) dictates that

$$(T_q^{(k)})' = U_R T_q^{(k)} U_R^+ = \sum_{q'=-k}^{k} T_q^{(k)} D_{q'q}^{(k)}(R). \tag{H.8}$$

Substituting the first-order expression for the rotation given in Eq. (H.7), namely

$$U_R = 1 - \frac{i}{\hbar}\bar{\varepsilon} \cdot \bar{J},$$

into Eq. (H.8), the left hand side becomes

$$\left(1 - \frac{i}{\hbar}\bar{\varepsilon} \cdot \bar{J}\right) T_q^{(k)} \left(1 + \frac{i}{\hbar}\bar{\varepsilon} \cdot \bar{J}\right)$$

$$= T_q^{(k)} - \frac{i}{\hbar}\bar{\varepsilon} \cdot \bar{J}T_q^{(k)} + \frac{i}{\hbar}T_q^{(k)}\bar{\varepsilon} \cdot \bar{J} + \frac{1}{\hbar^2}\bar{\varepsilon} \cdot \bar{J}T_q^{(k)}\bar{\varepsilon} \cdot \bar{J}$$

$$\approx T_q^{(k)} - \frac{i}{\hbar}\varepsilon_x\left[J_x, T_q^{(k)}\right] - \frac{i}{\hbar}\varepsilon_y\left[J_y, T_q^{(k)}\right] - \frac{i}{\hbar}\varepsilon_z\left[J_z, T_q^{(k)}\right]. \tag{H.9}$$

The right hand side yields

$$\sum_{q'=-k}^{k} T_{q'}^{(k)} D_{q'q}^{(k)}(R)$$

$$= \sum_{q'=-k}^{k} T_{q'}^{(k)} \left\{ \delta_{q'q} - \frac{i\varepsilon_x + \varepsilon_y}{2} \sqrt{(k-q)\,(k+q+1)}\delta_{q',q+1} \right.$$

$$\left. - \frac{i\varepsilon_x - \varepsilon_y}{2} \sqrt{(k+q)\,(k-q+1)}\delta_{q',q-1} - i\varepsilon_z q \delta_{q'q} \right\}$$

$$= T_q^{(k)} + \frac{i\varepsilon_x}{\hbar} \left\{ -\frac{\hbar}{2} \sqrt{(k-q)\,(k+q+1)}T_{q+1}^{(k)} - \frac{\hbar}{2} \sqrt{(k+q)\,(k-q+1)}T_{q-1}^{(k)} \right\}$$

$$+ \frac{i\varepsilon_y}{\hbar} \left\{ -\frac{\hbar}{2i} \sqrt{(k-q)\,(k+q+1)}T_{q+1}^{(k)} + \frac{\hbar}{2i} \sqrt{(k+q)\,(k-q+1)}T_{q-1}^{(k)} \right\}$$

$$+ \frac{i}{\hbar} \left(-\hbar\varepsilon_z q \right) T_q^{(k)}. \tag{H.10}$$

Equating left and right sides, and comparing coefficients of $\varepsilon_x, \varepsilon_y, \varepsilon_z$, we obtain

$$\left[J_x, T_q^{(k)} \right] = \frac{\hbar}{2} \left\{ \sqrt{(k-q)\,(k+q+1)}T_{q+1}^{(k)} + \sqrt{(k+q)\,(k-q+1)}T_{q-1}^{(k)} \right\}, \tag{H.11}$$

$$\left[J_y, T_q^{(k)} \right] = \frac{\hbar}{2i} \left\{ \sqrt{(k-q)\,(k+q+1)}T_{q+1}^{(k)} - \sqrt{(k+q)\,(k-q+1)}T_{q-1}^{(k)} \right\}, \tag{H.12}$$

$$\left[J_z, T_q^{(k)} \right] = \hbar q T_q^{(k)}. \tag{H.13}$$

Now $J_\pm = J_x \pm iJ_y$, so that

$$\left[J_+, T_q^{(k)} \right] = \hbar \sqrt{(k-q)\,(k+q+1)}T_{q+1}^{(k)}, \tag{H.14}$$

$$\left[J_-, T_q^{(k)} \right] = \hbar \sqrt{(k+q)\,(k-q+1)}T_{q-1}^{(k)}. \tag{H.15}$$

Hence Eqs. (H.13)–(H.15) are completely equivalent (for infinitesimal rotations) to the required transformation relations in Eq. (H.8) for irreducible tensor operators. This is sufficient to establish the equivalence between Eq. (H.8) and the commutation relations for all rotations, and make it clear that the rotation properties of any operator are determined by its commutator with the angular momentum. This is fortunate, because in practice we could not have applied Eq. (H.8) for *all* possible rotations R! We now turn to the problem of relating irreducible tensor components to the Cartesian components of rank zero, rank one, rank two, etc. tensors, using Eqs. (H.13)–(H.15).

The procedure for constructing spherical tensors is illustrated for rank one (vectors) below. Because the tensor components $T^{(k)}$ and the Cartesian vector components V_i both span the space, and obey linear transformation equations, they must be linear combinations of one another.

$$\left.\begin{aligned} T_1^{(1)} &= aV_x + bV_y + cV_z \\ T_0^{(1)} &= dV_x + eV_y + fV_z \\ T_{-1}^{(1)} &= gV_x + mV_y + nV_z \end{aligned}\right\}. \tag{H.16}$$

Substitution of Eq. (H.16) into Eqs. (H.13)–(H.15) yields nine equations in nine unknowns. We assume that the vector V satisfies the usual angular momentum commutation relations. Each equation can then be simplified by using the relations $[J_i, V_j] = i\hbar\varepsilon_{ijk}V_k$, where ϵ_{ijk} is the Levi-Civita pseudotensor. Its value is $+1$ for cyclic permutations of the indices, -1 for anti-cyclic permutations, and zero if two or more indices are equal.

$$\left[J_z, T_{-1}^{(1)}\right] = [J_z, (gV_x + mV_y + nV_z)] = -\hbar T_{-1}^{(1)},$$

$$i\left(gV_y - mV_x\right) = T_{-1}^{(1)}, \tag{H.17}$$

$$\left[J_z, T_0^{(1)}\right] = [J_z, (dV_x + eV_y + fV_z)] = 0,$$

$$dV_y - eV_x = 0, \tag{H.18}$$

$$\left[J_z, T_1^{(1)}\right] = [J_z, (aV_x + bV_y + cV_z)] = \hbar T_1^{(1)},$$

$$i\left(aV_y - bV_x\right) = T_1^{(1)}, \tag{H.19}$$

$$\left[J_+, T_{-1}^{(1)}\right] = [J_+, (gV_x + mV_y + nV_z)] = \sqrt{2}\hbar T_0^{(1)},$$

$$-n\left(V_x + iV_y\right) + (g + im)V_z = \sqrt{2}T_0^{(1)}, \tag{H.20}$$

$$\left[J_+, T_0^{(1)}\right] = [J_+, (dV_x + eV_y + fV_z)] = \sqrt{2}\hbar T_1^{(1)},$$

$$-f\left(V_x + iV_y\right) + (d + ie)V_z = \sqrt{2}T_1^{(1)}, \tag{H.21}$$

$$\left[J_+, T_1^{(1)}\right] = [J_x + J_y, (aV_x + bV_y + cV_z)] = 0,$$

$$-c\left(V_x + iV_y\right) + (a + ib)V_z = 0, \tag{H.22}$$

$$\left[J_-, T_{-1}^{(1)}\right] = [J_x - iJ_y, (gV_x + mV_y + nV_z)] = 0,$$

$$n\left(V_x - iV_y\right) + (-g + im)V_z = 0, \tag{H.23}$$

$$\left[J_-, T_0^{(1)}\right] = [J_-, (dV_x + eV_y + fV_z)] = \sqrt{2}\hbar T_{-1}^{(1)},$$

$$f(V_x - iV_y) + (-d + ie)V_z = \sqrt{2}T_{-1}^{(1)}, \tag{H.24}$$

$$\left[J_-, T_1^{(1)}\right] = [J_-, (aV_x + bV_y + cV_z)] = \sqrt{2}\hbar T_0^{(1)},$$

$$c(V_x - iV_y) + (-a + ib)V_z = \sqrt{2}T_0^{(1)}. \tag{H.25}$$

These relations are completely general. But notice from Eq. (H.18) that

$$dV_y - eV_x = 0 \rightarrow d = e = 0, \tag{H.26}$$

since $V_y \neq V_x$. Hence, from Eq. (H.16) we find

$$T_0^{(1)} = fV_z. \tag{H.27}$$

Also from Eq. (H.21) we can write

$$T_1^{(1)} = -f\frac{(V_x + iV_y)}{\sqrt{2}}, \tag{H.28}$$

and from Eq. (H.24) we find

$$T_{-1}^{(1)} = f\frac{(V_x - iV_y)}{\sqrt{2}}. \tag{H.29}$$

The simplest choice is $f = 1$, for which we obtain

$$T_1^{(1)} = -\frac{(V_x + iV_y)}{\sqrt{2}}, \tag{H.30}$$

$$T_0^{(1)} = V_z, \tag{H.31}$$

$$T_{-1}^{(1)} = \frac{(V_x - iV_y)}{\sqrt{2}}. \tag{H.32}$$

Based on Eqs. (H.30)–(H.32), the general form of irreducible rank one spherical tensors is

$$V_1^{(1)} = -\frac{(V_x + iV_y)}{\sqrt{2}}, \tag{H.33}$$

$$V_0^{(1)} = V_z, \tag{H.34}$$

$$V_{-1}^{(1)} = \frac{(V_x - iV_y)}{\sqrt{2}}. \tag{H.35}$$

Inverse relations are provided by solving Eq. (H.33)–(H.35) for V_x, V_y, and V_z.

$$V_y = +i\left(\frac{V_1^{(1)} + V_{-1}^{(1)}}{\sqrt{2}}\right), \tag{H.36}$$

$$V_z = V_0^{(1)}, \tag{H.37}$$

$$V_x = -\left(\frac{V_1^{(1)} - V_{-1}^{(1)}}{\sqrt{2}}\right). \tag{H.38}$$

From Eq. (H.36)–(H.38) we can now derive an expression for the scalar product of two vectors $\bar{A}$, $\bar{B}$ in terms of tensor components A_q, B_q adapted to spherical coordinates.

Scalar product

$$\bar{A} \cdot \bar{B} = A_x B_x + A_y B_y + A_z B_z$$

$$= \left(\frac{A_1^{(1)} - A_{-1}^{(1)}}{\sqrt{2}}\right)\left(\frac{B_1^{(1)} - B_{-1}^{(1)}}{\sqrt{2}}\right) - \left(\frac{A_1^{(1)} - A_{-1}^{(1)}}{\sqrt{2}}\right)\left(\frac{B_1^{(1)} - B_{-1}^{(1)}}{\sqrt{2}}\right) + A_0^{(1)} B_0^{(1)}$$

$$= -A_1^{(1)} B_{-1}^{(1)} - A_{-1}^{(1)} B_1^{(1)} + A_0^{(1)} B_0^{(1)}, \tag{H.39}$$

$$\bar{A} \cdot \bar{B} = \sum_{q=-1}^{1} (-1)^q A_q B_{-q}. \tag{H.40}$$

To specify individual vectors like $\bar{A}$ or $\bar{B}$ completely in spherical tensor notation, expressions for the basis vectors as well as the amplitudes are needed. Because their magnitude is unity, the spherical basis vectors may be obtained directly from Eq. (H.33)–(H.35), and are denoted by

$$\hat{\varepsilon}_1^{(1)} = -\frac{1}{\sqrt{2}}\left(\hat{x} + i\hat{y}\right), \tag{H.41}$$

$$\hat{\varepsilon}_0^{(1)} = \hat{z}, \tag{H.42}$$

and

$$\hat{\varepsilon}_{-1}^{(1)} = \frac{1}{\sqrt{2}}\left(\hat{x} - i\hat{y}\right). \tag{H.43}$$

The coefficients of a general vector $\bar{A}$ can then be obtained by replacing all the Cartesian components introduced in the defining expression for $\bar{A}$ with their spherical tensor equivalents given by Eq. (H.36)–(H.38).

$$\bar{A} = A_x \hat{x} + A_y \hat{y} + A_z \hat{z}$$

$$= \left(\frac{-A_1^{(1)} + A_{-1}^{(1)}}{\sqrt{2}}\right)\hat{x} + i\left(\frac{A_1^{(1)} + A_{-1}^{(1)}}{\sqrt{2}}\right)\hat{y} + A_0^{(1)}\hat{z}$$

$$= A_1^{(1)}\left(-\frac{\hat{x} - i\hat{y}}{\sqrt{2}}\right) + A_{-1}^{(1)}\left(\frac{\hat{x} + i\hat{y}}{\sqrt{2}}\right) + A_0^{(1)}\hat{z}$$

$$= (-1)^1 A_1^{(1)}\hat{\varepsilon}_{-1} + (-1)^{-1} A_{-1}^{(1)}\hat{\varepsilon}_1 + (-1)^0 A_0^{(1)}\hat{\varepsilon}_0$$

$$= \sum_{q=-1}^{1} (-1)^q A_q \hat{\varepsilon}_{-q}. \tag{H.44}$$

Irreducible representation of V :

  The electric dipole moment operator is

$$\bar{\mu} = e\bar{r} = e\left[x\hat{x} + y\hat{y} + z\hat{z}\right]$$

$$= er\left[\sin\theta\left(\hat{x}\cos\phi + \hat{y}\sin\phi\right) + \hat{z}\cos\phi\right]$$

$$= er\left(\frac{1}{2}\sin\theta\right)\left[(\hat{x} - i\hat{y})\exp(i\phi) + (\hat{x} + i\hat{y})\exp(-i\phi)\right] + \hat{z}er\cos\theta$$

$$= er\left\{\frac{\sin\theta}{\sqrt{2}}\left[\hat{\varepsilon}_{-1}\exp(i\phi) - \hat{\varepsilon}_1\exp(-i\phi)\right] + \hat{\varepsilon}_0\cos\theta\right\}$$

$$= er\left\{-\hat{\varepsilon}_{-1}Y_1^{(1)}\sqrt{\frac{4\pi}{3}} - \hat{\varepsilon}_1 Y_{-1}^{(1)}\sqrt{\frac{4\pi}{3}} + \hat{\varepsilon}_0 Y_0^{(1)}\sqrt{\frac{4\pi}{3}}\right\}$$

$$= er\left\{\sum_q (-1)^q \left(\frac{4\pi}{3}\right)^{1/2} Y_q^{(1)}\hat{\varepsilon}_{-q}\right\}. \tag{H.45}$$

Consequently, it has three irreducible tensor components given by

$$\mu_{\pm 1} = -erC_{\pm 1}^{(1)}, \tag{H.46}$$

$$\mu_0 = -erC_0^{(1)}, \tag{H.47}$$

where

$$C_q^{(1)} \equiv \left(\frac{4\pi}{3}\right)^{1/2} Y_q^{(1)} \tag{H.48}$$

is the Racah tensor. In the same way, we can write out the field in irreducible form as

$$\bar{E} = -\frac{1}{2}\left\{E_{+1}\hat{\varepsilon}_{-1} + E_{-1}\hat{\varepsilon}_1\right\}\exp[-i(\omega t - kz)t] + c.c. \tag{H.49}$$

Using these results, the interaction Hamiltonian becomes

$$V(t) = -\bar{\mu}\cdot\bar{E}(t)$$

$$= er\sum_q (-1)^q \left(\frac{4\pi}{3}\right)^{1/2} Y_q^{(1)}\hat{\varepsilon}_{-q}\cdot\left(\frac{1}{2}\right)\left\{(E_+\hat{\varepsilon}_- + E_-\hat{\varepsilon}_+)\exp[-i(\omega t - kz)t] + c.c.\right\}$$

$$= er\frac{1}{2}\sqrt{\frac{4\pi}{3}}\left\{(E_+Y_{-1}^{(1)} + Y_1^{(1)}E_-)\exp[-i(\omega t - kz)t] + c.c.\right\}$$

$$= -\frac{1}{2}\left\{\mu_- E_+ + \mu_+ E_-\right\}\exp[-i(\omega t - kz)t] + c.c.$$

$$= (V_+ + V_-)\exp[-i(\omega t - kz)t] + c.c. \tag{H.50}$$

We need matrix elements for V starting from a state i and ending in state f. Let the states themselves be represented by

$$|i\rangle = |\alpha' j' m'\rangle,$$

$$|f\rangle = |\alpha j m\rangle,$$

where j, j' are the angular momenta of the two states and m, m' specify their projections on the axis of quantization. α, α' denote other quantum numbers (like the principle quantum number n) required to specify each state completely. Then

$$\langle f\,|V_-|\,i\rangle = -\frac{1}{2}\,\langle \alpha\,jm\,|\mu_+ E_-|\,\alpha' j' m'\rangle,$$

$$= \frac{1}{2}\,eE_-\,\Big\langle \alpha\,jm\,\Big|rC_+^{(1)}\Big|\,\alpha' j' m'\Big\rangle. \tag{H.51}$$

Using the Wigner–Eckart (W–E) theorem (see Eq. (H.63)), this reduces to

$$\langle f|\,V_-\,|i\rangle = (-1)^{J-m}\frac{1}{2}\,eE_-\,\Big\langle \alpha j\,\Big\|rC^{(1)}\Big\|\,\alpha' j'\Big\rangle \begin{pmatrix} j & 1 & j' \\ -m & 1 & m' \end{pmatrix}, \tag{H.52}$$

where $\langle \alpha j\|rC^{(1)}\|\alpha' j'\rangle$ is the so-called reduced matrix element (independent of m, m'), and $\begin{pmatrix} j & 1 & j' \\ -m & 1 & m' \end{pmatrix}$ is a 3-j symbol that assures that momentum is conserved.

This particular 3-j symbol is nonzero, and specifies that the interaction can take place only if

$$\Delta j = j - j' = \pm 1, \tag{H.53}$$

$$\Delta m = m - m' = +1. \tag{H.54}$$

Hence Eqs. (H.53) and (H.54) constitute selection rules for electric dipole transitions excited by circularly polarized light. Transitions from $j' = 0$ to $j = 0$ are also excluded.

In writing Eq. (H.52) we used the W–E theorem to clarify as much as possible the dependence of the matrix element on the J and m values of the states involved. This theorem is readily proved starting from the transformation relation Eq. (H.8):

$$U_R T_q^{(k)} U_R^+ = \sum_{q'=-k}^{k} T_{q'}^{(k)} D_{q'q}^{(k)}(R).$$

Evaluating both sides for the states considered above, we find

$$\Big\langle \alpha' j' m'\,\Big|U_R T_q^{(k)} U_R^+\Big|\,\alpha\,jm\Big\rangle = \sum_{q'=-k}^{k} \Big\langle \alpha' j' m'\,\Big|T_q^{(k)}\Big|\,\alpha\,jm\Big\rangle D_{q'q}^{(k)}(R). \tag{H.55}$$

On the left side we can make the replacements

$$U_R^+ \,|\alpha\, jm\rangle = \sum_{\mu} |\alpha j\mu\rangle D_{m\mu}^{(j)}(R) \tag{H.56}$$

and

$$\langle \alpha' j'm'|\, U_R^+ = \sum_{\mu'} D_{m'\mu'}^{(j')}(R)\, \langle \alpha' j'm'|\,. \tag{H.57}$$

These relations follow directly from the definition of $D_{m'\mu}^{(j')}$ as the expansion coefficients of a rotated representation of the wavefunction. (See, for example, the defining relation and form of $D_{m'\mu}^{(j')}$ given by Eqs. (16.43) and (16.50) of Ref. [H.2], respectively.)

Using Eqs. (H.56) and (H.57) in Eq. (H.55), we find

$$\sum_{\mu\mu'} D_{m'\mu'}^{(j')}(R) \left\langle \alpha' j'\mu' \left| T_q^{(k)} \right| \alpha j\mu \right\rangle D_{m\mu}^{(j)}(R) = \sum_{q'} \left\langle \alpha' j'm' \left| T_q^{(k)} \right| \alpha\, jm \right\rangle D_{q'q}^{(k)}(R). \tag{H.58}$$

This equation has exactly the same form as an important transformation identity in which Clebsch–Gordan (C–G) coefficients replace the matrix elements on both sides of Eq. (H.58) (see, for example, Eq. (16.91) in Ref. [H.2]).

C–G coefficients furnish the unitary transformation from basis states $|j_1 j_2 m_1 m_2\rangle = |j_1 m_1\rangle |j_2 m_2\rangle$ to basis states $|j_1 j_2 jm\rangle$. That is,

$$|j_1 j_2 jm\rangle = \sum_{m=m_1+m_2} C_{m_1 m_2}^{j}\, |j_1 j_2 m_1 m_2\rangle\,. \tag{H.59}$$

From Eq. (H.59) we see that the $C_{m_1 m_2}^{j}$ have the values

$$C_{m_1 m_2}^{j} = \langle j_1 j_2 m_1 m_2|\, j_1 j_2 jm\rangle\,. \tag{H.60}$$

These coefficients have been extensively tabulated, but are often listed instead in terms of 3-j symbols that have simpler permutation properties. The 3-j symbols are defined by

$$\langle j_1 j_2 m_1 m_2|\, j_1 j_2 jm\rangle = (-1)^{-j_1+j_2-m}\sqrt{2j+1} \begin{pmatrix} j_1 & j_2 & j \\ m_1 & m_2 & -m \end{pmatrix}. \tag{H.61}$$

The fact that the form of Eq. (H.58) is the same as the formula derived from the C–G series simply means that the matrix element $\langle \alpha' j'm'|T_q^{(k)}|\alpha jm\rangle$ we are interested in is proportional to the C–G coefficient. That is,

$$\langle \alpha' j'm'|T_q^{(k)}|\alpha jm\rangle \propto \langle jkmq|jkj'm'\rangle. \tag{H.62}$$

The constant of proportionality in Eq. (H.62) does not depend on m, m', or q and is called the "reduced" matrix element, denoted $\langle \alpha' j'\|T^{(k)}\|\alpha j\rangle$. With this notation, the W–E theorem can be stated as

$$\left\langle \alpha' j'm' \left| T_q^{(k)} \right| \alpha\, jm \right\rangle = \langle jkmq\,|jkj'm'\rangle \left\langle \alpha' j' \left\| T^{(k)} \right\| \alpha j \right\rangle. \tag{H.63}$$

Equation (H.59) has two important implications. First, since transition probabilities depend on $|\langle\alpha'j'm'|T_q^{(k)}|\alpha\,jm\rangle|^2$, it is apparent from the right side of Eq. (H.59) that the relative strengths of optical transitions between different magnetic substates of the same $\alpha j \to \alpha'j'$ transition depend only on squared ratios of C–G coefficients. Second, since the reduced matrix element $\langle\alpha'j'\|T^{(k)}\|\alpha j\rangle$ does not depend on m, m', or q, it represents a transition multipole moment that is independent of the choice of origin. This resolves the issue that standard integral definitions of individual moments yield values of the moments that change with a shift of coordinates.

Our main interest in this book is in the tensor describing the interaction of light with matter as Hamiltonian operator $\hat{V} = -\bar{\mu}\cdot\bar{E}$. How can reduced matrix elements like the one in Eq. (H.52) be evaluated in the simplest, most general way? To explore this question, we first factor out and perform the radial integration for the case of an electric dipole operator. All the radially dependent quantities in the integral are well defined so one can write

$$\langle\alpha'j'\|T^{(1)}\|\alpha j\rangle = \langle\alpha'j'\|rC^{(1)}\|\alpha j\rangle$$

$$= \int_0^\infty \psi^*_{\alpha j}r\psi^*_{\alpha'j'}r^2\,dr\langle\alpha'j'\|C^{(1)}\|\alpha j\rangle_{\theta\phi}$$

$$\equiv \langle\alpha'j'\|r\|\alpha j\rangle_r\langle\alpha'j'\|C^{(1)}\|\alpha j\rangle_{\theta\phi}. \tag{H.64}$$

In the final expression $\langle\alpha'j'\|r\|\alpha j\rangle_r$ is a purely radial integral of r between the specified states. Note, however, that the angular integral over the undetermined quantity $C^{(1)}$ must be worked out by inverting the W–E theorem. This is necessitated by the fact that $\langle\alpha'j'\|C^{(1)}\|\alpha j\rangle_{\theta\phi}$ is not just the angular integral of a known combination of $Y_m^{(1)}$ or other functions. As mentioned above it is in fact independent of q, m, m'.

The radial dependence can be factored out of the general W–E relation (Eq. (H.63)) in the same way as above. From

$$\langle\alpha'j'm'|T_q^{(k)}|\alpha\,jm\rangle = \langle jkmq|jkj'm'\rangle\langle\alpha'j'\|T^{(k)}\|\alpha j\rangle,$$

we thus obtain

$$\langle\alpha'j'm'|C_+^{(1)}|\alpha\,jm\rangle_{\theta\phi} = (-1)^{J'-m'}\,\langle\alpha'j'\|C^{(1)}\|\alpha j\rangle_{\theta\phi}\begin{pmatrix} j' & 1 & j \\ -m' & 1 & m \end{pmatrix}. \tag{H.65}$$

Since we don't know the exact form of $\langle\alpha'j'\|C^{(1)}\|\alpha j\rangle_{\theta\phi}$, we must proceed by evaluating the angular integral on the left of expressions like Eq. (H.65) in order to find the reduced matrix element. Following Sobelman [H.3], the left hand side of Eq. (H.65) is

$$\int Y_{lm}^* Y_q^{(1)} Y_{l'm'}\sin\theta d\theta d\phi$$

$$= (-)^m\sqrt{\frac{(2l+1)\,(2k+1)\,(2l'+1)}{4\pi}}\begin{pmatrix} l & k & l' \\ 0 & 0 & 0 \end{pmatrix}\begin{pmatrix} l & k & l' \\ -m & q & m' \end{pmatrix},$$

so that the reduced matrix element obtained by inverting Eq. (H.65) is

$$\langle \alpha' j' m' | \, \big| C^{(1)} \big| \, | \alpha\, jm \rangle = (-)^{j'} \sqrt{(2j'+1)\,(2j+1)} \begin{pmatrix} j' & 1 & j \\ 0 & 0 & 0 \end{pmatrix}. \qquad \text{(H.66)}$$

The 3-j symbol in the expression Eq. (H.66) for the reduced matrix element dictates that $\Delta j = \pm 1$. The selection rule with respect to magnetic quantum number m arises from the 3-j symbol in Eq. (H.65) and dictates that $\Delta m = m' - m = 1$ in the example of circularly polarized light above. For linearly polarized light, the 3-j symbol in Eq. (H.65) would be

$$\begin{pmatrix} j' & 1 & j \\ -m' & 0 & m \end{pmatrix},$$

changing the magnetic quantum number selection rule to $\Delta m = m' - m = 0$. Additional discussion of the relationship betweenC–G coefficients and 3-j symbols can be found in Ref. [H.4] and formulas for their evaluation are on p. 60–6 of Ref. [H.3]. The choice of phase in Ref. [H.3] and Ref. [H.4] is that of Condon and Shortley [H.5] which renders the C–G coefficients real.

References

H.1. See, for example, G. Arfken, *Mathematical Methods for Physicists*, 2nd edition, Academic Press, New York, 1970, pp. 8–11 and 121–36.

H.2. E. Merzbacher, *Quantum Mechanics*, 2nd edition, Wiley & Sons, New York, 1970.

H.3. I.I. Sobelman, *Atomic Spectra and Radiative Transitions*, Springer-Verlag, New York, 1979, p. 78

H.4. L.I. Schiff, *Quantum Mechanics*, 3rd edition, McGraw-Hill, New York, pp. 214–24.

H.5. E. Condon and G. Shortley, *The Theory of Atomic Spectra*, Cambridge University Press, Cambridge, 1951.

Appendix I

Derivation of Effective Hamiltonians

To treat the dynamics of fully-quantized optical interactions consistently in a single reference frame, one can transform the unperturbed atom into the rotating frame of the light. In cavity QED this calls for transformation of the static atomic Hamiltonian into the rotating frame of the cavity mode.

Consider rotating the wavefunction of the atom into the frame of a cavity field at frequency Ω_c. This is given by

$$\psi(t)' = \begin{bmatrix} \psi_1(t) \exp(-i\Omega_c t/2) \\ \psi_2(t) \exp(i\Omega_c t/2) \end{bmatrix}. \qquad \text{(I.1)}$$

According to Eq. (2.4.12) of Chapter 2, which describes the temporal evolution of ψ for a time-independent Hamiltonian H_0, the components of ψ' in (I.1) progress according to

$$|\psi_1(t)\rangle = C_1(t) \exp(-i\omega_1 t) |1\rangle \tag{I.2}$$

$$|\psi_2(t)\rangle = C_2(t) \exp(-i\omega_2 t) |2\rangle \tag{I.3}$$

Hence the first component changes to

$$|\psi_1(t)'\rangle = C_1(t) \exp(i\Delta t/2) |1\rangle, \tag{I.4}$$

where $\Delta \equiv \omega_2 - \omega_1 - \Omega_c$. Here the zero of energy has been chosen such that $(\omega_1 + \omega_2)/2 = 0$. Similarly, the other component of the wavefunction transforms to

$$|\psi_2(t)'\rangle = C_2(t) \exp(-i\Delta t/2) |2\rangle \tag{I.5}$$

The frequency factor in the argument of the exponential functions in (I.4) and (I.5) can now be interpreted as new effective frequencies of the energy levels in the rotating frame. Hence we can write an effective Hamiltonian in this frame that is given by

$$H_{eff} = \frac{\hbar}{2} \begin{bmatrix} -\Delta & 0 \\ 0 & \Delta \end{bmatrix} = -\frac{\hbar}{2}\Delta\sigma_z, \tag{I.6}$$

where σ_z is one of the Pauli spin matrices.

It is left to the reader to verify that the use of Eq. (I.6) in the equation of motion for the density matrix gives the same result for the slowly-varying amplitude $\tilde{\rho}_{12}$ of the coherence as that in Eq. (7.7.18). This establishes the validity of calculations based on effective Hamiltonians such as that in (I.6). The derivation above also provides a general approach to deriving simplified Hamiltonians for fully quantized systems in a single reference frame. Another example of this approach was given in Chapter 7 where the effective Hamiltonian method was used to reduce the more serious level of complexity of coherent population transfer in a 2-field interaction (Eq. (7.3.2)).

Index